Probing ground and excited state properties of Ruthenium(II) and Osmium(II) polypyridyl complexes

Wesley R. Browne

A Thesis presented to Dublin City University for the degree of Doctor of Philosophy.

2002

Probing ground and excited state properties of Ruthenium(II) and Osmium(II) polypyridyl complexes

Isotope, pH, solvent and temperature effects.

by

Wesley R. Browne, BSc.(Hons), AMRSC

A Thesis presented to Dublin City University for the degree of

Doctor of Philosophy.

Supervisor: Professor Johannes G. Vos

School of Chemical Sciences

Dublin City University

August 2002

Dedicated to Matthew &
to the memory of
Ross and Mick

"Caste a cold eye on life,
on death.
Horseman pass by"

Epitaph for William Butler Yeats

I hereby certify that this material, which I now submit for assessment on the programme of study leading to the award of Doctor of Philosophy by research and thesis, is entirely my own work and has not been taken from work of others, save and to the extent that such work has been cited within the text of my work.

Signed: 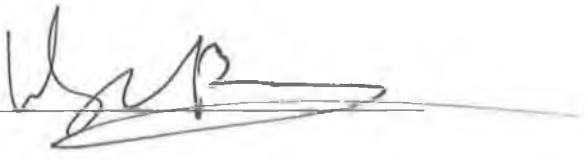

Wesley R. Browne

I.D. No. **95478965**

Date: 11/9/2002

Abstract

The area of ruthenium(II) and osmium(II) polypyridyl chemistry has been the subject of intense investigation over the last half century. In chapter 1, topics relevant to the studies presented in this thesis are introduced. These areas include the basic principles behind the ground and excited state properties of Ru(II) and Os(II) polypyridyl complexes, complexes incorporating the 1,2,4-triazole moiety and the application of deuteriation to inorganic photophysics.

Chapter 2 details experimental and basic synthetic procedures employed in the studies presented in later chapters. A limited discussion of practical aspects of both synthetic procedures and physical measurements is included, in particular where major difficulties were encountered and where improvements to standard procedures were made.

A central theme to this thesis is the application of deuteriation as a spectroscopic probe. In order to fully exploit its potential fully, a general and systematic approach to the deuteriation of polypyridyl type ligands is required. In chapter 3 a range of isotopomers of heteroaromatic compounds containing pyrazyl-, pyridyl-, 1,2,4-triazole-, thienyl-, methyl-, and phenyl- moieties, are reported.

The application of deuteriation in inorganic chemistry as a spectroscopic probe both in simplification of NMR and Raman spectra and as a probe into the excited state structure of heteroleptic complexes is the focus of chapter 4. Deuteriation is employed extensively to probe the excited state structure of several series of Ru(II) and Os(II) polypyridyl complexes. In particular the effect of deuteriation on emission lifetime and ground and excited state resonance Raman spectra is investigated.

In chapter 5, the phenomena of temperature dependent dual luminescence observed for the mononuclear complex $[Ru(bpy)_2(pztr)]^+$ forms the basis of a wider investigation of related complexes in an effort to gain more insight into the nature of the phenomenon. In addition some fundamental studies into the picosecond excited state processes of $[Ru(bpy)_3]^{2+}$ are presented. In these studies deuteriation shows itself as a powerful tool in effecting small but important perturbations.

In Chapter 6 the separation, characterisation and photophysical properties of the stereoisomers of mono- and bi-nuclear Ru(II) polypyridyl complexes is examined. In particular the importance of chirality both in terms of solvent and in complex in determining the circular dichroism, ^{1}H NMR spectroscopy and photophysical properties is investigated.

In chapters 7 and 8, attention is turned to binuclear systems incorporating 1,2,4-triazole moieties. The effects of variations in the bridging ligand in these systems (*e.g.*, distance and spacer groups, pyrazine vs. triazole *etc.*) are examined. Deuteriation is employed in some of these systems as a tool in assessing the localisation of the lowest emissive excited state on particular moieties of the complexes.

Acknowledgements

Where do I start! At the beginning I suppose.

My Family: Thank you Mum for unrelenting support throughout that epic 21 year quest that is known as an education and for the many heated discussions we have had over those years. I won't forget it in your twilight years (I am sure I will be able to arrange a job in an old folks home for you). To my sister "Garda Nicola Browne" for always being there for me, despite the fact I manage to get on your nerves without even trying. Next to Mick for all the trouble you've caused in the few years I have known you (namely Ross and Matthew), thank you for being a friend; you are not forgotten. To Ross, whom is always there like the warm glow of an open hearth. And last but by no means least to Matthew for being, well, Matthew, the ultimate in long-lived excited states.

My Mentors: the main man, Han, the boss, a.k.a Prof. J.G. Vos. The first day I started my postgrad you said something that set the tone for the following three years- "*Of course you can harass me – but come in and close the door first*". And it went downhill after that. Thanks for the enthusiasm, interest and encouragement over the years and for the freedom to do what I was interested in. Also thanks Ronald (Dr. Ronald Hage), for convincing me to do a Phd in the first place and for being the perfect boss (*i.e.* leaving me alone to get on with it; must be a dutch trait). And finally to my Sensei (Mr. John Sweeney) for teaching me self-discipline, how to be a true martial artist and for keeping me focused through my teenage years.

My friends in the North: Firstly to Prof. J.J. McGarvey for allowing me to use his Raman facilities at Queen's University Belfast and sending me to R.A.L.. Thanks Colin (take a break) Coates and Clare (how did you survive the years with Colin!!) Brady. Oh, and thanks Pavel, Mike and Stan with those ultrafast thingies. And also to Kate, Ali and Murph for making Belfast more welcoming.

On the International seen: Bologna, Italy – Firstly thanks to Mama (Prof) Teresa and Papa (Prof) Roberto for helping me learn something about real photophysics and for making me feel welcome on my visits to Bologna. To the family Passaniti, for putting me up in Bologna and for welcoming me with open arms. And to Paolo, a gentleman and a scholar (and a stirrer if ever there was one). To Cincia and Sebastiano in Messina thanks for an interesting adventure that was the DPY/DPZ saga! To Dr. Dusan Hesek and Dr. Claudio Villani (maybe we will actually meet some day) for help with chiral separations.

My proof readers Jennifer McKenna and Aine Connolly (you didn't know what you were letting yourselves in for!). This thesis would not have read near as good without your help. As for the mistakes still in it, I take full responsibility as they are entirely my own (and Han's).

Thanks also go Sligo VEC and Enterprise Ireland for helping me out with a few quid over the years and to the SCS for the facilities in which to do the work.

On the Technical side; I would like to thank all the technicians in the School of Chemical Sciences for being the most capable and professional group of people I will probably ever have the pleasure of working with. My thanks to Mick (an all round good egg if ever their was one), Maurice (Jim'ill fix it for you), Damien (scuba boy), Veronica and Ann (for

sorting out the mess that is the ordering system and more importantly the mess I usually made of it), Ambrose, Vinny, John, Mary and Tony.

On the staff side, I thank especially Dr. Mary Pryce, Dr. Paraic James, Dr. Peter Kenny, Dr John Gallagher, Dr. Josh Howarth and Dr. Kieran Nolan for the invaluable advice they have given over the years.

On the PGAC side, Prof. Malcolm Smyth, Prof. Robert Forster, Mick Burke (again!) Kathleen Greenan, Ger McDermott, Marion King, Jennifer Brennan, Dr. Brett Paul and Dr Dermot Brougham. It was an interesting experience that I am thankfully none the worse for. Keep up the good work.

My friends/colleagues- there are too many to name but a few bear special mention:
Firstly, in the HVRG past and present, again in no particular order. Dr Christine (have you got another paper written for me yet) O'Connor (is it D.O'C or C.O'C), Dr Francis Weldon, Dr Luke O'Brien, Dr. J. Scott Killeen, thanks for getting me started. To Adrian, Dec, Helen and Marco – I could not have done it without you, good luck in the future. I must point out that both Adrian and Dec are in no small measure responsible for me being able to work with purish compounds, thanks for the help lads. Marco deserves an extra mention (if only for his hair's chameleon properties), thanks for challenging my thoughts and interpretations not just in chemistry. Thanks to Gillian Whitaker for helping me (doing the donkey work) on the osmium monomers. Also thanks to Carl and Jennifer, who have managed to stay friends with me for SEVEN years, that's staying power. Oh, and thanks Noel for the CHN's and for proving chemistry can be amusing, and Clare (where's my paper) Brennan for making purple the new orange!

My closest (non-chemistry) friends, in no particular order, Aine Connolly, Lorraine O'Reilly, Alan Pearson, Ed Walsh, Jupe Van den Broeke (technically your chemistry but I've never seen you do anything so the jury is still out), Tom Roberts, Fenton Ewing, Gareth Wynne. Thanks for helping me over the years.

My undergrad days; those were Halcyon days, thanks to that AC shower! Hopefully we will stay in touch.

And last I guess I should mention my housemates in Albert College park. Mark (physics), Kevin (Chemistry), and Henry (biology). It has been an interesting few years. Thankfully in the good sense. Thanks also to Phyllis (my Clare mother) and the girls! in Santry and Fran (I vont to be aloon) in Beaumont

And to the people I haven't mentioned, I have done so on purpose (I've got writers cramp and there are too many of you).

Table of contents

Glossary

Abbreviations used throughout this thesis

CD	Circular Dichroism
COSY	Correlated spectroscopy
CSFE	crystal field stabilization energy
CT	Charge Transfer
CT	Creutz Taube ion: $[(NH_3)_5Ru(\mu\text{-pz})Ru(NH_3)_5]^{6+}$
FC	Franck-Condon
GS	Ground state
HMBC	Heteronuclear multiple bond coherence
HMQC	Heteronuclear multiple quantum coherence
HOMO	Highest occupied molecular orbital
IT/MMCT	Intervalence Transition/ metal to metal charge transfer
LUMO	Lowest unoccupied molecular orbital
^{1}MLCT	singlet metal to ligand charge transfer state
^{3}MLCT	triplet metal to ligand charge transfer state
^{1}MC/^{1}dd	singlet metal centred
^{3}MC/^{3}dd	triplet metal centred
NOE	Nuclear Overhauser Effect enhancement
OTTLE	Optically transparent thin layer electrode
PMD's	Photomolecular devices
π-π*/IL/LC	intraligand or ligand centred transition
CTTS	Charge transfer to solvent
S	Huang Rhys Factor
SCE	supercritical fluid H/D exchange (Chapter 3 only)
SCE	Saturated Calomel electrode (all chapters except chapter 3)
vide infra	see below
vide supra	see above

N.B. For the ruthenium(II) complex based on the ligand Hppt the abbreviations ppt1and ppt2 refer to the binding mode.

ppt1	Refers to binding via N1 of triazole and pyridine
ppt2	Refers to binding via N2 of triazole and pyrazine

Abbreviations and molecular structures of compounds discussed in this thesis

bpy	2,2'-bipyridine
4,4'-bpy	4,4'-bipyridine
2,2'-bpy-N,N-dioxide	2,2'-bipyridine-N,N'-dioxide
H_2dcb	4,4'-dicarboxy-2,2'-bipyridine
dmb	4,4'-dimethyl-2,2'-bipyridine
dpb	4,4'-diphenyl-2,2'-bipyridine
phen	1,10-phenanthroline
ph_2phen	4,7-diphenyl-1,10-phenanthroline
biq	2,2'-biquinoline
dpp	2,3-bis(pyrid-2'-yl)-pyrazine
terpy	2,2';6,2'-terpyridine
pyth	2-(thien-2'-yl)-pyridine
ppy	2-(phenyl)-pyridine

pypz	2-(pyridin-2'-yl)-pyrazine
dppz	dipyridophenazine
phi	1,10-Phenanthroline-5,6-dione
HDPA	2,2'-dipyridyl-amine
Hpytr	3-(pyridin-2'-yl)-1H-1,2,4-triazole
Hpztr	3-(pyrazin-2'-yl)-1H-1,2,4-triazole
HMepytr	5-methyl-3-(pyridin-2'-yl)-1H-1,2,4-triazole
HMepztr	5-methyl-3-(pyrazin-2'-yl)-1H-1,2,4-triazole
1-Mepytr	1-methyl-3-(pyridin-2'-yl)-1H-1,2,4-triazole
1-Mepztr	1-methyl-3-(pyrazin-2'-yl)-1H-1,2,4-triazole
Hphpytr	5-phenyl-3-(pyridin-2'-yl)-1H-1,2,4-triazole
Hphpztr	5-phenyl-3-(pyrazin-2'-yl)-1H-1,2,4-triazole
Htolpztr	5-toluyl-3-(pyrazin-2'-yl)-1H-1,2,4-triazole
Hbpt	3,5-bis(pyridin-2'-yl)-1H-1,2,4-triazole
Hbpzt	3,5-bis(pyrazin-2'-yl)-1H-1,2,4-triazole
Hppt	3-(pyrazin-2'-yl)-5-(pyridin-2'-yl)-1H-1,2,4-triazole

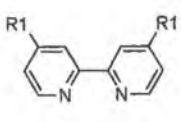

R1
bpy = H
dmb = CH_3
dpb = phenyl
H_2dcb = CO_2H

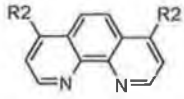

R2
phen = H
ph_2phen = phenyl

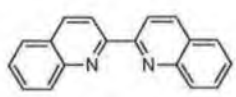

biq

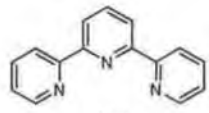

trpy

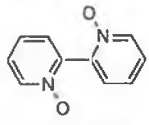

2,2'-bpy-*NN'*-dioxide

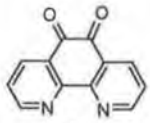

phi

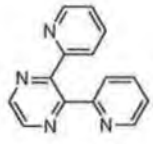

dpp

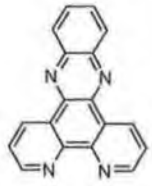

dppz

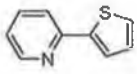

pyth

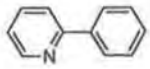

ppy

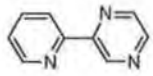

pypz

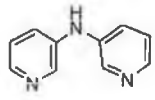

HDPA

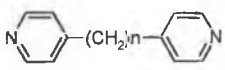

4,4-bpy n =0
P2P n = 2

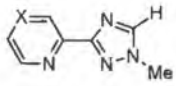

1-Mepytr = CH
1-Mepztr = N

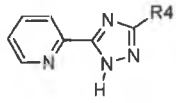

R4
Hpytr = H
HMepytr = methyl
Hphpytr =phenyl
Hbpt = pyridyl-

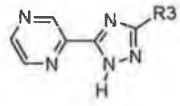

R3
Hpztr = H
HMepztr = methyl
Hphpztr = phenyl
Htolpztr = *p*-tolyl
Hbpzt = pyrazinyl
Hppt = pyridinyl

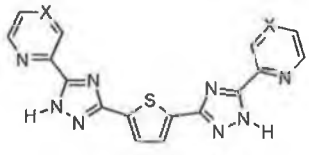

X
$H_2(pytr)_2th$ = CH
$H_2(pztr)_2th$ = N

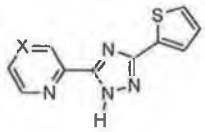

X
Hpytrth = CH
Hpztrth = N

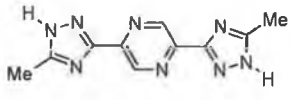

$H_2(Metr)_2pz$

Chapter 1

Introduction

The area of Ru(II) and Os(II) polypyridyl chemistry has been the subject of intense investigation over the last half century. In this chapter, no attempt to include the whole of this area is made, rather areas relevant to the studies presented in the remaining chapters will be introduced. These areas include the basic principles behind the ground and excited state properties of Ru(II) and Os(II) polypyridyl complexes, focusing on the 1,2,4-triazole based complexes and the application of deuteriation to inorganic photophysics. Other areas, which have specific relevance to individual chapters, will be introduced in those chapters.

1.0 Introduction

Since the early 1950's, there has been extensive interest in ruthenium(II) and osmium(II) diimine complexes, primarily because of their extensive photophysical and photochemical properties.[1,2,3] The lowest excited states of these complexes are luminescent and are generally sufficiently long-lived to be capable of engaging in photo-redox and -chemical reactions. In addition it has been found that in an electronically excited state these complexes are both very strong oxidants and reductants compared with the complexes in their electronic ground state (see Figure 1.1).[1,2] These properties have been extensively investigated and are relatively well understood.[1,2] They have been found to be controllable not only by varying external perturbations such as pH and solvent but also by judicious choice of the diimine ligands employed.[4] Ru(II) polypyridyl complexes have also received extensive attention as models for photo-system II and in the catalytic photochemical cleavage of water.[5] Of particular interest therefore is the design of multinuclear structures capable of directing and modulating electron and energy transfer processes.[1,6] Tailoring of the excited state properties of these complexes is central to their adaptation for useful practical application.

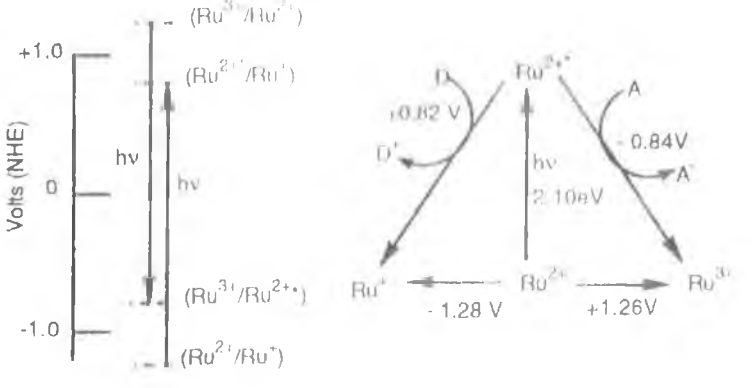

Figure 1.1 *Relationship between ground and excited state redox properties for $[Ru(bpy)_3]^{2+}$ from ref. 1*

With the plethora of diimine ligands and the many techniques available for the synthesis and isolation of both homo- and heteroleptic complexes, preparation of complexes with user-defined properties has become possible.[7] This has allowed for the application of Ru(II) and Os(II) diimine complexes as potential photo-oxidants and reductants, in optical storage systems, in photochemical solar energy conversion devices and as photo-molecular devices.[8] In addition the vast array of symmetric and asymmetric bridging ligands available for the synthesis of polynuclear complexes and mixed metal polynuclear

complexes has allowed for their extensive application in the development of supramolecular chemistry.[8]

1.1 Supramolecular chemistry – modeling the future

Whereas the 20th century is generally regarded as the era of the silicon revolution and of micro-scale electronics, the 21st century is becoming known as the nano-age, with "science fiction" becoming "science-fact" at an ever-increasing rate. The remorseless drive to miniaturization in particular in the field of electronics, witnessed in the 2nd half of the 20th century, is rapidly approaching the "quantum wall" where bulk properties become less certain and quantum mechanics 'kicks in'.[9] This large to small approach of electronics and materials science, which led physicists to deal with sub-micron dimensions, has in the last decade reached the nano-scale.[9] In contrast, molecular chemistry and in particular supramolecular chemistry has worked in the opposite direction creating ever-larger molecules and assemblies. In this approach, molecular "building blocks" are employed to create assemblies, which allow for control of molecular and supramolecular properties and allow for the creation of user-defined properties.[8,10]

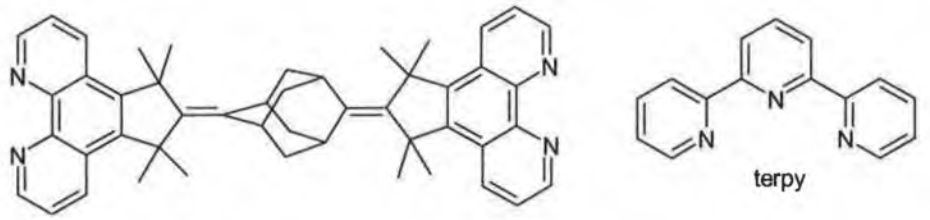

Figure 1.2 *Ligands used in the preparation of molecular wires*

However, despite the advantage, in terms of controlling the properties of molecular aggregates achievable by this bottom-up approach, a conjugate problem is created in the characterization of these systems.[10] Controlling the structure of aggregates, in particular inorganic complexes, by stepwise building of the aggregates has been demonstrated by Serroni *et al.* in the so-called "complexes-as-ligands/complexes as metals" strategy where metals or "complex-metals" are reacted with ligands or "complex ligands".[11] Other strategies include the use of linear aggregates, which are a particular feature of PAP and terpyridine systems (see Figure 1.2).[12] Approaches taken include the "divergent" and "convergent" approaches, the former being a stepwise method in which the peripheral ligands are selectively protected to limit the number of binding sites available and the latter approach is to use a large excess of ligand to prevent multiple binding.[13]

Several issues arise in the preparation and study of large and complex systems, in particular those possessing centres of chirality and asymmetric ligands. The most important of these are the formation of stereo- and coordination- isomers and the effect of isomerism on the NMR spectra, and hence characterisation of such systems.[14,15] The properties of nano-sized systems such as supramolecular assemblies are potentially sensitive to very small variations in structure. In addition to the bottom up development of molecular devices, the development of new characterisation techniques and an understanding of the properties of not only the components of such systems but also their interactions within the assemblies formed, are required.

1.2 Group VIII photophysics (Fe, Ru, Os)

The Group VIII (*i.e.* Fe, Ru, Os) transition metal elements and their cations have dominated the area of transition metal supramolecular chemistry, since the 1960's and 70's.1 In contrast to the first row transition metals (*e.g.* Fe), the second and third row members of the group VIII are rare in the earths crust.[16] Ironically it is these rare elements which show the most interesting photophysical properties, in particular their d^6 ions, whose complexes' tunability has led to intensive interest in potential applications in photo-molecular devices,[8] photocatalysis,[1] and artificial photosynthesis.[5,8] The entire group VIII metals show rich and diverse coordination chemistry and in particular their d^6 ion complexes with imine ligands have received considerable attention over the past 40 years.[1] This has been to a large extent due to the varied character of their emissive excited states, which are generally long lived and undergo not only luminescence but also photochemistry, excited state electron transfer and photo-oxidation and -reduction as well as energy transfer processes.[1,2,3]

1.2.1 Group VIII electronic structure and transitions

Figure 1.3 shows a basic ligand field model for a transition metal complex and the possible transitions, which may occur. In reality such diagrams do not describe the electronic structure of transition metal complexes very well, however it does serve to illustrate the transitions responsible for the electronic absorption spectra of, in this case d^5 and d^6 polypyridyl complexes.

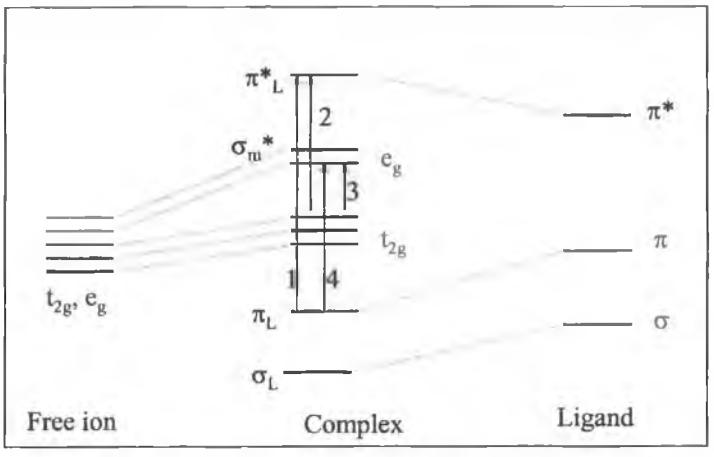

1) ππ* (LC); 2) dπ* (MLCT); 3)dd* (MC); 4) πd* (LMCT)

Figure 1.3 *Jablonski diagram showing the relative disposition of metal and ligand orbitals and possible electronic transitions in for an octahedral ligand field transition metal complex*

The four transitions shown in Figure 1.3 are

1) Ligand centred (LC) or intraligand (IL) are equivalent to that observed for the free ligand
2) Metal to ligand charge transfer (MLCT) where the metal centre is formally oxidised and the ligand reduced
3) Metal centred (MC or dd): a transition from the t_{2g} to the e_g orbitals
4) Ligand to metal charge transfer (LMCT) where the ligand is oxidised and the metal reduced

Other transitions not shown in Figure 1.3 are ligand to ligand (LLCT) and metal-to-metal charge transfer (MMCT). These transitions will be discussed later.

1.2.2 Luminescence from excited electronic states: classification and identification

Before discussing the trends observed in group VIII photophysics, a brief summary of the nature and general properties of luminescence {arising from intra ligand (^{3}IL), ligand to metal charge transfer (^{3}LMCT), metal to ligand charge transfer (^{3}MLCT), ligand to ligand charge transfer (^{3}LLCT) and metal centred (^{3}MC) transitions} is pertinent.[17]

^{3}MC excited states are strongly distorted with respect to the ground state, due to increased electron density in the e_g orbitals and reduced backbonding from the t_{2g} orbitals (see Figure 1.4). Such distortion increases radiationless deactivation rates (greater vibrational overlap at the edges of the potential well, *vide infra*). Emission from the ^{3}MC excited state is generally devoid of vibrational structure (gaussian shaped emission band) and due to the effect of its geometric distortion on Franck-Condon (FC) transitions suffers a

considerable red shift compared with the lowest energy absorption. Such emission has a relatively long lifetime (10 ms to 1 ms) in rigid matrices at 77 K but falls off very quickly with increasing temperature and is not usually observed in fluid solution.

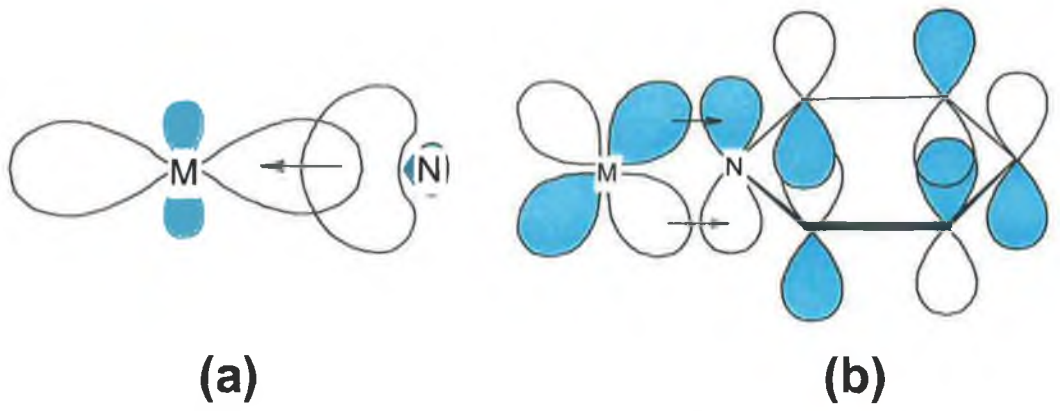

Figure 1.4 *Overlap between (a) σ-donor bond of ligand and metal d_{z^2} or $d_{x^2-y^2}$ orbital of the metal (b) back donation or backbonding from metal to ligand via overlap of metal based d_{xy}, d_{xz} or d_{yz} orbital and ligand π* orbital*

^{3}MLCT states of Ru(II) and Os(II) show little distortion with respect to the ground state and hence slower radiative processes can compete effectively with non-radiative deactivation.[2] Emission from ^{3}MLCT excited states are generally highly structured with prominent vibrational progressions at 77 K and usually show a sizeable Stoke's shift from the lowest energy absorption bands. Emission lifetimes are in the range of 1-50 μs, however natural radiative lifetimes can be 10 times longer. Increasing temperature slowly decreases intensities and lifetimes of ^{3}MLCT emissions such that at 292 K emission lifetimes of 10 ns to 10 μs are normal.

^{3}LC excited states generally show little geometric distortion from ground state geometry and very slow non-radiative decay. ^{3}LC emission is normally highly structured at low temperatures and occurs quite close to free ligand emission (1000 cm^{-1} red shifted). The ^{3}LC excited state is less influenced by the metal centre, hence spin forbidden transitions remain more so than for ^{3}MLCT emission. Emission lifetimes at 77 K are generally found to be greater than 0.1 ms and are seldom observed at 292 K.

^{3}LMCT excited states are rare for d^3 and d^6 transitions (although more common for d^0 {CH_3ReO_3) and d^5 ($[Ru(CN)_6]^{3-}$) transition metal complexes).[18] Emission from such states occurs with considerable Stoke's shift due to the distortion caused by an electron occupying metal centred orbitals.

A point relevant to the assignment of emission bands is the effect of glassy matrices.[19] A glass matrix is not homogeneous and hence charge transfer transitions, which induce considerable changes in the dipole moments of complexes, can show a range of emissive states in such media. In contrast ^{3}IL emissions show much less dependence on the external environment and are less likely to be affected by the matrix. The reason for this lack of sensitivity to solvent a changing solvent environment is due to the negligible dipole change associated with the transition and hence the ground and excited state solvation spheres are generally the same. Multi-exponential emission behaviour has been reported up to 110 K in EtOH/MeOH glasses (glass transition region (or T_g) 115-145 K) by Wallace *et al.*[19] for $[Ru(LL)CO_3Py]^+$ (where LL is a 1,10-phenathroline based ligand). However, above 115 K the matrix can be considered as a viscose fluid and such multi-exponential behaviour has been found to cease above this temperature.

In general above 135 K such a matrix can be viewed as a fluid solution and has been found to behave in such a way.[20] Awareness of the effect of the matrix particularly below the T_g is crucial. The effect of the glass matrix on excited states (in particular the charge transfer excited states) can be explained in terms of rigidochromic effects.[21] As the matrix becomes less fluid on lowering the temperature, its ability to reorientate to take account of the change in electron distribution reduces. Hence in frozen matrices the stabilisation of excited states by solvent sphere reorganisation is not possible. This results in a blue shift in the emission energy on lowering temperature. The extent of this shift depends very much on the nature of the emissive state and the difference in the electronic charge, and hence solvent, distribution between the ground and emissive excited states.

For charge transfer transitions the movement of charge requires significant solvent reorganisation to accommodate the change in charge distribution. In frozen matrices such reorganisation is not normally possible and hence the emission energy in frozen matrices is higher than in fluid solution. For localised excited states such as intra ligand (IL) excited states, no large change in charge distribution and hence solvation sphere is required. As a result, the effect of a rigid matrix on the excited state energy is minimal and only minor differences are observed in the emission energy between fluid and glassy matrices. Solvatochromic effects operate on a similar principle. Polar solvents stabilise charge transfer (CT) states more so than nonpolar solvents and by varying the solvent used, the energy of the observed emission varies also. For non-CT transitions solvent effects are unimportant.[22]

1.2.3 $[Ru(bpy)_3]^{2+}$: the parent ion

$[Ru(bpy)_3]^{2+}$ is perhaps the most extensively studied of the myriad of Ru(II) diimine complexes, with the first reported emission from this complex made by Paris and Brandt in 1959.[23] Since then the interest in $[Ru(bpy)_3]^{2+}$ has flourished and as a result much is known about the photophysical and photochemical properties of the complex.[1,2,3] The chemical stability and redox properties together with its excited state luminescence lifetime and reactivity are just a few of the reasons for the extent of interest in $[Ru(bpy)_3]^{2+}$. The photophysical properties of $[Ru(bpy)_3]^{2+}$ are generally well understood and it has become a standard model and reference complex for comparison with the many other Ru(II) diimine complexes, including those described in this thesis. In this section the excited state structure, photophysical processes and photochemistry of $[Ru(bpy)_3]^{2+}$ are discussed.

1.2.3.1 Singlet or triplet?

Prior to discussing the excited state electronic structure of $[Ru(bpy)_3]^{2+}$, it may be of use to clarify the meaning of the assignment of spin state to electronically excited states. In contrast to the electronically excited states of organic molecules, the assignment of excited states of inorganic complexes as triplet and singlet can be problematic. The heavy atom effect of the ruthenium centre makes the assignment of states as singlet or triplet tentative since the heavy atom induces a considerable amount of spin-orbit coupling. The mixing of singlet and triplet levels which results from spin-orbit coupling is unimportant for first row transition metals but becomes more important for the heavier second row and third row transition metals such as ruthenium and osmium.

Spin-orbit coupling has a significant effect on transitions which are formally spin forbidden *i.e.* $\Delta J = 0$. These can become partially allowed since if L (orbital quantum number) and S (spin quantum number) vary in opposite directions then J (where J = L + S) will remain unchanged. The spin-orbit coupling which increases with the atomic number of an atom (electrons move faster around nuclei with a large positive charge so the interaction between the electric currents and the associated magnetic fields increases) provides the link between L and S. The overall effect of this is to enhance the rate of both radiative and non-radiative transitions, which are formally spin forbidden. Hence for $[Ru(bpy)_3]^{2+}$ excitation to all higher excited states regardless of their formal multiplicity is followed by rapid internal conversion (IC) and inter-system crossing (ISC) to the lowest lying manifold of ^{3}MLCT excited states with near unit efficiency.[2]

1.2.3.2 Excited state electronic structure of $[Ru(bpy)_3]^{2+}$

It is generally agreed in the literature that the lowest excited states of $[Ru(bpy)_3]^{2+}$ can be classified as triplet Metal to Ligand Charge Transfer states (^{3}MLCT) which lie below the triplet ^{3}MC and ^{1}MLCT excited states.[24] The lowest ^{3}MLCT excited state has been found to be a manifold of three close lying excited states (10 and 60 cm^{-1}), which are thermally equilibrated at and above 77 K and are distinguishable only at very low temperatures (< 5 K).[25] A fourth ^{3}MLCT excited state lies approximately 600 cm^{-1} above these lower states and is only thermally populated at higher temperatures (~> 200 K).[24] This fourth ^{3}MLCT state has considerably more singlet character than the lower lying ^{3}MLCT states and hence ISC rates to the ground state by non-radiative processes are considerably enhanced by its presence.

Higher still lies the ^{3}MC excited state which can be populated thermally from the lowest ^{3}MLCT manifold and from which much of $[Ru(bpy)_3]^{2+}$ photochemistry arises. This ^{3}MC state is distorted with respect to the Ru-N bond distance compared with the ^{3}MLCT excited states and the ground state. This can be primarily attributed to the fact that the ^{3}MC-excited state has considerable e_g orbital character and hence places electron density between the ruthenium centre and the nitrogen donor atoms (the ^{3}MC state essentially involves transfer of electron density from the bonding t_{2g}-π^* orbital to an antibonding e_g orbital). The resulting electronic repulsion of placing electron density in the e_g orbitals and the loss of backbonding from the t_{2g}-π^* orbital (

Figure ***1.4***), weakens the Ru-N bonds and increases the Ru-N bond length. As a result of this weakening of the Ru-N bond, dissociation of the ligands can and does occur (*vide infra*). Above the ^{3}MC state lie the ^{1}MLCT, ^{1}MC and π-π^* transitions. Transitions from the ground state to these states can be observed in the electronic absorption spectrum of $[Ru(bpy)_3]^{2+}$ (vide infra).

1.2.3.3 Electronic absorption spectrum

Ru(II) diimine complexes are normally stable low-spin species and form octahedral coordination complexes with a diamagnetic t_{2g}^6 electronic configuration. The absorption spectrum[2] of $[Ru(bpy)_3]^{2+}$ exhibits intense absorption bands at 185 nm and 285 nm, assigned to LC (π-π^*) transitions by comparison with the spectrum of the protonated ligand H_2bpy^{2+}.[26] The remaining intense bands at 240 and 452 nm are assigned to a metal-to-ligand charge-transfer (^{1}MLCT, log ε_{450} = 4.16) transition.

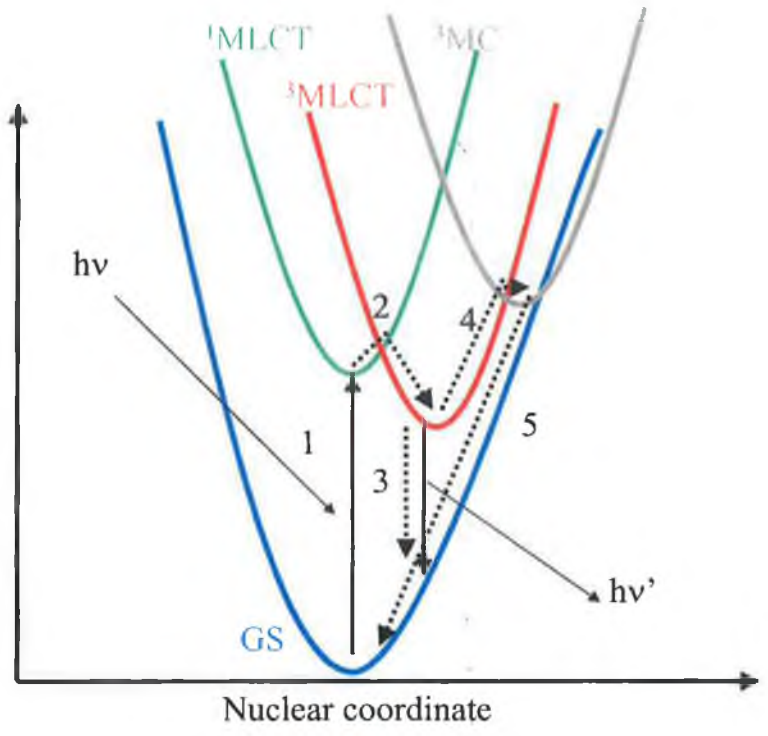

Figure 1.5 *Excited state structure of $[Ru(bpy)_3]^{2+}$. Excited state processes: 1) absorption of light with excitation from GS to the ^{1}MLCT state, 2) ISC, 3) radiative (hν') and non-radiative relaxation to GS from ^{3}MLCT, 4) Thermal population of the ^{3}MC state, 5) radiationless deactivation of the ^{3}MC state to the ground state.*[2]

This latter band is in fact a manifold of at least five overlapping absorption bands. The shoulders at 322 nm and 344 nm are not fully understood and may be metal centred transitions. At low temperatures (77 K) a weak band at 550 nm is observable and has been assigned as a spin forbidden ^{3}MLCT band.[27]

1.2.3.4 Luminescence

The emission spectrum of $[Ru(bpy)_3]^{2+}$ shows considerable temperature dependence between 2 and 300 K. Detailed studies of the emission properties of $[Ru(bpy)_3]^{2+}$ have been made by several research groups.[2] Luminescence occurs from a set of three closely spaced excited states. The detailed description of this manifold is still a matter of debate and for the purposes of this thesis is treated as a single state. In alcoholic glasses the emission lifetime at 77 K is of the order of 5 μs and has a quantum yield of 0.4. Above the glass transition temperature there is a dramatic reduction in emission intensity and quantum yield due to the contribution of solvent vibrational modes to the non-radiative decay of the ^{3}MLCT. At room temperature in deaerated aqueous solution the emission lifetime is reduced to 540 ns and the quantum yield is less than 0.02.

1.2.3.5 Lifetime of the emitting state and its temperature dependence

Figure 1.5 shows the various excited state processes that occur for $[Ru(bpy)_3]^{2+}$. The quantum yield of the emission is the fraction of the absorbed light, which is reemitted and can be expressed as:

$$\textbf{Equation 1.1} \quad \phi_{em} = k_r / (k_r + \Sigma k_{nr})$$

where k_r is the natural radiative rate constant and Σk_{nr} is the sum of the non-radiative rate constants. From this the natural radiative rate constant for $[Ru(bpy)_3]^{2+}$ can be determined (13 μs).[2]

This equation is derived from the general equation[28] for the quantum yield of phosphorescence:

$$\textbf{Equation 1.2} \quad \phi_p = \eta_{isc} k_p \tau_{obs}$$

where ϕ_p is the quantum yield of phosphorescence, η_{isc} is the efficiency of intersystem crossing (ISC), k_p is the natural radiative rate of phosphorescence and τ_{obs} is the measured lifetime of the emitting state. Since the efficiency of ISC is taken to be very close to unity for Ru(II) and Os(II) polypyridine complexes and the measured lifetime is equal to the inverse of the sum of all excited state deactivation processes then Equation 1.1 as written above is valid.

The temperature dependence of the emission lifetime has been accounted for by a stepwise term and two Arrhenius terms (Equation 1.3):

$$\textbf{Equation 1.3} \qquad 1/\tau = k_o + B/\{1+exp[C_i(1/T-1/T_B)]\} + A_1 e^{-\Delta E_1/RT} + A_2 e^{-\Delta E_2/RT}$$

Where τ is the observed emission lifetime, k_o is the natural radiative rate constant, $k_i^{nr} = A_i e^{-\Delta E_i/RT}$ describes the activated surface crossing to another excited state and $k_i^{nr} = B/(1+\exp[C_i(1/T-1/T_B)])$ describes vibrational modes that favour radiationless deactivation (*e.g.* solvent), which are inhibited at low temperature due to the frozen molecular environment. This term describes the stepwise behaviour centred at a temperature T_{Bi}, C_i is the temperature related to the smoothness of the step and B_i is the value attained by k_i at $T >> T_{Bi}$. This term is only of importance in the region of the glass/fluid transition (T_g).

Non- radiative relaxation processes can occur in one of the following ways:

(1) vibrational relaxation of an excited state species within one electronic state by collisional interaction with the surrounding medium

(2) internal conversion from one electronic state to another state of the same multiplicity; IC

(3) intersystem crossing between states of different multiplicity; ISC

The mechanisms by which electronically excited states transfer excess vibrational energy during radiationless transitions have been of much theoretical interest. In general M-N, C-C and X-H stretching modes are considered as principal "accepting" modes, the vibrational modes into which the majority of the excited state energy is disposed. The role this concept plays in the effect of deuteriation on excited states will be discussed below and in Chapters 4 and 5.

1.2.3.6 Redox properties

Ru(II) compounds are redox active and can be oxidised (removal of a metal-localised electron) or reduced (addition of an electron in a ligand π* orbital). Table 1.1 shows the redox potentials in acetonitrile (vs. SCE) for $[M(bpy)_3]^{2+}$ (M = Fe, Ru, Os).

Metal complex	M^{II}/M^{III}	Ligand reduction
$[Fe(bpy)_3]^{2+}$	1.05 V[29]	--
$[Ru(bpy)_3]^{2+}$	1.26 V	-1.35
$[Os(bpy)_3]^{2+}$	0.83 V	-1.28

Table 1.1 *Redox properties of $[M(bpy)_3]^{2+}$ complexes (vs. SCE)*

The most interesting feature of both Ru(II) and Os(II) polypyridyl redox chemistry is that typically both metal and ligand redox processes are fully reversible. This is advantageous in that it allows for the investigation of the spectroscopic properties of the oxidised and reduced forms of the complex by bulk electrolysis.

1.2.3.7 Photochemistry

The photochemistry of $[Ru(bpy)_3]^{2+}$ has been extensively studied.[2,1] Its photoreactivity arises from both the ^{3}MLCT excited states, which have a sufficiently long lifetime to engage in both energy and electron transfer processes, and the ^{3}MC excited states from which ligand dissociation can occur.[2] The photochemistry, which arises from the ^{3}MC excited state is of most interest to the studies described in this thesis and hence will be

discussed in some depth here. Processes arising from the ^{1}MLCT/^{3}MLCT excited states will not be discussed further (*e.g.* electron transfer).

As mentioned above, when $[Ru(bpy)_3]^{2+}$ is in the ^{3}MC excited state, Ru-N bond lengths are considerable distorted with respect to the ground state (Figure 1.5). This has an important consequence in terms of the rate of vibrational deactivation of the excited state. The Franck-Condon (FC) sum of the vibrionic overlap integral term is important in determining the contribution of vibrational deactivation to the overall rate of non-radiative excited state decay (*vide infra*). The amplitude of the vibrational levels are greatest at the "edges" of the potential well, hence when the "edges" of two electronic states are close, *i.e.* ^{3}MC and GS, then the vibrionic overlap will be much greater than for the ^{3}MLCT and the ground state (GS). As a result the FC Factor and the rate of radiationless deactivation will be enhanced. This has been shown to be the case by Van Houten and Watts,[30] by examination of the temperature dependence of $[Ru(bpy)_3]^{2+}$ and they found that the deactivation of the ^{3}MC state was extremely fast. It should be noted that it is the ^{3}MC excited from which photochemical decomposition occurs, however Van Houten *et al.* found that this was a thermally activated process and was very much a minor deactivation process of the ^{3}MC excited state. This is important as it implies that the effect of the ^{3}MC state on the ^{3}MLCT states is not restricted to a route of Ru-N bond rupture, rather it forms a very efficient channel for non-radiative excited state relaxation. These results also suggest that the ^{3}MC excited states are associative rather than dissociative, and that photo-reactivity from these states is a thermally activated process in itself. The implications of this, is that by raising or lowering the ^{3}MC excited state energy, the photoreactivity and the ^{3}MLCT-GS emission intensity and lifetime may be tuned. For most applications such as in photovoltaics,[5c,31] where electron transfer processes from the ^{3}MLCT are of interest and an increase in stability as regards photochemical decomposition is desirable, then the raising of the ^{3}MC excited states is equally desirable.[5,8] However for other applications such as photo-molecular devices the ability to induce a structural change with light (preferably reversible) is of interest, hence population of the ^{3}MC may be desirable and lowering its energy relative to the ^{3}MLCT excited state would be preferred.[8]

The photophysics and photochemistry of Ru(II) and Os(II) complexes are dominated by the relative energies of the ^{3}MLCT and ^{3}MC excited states to the ground electronic state and by the relative energy separation between the ^{3}MLCT and ^{3}MC themselves. For

applications such as photosensitisers and as photochemically driven redox catalysts, photostability is very desirable, requiring as a large a separation between the GS/^{3}MLCT excited states and the ^{3}MC excited states as is possible. However by increasing the energy of the ^{3}MC excited states by the use of osmium a loss in the energy gap between the ground state and the ^{3}MLCT excited states occurs (due to the higher lying 5d orbitals relative to the 4d orbitals of ruthenium). This has important consequences, as the energy gap law states that the closer two energy levels are, the larger the rate of both radiative and non-radiative deactivation.[2,32] Hence for Os(II) complexes' ^{3}MLCT excited state, the radiative lifetime is considerably reduced to ten's of nanoseconds from the several hundreds of nanoseconds observed for $[Ru(bpy)_3]^{2+}$.[2]

1.2.4 $[Fe(bpy)_3]^{2+}$, $[Ru(bpy)_3]^{2+}$, $[Os(bpy)_3]^{2+}$: excited state structures

In addition to $[Ru(bpy)_3]^{2+}$, complexes of other group VIII metals *i.e.* iron and osmium are of interest. Iron, being readily available and inexpensive, would be a very attractive alternative to ruthenium, but that the chemistry of its complexes demonstrate much greater lability in contrast to those of their ruthenium based analogues.

Metal complex	Lowest excited state	Luminescence (energy)
$[Fe(bpy)_3]^{2+}$	^{3}MC	No!
$[Ru(bpy)_3]^{2+}$	^{3}MLCT	Yes (610 nm at 298 K)
$[Os(bpy)_3]^{2+}$	^{3}MLCT	Weakly (720 nm at 298 K)
$[Rh(bpy)_3]^{3+}$	^{3}LC	Yes (77 K)
$[Ir(bpy)_3]^{3+}$	^{3}LC	Yes (450 nm at 77 K)

***Table 1.2** from ref. 1*

$[Fe(bpy)_3]^{2+}$ is deep red in colour and absorbs strongly in the visible region, however, it is not luminescent to any appreciable extent.[24] Its lowest excited state is ligand field (^{3}MC) rather than charge transfer in nature rendering its complexes inherently photochemically unstable. Osmium analogues, on the other hand, exhibit chemistry closely related to that of ruthenium, although for $[Os(bpy)_3]^{2+}$ the ^{3}MLCT excited state lifetime is 10-30 times shorter than for $[Ru(bpy)_3]^{2+}$. The ^{3}MC state of $[Os(bpy)_3]^{2+}$ lies at higher energy than that of $[Ru(bpy)_3]^{2+}$, and for this reason, osmium complexes are photochemically inert. The effect of metal substitution on the lowest excited state and on the emission energy of a series of bpy-based complexes is shown in Table 1.2:

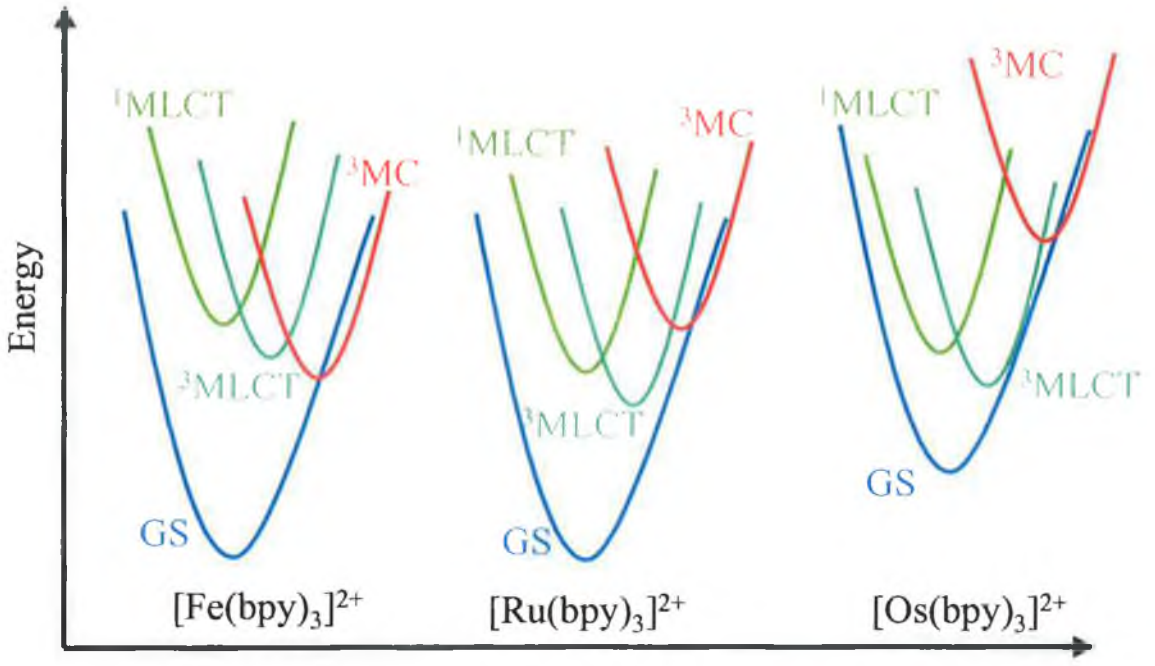

Figure 1.6 *Excited state structure of $[M^{II}(bpy)_3]^{2+}$ (M = Fe, Ru, Os)*

1.2.4.1 Photophysical properties

The excited state structures of $[M^{II}(bpy)_3]^{2+}$ (M = Fe, Ru, Os) are described in Figure 1.6. For low spin M^{II} complexes the ground electronic state is a singlet state, hence only transitions to singlet-excited states are formally allowed. As discussed above the effect of spin orbit coupling is such that formally forbidden spin transitions *e.g.* spin forbidden transitions become more allowed as the atomic number increases. Hence for Os(II) and to a lesser extent Ru(II), ^{3}MLCT absorption transitions are observed in the visible region of their UV.Vis absorption spectrum.

In order to understand why Ru(II) complexes are of interest towards many photophysical and photochemical applications, the relative energies of the various low-lying excited states must be examined. For Fe(II) diimine complexes the lowest excited state is principally the ^{3}MC excited state, lying lower than either the lowest ^{3}MLCT or ^{1}MLCT excited states. Although ISC is weaker for Fe(II) complexes than for Ru(II) or Os(II), efficient population of the ^{3}MLCT excited states occurs followed by rapid internal conversion to the non-emissive ^{3}MC excited states. For Ru(II) and Os(II) emission from the lowest ^{3}MLCT excited states is an important deactivation pathway, however, for Fe(II) this is not the case, since non-radiative deactivation and photo-decomposition via the ^{3}MC excited state are the dominant decay pathways. Population of the ^{3}MC excited states of Ru(II) complexes is a thermally activated process and is important only at elevated temperatures (> 30 °C). For $[Os(bpy)_3]^{2+}$ population of such states is possible

thermally but due to the large energy gap requires much higher temperatures than for Ru(II).[30]

1.2.5 Tris heteroleptic Ru(II) diimine complexes

As the number of suitable metals is very limited, the search for alternatives to $[Ru(bpy)_3]^{2+}$ has thus far focussed mainly on the ligand system, with the maintenance of the Ru(II) centre and the presence of three bidentate ligands allowing for fine-tuning of the properties.[2] A considerable amount of effort has been directed towards modification of the polypyridine ligand systems, with a view to obtaining more robust complexes with tuneable spectroscopic and electrochemical properties.[2] Approaches have included attachment of electron mediating substituents to the pyridine rings, employing ligands with different electronic contributions, ligands with varying σ-donor and π-acceptor properties, in homoleptic and heteroleptic configurations.[2] The nature of the lowest excited states of heteroleptic complexes is the subject of extensive investigation and debate.[33] In particular the localisation/delocalisation, over all three ligands, of the lowest lying ^{3}MLCT excited state (Figure 1.7).

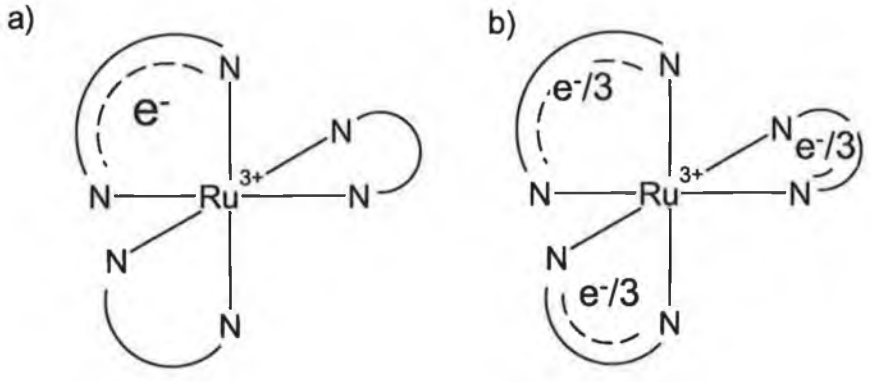

Figure 1.7 *a) Localised versus b) delocalised excited state model*

Localisation vs. Delocalisation.

Various techniques have been employed in an attempt to answer the question of localisation of the excited state on individual ligands, in particular high resolution emission spectroscopy and Raman spectroscopies. In order to aid interpretation of the data obtained from these studies, deuteriation has been employed to effect perturbation of the vibrational structure of Ru(II) complexes with only minimal perturbation of their electronic structure.[33]

The primary difficulty with answering this issue of excited state location has been the fact that for homoleptic complexes each of the ligands are equivalent and spectral and temporal resolution of the emission, excited state absorption (ESA) and resonance Raman

spectra are impossible. Some attempts at spectral resolution have been made in vibrational studies using selective deuteriation of ligands,[33] however these studies have been far from conclusive and are themselves subject to controversy. Of primary interest is the effectiveness of the ruthenium metal centre in mediating electronic communication between the ligands. For isoelectronic Rh(III) complexes this interaction is generally accepted as being minimal, which is demonstrated by the presence of a dual ^{3}IL emission from some of its heteroleptic complexes (see Chapter 6).[34] This is also true for Ir(III) complexes although the level of interaction mediated by the metal centre is greater than for Rh(III). In contrast Os(II) complexes show extensive metal mediated interaction between ligands.

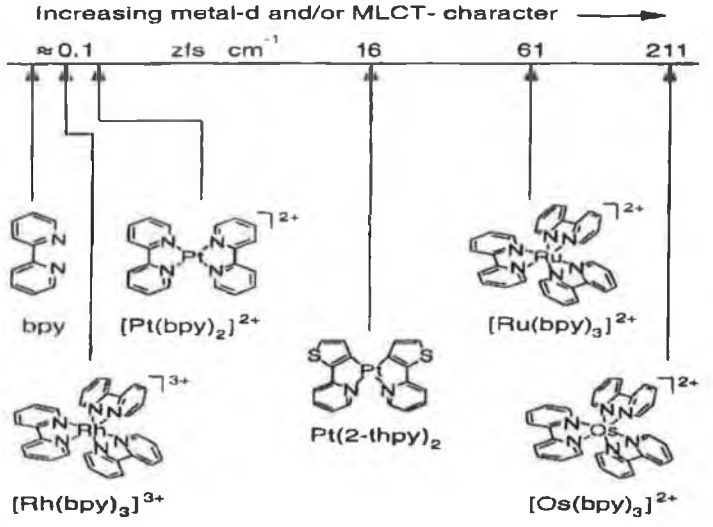

Figure 1.8 *Chart showing relative interligand coupling for several platinum group complexes (zfs = zero field splitting reflects the importance of metal character to the lowest excited state)* [35]

Ru(II) complexes are somewhat intermediate in the degree of communication between ligands in its complexes. Substitution of a bpy ligand of $[Ru(bpy)_3]^{2+}$ for 2,2'-bipyrazine or 2-(pyrid-2'-yl)-pyrazine[36] has been shown by resonance Raman (rR) to localise the excited state on the 2,2'-bipyrazine ligand and pyrazine moiety respectively, clearly demonstrating that given a sufficient difference in the ^{3}MLCT levels of the ligands in a heteroleptic ruthenium complex, localisation on a particular ligand will take place. However the fact that the emission quantum yields in such complexes are independent of excitation wavelength shows that the interaction between ligands is sufficient to allow for fast intramolecular energy transfer.

It has been shown that in heteroleptic complexes the excited state can be ligand localised given a sufficient difference in the relative LUMO (lowest unoccupied molecular orbital)

energies of the ligands.[37] This does not address the question as to whether the photophysical properties of the lowest excited ^{3}MLCT states are an average of the properties of the ligand localised excited states or due to a delocalised ^{3}MLCT excited state over all or some of the ligands.

Assuming that the excited states of these complexes are predominantly localised on individual ligands, then two limiting situations are possible for the excited state properties of such complexes. If the electronic communication between the ligands is weak then the rate of energy transfer between the excited states based on individual ligands will not be sufficient to allow the system to reach equilibrium within the emission lifetime of the excited states. If however the electronic communication is strong, then the system will reach equilibrium within the emission lifetime of the complex and will emit from the lowest excited state (Kasha's rule).[38] The former situation will give rise to multiple emissions from the complex (or rather from the excited states based on the ligands). This does not violate Kasha's rule as the excited states are effectively independent and hence can be viewed as separate systems. If however a delocalised model is proposed then dual emission should not be observed since the electronic communication between the ligands is inherently strong. The delocalised model is not however the same as for the second (strong communication) limit of the localised model, since the individual excited states have character due to all of the ligands and are not based on any specific ligand.

Heteroleptic complexes of the type $[Ru(bpy)_{3-x}(phen)_x]^{2+}$, $[Ru(bpy)_{3-x}(ph_2phen)_x]^{2+}$ (X = 1 or 2)have been employed by several groups to assess the level of interaction between the ligands of heteroleptic complexes and by inference homoleptic complexes.[39] The ligands bpy, phen and ph_2phen are structurally very similar. They all possess C_{2v} symmetry and hence the vibrational properties of their complexes are expected to be similar. However the increased structural rigidity of the ligands, and possibly more importantly by elimination of promoter modes (see Chapter 4), in the order bpy, phen, ph_2phen, results in a decrease in the vibrational contribution to the overall non-radiative decay rate constant k_{nr} of the lowest ^{3}MLCT excited states of their respective ruthenium (II) complexes.

Kumar *et al.*[39] have examined the excited state absorption spectra (ESA) and resonance Raman (rR) spectra of mixed ligand complexes of these types. They found that the excited state lifetimes of the mixed ligand complexes $[Ru(bpy)_x(phen)_{3-x}]^{2+}$ are statistical averages of the parent homoleptic complexes.[25] In addition, emission quantum yields and spectral maxima suggest rapid thermal equilibration. It has been suggested that moving

the equilibrium in favour of one ligand could localise the excited state of a Ru(II) polypyridyl complex.[40] To this end they employed ph_2phen to prepare the complexes $[Ru(bpy)_x(ph_2phen)_{3-x}]^{2+}$. Using both ESA and rR studies they found the following:

1. The ESA spectra of $[Ru(bpy)_x(phen)_{3-x}]^{2+}$ complexes are unaffected by excitation wavelength whereas the nanosecond ESA spectra of mixtures of $[Ru(bpy)_3]^{2+}$ and $[Ru(phen)_3]^{2+}$ critically depend on the relative absorption at the excitation wavelength employed. The ESA spectrum of $[Ru(bpy)_2(phen)]^{2+}$ is super-imposable on $[Ru(bpy)_3]^{2+}$ / $[Ru(phen)_3]^{2+}$ mixtures of 2:1 ratio (ABS) at 355 nm. This indicates that an initial population of the bpy or phen ligand is quickly equilibrated in the case of the mixed ligand complexes whereas for the mixtures of the parent homoleptic complexes this does not occur. Hence it can be assumed that intramolecular energy transfer is faster than intermolecular energy transfer.
2. The ESA spectrum $[Ru(bpy)_x(ph_2phen)_{3-x}]^{2+}$ (x = 1 or 2) at 20 ns, at 355 nm excitation, is very similar to $[Ru(ph_2phen)_3]^{2+}$ and is distinct from a 2:1 mixture of the parent homoleptic complexes. Therefore, the equilibrium favours a ph_2phen based excited state over a bpy based excited state. The transient spectra of both complexes, $[Ru(bpy)_2(ph_2phen)]^{2+}$ and $[Ru(bpy)(ph_2phen)_2]^{2+}$, are independent of excitation wavelength.

Excited state rR of $[Ru(bpy)_x(phen)_{3-x}]^{2+}$ are in agreement with the ESA spectra for the complexes. The excited state rR spectra is superimposable with spectra for the parent complexes albeit with phen appearing weaker (due to low resonance Raman enhancement).[41] Excited state rR spectra of $[Ru(bpy)_x(ph_2phen)_{3-x}]^{2+}$ show characteristic ph_2phen resonances with weaker bpy based bands suggesting ph_2phen is dominant and the excited state is localised on ph_2phen.

The photophysical properties of the $[Ru(bpy)_2(phen)]^{2+}$ complex demonstrate that when the excited state energies of the ligand based ^{3}MLCT are very close, under conditions where electronic communication is strong, excitation into either bpy or phen based ^{1}MLCT or ^{1}IL excited states results in a near statistical population of the bpy and phen based ^{3}MLCT excited states well within the overall lifetime of both ^{3}MLCT excited states.[42] Emission from both states is observed, as the energy difference (100 cm^{-1}) between the excited states is insufficient to favour emission from one over the other. For $[Ru(bpy)_{3-x}(ph_2phen)_x]^{2+}$ in contrast, the energy gap is much larger and hence emission from a ph_2phen based excited state occurs.

In Chapter 4 the effect of systematic partial and complete deuteriation on the complexes of the type $[M(bpy)_{3-x}(ph_2phen)_x]^{2+}$ will be examined in order to assess whether the location of the excited state can be determined by the effect of deuteriation on emission lifetimes.

1.3 Triazole based heteroleptic ruthenium (II) and osmium (II) polypyridyl complexes: Photochemical, Electrochemical, Photophysical, ^{1}H NMR spectroscopic properties

The properties of Ru(II) compounds are governed by the σ-donor and π-acceptor properties of the ligands. The σ-donor capacities of the ligands can be estimated by measuring the pK_a of the free ligand,[43] whilst the π-acceptor properties are related to the reduction potential of the ligands.[43] Ligands that are stronger σ-donor ligands (Class A) or better π-acceptors (Class B) (see Figure 1.4) than bpy are of interest as they allow for the tuning of both the ground and excited state properties. An increase in the σ-donor properties compared with bpy results in a greater crystal field splitting (*i.e.* a stabilisation of the metal based ground state and a raising of the potentially photoactive ^{3}MC state).

Apart from bpy, several Ru(II) complexes containing strong π-accepting ligands such as 2,2'-bipyrazine (bpz), 2,2'-bipyrimidine (bpm) and 2,2'-biquinoline (biq) have been reported in the literature.[2] The increased π-acceptor properties of the ligands relative to bpy result in a decrease in the electron density of the metal centre and hence a reduction in the crystal field splitting of the complex. This can be observed in their electrochemical properties in that their metal oxidation potentials and ligand reduction potentials are more positive than for $[Ru(bpy)_3]^{2+}$. This loss in crystal field splitting results in a reduction in the level of the ^{3}MC states, rendering the ligands photo-unstable and reducing their quantum yield of emission.

In contrast class B ligands (strong σ-donors, weak π-acceptors) have the reverse effect on the ground and excited state properties. In Ru(II) complexes possessing 'class B ligands' electron density is donated into the d orbitals, reducing the metal oxidation potentials and shifting the ligand reductions to more negative potentials. Ligands with these characteristics (strong σ-donor capacity) include 2-(pyridin-2-yl)-imidazole and 2-(pyridin-2'-yl)-pyrazole.[44] Their strong σ-donor capacities result in larger ligand-field

splitting, raising the energy of the ^{3}MC excited state and thus preventing photodecomposition. Due to their strong σ-donor capabilities, the ligands possess π* levels of much higher energy than bpy and as a result the excited state is always bpy based in mixed chelate complexes containing both bpy and class B ligands.

Included in class B is the strong σ-donor/weak π-electron ligand 1,2,4-triazole. The first report of 1,2,4-triazole ligands and their ruthenium complexes was by Vos and co-workers in 1983.[45] It is noted that the 1,2,4-triazole's weak π-acceptor properties, compared to 2,2'-bipyridine, increase on protonation of the triazole ligand and its σ-donor properties decrease. More recently, the combination of class A and B type ligands, *e.g.* 2,2'-biquinoline and 1,2,4-triazoles, was shown to result in pH dependent photochemical reactivity.[46]

Pyridyl-1,2,4-triazole ligands possess an acid-base chemistry that can be utilised to manipulate the properties of their Ru(II) complexes. Protonation/deprotonation of the uncoordinated nitrogen of the triazole leads to important changes in the properties of the complexes. Protonation reduces the σ-donor capacity of the ligand that results in marked effects on the ground and excited state properties of the complexes. In the deprotonated state the pyridyl-1,2,4-triazole complexes are in general photostable, whilst in the protonated state they exhibit a marked photochemical reactivity due to their decreased σ-donating ability (and hence a lowered ^{3}MC level).[47]

Another important feature of pyridyl-1,2,4-triazole type complexes is the asymmetry of the coordination sites of the triazole whereby the specific sites chosen affect the magnitude of σ-donation experienced by the metal. Hage and co-workers have investigated the syntheses and structures of Ru(II) complexes with six substituted 3-(pyridin-2'-yl)-1,2,4-triazole ligands.[48] It was deduced from ^{1}H-NMR and X-ray analysis that the metal ion can bind via N2 or N4 of the triazole ring with the most favourable coordination mode depending on the position of the ring substituents. For example, the ligand 3-(pyrid-2'-yl)-1H-1,2,4-triazole exhibits both coordination modes, 3-methyl-5-(pyrid-2'-yl)-1H-1,2,4-triazole exhibits predominantly the N2 coordination mode, and 1-methyl-5-(pyrid-2'-yl)-1,2,4-triazole exhibits predominantly the N4 coordination mode.

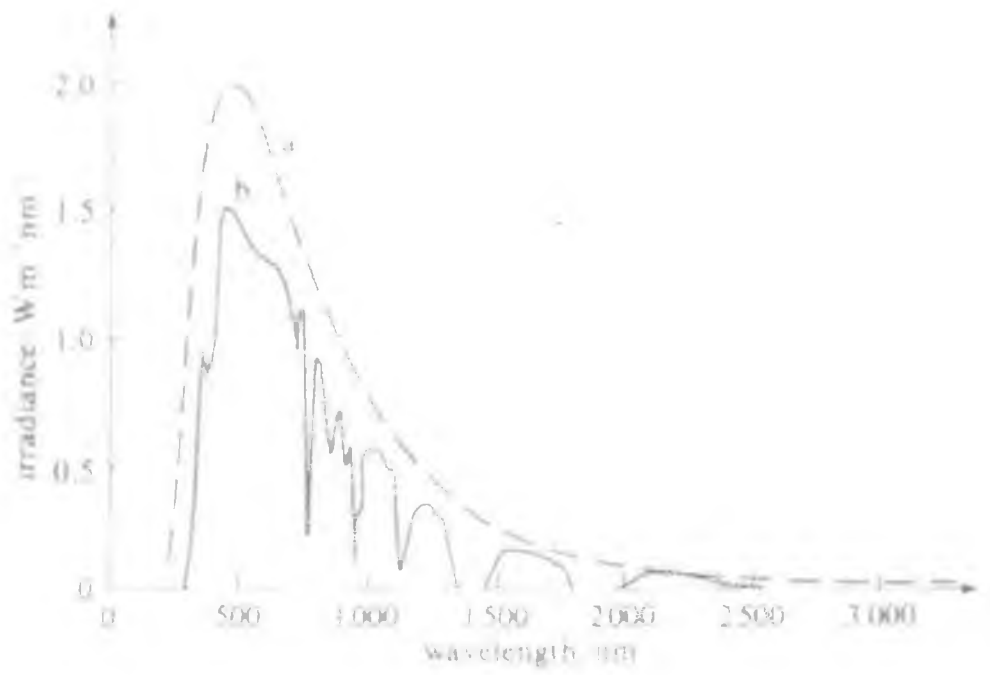

Figure 1.9 *Solar spectrum at sea level (curve b)*[49]

The complexes formed with these ligands have absorption and emission spectra, which are red-shifted compared to that of $[Ru(bpy)_3]^{2+}$, resulting in better overlap with the solar spectrum (Figure 1.9). As the π-acceptor strength of these ligands is increased (estimated on the basis of reduction potentials), the absorbance and emission spectra are shifted further into the red.[20] Correlation between the lowest unoccupied molecular orbital (LUMO) energy, reduction potential and absorption and emission energy have shown to be linearly dependent on each other.[2] Hence the red shift observed is indicative of a lowering of the LUMO's in these complexes. In the case of mixed ligand complexes, the MLCT excited state has been shown to be localised on the most easily reduced ligand and that emission occurs solely from this state, as seen for $[Ru(biq)(bpy)_2]^{2+}$, $[Ru(bpz)(bpy)_2]^{2+}$ and $[Ru(bpm)(bpy)_2]^{2+}$, where emission originated only from the biq, bpz and bpm based MLCT states, respectively.[50]

Interestingly, absorption spectra of the above mentioned complexes showed ^{1}MLCT bands characteristic of both ligands in the complex. Emission from these complexes occurs entirely from the lowest ^{3}MLCT excited state. While the red-shifted absorption of the class A type ligands, as a consequence of lower lying LUMO's, is advantageous, these ligands are usually weaker σ-donors than 2,2'-bipyridine, and the ligand field splitting is reduced in their metal complexes. This effect renders them, in general, less photostable as a result of the more accessible ^{3}MC decay pathway. Homoleptic complexes can be particularly problematic in this regard, the photodissociative ^{3}MC state of $[Ru(biq)_3]^{2+}$ is

shown to be easily populated at room temperature.[2] Mixed ligand complexes have circumvented this problem to some degree as weak and strong σ-donors can be combined in the same complex. This allows for the lowering of the LUMO energies without seriously affecting the ligand field splitting.

1.3.1 ^{1}H NMR spectroscopy

^{1}H NMR has proven an invaluable tool in the determination of the coordination mode of 1,2,4-triazole based ruthenium and osmium polypyridyl complexes.[20,57,58,67] Simplification of spectra by selective deuteriation allows for the suppression of peaks, which yield relatively little information (*e.g.* bpy) and allow for accurate assignment of 1,2,4-triazole based ligand resonances. This can be seen in Figure 1.10 and 1.12, where the deuteriation of bpy greatly simplifies the spectra of ppt1 and ppt2 (see Figure 1.13)

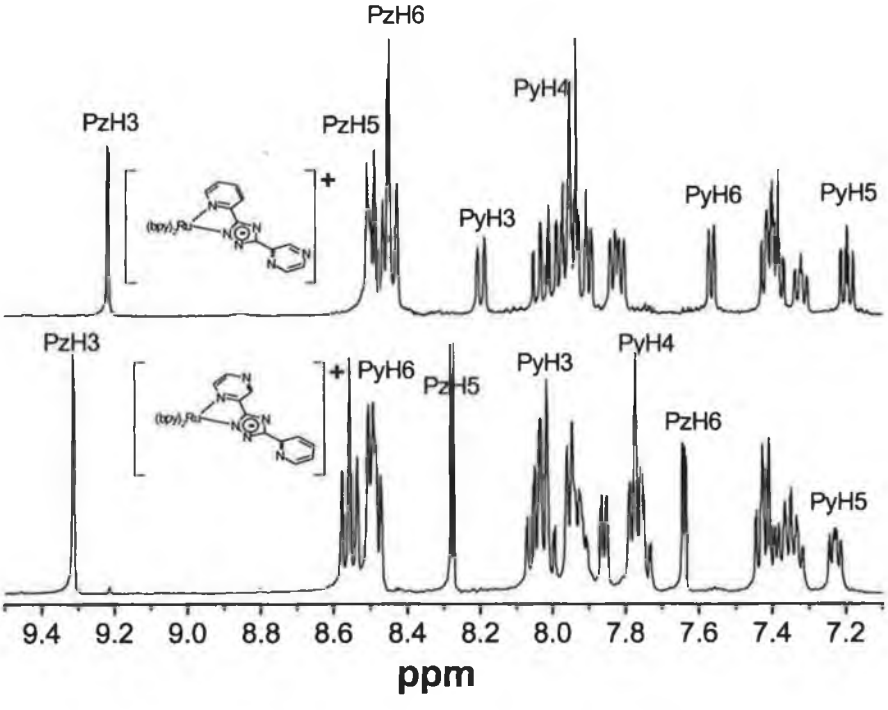

Figure 1.10 *^{1}H NMR (400 MHz) spectra of [Ru(bpy)$_2$ppt1]PF$_6$ (upper spectrum) and [Ru(bpy)$_2$ppt2]PF$_6$ (lower spectrum) in CD$_3$CN*[57]

The most striking feature in Figure 1.12 is the effect of complexation on the H_6 proton of the pyridine/pyrazine ring, which is coordinated to the metal centre. In each case the resonance is shifted upfield by as much as 1 ppm.

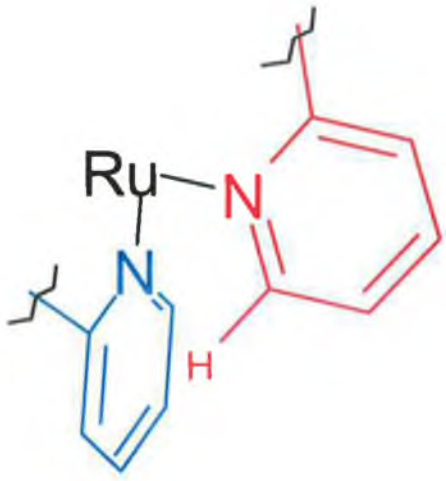

Figure 1.11 *Position of H_6 of pyridyl ring relative to neighbouring pyridyl ring*

This is opposite to what is observed for every other resonance, which suffers a downfield shift due to the increased ring current resulting from backbonding from the metal d-orbitals into the π-system of the ring. The origin of this effect on the H_6 proton is due to the shielding effect of a neighbouring pyridyl ring. The proton is positioned so that it is close to the centre of the ring (see Figure 1.11) and feels a stronger magnetic field due to the additive effect of the ring current and the bulk magnetic field of the NMR spectrometer.

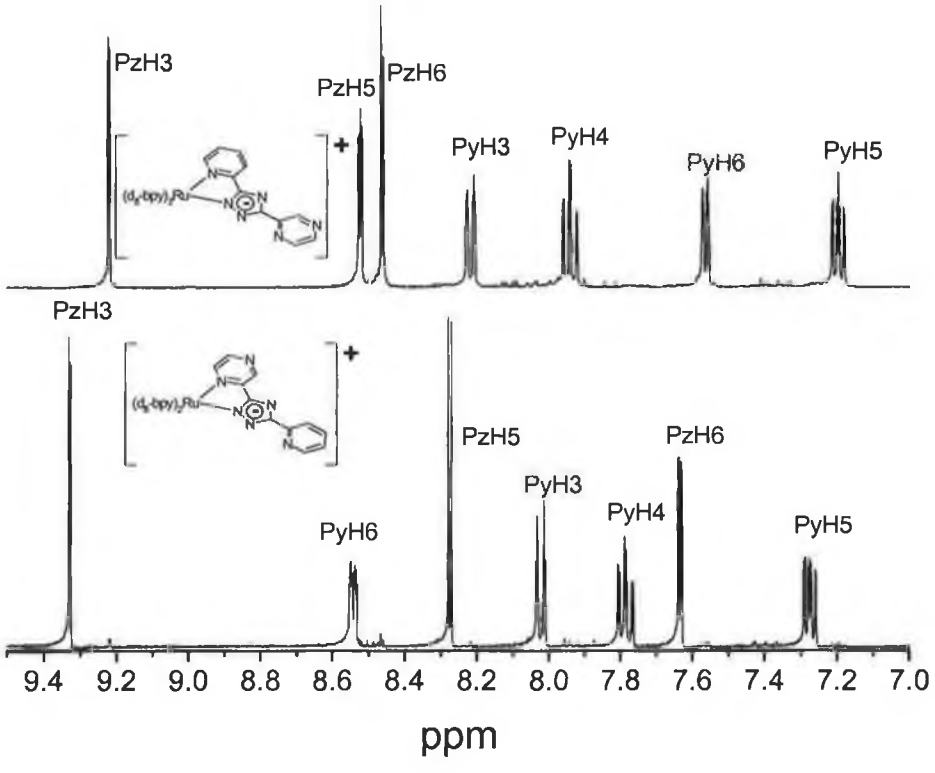

Figure 1.12 *^1H NMR (400 MHz) spectra of $[Ru([D_8]\text{-bpy})_2ppt1]PF_6$ (upper spectrum) and $[Ru([D_8]\text{-bpy})_2ppt2]PF_6$ (lower spectrum) in CD_3CN*

1.3.2 Absorption and emission spectroscopy

The absorption and emission spectra of 1,2,4-triazole based complexes show a striking similarity with the parent complex $[Ru(bpy)_3]^{2+}$. The lowest energy absorption feature for the ruthenium complexes is assigned to a ^{1}MLCT transition (log $\varepsilon \sim 4$) by comparison with other ruthenium polypyridyl complexes.[2] The complexes show strong absorptions (log $\varepsilon \sim 5$) at about 280 nm which are π-π^* in nature. For the Os(II) based 1,2,4-triazole complexes formally forbidden ^{3}MLCT transitions are present at longer wavelengths (550 nm to 750 nm) similar to those observed for related complexes *e.g.* $[Os(bpy)_3]^{2+}$.[51] However, there are some significant differences in the electronic properties of the pyridine and pyrazine based complexes (*vide infra*).

Overall the electronic properties of all complexes are typical for ruthenium and Os(II) polypyridyl complexes.[2] For the pyridine bound complexes (*e.g.* bpt$^-$), the absorption spectra undergo a large blue shift upon protonation (~ 40 nm). For the pyrazine based complexes (*e.g.* bpzt$^-$) a smaller blue shift is also observed upon protonation (~ 10 nm). Overall as is typical of pyrazine-triazole based complexes, only minor changes in the electronic spectrum are observed upon protonation compared with those observed for the pyridine bound complexes. For the osmium analogues a similar situation is observed, although, the presence of formally spin forbidden transitions (^{3}MLCT) results in more complex spectra.

All 1,2,4-triazole based complexes examined are luminescent in acetonitrile both at room temperature and at 77 K. The ruthenium complexes emit in the 650 to 700 nm region and a large blue shift is observed between 300 and 77 K, typical for ^{3}MLCT emission. For the osmium complexes emission is observed at much lower energy (> 700 nm) as expected.[51] For pyridine based complexes protonation results in a large blue shift in the emission energy with a dramatic shortening of emission lifetime (due to lowering of the ^{3}MC excited state). In contrast the emission of the pyrazine based complexes is less affected by protonation and the lifetime actually increases upon protonation.

1.3.3 Redox potentials

Both pyrazine and pyridine 1,2,4-triazole based Ru(II) and Os(II) complexes exhibit redox chemistry similar to $[Ru(bpy)_3]^{2+}$ and $[Os(bpy)_3]^{2+}$ respectively. Pyrazine based complexes exhibit a more positive metal-based oxidation potential than their pyridine analogues. This is due mainly to the weaker σ-donor/stronger π-acceptor properties of the

pyrazine over the pyridine ligand,[50,52] which reduces the relative electron density on the metal centre. The first two reduction potentials of the deprotonated complexes are generally reversible and are similar to those of $[Ru(bpy)_3]^{2+}$, suggesting they are bpy based reductions.[53] Upon protonation both pyridine and pyrazine based complexes exhibit a cathodic shift in the metal oxidation wave. This is due to the reduction of the 1,2,4-triazoles σ-donor strength upon protonation and hence a reduction in the effective electron density on the metal. Due to hydrogen formation, reduction potentials are not usually obtained for protonated complexes. The oxidation potentials of the osmium based 1,2,4-triazole complexes are approximately 400 mV lower than those of the corresponding ruthenium complexes. This is normal behaviour for these types of systems and is attributed to the higher energy of the 5d orbitals compared to the 4d orbitals.[51,54]

Coordination via the N4 of the 1,2,4-triazole ring rather than the N2 nitrogen results in a small increase in the observed oxidation potential (see Table 1.3). This indicates that the 1,2,4-triazole ring is a stronger σ-donor when bound through the N2 nitrogen rather than the N4.

Deprotonated complexes			**Protonated complexes**		
	N2	N4		N2	N4
$[Ru(bpy)_2(pytr)]^+$	0.83	0.90	$[Ru(bpy)_2(Hpytr)]^{2+}$	1.14	1.20
$[Ru(bpy)_2(pztr)]^+$	1.01	1.10	$[Ru(bpy)_2(Hpztr)]^{2+}$	1.25	1.30
$[Ru(phen)_2(pztr)]^+$	0.87	0.94	$[Ru(phen)_2(Hpztr)]^{2+}$	0.82	0.86
$[Ru(biq)_2(pztr)]^+$	1.02	1.04	$[Ru(biq)_2(Hpztr)]^{2+}$	0.87	1.29

Table 1.3 *Data obtained from reference 20*

It is interesting to note that the presence of electron withdrawing/donating groups influences the metal redox potentials, in particular substitution of the 5 position of the 1,2,4-triazole ring (*vide infra*-acid/base properties). The metal oxidation potentials for a series of substituted 1,2,4-triazole complexes are given in Table 1.4.

The nature of the effect of the various substituents can be considered analogous to the 'Hammett' effects encountered in organic chemistry. The effect of electron withdrawing groups and electron donating groups, relative to –H, on the metal oxidation potential is such that the electron donating groups effect a diminution of electron density on the metal centre and lower the metal oxidation potential.

Pyrazine bound complexes	$E_{1/2}$ (V)	ΔE (mV)	Pyridine bound complexes	$E_{1/2}$ (V)	ΔE (mV)
Deprotonated complexes					
[a][Ru(bpy)$_2$(pztr)]$^+$	1.01	0	[a][Ru(bpy)$_2$(pytr)]$^+$	0.83	0
[a][Ru(bpy)$_2$(bpzt)]$^+$	0.99	-10	[b] Ru(bpy)$_2$(ppt1)]$^+$	0.95	+120
[b][Ru(bpy)$_2$(ppt2)]$^+$	1.05	+50	[a][Ru(bpy)$_2$(bpt)]$^+$	0.85	+20
[a][Ru(bpy)$_2$(Mepztr)]$^+$	0.92	-80	[a][Ru(bpy)$_2$(Mepytr)]$^+$	0.80	-30
[b][Os(bpy)$_2$(bpzt)]$^+$	0.64	-370	[b][Os(bpy)$_2$(ppt1)]$^+$	0.52	-310
[b][Os(bpy)$_2$(ppt2)]$^+$	0.63	-380	[a][Os(bpy)$_2$(bpt)]$^+$	0.49	-340
Protonated complexes					
[a][Ru(bpy)$_2$(Hpztr)]$^{2+}$	1.25	0	[a][Ru(bpy)$_2$(Hpytr)]$^{2+}$	1.14	0
[a][Ru(bpy)$_2$(Hbpzt)]$^{2+}$	1.24	-10	[b][Ru(bpy)$_2$(Hppt1)]$^{2+}$	1.25	+110
[b][Ru(bpy)$_2$(Hppt2)]$^{2+}$	1.20	-50	[a][Ru(bpy)$_2$(Hbpt)]$^{2+}$	1.06	- 80
[a][Ru(bpy)$_2$(HMepztr)]$^{2+}$	1.29	+40	[a][Ru(bpy)$_2$(HMepytr)]$^{2+}$	1.20	+140
[b][Os(bpy)$_2$(Hbpzt)]$^{2+}$	1.08	-170	[b][Os(bpy)$_2$(Hppt1)]$^{2+}$	0.80	-340
[b][Os(bpy)$_2$(Hppt2)]$^{2+}$	0.77	-480	[a][Os(bpy)$_2$(Hbpt)]$^{2+}$	0.89	-250

Table 1.4 *Metal redox potentials (vs. SCE) for selected complexes Redox potentials (vs. SCE). Protonation by addition of concentrated $HClO_4$. [a]values obtained from ref.20. [b]values obtained from ref.57. ΔE values are relative to pytr$^-$ and pztr$^-$ based complexes.*

1.3.4 Acid-base properties

1.3.4.1 Ground-state acid-base properties

Coordination of a 1,2,4-triazole ring to a metal centre *e.g.* Ru(II) or Os(II) results in a dramatic increase in the acidity of the triazole NH.[20] The 1,2,4-triazole ring is a stronger σ-donor ligand and weaker π-acceptor ligand than bpy, *i.e.* electron density is transferred from the ring to the metal centre upon coordination and very little electron density is regained through backbonding. Typically the pK_a for a coordinated triazole ring is in the region of pH 3 to pH 5 but may be as low as pH 1, depending on the ring substituents. The effect of protonation on both ground and excited state properties is quite large in the case of 1,2,4-triazole complexes. This arises from the dramatic change in σ-donor/ π-acceptor properties of the 1,2,4-triazole on protonation. Since protonation results in reduction of the electron density on the 1,2,4-triazole ring, the ligand becomes a weaker σ-donor and better π-acceptor than the deprotonated form.

1.3.4.2 Excited state acid base properties

An excited state molecule may be considered as a new chemical entity with physical and chemical properties quite different from those of the ground state. One such chemical

property that can change is the overall acidity/basicity of the complex.[55] For complexes, which possess long-lived charge transfer excited states, the excited state pK_a (pK_a*) will be dependent on the change in electron distribution on excitation. The direction of the change of the pK_a from the ground to the excited state is determined by the nature of the location of the lowest excited emissive state.[4] Two possible situations may be envisaged:

(i) If the lowest CT excited state is based on the ligand which is responsible for the acid/base behaviour then excitation will result in an increase in the electron density on that ligand and hence an increase in pK_a.

(ii) If, however, the excited state is based on a ligand other than that responsible for the acid base chemistry then upon excitation the electron density on the metal centre will be reduced. This will in turn reduce the electron density of the protonatable ligand and hence lower the pK_a.

The use of comparison of excited and ground state acid base properties as a tool in determining the localisation of emitting states has been proposed by Vos and others,[4] however its application is somewhat troublesome in that the determination of the actual excited state pK_a (pK_a*) rather than the pH_i (the inflection point of the emission titration curve), is often not possible.[56] Since protonation changes the energy levels of a molecule, changes in electronic transitions will also be observed. The acid base properties (in particular the excited state acid-base properties) may therefore be probed by absorption and emission spectroscopy.

1.3.4.3 Factors affecting the acid/base properties of pyrazinyl- and pyridinyl-1,2,4-triazole based Ru(II) and Os(II) Polypyridyl Complexes

The acid-base properties of 1,2,4-triazole based Ru(II) and Os(II) complexes have been investigated by studying the pH dependence of their absorption spectra.[20,57,58,67] The pK_a values obtained from these studies are presented in Table 1.5. In every case the acid/base behaviour observed can be explained by protonation/deprotonation of the triazole moiety as indicated in Equation 1.4; [i]

Equation 1.4 $[Ru(bpy)_2(tr)]^+ + H^+ \quad [Ru(bpy)_2(Htr)]^{2+}$

[i] Although, in the case of pyrazine based complexes protonation of the coordinated pyrazine ring is possible, this occurs at only at negative pH ($pKa \sim -1.5$).[20]

In the case of two mononuclear coordination isomers based on the ligand Hppt (see Figure 1.13) an interesting acid base chemistry is observed. To a first approximation the acid-base properties of the pyridine bound complex **ppt1** would be expected to be similar to that of the bpt⁻ based mononuclear complex. Likewise the acid-base properties of the pyrazine bound isomer **ppt2** would be expected to be similar to the bpzt⁻ based complex. Unusually the acid-base properties of **ppt1**/**ppt2** are found to display behaviour quite different to that initially expected.

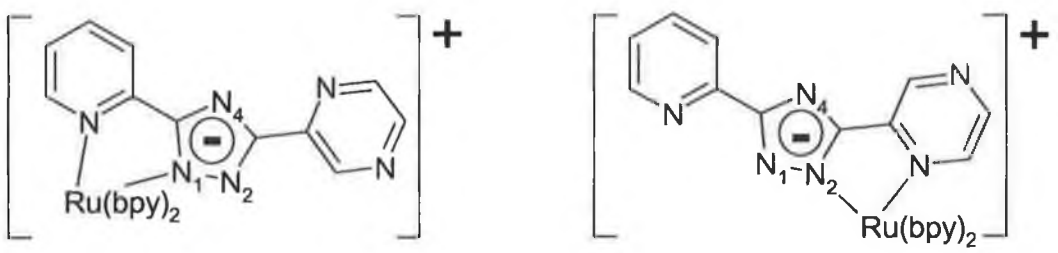

ppt1 **ppt2**

Figure 1.13 *N2 bound coordination isomers of* $[Ru(bpy)_2ppt]^+$.

By examination of Table 1.5 it can be shown that the acidity of the coordinated triazole ring is strongly dependent on the nature of the non-coordinated substituent in the C5 position. This dependence is reflected in the ΔpK_a values, with respect to the unsubstituted C-H analogues, given in Table 1.5. The effect of the introduction of a pyridine or pyrazine ring is particularly relevant. A comparison of the pK_a values of the pztr⁻ and bpzt⁻ complexes shows that the triazole ring becomes more acidic by 1.7 pH units in the presence of an additional, free, pyrazine ring.

Pyrazine bound complexes	**pK_a**	**ΔpK_a**	**Pyridine bound complexes**	**pK_a**	**ΔpK_a**
[a]$[Ru(bpy)_2(pztr)]^+$	3.7	0	[a]$[Ru(bpy)_2(pytr)]^+$	4.1	0
[a]$[Ru(bpy)_2(bpzt)]^+$	2.0	-1.7	[b]**Ruppt1**	2.7	-1.4
[b]**Ruppt2**	3.8	+0.1	[a]$[Ru(bpy)_2(bpt)]^+$	4.2	+0.1
[a]$[Ru(bpy)_2(Mepztr)]^+$	4.2	+0.5	[a]$[Ru(bpy)_2(Mepytr)]^+$	4.9	+0.8
[c]$[Ru(bpy)_2(Brpztr)]^+$	1.4	-2.3	[c]$[Ru(bpy)_2(Brpytr)]^+$	1.3	-2.8
[b]$[Os(bpy)_2(bpzt)]^+$	1.2	-2.5	[b]**Osppt1**	2.1	-2.0
[b]**Osppt2**	3.5	-0.2	[a]$[Os(bpy)_2(bpt)]^+$	n/a	--

Table 1.5 *Ground state pK_a values of 1,2,4-triazole based mononuclear complexes. All measurements are carried out in Britton-Robinson buffer, values ± 0.1. a) from ref 20, b) from ref 57, c) from ref 58.*

A comparison of the values observed for the pytr⁻ and bpt⁻ complexes shows that the effect of the introduction of a pyridine ring is far less dramatic and does not result in a significant change in the pK_a (+ 0.1 pH unit). This indicates that the free pyrazine group acts as a strong electron-withdrawing group. Within this framework the pK_a values are as expected and indicate that there is substantial interaction between the different components of the Hppt ligand. Similar trends are observed for the analogous Os(II) complexes. It is interesting to note the comparison of the substituent effect on the acid base properties of the complexes and similar effects observed for organic systems such as benzoic acid

1.3.5 Photochemistry

Mixed ligand ruthenium polypyridyl complexes have been studied extensively as a result of their potential as components for supramolecular devices.[4,8] A vast array of ligands are available to this end, allowing for the optimisation of any particular photophysical and/or electrochemical properties.[2] Of particular concern to supramolecular chemistry is the control of photochemical properties. As has been discussed above the archetypal $[Ru(bpy)_3]^{2+}$ has a small but significant photochemistry. Such instability is undesirable for most systems where decomposition would result in degradation and loss of function. However, reversible photochemical changes in complexes are highly desirable in many areas, in particular in rewriteable data storage, molecular switches and photo-molecular devices.[8]

In an attempt to reduce or eliminate photo-decomposition of ruthenium photo-sensitisers, used in photovoltaics and photo-chemically driven catalysis, mixed ligand complexes containing a relatively weak σ-donor ligand with a relatively low π* level and a single strong σ-donor ligand have been prepared.[59] This results an increase of the ^{3}MLCT-^{3}MC energy gap (from which ligand loss takes place by thermal population of the ^{3}MC).[60] It is ironic that many of the mixed ligand complexes containing the strong σ-donor ligands have been found to display a surprisingly rich and varied photochemistry.[59]

The difference in photo-reactivity of the protonated and deprotonated complexes containing 1,2,4-triazole based ligands has been explained in terms of the accessibility of the ^{3}MC excited state. Temperature dependent emission studies have shown that the activation energy for the cross over from the ^{3}MLCT to the ^{3}MC excited state is much lower for the protonated complex than for the deprotonated complex. Since photo-

dissociation occurs from the ^{3}MC excited state, the results of the photolysis studies are as expected. Protonation withdraws electron density from the triazole making it a weaker σ-donor and hence reducing the crystal field splitting (and the ^{3}MC-GS gap) whilst raising the ^{3}MLCT excited state energy level. This occurs because the Ru(II) centre becomes electron poor and the backbonding stabilisation of the π* orbitals is reduced. The diimine ligands can be divided into two groups i) strong π-acceptor ligands and ii) strong σ-donor ligands. The former ligands have low lying π* levels (*e.g.* pyrazine, pyrimidine and pyridine). However these ligands tend to be weak σ-donors, which results in smaller crystal field splitting. An increase in σ-donor properties of these ligands can be achieved by the use of methyl and phenyl groups. The latter class of ligands are strong σ-donors, which give rise to large crystal field splitting. For these ligand the π* energy levels are inaccessible.

In basic conditions, heteroleptic Ru(II) complexes containing 1,2,4-triazole based ligands have proven to be amongst the most photo-stable Ru(II) diimine complexes known.[4a] Therefore, application of such complexes in photochemically driven systems is very promising due to their stability as regards decomposition. Under protonating conditions these complexes exhibit an extensive and interesting photochemistry, which includes coordination isomerisation, and reversible ligand substitution.[56,59] The photochemistry of several complexes is discussed in this section.

1.3.5.1 Mononuclear Pyridyl triazole complexes

Mononuclear ruthenium polypyridyl complexes incorporating the ligands based on pyridyl-triazoles have been the subject of extensive investigations into the factors effecting their photostability/reactivity.[61,62,63]

$[Ru(bpy)_2(pytr)]^+$: The photochemical reactivity of both N2 and N4 coordination isomers of $[Ru(bpy)_2(pytr)]^+$ has been investigated in some detail.[59] In the deprotonated state neither the N2 isomer nor the N4 isomer of $[Ru(bpy)_2(pytr)]^+$ demonstrated any photochemical reactivity in dichloromethane upon extended photolysis and even in the presence of bromide ions. Under protonating conditions both N2 and N4 isomers demonstrated linkage isomerisation to give a final mixture of 20% to 80% respectively, regardless of the initial coordination mode of the complex. Under protonating conditions in the presence of bromide ions the formation of *cis*-$[Ru(bpy)_2Br_2]$ (and the small amounts of the N4 isomer in the case of photolysis of the N2 isomer) occurred. HPLC

analysis found that in addition to the main photo-product and the free ligand an additional product was formed which had a spectrum very similar to *cis*-$[Ru(bpy)_2Br_2]$. It was proposed that this was a complex containing a monodentate bound Hpytr ligand.[59] A strong correlation was observed between the results of temperature dependent luminescence studies and the results of photochemical studies as has been found in earlier studies.[64] For the deprotonated complexes the prefactors for the activated crossing to the photo-reactive ^{3}MC state are small ($k' \sim 10^7$) and population of the ^{3}MC from the lowest ^{3}MLCT states is not efficient. For the protonated complexes in contrast, large prefactors ($k' \sim 10^{10}$ to 10^{13}) have been determined for this process indicating that deactivation of the emissive ^{3}MLCT states via the ^{3}MC is important.

$[Ru(bpy)_2(5\text{-}Mepytr)]^+$ and $[Ru(bpy)_2(bpt)]^+$: In contrast with $[Ru(bpy)_2(pytr)]^+$ which is formed in approximately a 1:1 ratio (N2/N4) during synthesis, only the N2 isomers of $[Ru(bpy)_2(5\text{-}Mepytr)]^+$ [65] and $[Ru(bpy)_2(bpt)]^+$ [61] are formed in appreciable amounts. This suggests that the thermal equilibrium is influenced heavily by steric considerations, namely the bulky methyl group. As for $[Ru(bpy)_2(pytr)]^+$, $[Ru(bpy)_2(5\text{-}Mepytr)]^+$ displays no photo-reactivity under deprotonating conditions in dichloromethane. When protonated the complex undergoes coordination isomerisation to form the N4 isomer. In the presence of acid and bromide ions in dichloromethane, the final photoproduct formed is the complex *cis*-$[Ru(bpy)_2Br_2]$.

$[Ru(bpy)_2(1\text{-}Mepytr)]^{2+}$ and $[Ru(bpy)_2(4\text{-}Mepytr)]^{2+}$: The photochemistry of the N-methylated pyridine triazole complexes has recently been examined by Buchannan *et al.*[62] and Fanni *et al.*.[66] For the N2 coordinated N4 methylated complex photochemical decomposition was observed via a monodentate intermediate. Not unexpectedly, no N2-N4 isomerisation was found to take place. Of more interest was the thermal and photochemistry of the N1-methylated complexes.

When $[Ru(bpy)_2(1\text{-}Mepytr)]^{2+}$ was prepared from the methylated ligand, only the N4 coordinated isomer was formed on complexation, however the N2 isomer could be prepared (together with the N2 (N4 methylated) complex) by methylation of the N2-$[Ru(bpy)_2(pytr)]^+$ complex.[66] As methylation can be viewed as a form of irreversible protonation (albeit to a first approximation) the methylated complexes would be expected to undergo similar photochemistry to the N2-$[Ru(bpy)_2(pytr)]^+$ complex.

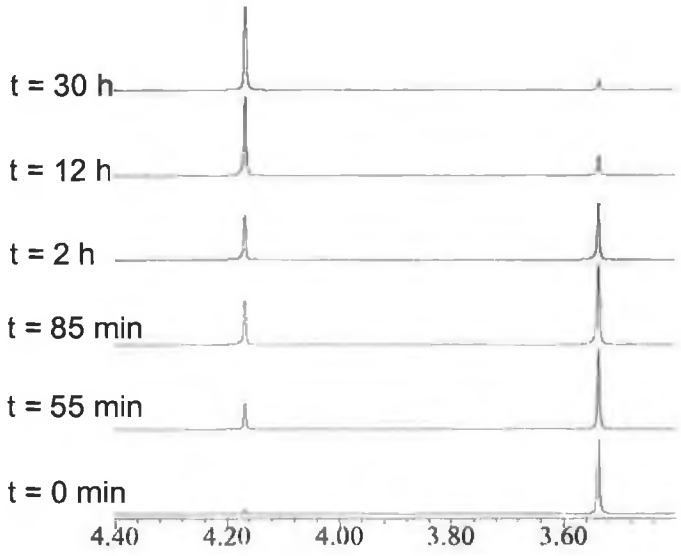

Figure 1.14 *^{1}H NMR spectroscopy following the photochemically induced coordination isomerisation of $[Ru(bpy)_2(1\text{-}Mepytr)](PF_6)_2$ N2 isomer to the N4 isomer: from ref 66*

It was found however that although both the N2 and N4 isomer underwent decomposition in strongly coordinating solvents such as acetonitrile, in weaker solvents such as acetone the N2 isomer isomerised to form the N4 isomer. Conversion of the N4 isomer to the N2 isomer did not take place. The photochemical N2–N4 isomerisation of $[Ru(bpy)_2(1\text{-}Mepytr)]^+$ was monitored by UV.Vis Spectroscopy and ^{1}H NMR spectroscopy (Figure 1.14 and Figure 1.15).

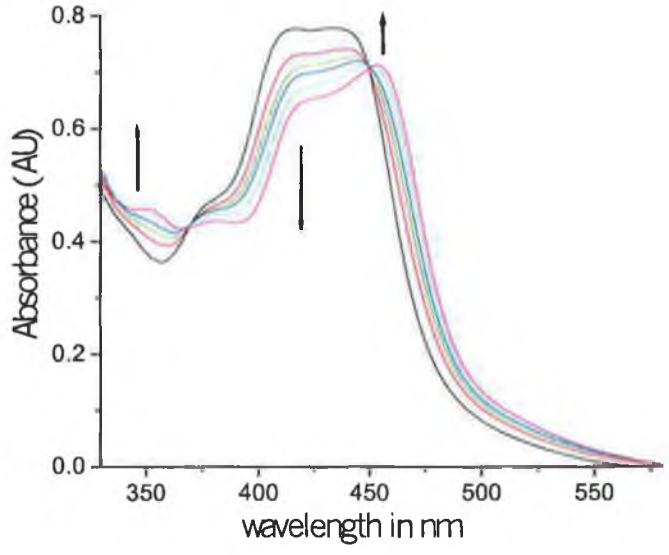

Figure 1.15 *The photolysis of N2 co-ordination isomer $[Ru(bpy)_2(1\text{-}Mepytr)](PF_6)_2$ in acetone, followed by UV.Vis spectroscopy after a) 0 min, b) 5 min, c) 10 min, d) 17.5 min e) 27.5 min and f) 120 min: Isosbestic points at 367 and 450 nm, from ref 66.*

$[Ru(biq)_2(1\text{-}Mepytr)]^{2+}$ & $[Ru(biq)_2(5\text{-}Mepytr)]^{+}$: Keyes *et al.*[46] have examined the effect of variation of the bpy ligand on the photochemical properties of pyridyl-1,2,4-triazoles. Due to the weaker σ-donor properties of the biq ligand a lowering of the ^{3}MC excited state would be expected and the complex formed should exhibit greater photochemical instability as a result. As expected for $[Ru(biq)_2(1\text{-}Mepytr)]^{2+}$ and $[Ru(biq)_2(5\text{-}HMepytr)]^{2+}$ in both acetonitrile and in dichloromethane containing bromide ions, fast photodecomposition was observed. Surprisingly the deprotonated complex $[Ru(biq)_2(5\text{-}Mepytr)]^{+}$ did not show any photochemical activity under extended photolysis.

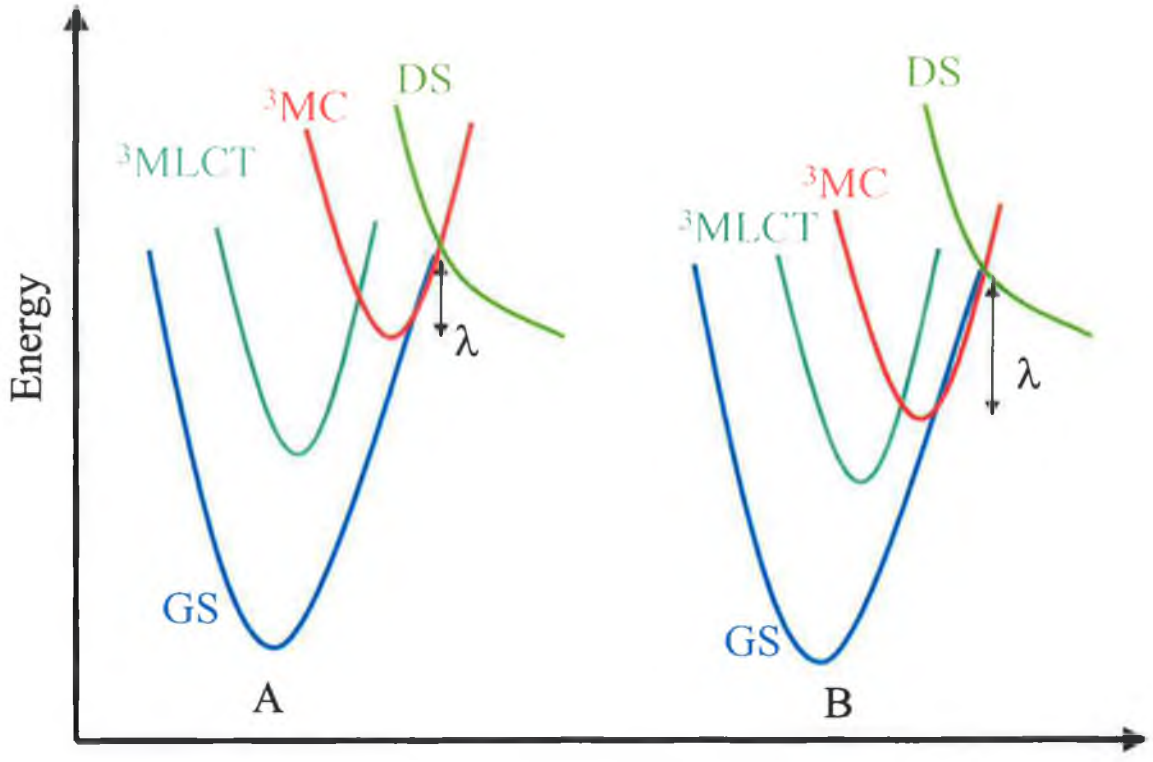

Figure 1.16 *Excited state structure and thermal cross-over from the ^{3}MC state to a dissociative state a) low thermal activation (λ) i.e. photochemistry is competitive b) high activation energy (λ) i.e. photochemistry is unimportant. DS = dissociative state*

The importance of steric factors in the photochemistry of pyridyl-1,2,4-triazoles can be seen clearly from these results. Steric effects prevent the N4-N2 coordination isomerism of the complex $[Ru(bpy)_2(4\text{-}Mepytr)](PF_6)_2$, but cannot explain the N2/N4 equilibrium established by the complex $[Ru(bpy)_2(pytr)]PF_6$ of 20/80. On steric grounds the reverse would be expected, however the limiting factor in this case appears to be the relative σ-donor strengths of the N2 and N4 coordination sites. From electrochemical measurements it can be deduced that the N4 site is a weaker σ-donor than the N2 site. This results in a destabilisation of the metal centred orbitals and results in a lowering in energy of the ^{3}MC excited state from which the isomerisation is believed to originate. Figure 1.16 shows the

effect of lowering the ^{3}MC excited state on the coupling with a dissociative state. By lowering the ^{3}MC level the thermal activation barrier between the two states is increased and the photochemical activity is also reduced. Hence the equilibrium of the isomerisation is shifted in favour of the N4 isomer over the N2 isomer.

1.3.5.2 Mononuclear Pyrazyl-1,2,4-triazole complexes

A comparative study into the photochemistry of $[Ru(bpy)_2(pztr)]^+$ (N2 and N4 isomers) and $[Ru(bpy)_2(3\text{-}Mepztr)]^{2+}$ has been carried out by Hughes.[67] In acetonitrile $[Ru(bpy)_2(pztr)]^+$ was found to be completely photochemically inert, whilst in contrast both $[Ru(bpy)_2(3\text{-}Mepztr)]^{2+}$, and $[Ru(bpy)_2(Hpztr)]^{2+}$ (N2 and N4 isomers) resulted in complete loss of the 1,2,4-triazole ligand. In dichloromethane neither $[Ru(bpy)_2(pztr)]^+$ (N2 and N4 isomers) nor $[Ru(bpy)_2(3\text{-}Mepztr)]^{2+}$ demonstrated photoreactivity, however for $[Ru(bpy)_2(Hpztr)]^{2+}$ both the N2 and N4 coordination isomers underwent isomerisation (N2-N4) with a final ratio of 20:80 (N2:N4) in both cases regardless of the initial coordination mode of the isomer examined. Similarly Hughes *et al.*[68] have reported that as for the deprotonated mononuclear pyrazinyl-1,2,4-triazole complex based on the bpzt$^-$ ligand no photo-reactivity in either acetonitrile or dichloromethane and in the presence of chloride ions was observed.

Binuclear 1,2,4-triazole complexes: The photochemical properties of complexes of the type $[Ru(LL_1)_2bptRu(LL_2)_2]^{3+}$ [61,69] and $[Ru(LL_1)_2bpztRu(LL_2)_2]^{3+}$ [68] have been investigated (where LL_1 and LL_2 are either bpy or phen).

For both $[Ru(bpy)_2bptRu(bpy)_2]^{3+}$ [61] and $[Ru(bpy)_2bpztRu(bpy)_2]^{3+}$ [68] photolysis in either acetonitrile or in dichloromethane results in dissociation of the N4 $Ru(bpy)_2$- moiety only. Likewise for the mixed ligand systems $[Ru(bpy)_2bptRu(phen)_2]^{3+}$ and $[Ru(phen)_2bptRu(bpy)_2]^{3+}$ in acetonitrile, the N2 isomer was formed upon photolysis only.[69] Interestingly, for complexes of the type $[Ru(bpy)_2bptRu(bpy)_2]^{3+}$ both the N2 and N4 sites appear to undergo dissociation in the presence of Cl^-. However it is possible that in this case further reaction of the mononuclear photoproducts results in formation of the N4 isomer as a secondary rather than a primary product.

In Chapter 8, the photochemistry of both a novel pyrazine bridged binuclear triazole complex is examined. Of interest is the effect of the stabilisation of the pyrazine π^* orbital on the pH dependence of its photochemistry.

1.4 The application of deuteriation to inorganic photophysical studies

The significance of the deuterium isotope effect on the photophysical properties of organic systems was recognised as early as 1960.[70,71] Since then many polyaromatic hydrocarbons have been investigated and a theoretical understanding has been developed.[72,73,74] The application of deuteriation in organic photophysics has been concerned primarily with probing electronically excited state decay pathways and as such has proven to be an invaluable tool in the study of the nature of these processes. Far fewer investigations of this type have been reported in inorganic chemistry. The earliest applications of deuteriation to inorganic photophysics can be found in the work of Kropp and Windsor,[75] who investigated the effects of deuteriation on the fluorescence of rare earth ions, and of Watts and co-workers on the emission lifetimes of the lowest ^{3}dd (metal centred) excited state of $[Rh(NH_3)_{6-n}X_n]^{(3-n)+}$ (X = Cl, Br, I, n =0,1)[76] and the ^{3}MLCT (Metal to Ligand Charge Transfer) excited state of $[Ru(bpy)_3]^{3+}$.[77]

The effect of deuteriation, via vibrational coupling, on the excited state decay processes in platinum group metal ions and complexes is discussed in this section. Of particular interest is the use of deuteriation in probing both the emissive excited states and indirectly in probing other low lying excited states, which attain a significant Boltzmann population. In addition, brief overviews concerning the use of deuteriation as a probe in vibrational spectroscopies such as resonance Raman, Stark effect, low temperature high-resolution emission spectroscopies and line narrowing techniques have been included.

1.4.1 Theoretical considerations on the effect of deuteriation on excited state deactivation.

In 1960, Hutchinson,[70] Wright,[71] and co-workers reported the involvement of C-H vibrational modes in the radiationless deactivation of the phosphorescent triplet excited states of naphthalene and benzene. At 77 K in a durene matrix deuteriation of naphthalene leads to an eight-fold increase in the triplet lifetime.[70] At that temperature matrix deuteriation had no effect on the decay lifetimes. At temperatures above 100 K a significant difference was observed in the temperature dependence of the triplet excited state lifetime.[78] These studies demonstrate that C-H vibrational modes of both the compound under examination and the matrix may participate in radiationless deactivation processes. These observations have stimulated the development of a theoretical understanding of the effect of deuteriation.[72b]

The theoretical understanding of the nature of non-radiative deactivation processes initiated by Robinson and Frosch[72b] has since been further developed by Gelbart *et al.*,[73] Jortner and coworkers,[74] and Siebrand.[72c] Several groups have extended the theoretical models developed for aromatic hydrocarbons to investigate non-radiative transitions in inorganic systems. [79] In this section a general overview of the results obtained in these theoretical studies will be given. However, a detailed mathematical basis for these results is beyond the scope of this thesis and more detailed analyses may be found in the original work in this area. [72,73,74,79]

1.4.1.1 Competing processes in the deactivation of electronically excited states.

To understand the origins of the effect of deuteriation on excited state transitions, it is pertinent to first discuss the nature of the interaction between electronic states and the mechanisms, which result in their deactivation. The lifetime of an excited state may be expressed by Equation 1.5:

Equation 1.5 $$1/\tau_{obs} = k_r + \Sigma k_{nr}$$

where k_r is the natural radiative lifetime and Σk_{nr} is the sum of the rates of all non-radiative relaxation processes. The component k_r has been shown to follow an exponential dependence on the energy gap between the emitting state and the ground state.[32,74,80] The component Σk_{nr} incorporates all other temperature dependent and independent terms, which contribute to the overall decay rate, such as thermal population of higher energy excited state/s, unimolecular photochemical deactivation, bimolecular (*e.g.* $^3O_2$) quenching, vibrionically coupled radiationless deactivation *etc.*. The relative contribution of each component of the term k_{nr} is dependent on several factors, the principle of which are the relative energies of the various interacting excited states and the relative vibrionic and electronic coupling between the states (*vide infra*).[ii]

[ii] The equation (a) described by Jortner and coworkers[72] for the vibrationally induced non-radiative excited state decay rate has been furthered by Gelbart *et al.*[73]

$$k_{nr} = (2\pi/\hbar)\,\Sigma_r\Sigma_s\, p(mr)|\nu_{mr,ns}|^2\delta(E_{mr}-E_{ns}) \qquad \text{eq. (a)}$$

Where p(mr) is the Boltzman factor for the state of energy Emr, $\nu_{mr,ns}$ is the matrix element for the total Hamiltonian for the zero order Born-Oppenheimer state, Emr and E_{ns} is the energy of the donor and acceptor states respectively. By applying the low temperature limit the term r is only r = 0 and hence $\delta(E_{mr}-E_{ns})$, the weighted sum of the energy gap, becomes δ(Em0-Ens) and thence equation (a) may be written as eq. (b):

$$k_{nr} = (2\pi/\hbar)\Sigma_s\, p(m0)|\nu_{m0,ns}|^2\delta(E_{m0}-E_{ns}) \qquad \text{eq. (b)}$$

and hence:

$$k_{nr} = (2\pi/\hbar)\,\rho\,\nu_{mn}^2 \qquad \text{eq. (c)} \qquad \{\text{where } \nu_{mn}^2 \approx |\nu_{m0,ns}|^2 \text{ and } \rho \approx \Sigma_s\delta(E_{m0}-E_{ns})\}$$

ν_{mn}^2 is a simple function of electronic factors and vibrational overlaps ($\nu(mr\text{-}ns) = \Sigma_k J_k(m,n)F_k(mr,ns)$). By separating ν_{mn}^2 into its electronic {J or $J_k(m,n)$} and vibrational components {F(E) or Fk(mr,ns) } equation 2 is obtained:

$$k_{X\text{-}H} = (2\pi/\hbar)\rho JF(E) \qquad \text{eq 2}$$

1.4.1.2 Coupling between electronically excited states

Jortner and co-workers have proposed two limiting cases for the coupling of electronically excited states.[74b,c] In the strong coupling limit, a large horizontal displacement of the excited state potential well is proposed (see Figure 1.17).[74b] The strong coupling limit can be used to describe systems (*e.g.* the ^{3}MC state of M^{II} platinum group complexes) where large distortions in the geometry of M-L bonds are observed (*e.g.* Ru-N, Rh-Cl).

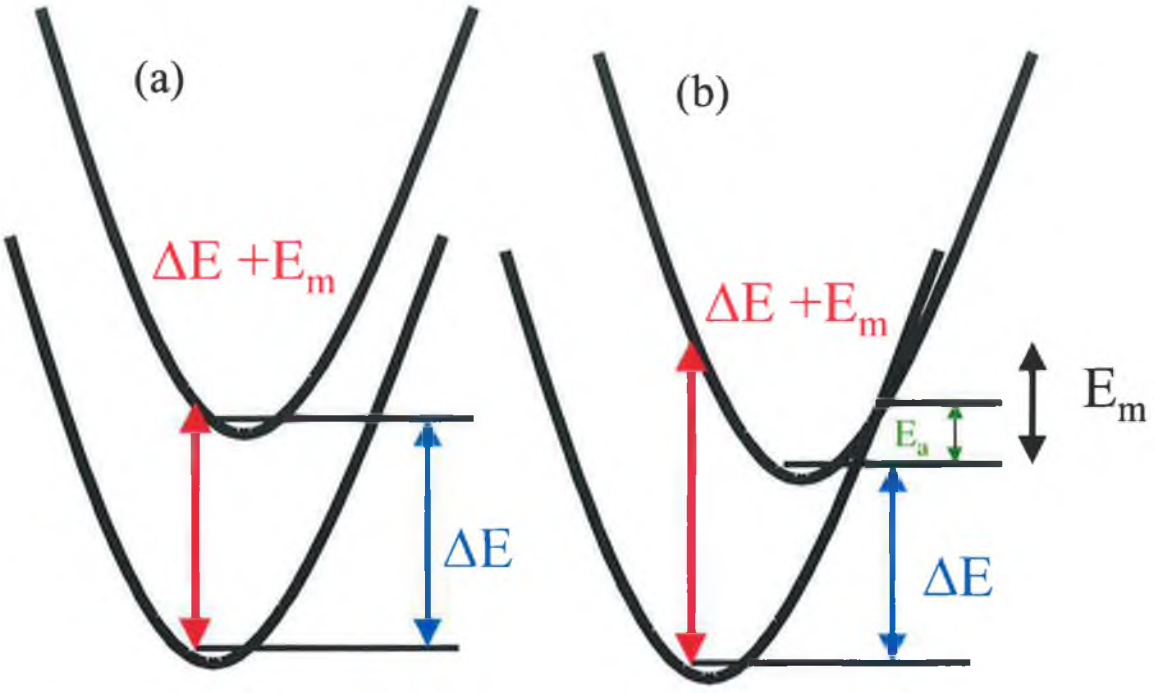

Figure 1.17 *(a) Weak coupling limit and (b) strong coupling limit between electronic states. The Franck-Condon absorption ($\Delta E + E_m = h\nu_{abs}$) and emission energies ($\Delta E - E_m = h\nu_{em}$), allow for the approximate calculation of the Stoke's shift $\approx (\Delta E + E_m) - (\Delta E - E_m) = 2E_m$*

In addition to large geometric distortions between the ground and excited state, the potential energy curves of the donor and acceptor states have a cross-over point close to the minimum of the excited state potential well (see *Figure 1.17*(b)).[iii] Due to the greater contribution of low energy vibrational modes to the Franck-Condon overlap term F(E) for the strong coupling case, all vibrational modes are in principle available to accept

[iii] Two consequences of the low value of Ea (fig.1) are (a) the thermal energy required to overcome the potential barrier is generally available at low temperatures and (b) as the probability of the vibrionic state is greatest at the edge of the potential well then the excited state distortion will result in large overlaps of the lowest vibrionic states of the excited state with the isoenergetic ground vibrionic states.

electronic energy.[iiib] In this case the lack of a large isotope effect is expected, as the transition probability is dependent on the mean vibrational frequency, which is expected to show only minor perturbation on isotopic substitution.[iv]

Coupling between excited states can be described by a weak coupling limit if the horizontal displacement of the potential wells is small and the potential energy curves of the states do not cross close to the energy minimum of the excited state potential well (see Figure 1.17 (a)). Radiationless deactivation between weakly coupled excited states is expected to involve conversion of electronic energy to vibrational energy. As a result of the relatively large amount of energy (compared to the typical energy difference between vibrationally excited states) that is converted by deactivation by such a route, overlap considerations favour high frequency vibrations and the application of the low temperature limit (*i.e.* only the lowest excited vibrionic state is populated significantly).

1.4.1.3 Weak or strong limit!

The question as to which limit is applicable in specific cases has been considered by Jortner and coworkers.[74b] They suggested that the energy of the Stokes shift can be used crudely in estimating the value E_m (see Figure 1.17), which in turn can be related to the geometric distortion between the excited and ground state and thereby discriminate between the weak and strong coupling limits.[74b] The weak coupling limit is the limit normally described by radiationless deactivation theory and is dominant when the Stokes' shift is less than the mean vibrational frequency of the molecule ($S < 1$).[v] In this limit the rate of radiationless decay is normally largely dependent on the frequency of the highest energy vibrational modes of the molecule *e.g.* O-H, N-H and C-H stretching modes. If the Stokes shift exceeds twice the mean frequency of the molecular vibrations ($S > 2$) then the strong coupling limit is relevant, and vice versa.[v] The use of the Stokes shift as a diagnostic tool although generally applicable in the case of polyaromatic systems, is problematic in the case of transition metal complexes where spin orbit coupling factors

[iv] The mean vibrational frequency of a molecule is given by the weighted average of all vibrational frequencies (*i.e.* $\Sigma_j\Delta_j^2\omega_j/\Sigma_j\Delta_j^2$ where Δ_j is the excited state fractional displacement w.r.t. the ground state and ωm is the frequency of the deactivating vibrational mode). Due to the large contribution of C-C (and in the case of transition metal complexes metal ligand vibrations *e.g.* Ru-N, Ru-Cl etc.) to the overall value of the mean molecular vibrational frequency then deuteriation of a large molecule would be expected to show only very minor perturbations to this value.

[v] The Huang Rhys factor (S) corresponds to the electron vibrational coupling constant, which is related to the displacement of the excited state potential well along the molecular co-ordinates corresponding to the vibrational mode in question. $S = \frac{1}{2}\Sigma_j\Delta_j^2$ or ½ the sum of the square of the fractional displacement of the ground and excited states for the deactivating mode/s.

become significant. In particular when phosphorescent excited states are considered, direct absorption into the emitting state is spin-forbidden and hence population of the excited state must occur via a higher lying state of identical spin multiplicity to the ground state, increasing the observed Stokes' shift.

A further complication to the assignment of weak and strong coupling limits is their temperature dependence. Gelbart *et al.*[73] have considered both strong and weak coupling of electronic states and their implications towards photoisomerism, in particular stilbene type *cis-trans* photo-isomerisation.[vi] The energy of the lowest triplet excited state of stilbene can be dissipated either via torsional and vibrational processes, with the former resulting in isomerisation. They concluded that the non-radiative transition rate (k_{nr}) is proportional to the energy gap between the ground and excited electronic states (ΔE) and any changes in the equilibrium configuration (Δ_j).[iv] For large displacements between ground and excited states, which may result in intramolecular rearrangements, the strong coupling limit is applicable (*e.g.* photoisomerism of stilbene results in radiationless deactivation of the lowest triplet (twisted) state). However, in glassy matrices at low temperature (77 K) where *cis-trans* isomerism is "frozen out" or where such isomerisation if sterically hindered, more of the electronic energy is forced to dissipate through vibrational modes rather than torsional modes. The system is better described by the weak-coupling limit as purely vibrational modes have an increased role in excited state deactivation.

1.4.2 Origin of the deuterium induced perturbation of electronic excited state decay processes

It has been suggested that in the case of the weak coupling limit, the vibrational contribution to the overall rate of non-radiative deactivation ($\sum k_{nr}$) depends in part on the magnitude of the vibrational overlap integrals between the initial and final states of a transition.[72b,e,74b,ii] Stretching modes have been suggested to be important channels for radiationless deactivation and as a result Σk_{nr} includes the term $k_{X\text{-}H}$ (X = C, N or O), the rate of radiationless deactivation due to X-H vibrational coupling.[74b] This term can in turn be expressed in terms of Equation 1.6:

Equation 1.6 $k_{X\text{-}H} = (2\pi/\hbar)\rho J F(E)$ [ii]

[vi] The energy of the lowest triplet excited state of stilbene is can be dissipated either via torsional and vibrational processes, with the former resulting in isomerisation. The non-radiative rate constant in such systems contains contributions from both torsional (which may result in photochemical deactivation) and vibrational modes.

where ρ is the weighted sum of the energy gap between the vibrionic states, J is the electronic coupling between the two electronic states, and F(E) is the Franck-Condon sum of the products of the overlap integrals.[iv] Deuteriation reduces both the amplitude and frequency of X-H vibrational modes and hence C-D vibrations are of lower frequency and amplitude than the equivalent C-H vibrations. As a result, the vibrational overlap between two states will be diminished for the same energy gap (Equation 1.6). Hence the Franck-Condon factor component F(E) and k_{X-H} are reduced.[72,,81,vii] This results in an increase in the observed lifetime of the electronically excited state (since non-radiative deactivation is less effective). In addition when X-H vibrational modes are available to act as promoting modes, the electronic coupling term (J) is also reduced by deuteriation.[79f]

If deuteriation effects were solely due to Franck-Condon factors F(E) (and to a lesser extent electronic coupling, J) then in principle, each X-H vibrational mode would have equal probability of accepting electronic energy and hence isotopomers would exhibit equal deuterium effects. This was first investigated in detail for naphthalene by Lin *et al.*,[82] who have suggested that the principle promoting modes in aromatic hydrocarbons are a small number of low energy C-C skeletal vibrations whilst the principle accepting modes are a large number of C-H high frequency stretching modes. They reported no positional dependence of deuteriation and that each position regardless of electron density contributes equally.[82]

Later studies of the positional dependence of deuteriation, which have been performed by several groups for both organic and inorganic compounds (*vide infra*).[83,84] Henry *et al.* have reported that location of the excited state electron density distribution is critical to the effect of deuteriation on emission lifetimes.[83,84] For example, for anthracene deuteriation of the alpha position has an increased effect over deuteriation of the beta position. This effect has also been observed for trans-stilbene.[ii,85]

---

systems contains contributions from both torsional (which may result in photochemical deactivation) and vibrational modes.

[vii] The integral in eq. (d) is only significant when ζ_{mn} is large in the region of the vibrating nuclei and hence increasing electron density (ζ_{mn}) in the region where vibrations act as promoting modes should therefore lead to larger values of knr.

$$J \propto \int \zeta_{mn}(r)(dV/dQ_k)\, dr \qquad \text{eq. (d)}$$

where ζ_{mn} is the electronic transition density from ψ_m-ψ_n, dQ_k are the nuclear coordinates of the promoting modes and V is the one electron electron-nuclear interaction. {Promoting modes undergo change of one quantum in the radiative transition; accepting modes appear in the FC overlap integral in eq 2}.

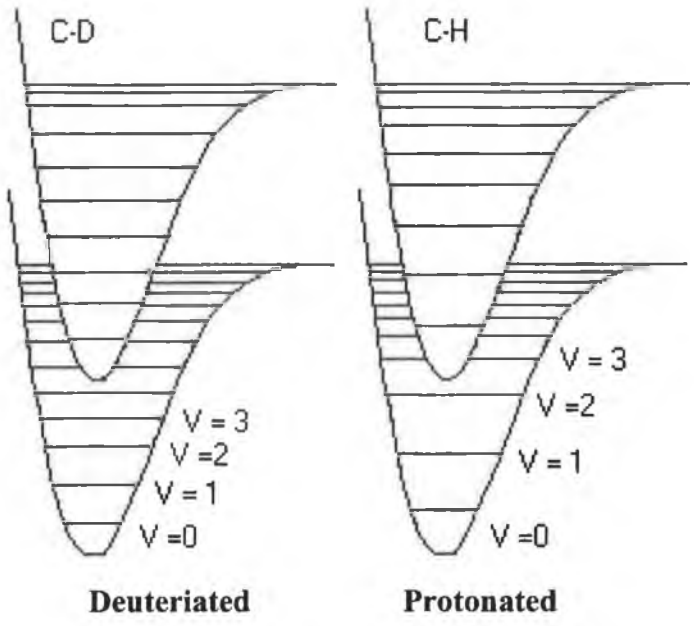

Figure 1.18 *Changes in vibrational levels and overlap, which occur upon deuteriation*

Although the role of high energy vibrational modes, in particular X-H (X = N, C, O) modes as acceptors of electronic energy (energy sinks), is primarily due to the larger F(E) values for these modes compared with lower energy skeletal modes, the role of such vibrational modes in promoting non-radiative transitions is less clear. Promoting modes can be loosely described as vibrational modes (usually symmetric), which stimulate transitions between excited states and undergo a single quantum (vibrational) change during the transition. Robbins *et al.* have examined the effect of the number of near neighbour hydrogens on the emission properties of octahedral Cr(III) complexes in glass matrices.[79f] The ^{3}dd emission originates from the $^{2}E_g$ (excited state) to $^{4}A_{ug}$ (ground state) transition, both of which are T_{2g} based and shows only minimal perturbation by variations in ligand field strength. Hence in a series of complexes {$[Cr(NH_3)_x(Y)_{6-x}]^{(3-x)+}$ (where x = 0,2 and Y = NCS); $[Cr(LL)_3]^{3+}$ (where LL = acetylacetate, formoacetate and malonate)} the ground–excited state energy gap is generally invariant, and the rate of radiationless decay is dependent only on the number of high-frequency acceptor modes and low frequency promoter modes. The results of these studies have suggested that involvement of C-H vibrational modes not only as acceptor modes but also as promoter modes. In the case of the latter set of complexes ($[Cr(LL)_3]^{3+}$) where the delocalisation of the excited state by π-conjugation occurs, the contribution of α-C-H vibrational modes as promotor modes is apparent. The rate of radiationless decay is dramatically reduced by their substitution by methyl groups. The existence of such "active H-atom" vibrational modes *i.e.* C-H bending modes capable of promoting electronic relaxation was already suggested

by Henry[83] and Siebrand.[72c] This explanation of the observed effect of removal of C-H oscillators may according to the Robbins *et al.* also explain the effect of phenyl or methyl substitution of bipyridyl and phenanthroline complexes of d^6 Ru(II) and Os(II) in reducing k_{nr} as being due to loss of promoting C-H modes.[79f, iib]

Deuteriation has shown in many cases, in particular in organic systems, to have a significant effect on vibrationally induced excited state non-radiative decay processes. In the case of inorganic systems, the effect of deuteriation may not be as apparent. It can be said, however, that provided the coupling between electronic states can be described by the weak coupling limit,[74] and provided that X-H vibrational modes make a significant contribution to the overall non-radiative rate constant ($\sum k_{nr}$), an effect of deuteriation will be observed. In addition, an important observation is that the location of the excited state on a particular moiety of a compound (*i.e.* the electron density in the region of the promoting X-H oscillator), determines the extent of the effect of isotopic substitution. This point is of particular relevance to the application of deuteriation in the study of excited state electronic structure of transition metal complexes.

1.4.3 Deuteriation studies: probing excited state decay processes.

Although deuteriation is widely applied to the study of ground state properties of both organic and inorganic complexes its application to the study of photophysical properties, in particular as a probe into excited state processes, is much less extensive. The majority of the studies that have been reported in the literature involve metal complexes based on lanthanides and platinum group metals. The latter area is of most relevance to the studies described in this thesis and hence the effect of deuteriation is centred on the platinum group metals.

1.4.4 Photophysical properties of deuteriated platinum group metal compounds.

Within the platinum group metals the majority of the more recent investigations have been carried out on Ru(II) polypyridyl complexes. This is not surprising since these compounds have well-defined excited state properties and an extensive synthetic chemistry allows for the systematic variation of the ligands around the metal centre.[2,1] Deuteriation has also been applied to the study of platinum, rhodium, chromium and molybdenum complexes. The application of deuteriation in inorganic photophysics can be broadly divided into two areas. In the first deuteriation has been applied to probing excited state decay processes. In these studies the effect of deuteriation on emission lifetimes (and occasionally unimolecular photochemical activity) has been studied. The

second area deuteriation has been used is as a tool in spectroscopic techniques such as resonance Raman[86,87,88,89] and high resolution emission spectroscopy,[90] due to its significant isotopic effect on the energies of vibrational transitions. These latter studies are aimed at obtaining detailed information on the nature of electronically exited states through a study of their vibrational properties.

1.4.4.1 Deuteriation and Luminescence lifetimes

Thomas *et al.* have examined the effect of deuteriation on the lifetime of the lowest energy ^{3}dd excited state, for a series of related Rh(III) complexes of the type $[Rh(NH_3)_{6-n}X_n]^{(3-n)+}$ (X = Cl, Br, I, n =0,1).[76] The increase in the emission lifetime (at 77K and 110 K in H_2O/MeOH 1:4 v/v) observed for these complexes upon solvent and ligand deuteriation is between 12 and 62 fold {for X = NH_3-τ_D/τ_H = 62, Cl-τ_D/τ_H = 52, Br-τ_D/τ_H = 36, I-τ_D/τ_H = 12}. The decrease in effect with increasing mass of X is most likely due to the increased importance of spin orbit coupling effect of the heavy halide atom, which facilitates deactivation by increasing the contribution of the radiative rate constant (k_r, see eq. 1).[91] Ford and coworkers have also studied the effect of deuteriation on the ^{3}dd emission of $[Rh(NH_3)_{6-n}X_n]^{(3-n)+}$ (X = Cl, Br, n = 0,1) in acidic aqueous solutions (to prevent H-D exchange of amine protons) at 298 K. [92] For both chloro- and bromo-complexes ligand (NH_3-ND_3) deuteriation resulted in a doubling of the emission lifetime in all solvents examined whilst solvent deuteriation resulted at most in a 20 % increase.

When the effect of ligand deuteriation on the photochemistry of the complexes was examined the value of k_p, the rate constant for photochemical deactivation, increased in all cases by 20-25 %. It was proposed that this increase in the rate k_p is due to a significant reduction in the k_{N-H} term (upon deuteriation) contribution to the overall non-radiative excited state decay rate $\sum k_{nr}$ and hence a relative increase in the importance of other terms. The effect of both ligand and solvent deuteriation on the ^{3}dd emission (at 77 K in H_2O/MeOH 1:4 v/v) of the complex *trans*-$[Rh(py)_4Br_2]Br$ (where py = pyridine) has also been examined.[76,93] Solvent deuteriation results in a 1.16-1.92 fold increase, whereas ligand deuteriation results in a more substantial 2.7 – 4.5 fold increase in the emission lifetime. In a similar study, Islam *et al.* have used deuteriation of the amine groups in the complex [*trans*-$Rh(en)_2Cl_2]Cl$ (where en = ethylene diamine) to compare the efficiency of excited state deactivation due to N-D/N-H vibrational modes and the symmetric Cl-Rh-Cl stretching vibrational modes and have found the latter to be the most important.[94] The two primary accepting modes were determined using spectral fitting and temperature

dependent lifetime studies. Huang Rhys factors (S) of 0.1 and 21 were determined for N-H/D and Cl-Rh-Cl stretching vibrational modes respectively.[viii] The weak coupling nature of the former was expected to result in an observable deuteriation effect, which was found to be the case. Deuteriation of N-H leads to a 3.4 to 11 μs increase at 298 K and 17 to 274 μs increase in emission lifetime at 80 K.

Krausz *et al.* have shown that such dramatic effects of deuteriation on the emission lifetime of rhodium complexes are not restricted to systems exhibiting ^{3}dd emission. [95] The emission of rhodium tris diimine complexes (*e.g.* $[Rh(bpy)_3]^{3+}$) has been classified as ^{3}IL in origin. Upon ligand deuteriation of $[Rh(bpy)_3]^{3+}$ an increase in emission lifetime of 280 to 570 μs (at 77K) has been observed.[95] Watts *et al.* have examined the effect of deuteriation on $[Ir(bpy)_2Cl_2]^+$.[93] This complex has demonstrated a dual emissive behaviour arising from two close lying weakly interacting excited states (*i.e.* metal centred ^{3}dd emission and a higher energy ^{3}dπ* charge transfer state). At 77 K the two excited states are not equilibrated and exhibit different emission lifetimes (^{3}dd (5.9 μs) and ^{3}dπ* (4.8 μs)) and upon deuteriation the ^{3}dd emission lifetime increases to 12.2 μs. Above 231 K the excited states are thermally equilibrated and show equal emission lifetimes, as the lifetimes of both emissions increase equally upon deuteriation (570 to 1190 ns).

2-thiopyridine (2-thpy) dipyridophenazine (dppz)

Figure 1.19 *Ligands described in the text*

The origins of this difference in the effect of deuteriation has been explained on the basis of reduced involvement of C-H modes in deactivating the ^{3}dπ* excited state arising from the change in vibrational force constants due to increased electron density on the aromatic ligands. This reduces the interaction between ground and excited vibrionic states. In contrast for the metal centred transition, less change in electron density on the aromatic

[viii] The Huang-Rhys Factor is a measure of the relative displacement of the donor and acceptor state and reflects the expected coupling between those states, *e.g.* S<1 weak coupling, S >2 strong coupling.

ligands occurs, and hence vibrational force constants are similar in both ground and excited states.

Riesen *et al.* have examined the role of C-H oscillators as acceptor modes in the non-radiative decay of the ^{3}dd excited state of ruthenocene by per-deuteriation and per-methylation of the cyclopentadienyl rings.[96] The emission lifetimes of ruthenocene (127 μs) is increased to 627 μs upon per-methylation (decamethylruthenocene) and 990 μs upon perdeuteriation ([D_{10}]-ruthenocene) at 1.5 K. The large increase in emission lifetime lends considerable support to the hypothesis that C-H modes act as energy acceptors.

Milder *et al.* have studied the effect of solvent and ligand deuteriation on the complex $[Pt_2(POP)_2]^{4-}$ (POP = μ-$P_2O_5H_2$).[97] The complex shows both phosphorescence ($^3A_{2u}(E_u)$-$^1A_{1g}$) and fluorescence ($^1A_{2u}$-$^1A_{1g}$) at 293 K. The very low quantum yield of fluorescence is due to the rapid ISC to a slightly higher energy state ($^3B_{2u}$) with which it is "strongly coupled" and "weakly coupled" to the phosphorescent $^3A_{2u}$ state. The coupling in both cases refers to the displacement with respect to the fluorescent $^1A_{2u}$ state and not the ground state. Ligand deuteriation did not result in significant changes in the fluorescence lifetime of the complex, either in propionitrile/2-methytetrahydrofuran glass or in polymethylmethacrylate at 77 K. However, solvent deuteriation in the case of ethanol/methanol matrices resulted in dramatic increases in fluorescence lifetimes; C_2H_5OH/CH_3OH - 750 ps, C_2H_5OD/CH_3OD - 1900 ps, C_2D_5OD/CD_3OD - 2170 ps. The origin of this increase in fluorescence lifetime was determined to be primarily due to the reduction in the rate of ISC to the weak coupling phosphorescent $^3A_{2u}$ excited state from the fluorescent $^1A_{2u}$, a process that is suggested to be coupled to O-H and C-H solvent vibrational modes.

Although the effect of deuteriation on several transition metal systems has been examined in the past, more recently significant attention has been given to Ru(II) diimine complexes. The first observation of an effect of deuteriation on the emission lifetime of $[Ru(bpy)_3]^{2+}$ was made by Watts *et al.*.[76,93] They have found that deuteriation of bpy results in a doubling of its emission lifetime (0.9 s to 2.2 s at 77K), whilst deuteriation of the complex $[Ru(bpy)_3]^{2+}$ results in a more modest 20 % increase in (5.1 to 6.1 μs at 77 K in EtOH/MeOH and 0.58 to 0.69 μs at 298 K in H_2O). In contrast solvent deuteriation (H_2O to D_2O) leads to a doubling of the emission lifetime of $[Ru(bpy)_3]^{2+}$ (0.58 to 1.02 μs at 298 K). It was suggested, based on the theories of radiationless transitions developed

for organic compounds[72,73,74] that this difference between ligand C-H and solvent O-H vibrational modes' ability to deactivate the lowest ^{3}MLCT states is due to the charge-transfer-to-solvent character (CTTS) of the ^{3}MLCT state. In such a case a significant proportion of the excited state's electron density is distributed over the solvent cage, facilitating transfer of electronic energy to solvent vibrational modes. A similar difference in the effect of solvent and ligand X-H vibrational modes on the emitting states of rare earth ions has also been observed (see Appendix A). In addition, O-H vibrational modes tend not to be as well defined as C-H vibrations and hence the energy match between the excited and ground state of the complex and the vibrational transition of the solvent is more easily attained. More recently Krausz *et al.* (Table 1.6) have examined the effect of partial and complete deuteriation of $[Ru(bpy)_3]^{2+}$ on emission lifetime in a range of matrices.[95] The results show a linear dependence of emission lifetime on the number of hydrogen atoms exchanged in agreement with the findings of Robbins *et al* (*vide supra*).[79f]

Matrix	Temperature	$[D_0]$-	$[D_8]$-	$[D_{16}]$-	$[D_{24}]$-
H_2O	298 K	610 ns	640 ns	690 ns	760 ns
D_2O	298 K	950 ns	1080 ns	1180 ns	1340 ns
Single crystal	5 K	64 μs	68 μs	75 μs	80 μs
PVA	77 K	5.2 μs	5.7 μs	6.1 μs	6.7 μs

Table 1.6 *The effect of extent of deuteriation and matrix on the emission lifetime of* $[Ru(bpy)_3]^{2+}$

Kincaid and coworkers have examined the positional dependence of the deuteriation effect in $[Ru(bpy)_3]^{2+}$.[86,98] The studies showed that deuteriation of the 3,3' or 4,4' positions of the bpy ligand had no observable effect on the emission lifetimes (610 and 605 ns respectively) compared with non-deuteriated $[Ru(bpy)_3]^{2+}$ (590 ns). Deuteriation of the 5,5' or 6,6' positions in contrast increased the emission lifetime to 635 and 645 ns respectively. Similar trends were observed when two or three of the available positions were deuteriated. These studies are in agreement with similar studies carried out on organic compounds (*vide supra*) and again suggest that the ability of X-H vibrational modes to deactivate an excited state is dependent on the electron density distribution in the excited state.

Studies of the effect of deuteriation on the photochemical properties of $[Ru(bpy)_3]^{2+}$ demonstrated that at elevated temperatures competing processes for excited state

deactivation become more important and the effects of ligand and solvent deuteriation are equally reduced.[76,93,99] It was suggested that a set of excited states (^{3}MC or metal centred) lying higher than the lowest excited states (^{3}MLCT) are thermally populated from the same. Importantly, deactivation via these states (^{3}MC) was found to be independent of both ligand and solvent deuteriation,[99] as would be expected for a strong coupling system. These results are in agreement with the conclusions reached in section 3 in that in order for a deuteriation effect to be observed, X-H vibrational coupling must make a significant contribution to the overall non-radiative decay rate constant of the excited state.

1.4.4.2 Deuteriation and localised emissive excited states in heteroleptic Ru(II) complexes

The studies on ruthenium polypyridyl complexes discussed above are concerned with the excited state properties of homoleptic complexes. The effect of partial and complete deuteriation on the emission lifetimes of heteroleptic Ru(II) and Os(II) diimine complexes has also been examined. Krausz *et al.* have observed an increase in the emission lifetime of $[Ru(bpy)_2(5,5\text{-dicarboxybipyridine})]^{2+}$ (6.3-6.9 μs at 77 K in EtOH/MeOH 4:1 v/v) upon deuteriation of the bpy ligand. [95] This increase is close to the increase in emission lifetime from $[Ru([H_8]\text{-bpy})_2(bpy)]^{2+}$ to $[Ru([D_8]\text{-bpy})_2(bpy)]^{2+}$ (5.2-6.1 μs at 77 K in PVA)[95].

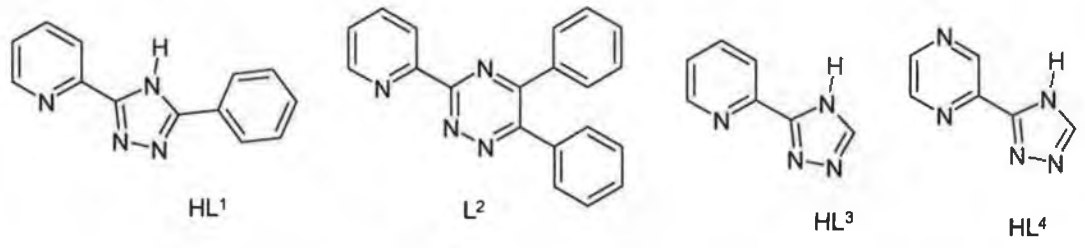

Figure 1.20 *Triazole and triazine based ligands used in the study of the effect of partial deuteriation on mixed ligand ruthenium polypyridyl complexes*

Kober *et al.* have reported the effect of bpy deuteriation on a range of heteroleptic Os(II) complexes ($[Os(bpy)_2(LL)]^{2+}$, LL = dppy, dppm, diars, bpy).[100] They observed increases of between 40 and 100% in the emission lifetime, demonstrating that the relative effect of ligand deuteriation for Os(II) complexes is greater than that observed for of $[Ru(bpy)_3]^{2+}$. Bergkamp *et al.* have found similar increases in emission lifetime upon perdeuteriation of $[Os(bpy)_3]^{2+}$ at 10 K (1.05 μs to 2.5 μs).[101]

In mixed ligand compounds the issue as to which ligand the emitting ^{3}MLCT state is localised on is of interest. The nature and location of the lowest excited state is often a

controlling factor where energy vectoring is of significant interest and where the design of suitable molecular assemblies is concerned.[2] As a consequence the location of excited states is of particular interest to the field of supramolecular chemistry. In heteroleptic complexes, such as $[Ru(bpy)_2(LL)]^{n+}$, the excited state may lie on either the bpy ligand or the ligand (LL) or even on a component of a ligand.[88] Methods of determining its location are required for the correct assignment of spectroscopic bands and LUMO energies. Resonance Raman spectroscopy,[88] electrochemistry[2] and acid base studies,[4] have proven useful in determining excited state electronic distribution, however a more recent approach has investigated the application of deuteriation of ligands for this purpose. Partial deuteriation in combination with the measurement of the excited state lifetime has been proposed as a method for the location of the emitting states of hetereoleptic ruthenium polypyridyl complexes.[88,102] It has been suggested that deuteriation of one of the ligands in a mixed ligand complex will only affect the emission lifetime if the emitting state is based on that ligand.

		τ (ns)		τ (ns)
1	$[Ru(bpy)_2(L^1)]^+$	**225**	$[Ru([D_8]\text{-}bpy)_2(L^1)]^+$	**480**
2	$[Ru(bpy)_2(L^2)]^{2+}$	**740**	$[Ru([D_8]\text{-}bpy)_2(L^2)]^{2+}$	**780**
3	$[Ru(bpy)_2(L^3)]^+$	**145**	$[Ru([D_8]\text{-}bpy)_2(L^3)]^+$	**250**
4	$[Ru(bpy)_2(L^4)]^+$	**230**	$[Ru([D_8]\text{-}bpy)_2(L^4)]^+$	**290**
5	$[Ru(bpy)_2(HL^4)]^{2+}$	**230**	$[Ru(bpy)_2([D_4]\text{-}HL^4)]^{2+}$	**470**

Table 1.7 *Effect of deuteriation on the emission lifetime of complexes 1 to 5. Measured in N_2 degassed acetonitrile*

To illustrate this Vos and co-workers have carried out partial deuteriation of two mixed ligand complexes, $[Ru(bpy)_2(L^1)]^+$ (**1**), $[Ru(bpy)_2(L^2)]^{2+}$ (**2**) (see Figure 1.20). [102] For the non-deuteriated complexes the emission lifetimes of 225 (**1**) and 740 ns (**2**) were obtained, deuteriation of the bpy ligands leads to lifetimes of 480 (**1**) and 780 ns (**2**). So deuteriation of (**1**) leads to almost a doubling of the emission lifetime while for complex (**2**) deuteriation has little effect (Table 1.7). It was concluded from this that the emitting states were located on the bpy ligand for complex (**1**) and electron poor triazine ring L^2 ligand for complex (**2**).[102a,b] These observations were in agreement with resonance Raman studies on these compounds.

In a similar study partial deuteriation of the complexes, $[Ru(bpy)_2(L^3)]^+$ (**3**), $[Ru(bpy)_2(L^4)]^+$ (**4**) and $[Ru(bpy)_2(HL^4)]^{2+}$ (**5**) (Figure 1.21) was carried out and lifetime measurements in conjunction with excited state rR were carried out to determine the

nature of the emitting state.[102c] For complex (**3**) deuteriation of the bpy ligand leads to an increase in the emission lifetime from 145 ns to 250 ns, (Figure 1.20) whilst deuteriation of the L^3 had no effect. For complex (**4**) deuteriation of the bpy ligand leads to a small increase in emission lifetime (230 ns to 290 ns) whilst deuteriation of L^4 had little or no effect on the emission lifetime. RR suggests that in both (**3**) and (**4**) the emitting state is bpy based. The increase observed for bpy deuteriation in (**4**) was however less than expected. Detailed studies carried on this compound suggest that this reduced sensitivity is explained by the presence of two emitting states, one bpy and one pyrazine based. Complex (**5**) showed no increase in emission lifetime upon deuteriation of the bpy. Deuteriation of HL^4 however did result in a doubling of the emission lifetime (230 to 470 ns) indicating that in the protonated form the lowest excited state is HL^4 based, again in agreement with resonance Raman studies.[102c]

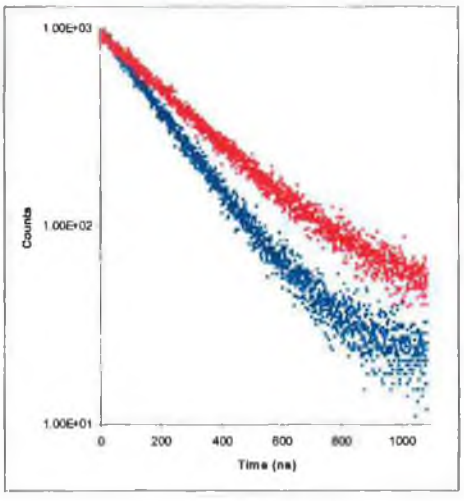

Figure 1.21 *Time Correlated Single Photon Counting traces of the complexes* $[Ru(bpy)_2(L^3)]^+$ *(lower trace) and* $[Ru([D_8]\text{-}bpy)_2(L^3)]^+$ *(upper trace)*

The issue of the temperature at which measurements are made was raised by Krausz *et al.*.[95] At low temperatures where only the lowest excited state has a significant Boltzmann population, the effect of deuteriation observed is the effect on that state alone. At higher temperatures when several low-lying electronically excited states of similar orbital parentage are populated then the effect of deuteriation observed is an averaged effect on the populated states. At even higher temperatures thermal population of states, which exhibit strong coupling with the ground state and undergo fast decay directly to the ground state may result in a reduction or even elimination of any observable effect of deuteriation. This is particularly important when assignment of excited state localisation is being attempted by selective deuteriation techniques, where excited states of similar character (*e.g.* ^{3}MLCT) but different orbital parentage are close in energy. The effect of

deuteriation on the emission lifetime of platinum group transition metal complexes shows a strong dependence on the deactivating ability of X-H vibrational modes. In addition the effect of selective deuteriation experiments can potentially provide information on the nature of the emissive states and can be applied to investigating the localisation of excited state on specific ligands. However, in contrast to many organic systems, X-H vibrational modes are seldom the primary route towards radiationless deactivation. For example, in the case of $[Ru(bpy)_3]^{2+}$, it has been found that with skeletal C-C-C vibrational modes deactivation via the lowest ^3MC excited state and quenching (*e.g.* $^3O_2$ quenching) constitute a dominant contribution towards radiationless deactivation, with C-H vibrational modes only being of secondary importance.[86,98] As would be expected based on Equation 1.1, this limits the observable effects of deuteriation and as a result the application of deuteriation as a probe in these studies may not be universally applicable, particularly in systems which can be described best by the strong coupling limit of Jortner *et al.*.[74]

1.4.5 Application of deuteriation to vibrational spectroscopies

The use of isotope exchange and in particular deuteriation in assigning vibrational modes is of significant interest. An extensive discussion of the results of studies involving the use of deuteriation in vibrational spectroscopies is beyond the scope of this chapter and is dealt with elsewhere and in Chapter 4.[90] However some notable examples of the use of deuteriation in assigning vibrational bands are presented to illustrate the effectiveness of deuteriation in both interpreting vibrational spectra and in applying the results to understanding photophysical processes and electronic excited state structure.

The application of H-D exchange to vibrational spectroscopy has been well demonstrated in the study of the complexes $[Mo_2(O_2CCH_3)_4]$ and $[Mo_2(O_2CCD_3)_4]$ by Hempleman *et al.*.[103] In the Raman spectra (at 20 K) of these complexes the band at 404 cm^{-1}, which had been assigned to Mo-Mo stretching modes by metal isotope substitution, is essentially unchanged by deuteriation whilst Mo-O and OCO bands are noticeably shifted to lower energy. Clark *et al.* have extended the use of isotopic labelling as a tool for the unambiguous assignment of vibrational bands of Raman and Resonance Raman spectra to the complex $[Rh_2(O_2CCH_3)_4(PPh_3)_2]$.[104] Deuteriation has also been used to probe the excited state (T_1) structure of copper(II) porphyrins using time resolved resonance Raman (TR^3) spectroscopy.[105]

Coates *et al.* have used the partial deuteriation of dppz to [D_6]-dppz to aid assignment of the transient resonance Raman spectra of $[Ru(ph_2phen)_2(dppz)]^{2+}$ and $[Ru(ph_2phen)_2([D_6]\text{-dppz})]^{2+}$ in H_2O, DNA and CH_3CN. [88b] These studies have shown that although many of the bands observed are attributable to vibrations which involve the entire dppz ligand skeleton, isotopic substitution suggests the involvement of vibrational modes more confined to a particular moiety of the dppz ligand.

In addition to providing information on the origin of vibrational modes by isotopic shift effects, the use of deuteriation has been extended by Kincaid *et al.* to provide additional data to allow for refinement of ground state force field calculations obtained from normal co-ordinate analysis (NCA).[86,98] They have carried out rR and TR^3 studies in fluid solution on a series of isotopomers of $[Ru(bpy)_3]^{2+}$ using selective deuteriation and ^{15}N labelling. The data obtained has allowed for the derivation of a corresponding force field for the anion radical fragment of the ^{3}MLCT excited state. This has allowed identification of the presence of vibrations in the excited state Raman spectra of $[Ru(bpy)_3]^{2+}$, which are similar to those observed for the bpy^{-*} radical anion. Based on the results of these empirical and theoretical studies, Kincaid *et al.*[86,98] have suggested that for $*[Ru(bpy)_3]^{2+}$ a localised excited state with the formula $[Ru^{III}(bpy)_2(bpy^-)]^{2+}$ exists, in agreement with the conclusions of Krausz *et al.*.[90b,c]

The use of vibrational spectroscopy, in particular resonance Raman and TR^3, in probing excited states, although useful, may be ambiguous as has been demonstrated by Humbs *et al.* in the study of the complexes $[Pt([H_8]\text{-bpy})_{2-n}([D_8]\text{-bpy})_n]^{2+}$ (where n = 0,1,2). [89] Raman spectra of these complexes were obtained as their neat perchlorate powders and interestingly the Raman scattering intensities due to the per-deuterio ligand in the mixed ligand complex were found to be significantly higher than for the per-protio ligand. This is not an unusual occurrence and has also been found the Humbs *et al.* to occur in the analogous $[Rh([H_8]\text{-bpy})_{3-n}([D_8]\text{-bpy})_n]^{2+}$ (where n = 1,2) complexes. The results of these Raman studies were then used to aid assignment of vibrational features of the highly resolved low temperature emission spectrum (*vide infra*) of the Pt(II) complexes {$[Pt([H_8]\text{-bpy})_{2-n}([D_8]\text{-bpy})_n]^{2+}$ (where n = 0,1,2)}, where only vibrational modes due to the per-protio ligands were observed in all but the perdeuteriated complex, indicating that emission from the per-protio ligand based excited state alone is occurring. Danzer *et al.* have examined the rR and TR^3 spectra of ruthenium complexes containing bpy, pypz, bpz and their partially deuteriated analogues in order to assign Raman bands and assign the

location of the excited state.[88] The results of these studies allowed for the confirmation of the localisation of the excited state on the pyrazine moiety in hetereoleptic complexes. Similar studies on the pyridinyl- and pyrazinyl-1,2,4-triazole complexes (*vida supra*) described in above have been carried out. In these studies partial and complete deuteriation has allowed for the determination of the emitting state for these compounds.[102]

Low temperature (< 5 K) high resolution emission studies on a series of platinum group complexes have been carried out by Yersin *et al.*[90a] and Krausz *et al.*.[106,107] Both matrix and ligand deuteriation have been employed in these studies. The results of these studies have recently been reviewed in detail by Yersin *et al.* [90a] and Krausz *et al.*[90b,c] and only experimental effects of deuteriation will be dealt with here.

Obtaining highly resolved emission and excitation spectra of transition metal complexes is often hampered by the lack of adequate matrices. However several matrices have been found that are suitable such as $[Pt(bpy)_2](ClO_4)_2$, $[Zn(bpy)_3](ClO_4)_2$, $[Rh(bpy)_3](ClO_4)_2$, $[Ru(bpy)_3[(ClO_4)_2$ and $[Os(bpy)_3](ClO_4)_2$.[90] These are suitable due to the presence of inequivalent sites, the so called X traps, which allow the transition metal complexes in neat crystal matrices to have their emitting states several tens of cm^{-1} lower than those of the majority of complexes and/or below the exciton band. At very low temperatures these "sites" can be populated selectively and hence highly resolved spectra obtained.[90a] A second strategy for isolating transition metal complexes is based on the effect of deuteriation on electronic transition energies. By doping per-deuteriated matrices with the partially or completely per-protonated metal complexes a similar effect to the X-trap effect can be observed,[90a] *i.e.* the electronic origins of the nondeuteriated and partially deuteriated complexes are several 10's of cm^{-1} lower than those of the completely deuteriated matrices.

Deuteriation has been applied to similar studies of Cr(III) amine complexes by Flint *et al.*[108] and later Kirk *et al.*[109], of ruthenocene by Riesen *et al.*,[96] of vanadium(II) hexaaquo complex by Mcdonald *et al.*,[110] of $Pd(2\text{-thpy})_2$[111] and of $[Rh([H_8]\text{-bpy})_{3-x}([D_8]\text{-bpy})_x]^{2+}$ (x = 0 to 3) by Yersin *et al.*.[89a] In general the application of deuteriation to these studies have been to allow for the assignment of vibrational bands rather than as a direct probe into electronically excited state decay processes. In a similar manner deuteriation has also been applied in investigations involving Stark effect spectroscopy,[112] fluorescence and excitation line narrowing and transient spectral hole burning.[89a,112,113,114]

1.5 Scope of thesis

Over the last half-century ruthenium and osmium have formed an important part in the development of supramolecular chemistry, in particular, in the development of artificial photosynthesis and in the exploration of energy and electron transfer processes. In this latter aspect, the application of Ru(II) complexes have proven exceptional application towards heterogeneous supramolecular chemistry (*e.g.* photovoltaics). The use of ruthenium is no small part due to its synthetic versatility and the stability of its polypyridyl complexes. This allowed for the synthesis of ever-larger molecular assemblies and multicomponent systems. In order to fully exploit the synthetic control available, the ability to understand these systems reliably require new approaches to traditional methods of characterisation. This is not restricted to improvements in approaches taken in their structural characterisation, but equally the need to understand the factors that affect intercomponent interactions and excited state properties is clear.

The scope of this thesis covers four main areas. The first area considered is the development of facile and efficient methods allowing for isotope exchange (Chapter 3) together with the synthesis and characterisation of selectively deuteriated Ru(II) and Os(II) polypyridyl complexes (Chapter 4). Secondly the use of deuteriation as a routine spectroscopic tool not only in simplification of NMR spectra and in interpreting vibrational spectra but also in probing excited electronic state processes (Chapters 4 and 5). Thirdly the issue of isomerism is examined, both in terms of stereochemistry and coordination isomerisation (Chapter 6). Although the effect of stereochemistry on ground state properties has been examined by several groups, in particular Keene and coworkers,[14] its importance in photophysical processes has received little attention and it is this area that is considered here. Finally, systematic variation of internuclear interaction both by variation of the bridging ligand and of pH, is explored (Chapter 7 and 8).

In Chapter 2, details of the experimental techniques employed together with practical considerations are described. The preparation of some of the more common ruthenium and osmium complexes, used as precursors throughout the remaining chapters of the thesis, is examined from a practical viewpoint and the utility of microwave radiation as a heat source briefly examined. A short discussion of some of the fundamental aspects of the various techniques employed has been included together with references to more

detailed texts on the subjects touched upon. The synthesis and characterisation of all ligands employed in Chapters 4 to 7 is also described.

1.6 Bibliography

1. (a) K. Kalyanasundaram, *Coord. Chem. Rev.*, **1982**, *46*, 159 (b) J. M. Lehn, *Angew. Chem., Int. Ed. Engl.*, **1988**, *27*, 89 (c) V. Balzani, S. Campagna, G. Denti, A. Juris, S. Serroni and M. Ventura, *Coord. Chem. Rev.* **1994**, *132*, 1 (d) V. Balzani, A. Juris, M. Venturi, S. Campagna and S. Serroni, *Chem. Rev.*, **1996**, *96*, 759 (e) V. Balzani, A. Juris, M. Venturi, S. Campagna and S. Serroni, *Acc. Chem. Res.*, **1998**, *31*, 26 (f) C. A. Slate, D. R. Striplin, J. A. Moss, P. Chen, B. W. Erickson and T. J. Meyer, *J. Am. Chem. Soc.* **1998**, *120*, 4885 (g) Y.-Z. Hu, S. Tsukiji, S. Shinkai, S. Oishi and I. Hamachi, *J. Am. Chem. Soc.* **2000**, *122*, 241 (h) J-P. Sauvage, J-P. Collin, J-C. Chambron, S. Guillerez, C. Coudret, V. Balzani, F. Barigelletti, L. De Cola and L. Fannigni, *Chem. Rev.*, **1994**, *94*, 993 (i) J. N. Demas and D. A. DeGraff, *Analytical Chem.*, **1991**, *63*, 829

2. A. Juris, V. Balzani, F. Barigelletti, S. Campagna, P. Belser and A. von Zelewsky *Coord. Chem. Rev.* **1988**, *84*, 85

3. K. Kalyanasundaram, *Photochemistry of Polypyridine and Porphyrin Complexes*, Academic Press, London, **1992**

4. (a) J. G. Vos, *Polyhedron* **1992**, *11*, 2285 (b) Md. D. Hossain, R. Ueno and M. Haga, *Inorg. Chem. Commun.*, **2000**, *3*, 35 (c) M. Haga, Md. M. Ali, H. Maegawa, K. Nozaki, A. Yoshimura and T. Ohno, *Coord. Chem. Rev.* **1994**, *132*, 99

5. (a) H. Dürr and S. Bossmann, *Acc. Chem. Res.*, **2001**, *34*, 905 (b) T. J, Meyer, *Acc. Chem. Res.*, **1989**, *22*, 163 (c) B. O'Regan and M. Graetzel, *Nature*, **1991**, *335*, 737 (d) L. De Cola and P. Belser, *Coord. Chem. Rev.*, **1998**, *177*, 301 (e) C. A. Bignozzi, J. R. Schoonover and F. Scandola, *Progr. Inorg. Chem.*, **1997**, *44*, 1 (f) M-J. Blanco, M. C. Jiménez, J-C. Chambron, V. Heitz, M. Linke and J-P. Sauvage, *Chem. Soc. Rev.*, **1999**, *28*, 293 (g) L. Sun, L. Hammarström, B. Åkermark and S. Styring, *Chem. Soc. Rev.*, **2001**, *30*, 36 (h) A. Magnunson, Y. Frapart, M. Abrahamsson, O. Horner, B. Åkermark, L. Sun, J.-J Girerd, L. Hammarström and S. Styring, *J. Am. Chem. Soc.*, **1999**, *121*, 89 (i) J-P. Collin, A. Harriman, V. Heitz, F. Odobel and J-P. Sauvage, *Coord. Chem. Rev.*, **1996**, *148*, 63

6. (a) P. D. Beer, F. Szemes, V. Balzani, C. M. Salà, M. G. Drew, S. W. Dent and M. Maestri, *J. Am. Chem. Soc.*, **1997**, *119*, 11864 (b) F. Barigelletti, L. Flamigni, J-P. Collin and J-P. Sauvage, *Chem. Commun.*, **1997**, 333 (c) O. Waldmann, J. Hassmann, P. Müller, G. S. Hanan, D. Volkmer, U. S. Schubert and J-M. Lehn, *Phys. Rev. Lett.*, **1997**, *78*, 3390 (d) E. Zahavy and M. A. Fox, *Chem. Eur. J.* **1998**, *4*, 1647 (e) V. Balzani, A. Credi and M. Venturi, *Curr. Opin. Chem. Biol.*, **1997**, *1*, 506 (f) L. Flamigni, F. Barigelletti, N. Armaroli, J-P. Collin, I. M. Dixon, J-P. Sauvage and J. A. G. Williams, *Coord. Chem. Rev.*, **1999**, *190*, 671 (g) J-C. Chambron, J-P. Collin, J-O. Balbavie, C. O. Dietrich-Buchecker, V. Heitz, F. Odobel, N. Solladie and J-P. Sauvage, *Coord. Chem. Rev.*, **1998**, *178*, 1299

7. G. Wilkinson, *Comprehensive Coordination Chemistry*, Vol. 4, Chap. 45/46, pp 327-345

8. (a) V. Balzani and F. Scandola, *Supramolecular Photochemistry*, Ellis Horwood: Chichester, UK, **1991** (b) Balzani, V. Ed., *Supramolecular Photochemistry*, Reidel, Dordrecht, **1997** (c) J-M. Lehn, *Supramolecular Chemistry*, Wiley-VCH, Weinheim, **1995** (d) A. K –D. Mesmacker, J-P. Lecomte and J. M. Kelly, *Top. Curr. Chem.*, **1996**, *177*, 25

9. M. Gross, *Chemistry in Britain*, **2002**, *38*, 36

10. (a) D. J. Cárdenas, P. Gavi a and J-P. Sauvage, *J. Am. Chem. Soc.*, **1997**, *119*, 2656 (b) J-P. Sauvage and C. Dietrich, *Molecular Catenanes, Rotaxanes and Knots*, Wiley-VCH, Weinheim, **1999** (c) P. Belser, A. von Zelewsky, M. Frank, C. Seel, F. Vögtle, L. de Cola, F. Barigelletti and V. Balzani, *J. Am. Chem. Soc.*,**1993**, *115*, 4076 (d) C. Dietrich-Buchecker, G. Rapenne and J-P. Sauvage, *Cord. Chem. Rev.*, **1999**, *185*, 167

11. S. Serroni, S. Campagna, F. Puntoriero, C. di. Pietro, N. D. McGlenaghan and F. Loiseau, *Chem. Soc. Rev.*, **2001**, *30*, 367

12. (a) V. Balzani, F. Barigelletti, P. Belser, S. Bernhard, L. de Cola and L. Flamigni, *J. Phys. Chem.*, **1996**, *100*, 16786 (b) E. C. Constable, *Prog. Inorg. Chem.*, **1994**, *42*, 67 (c) S. Chodorowski-Kimmes, M. Beley, J-P. Collin and J-P. Sauvage, *Tet. Lett.*, **1996**, *37*, 2963

13. (a) S. Serroni and G. Denti, *Inorg. Chem.*, **1992**, *31*, 4251 (b) S. Campagna, G. Denti, S. Serroni, A. Juris, M. Venturi, V. Ricevieto and V. Balzani, *Chem. Eur. J.*, **1995**, *1*, 211 and ref therein

14. (a) F. R. Keene, *Coord. Chem. Rev.*, **1997**, *166*, 121 (b) F. R. Keene, *Chem. Soc. Rev.*, **1998**, *27*, 185

15. (a) R. P. Thummel, D. Williamson and C. Hery, *Inorg. Chem.*, **1993**, *32*,1587 (b) S. Chirayil and R. P. Thummel, *Inorg. Chem.*, **1989**, *28*, 812 (c) J. E. O'Brien, T. B. H. McMurry and C. N. O'Callaghan, *J. Chem. Research (s)*, **1998**, 448 and ref. therein (d) C. K. Brush, M. P. Stone and T. M. Harris, *J. Am. Chem. Soc.*, **1988**, *110*, 4405

16. E. A. Seddon and K. R. Seddon, *The Chemistry Of Ruthenium*, Elsevier, Amsterdam, **1984**, *Chap. 15*

17. K. Kalyansundaram and M. Graetzel, Ed.s, *Photosensitisation and photocatalysis using inorganic and organometallic compounds*, Kluwer Academic Publishers, Dordrecht, **1993**

18. D. P. Segers and M. K. DeArmond, *J. Phys. Chem.*, **1982**, *86*, 3766

19. L. Wallace, D. C. Jackman, D. P. Rillema and J. W. Merkert, *Inorg. Chem.*, **1995**, *34*, 5210

20. R. Hage, *Ph.D. Thesis,* Leiden University, The Netherlands, **1991**

21. J. N. Demas, *Excited state lifetime Measurements*, Academic Press, New York, **1983**

22. E. Kober, B. P. Sulivan and T. J. Meyer, *Inorg. Chem.*, **1984**, *23*, 2098

23. J. P. Paris and W. W. Brandt, *J. Am. Chem. Soc.*, **1959**, *81*, 5001

24 .E. Kober and T. J. Meyer, *Inorg. Chem.*, **1983**, *22*, 1614

25. (a) G. A.Crosby and W.H. Elfring Jr, *J. Phys. Chem.*, **1976**, *80*, 2206 (b) C. Dual, E.J. Baerends and P. Vernooijs, *Inorg. Chem.*, **1994**, *33*, 3538

26. F. E. Lytle, and D.M. Hercules, *J. Am. Chem. Soc.*, **1969**, *91*, 253

27. D. M. Klassen and G. A. Crosby, *J. Chem. Phys.*, **1968**, *48*, 1853

28. P. Chen and T. J. Meyer, *Chem.Rev.*, **1998**, *98*, 1439

29. M. H. Ford-Smith and N. Sutin,, *J. Am. Chem. Soc.*, **1961**, *83*, 1830

30. J. Van Houten, and R. J. Watts, *J. Am. Chem. Soc.*, **1976**, *98*, 4853

31. M. Graetzel and B. O'Regan, *J. Am. Chem. Soc.*, **1993**, *115*, 6382

32. (a) J. V. Casper and T. J. Meyer, *Inorg. Chem.*, **1983**, *22*, 2444 (b) J. V. Casper and T. J. Meyer, *J. Am. Chem. Soc.*, **1983**, *105*, 5583

33. H. Yersin, W. Humbs and J. Strasser, *Topics in Current Chemistry*, **1997**, *191* 154

34. R. J. Watts and J. van Houten, *J. Am. Chem. Soc.*, **1978**, *100*, 1718

35. H. Yersin and W. Humbs, *Inorg. Chem.*, **1999**, *38*, 5820

36. G. D. Danzer, J. A. Golus and J. R. Kincaid, *J. Am. Chem. Soc.*, **1993**, *115*, 8643

37. F. Barigelletti, A. Juris, V. Balzani, P. Belser, A. von Zelewsky, *Inorg. Chem.*, **1983**, *22*, 3335

38. M. Kasha, *Discuss. Faraday Soc.*, **1950**, *9*, 14

39. C. V. Kumar, J. K. Barton, I. R. Gould, N. J. Turro, and J. van Houten, *Inorg. Chem.*, **1988**, *27*, 648

40. (a) S. F. McClanahan, R. F. Dallinger, F. J. Holler and J. R. Kincaid, *J. Am. Chem. Soc.*, **1985**, *107*, 4853 (b) P. A. Mabrouk and M. S. Wrighton, *Inorg. Chem.*, **1986**, *25*, 526

41. C. V. Kumar, J. K. Barton, N. J. Turro and I. R. Gould, *Inorg. Chem.*, **1987**, *26*, 1455

42. H. Hughes, D. Martin, S. Bell, J. J. McGarvey and J.G. Vos, *Inorg. Chem.* **1993**, *32*, 4402

43. R. Hage, J. G. Haasnoot, J. Reedijk and J. G. Vos, *Chemtracts-Inorg. Chem.*, **1992**, *4*, 75 and ref. therein

44 P. J. Steel and E. C. Constable, *J. Chem. Soc., Dalton Trans*, **1990**, 1389

45. J. G. Vos and J. G. Haasnoot, *Inorg. Chim. Acta*, **1983**, *71*, 155

46. T. E. Keyes, J. G. Vos, J. A. Kolnaar, J. G. Haasnoot, J. Reedijk and R. Hage, *Inorg. Chim. Acta,* **1996**, 245, 237

47. R. Wang, J. G. Vos, R. H. Schmehl and R. Hage, *J. Am. Chem. Soc.,* **1992**, *114*, 1964

48. H. A. Nieuwenhuis, J. G. Haasnoot, R. Hage, J. Reedijk, T. L. Snoeck, D. J. Stufkens and J. G. Vos, *Inorg. Chem.,* **1991**, *30*, 48

49. S. L. Valley ed., *Handbook of Geophysics and Space environment*, McGraw Hill, **1965**

50. D. P. Rillema, G. Allen, T. J. Meyer and D. Conrad, *Inorg. Chem.*, **1983**, *22*, 1617

51. G. M. Bryant, J. E. Fergusson and H. K. J. Dowell, *Aust. J. Chem.*, **1971**, *24*, 257

52. E. S. Dodsworth and A. B. P. Lever, *Chem. Phys. Lett.*, **1986**, *124*, 152

53. (a) C. M. Elliot and E. J. Hershenhart, *J. Am. Chem. Soc.*, **1982**, *104*, 7519 (b) R. Hage, J. G. Haasnoot, D. J. Stufkens, T. L. Snoeck, J. G. Vos and J. Reedijk, *Inorg. Chem.*, **1989**, *28*, 1413

54. (a) Y. Ohsawa, M. K. DeArmond, K. W. Hanck and C. G. Moreland, *J. Am. Chem. Soc.*, **1985**, *107*, 5383 (b) J. M. de Wolf, R. Hage, J. G. Haasnoot, J. Reedijk and J.G. Vos, *New J. Chem.*, **1991**, *15*, 501

55. (a) T. Förster, *Naturwiss*. **1949**, *36*, 186 (b) K. Weber, *Z. Phys. Chem.* **1931**, *B15,* 18 (c) Md. K. Nazeeruddin and K. Kalyanasundaram, *Inorg. Chem.*, **1989**, *28*, 4251

56. J. F. Ireland and P. A. H. Wyatt, *Adv. Phys. Org. Chem.* **1976**, *12*, 131

57. W. R. Browne, C. M. O'Connor, H. P. Hughes, R. Hage, O. Walter, M. Doering, J.F. Gallagher and J. G. Vos, *J. Chem. Soc., Dalton Trans*., **2002**, accepted Sept.

58. (a) S. Fanni, C. Di Pietro, S. Serroni, S. Campagna and J. G. Vos, *Inorg. Chem. Commun*., **2000**, *3*, 42 and (b) C. Di Pietro, S. Serroni, S. Campagna, M. T. Gandolfi, R. Ballardini, S. Fanni, W. R. Browne and J.G. Vos, *Inorg. Chem.*, **2002**, *41, 2871*

59. R. Wang, J. G. Vos, R. H. Schmehl and R. Hage, *J. Am. Chem. Soc.*, **1992**, *114*, 1965

60. P. J. Giordano, S. M. Fredricks, M. S. Wrighton, D. C. Morse, *J. Am. Chem. Soc.,* **1978**, *100*, 2257 and ref 9 to 17 therein

61. F. Barigelletti, L. De Cola, V. Balzani, R. Hage, J.G. Haasnoot, J. Reedijk and J. G. Vos, *Inorg. Chem.*, **1989**, *28*, 4344

62. B. E. Buchanan, H. Hughes, J. H. Van Diemen, R. Hage, J. G. Haasnoot, J. Reedijk and J. G. Vos, *J. Chem. Soc., Chem. Commun.*, **1991**, 300

63. B. E. Buchanan, P. Degn, J. M. P. Velasco, H. Hughes, B. S. Creaven, C. Long, J. G. Vos, R. A. Howie, R. Hage, J. H. van Diemen, J. G. Haasnoot, and J. Reedijk, *J. Chem. Soc., Dalton Trans.*, **1992**, 1177

64. W. F. Wacholtz, R. A. Auerbach and R. H. Schmehl, *Inorg. Chem.*, **1986**, *25*, 227

65. R. Wang, *Ph.D. Thesis*, Dublin City University, Ireland, **1990**

66. S. Fanni, F. Weldon, L. Hammarström, E. Muktar, W. R. Browne, T. E. Keyes and J. G. Vos, *Euro. J. Inorg. Chem.*, **2001**, 529

67. H. Hughes, *Ph.D. Thesis*, Dublin City University, Ireland, **1993**

68. H. P. Hughes and J. G. Vos, *Inorg. Chem.*, **1995**, *34*, 4001

69. H. Hughes, D. Martin, S. Bell, J. J. McGarvey and J. G. Vos, *Inorg. Chem.*, **1993**, *32*, 4402

70. C. A. Hutchinson, Jr. and B. W. Mangum, *J. Chem. Phys.*, **1960**, *32*, 1261

71. M. R. Wright, R. P. Frosch and G. W. Robinson, *J. Chem. Phys.*, **1960**, *33*, 934

72. (a) G. W. Robinson and R. P. Frosch, *J. Chem. Phys.*, **1962**, *37*, 1962 (b) G. W. Robinson and R. P. Frosch, *J. Chem. Phys.*, **1963**, *38*, 1187 (c) W. Siebrand, *J. Chem. Phys.*, **1967**, *46*, 440 (d) W. Siebrand, *J. Chem. Phys.*, **1966**, *44*, 4055

73. W. M. Gelbart, K. F. Freed and S. A. Rice, *J. Chem. Phys.*, **1970**, *52*, 2460

74. (a) J. Jortner, S. A. Rice and R. M. Hochstrasser, *Adv. Photochemistry*, **1969**, *7*, 149 (b) K. F. Freed and J. Jortner, *J. Chem. Phys.*, **1970**, *52*, 6272 (c) R. Englman and J. Jortner, *Mol. Physics*, **1970**, *18*, 145

75. (a) J. L. Kropp and M. W. Windsor, *J. Chem. Phys.*, **1963**, *39*, 2769 (b) J. L. Kropp and M. W. Windsor, *J. Chem. Phys.*, **1965**, *42*, 1599

76. T. R. Thomas, R. J. Watts and G. A. Crosby, *J. Chem. Phys.*, **1973**, *59*, 2123

77. J. van Houten and R. J. Watts, *J. Am. Chem. Soc.*, **1975**, *97*, 3843

78. N. Hirota and C. A Hutchinson, Jr, *J. Chem. Phys.*, **1965**, *43*, 1561

79. (a) H. Kupka, *Mol. Physics*, **1979**, *37*, 1673 (b) H. Kupka, *Mol. Physics*, **1979**, *37*, 1683 (c) H. Kupka, W. Ensslin, R. Wernicke and H. Schmidtke, *Mol. Physics*, **1979**, *37*, 1693 (d) H. Kupka, *Mol. Physics*, **1978**, *36*, 685 (e) V. L. Ermolaev and E. B. Sveshnikova, *Chem. Phys. Lett.*, **1973**, *23*, 349 (f) D. J. Robbins and A. J. Thomson, *Mol. Physics*, **1973**, *25*, 1103

80. J. V. Casper, E. M. Kober, B. P. Sullivan and T. J. Meyer, *J. Am. Chem. Soc.*, **1982**, *104*, 630

81. Y. Hasegawa, K. Murakoshi, Y. Wada, S. Yanagida, J. Kim, N. Nakashima and T. Yamanaka, *Chem. Phys. Lett.*, **1996**, *248*, 8

82. S. H. Lin, *J. Chem. Phys.*, **1966**, *44*, 3759 (c) S. H. Lin and R. Bersohn, *J. Chem. Phys.*, **1968**, *48*, 2732

83. B. R. Henry and J. L. Charlton, *J. Am. Chem. Soc.*, **1973**, *95*, 2782

84. (a) R. J. Watts and S. J. Strickler, *J. Chem. Phys.*, **1968**, *49*, 3867 (b) T. D. Gierke, R. J. Watts and S. J. Strickler, *J. Chem. Phys.*, **1969**, *50*, 5425 (c) J. D. Simpson, H. W. Offen and J. G. Burr, *Chem. Phys. Lett.*, **1968**, *2*, 383

85. V. G. Heinrich, H. Gusten, F. Mark, G. Olbrich and D. Schulte-Frohlinde, *Ber. Bunsenges. Phys. Chem.*, **1973**, *77*, 103

86. (a) P. K. Mallick, G. D. Danzer, D. P. Strommen and J. R. Kincaid, *J. Phys. Chem.*, **1988**, *92*, 5628 (b) K. Maruszewski, K. Bajdor, D. P. Strommen and J. R. Kincaid, *J. Phys. Chem.*, **1995**, *99*, 6286 (c) S. F. McClanahan and J. R. Kincaid, *J. Am. Chem. Soc.*, **1986**, *108*, 3840

87. M. Asano-Someda, S. Sato, K. Aoyagi and T. Kitagawa, *J. Phys. Chem.*, **1995**, 99, 13800

88. (a) G. D. Danzer, J. A. Golus and J. R. Kincaid, *J. Am. Chem. Soc.*, **1993**, *115*, 8643 (b) C. G. Coates, P. L. Callaghan, J. J. McGarvey, J. M. Kelly, P. E. Kruger and M. E. Higgins, *J. Raman Spect.*, **2000**, *31*, 283

89. (a) W. Humbs and H. Yersin, *Inorg. Chem.*, **1996**, *35*, 2220 (b) W. Humbs and H. Yersin, *Inorg. Chim. Acta*, **1997**, *265*, 139

90. (a) H. Yersin, W. Humbs and J. Strasser, *Topics in Current Chemistry*, **1997**, *191*, 154 (b) H. Riesen and E. Krauz, *Comments on Coord. Chem.*, **1995**, *18*, 27 (c) H. Riesen and E. Krauz, *Int. Rev. Phys. Chem.*, **1997**, *16*, 291

91. J. N. Demas and G. A. Crosby, *J. Am. Chem. Soc.*, **1970**, *92*, 7262

92. (a) J. D. Petersen and P. C. Ford, *J. Phys. Chem.*, **1974**, *78*, 1144 (b) M. E. Frink and P. C. Ford, *Inorg. Chem.*, **1985**, *24*, 1033 (c) M. A. Bergkamp, J. Brannon, D. Magde, R. J. Watts and P. C. Ford, *J. Am. Chem. Soc.*, **1979**, *101*, 4549 (d) M. A. Bergkamp, R. J. Watts and P. C. Ford, *J. Am. Chem. Soc.*, **1980**, *102*, 2627 (e) W. Weber, R. Van Eldik, H. Helm, J. Di Benedetto, Y. Du Commun, H. Offen and P. C. Ford, *Inorg. Chem.*, **1983**, *22*, 623

93. R. J. Watts, S. Efrima and H. Metiu, *J. Am. Chem. Soc.*, **1979**, *101*, 2742

94. A. Islam, N. Ikeda, K. Nozaki and T. Ohno, *J. Chem. Phys.*, **1998**, *109*, 4900

95. E. Krausz, G. Moran and H. Riesen, *Chem. Phys. Lett.*, **1990**, *165*, 401

96. H. Riesen, E. Krausz, W. Luginbuhl, M. Biner, H. U. Gudel and A. Ludi, *J. Chem. Phys.*, **1992**, *96*, 4131

97. S. J. Milder and B. S. Brunschwig, *J. Phys. Chem.*, **1992**, *96*, 2189

98. D. P. Strommen, P. K. Mallick, G. D. Danzer, R. S. Lumpkin and J. R. Kincaid, *J. Phys. Chem.*, **1990**, *94*, 1357

99. (a) J. van Houten and R. J. Watts, *J. Am. Chem. Soc.*, **1976**, *98*, 4853 (b) J. Van Houten and R. J. Watts, *Inorg. Chem.*, **1978**, *17*, 3381

100. E. M. Kober, J. V. Casper, R. S. Lumpkin and T. J. Meyer, *J. Phys. Chem.*, **1986**, *90*, 3722

101. M. A. Bergkamp, P. Gutlich, T. L. Netgel and N. Sutin, *J. Phys. Chem.*, **1983**, *87*, 3877

102. (a) T. E. Keyes, F. Weldon, E. Müller, P. Pechy, M. Grätzel and J. G. Vos, *J. Chem. Soc. Dalton Trans.*, **1995**, 2705 (b) S. Fanni, T. E. Keyes, C. M. O'Connor, H. Hughes, R. Wang and J. G. Vos, *Coord. Chem. Rev.*, **2000**, *208*, 77 (c) T. E. Keyes, C. M. O'Connor, U. O'Dwyer, C. G. Coates, P. Callaghan, J. J. McGarvey and J. G. Vos, *J. Phys. Chem. A*, **1999**, *103*, 8915

103. A. J. Hempleman, R. J. H. Clark and C. D. Flint, *Inorg. Chem.*, **1986**, *25*, 2915

104. R. J. H. Clark, A. J. Hempleman and C.D. Flint, *J. Am. Chem. Soc.*, **1986**, *108*, 518

105. P. Dro d ewski and E. Kordon, *Spectrochimica Acta Part A*, **2000**, *56*, 1299

106. H. Riesen, L. Wallace and E. Krausz, *J. Phys. Chem.*, **1996**, *100*, 17138

107. H. Riesen, L. Wallace and E. Krausz, *J. Phys. Chem.*, **1995**, *99*, 16807

108. (a) C. D. Flint and P. Greenhough, *J. Chem. Soc., Faraday Trans. 2*, **1972**, *68*, 897 (b) C. D. Flint, A. P. Matthews and P. J. O'Grady, *J. Chem. Soc., Faraday Trans. 2*, **1977**, *73*, 655

109. A. D. Kirk and H. U. Güdel, *Inorg. Chem.*, **1992**, *31*, 4564

110. R. G. Mcdonald, R. Starnger, M. A. Hitchman and P. W. Smith, *Chem. Phys.*, **1991**, *154*, 179

111. D. Becker, H. Yersin and A. von Zelewsky, *Chem. Phys. Lett.*, **1995**, *235*, 490

112. (a) H. Riesen and E. Krausz, *J. Chem. Phys.*, **1993**, *99*, 7614 (b) H. Riesen, L. Wallace and E. Krausz, *J. Chem. Phys.*, **1995**, *102*, 4823 (c) H. Riesen and E. Krausz, *Chem. Phys. Lett.*, **1996**, *260*, 130 (d) H. Riesen and E. Krausz, *Chem. Phys. Lett.*, **1998**, *287*, 388

113. H. Riesen, E. Wallace and L. Krausz, *Inorg. Chem.,* **2000**, *39*, 5044 and references 13-16 therein

114. (a) H. Riesen and E. Krausz, *Chem. Phys Lett.*, **1988**, *151*, 65 (b) H. Riesen, L. Wallace and E. Krausz, *J. Phys. Chem.,* **1996**, *100*, 4390

Chapter 2

General introduction to synthetic and purification procedures, physical techniques and measurements

In this chapter details of experimental and basic synthetic procedures used in subsequent chapters are described. In addition a limited discussion of practical aspects of both synthetic procedures and physical measurements is included, in particular where major difficulties were encountered and where improvements to standard procedures were made. For selected techniques a very brief summary of their theoretical basis is included together with references to useful literature sources.

2.1 General synthetic procedures and considerations

All synthetic reagents were of commercial grade and no further purification was employed, unless otherwise stated. All solvents used for spectroscopic measurements were of HPLC or UVASOL (Merck) grade. For luminescence measurements UVASOL grade solvents have been found to be the purest with respect to emissive contaminants. D_2O (99.9%) and 10% w/w Pd/C (Sigma-Aldrich) were used as received. 1 M NaOD/D_2O solution were prepared *in situ* by addition of 460 mg of sodium metal to 20 cm^3 of D_2O. 2,2'-Bipyridine, 4,4'-bipyridine, 4,4'-dimethyl-2,2'-bipyridine, 4,4'-diphenyl-2,2'-bipyridine, 1,10-phenanthroline, 4,7-diphenyl-1,10-phenanthroline (ph_2phen), 2,2'-biquinoline (Sigma-Aldrich) and 2-(thien-2'-yl)-pyridine (2-thpy) (Lancaster) were obtained from commercial sources and used as received without further purification. The synthesis of 2,3-bis(pyrid-2'-yl)-pyrazine,[1] 3-(pyrazin-2'-yl)-1,2,4-triazole (Hpztr), 3-methyl-5-(pyrazin-2'-yl)-1,2,4-triazole (Hmepztr), 3-(pyridin-2'-yl)-1,2,4-triazole (Hpytr), 3-methyl-5-(pyridin-2'-yl)-1,2,4-triazole (Hmepytr), and 3-phenyl-5-(pyridin-2'-yl)-1,2,4-triazole (Hphpytr) have been carried out using previously reported procedures.[2]

2.1.1 Preparation of ligands

The syntheses of 1,2,4-triazole based ligands were carried out by literature procedures.[3] No attempts at optimization of yields or investigations into alternative synthetic procedures were made except where stated. The synthesis of 1,2,4-triazole based ligands exploits the strong nucleophilicity of primary amines towards carbonyls.

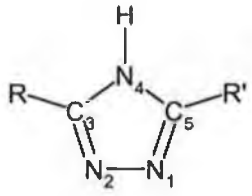

Figure 2.1 *Triazole moiety, which forms a basic unit in many of the ligands described in this chapter.*

Procedures for the synthesis of ligands containing triazole moieties are already well developed and the methods available allow for the synthesis of triazole ligands substituted in either or both of the 3 and 5 positions (see Figure 2.1). Not only can symmetric ligands such as Hbpt and Hbpzt be prepared by general routes outlined below (Schemes A & B) but also asymmetric ligands such as Hpztr, Hppt, 3-Hmepztr (mepztr), and 3-Hphpztr (phpztr).

Although alternative routes towards synthesis of the ligands described in this thesis are available they have not been investigated and will not be discussed here.[3]

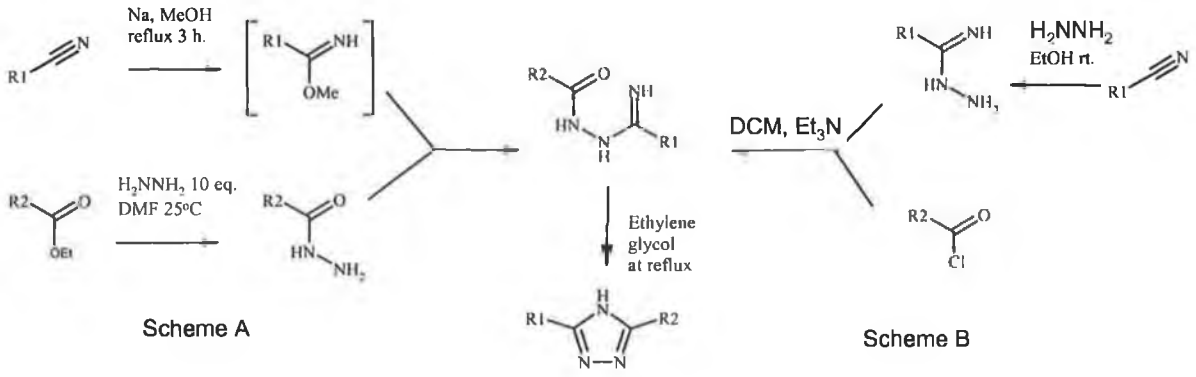

Figure 2.2 *General synthetic routes used in preparation of 1,2,4-triazole ligands.*

2.1.2 Synthetic procedures and characterisation of ligands

2-(5'-phenyl-4'H-[1,2,4]triazol-3'-yl)-pyrazine (Hphpztr). 0.8 g of sodium metal were added (carefully) to 35 cm^3 of methanol followed by the addition of 10.9 g (104 mmoles) of 2-pyrazine carbonitrile. The solution was heated at reflux for 3 h after which, it was allowed to cool and 17 g (104 mmoles) of phenyl hydrazide was added and the solution refluxed for a further 15 min yielding a dark yellow solution. Yellow crystals formed on cooling at room temperature overnight and were filtered under vacuum and air dried for one hour. The crystals were dissolved in 40 cm^3 of ethylene glycol and refluxed for 3 h. On cooling overnight the white target ligand precipitated and was collected by vacuum filtration, followed by washing with 50 cm^3 methanol. The product was recrystallised from hot ethanol. Yield of Hphpztr 15 g (64.4 mmol, 64 %). Mass spectrometry HM^+ ion at 224 m/z (calc. for $C_{12}H_{10}N_5^+ = 224$). ^1H NMR (D_6-DMSO) δ in ppm: 9.35 (d, 1H, pz-H3), 8.795 (dd, 1H, pz-H5), 8.765 (d, 1H, pz-H6), 8.11 (d, 2H, ph-H2/H6), 7.54 (dd, 2H, ph-H3/H5) 7.49 (t, 1H, ph-H4)

2-(5'-p-tolyl-4'H-[1,2,4]triazol-3'-yl)-pyrazine (Htolpztr). As for Hphpztr except 17 g (110 mmol) *p*-toluic hydrazide was used instead of phenyl hydrazide. Yield: 16.8 g (70 mmol, 63.5 %). Mass spectrometry HM^+ ion at 238 m/z (calc. for $C_{13}H_{12}N_5^+ = 238$). ^1H NMR (D_6-

DMSO) δ in ppm: 9.33 (d, 1H, pz-H3), 8.77 (m, 2H, pz-H5/H6), 7.34 (d, 2H, ph-H2/H6), 8.00 (dd, 2H, ph-H3/H5), 2.36 (s, 3H, $-CH_3$)

2-(5-thiophen-2-yl-4H-[1,2,4]triazol-3-yl)-pyridine (Hpytrth). 4 cm^3 (36 mmol) of 2-thiophene acid chloride were added dropwise to a stirred solution of 4 cm^3 of Et_3N and 3 g (22 mmol) of pyridin-2-yl amidrazone in 50 cm^3 of THF. The yellow suspension formed was stirred for 2 h at room temperature followed by addition of 30 cm^3 of ethanol. The precipitate was collected under vacuum and air-dried overnight. The yellow precipitate was heated at reflux in 30 cm^3 of ethylene glycol for 1 h and the solution was cooled to room temperature. 50 cm^3 of water was added to the thick off-white suspension and the product filtered under vacuum and recrystallised twice from hot ethanol. Yield 2.5 g (11 mmol, 50 %). ^1H NMR (400 MHz) in D_6-DMSO; 8.73 (1H, d, pyH6), 8.14 (1H, d, pyH3), 8.01 (1H, dd, pyH4), 7.69 (1H, d, th), 7.65 (1H, d, th), 7.55 (1H, dd, pyH5), 7.185 (1H, dd, th).

2-(5-thiophen-2-yl-4H-[1,2,4]triazol-3-yl)-pyrazine (Hpztrth). As for Hpytrth except: 3 g (22 mmol) of pyazin-2-yl amidrazone was employed. Yield 1.15 g (5 mmol, 22 %). ^1H NMR (400 MHz) in D_6-DMSO; 9.29 (1H, d, pzH3), 8.77 (1H, d, pzH5), 8.76 (1H, dd, pzH6), 7.74 (1H, d, th), 7.69 (1H, d, th), 7.21 (1H, dd, th)

2,5-bis-(5'-(pyridin-2''-yl)- 1'H-1',2',4'-triaz-3'-yl)-thiophene ($(Hpytr)_2th$). As for Hpytrth except: 2,5-thiophene-diacylchloride (prepared by heating at reflux 1.5 g (8.7 mmol) of 2,5-dicarboxy-thiophene in 30 cm^3 of $SOCl_2$) was reacted with 3 g (22 mmol) of pyidin-2-yl amidrazone was employed. Yield 674 mg (1.8 mmol, 21 %). ^1H NMR (400 MHz) in D_6-DMSO; 8.74 (1H, d, pyH6), 8.17 (1H, d, pyH3), 8.06 (1H, dd, pyH4), 7.73 (1H, s, th), 7.57 (1H, dd, pyH5)

2,5-bis-(5'-(pyrazin-2''-yl)- 1'H-1',2',4'-triaz-3'-yl)-thiophene- ($(Hpztr)_2th$). As for Py-tr-th except: 2,5-thiophene-diacylchloride (prepared by heating at reflux 1.2 g (6 mmol) of 2,5-dicarboxy-thiophene in 30 cm^3 of $SOCl_2$) was reacted with 2.4 g (18 mmol) of pyazin-2-yl amidrazone was employed. Yield 334 mg (0.9 mmol, 15 %). ^1H NMR (400 MHz) in D_6-DMSO; 9.30 (1H, d, pzH3), 8.775 (1H, d, pzH5), 8.765 (1H, dd, pzH6), 7.61 (1H, d, th)

Pyrazine-2,5-dicarbonitrile. 1 g (6 mmol) of pyrazine-2,5-dicarboxylic acid (Aldrich) was heated at reflux in 5 cm^3 of DMF and 20 cm^3 of $SOCl_2$ for 3 h. $SOCl_2$ was removed by vacuum distillation and the residue cooled in ice. 25 cm^3 of ice-cold concentrated NH_4OH solution was added dropwise and the solution stirred at room temperature overnight. The tan precipitate (pyrazine-2,5-dicarboxamide, 0.9 g (5.4 mmol)) was filtered and washed with 20 cm^3 of ice cold methanol and air-dried. The diamide was then suspended in 20 cm^3 of DMF at -10 °C and 25 cm^3 of $SOCl_2$ added dropwise over 30 min. The temperature was raised to room temperature and the solution stirred for a further 2 days. The contents were added, slowly, to ice and the solid formed was collected by vacuum filtration. Yield 0.6 g (4.6 mmol, 75 %) ^{1}H NMR in [D_6]-DMSO; 9.48 (2H, s)

2,5-bis(5'-methyl-4'H-[1,2,4]triaz-3'-yl)-pyrazine ((Metr)$_2$pz). 0.6 g (4.6 mmol) of 2,5-dicyanopyrazine was dissolved in 5 cm^3 of ethanol. 3 cm^3 of hydrazine hydrate were added and the solution stirred for 3 h at room temperature. The yellow precipitate was filtered and air-dried. The *bis*-amidrazone was then added to 10 cm^3 of acetic acid/acetic anhydride (50/50 v/v) at 0 °C. The temperature was raised slowly to 30 °C and the solution stirred for 2 h. The solution was then evaporated to near dryness and 2 cm^3 of ethylene glycol added and the solution boiled for 15 min. On cooling 10 cm^3 of water was added and the precipitate collected by vacuum filtration and washed with 10 cm^3 of methanol and air-dried. Yield 320 mg (1.32 mmol, 29 %). ^{1}H NMR in [D_6]-DMSO; 9.41 (2H, s), 2.79 (6H, s)

[D$_6$]-2,2'-bipyridine-4,4'-dicarboxylic acid.[4] 4.5 g (23 mmol) of [D_{12}]- 4,4'-dimethyl-2,2'-bipyridine was added slowly to 120 cm^3 of 98% H_2SO_4, followed by 24 g of sodium dichromate (92 mmol). The reaction temperature was maintained at 70 °C for 3 h followed by cooling to 20 °C. The reaction mixture was poured over 800 g of ice, stirred for 20 min and the yellow [D_6]-2,2'-bipyridine-4,4'-dicarboxylic acid collected by vacuum filtration. The crude product was suspended in 120 cm^3 of 50% nitric acid and heated to reflux for 4 h. After cooling the solution to room temperature it was added to 200g of ice and 500 cm^3 of water. On cooling to 5 °C a white precipitate formed. This was collected under vacuum and air-dried. Yield 4.2 g (16 mmol, 70 %). ^{1}H NMR ([D_6]-DMSO): 8.92 (*resid.* s), 8.85 (*resid.* s), 7.92 (*resid.* s)

2.1.2 Deuteriation of ligands

The deuteriation of ligands was carried out in a general-purpose dissolution Bomb P/N 4744 from Scientific Medical Products, which included a Teflon cup and cover. Calculation of the extent of H/D exchange has been carried out using ^{1}H NMR spectroscopy. The procedure used for the determination of the % deuteriation of the ligands described is as follows.[5] A known mass (and hence number of moles) of both the non-deuteriated and deuteriated sample is dissolved in 0.75 cm^3 of a suitable deuteriated solvent and the ^{1}H NMR spectra of both samples is obtained. The ratio of the integrated peak areas of the samples (relative to the residual solvent peak) is then obtained and the % H/D exchange calculated as in Equation 2.1. For example, the ^{1}H NMR spectra of the non-deuteriated ligand (6 mg) and the deuteriated ligand (12 mg) were obtained using the same sample of $CDCl_3$ or $(CD_3)_2SO$ to ensure the solvent peaks in each spectra reflected identical concentrations of residual non-deuteriated solvents (internal standards). The integration values of the ligand resonances (L) and the integration values of the solvent peaks (S) were determined. Since the integration values are proportional to the number of protons in the sample then the percentage deuteriation is determined by using the following equation:

$$\textbf{Equation 2.1} \quad \%Deuteriation = 100 - \frac{[(L_D/S_D)/6]}{[(L_H/S_H)/12]} * 100$$

Where the subscripts H and D refer to the non-deuteriated ligand and the deuteriated ligand respectively and the factors 6 and 12 account for the differences in ligand concentrations in the two samples. Determination of the extent of deuteriation by this procedure is subject to several major sources of error. Due to the small quantities employed in the sample preparation, the error in concentration would be expected to be ± 5 %. More accurate determination of the overall extent of deuteriation is available by analysis of the isotopic pattern of the mass spectra of the deuteriated complexes. Additional confirmation of the extent of deuteriation can be gleaned from the ^{1}H NMR spectra of partially deuteriated complexes (see Chapter 3).

2.1.3 Preparation of ruthenium(II) and osmium(II), cis-[M(LL)$_2$Cl$_2$] complexes by standard reflux

Cis-[Ru(LL)$_2$Cl$_2$].2H$_2$O and *cis*-[Os(LL)$_2$Cl$_2$].2H$_2$O are probably the most frequently employed precursor materials in the synthesis of Ru(II) and Os(II) polypyridyl complexes.[6] *cis*-[Ru(LL)$_2$Cl$_2$].2H$_2$O[7] and *cis*-[Os(LL)$_2$Cl$_2$]2H$_2$O[8] were prepared by the literature methods (where LL = bpy, phen, ph$_2$phen, [D$_8$]-bpy, [D$_8$]-phen, or [D$_{16}$]-ph$_2$phen). The synthesis of *cis*-[Ru(LL)$_2$Cl$_2$] complexes normally results in yields of 60 to 80 %, however, when the reaction is not kept at a vigorous reflux, yields drop dramatically. *N.B.* In contrast to previously reported procedures deoxygenation by argon or nitrogen purge of the reaction solution was not carried out, as it was noted in several cases that the cooling effect of the N_2 stream reduced the reaction temperature and hence inhibited the reaction. In the early stages of the reaction the reaction mixture is first dark green becoming dark red-brown after a few minutes reflux. Typically after 30 min gentle reflux the solution becomes lighter in colour. At this stage a mixture of products is present including possibly [Ru(LL)Cl$_3$] and certainly some [Ru(LL)$_3$]$^{2+}$ (as determined by emission spectroscopy). Extended heating at gentle reflux results in a slow darkening of the solution to a reddish colour. By allowing a more vigorous reflux the solution quickly (usually within 20 to 30 min) becomes the desired intense purple colour.[8] For *cis*-[Ru(ph$_2$phen)$_2$Cl$_2$] some problems do occur due to the poor solubility of the ligand. During the reaction sufficient solvent should be used (together with extended reaction times) to ensure reaction completion. A second problem encountered is that it is difficult to remove unreacted ph$_2$phen from the product due to the low solubility of ph$_2$phen in diethylether. The water of crystallization indicated for all complexes was estimated from the relative intensity of the proton resonance of the water peak in (CD$_3$)$_2$SO in the ^{1}H NMR spectra. The actual amount varied between 1.5 and 2.5 water molecules per molecule of complex.

cis-[Ru(bpy)$_2$Cl$_2$].2H$_2$O.

10.3 g (66 mmoles) of bpy, 8 g (33 mmoles) of RuCl$_3$.H$_2$O and 2 g LiCl in 60 cm^3 of DMF were heated at reflux for 8 h. The solution was then cooled to 25 °C and transferred to 100 cm^3 of acetone and kept at – 4 °C overnight. The product was filtered and washed with ice water (until the filtrate becomes colourless) and 50 cm^3 cooled diethyl ether yielding a dark purple powder. Yield 12.9 g (25 mmoles, 76 %). ^{1}NMR (400 MHz) in (CD$_3$)$_2$SO; 9.97 (2H,

d), 8.64 (2H, d), 8.49 (2H, d), 8.07 (2H, dd), 7.79 (2H, dd), 7.685 (2H, dd), 7.51(2H, d), 7.10 (2H, dd).

cis-[Ru([D$_8$]-bpy)$_2$Cl$_2$].2H$_2$O

As for *cis*-[Ru(bpy)$_2$Cl$_2$].2H$_2$O except 4.1 g (25 mmoles) of [D$_8$]-bpy, 3.04 g (12.5 mmoles) of RuCl$_3$.H$_2$O and 1.5 g LiCl in 50 cm^3 DMF. Yield 3.67 g (6.8 mmoles, 54 %).

cis-[Ru(ph$_2$phen)$_2$Cl$_2$].2H$_2$O

As for *cis*-[Ru(bpy)$_2$Cl$_2$].2H$_2$O except 2 g (6 mmoles) of ph$_2$phen, 690 mg (2.84 mmoles) of RuCl$_3$.H$_2$O and 2 g LiCl in 50 cm^3 DMF. Yield 1.9 g (2.15 mmoles 75 %). ^{1}NMR (400 MHz) in (CD$_3$)$_2$SO; 10.44 (2H, d), 8.27 (2H, d), 8.23 (2H, d), 8.1 (2H, d), 8.05 (2H, d), 7.86 (4H, d), 7.74(4H, t), 7.72 (2H, d), 7.56 (10H, m), 7.41(2H, d).

cis-[Ru([D$_{16}$]- ph$_2$phen)$_2$Cl$_2$].2H$_2$O

As for *cis*-[Ru(bpy)$_2$Cl$_2$].2H$_2$O except 0.8 g (2.3 mmoles) of [D$_{16}$]-4,7-diphenyl-1,10-phenanthroline ([D$_{16}$]-ph$_2$phen), 0.29 g (1.2 mmoles) of RuCl$_3$.H$_2$O and 0.1 g LiCl in 20 cm^3 DMF. Yield 600 mg (0.67 mmoles, 56 %).

cis-[Ru(phen)$_2$Cl$_2$].2H$_2$O

As for *cis*-[Ru(bpy)$_2$Cl$_2$].2H$_2$O except 720 mg (4 mmoles) of phen and 490 mg (2 mmoles) of with 2 g of LiCl were dissolved in 50 cm^3 DMF. Yield 550 mg (0.96 mmoles, 48%).^{1}NMR (400 MHz) in (CD$_3$)$_2$SO; 10.27 (2H, d), 8.73 (2H, d), 8.29 (2H, d), 8.24 (2H, d), 8.22 (2H, d), 8.14 (2H, d), 7.76 (2H, d), 7.35 (2H, d), 7.33 (2H, d).

cis-[Os(bpy)$_2$Cl$_2$].2H$_2$O

193 mg (1.24 mmoles) of bpy and 300 g (0.62 mmoles) of K$_2$OsCl$_6$ were dissolved in 3 cm^3 of ethylene glycol and heated at reflux for 45 min. The reaction mixture was cooled to room temperature and 5 cm^3 of saturated sodium dithionite solution was added. The mixture was stirred for a further 30 min and the black precipitate formed was filtered and washed with water (until the filtrate became colourless) and then 50 cm^3 of diethyl ether. Yield 320 mg (0.52 mmoles, 83%). ^{1}NMR (400 MHz) in (CD$_3$)$_2$SO; 9.61 (2H, d), 8.59 (2H, d), 8.37 (2H, d), 7.61 (2H, dd), 7.58 (2H, dd), 7.29 (4H, m), 6.8 (2H, dd).

cis-[Os([D$_8$]-bpy)$_2$Cl$_2$].2H$_2$O

450 mg (2.74 mmoles) of [D$_8$]-bpy and 600 g (1.37 mmoles) of $(NH_3)_2OsCl_6$ were dissolved in 3 cm^3 of ethylene glycol and heated at reflux for 45 min. The reaction mixture was cooled to room temperature and 5 cm^3 of saturated sodium dithionite solution was added. The mixture was stirred for a further 30 min and the black precipitate formed was filtered and washed with water (until the filtrate became colourless) and then 50 cm^3 of diethyl ether. Yield 620 mg (0.99 mmoles, 72 %).

cis-[Os(phen)$_2$Cl$_2$].2H$_2$O

493 mg (2.74 mmoles) of phen and 600 g (1.37 mmoles) of $(NH_3)_2OsCl_6$ were dissolved in 3 cm^3 of ethylene glycol. Yield 750 mg (1.14 mmoles, 83 %). ^{1}NMR (400 MHz) in $(CD_3)_2SO$; 10.10 (2H, d), 8.62 (2H, d), 8.31 (2H, d), 8.25 (2H, d), 8.20 (2H, d), 8.09 (2H, d), 7.72 (2H, d), 7.31 (2H, d), 7.28 (2H, d).

cis-[Os([D$_8$]-phen)$_2$Cl$_2$].2H$_2$O

256 mg (1.37 mmoles) of [D$_8$]-phen and 300 g (0.68 mmoles) of $(NH_3)_2OsCl_6$ were dissolved in 3 cm^3 of ethylene glycol. Yield 310 mg (0.52 mmoles, 76 %).

2.1.4 Preparation of Ru(II) and Os(II), cis-[M(LL)$_2$Cl$_2$] complexes by microwave reflux

Although potentially an excellent method for carrying out reactions quickly and efficiently, it should be noted that several hazards are present in the use of microwave radiation. The solvent employed must be able to absorb microwave radiation efficiently. A good rule of thumb is that the solvent must have an permanent electric dipole moment *e.g. N,N*-DMF, ethylene glycol, EtOH, H_2O etc. Some problems with microwave reactions are that anti-bumping agents are ineffective and may in actual fact create problems with bumping, and several solvents decompose (*e.g. N,N*-DMF to CO and Me_2NH) giving rise to potentially hazardous gases. A further concern is in cases where regulation of the reaction temperature is necessary since superheating of the reaction solution normally occurs. Despite these pitfalls, the use of microwave radiation is becoming more prevalent[9] and with reasonable precautions it can be used safely and effectively. In order to assess the potential usage of microwave radiation in preparation of *cis*-$[M^{II}(LL)_2Cl_2]$ complexes the following reactions were carried out.

cis-[Ru(bpy)$_2$Cl$_2$].2H$_2$O

0.249 g (1.6 mmoles) of bpy, 0.20 g (0.82 mmoles) of $RuCl_3.H_2O$ and 0.4 g LiCl were heated at 120 W power for 2 × 10 min at 120 W in 15 cm^3 DMF. The solution was then cooled to 25 °C and transferred to 100 cm^3 of acetone and kept at – 4 °C overnight. The product was filtered and washed with 200 cm^3 of ice water and 50 cm^3 cooled diethyl ether yielding a dark purple powder. Yield 110 mg (0.2 mmoles, 12.5 %). As for cis-$[Ru(bpy)_2Cl_2].2H_2O$, see above. Due to the small scale of the reaction and the large volumes employed, the yield does not represent an optimised yield for the reaction.

cis-[Ru(dcb)$_2$Cl$_2$].2H$_2$O

540 mg (2.25 mmol) of 4,4'-dicarboxy-2,2'-bipyridine (dcb) and 375 mg (1.5 mmol) of $RuCl_3.H_2O$ were heated at 120 W power for 2 × 10 min in 15 cm^3 DMF. The solution was then filtered, reduced in volume and cooled to 25 °C and transferred to 50 cm^3 of acetone and kept at – 4 °C overnight. The product was filtered and washed with 200 cm^3 of ice water and 50 cm^3 cooled diethyl ether yielding a dark purple powder. Yield 850 mg (1.29 mmol, 53 %). ^{1}H NMR spectroscopy (in DMSO-d_6): 10.08 (2H, d), 9.058 (2H, s), 8.88 (2H, s), 8.22 (2H, d), 7.74 (2H, d), 7.49 (2H, d).

2.1.5 Preparation of Ru(II) and Os(II), $[M(LL)_3]^{2+}$ and $[M(LL)_2(LL')]^{2+}$ complexes

Homoleptic complexes are easily prepared directly from the reaction of either $RuCl_3.H_2O$[10], K_2OsCl_6 or $(NH_4)_2OsCl_6$ by heating at reflux with 3 mole equivalents of the diimine ligand in either ethanol/water or ethylene glycol in the presence of a reducing agent (ascorbic acid, sodium hydrogen phosphite or sodium dithionite). Alternatively homoleptic complexes can be prepared from the *cis*-$[M(LL)_2Cl_2].2H_2O$ (M = Os, Ru) complexes by heating at reflux in ethanol/water (50/50 v/v) with one equivalent of diimine ligand (LL). Heteroleptic complexes were prepared by the latter method using 1 equivalent of a different diimine ligand (LL'). For osmium complexes the reactions were carried out in the presence of powdered zinc metal to aid reduction from Os(III) and Os(II). Again microwave radiation can be used to significantly reduce the reaction times involved in all these synthesis, without significant modification of the reaction mixtures employed.[11]

2.2 Chromatographic techniques

2.2.1 Analytical HPLC

Analytical High Performance Liquid Chromatography (HPLC) experiments were carried out using a JVA analytical HPLC system consisting of a Varian Prostar HPLC pump fitted with a 20 μL injection loop, a Varian Prostar PDA detector connected to a dedicated PC, and a HiChrom Partisil P10SCX-3095 cation exchange column. The mobile phase used was 80:20 CH_3CN:H_2O containing typically 0.08-0.01 M $LiClO_4$ ***(Explosive!)***, the flow rate was either 1.8 or 2.5 cm^3/min.

2.2.2 Column Chromatography

Column chromatography was carried out on activated neutral alumina (Al_2O_3, 150 mesh) or on Silica gel (65/35 CH_3CN/H_2O saturated with KNO_3) except where otherwise stated. In the case of separations carried out using alumina, typically elution first with acetonitrile (for tris-homoleptic and heteroleptic polypyridyl complexes and N2 bound isomers of 1,2,4-triazoles) followed by methanol (for N4 bound isomers of 1,2,4-triazoles) was carried out.

2.2.3 Separation of Stereoisomers

The separation of the stereoisomers of the complex $[Ru(bpy)_2(phpztr)]PF_6$ was carried out by Dr. D. Hesek using a DaiCel CHIRALCEL OD-RH carbamate based semi-preparative column. Elution was with 0.1 M $NaPF_6$ CH_3CN/MeOH 80/20 v/v. The stereoisomers of $[Ru(phen)_2(pztr)]PF_6$ and $[(Ru(bpy)_2)_2(bpt)](PF_6)_3$ were separated by Dr. C. Villiani using semi-preparative HPLC using a chiral stationary phase (CSP 1) containing Teicoplanin bonded to silica gel microparticles,[12] packed in a 250*10 mm I.D. column. A Waters Delta Prep 3000 preparative HPLC apparatus, equipped with Knauer UV and RI detectors and a 7010 Rheodyne injector, was employed for the separation. Analytical control of the collected fractions was carried out on a Waters 2690 Separation Module equipped with a UV 481 detector set at 288 nm. Samples of $[Ru(phen)_2(pztr)]^+$ or $[(Ru(bpy)_2)_2(bpt)]^{3+}$ were dissolved in the eluent (40 mg/cm^3) and filtered through a 0.45-micron filter prior to injection. Typical column loadings were 20-30 mg per run, using $CH_3CN/RCH_2OH/AcONH_4$ 0.5 M 60/20/20 mobile phase (where R =, H or CH_3).

2.3 Nuclear Magnetic Resonance spectroscopy

NMR spectroscopy is an invaluable tool not only in the identification of compounds but also in the monitoring of reactions and the determination of purity. It is used extensively throughout this thesis and where practical full assignment of ^{1}H and ^{13}C NMR spectra have been made using a combination of 2-dimensional techniques.[13]

2.3.1 ^{1}H, ^{13}C and ^{1}H CoSy Spectroscopy

All ^{1}H (400 MHz), ^{13}C (100 MHz) and ^{2}D (75 MHz) NMR experiments were recorded on a Bruker Avance 400 NMR Spectrometer and the free induction decay (FID) profiles processed using XWIN-NMR software package. All measurements were carried out in $(CD_3)_2SO$, CD_3Cl or $(CD_3)_2CO$ for ligands and CD_3CN or $(CD_3)_2CO$ for complexes. Peak positions are relative to residual solvent peaks. For ^{1}H Cosy NMR experiments 256 FID's, each of 8 scans, consisting of 1K data points were accumulated. After digital filtering using a sine bell squared function, the FID's were zero filled in the F1 dimension. Acquisition parameters were F1 = ! 500 Hz, F2 = 1000 Hz, $t_{1/2}$ = 0.001 s and the recycle delay was 1.5 s.

2.3.2 HMBC & HMQC experiments

HMQC (Heteronuclear Multiple Quantum Coherence) and HMBC (Heteronuclear Multiple Bond Coherence) NMR experiments were carried in order to assign ^{13}C NMR spectra. Both experiments are cross-correlated experiments comparable to ^{1}H-^{13}C heteroatom correlation spectroscopy (HETCOR) and COLOC respectively, in that they allow for the identification of the through bond distances between protons and carbon nuclei. For a HETCOR experiment detection is made through the ^{13}C signals whilst for HMBC and HMQC detection is made through the more sensitive ^{1}H signals. This results in the latter techniques being by far, more sensitive, and is less demanding in terms of experiment duration, being equivalent to ^{1}H COSY NMR experiments in duration.

2.3.3 ^{2}D NMR spectroscopy

Deuterium NMR spectra were recorded as for other experiments except that perprotio solvents were employed. Spectra are typically an accumulation of between 16 and 128 scans and are referenced to the residual solvent peak. Since the gyromagnetic ratio for deuterium is three orders of magnitude ($\gamma = 1.5\times10^{-6}$) less than that for hydrogen, ^{2}D NMR spectra require

much higher concentrations of sample than do ^{1}H NMR experiments. This is often impractical and to compensate for lower sensitivity experiments require a greater number of scans. This in itself is problematic since no signal lock is available during acquisition and hence compensation for magnetic field fluctuations cannot be made. This can and does result in asymmetric peaks and severe broadening.

As an example of the potential of both 1D and 2D experiments in the elucidation of ^{1}H and ^{13}C NMR spectra the following example is described in some detail. The compound ***2-Thiophen-2-yl-pyridine*** (pyth, Lancaster) contains a pyridyl- and a thienyl- moiety. The ^{1}H NMR spectrum is divided in two sets of three peaks. The higher electron density of the pyridyl ring, and hence the larger ring current, results in a greater downfield shift of its proton resonances when compared with the thienyl proton resonances. The H_6 and H_3 resonances of the pyridyl ring is shifted downfield, with respect to the H_4 and H_5 protons, due to the proximity of the H_3 to the thienyl ring and its associated deshielding ring current and of the H_6 with the electron withdrawing nitrogen atom of the pyridyl ring. ^{1}H CoSy NMR spectroscopy (*Figure 2.5*) shows two examples as to the correlation between resonances using the "box" relationship. This allows for assignment of all peaks as shown in Figure 2.3.

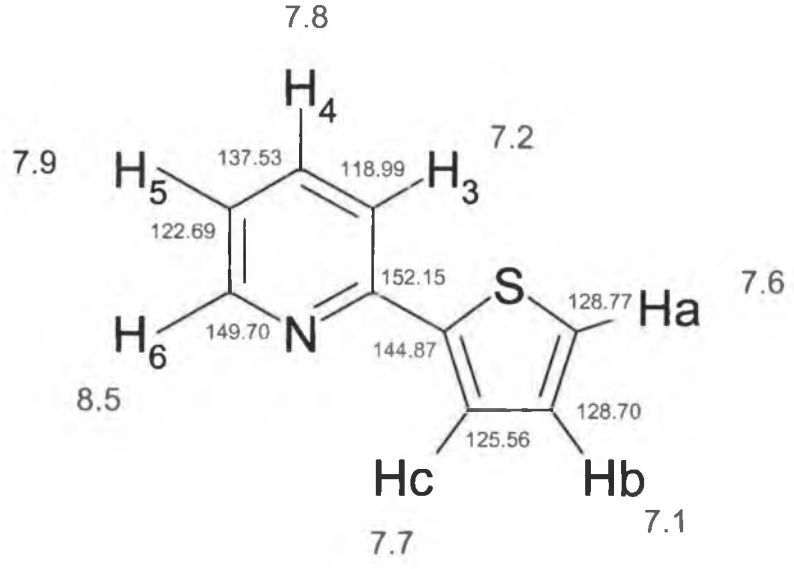

Figure 2.3 *Structure of pyth (2-Thiophen-2-yl-pyridine). δ in ppm*

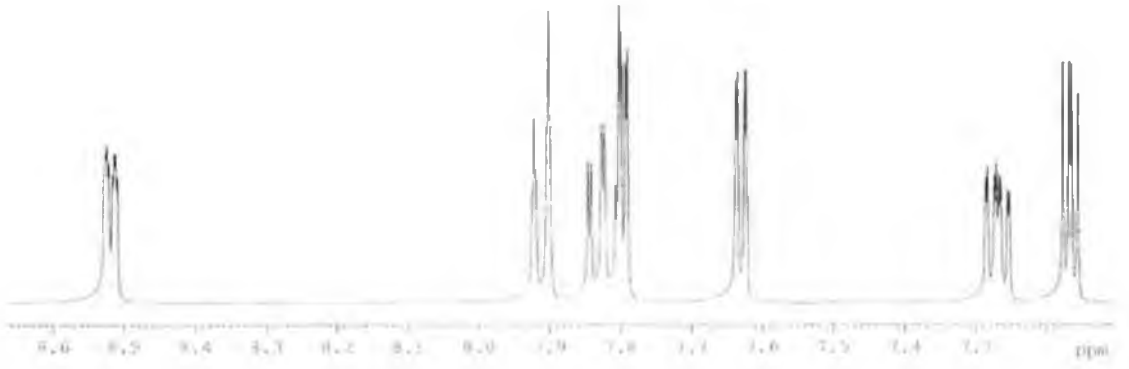

Figure 2.4 *^{1}H NMR spectra (400 MHz) of pyth in $(CD_3)_2SO$*

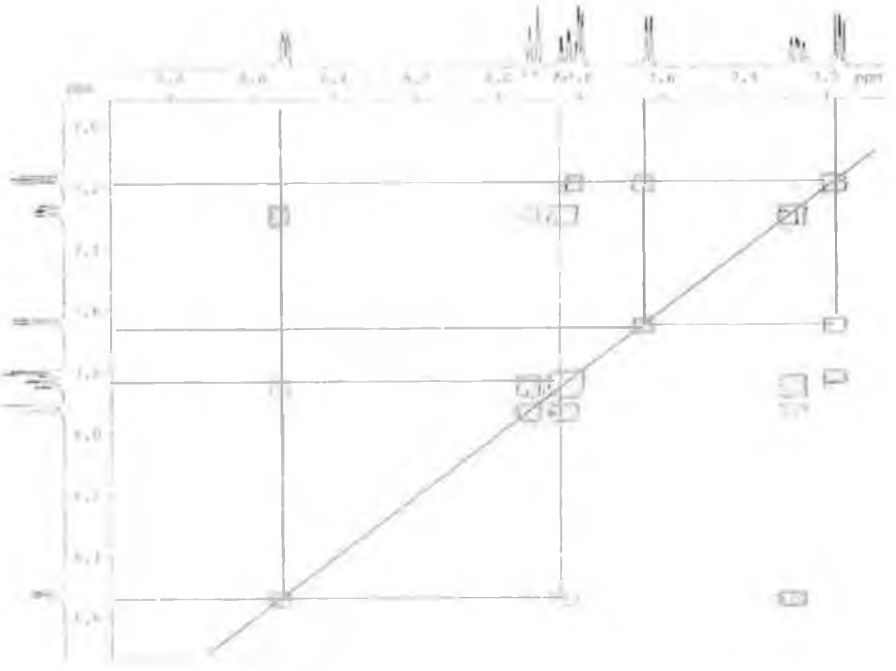

Figure 2.5 *^{1}H COSY NMR spectrum (400 MHz) of pyth in $(CD_3)_2SO$*

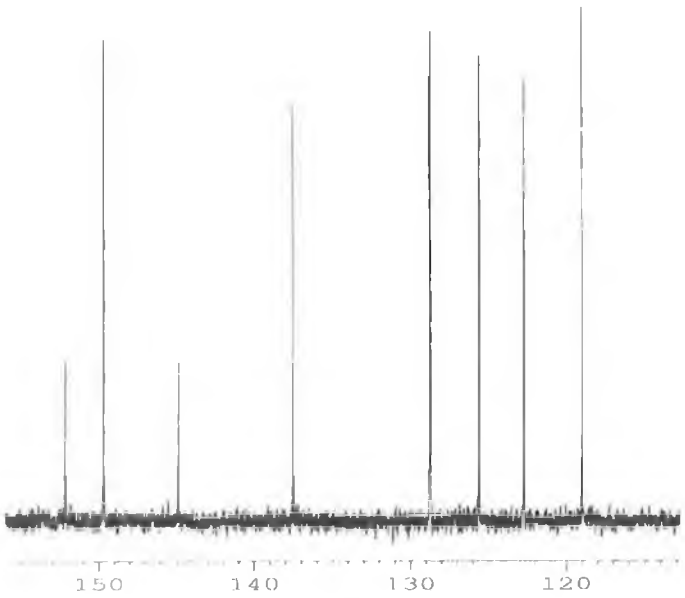

Figure 2.6 *^{13}C NMR spectrum (400 MHz) of pyth in $(CD_3)_2SO$*

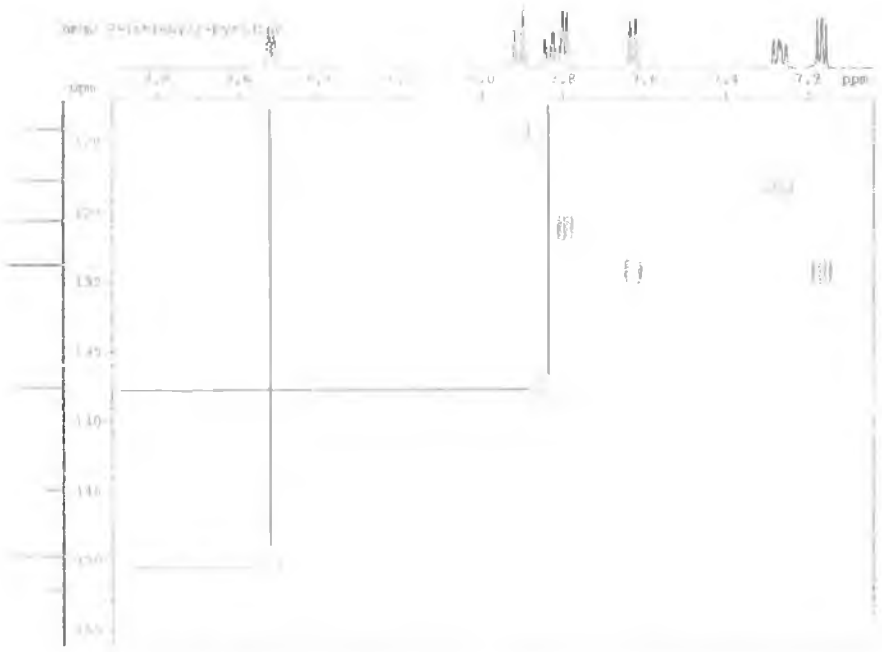

Figure 2.7 *^{1}H-^{13}C HMQC NMR spectrum (400 MHz) of pyth in $(CD_3)_2SO$*

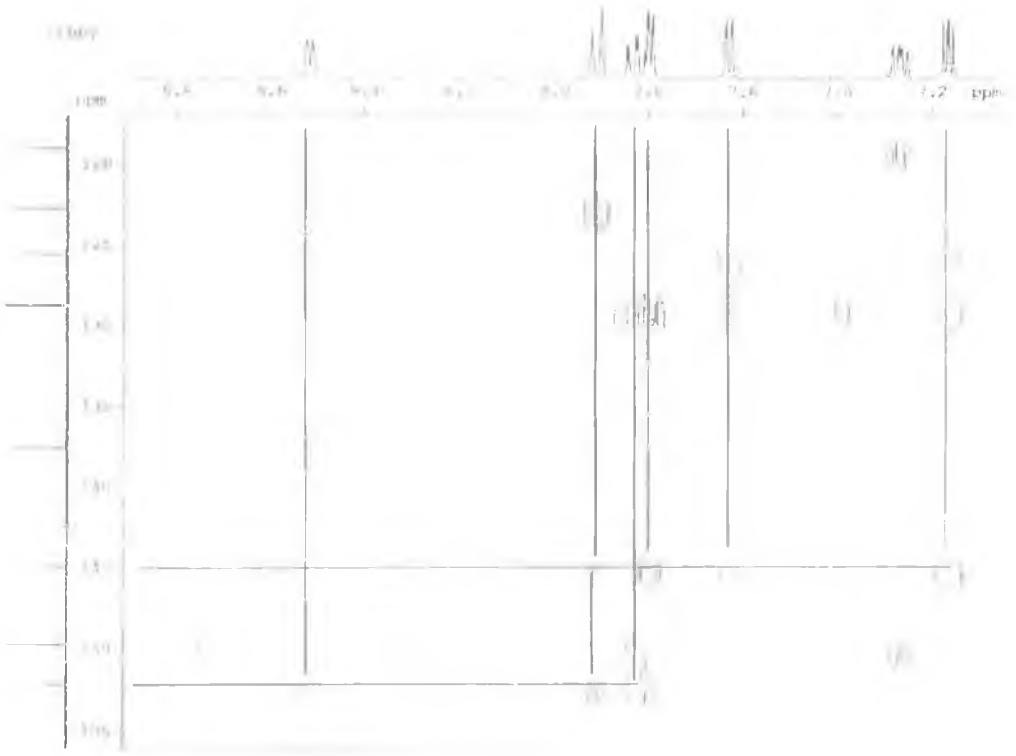

Figure 2.8 *^{1}H-^{13}C HMBC NMR spectrum (400 MHz) of pyth in $(CD_3)_2SO$*

Assignment of the ^{13}C spectrum (Figure 2.6) using HMQC (Figure 2.7) and HMBC (Figure 2.8) allows for identification of ternary and quaternary carbons. In contrast to ^{1}H COSY NMR spectra the associations are drawn not from a box pattern but rather by direct vertical and horizontal correlation. It can be seen from the HMQC spectrum the H6 (at 8.5 ppm) is coupled with C6 (at 149.70 ppm), H4 (at 7.8 ppm) with C4 (at 137.53 ppm). From the HMBC spectrum the quaternary carbons may be assigned. It should be noted that this technique shows interaction through two (and often three) bonds. As a result interpretation of these spectra must be done with considerable caution.

Accurate assignment of ^{1}H NMR spectra is essential in interpreting the spectra of partially deuteriated ligands as although mass spectrometry allows for the determination of the overall extent of deuteriation from the isotopic pattern, the identification of the positions exchanged can only be made on the basis of the suppression of NMR resonances.

2.4 Electronic spectroscopy

Electronic spectroscopy is principally concerned with the absorption of electromagnetic (EM) radiation resulting in direct excitation of molecules to higher electronic energy states. Such transitions may, in the case of gaseous samples of simple molecules, result in very sharp well-defined spectra. However in condensed phases the bands observed are considerably broadened. This broadening arises primarily from three sources: Doppler broadening, rotational energy level transitions and vibrational energy level transitions. Perturbation of energy levels by solvation adds to this broadening significantly. A detailed discussion of these effects is beyond the scope of this thesis, however the area has been dealt with in detail by several authors.[14] As a result of this broadening (and often the presence of overlapping absorption bands) detailed analysis of the bands is generally impossible except for the simplest molecules. Despite this electronic spectroscopy is an invaluable tool in the characterization of the electronic properties and excited state processes of molecules and, in the case of this thesis, of ruthenium and osmium polypyridyl complexes.[15]

2.4.1 Absorption spectroscopy

Electronic absorption spectra of molecules are found in the wavelength range 100 to 2500 nm (100,000 to 4,000 cm^{-1}) stretching from the ultraviolet to the near infrared region. In the following chapters, electronic spectra can be divided into three main regions; 190 – 300 nm: generally $\pi\pi^*$ transitions of ligands and complexes, 300 - 400 nm: ^{1}MC transitions, 350 - 700 nm: ^{1}MLCT and ^{3}MLCT transitions of Ru(II) and Os(II) complexes and 800 – 2500 nm: ligand to metal charge transfer (LMCT) transitions of Ru(III) and Os(III) species and intervalence transitions involving mixed valence ($M^{II}M^{III}$) species. As has been discussed in Chapter 1 the absorption spectrum of Os(II) and Os(III) complexes is considerably more complicated than those of their corresponding Ru(II) and Ru(III) complexes due to larger spin-orbit coupling, resulting in formally spin forbidden transitions appearing in the spectra of the former.

Although the energy of a transition can easily be ascertained from the measurement of the absorption maximum, of equal importance, in the characterization of compounds, is the intensity of the absorption. The Beer-Lambert law is most often used in the determination of the intensity of a transition. The law (*Equation 2.2*) states that the absorption or optical

density (A) is proportional to the concentration of the sample (c) and the pathlength (l) through which the incident light must pass (the constant of proportionality (ε, the molar absorptivity) usually having the units $Lmol^{-1}cm^{-1}$). This rule is of course limited in that it only holds within a narrow range of concentrations. At low concentrations only a very small amount of light is absorbed and hence detector noise will interfere and at high concentrations all light will be absorbed. A general rule of thumb, however is that the intensity should be between 0.2 and 1.2 absorbance units.

Equation 2.2 $$A = -\log_{10} I / I_0 = \varepsilon c l$$

The measuring of the molar absorptivity at a single wavelength is however problematic in that it is often dependent on the resolution of the spectrum. At low resolution peaks become broadened and reduced in measured intensity and troughs increase in intensity. In order to counter this source of error then the spectrum should be recorded at several levels of resolution (2 nm, 1 nm, .5 nm, .2 nm etc) until the differences in the values obtained are insignificant.

Unless otherwise stated, UV.Vis spectra were recorded on a Shimadzu UV.Vis/NIR 3100 spectrophotometer interfaced with an Elonex-466 PC using UV.Vis data manager. Samples were held in 0.1 or 1cm pathlength quartz cuvettes.

2.4.2 Emission spectroscopy

Emission spectroscopy is concerned with the light emitted as a result of the relaxation of electronically excited molecules to their ground electronic states. Emission spectroscopy by its nature does not suffer many of the limitations of absorption spectroscopy. Although most organic compounds emit either at room temperature or at 77 K, only a relatively small number of inorganic complexes dissipate electronic energy as light. The most commonly encountered emissive complexes are those of the 2^{nd} and 3^{rd} row transition metals and the lanthanide metals. The ground state and excited state nuclear geometries of a compound are normally different and, due to the FC rule electronic excitation, is normally followed by fast relaxation to the lowest vibrational level of the excited electronic state (the excess energy being lost as thermal energy). The transition to the ground electronic state also occurs vertically (FC principle) and hence to a vibrationally excited state. Overall the result is that

the energy of the absorbed light is greater than that of the emitted light. The resulting difference between the lowest absorption and the emission bands is referred to as the Stokes' shift and may be used as a measure of the excited state distortion. For fluorescence spectroscopy *i.e.* emission from an excited state with the same spin multiplicity as the ground state this assumption is normally correct, however when the emission arises from a formally spin forbidden transition such as a ^{3}MLCT excited state of a Ru(II) polypyridyl complex, then the shift in energy between the absorption and emission band will not reflect the excited state distortion accurately (it will overestimate it).

Unless otherwise stated, emission spectra were recorded at all temperatures using a Perkin-Elmer LS50 or LS50-B Luminescence spectrophotometer interfaced with an Elonex-466 PC using windows 3.1 based fluorescence data manager software. Emission and excitation slit widths were typically 3, 5 or 10 nm depending on conditions. Measurements at 77 K were carried out in liquid nitrogen filled glass cryostat, with sample held in a NMR tube. Measurements between 90 K and 280 K were carried out using an Oxford Instruments liquid nitrogen cooled cryostat model 39426 with samples being held in a home-made quartz or glass cuvette. Spectra are uncorrected for photomultiplier response.

2.4.3 Emission Quantum yield measurements

Quantum yield measurements were carried out by the optically dilute method[16] by comparison with $[Ru(bpy)_3](PF_6)_2$[17] in aerated acetonitrile. Emission spectra were obtained at a wavelength where the absorption by $[Ru(bpy)_3](PF_6)_2$ and the sample under examination are equal. The area under the emission spectrum (A) of each sample was calculated using the spectrometer supplied software and the quantum yield was calculated from Equation 2.3:

$$\textbf{Equation 2.3} \quad \frac{\Phi_{unknown}}{\Phi_{[Ru(bpy)_3](PF_6)_2}} = \frac{A_{unknown}}{A_{[Ru(bpy)_3](PF_6)_2}}$$

Where Φ is the quantum yield and A is the area under the emission spectrum. As all quantum yield measurements were carried out in acetonitrile, compensation for refractive indices is unnecessary.

Several factors must be accounted for in the determination of quantum yield values. Measurements must be carried out at the same temperature (preferably in a thermostatic bath

when a large temperature dependence of emission intensity is observed). Quenching of emission is another problem and can arise from one or more sources (usually more!) *e.g.* dissolved gases $^3O_2$, electron transfer agents (*e.g.* methyl-viologen), concentration quenching (inner filter effects) and the presence of impurities such as water and protic solvents. Another common error is that of over concentrated samples. These effects are most noticeable at high concentration. To avoid this, the concentration dependence of the emission should be examined to determine the linear region where concentration is proportional to luminescence intensity.

2.4.4 pK_a and pK_a determinations*

pH titrations of 1,2,4-triazole based ruthenium complexes were carried out in Britton-Robinson buffer (0.04 M H_3BO_3, 0.04 M H_3PO_4, 0.04 M CH_3CO_2H). The pH of the solutions was adjusted using concentrated sulphuric acid or sodium hydroxide solution. The appropriate isosbestic point from the absorption spectra was used as the excitation wavelength for pH titrations followed by emission spectroscopy.

In special cases where the solubility of a complex is very low or where its emission is very weak in aqueous solution then titrations may be carried out in non-aqueous solvents by adding known amounts of acid ($HClO_4$) or base (NH_4OH) and calculating the pH. Although the correlation between the pH in water and in solvents such as acetonitrile is dubious, it has been found in previous studies that the pK_a values calculated are in very close agreement with values obtained by other methods.[18] In determining the pK_a from a plot of absorbance (at a point of greatest change) against pH, a sigmoidal curve was fit using Origin (Microcal software).

The pK_a is determined from changes in the absorption spectra of the complexes examined using the Henderson-Hasslebach equation (Equation 2.4) as being the point at which the concentration of the protonated and deprotonated analyte are equal, which equals the inflection point of the sigmoidal curve.

Equation 2.4 *Henderson-Hasselbach equation* $pH = pK_a + log_{10}([HA]/[A^-])$

*Determination of pK_a**

In order to quantify the pK_a* of a compound two methods are frequently employed; *i.e.* the Förster cycle based on thermodynamics, and a kinetic treatment.[19]

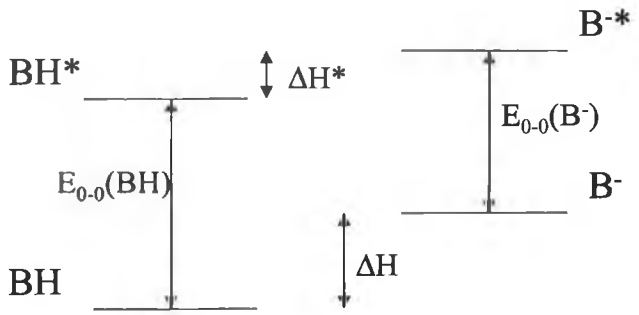

***Figure 2.9** The Förster relationship between enthalpy changes and electronic transitions*

Figure 2.9 shows relationship between the enthalpy changes and the electronic transitions for a system where the protonated species is stabilised relative to the deprotonated species. From the diagram the relationships given by Equation 2.5, Equation 2.6 and Equation *2.7* may be considered (where N_A is Avogadro's number, h is Planck's constant and v_x is the energy of the $E_{0\text{-}0}(x)$ transition in cm^{-1})

Equation 2.5 $\Delta H^* + E_{0\text{-}0}(HB) = \Delta H + E_{0\text{-}0}(B^-)$

Equation 2.6 $\Delta H^* + N_A h\nu_{HB} = \Delta H + N_A h\nu_{B^-}$

Equation 2.7 $\Delta H^* - \Delta H = N_A h(\nu_{B^-} - \nu_{HB})$

Assuming that the ΔH approximates ΔH^o under the experimental conditions employed and ΔS for each reaction is equal then ΔH can be equated to ΔG^o the Gibbs free energy by Equation 2.8.

Equation 2.8 $\Delta H \sim \Delta G^o = RT\ln K = 2.303RTpK$

Together with Equation *2.7* this yields:

Equation 2.9 $pK_a^* = pKa + (0.625/T)(\nu_{B^-} - \nu_{HB})$

or

$$\Delta pK_a = 0.00209(\nu_{B^-} - \nu_{BH}) \text{ at } 298\ K$$

There are several aspects to this treatment that are problematic. Firstly the values of V_{B^-} and V_{BH} used must be accurate, as small inaccuracies may lead to a large distortion of the true value. Secondly the excited state under examination is of considerable importance. Since only the lowest excited singlet and triplet states are normally populated on the timescale of protonation/deprotonation (10^{-10} to 10^{-8} s) then only these states need be considered. For an excited singlet state either the absorption or fluorescence bands may be used for the determination of change in the $E_{0\text{-}0}$, however, for triplet excited states only the phosphorescence spectra may be employed. A third aspect of the Förster treatment that is important is that the derivation is thermodynamic in basis and assumes an equilibrated system. This approximation is acceptable when the lifetime of both protonated and deprotonated excited states is much longer than the equilibration time and also when they are very close. These conditions are seldom fulfilled.

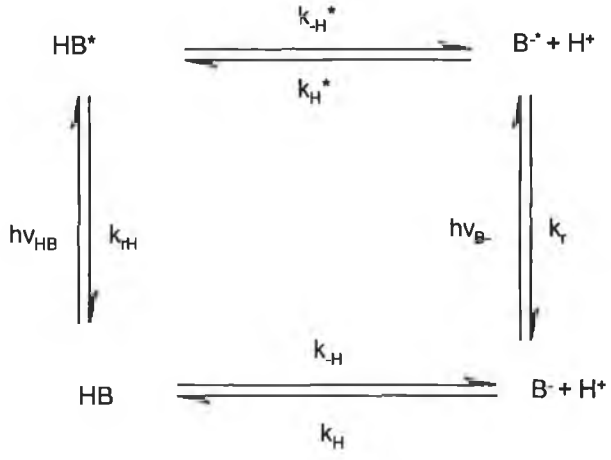

Figure 2.10 *Ground and excited state acid/base processes*

Kinetic considerations

Figure 2.10 shows the ground and excited state acid/base process for a monoprotic acid. k_H, k_{-H}, k_H*, and k_{-H}* are the rate constants for the protonation/deprotonation in the ground and excited state respectively and k_r and k_{rH} the observed excited state decay rates. In order to reach excited state equilibrium the following conditions must be observed: $k_r << k_H$* and $k_{rH} << k\text{-}_H$*. When these conditions are met then Equation 2.10 can be used to calculate the excited state pK_a(*) from the inflection point of the emission titration curve pH_i.

Equation 2.10 $pK_a^* = pH_i + \log(\tau_{HB}/\tau_{B^-})$

2.4.5 Circular dichroism (CD) spectroscopy[20]

CD spectra of the stereoisomers of $[Ru(bpy)_2(phpztr)](PF_6)$ and $[Ru(phen)_2(pztr)](PF_6)$ were recorded on a Jasco J-720 spectropolarimeter in acetonitrile at 25 °C. CD spectra of the four stereoisomers of $[(Ru(bpy)_2)_2(bpt)](PF_6)_3$ were recorded on a Jasco J-710 spectropolarimeter in CH_3CN at 25 °C by Dr. C. Villiani. (University of Rome) For these measurements, impure fractions were resubmitted for HPLC on the chiral stationary phase to obtain single stereoisomers with greater than 99% purity. Acetonitrile solution of the four stereoisomers of $[(Ru(bpy)_2)_2bpt)](PF_6)_3$ were used at concentrations in the 5 to 8 $\times 10^{-6}$ M range.

2.5 Time Correlated Single Photon counting (TCPSC) techniques, nanosecond time resolved emission spectroscopy and picosecond time resolved emission spectroscopy

All lifetime measurements reported have been determined using TCSPC either at DCU using an Edinburgh Instruments nf900 ns flashlamp and CD900 TAC (time to amplitude converter) or at the Department of Photochemistry, "G. Ciamician" University of Bologna, Italy using an Edinburgh Instruments instrument of similar design but with manual TAC control. Lifetimes were measured using Uvasol Solvents (Lennox chemicals) and either degassed using Ar purge for 20 min or by undergoing four freeze-pump-thaw cycles. Deconvulution of the lamp profile was carried out for samples, which showed either very weak emission and/or had emission lifetimes < 50 ns. The lamp profile was obtained using a colloidal suspension of silica in water as scattering agent.

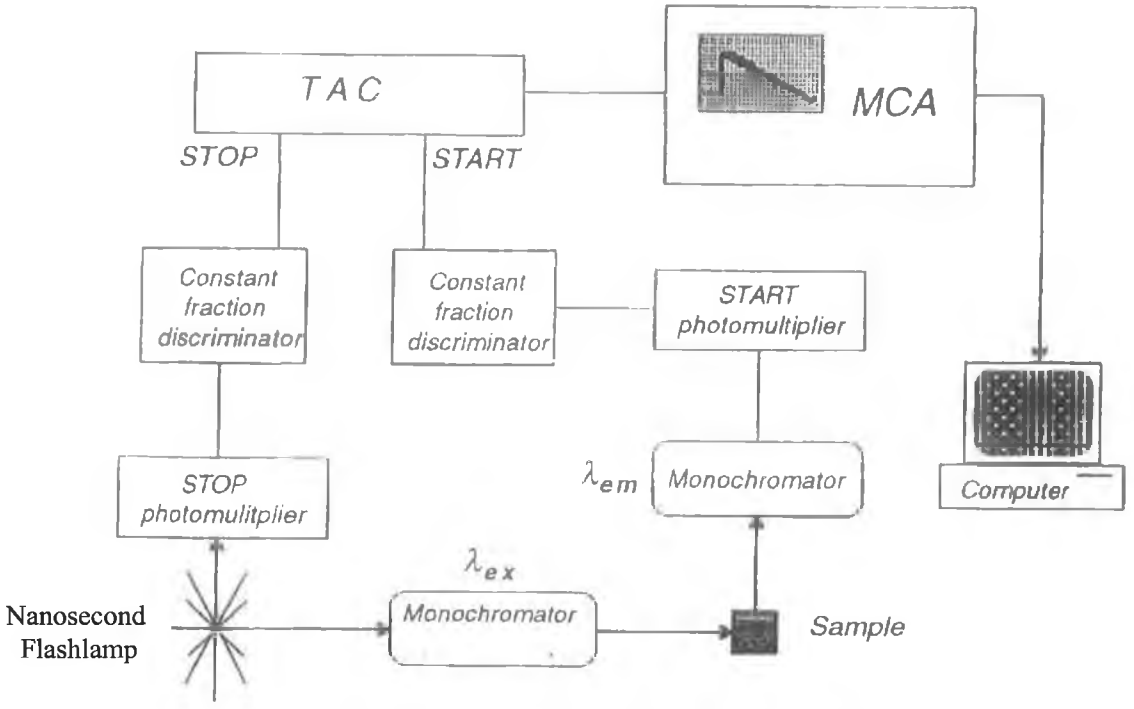

Figure 2.11 *Schematic diagram of TCSPC apparatus*

The system illustrated in Figure 2.11 operates as follows. The when the START photomultiplier detects a photon of emitted light it triggers the TAC to initiate a voltage ramp. This ramp is halted when the STOP photomultiplier detects a photon from the reference beam (*i.e.* the nanosecond flashlamp pulse). The multi channel analyser (MCA) records the number of times a specific voltage is obtained in each of between 1024 and 4096 channels (depending on settings employed). A spectrum of voltages, and hence time differences, is produced by the MCA memory and the experiment is terminated when a sufficient number of counts are collected (typically 1000 in the peak channel). The spectrum of voltages is directly related to the emission decay allowing for measurement of the emission. The quality of the lifetime data obtained is judged primarily by two criteria: the χ^2, and the random nature of the residuals plot. A χ^2 as close to 1 as possible (but not below one) is ideal.

Time resolved emission spectra were obtained using a Q-Switched Nd-YAG Spectrum laser system using the third Harmonic (355 nm) as excitation source. Emission was detected at right angles to the excitation beam using an Oriel Model IS520 gated intensified CCD

coupled to an Oriel model MS125 spectrograph. Data was collected using a dedicated PC and processed using Origin (MicroCal).

Picosecond emission spectroscopy was carried out at the Central laboratories of the Research Council, Rutherford-Appleton laboratories at Oxford, UK. The experiments were carried out using time resolved fluorescence (TRF) setups based on optical parametric amplifiers (OPAs) as described in detail in the literature.[21] For TRF measurements the following changes were made. The Raman probe pulse was blocked and the Kerr gate opened to sample the fluorescence spectrum at various time delays following the excitation pulse. The excitation laser system employed produces pulses of 70 ps FWHM at a frequency of 41.13 MHz. A mode locked Nd-YAG IR laser produces radiation at 1064 nm, which is frequency doubled and tripled to produce 532 nm and 355 nm radiation. The instrument response time was ~3 ps (rise from 10% to 90%). All TRF spectra were obtained by subtraction of the negative time delay signal from the positive time delay signal. Samples were measured in either acetonitrile or in water. Protonation was achieved using trifluoroacetic acid. Due to the very high power of the laser pulse employed, samples were analysed using a continuous flow system employing a peristaltic pump, ensuring a continuous supply of fresh sample. A vertically flowing open jet (500 μm diameter) sample arrangement was employed, requiring sample volumes of the order of 20 cm^3.

2.6 Resonance Raman (rR) and time resolved resonance Raman spectroscopy

In contrast to IR spectroscopy where the vibrational structure is probed by direct excitation into vibrational transitions, rR relies on the indirect probing of vibrational structure through electronic spectroscopy. In a typical experiment (ground state rR) the sample is irradiated with monochromatic laser light (at a wavelength resonant with an allowed electronic transition). When resonance is achieved symmetric vibrational modes (*e.g.* Raman active stretching vibrations) show enhanced Raman intensities.[22] The process by which this takes place is very different to IR spectroscopy. Excitation results in the formation of a virtual excited state, which almost instantly relaxes either to the ground vibrionic state or to a higher vibrionic state (see Figure 2.12).

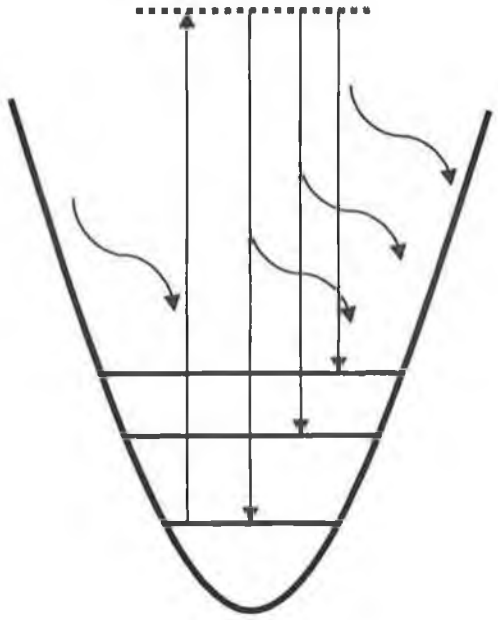

Figure 2.12 *Diagram showing the process by which Raman scattering occurs.*

This technique has proven invaluable in the assignment of ^{1}MLCT transitions in mixed ligand ruthenium polypyridyl complexes.[23] In addition to the assignment of ground state electronic spectra, excited state rR and time resolved rR can be used in studies of the lowest excited state of homo- and hetero-leptic transition metal complexes. In these experiments either a single colour or two colour pump and probe technique is employed. In the former the leading edge of the laser pulse generates a population inversion and the trailing edge probes the metastable state formed. In the later technique two laser pulses of different wavelength are employed. The first again creates the population inversion whist the later pulse probes the excited molecules.

Ground state and nanosecond timescale excited state rR spectroscopy was carried out with Prof. John J. McGarvey and Dr. Colin Coates at the Chemistry department, Queen's University of Belfast. Ground state spectra were obtained using a Spectra Physics Argon Laser at 457.9 nm and 514.5 nm. Most excited state resonance Raman measurements were carried out using a single colour pump and probe method.[24] A Q-switched Nd/Yag laser (Quanta-Ray GCR2, pulse width ca. 9 ns) was used to populate and probe the excited states of the complexes at an excitation wavelength of 355 nm. In single colour pump and probe measurements, the leading edge of the laser pulse pumps the molecules into an excited state

and the remainder of the pulse probes the excited species formed. Samples were held in an NMR tube and spun to reduce localized sample heating and thermal decomposition. Two colour experiments were carried out by pumping at 532 nm and probing the excited species formed using a 355 nm pulse. All measurements were carried out in CD_3CN, unless otherwise stated. Protonation of samples was achieved using trifluoroacetic acid (0.1 M in CD_3CN).

2.7 Mass spectrometry

Mass spectral measurements of the ligand Hphpztr and the complex $[Ru(bpy)_2(phpztr)](PF_6)$ were carried out by the Mass Spectrometry department at Berlin University. The spectrum of Hphpztr was obtained using electrospray ionisation mass spectrometry, 80 eV ionisation potential. Complex spectra were obtained from Fast Atom Bombardment technique, using Xenon atoms and MNBA/CH_2Cl_2 matrix. All other mass spectra were obtained by Mr. Maurice Burke at Dublin City University, using a Bruker-Esquire LC_00050 electrospray ionisation mass spectrometer at positive polarity with cap-exit voltage of 167 V. Spectra were recorded in the scan range of 50-2200 m/z with an acquisition time of between 300 and 900 μs and a potential of between 30 and 70 V. Each spectrum was recorded by summation of 20 scans.

2.8 Photochemical studies

Photolysis studies were carried out by placing samples in either Quartz matched cuvettes or NMR tubes (for NMR studies) and placing them before a 20 W Tungsten filament light source slide projector (Kodak Carousel S-AV2020). Sample heating was prevented using a water filter. Photolysis was followed using emission, absorption and ^1H NMR spectroscopies as outlined in chapter 8.

2.9 Electrochemical measurements[25]

Electrochemical measurements were made on a Model 660 Electrochemical Workstation (CH Instruments). Typical complex concentrations were 0.5 to 1 mM in anhydrous acetonitrile (Aldrich 99.8%), containing 0.1 M tetraethyl ammonium perchlorate (TEAP) as the support electrolyte. A glassy carbon working electrode, a Pt wire the auxiliary electrode and Saturated Calomel Electrode (SCE) reference were employed. Solutions for reduction

measurements were deoxygenated by purging the solution with N_2 or Ar gas for 15 min prior to the measurement. Typically measurements were taken in the range of –1.8 to 1.8 V. Protonation of complexes was achieved by addition of 0.1 M $HClO_4$ or 0.1 M CF_3CO_2H to the electrolyte solution. The scan rates used were 0.1 or 0.5 V/s. Spectroelectrochemistry was carried out using an optically transparent thin layer electrode (OTTLE) set-up comprising of a homemade Pyrex glass, thin layer cell (1mm). The optically transparent working electrode was made from platinum gauze, the counter electrode used was a platinum wire, and the reference electrode was a pseudo Ag/AgCl reference electrode. The Ag/AgCl electrode was prepared by dipping it into a 1 M KCl_{aq} solution and holding for 60 s at 9V (generated using a 9V battery) with a platinum wire acting as the second electrode. Spectroelectrochemistry[26] was carried out in anhydrous acetonitrile (Aldrich), and the electrolyte employed was 0.1 M TEAP perchlorate. The working electrode was held at the required potential throughout the measurement using an EG&G PAR Model 362 scanning potentiostat. Absorption spectra of the species generated in the OTTLE cell were recorded on a Shimadzu 3100 UV-Vis/NIR spectrophotometer interfaced with an Elonex PC-433. Protonation of complexes under bulk electrolysis was achieved by addition of 1 M trifluoroacetic acid in acetonitrile.

TEAP was prepared by dissolving tetraethylammonium bromide in Millipore water to 1 M concentration, followed by precipitation with drop wise addition of 1 mole equivalent of perchloric acid (70 % w/v). The precipitate was collected under vacuum, redissolved in hot water and the solution neutralized with conc. NaOH solution. On cooling the TEAP rerystallised and was again collected under vacuum and washed with 20 cm^3 water, followed by recrystallisation three times from hot water.

Chemical oxidation (using Ce(IV)) was carried out by addition of controlled amounts of ammonium cerium(IV) nitrate, dissolved in acetonitrile (freshly prepared), to an acetonitrile solution of the complexes being examined.

2.10 Elemental Analysis

Elemental analysis on C, H and N was carried out at the Microanalytical Laboratory of University college Dublin (UCD). The CHN analyser used is an Exador analytical CE440. In the analysis of compounds containing deuterium, interpretation of results is complicated by the fact that although calculation of the overall mass of the complex takes into account the

additional mass of the deuterium, in calculating the percentage of hydrogen and deuterium in the sample all protons and deuterons are treated as protons. In determining the hydrogen content of a sample the number of water molecules formed and not the mass of water formed is measured, resulting in the correction being required in the case of deuteriated samples.

2.11 Bibliography

1. H. A. Goodwin and F. Lions, *J. Am. Chem. Soc.*, **1959**, *81*, 6415

2. R. Hage, *Ph.D. Thesis*, Leiden University, The Netherlands, **1991**

3. D. Hughes, *Ph.D. Thesis*, Dublin City University, Ireland, **1999**

4. A. R. Oki and R. J. Morgan, *Synthetic Commun.*, **1995**, *25*, 4093

5. C. O'Connor, *Ph.D. Thesis*, Dublin City University, Ireland, **1999**

6. P. Belser and A. von Zelewsky, *Helv. Chim. Acta,* **1980**, *63*, 1675

7. B. P. Sullivan, D. J. Salmon and T. J. Meyer, *Inorg. Chem.*, **1978**, *17*, 3334

8. P. Lay, A. M. Sargeson, H. Taube, M. H. Chou and C. Creutz, *Inorg. Synth.*, **1986**, 24, *John Wiley and Sons (Publishers)*

9. (a) J. R. Jones, W. J. S. Lockley, S. Y. Lu and S. P. Thompson, *Tet. Lett.*, **2001**, *42*, 331 (b) N. Elander, J. R. Jones, S. Y. Lu and S. Stone-Elandor, *Chem. Soc. Rev.*, **2000**, *29*, 239 (c) S. Anto, G. S. Getvoldsen, J. R. Harding, J. R. Jones, S-Y. Lu and J. C. Russell, *J. Chem, Soc., Perkin Trans. 2*, **2000**, 2208 (d) W. J. S. Lockley, *Tet. Lett.*, **1982**, *23*, 3819 (e) W. T. Erb, J. R. Jones and S-Y. Lu, *J. Chem. Res. (S)*, **1999**, 728

10. N. C. Fletcher, M. Nieuwenhuyzen and S. Rainey, *J. Chem. Soc., Dalton Trans.*, **2001**, 2641

11. (a) P. Belser and A. von Zelewsky, *Helv. Chimica Acta*, **1980**, *63*, 1675 (b) D.M. Klassen, *Inorg. Chem.*, **1976**, *15*, 3166 (c) M. Kakoti, A. K. Deb and S. Goswami, *Inorg. Chem.*, **1992**, *31*, 1302 (d) G. F. Strouse, P. A. Anderson, J.R. Schoonover, T.J. Meyer and F.R. Keene, *Inorg. Chem.*, **1992**, *31*, 3004

12. (a) I. D'Acquarica, F. Gasparrini, D. Misiti, C. Villani, A. Carotti, S. Cellamare and S. Muck, *J. Chromatogr. A*, **1999**, *857*, 145 (b) F. Gasparrini, I. D'Acquarica, J. G. Vos, C. M. O'Connor and C. Villani, *Tet.: Assymetry*, **2001**, *11*, 3535

13. (a) G. Binsch and H. Kessler, *Angew. Chem., Int. Ed. Engl.*, **1980**, *19*, 411 (b) R. W. King and K. R. Williams, *J. Chem. Ed.*, **1990**, *67*, A101 (useful glossary of NMR terms) (c) C. Dybowski, A. Glatfelter and H. N. Cheng, *Encyclopaedia of Analytical Chemistry*, Academic

press, 149 (d) K. R. Williams and R. W. King, *J. Chem. Ed.*, **1990**, *67*, A125 (e) P. Crews, J. Rodriguez, *Organic Structural Analysis*, Oxford University press, Oxford, 1998

14. (a) C. N. R. Rao, *"Ultraviolet and visible spectroscopy: chemical applications"*, Butterworth and Co. Ltd., UK, **1975** (b) R. J. H. Clark, T. Frost and M. A. Russell, ed., "*Techniques in visible and ultraviolet spectroscopy*", Vol. 4, Chapman and Hall, UK, **1993** (c) A. Gilbert and J. Baggot, "*Essentials of molecular photochemistry*", Blackwell Scientific Publications, UK, **1991** (d) H-H. Perkampus, *"UV-VIS Spectroscopy and its applications"*, Springer Laboratory, Dusseldorf, **1992**

15. M. Z. Hoffman, *J. Chem. Ed.*, **1983**, *60*, 784

16. J. N. Demas and G. A. Crosby, *J. Phys. Chem.*, **1971**, *75*, 991

17. N. Nakamaru, *Bull. Chem. Soc. Jpn.*, **1982**, *55*, 2697

18. M. Haga, T. Ano, K. Kano and S. Yamabe, *Inorg. Chem.*, **1991**, *30*, 3843

19. J. F. Ireland and P. A. H. Wyatt, *Adv. Phys. Org. Chem.* **1976**, *12*, 131

20. " Circular Dichroism; Principles and applications", eds., K. Nakanishi, N. Berova and R.W. Woody, VCH publishers UK Ltd., UK, **1994**

21. (a) M. Towrie, A. W. Parker, W. Shaikh and P. Matousek, *Meas. Sci. Technol.* **1998**, *9*, 816 (b) P. Matousek, A. W. Parker, P. F. Taday, W. T. Toner and M. Towrie, *Opt. Commun.* **1996**, *127*, 307

22. J. R. Schoonover and G. F. Strouse, *Chem. Rev.*, **1998**, *98*, 1335

23. G. D. Danzer, J. A. Golus and J. R. Kincaid, *J. Am. Chem. Soc.*, **1993**, *115*, 8643

24. K. C. Gordon and J. J. McGarvey, *Inorg. Chem.*, **1991**, *30*, 2986

25. (a) G. A. Mabbott, *J. Chem. Ed.*, **1983**, *60*, 697 (b) D. H. Evans, K. M. O'Connell, R. A. Peterson and M. J. Kelly, *J. Chem. Ed.*, **1986**, *60*, 290

26. W. R. Heineman, *J. Chem. Ed.*, **1983**, *60*, 4

Chapter 3

Routes to regioselective deuteriation of heteroaromatic compounds

In this chapter a systematic approach to the deuteriation of polypyridyl type ligands is reported. A range of isotopologues of heteroaromatic compounds containing pyrazyl-, pyridyl-, 1,2,4-triazole-, thienyl-, methyl-, and phenyl- moieties, have been prepared in a cost effective manner, using a range of methods based on subcritical aqueous media. Selectively and fully deuteriated ligands are characterized by mass spectrometry, ^{1}H, ^{2}D and ^{13}C NMR spectroscopy. The application of deuteriation in supramolecular chemistry is also discussed briefly and some of the points raised will be dealt with in detail in the subsequent chapters.

3.1 Introduction

The application of transition metal complexes incorporating polypyridyl type ligands in inorganic photochemistry and in supramolecular chemistry has increased rapidly since the 1970's.[1] Ruthenium(II) and osmium(II) based polypyridyl complexes have been utilized as building blocks for large multinuclear structures, mostly because of their synthetic versatility and suitable photophysical and electrochemical properties.[2] However, with the ever-increasing complexity of supramolecular systems, the ability to characterize these molecules fully by standard NMR techniques has become difficult.[3] An additional challenge often encountered is the identification of the nature of the emitting state, which for heteroleptic compounds, may be located on different parts of the molecular assembly. Deuteriation of ligands has been proposed as a spectroscopic tool to, at least in part, help overcome these problems.[4]

To date however, the widespread use of deuteriation as a general spectroscopic aid has been limited, due the lack of generally applicable, high yield and low cost H/D exchange procedures for polypyridyl type ligands. In this chapter, a general and systematic approach to the deuteriation of polypyridyl type heteroaromatic compounds is described. This approach is based on the use of subcritical D_2O. The methods reported in this chapter are a significant improvement on traditional routes reported for the deuteriation of 2,2'-bipyridyl, which require several synthetic steps or the use of the environmentally unfriendly material asbestos.[5,6] Both methods yield only fully deuteriated compounds, in low to moderate yields. By modification of the reaction conditions employed, more than 30 partially and fully deuteriated compounds (Figure 3.1) are obtained in high yields (~90%). The procedures used are relatively low cost and straightforward and can be carried out on at least a 1 g scale. The approach described is of a general nature and can be applied to a wide range of compounds and as a result the widespread use of partial deuteriation to elucidate the properties of supramolecular structures is now possible. Earlier studies on the deuteriation of 2,2'-bipyridyl using a Pd/C catalyst and D_2O as deuterium source were reported by Keyes *et al.*.[7] Subsequently this approach was applied to the full deuteriation of 1,10-phenanthroline,[7,8] pyridyl- and pyrazyl-1,2,4-triazole,[9] imidazoles,[10] and 2-(thien-2'-yl)-pyridine.[11]

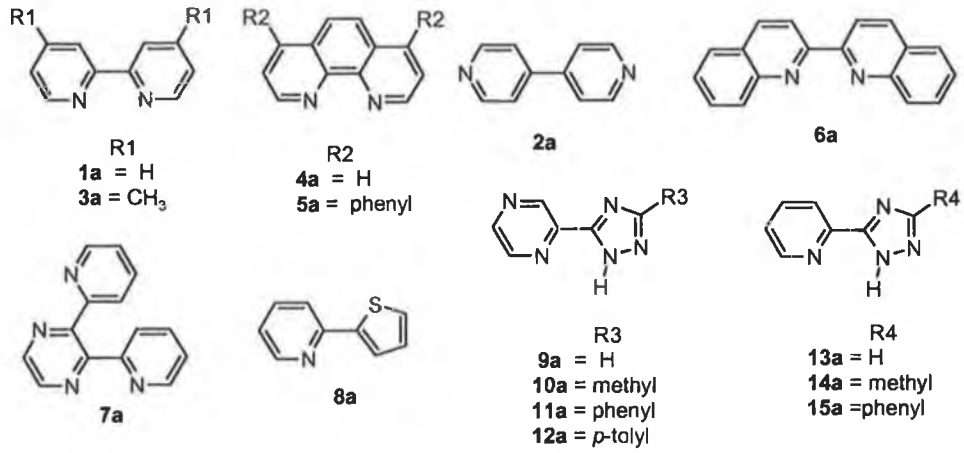

Figure 3.1 *Structures of compounds examined for H/D exchange*

3.1.1 Hydrogen/deuterium exchange reactions

The area of hydrogen/deuterium exchange reactions has been of interest since the late 1950's when commercially available sources of useable deuterium became widely available. One of the most common methods of deuteriation is that of ^{1}H-^{2}D exchange of labile hydrogens, such as N-H, O-H,[12] terminal acetylenes,[13] α-methylenic protons,[12d,14] bpy (C6 position only)[15] and heteroaromatic *N*-oxides such as 2,2'-bipyridyl-*N,N*-dioxide.[5] This H-D exchange can be effected simply by dissolution in D_2O (or in a binary protic solvent system using CD_3OD or $(CD_3)_2SO$) with heat, pressure and/or acid/base.[13] Both partial[16,17,18] and complete,[18,19] deuteriation of transition metal complexes has been achieved in this manner.

Somewhat limited methods for the deuteriation of polyaromatic hydrocarbons employing BF_3/D_2O,[20] Bu_3SnD (in ether),[21] $EtAlCl_2$ (in C_6D_6)[22] and platinum[23] catalysts, hydrogenation catalysts such as Lindler's catalyst (deuteriation of alkenes)[24], Adam's catalyst ($PtO_2.H_2O$),[25] $RhCl_3$,[26] palladium/carbon (reductive deuteriation of aryl-carbonyls),[27] $RuCl_3$ and $IrCl_3$[28] (deuteriation of mono-substituted aromatics and α,β-unsaturated acids) have been reported in the literature since the early 1960's and more recently, microwave radiation has been employed in promoting deuteriation of polyaromatic, heterocyclic aromatic compounds[29] and reductive deuteriation of ketones.[30]

The use of high temperature aqueous media, both sub- and super-critical water in organic chemistry is extensive and has recently been reviewed by Kratritzky *et al.*.[31] In particular the use of D_2O in supercritical H/D exchange reactions has also been the focus of a review by

Junk *et al.*.[32] Supercritical water has been shown by several groups to effective H/D exchange of both aliphatic[33] and heteroaromatic[34] compounds even in the presence of functional groups, such as ketones[20b] and has shown particular sensitivity to acid and base concentration in its selectivity.[35] Of particular interest is the rapid H/D exchange observed for pyrazine and pyridine in supercritical D_2O.[35] Despite the potential utility of supercritical fluid H/D exchange (SCE), the requirement for high temperatures and pressures somewhat limits its practicality and its applicability to less stable compounds.[20b,35]

The use of subcritical DCl/D_2O and OD^-/D_2O to effect H/D exchange has been successfully employed in the both partial and complete deuteriation of pyridyl containing compounds,[36] flavinones,[14c] imidazoles,[10,37] fluorenes,[38] thiazoles (MeO^-/MeOD)[39] and 2,2'-bipyridine-*N,N'*-dioxide.[5] Fischer *et al.* have reported the use of a Pt/asbestos catalyst for the deuteriation of a range of nitrogen based heterocyclic polyaromatic hydrocarbons using pressure, heat and D_2O as the deuterium source.[6] This method shows wide range applicability for pyridine type aromatic systems. More recently, Vos and co-workers and others have reported the use of a more "user-friendly" catalyst of 10% w/w Pd/C and D_2O under pressure and high temperature (~200 °C) as an effective and general procedure for the deuteriation of a number of hetero-aromatic compounds, *e.g.* pyridyls, pyrazyls, triazoles[7,9] and imidazoles.[10] This latter method, which produces yields in excess of 80%[7,9] without the need for derivitisation, has the advantage over the method of Fischer *et al.* in that the catalyst is commercially available and requires no pre-treatment.

Incorporation of deuteriated precursors has also been used in the preparation of partially deuteriated dppz ([D_6]-dipyridophenazine) where oxidation of [D_8]-1,10-phenanthroline to the 5,6-diphenone was followed by condensation with o-phenylenediamine to form the target ligand,[8] in the partial deuteriation of poly-aromatic hydrocarbons via Diels-Alder reactions[40] and in the preparation of "dionate" type ligands.[41]

3.1.2 Deuteriation and NMR spectroscopy

Ru^{II}, like Rh^{III}, Ir^{III}, Os^{II}, Fe^{II} and Re^{I}, is a d^6 transition metal ion and possesses 6 electrons in its 4d electronic orbital. The 4d level has a degeneracy of 5 in the gaseous state, but according to crystal field theory this degeneracy is lost in the presence of co-coordinating ligands *e.g.* bpy. The coordinating ligand places electron density between the donor atom and the Ru^{II}

centre, resulting in a raising in the energy of the two 4d orbitals (e_g), which are in these regions *i.e.* destabilising them. In addition backbonding into * orbitals stabilises the other three d orbitals (t_{2g}). This results in crystal field splitting of the 4d orbitals in to the t_{2g} (triply degenerate) and e_g (doubly degenerate) states. In this environment, assuming the total spin pairing energy is less than that of the crystal field stabilization energy (CFSE), the six 4d electrons fill the t_{2g} orbitals (low spin state s = 0). As a consequence of this ruthenium(II) complexes are diamagnetic. This is of crucial advantage to the characterisation and study of ruthenium(II) complexes in that it allows for the extensive use of NMR spectroscopy of not only ^{1}H and ^{13}C nuclei but also more recently ^{99}Ru nuclei and hence has facilitated the extensive research which has been carried out on ruthenium complexes.[9]

Partial deuteriation of inorganic complexes has been shown to be useful in the structural elucidation of the large molecules and large ruthenium(II) complexes. Assignment of not only the ^{1}H NMR spectrum but also the ^{13}C NMR spectrum of complexes is simplified significantly.[3]

^{13}C NMR spectroscopy is hampered by both the small gyromagnetic ratio of the nuclei and its low natural abundance, resulting in very weak signals in the ^{13}C NMR spectra of compounds compared with ^{1}H NMR spectroscopy. In order to maximise the intensity of ^{13}C NMR resonances, the coupling between the ^{1}H nuclei and the ^{13}C nuclei (which results in peak splitting) is eliminated by saturation of the ^{1}H nuclei with microwave radiation (coupling due to adjacent ^{13}C nuclei is unimportant due to its low natural abundance). This results in the collapse of the splitting of the ^{13}C peaks and hence an increase in the observed intensity. An additional increase in intensity is achieved through Nuclear Overhauser Effect enhancement (NOE). Splitting from ^{1}H nuclei does not affect quaternary carbons *i.e.* carbons, which are not bonded directly to ^{1}H nuclei, whilst the NOE enhancement is a much reduced effect. This and the longer relaxation times results in their intensities being much lower than for 1°, 2° or 3° carbon nuclei.

When ^{1}H nuclei are replaced by ^{2}D nuclei the strength of the ^{13}C signal of carbons close to the ^{2}D nuclei is reduced. This is due to two reasons. Firstly the signal of the ^{13}C nuclei is split into a triplet (1 deuterium), pentuplet (2 deuterium nuclei) etc., which diminishes the intensity of the signal significantly. Since ^{2}D nuclei resonate at much higher energy than ^{1}H nuclei, irradiation in the region of the resonance of ^{1}H nuclei does not affect the splitting due

to ^{2}D nuclei. Secondly a loss in intensity is observed due to the loss of the NOE enhancement, from saturating the ^{1}H nuclei. Upon partial or full deuteriation of a complex, not only are the ^{1}H resonances lost or diminished, so too are the ^{13}C resonances. Hence deuteriation can be utilized in simplifying both ^{1}H and ^{13}C NMR spectra of ruthenium(II) complexes.[3]

Figure 3.2 demonstrated the results of both loss of NOE enhancement and the splitting upon deuteriation of 1,10-phenanthroline. This allows for immediate assignment of the resonances at 127 and 146 ppm as those of the quaternary carbon nuclei at the bridge points. Each of the remaining C-H carbon nuclei (C-H) show a dramatic loss in intensity and splitting (triplets) by coupling with ^{2}D nuclei. The application of deuteriation to other forms of spectroscopy such as resonance Raman, will be discussed in subsequent chapters.

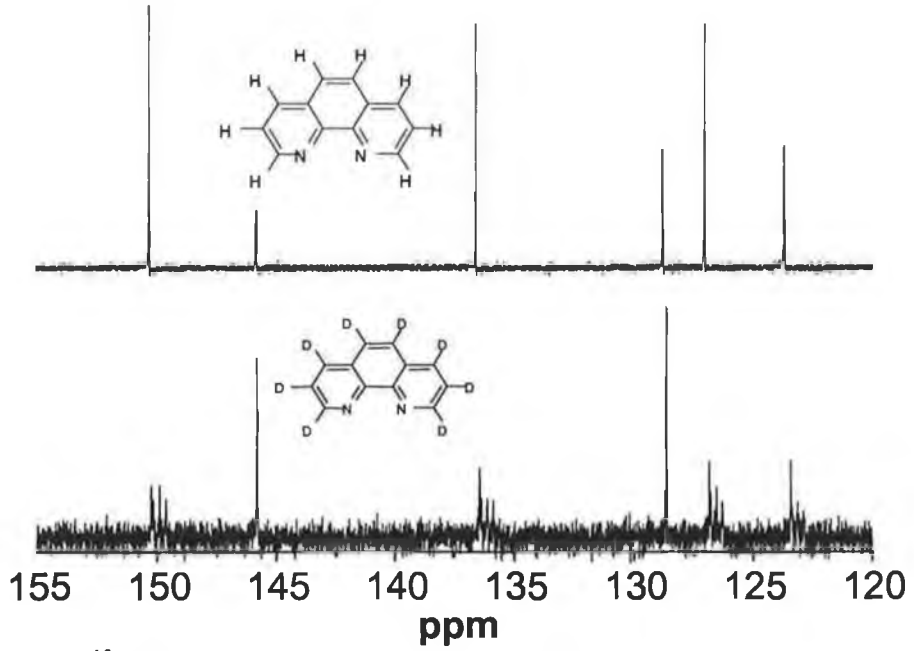

Figure 3.2 *^{13}C (proton decoupled) NMR spectra of [H_8]-1,10-phenanthroline (5a) {upper spectrum} and [D_8]-1,10-phenanthroline (5b){lower spectrum} in $(CD_3)_2SO$.*

3.2 Results

3.2.1 Synthesis and characterisation of deuteriated compounds

The synthetic procedures employed in the synthesis of the 1,2,4-triazole ligands were standard and no attempts at optimisation were made. Synthetic methods and the characterisation of the compounds employed in this chapter are described in Chapter 2. All

compounds were characterized by ^{1}H NMR spectroscopy and Mass spectrometry and were as expected. Where possible additional characterisation by ^{13}C, ^{2}D, ^{1}H COSY, HMQC and HMBC (for assignment of ^{13}C spectra) spectroscopy was carried out. Assignment of all spectral data is presented in the experimental section of this chapter.

As outlined in the experimental part, several H/D exchange procedures, methods A, B and C have been developed. In method A, Pd/C is used as a catalyst in the presence of D_2O, in method B only D_2O is used, while method C is based on the use of basic D_2O (pD = 10/11). In addition, "reverse" D/H exchange has been used to achieve further regioselectivity. The approaches taken are basic H_2O, method D, neutral H_2O, method E, and neutral H_2O in the presence of Pd/C, method F. In all methods the reaction is carried out in a sealed steel container with a Teflon liner at 200 °C. The products obtained, together with yields, the degree of deuteriation and experimental conditions are given in Tables 3.1 and 3.2.

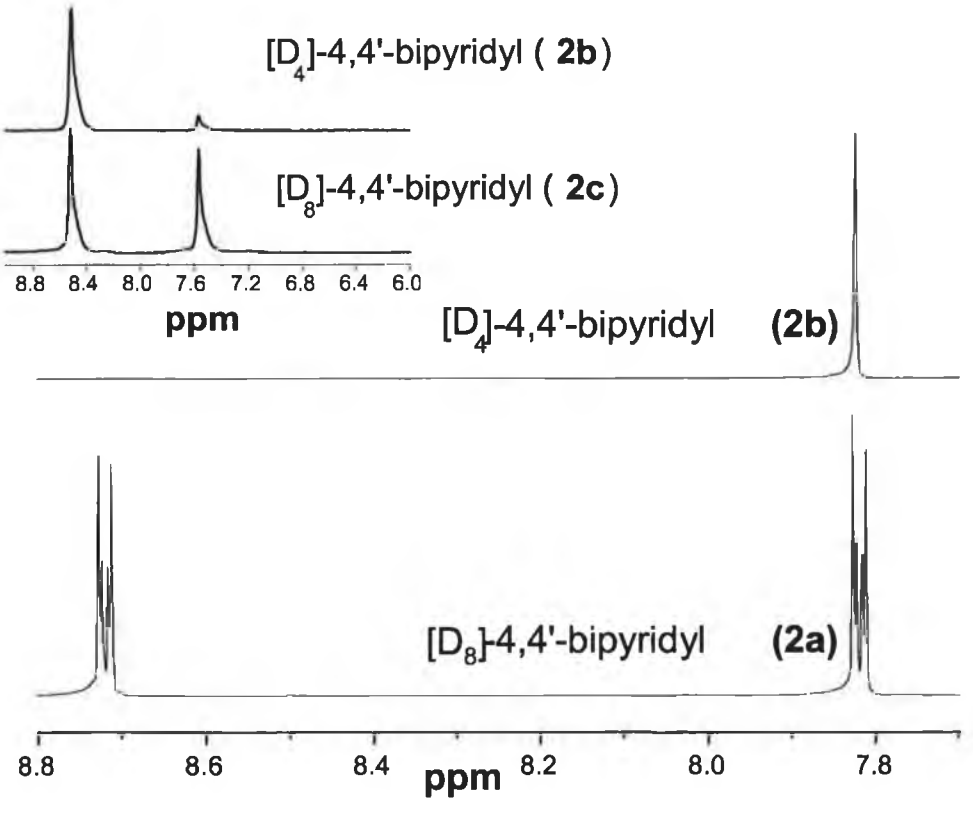

Figure 3.3 *^{1}H NMR spectra of [H_8]-4,4'-bipyridine (**2a**) (lower spectrum) and [D_4]-4,4'-bipyridine (**2b**) (upper spectrum) in $(CD_3)_2CO$ {inset; ^{2}D NMR spectra of [D_8]-4,4'-bipyridine (**2c**) (lower spectrum) and [D_4]-4,4'-bipyridine (**2b**) (upper spectrum) in $(CH_3)_2CO$}*

The three methods employed vary in the regioselectively obtained. This is exemplified by deuteriation of **2a** (Figure 3.3). Together ^{1}H and ^{2}D NMR spectroscopy were employed in characterisation. It is clear from the ^{1}H NMR spectra that method B results in exchange at the C2/6 position almost exclusively with relatively little exchange at the C3/5 position (as evidenced by the very small peak at 7.5 ppm in the ^{2}D NMR spectrum (Figure 3.3 inset). When either Method A or C is employed complete exchange is observed. In Tables 3.1 and 3.2 (and for convenience throughout this thesis) the exchange of the N-H proton of 1,2,4-triazole rings is not considered since exchange at this position is fast and occurs under ambient conditions in protic solvents.

3.3 Discussion

The application of high temperature and supercritical aqueous media in organic reactions has attracted significant interest in recent years.[31a] Much less attention has been focused on medium temperature (150 to 250 °C) aqueous media despite it being the more accessible temperature range. H/D exchange of pyridine under acidic, neutral and basic conditions was investigated in some detail in the medium (150 to 250 °C) and low (< 150°C) temperature range.[29c,36] The usefulness of transition metal catalysts was examined, with Pt and Pd receiving the most attention. However, to the best of my knowledge, no detailed study on the general application of such methods has been reported. The motivation behind the interest in the deuteriation of polypyridyl ligands is their potential applicability in the study of supramolecular systems. One approach taken has been the direct deuteriation of the metal complexes.[42] For example, deuteriation of $[Ru(bpy)_3]^{2+}$ in 0.1 M $NaOCD_3/(CD_3)_2SO/CD_3OD$ at 35 °C was found to occur rapidly at the 3,3'-positions and more slowly at the 5,5'-positions. In the present study $[Ru(bpy)_3]^{2+}$ is found to be inert to H/D exchange in both neutral and basic D_2O (***Table 3.2***). When using method B, $[Ru(bpy)_2(\mathbf{12a})]^{+}$ shows a very slow exchange at the H6 position of the pyrazyl ring (adjacent to the coordinating nitrogen), whereas the H3 and H5 positions of the pyrazine ring undergo complete exchange. Overall deuteriation of metal complexes is slow and has severe limitations especially in the case of heteroleptic complexes, for this reason a general strategy for the H/D exchange of ligands is needed.

Table 3.1 Conditions, yields and extent of isotope exchange reactions.

	Compound	[a]Overall % H-D exchange (site)	[b]Method	[c]% Yield	Reaction time (days)
1b	[D_8]-2,2'-bipyridine	> 98	A	80	3
		> 98	C	90	6
2b	[D_4]-4,4'-bipyridine	> 98 (C2/C6): < 15 (C3/C5)	B	95	3
2c	[D_8]-4,4'-bipyridine	> 98	A	80	4
		> 98	C	90	6
3b	[D_{16}]-4,4'-diphenyl-2,2'-bipyridine	> 98	A	90	6
4b	[D_{12}]-4,4'-dimethyl-2,2'-bipyridine	> 98 (50 % exchange at C3)	A	70	4
		> 98	C	95	6
5b	[D_8]-1,10-phenanthroline	> 98	A	70	4
		> 98	C	95	6
6b	[D_6]-4,7-diphenyl-1,10-phenanthroline	> 98 phenanthroline protons (< 5 % for phenyl rings, C5/C6 show incomplete exchange)	C	95	6
6c	[D_{10}]-4,7-diphenyl-1,10-phenanthroline	~95 % for phenyl rings	D(from **5d**)	95	6
6d	[D_{14}]-4,7-diphenyl-1,10-phenanthroline	> 98 (< 5 at C5/C6)	A	60	6
6e	[D_{16}]-4,7-diphenyl-1,10-phenanthroline	> 98	A then C	80	2 x 3 days
7b	[D_{12}]-2,2'-biquinoline	> 98	A	80	3
7c	[D_4]-2,2'-biquinoline	> 98 C2/C3/C4 (< 10 at remaining positions)	C	60	4
8b	[D_{10}]-2,3-Di-(pyrid-2yl)-pyrazine	> 98	C	90	6
9b	[D_2]-2-(thien-2'-yl)-pyridine	> 98 (py-H6/th-H5')	B	85	6
9c	[D_7]-2-(thien-2'-yl)-pyridine	> 98	C	95	6

a) in the case of partially deuteriated compounds exchange at individual positions are given in parentheses. b) **A** 0.1 g of 10 % Pd/C in 20 mL of D_2O at 200 °C; **B** in 20 mL of D_2O at 200 °C; **C** in 20 mL of 1 M NaOD/D_2O at 200 °C; **D** in 20 mL of 1 M NaOH/H_2O at 200 °C. c) based on recovered yield.

Table 3.2 *Conditions, yields and extent of hydrogen/deuterium exchange reactions.*

	Compound	[a]Overall % H-D exchange (site)	[b]Method	[c]% Yield	Reaction time (days)
10b	$[D_4]$-Hpztr	> 98%	B	95	3
11b	$[D_6]$-Hmepztr	> 98%	B	95	3
12b	$[D_3]$-Hphpztr	> 98% (pz-)	B	95	3
12c	$[D_5]$-Hphpztr	> 98% (ph-)	E (#)	95	3
12d	$[D_8]$-Hphpztr	> 98%	A	80	2 x 3 days
13b	$[D_3]$-Htolpztr	>98 % (pz-)	B	95	3
13c	$[D_3]$-Htolpztr	>98 % (Me-)	E (prep. From **12e**)	95	2
13d	$[D_4]$-Htolpztr	> 80 % (tolyl: see scheme 2)	F (#)	95	6
13e	$[D_6]$-Htolpztr	> 98 % (pz- & Me-)	A	95	6
13f	$[D_7]$-Htolpztr	> 98% (tolyl-)	E (#)	95	3(§)
13g	$[D_{10}]$-Htolpztr	> 98%	C	95	2x10 days
14b	$[D_5]$-Hpytr	> 98%	C	80	3
15b	$[D_7]$-Hmepytr	> 98%	C	80	3
16b	$[D_1]$-Hphpytr	> 95 % (py- H6)	B	95	30
16c	$[D_4]$-Hphpytr	>95% (py), < 15 % (ph)	C	90	3
16d	$[D_5]$-Hphpytr	>95% (ph), < 15 % (py)	E (#)	90	3
16e	$[D_9]$-Hphpytr	> 98 %	A	80	6
17b	$[D_7]$-Hppt	> 98 %	A	80	6
		> 98 %	C	85	3
17c	$[D_4]$-Hppt	> 98 %(pz, pyC6)	A	80	6
	$[Ru(bpy)_2$(**12a**)$](PF_6)$	> 98 % pz C3/5, < 20 % at pz C6	B	70	3
	$[Ru(bpy)_3](PF_6)$	No exchange observed	B	90	3
		No exchange observed	B	90	3

a) in the case of partially deuteriated compounds exchange at individual positions are given in parentheses. b) **E** in 20 mL of H_2O at 200 °C; **F** 0.1 g of 10 % Pd/C in 20 mL of H_2O at 200 °C; **#** prepared from perdeuteriated reagents (see experimental); For other reaction conditions (see Table 1.) c) based on recovered yield, (§) when reacted for 30 days no further exchange was observed. For **13b-g** see scheme 2 for further information.

With the strategy employed in this chapter, deuteriation has been achieved on the gram scale, with high yields (typically >80 % after purification) and to high degrees of isotopic purity (typically >98 %). By careful manipulation of the conditions employed and by the combination of different methods regioselective deuteriation is achieved. The behaviour of the compounds studied is discussed in more detail in the next sections. It is worth pointing out that in certain instances the reported yield is somewhat lower than 80%. The lower yields in the case of **4b** and **5d** are not due to decomposition (no evidence for this has been observed) but rather reflect the difficulty in removing the compounds from the Pd/C catalyst. A second point that should be considered is the extent of deuterium incorporation. There is a theoretical limit to the extent of deuteriation achievable under the conditions employed, which is dependent on the molar ratio of the substrate and solvent employed. For example, 3g of **1a** contains 0.154 mole equivalents of ^{1}H and 20 cm^{3} of $^{2}H_2O$ contains 2.11 mole equivalents of ^{2}H. Under these conditions the theoretical limit for exchange is 93.5% and the resulting deuteriated sample should be submitted for a second cycle. In contrast if 1 g of **1a** is employed then the equilibrium limit is raised to 98%.

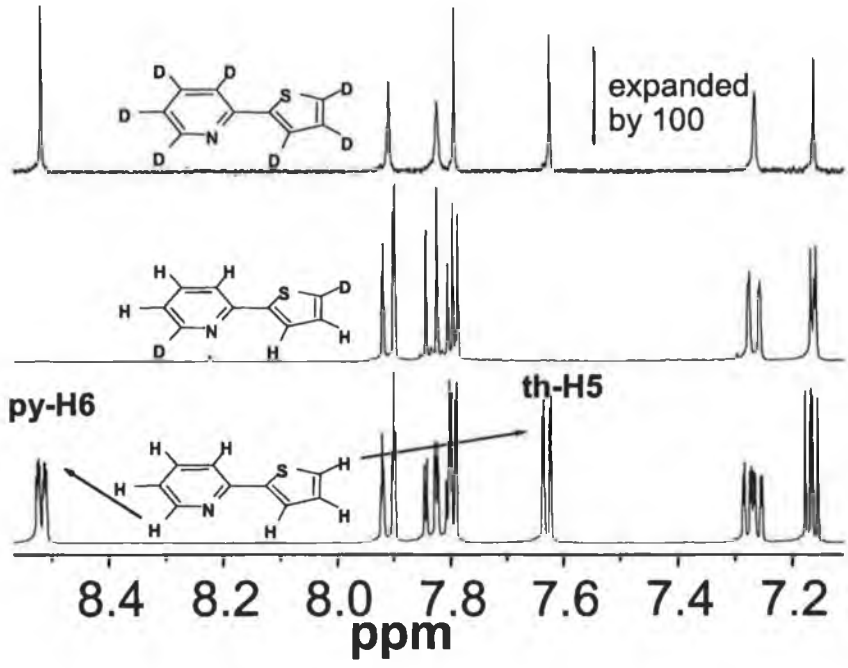

Figure 3.4 *^{1}H NMR spectra of [H_7]-2-(thien-2'-yl)-pyridine (**9a**) (lower spectrum) [D_2]-2-(thien-2'-yl) pyridine (**9b**) (middle spectrum) and [D_7]-2-(thien-2'-yl)-pyridine (**9c**) (upper spectrum) in [D_6]-DMSO (all spectra were obtained at equal concentrations).*

3.3.1 Deuteriation of heterocyclic groups.

Compounds **1a** to **9a** (Table 3.1) are amongst the most commonly employed bidentate ligands in the preparation of inorganic polypyridyl complexes[1]. Table 1 shows that Pd/C is not needed to achieve full deuteriation. Neutral and basic D_2O solutions also yield high deuteriation ratios and high yields. The absence of a catalyst has the advantage that the work-up of the reaction mixture is easier, and hence yields improve (See Table 3.1). The effect of the reaction conditions used (*e.g.* time, pH/pD and catalyst) is found to be dependent on the type of proton to be exchanged. For example as shown in Figure 3.1, by using method B, little exchange is observed for the H3/H5 position of 4,4'-bipyridine (**2a**). Another example is illustrated in Figure 3.9 for compound **9a-c**. This figure shows that after use of method B only the pyridine H6 and the thienyl H5 are exchanged, while full exchange is obtained with method C. In general, with method B, only exchange at the positions adjacent to heteroatoms (*e.g.* N and S) takes place even with extended reaction times (see Table 3.1 and Table 3.2). Pyrazyl groups (compounds **10a-13a**) readily undergo complete exchange. This is not unexpected since every position can be considered as analogous to the H2/H6 position of pyridine.

Under basic conditions much less variation is observed in exchange rates at different positions, with thienyl-, pyridyl and pyrazyl groups showing complete H/D exchange. However, with this method a significant level of control over the deuteriation of the aryl- and pyridyl- moieties in **6a** and **7a** can be achieved. It should be noted that with method C the regioselectivity observed for **6a** is different than observed for method B. This is discussed below in more detail.

3.3.2 Deuteriation of aromatic and aliphatic groups

H/D exchange of methyl groups depends on the nature of the moiety to which they are attached. When bound directly to pyridyl- (**4a**) or 1,2,4-triazole (**11a**, **15a**) groups, complete exchange occurs under all conditions examined (Table 3.1 and Table 3.2). In contrast methyl groups attached to phenyl rings (**13a**) show no exchange using method B, but is deuteriated completely in basic media and with method A. Phenyl- (**6a**, **12a** and **16a**) and tolyl- groups (**13a**) are the least reactive moieties. No exchange of aromatic protons was observed using method B, but phenyl groups do exchange in the presence of Pd/C catalyst (method A). Using

method C complete exchange of both phenyl and methyl protons is observed, albeit at a much slower rate than for heteroaromatic groups.

3.3.3 Regioselective deuteriation

The differences in the reactivity of the various moieties allow for the development of strategies for the regioselective isotope exchange. Two examples of the combination different methods to achieve selectively deuteriated compounds are shown in Schemes 3.1 and 3.2. Scheme 3.1 (and Table 3.1) illustrates the routes taken in the preparation of four isotopologues of ph_2phen, namely $[D_6]$-ph_2phen (**6b**), $[D_{10}]$-ph_2phen (**6c**), $[D_{14}]$-ph_2phen (**6d**), and $[D_{16}]$-ph_2phen (**6e**). H/D exchange of the phenyl groups is achieved in the presence of the Pd/C catalyst in neutral D_2O, but occurs only very slowly in basic D_2O.

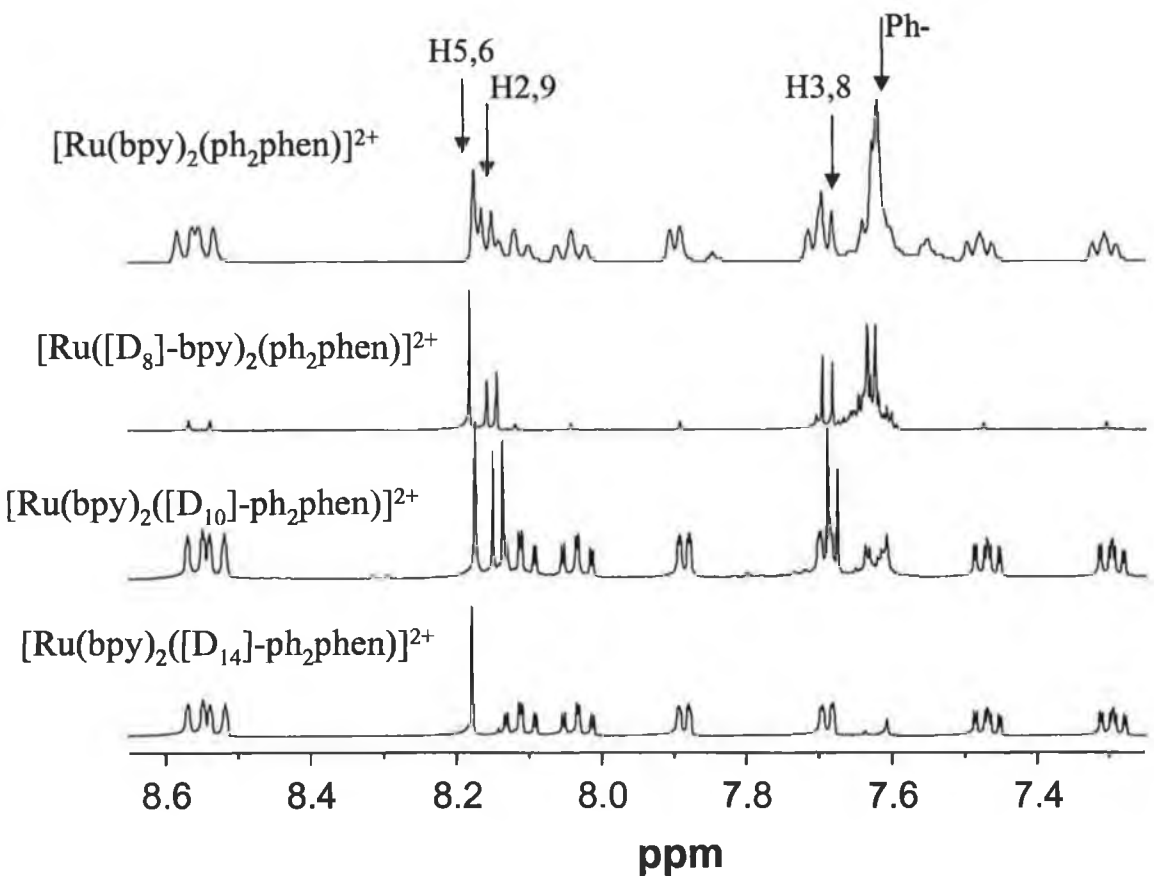

Figure 3.5 *^1H NMR spectra (400 MHz) of $[Ru([D_x]\text{-bpy})([D_y]\text{-}ph_2phen)](PF_6)_2$ in CD_3CN. (x= 0 or 8, y = 10, 14, 16). Resonances due to ph_2phen ligand are indicated*

Consequently using method A, the $[D_{14}]$-isotopologue (**6d**) is obtained in good yield with excellent regioselectivity. Interestingly it is the phenanthroline H5 and H6 positions, which

do not exchange under these conditions. However, deuteration of the complete phenanthroline moiety takes place using method C. The fact that these reactions are high yield and can be carried out on a gram scale opens the possibility to use the products obtained as materials for further reaction. Therefore, a reverse D/H exchange as shown in Scheme 3.1 becomes a viable option. With this approach compounds such as **6c** can be prepared from **6d**. In this process the moiety that is most easily exchanged, namely the phenanthroline grouping, is regenerated in the perprotio form.

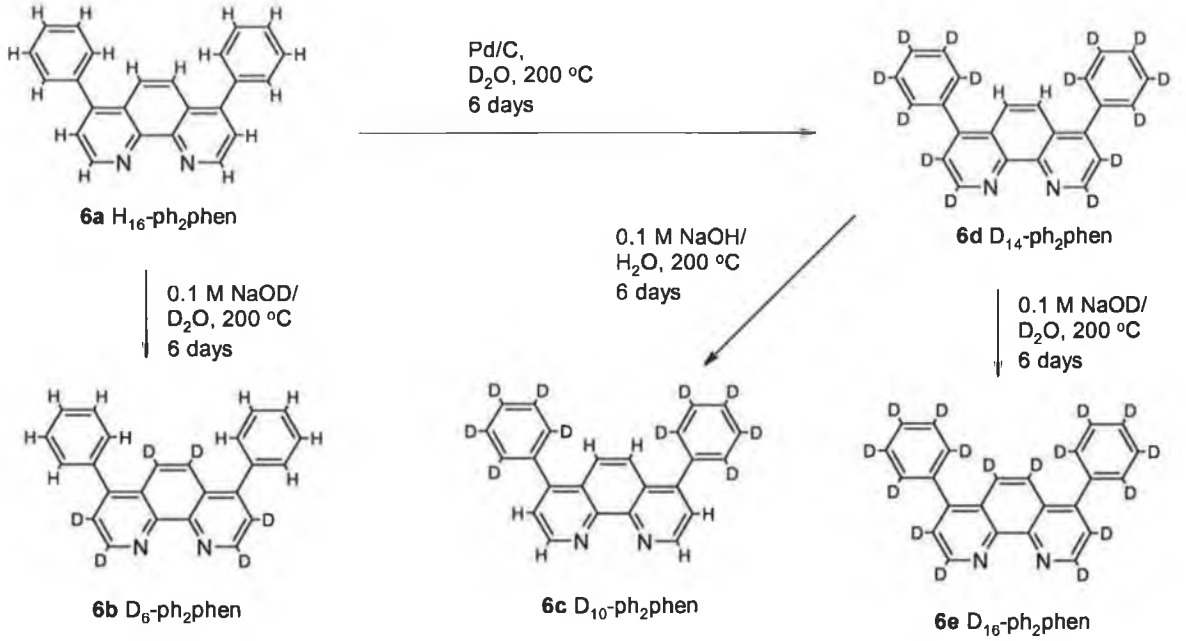

Scheme 3.1. *Routes examined in the deuteriation of* ***6a***

In Scheme 3.2 the different reactivity of pyrazine, aromatic and methyl groupings are illustrated. Based on the behavior observed in Scheme 3.1 it is surprising that the tolyl aromatic protons do not exchange in any significant manner using method A and this suggests that the methyl group deactivates the tolyl ring towards H/D exchange. Exchange of these protons is more efficient in the presence of base, albeit at a slower rate than for methyl or pyrazinyl- protons. In contrast to the results obtained for **4a** and **11a** the protons of the methyl group in **13a** can be exchanged using method A, but not by the use of method B. Again the reverse D/H exchange can be used to yield isotopologues, such as **13c**, **13d** and **13f**, which contain deuterium atoms in positions, which undergo H/D exchange with most difficulty.

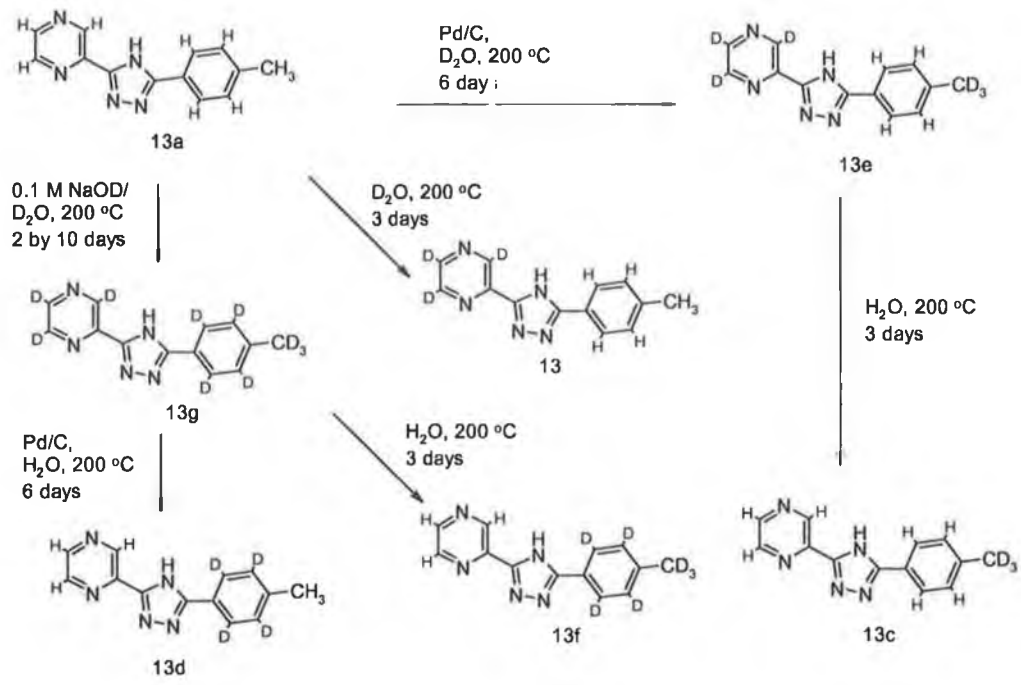

Scheme 3.2 *Routes examined for the deuteriation of* ***13a***

3.3.4 Application of deuteriation to supramolecular systems.

The effect of deuteriation on ^{1}H and ^{13}C NMR spectroscopy is already well known.[3,4] Deuteriation results not only in a loss in intensity but also the splitting of ^{13}C signals into multiplets. An example of this is shown in Figure 4, which shows the ^{13}C spectra for **5a** and **5b**. In the spectrum of **5b** only the signals that can be attributed to the quaternised carbon atoms remain as singlets, the others appear as triplets. Selective deuteriation is therefore useful in the assignment of ^{13}C resonances.[3c] In addition ^{2}D NMR spectroscopy can be used to monitor specific sites in complexes, which have complicated ^{1}H NMR spectra (see Figure 3.8 and 3.11). Furthermore, for large molecules such as ruthenium(II) and osmium(II) polypyridyl complexes, deuteriation has been shown to be very useful in simplifying ^{1}H NMR spectra[3] and an example of this can be seen in Figure 3.10, where ^{1}H NMR resonances are eliminated by selective deuteriation. The spectra shown illustrate how well defined NMR based information can be obtained for compounds, which contain a large number of hydrogen atoms. It is also important to point out that no evidence for H/D exchange was observed, under the reaction conditions employed to prepare ruthenium complexes from deuteriated ligands.[9] This is in agreement with the observed temperature dependence of the deuteriation methods discussed, which indicates that no measurable exchange occurs below 140 °C.[43]

The application of deuteriation is not limited to structural characterization. Isotope exchange has found application as a probe for studying excited state processes in transition metal complexes in time-resolved resonance Raman spectroscopy.[42] In addition deuteriation has received considerable attention, in the study of the excited state properties of rare earth ions and ruthenium(II) polypyridyl complexes.[4] Selective deuteriation of mixed ligand complexes was shown to yield important information about the location of the emitting state in mixed ligand complexes by its effect on emission lifetime.[7,8] For example this approach can now be applied in the study of dpp (**8a**) based multinuclear ruthenium and osmium based bis(bipyridyl) complexes.[44] Deuteriation of either **8a** or **1a** would allow for the detailed study of the possible isomers present and selective deuteriation could also be used to study the excited state behavior of such compounds.

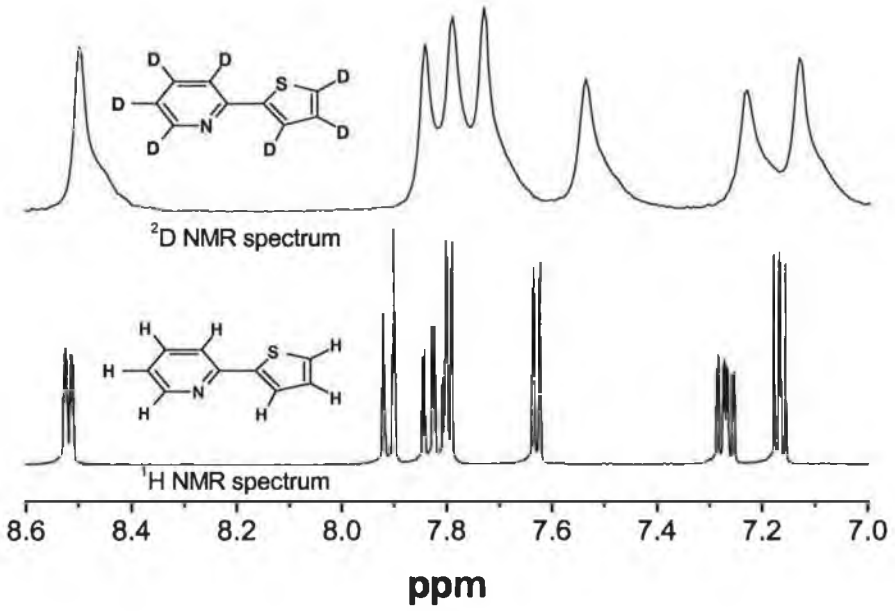

Figure 1.6 *^1H NMR spectra of [H_7]-2-(thein-2'-yl)-pyridine (**9a**) (lower spectrum) in $(CD_3)_2CO$ and ^2D NMR spectra of [D_7]-2-(thein-2'-yl)-pyridine (**9c**) (upper spectrum) in $(CH_3)_2CO$*

3.3.5 Limitations

During the course of this study, 1,2,4-triazines and compounds containing functional groups (*e.g.*-carboxylic acids, esters, and –carbonitriles) were found to decompose under the conditions employed. However, the deuteriation of relatively large amounts of material (up to 3 g in this study) coupled with high yields, allows for the preparation of a much larger range

of deuteriated compounds through the deuteriation of precursors in synthetically useful amounts. Therefore, the preparation of perdeuteriated compounds containing thermally unstable functional groups such as carboxylic acid, carbonitriles, amides etc., may be achieved indirectly via perdeuteriated methyl precursors (*e.g.* $[D_6]$-4,4'-dicarboxy-2,2'-bipyridine can be prepared from **4b,** see Chapter 2).

Regioselective deuteriation is also limited to systems possessing moieties showing large differences in reactivity. An example of a system, which does not show this, is the ligand Hppt (**17a**). Partial deuteriation can be achieved in the case of **17c** (Table 3.2). In order to prepare Hppt with only one ring deuteriated, deuteriation of that ring must take place prior to preparation of the ligand. Although materials such as pyrazine-carbonitrile and pyrazine-carboxylic acid are unstable towards deuteriation, the deuteriation of the ring may be achieved by deuteriation of picoline or methylpyrazine followed by oxidation to the corresponding carboxylic acid. This material can subsequently be employed for the synthesis of Hppt by standard procedures (see Chapter 2).

3.4 Conclusions

In this chapter a general approach to the deuteriation of heteroaromatic compounds is described. The potential for regioselective deuteriation is identified. The procedures employed allow for the reduction and often the complete elimination of the requirement for catalysts or derivitisation (*e.g.* via N-oxide intermediates[5]) and much-improved yields. The applicability of deuteriation in inorganic photophysics and supramolecular chemistry is already well known.[4] However, its use has been severely limited by the cost and difficulty in preparing well-defined deuteriated materials. In this regard the methods described here allow for the widespread application of deuteriation in such studies and provide an additional tool for the study of the spectroscopic and photophysical properties of supramolecular compounds.

3.5 Experimental

3.5.1 Hydrogen-Deuterium exchange reactions

Typical examples of each reaction type A to F are given below. Spectroscopic data for each partially and fully deuteriated compound are summarized as the supplementary material. In

the case of method A, the solvent employed to remove deuteriated compound from the catalyst varied depending on the solubility of the compound. The extent of isotope exchange was determined from the isotopic pattern of the mass spectra of the compounds and by comparison of the ^{1}H NMR spectra of the deuteriated compound with its perprotio analogue at known concentrations using the residual solvent peak as an internal standard.

Method A: [D_8]-2,2'-bipyridine **1b**. **1a** (3 g) was reacted with 50 mg of 10% Pd/C in 20 ml of D_2O at 200 °C under pressure for 3 days. On cooling the reaction mixture was filtered and the catalyst was washed with 2 × 50 ml of diethyl ether to remove any bpy from the catalyst surface. The diethyl ether washings and the aqueous filtrate were evaporated to dryness to yield the **1b**. It should be noted that with this method yields are sometimes lower than quantitative due to difficulties in removing the product from the catalyst.

Method B: [D_3]-Hphpztr **12b**. 1 g of **12a** was reacted at 200 °C in 20 ml of D_2O for 3 days. After cooling the compound precipitated and was filtered and air-dried.

Method C: [D_4]-Hphpytr **16c**. 1.5 g of **16a** was reacted at 200 °C in 20 ml of 1 M NaOD/D_2O for 3 days. On cooling, the reaction mixture was neutralized with concentrated HCl and the white precipitate was filtered and air-dried.

Method D: [D_5]-Hphpytr **16d**. 0.5 g of **16e** was reacted at 200 °C in 20 ml of 1 M NaOH/H_2O for 3 days. On cooling, the reaction mixture was neutralized with concentrated HCl and the white precipitate was filtered and air-dried.

Method E: [D_5]-Hphpztr **12c**. 0.5 g of **12d** was reacted at 200 °C in 20 ml of H_2O for 3 days. On cooling the reaction mixture, the white precipitate was filtered and air-dried.

Method F: As for method A except H_2O was used in place of D_2O.

3.5.2 ^{1}H, ^{13}C and ^{2}D NMR spectroscopic and mass spectral data

Assignment of ^{1}H and ^{2}D NMR resonances were made by comparison with assignments made for ^{1}H NMR spectra of their perprotio analogues. Assignment of ^{13}C spectra were made

on the basis of comparison with assignments made for their perprotio analogues using HMQC and HMBC NMR experiments and on the basis of the loss of intensity and splitting upon deuteriation. All measurements were carried out in $(CD_3)_2CO$ or $(CD_3)_2SO$. ^{2}D NMR spectra were acquired in $(CH_3)_2CO$ or $(CH_3)_2SO$. Peak positions are relative to residual solvent peaks. The limited solubility of some compounds precluded the measurement of their ^{2}D and ^{13}C NMR spectra.

^{1}H, ^{2}D ^{13}C NMR Spectroscopic data and Mass spectral data for all partially and fully deuteriated compounds described in Tables 1 and 2.

Symmetric Diimine compounds

[D_8]-2,2'-bipyridine **1b**: Mass spectrometry HM^+ ion at 165 m/z. ^{1}H NMR in [D_6]-DMSO δ ppm; 8.69 (H3, *resid.* s), 8.39 (H6, *resid.* s), 7.95 (H4, *resid.* s), 7.45 (H5, *resid.* s). ^{13}C NMR in [D_6]-DMSO δ ppm; 149.62 (C3, t), 120.79 (C6, t), 137.68 (C4, t), 124.56 (C5, t), 155.54 (C2, s). ^{2}D NMR in [H_6]-acetone δ ppm; 8.68 (D3), 8.5 (D6), 7.89 (D4), 7.39 (D5).

[D_4]-4,4'-bipyridine **2b**: Mass spectrometry HM^+ ion at 161 m/z. ^{1}H NMR in [D_6]-DMSO δ ppm; 8.72 (H2, *resid.* s), 7.82 (H3, s). ^{13}C NMR in [D_6]-DMSO δ ppm; 150.89 (C2/6, t), 121.64 (C3/5, s), 144.67 (C4, s). ^{2}D NMR in [H_6]-acetone δ ppm; 8.71 (H2/H6, s), 7.76 (H3/H5, *resid.* s).

[D_8]-4,4'-bipyridine **2c**: Mass spectrometry HM^+ ion at 165 m/z. ^{1}H NMR in [D_6]-DMSO δ ppm; 8.72 (H2/6, *resid.* s), 7.82 (H3/5, *resid.* s). ^{13}C NMR in [D_6]-DMSO δ ppm; 150.89 (C2/6, t), 121.64 (C3/5, t), 144.67 (C4, s). ^{2}D NMR in [H_6]-acetone δ ppm; 8.71 (H2/H6, s), 7.76 (H3/H5, s).

[D_{16}]-4,4'-diphenyl-2,2'-bipyridine **3b**: Mass spectrometry HM^+ ion at m/z. ^{1}H NMR in [D_6]-DMSO δ ppm; 8.76 (H6 py, *resid.* s), 8.67 (H3 py, *resid.* s), 7.77 (H5 py, *resid.* s), 8.85 (H2/6 ph, *resid.* s), 7.54 (H3/5 ph, *resid.* s), 7.7.49 (H4 ph, *resid.* s). ^{13}C NMR in [D_6]-DMSO δ ppm; 148.53 (C4 py, *resid.* s), 156.09 (C2 py, *resid.* s), 137.28 (C1 py, *resid.* s).

[D_{12}]-4,4'-dimethyl-2,2'-bipyridine **4b**: Mass spectrometry HM^+ ion at 197 m/z. ^{1}H NMR in [D_6]-DMSO δ ppm; 2.36 (Me, m), 8.51(H6, *resid.* s), 8.20 (H3, *resid.* s), 7.27 (H5, *resid.* s). ^{13}C NMR in [D_6]-DMSO δ ppm; 149.32 (C6, t), 121.58 (C3, t), 148.28 (C4, s), 125.25

(C5, t), 155.45(C2, s), 21.23 (Me, not observed). ^{2}D NMR in [H_6]-acetone δ ppm; 2.35 (CD_3-), 8.49 (D6), 8.29 (D3), 7.21 (D5).

[D_8]-1,10-phenanthroline **5b**: Mass spectrometry HM^+ ion at 189 m/z. ^{1}H NMR in [D_6]-DMSO δ ppm ; 9.10(H2/9, *resid.* s), 7.77(H3/8, *resid.* s), 8.49 (H4/7, *resid.* s), 7.99 (H5/6, *resid.* s). ^{13}C NMR in [D_6]-DMSO δ ppm; 150.31 (C2/9, t), 123.70 (C3/8, t), 136.58 (C4/7, t), 127.04 (C5/6, t), 128.75 (C11/13, s), 145.83 (C12/14, s). ^{2}D NMR in [H_6]-acetone δ ppm; 8.66 (D2/9), 8.46 (D4/7), 7.64 (D5/6 and D3/8)

[D_6]-4,7-diphenyl-1,10-phenanthroline **6b**: Mass spectrometry HM^+ ion at 339 m/z. ^{1}H NMR in [D_3]-chloroform δ ppm ; 9.36 (H2/9, *resid.* s), 7.70 (H3/8, *resid.* s), 7.64 (phenyl-4,7, *resid.* s), 7.96 (H5/6, s).

[D_{10}]-4,7-diphenyl-1,10-phenanthroline **6c**: Mass spectrometry HM^+ ion at 343 m/z. ^{1}H NMR in [D_3]-chloroform δ ppm ; 9.36 (H2/9, d), 7.70 (H3/8, d), 7.64 (phenyl-4,7, *resid.* s), 7.96 (H5/6, s).

[D_{14}]-4,7-diphenyl-1,10-phenanthroline **6d**: Mass spectrometry HM^+ ion at 347 m/z. ^{1}H NMR in [D_3]-chloroform δ ppm ; 9.36 (H2/9, *resid.* s), 7.70 (H3/8, *resid.* s), 7.64 (phenyl-4,7, *resid.* s), 7.96 (H5/6, s). ^{2}D NMR in [H_6]-acetone δ ppm; 9.2 (D2/9), 7.91 (D3/8), 7.63 (phenyl-4/7, *resid.* D5/6)

[D_{16}]-4,7-diphenyl-1,10-phenanthroline **6e**: Mass spectrometry HM^+ ion at 349 m/z. ^{1}H NMR in [D_3]-chloroform δ ppm; 9.36 (H2/9, *resid.* s), 7.70 (H3/8, *resid.* s), 7.64 (phenyl-4,7, *resid.* s), 7.96 (H5/6, *resid.* s). ^{2}D NMR in [H_6]-acetone δ ppm; 9.2 (D2/9), 7.91 (D3/8), 7.63 (phenyl-4/7, D5/6)

[D_{12}]-2,2'-biquinoline **7b**: Mass spectrometry HM^+ ion at 269 m/z. ^{1}H NMR in [D_6]-DMSO δ ppm; 7.69 (*resid.* s), 7.86 (*resid.* s), 8.08 (*resid.* s), 8.19 (*resid.* s), 8.58 (*resid.* s), 8.71 (*resid.* s).

[D_4]-2,2'-biquinoline **7c**: Mass spectrometry HM^+ ion at 261 m/z. ^{1}H NMR in [D_6]-DMSO δ ppm; 7.69 (dd), 7.86 (dd), 8.08 (d), 8.19 (d), 8.58 (*resid.* s), 8.71 (*resid.* s).

Pyrazinyl- and thienyl- pyridine compounds

[D_{10}]-2,3-Di-(pyrid-2yl)-pyrazine **8b**: Mass spectrometry HM^{+} ion at 245 m/z. ^{1}H NMR in [D_6]-acetone δ ppm; 8.79 (pz, *resid.* s), 8.25 (pyH6, *resid.* s), 7.86 (pyH3, *resid.* s), 7.91 (pyH4, *resid.* s), 7.32 (pyH5, *resid.* s). ^{13}C NMR in [D_6]-acetone δ ppm; 143.14 (pzC5/6, t), 152.1(pzC2/3, s), 148.49 (pyC6, t), 124.16 (pyC3, t), 137.13 (pyC4, t), 123.56 (pyC5, t), 157.2 (C2, s). ^{2}D NMR in [H_6]-acetone δ ppm; 8.71 (pz), 8.21 (pyD6), 7.88 (pyD3/D4), 7.27 (pyD5)

[D_2]-2-(thien-2'-yl)-pyridine **9b**: Mass spectrometry HM^{+} ion at 164 m/z. ^{1}H NMR in [D_6]-acetone δ ppm; 7.7 (thH3,d), 7.1 (thH4,d), 7.6(thH5, *resid.* s), 8.5 (pyH6, *resid.* s), 7.9 (pyH3,d), 7.8 (pyH4,dd), 7.2 (pyH5,d). ^{13}C NMR in [D_6]-acetone δ ppm; 144.87 (thC2,s), 125.56 (thC3, s), 128.70(thC4,s), 128.77(thC5,t), 152.15 (pyC2,s), 118.99 (pyC3,s), 137.53(pyC4,s), 122.69 (pyC5,s), 149.70 (pyC6,t). ^{2}D NMR in [H_6]-acetone δ ppm; 7.72 (*resid.* thD3 ~ 15%), 7.54 (thD5), 8.50 (pyD6).

[D_7]-2-(thien-2'-yl)-pyridine **9c**: Mass spectrometry HM^{+} ion at 169 m/z. ^{1}H NMR in [D_6]-acetone δ ppm ; 7.7 (thH3, *resid.* s), 7.1 (thH4, *resid.* s), 7.6 (thH5, *resid.* s), 8.5 (pyH6, *resid.* s), 7.9 (pyH3, *resid.* s), 7.8 (pyH4, *resid.* s), 7.2 (pyH5, *resid.* s). ^{13}C NMR in [D_6]-acetone δ ppm; 144.87 (thC2,s), 125.56 (thC3,t), 128.70(thC4,t), 128.77(thC5,t), 152.15 (pyC2,s), 118.99 (pyC3,s), 137.53(pyC4,s), 122.69 (pyC5,s), 149.70 (pyC6,s). ^{2}D NMR in [H_6]-acetone δ ppm; 7.73 (thD3), 7.13 (thD4), 7.54 (thD5), 8.50 (pyD6), 7.84 (pyD3), 7.79 (pyD4), 7.23 (pyD5).

Pyrazine-1,2,4-triazole based compounds

[D_4]-Hpztr **10b**: Mass spectrometry HM^{+} ion at 152 m/z. ^{1}H NMR in [D_6]-DMSO δ in ppm: 9.46 (*resid.* s, pz-H3), 8.70 (*resid.* s, pz-H5), 8.66 (*resid.* s, pz-H6), 8.25 (*resid.* s, tr-H5), ^{2}D NMR in [H_6]-DMSO δ ppm; 9.24 (pz-D3), 8.72 (pz-D5/D6), 8.49 (tr-D5)

[D_6]-Hmepztr **11b**: Mass spectrometry HM^{+} ion at 169 m/z. ^{1}H NMR in [D_6]-DMSO δ in ppm: (*resid.* s, pz-H3), (*resid.* s, pz-H5), (*resid.* s, pz-H6), (*resid.* m, Methyl). ^{2}D NMR in ([H_6]-DMSO) δ ppm; 9.07 (pz-D3), 8.63 (pz-D5/D6), 2.32 (Methyl)

[D_3]-Hphpztr **12b**: Mass spectrometry HM^+ ion at 227 m/z. ^{1}H NMR in [D_6]-DMSO δ in ppm: 9.35 (*resid.* s, pz-H3), 8.795 (*resid.* s, pz-H5), 8.765 (*resid.* S, pz-H6), 8.11 (d, 2H, ph-H2/H6), 7.54 (dd, 2H, ph-H3/H5) 7.49 (t, 1H, ph-H4). ^{2}D NMR in [H_6]-DMSO δ ppm; 9.33 (pz-D3), 8.75 (pz-D5/D6)

[D_5]-Hphpztr **12c**: Mass spectrometry HM^+ ion at 229 m/z. ^{1}H NMR in [D_6]-DMSO δ in ppm: 9.35 (d, 1H, pz-H3), 8.795 (dd, 1H, pz-H5), 8.765 (d, 1H, pz-H6), 8.11 (*resid.* s, ph-H2/H6), 7.54 (*resid.* s, ph-H3/H5) 7.49 (*resid.* s, ph-H4), ^{2}D NMR in [H_6]-DMSO δ ppm; 8.07 (ph-D2/D6), 7.48 (ph-D3/D4/D5)

[D_8]-Hphpztr **12d**: Mass spectrometry HM^+ ion at 332 m/z. ^{1}H NMR in [D_6]-DMSO δ in ppm: 9.35 (*resid.* s, pz-H3), 8.795 (*resid.* s, pz-H5), 8.765 (*resid.* s, pz-H6), 8.11 (*resid.* s, ph-H2/H6), 7.54 (*resid.* s, ph-H3/H5) 7.49 (*resid.* s, ph-H4). ^{2}D NMR in [H_6]-DMSO δ ppm; 9.33 (pz-D3), 8.75 (pz-D5/D6), 8.07 (ph-D2/D6), 7.48 (ph-D3/D4/D5).

[D_3]-Htolpztr **13b**: Mass spectrometry HM^+ ion at 241 m/z. ^{1}H NMR in [D_6]-DMSO δ in ppm: 9.33 (*resid.* s, pz-H3), 8.77 (*resid.* s, pz-H5/H6), 7.34 (d, 2H, ph-H2/H6), 8.00 (dd, 2H, ph-H3/H5), 2.36 (s, 3H, -CH_3). ^{2}D NMR in [H_6]-DMSO δ ppm; 9.34 (pz-D3), 8.74 (pz-D5/D6)

[D_3]-Htolpztr **13c**: Mass spectrometry HM^+ ion at 241 m/z. ^{1}H NMR in [D_6]-DMSO δ in ppm: 9.33 (d, 1H, pz-H3), 8.77 (m, 2H, pz-H5/H6), 7.34 (d, 2H, ph-H2/H6), 8.00 (dd, 2H, ph-H3/H5), 2.36 (*resid.* m, methyl). ^{2}D NMR in [H_6]-DMSO δ ppm; 2.28 (Methyl-)

[D_4]-Htolpztr **13d**: Mass spectrometry HM^+ ion at 242 m/z. ^{1}H NMR in [D_6]-DMSO δ in ppm: (d, 1H, pz-H3), (dd, 1H, pz-H5), (d, 1H, pz-H6), (*resid.* s, ph-H2/H6), (*resid.* s, ph-H3/H5), (s, 3H, methyl).

[D_6]-Htolpztr **13e**: Mass spectrometry HM^+ ion at 244 m/z. ^{1}H NMR in [D_6]-DMSO δ in ppm: 9.33 (*resid.* s, pz-H3), 8.77 (*resid.* s, pz-H5/H6), 7.34 (d, 2H, ph-H2/H6), 8.00 (dd, 2H, ph-H3/H5), 2.36 (*resid.* m, methyl). ^{2}D NMR in [H_6]-DMSO δ ppm; 9.34 (pz-D3), 8.74 (pz-D5/D6), 2.28 (Methyl-).

[D_7]-Htolpztr **13f**: Mass spectrometry HM^+ ion at 245 m/z. ^{1}H NMR in [D_6]-DMSO δ in ppm: 9.33 (d, 1H, pz-H3), 8.77 (m, 1H, pz-H5/H6), 7.34 (*resid.* s, ph-H2/H6), 8.00 (*resid.* s, ph-H3/H5) 2.36 (*resid.* m, methyl).

[D_{10}]-Htolpztr **13g**: Mass spectrometry HM^+ ion at 248 m/z. ^{1}H NMR in [D_6]-DMSO δ in ppm: 9.33 (*resid.* s, pz-H3), 8.77 (*resid.* s, pz-H5), (*resid.* s, pz-H6), 7.34 (*resid.* s, ph-H2/H6), 8.00 (*resid.* s, ph-H3/H5), 2.36 (*resid.* m, methyl)

Pyridine-1,2,4-triazole based compounds

[D_5]-Hpytr **14b**: Mass spectrometry HM^+ ion at 151 m/z. ^{1}H NMR in [D_6]-DMSO δ in ppm: 8.09 (*resid.* s, py-H3), 7.98 (*resid.* s, py-H4), 7.51 (*resid.* s, py-H5), 8.70 (*resid.*s, py-H6), 8.27 (*resid.* s, tr-H5). ^{2}D NMR in [H_6]-DMSO δ ppm; 7.99 (py-D3), 7.88 (py-D4), 7.51 (py-D5), 8.71 (D6), 8.12 (tr-D5)

[D_7]-Hmepytr **15b**: Mass spectrometry HM^+ ion at 168 m/z. ^{1}H NMR in [D_6]-DMSO δ in ppm: (*resid.* s, py-H3), (*resid.* s, py-H4), (*resid.* s, py-H5), (*resid.* s, py-H6), (*resid.* m, Methyl). ^{2}D NMR in [H_6]-DMSO δ ppm; 7.96 (py-D3), 7.84 (py-D4), 7.38 (py-D5), 8.58 (py-D6), 2.26 (Methyl)

[D_1]-Hphpytr **16b**: Mass spectrometry HM^+ ion at 224 m/z. ^{1}H NMR in [D_6]-DMSO δ in ppm: (d, 1H, py-H3), (dd, 1H, py-H4), (dd, 1H, py-H5), (*resid.* s, py-H6), (d, 2H, ph-H2/H6), 7.54 (dd, 2H, ph-H3/H5) 7.49 (t, 1H, ph-H4), ^{2}D NMR in [H_6]-DMSO δ ppm; 8.67 (py-D6)

[D_4]-Hphpytr **16c**: Mass spectrometry HM^+ ion at 227 m/z. ^{1}H NMR in [D_6]-DMSO δ in ppm: (*resid.* s, py-H3), (*resid.* s, pz-H4), (*resid.* s, py-H5), (*resid.* s, py-H6), (d, 2H, ph-H2/H6), 7.54 (dd, 2H, ph-H3/H5) 7.49 (t, 1H, ph-H4), ^{2}D NMR in [H_6]-DMSO δ ppm; 8.09 (py-H3/H4), 7.49 (py-H5), 8.70 (py-H6).

[D_5]-Hphpytr **16d**: Mass spectrometry HM^+ ion at 228 m/z. ^{1}H NMR in [D_6]-DMSO δ in ppm: (d, 1H, py-H3), (dd, 1H, py-H4), (dd, 1H, py-H5), (d, 1H, py-H6), (*resid.* s, ph-H2/H6), 7.54 (*resid.* s, ph-H3/H5) 7.49 (*resid.* s, ph-H4).

[D_9]-Hphpytr **16e**: Mass spectrometry HM^+ ion at 232 m/z. ^{1}H NMR in [D_6]-DMSO δ in ppm: (*resid.* s, py-H3), (*resid.* s, py-H4), (*resid.* s, py-H5), (*resid.* s, py-H6), (*resid.* s, ph-

H2/H6), 7.54 (*resid.* s, ph-H3/H5) 7.49 (*resid.* s, ph-H4). ^{2}D NMR in [H_6]-DMSO δ ppm; 8.08 (py-H3/H4), 7.48 (py-H5, ph-H3/H5/H4), 8.70 (py-H6), 8.01 (ph-H2/H6).

[D_7]-Hppt **17b**: Mass spectrometry HM^+ ion at 232 m/z. ^{1}H NMR [D_6]-DMSO δ in ppm: 8.17 (*resid.* s, py-H3), 8.01 (*resid.* s, py-H4), 7.54 (*resid.* s, py-H5), 8.77 (*resid.* s, py-H6), 9.33 (*resid.* s, pz-H3), 8.72 (*resid.* s, pz-H5), 8.71 (*resid.* s, pz-H6).

[D_4]-Hppt **17c**: Mass spectrometry HM^+ ion at 232 m/z. ^{1}H NMR [D_6]-DMSO δ in ppm: 8.17 (d, 1H, py-H3), 8.01 (dd, 1H, py-H4), 7.54 (d, 1H, py-H5), 8.77 (*resid.* s, py-H6), 9.33 (*resid.* s, pz-H3), 8.72 (*resid.* s, pz-H5), 8.71 (*resid.* s, pz-H6).

3.6 Bibliography

1. (a) A. Juris, V. Balzani, F. Barigelletti, S. Campagna, P. Belser and A. von Zelewsky *Coord. Chem. Rev.* **1988**, *84*, 85 (b) V. Balzani, S. Campagna, G. Denti, A. Juris, S. Serroni and M. Ventura, *Coord. Chem. Rev.* **1994**, *132*, 1 (c) V. Balzani and F. Scandola, *Supramolecular Photochemistry*, Ellis Horwood: Chichester, UK, **1991** (d) Balzani, V. Ed., *Supramolecular Photochemistry*, Reidel, Dordrecht, **1997** (e) K. Kalyanasundaram, *Coord. Chem. Rev.*, **1982**, *46*, 159

2. (a) V. Balzani, A. Juris, M. Venturi, S. Campagna and S. Serroni, *Acc. Chem. Res.* **1998**, *31*, 26 (b) C. A. Slate, D. R. Striplin, J. A. Moss, P. Chen, B. W. Erickson and T. J. Meyer, *J. Am. Chem. Soc.* **1998**, *120*, 4885 (c) Y.-Z. Hu, S. Tsukiji, S. Shinkai, S. Oishi and I. Hamachi, *J. Am. Chem. Soc.* **2000**, *122*, 241 (d) V. Balzani, A. Juris, M. Venturi, S. Campagna and S. Serroni, *Chem. Rev.*, **1996**, *96*, 759

3. (a) R. P. Thummel, D. Williamson and C. Hery, *Inorg. Chem.*, **1993**, *32*, 1587 (b) S. Chirayil and R. P. Thummel, *Inorg. Chem.*, **1989**, *28*, 812 (c) J. E. O'Brien, T. B. H. McMurry and C. N. O'Callaghan, *J. Chem. Research (s)*, **1998**, 448 and ref. therein (d) C. K. Brush, M. P. Stone and T. M. Harris, *J. Am. Chem. Soc.*, **1988**, *110*, 4405

4. For a recent review see W. R. Browne and J. G. Vos, *Coord. Chem. Rev.*, **2001**, *219*, 761 and ref therein

5. M. J. Cook, A. P. Lewis, G. S. G. McAuliffe, V. Skarda, A. J. Thomson, J. L. Glasper and D. J. Robbins, *J. Chem. Soc., Perkin Trans. 2*, **1984**, 1293

6. G. Fischer and M. Puza, *Synthesis*, **1973**, *4*, 218

7. T. E. Keyes, F. Weldon, E. Müller, P. Pechy, M. Grätzel and J. G. Vos, *J. Chem. Soc. Dalton Trans.*, **1995**, 2705

8. (a) R. M. Hartshorn and J. K. Barton, *J. Am. Chem. Soc.*, **1992**, *114*, 5919 (b) C. G. Coates, P. L. Callaghan, J. J. McGarvey, J. M. Kelly, P. E. Kruger and M. E. Higgins, *J. Raman Spect.*, 2000, **31**, 283

9. T. Keyes, C. M. O'Connor, U. O'Dwyer, C. G. Coates, P. Callaghan, J. J. McGarvey and J. G. Vos, *J. Phys. Chem. A*, **1999**, *103*, 8915

10. C. Hardacre, J. D. Holbrey and S. E. McMath, J. *Chem. Commun.*, **2001**, 367

11. H. Yersin and W. Humbs, *Inorg. Chem.*, **1999**, *38*, 5820

12.(a) T. R. Thomas, R. J. Watts and G. A. Crosby, *J. Chem. Phys.*, **1973**, *59*, 2123 (b) M. E. Frink and P. C. Ford, *Inorg. Chem.*, **1985**, *24*, 1033 (c) R. W. Henning, A. J. Schultz, M. A. Hitchman, G. Kelly and T. Astley, *Inorg. Chem.*, 2000, *39*, 765 (d) R. E. Echols and G. C. Levy, *J. Org. Chem.*, **1974**, *39*, 1321

13. G. W. Kabalka, R. M. Pagni, P. Bridwell, E. Walsh and H. M. Hassaneen, *J. Org. Chem.*, **1981**, *46*, 1513

14.(a) S. Rasku and K. Wähäla, *Tetrahedron*, **2000**, *56*, 913 (b) B. Kuhlmann, E. M. Arnett and M. Siskin, *J. Org. Chem.*, **1994**, *59*, 3098 (c) B. Kuhlmann, E. M. Arnett and M. Siskin, *J. Org. Chem.*, **1994**, *59*, 5377

15. H. Riesen, L. Wallace and E. Krausz, *J. Phys. Chem.*, **1996**, *100*, 17138

16. S.F. McClanahan and J.R. Kincaid, *J. Raman Spectroscopy*, **1984**, *15*, 173

17.(a) P. K. Mallick, G. D. Danzer, D. P. Strommen and J. R. Kincaid, *J Phys. Chem.*, **1988**, *92*, 5628 (b) D. P. Strommen, P. K. Mallick, G. D. Danzer, R. S. Lumpkin and J. R. Kincaid, *J. Phys. Chem.*, **1990**, *94*, 1357 (c) K. Maruszewski, K. Bajdor, D. P. Strommen and J. R. Kincaid, *J. Phys. Chem.*, **1995**, *99*, 6286 (d) S. F. McClanahan and J. R. Kincaid, *J. Am. Chem. Soc.*, **1986**, *108*, 3840

18. E. C. Constable and K. R. Seddon, *J. Chem. Soc., Chem. Commun.*, **1982**, 34

19. G. Stein and E. Würzburg, *J. Chem. Phys.*, **1975**, *62*, 208

20. J. W. Larsen and L.W. Chang, *J. Org. Chem.*, **1978**, *43*, 3602

21. G. Keck and D. Krishnamurthy, *J. Org. Chem.*, **1996**, *61*, 7638

22. J. L. Garnett, M. A. Long, R. F. W. Vining and T. Mole, *J. Am. Chem. Soc.*, **1972**, *94*, 5913

23.(a) L. C. Leitch, *Can. J. Chem*, **1954**, *32*, 813, (b) B. Chenon, L.C. Leitch, R.N. Renaud. L. Pichat, *Bull. Soc. Chim. Fr.*, **1964**, 38

24.(a) J. Saltiel, A. S. Waller, D. F. Sears, Jr. and C. Z. Garrett, *J. Phys. Chem.*, **1993**, *97*, 2516 (b) J. S. Chikos, *J. Org. Chem.*, **1986**, *51*, 53

25. R. R. Fraser and R. N. Renaud., *J. Am. Chem. Soc.*, **1966**, *88*, 4365

26. D. Hesk, J. R. Jones and W. J. S. Lockley, *J. Pharm. Chem.*, **1991**, *80*, 887

27. K. Ofusa-Asante and L. M. Stock, *J. Org. Chem.*, **1987**, *52*, 2938

28. W. J. S. Lockley, *Tet. Lett.*, **1982**, *23*, 3819

29.(a) J. R. Jones, W. J. S. Lockley, S. Y. Lu and S. P. Thompson, *Tet. Lett.*, **2001**, *42*, 331 (b) N. Elander, J. R. Jones, S. Y. Lu and S. Stone-Elandor, *Chem. Soc. Rev.*, **2000**, *29*, 239 (c) S. Anto, G. S. Getvoldsen, J. R. Harding, J. R. Jones, S-Y. Lu and J. C. Russell, *J. Chem, Soc., Perkin Trans. 2*, **2000**, 2208

30. W. T. Erb, J. R. Jones and S-Y. Lu, *J. Chem. Res. (S)*, **1999**, 728

31. A. R. Katritzky, D. A. Nichols, M. Siskin, R. Murugan and M. Balasubramanian, *Chem. Rev.*, **2001**, *101*, 837

32. T. Junk and W. J. Catallo, *Chem. Soc. Reviews*, **1997**, *26*, 401

33. Y. Yang and R. F. Evilia, *J. Supercritical. Fluids*, **1999**, *12*, 165

34.(a) T. Junk and W. J. Catallo, *Tet. Lett.*, **1996**, *37*, 3445 (b) T. Junk, W. J. Catallo and J. Elguero, *Tet. Lett.*, **1997**, *38*, 6309

35. J. Yao and R.F. Evilia, *J. Am. Chem. Soc.*, **1994**, *116*, 11229

36.(a) J. A. Zoltewicz and C. L. Smith, *J. Am. Chem. Soc.*, **1967**, *89*, 3358 (b) J.P. Schaefer and L. J. Bertram, *J. Am. Chem. Soc.*, **1967**, *89*, 4121

37.(a) A. Islam, N. Ikeda, K. Nozaki and T. Ohno, *J. Chem. Phys.*, **1998**, 109, 4900 (b) E. Krausz, G. Moran and H. Riesen, *Chem. Phys. Lett.*, **1990**, *165*, 401 (c) E. M. Kober, J. V. Casper, R. S. Lumpkin and T. J. Meyer, *J. Phys. Chem.*, **1986**, *90*, 3722 (d) M. A. Bergkamp, P. Gutlich, T. L. Netgel and N. Sutin, J. Phys. Chem., **1983**, *87*, 3877 (e) J. L. Wong and J. H. Heck Jr., *J. Org. Chem.*, **1974**, *39*, 2398 (f) R. A. Olofson and J. M. Landesberg, *J. Am Chem. Soc.*, **1966**, *88*, 4263 (g) R. A. Olofson, J. M. Landesberg, K. N. Houk and J. S. Michealman, *J. Am Chem. Soc.*, **1966**, *88*, 4265 (h) R. A. Coburn, J.M. Landesberg, D. S. Kemp and R. A. Olofson, *Tetrahedron*, **1970**, *26*, 685

38. A. Streitwieser, Jr., W. B. Hollyhead, A. H. Pudjaatmaka, P. H. Owens, T. L. Kruger, P. A. Rubenstein, R. A. MacQuarrie, M. L. Brokaw, W. K. C. Chu and H. M. Niemeyer, *J. Am. Chem. Soc.*, **1971**, *93*, 5088

39.(a) H. Riesen, E. Krausz, W. Luginbuhl, M. Biner, H. U. Güdel and A. Ludi, *J. Chem. Phys.*, **1992**, *96*, 4131 (b) S. J. Milder and B. S. Brunschwig, *J. Phys. Chem.*, **1992**, 96, 2189 (c) J. van Houten and R. J. Watts, *J. Am. Chem. Soc.*, **1976**, *98*, 4853 (b) J. van Houten and R. J. Watts, *Inorg. Chem.*, **1978**, 17, 3381 (d) E. Buncel, O. Clement and I. Onyido, *J. Am. Chem. Soc.*, **1994**, *116*, 2679 (e) O. Clement, A. W. Roszak and E. Buncel, *J. Am. Chem. Soc.*, **1996**, *118*, 612 (f) E. Buncel and O. Clement, *J. Chem. Soc. Perkins Trans. 2*, **1995**, 1333

40. B. R. Henry and J. L. Charlton, *J. Am. Chem. Soc.*, **1973**, *95*, 2782

41. T. C. Schwendemann, P. S. May, M. T. Berry, Y. Hou and C. Y. Meyers, *J. Phys. Chem. A*, **1998**, *102*, 8690

42. D. P. Strommen, P. K. Mallick, G. D. Danzer, R. S. Lumpkin and J. R. Kincaid, *J. Phys. Chem.*, **1990**, *94*, 1357

43. U. O'Dwyer, *MSc. Thesis*, Dublin City University, Dublin Ireland, **1997**

44. S. Campagna, A. Giannetto, S. Serroni, G. Denti, S Trusso, F. Mallamace, and N. Micalli, *J. Am. Chem. Soc.*, **1995**, *117*, 1754 and ref therein

Chapter 4

Probing excited state electronic structure of monomeric ruthenium(II) and osmium(II) tris heteroleptic complexes by selective deuteriation

The application of deuteriation in inorganic chemistry is discussed in Chapter 1. Its use as a spectroscopic probe both in simplification of NMR and Raman spectra and as a probe into the excited state structure of heteroleptic complexes is already well known. In this chapter, deuteriation will be employed extensively to probe the excited state structure of two series of Ru(II) and Os(II) polypyridyl complexes. In particular the effect of deuteriation on emission lifetime and ground and excited state resonance Raman spectra is considered.

4.1 Introduction

Room temperature luminescence from $[Ru(bpy)_3]^{2+}$ was first reported by Paris and Brandt.[1] Ru(II) tris-diimine complexes have since been studied intensively, in particular with respect to their photophysical and photochemical properties.[2] Despite the large number of studies carried out already, the nature of the lowest excited states of these complexes is still the subject of considerable attention and debate.[3] In particular the localisation/delocalisation, over all three ligands, of the lowest lying ^{3}MLCT excited state is of most interest.

4.1.1 Probing ground and excited electronic states - resonance Raman and deuteriation.

Resonance Raman has proven an invaluable tool in the study of both electronic absorption spectra of homo- and hetero-leptic Ru(II) polypyridyl complexes and in particular their lowest excited electronic states.[4,5,6,7] Kincaid and coworkers have carried out an extensive investigation of the parent complex $[Ru(bpy)_3]^{2+}$ and its selectively deuteriated isotopologues.[8] It was found through rR that the excited state of $[Ru(bpy)_3]^{2+}$ is best described as being spatially localised on a single bpy ligand rather than over all three ligands (see Figure 1.7).[8] The primary basis for this conclusion is that the excited state resonance Raman spectrum of the complex very closely resembles that of 2,2-bipyridyl anion radical (Li^+bpy^{-*}). In addition, the usefulness of resonance Raman in studying heteroleptic Ru(II) complexes has also been demonstrated in the complexes such as $[Ru(bpy)_2(pypz)]^{2+}$ (where pypz is 2-(2-pyridyl)-pyrazine), in which the lowest emissive excited state has been determined to be localised on the pyrazine moiety.[7b] These studies have provided an invaluable set of data by which the resonance Raman spectra of many bpy and pyrazine Ru(II) and Os(II) based complexes, including those described in this chapter, can be interpreted.

Several studies have been carried out on heteroleptic complexes analogous to $[Ru(bpy)_3]^{2+}$ (*e.g.* $[Ru(bpy)_x(LL)_{3-x}]^{2+}$ where LL = phen or ph_2phen and x = 0-3).[5,5] The results of these studies demonstrate the intricate nature of Ru(II) polypyridyl photophysics and the importance of environment to electronic excited state structure.

Turro and co-workers have reported several studies of the ground and excited state resonance Raman spectra of mixed ligand Ru(II) complexes $[Ru(bpy)_x(phen)_{3-x}]^{2+}$ and $[Ru(bpy)_x(ph_2phen)_{3-x}]^{2+}$ (where x = 1 or 2).[5] For the former complexes involving the

ligands bpy and phen, only excited state bpy^{*-} modes were observed in either aqueous or acetonitrile solution, indicating that the emitting state is a bpy based ^{3}MLCT. It should be noted however that the resonance enhancement of phen modes are generally much lower than for bpy at the excitation wavelength (355 nm).[5a] For the latter complexes both bpy^{*-} and ph_2phen^{*-} modes are observed, confirming that both bpy and ph_2phen based ^{3}MLCT excited states are populated, significantly.

Confirmation of the localisation of the emitting lowest excited state of $[Ru(bpy)_x(phen)_{3-x}]^{2+}$ (where x = 1 or 2) is bpy based has been obtained by Chang *et al.*, whom have examined their picosecond excited state Raman time resolved spectra in aqueous and acetonitrile solution. They have concluded that the excited state is completely localised on the lower energy bpy ligand in each case.[5a] In contrast, for $[Ru(bpy)_2(ph_2phen)]^{2+}$ in aqueous media localisation occurs on both the bpy and ph_2phen ligands. However localisation on one or other ligand may be readily achieved by variations in the solvent environment, and by the presence of surfactants, which serve to selectively stabilise either bpy or ph_2phen.[5]

Vos and co-workers have employed resonance Raman and excited state resonance Raman extensively in their investigations of the excited state properties of Ru(II) polypyridyl complexes containing 1,2,4-triazoles similar to the complexes employed reported in this chapter.[9] Ground state resonance Raman spectra of both the protonated and deprotonated complex $[Ru(bpy)_2(Mepztr)]^+$ in acetonitrile have been reported by Nieuwenhuis *et al.*.[10] For the deprotonated complex the wavelength dependence of the relative intensities of the bpy based and pyrazine based symmetrical stretching modes is not particularly strong with both sets of modes being observed at 458, 488 and 514.5 nm excitation. This indicates that a significant overlap between both sets of ^{1}MLCT states occurs in this complex. For the protonated complex a different situation was observed, with low energy excitation resulting in much better rR enhancement for the pyrazine based modes (1720, 1558, 1512, 1455 and 1277 cm^{-1}) than for the bpy based modes (1603, 1559, 1489, 1319 and 1185 cm^{-1}). These studies demonstrate clearly both the effect of protonation on the relative energy of the bpy and pyrazine based MLCT states, with the latter being stabilised by protonation. In addition they show the utility of rR in deconvoluting the broad set of ^{1}MLCT absorption bands observed for Ru(II) polypyridyl complexes. In contrast to ground state resonance Raman, excited state resonance Raman allows for the identification of the lowest long lived excited states of Ru(II) polypyridyl complexes. For

the complex $[Ru(bpy)_2(pztr)]^+$, three sets of vibrational features are observed under 355 nm excitation, neutral bpy modes, neutral pyrazine modes and bpy^- modes (1018, 1212, 1288, 1425 and 1548 cm^{-1}), confirming the assignment of the emitting excited state as being bpy based. For the protonated complex $[Ru(bpy)_2(Hpztr)]^{2+}$, the excited state rR spectra observed were considerably different with no evidence for bpy^- in the spectrum. Instead neutral bpy and $pyrazine^-$ modes (1409, 1431 and 1536 cm^{-1}) were observed. Selective deuteriation of the ligands was employed to confirm the assignments made.

4.1.2 Probing ground and excited electronic states – emission lifetimes and deuteriation.

The effect of deuteriation on the vibrationally coupled deactivation of electronically excited states of $[Ru(bpy)_3]^{2+}$ was first reported by Van Houten and Watts in 1975.[11] In contrast to the dramatic increase in emission lifetimes observed for the deuteriation of the free ligand (100% increase) only a more modest 20% increase was observed for $[Ru(bpy)_3]^{2+}$. The effect of partial regioselective deuteriation of $[Ru(bpy)_3]^{2+}$ is discussed in Chapter 1. Krausz *et al.* have shown that sequential deuteriation of one, two and three ligands resulted in a statistical increase in the emission lifetime at 298 K or rather a statistical decrease in the observed radiative rate constant (see Figure 4.1).[12]

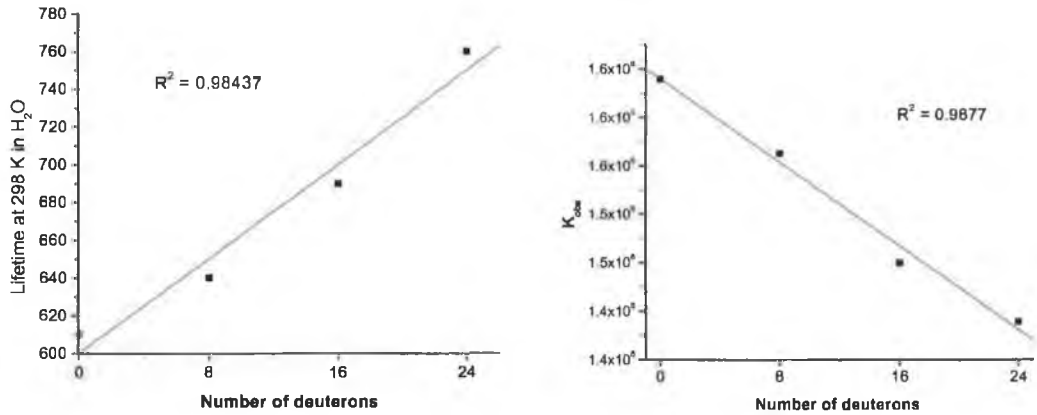

Figure 4.1 *Effect of deuteriation of 0, 1, 2 and 3 of the bpy ligands on the emission properties of* $[Ru(bpy)_3]^{2+}$*; left -* τ_{deg} *vs. No. of deuterons, right* k_{obs} *vs. No. of deuterons*[12]

Kincaid and coworkers have taken a different approach in examining the effect of selective deuteriation.[7c] Luminescence lifetime measurements for a series of tris complexes of selectively deuteriated bpy ligands are shown in Figure 4.2. It can be seen that as for the results obtained by Krausz *et al.* the increase in observed emission lifetime depends on the number of deuterons, however an additional observation is that

deuteriation at the 3 and 4 positions has relatively little effect, except when all other positions are deuteriated. No explanation for this anomaly was proposed by Kincaid and coworkers.

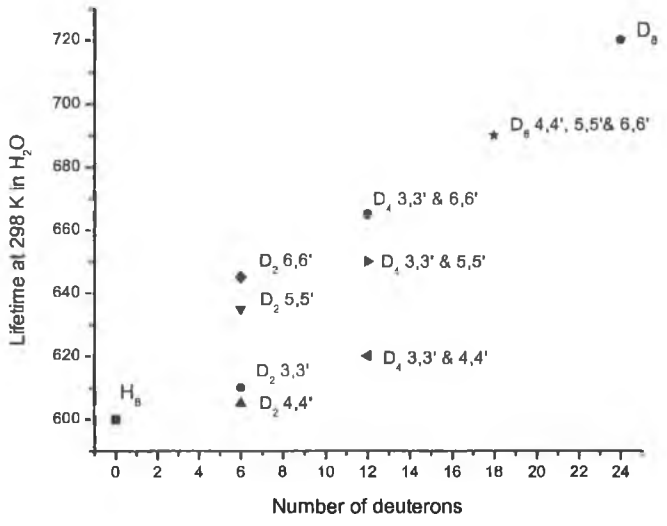

Figure 4.2 *Effect of deuteriation of 0, 1, 2 and 3 of the bpy ligands on the emission properties of* $[Ru(bpy)_3]^{2+}$ [7c]

These studies illustrate an important experimental aspect in the interpretation and comparison of independent studies. In both studies the values obtained for the deaerated emission lifetime of $[Ru(bpy)_3]^{2+}$ and $[Ru([D_8]\text{-}bpy)_3]^{2+}$ were 600/610 and 720/760, respectively. The discrepancy in values obtained may arise from several sources. The most likely are that of incomplete deuteriation, variations in solvent water content and use of different data fitting procedures. Nevertheless it serves as a warning against the over-analysis of relatively small data sets and the use of data from several sources without the use of standards for comparison.

One aspect of these studies is somewhat perplexing. For $[Ru(bpy)_3]^{2+}$ the effect of deuteriation although discernable is nevertheless quite small in comparison with its effect on the excited state lifetimes of rare earth ions and organic compounds.[13] The process of non-radiative deactivation by vibrational relaxation involves the vibrionic adiabatic coupling between excited state promoter modes and ground state acceptor modes.[8c] It has been determined from low temperature high resolution emission spectroscopy and from the absence of C-H stretching vibrations in the excited state resonance Raman spectrum of $[Ru(bpy)_3]^{2+}$ that principle acceptor modes for non-radiative vibrationally coupled deactivation are totally symmetric skeletal modes and not C-H symmetric stretching

vibrations. Comparison of experimentally determined non-radiative rate constants and the calculated vibrational modes (which are potential promoter modes) shows that the most important modes are non-totally symmetric in plane C-C-C and C-C-H bending motions of the bpy ligand. In summary, it is most likely that for $[Ru(bpy)_3]^{2+}$ the origin of the deuteriation effect may not be in inhibiting the dissipation of electronic energy but rather in reducing the vibrionic coupling between the excited state promoter vibrionic modes and the ground state acceptor vibrionic modes.

In contrast to $[Ru(bpy)_3]^{2+}$, for complexes containing 1,2,4-triazole moieties the effect of deuteriation has been reported to result in some cases in a doubling of emission lifetime.[14] To add further confusion to the standard excited state model for these complexes, temperature dependent studies on the emission properties of 1,2,4-triazoles resulted in the observation of a further oddity, dual emission! (see Chapter 5).

4.1.3 Osmium(II) polypyridyl complexes

Although Os(II) polypyridyl complexes show much greater stability towards photodecomposition compared to their ruthenium analogues, the luminescence properties have received much less attention, in part due to the shorter emission lifetimes (*cf.* energy gap law).[15] This, together with lower quantum yields of emission, makes investigation of the excited state Os(II) polypyridyl complexes by excited state and time resolved resonance Raman inherently difficult.

Deuteriation has been employed in several studies of the lifetime of both MLCT and LMCT excited states of Os(II) and Os(III) polypyridyl complexes.[15,16] In each of these studies a significant increase in the lifetime of these states was observed upon deuteriation. For several heteroleptic Os(II) polypyridyl complexes where the ligand on which the excited state is based is deuteriated a doubling of emission lifetime is observed.[15]

In this chapter, two series of selectively deuteriated Ru(II) and Os(II) complexes are examined in an attempt to answer several key questions. Firstly, is the small increase in emission lifetime observed for $[Ru(bpy)_3]^{2+}$ upon deuteriation, observed for complexes of the type $[Ru(bpy)_x(LL)_{3-x}]^{2+}$ where x = 0-3 and for their Os(II) analogues. Secondly, if this is the case can partial deuteriation be used in the locating the lowest lying emissive state on a particular ligand (*e.g.* ph_2phen). For $[Ru(bpy)_3]^{2+}$ the effect of deuteriation

although significant is small in comparison with its effect on the excited state lifetimes of rare earth ions and organic compounds.[13] Nevertheless, its potential as a spectroscopic probe, even for these systems, has been demonstrated by Vos and coworkers for 1,2,4-triazole and 1,2,4-triazine based Ru(II) complexes.[17] In addition selective deuteriation together with ground and excited state resonance Raman spectroscopy are employed in probing the excited state structure of the complexes $[Ru(bpy)_2(phpztr)]^+$and $[Ru(bpy)_2(phpytr)]^+$.

4.2 Results and Discussion

The non-deuteriated complexes of the type $[Ru(bpy)_x(ph_2phen)_{3-x}]^{2+}$ have been prepared previously and have been the focus of several detailed studies.[5,18] The osmium based heteroleptic complexes are very similar to the Ru(II) complexes with only minor changes to their ^1H NMR spectra. The synthesis and structural characterisation of these complexes is dealt with in Chapter 2 and will not be discussed in detail here. Likewise the electronic spectroscopic properties of the complexes are already known and will only be discussed briefly in relation to trends observed. The deuteriation dependence of the luminescence lifetime data for these complexes is, however, new and will be discussed in more detail.

4.2.1 Synthesis and structural characterisation

The ^1H NMR spectra of the complexes of type $[Ru(bpy)_x(ph_2phen)_{3-x}]^{2+}$ and $[Os(bpy)_x(phen)_{3-x}]^{2+}$ are relatively simple due to the highly symmetric nature of the complexes ($\sim C_{2v}$). Deuteriation allows for confirmation of assignments, which are readily made by ^1H COSY NMR spectroscopy. The ^1H NMR spectra of the complex $[Ru(bpy)_2(ph_2phen)]^{2+}$ and some of its isotopologues are shown in Figure 3.5. Heteroleptic complexes incorporating the 1,2,4-triazole moiety are much less symmetric and display more complicated ^1H NMR spectra with considerable overlap of ^1H NMR signals. For these complexes deuteriation becomes much more useful in the assignment of spectra as can be seen in Figure 4.3 where suppression of bpy resonances allows for accurate identification of $phpztr^-$ resonances.

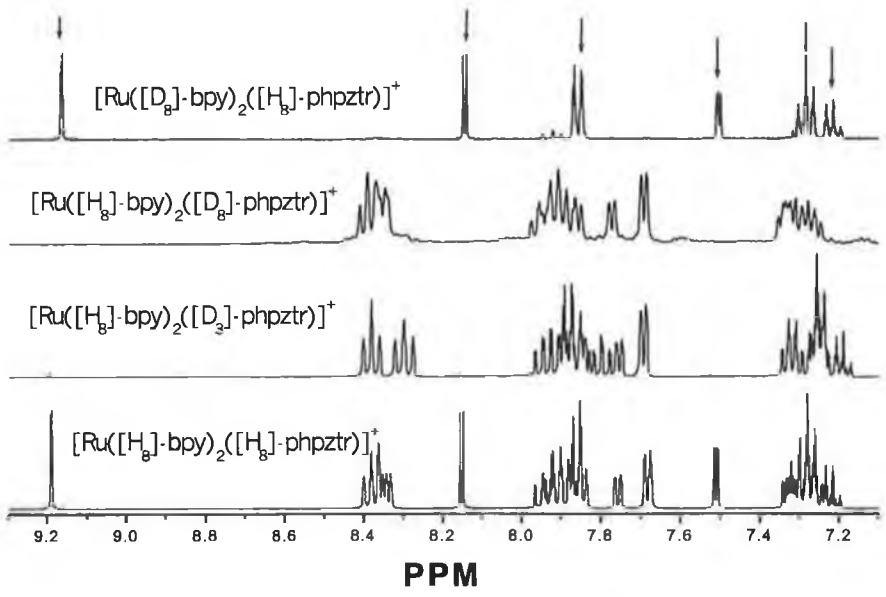

Figure 4.3 *^1H NMR spectra of $[Ru(bpy)_2(phpztr)]^+$ and some of its isotopologues in CD_3CN ($phpztr^-$ signals indicated by arrows)*

^2D NMR spectroscopy

As discussed in Chapter 3, deuterium has a nuclear spin greater than 0 ($I = 1$) and it is possible to obtain ^2D NMR spectra of complexes containing deuteriated ligands. Unfortunately, obtaining useful spectra is rendered difficult by practical problems, most notably that of low NMR sensitivity of ^2D compared with ^1H. Nevertheless ^2D NMR spectra of several partially and fully deuteriated complexes have been obtained and show broad signals at approximately the same chemical shift as the perprotio complex. The quality of the spectra is unfortunately quite poor and does not warrant further discussion.

4.2.2 UV.Vis Absorption and emission spectroscopy

The UV.Vis absorption and emission spectra of all complexes were found to be independent of the level of deuteriation to within the resolution of the spectra available. This is not unexpected as although deuteriation affects the vibrational fine structure of emission and absorption spectra, these differences are only observed at very low temperatures with high-resolution emission spectroscopic techniques (< 10 K).[19]

4.2.2.1 Heteroleptic complexes of bpy, phen and ph_2phen

The absorption and emission spectra of the complexes $[Ru(bpy)_x(ph_2phen)_{3-x}]^{2+}$ are shown in Figure 4.4. A progressive hypochromic shift in the absorption maximum is

observed on successive substitution of bpy with ph_2phen, suggesting the lowering of the MLCT bands of the complex by ph_2phen substitution, in agreement with the trends observed in the emission spectra. In addition the MLCT band (which is in reality several overlapping bands) broadens considerable on increasing substitution of bpy with ph_2phen.

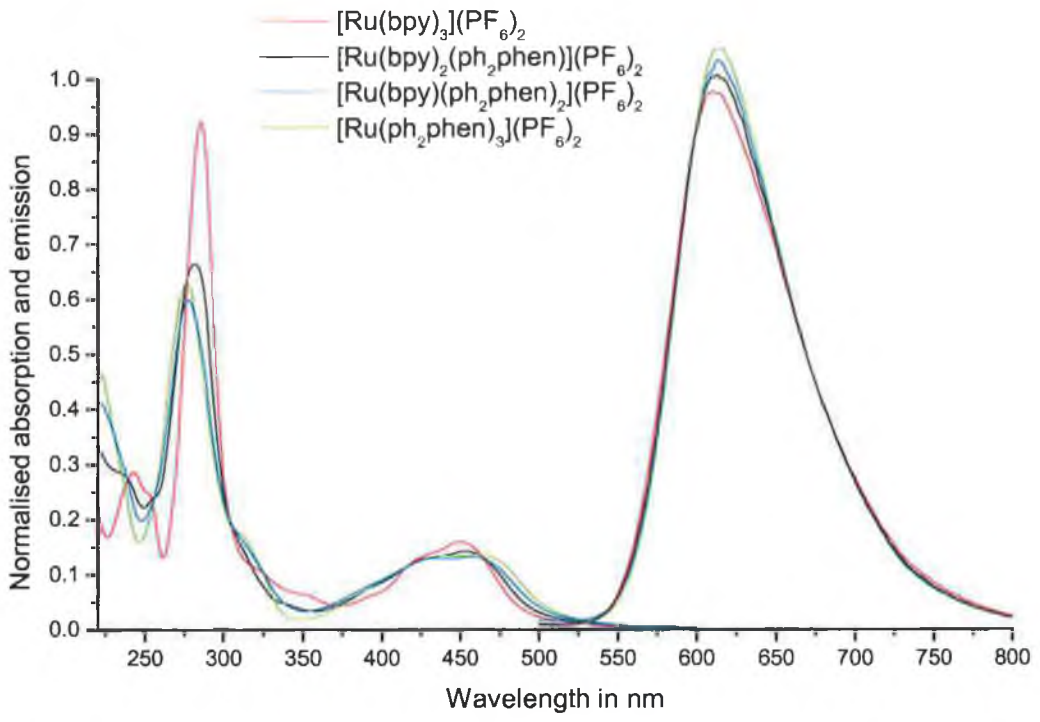

Figure 4.4 *Absorption and emission spectra of the four per-protonated Ru(II) complexes. (The spectral abs./intensity are adjusted for clarity)*

The shift to the red in the emission λ_{max} on increasing substitution of bpy with ph_2phen is also observed, which is as would be expected, considering that the MLCT excited states of ph_2phen are slightly lower in energy than that of bpy.[5d] However the change is of the order of 10 nm (~ 200 cm^{-1}) and hence represents only a minor change in terms of estimation of quantum yield of emission. Of more significance is the progressive change in the band shape of the emission spectrum. On increasing substitution of bpy for ph_2phen the emission full width at half maximum (FWHM) decreases. This can be attributed to the change in vibrational fine structure resulting from the increased rigidity of the ph_2phen ligand. This is of significance as it implies that the skeletal vibrational modes are restricted in amplitude and hence are less capable of mediating non-radiative excited state deactivation (*vide infra*).

The spectroscopic properties of Os(II) polypyridyl complexes are in general quite similar to their Ru(II) analogues. There are, however, important differences. The increase in spin orbit coupling observed for osmium complexes results in the formally spin forbidden ^{3}MLCT absorption bands (500 to 700 nm) having increased intensity. The higher energy 5d orbitals relative to the 4d orbitals results in a reduced energy gap between the metal based ground state and the lowest MLCT excited states and a significant lowering in the energy of the emission λ_{max}. As for the Ru(II) complexes increasing substitution of bpy with phen results in a blue-shift in the emission λ_{max}.[5] In contrast to the substitution of bpy with ph_2phen, the effect of substitution with phen is much larger (22 nm ~ 420 cm^{-1}). At 77 K however the shift in λ_{max} of the emission with increasing phen substitution is less pronounced, indicating phen is less affected by the solvent environment than bpy is. The energy of the emission bands relative to $[Ru(bpy)_3]^{2+}$ and $[Os(bpy)_3]^{2+}$, indicates that the relative energy of the MLCT transitions are in the order ph_2phen< bpy < phen.

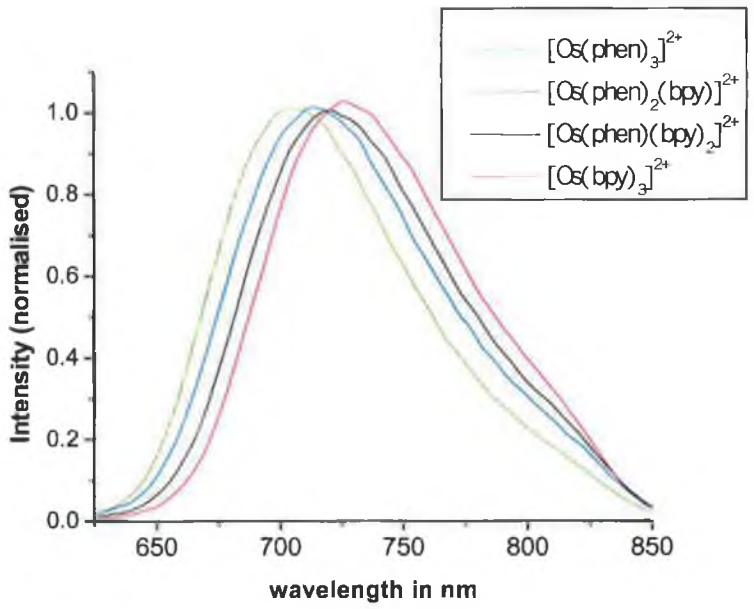

Figure 4.5 *Change in emission spectrum upon increasing substitution of bpy for phen at 298 K in acetonitrile solution*

4.2.2.2 1,2,4-Triazole and H_2dcb based complexes

The absorption and emission properties of Ru(II) polypyridyl complexes incorporating 1,2,4-triazole based ligands and H_2dcb are quite similar to the parent $[Ru(bpy)_3]^{2+}$ complexes. These complexes (see Table 4.4 and Table 4.5) do however exhibit acid/base properties in accessible pH ranges (see Chapter 1). In the case of pyrazine-triazole based

complexes protonation results in a blue shift in the absorption spectrum indicating that the majority of excited singlet states are destabilised (see Figure 4.6).

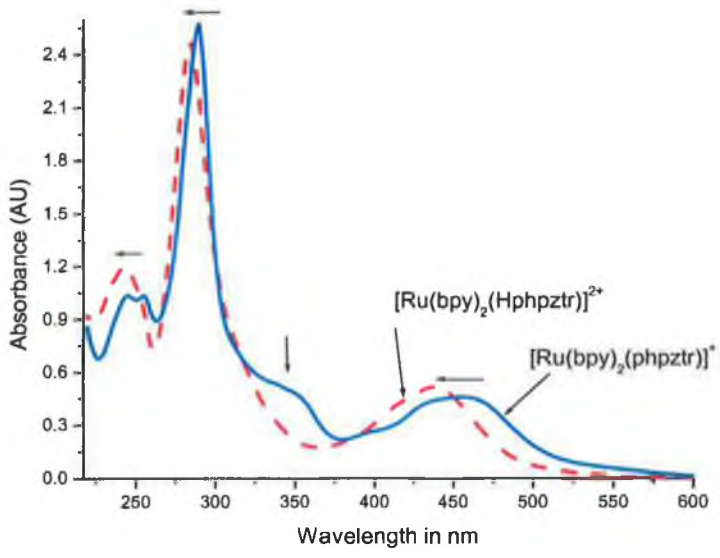

Figure 4.6 Absorption spectra of $[Ru(bpy)_2(phpztr)]^+$ (blue) and $[Ru(bpy)_2(Hphpztr)]^{2+}$ (red) in acetonitrile

In contrast, for these complexes the effect of protonation on the emission spectrum is more complicated. Addition of up to 6 mole equivalents of trifluoroacetic acid results in a red shift in the emission spectrum and an increase in emission intensity. Further addition of acid results in a blue shift in the emission λ_{max} and a significant reduction in emission intensity.

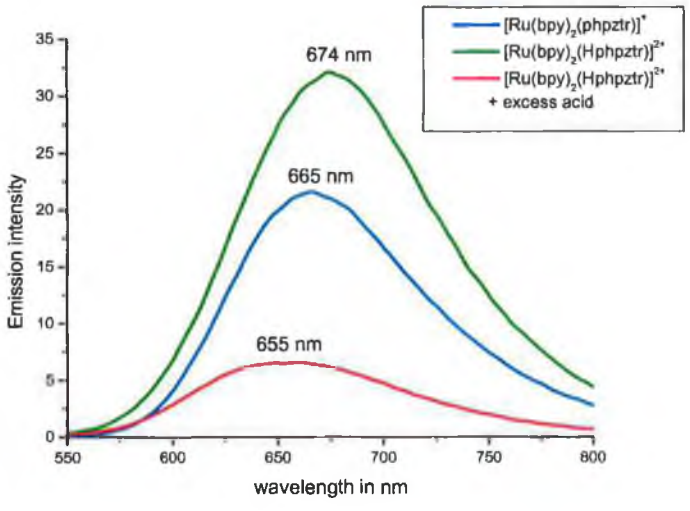

Figure 4.7 *Emission spectra of $[Ru(bpy)_2(phpztr)]^+$ (blue) and $[Ru(bpy)_2(Hphpztr)]^{2+}$ (green/red) in acetonitrile at 298 K*

For the complex [Ru(bpy)(dcb^{2-})] and its isotopologues, protonation results in a large red shift in the emission λ_{max} from 642 to 679 nm (see Table 4.4). In both cases the effect of protonation is to stabilise the lowest emissive state relative to the ground state. This is not unexpected and is due to destabilisation of the ground state (due to a reduction in the σ-donor strength of the ligand and hence reduction in CFSE) and to the stabilization of the ligand based π* orbitals involved in the ^{3}MLCT excited state.

4.2.3 Isotope effects on emission lifetimes

4.2.3.1 Ru(II) and Os(II) polypyridyl complexes of bpy, phen and ph_2phen

Lifetime measurements of Ru(II) polypyridyl complexes (and to a lesser extent Os(II) complexes) are particularly sensitive to oxygen. For some of the Ru(II) complexes displacement of O_2 by N_2 or Ar by gas purge was found to be insufficient and hence four freeze-pump-thaw cycles were carried out before sample lifetimes were measured. In several cases the measurements were repeated employing fresh solutions. In all cases the repeat measurements arrived at results well within the estimated experimental error (+/- 2.5 %).

	τ (ns)	ϕ (*10^{-2})		τ (ns)
$[Ru(bpy)_3]^{2+}$	163 (190)*	1.2*	$[Ru([D_8]\text{-}bpy)_3]^{2+}$	165
$[Ru(bpy)_2(ph_2phen)]^{2+}$	170	9.0	$[Ru([D_8]\text{-}bpy)_2(ph_2phen)]^{2+}$	162
			$[Ru(bpy)_2([D_{10}]\text{-}ph_2phen)]^{2+}$	161
			$[Ru(bpy)_2([D_{14}]\text{-}ph_2phen)]^{2+}$	167
			$[Ru(bpy)_2([D_{16}]\text{-}ph_2phen)]^{2+}$	170
			$[Ru([D_8]\text{-}bpy)_2([D_{16}]\text{-}ph_2phen)]^{2+}$	169
$[Ru(bpy)(ph_2phen)_2]^{2+}$	172	7.5	$[Ru([D_8]\text{-}bpy)(ph_2phen)_2]^{2+}$	174
			$[Ru(bpy)([D_{16}]\text{-}ph_2phen)_2]^{2+}$	171
			$[Ru([D_8]\text{-}bpy)([D_{16}]\text{-}ph_2phen)_2]^{2+}$	184
$[Ru(ph_2phen)_3]^{2+}$	175	8.0	$[Ru([D_{14}]\text{-}ph_2phen)_3]^{2+}$	179

***Table 4.1** Measurements in aerated acetonitrile at 25 °C. *literature value. All values assumed to have 5 % error.*

In the case of the complex $[Ru(bpy)_2([D_{14}]\text{-}ph_2phen)](PF_6)_2$ a significant emission was observed at higher energy than the Ru(II) based emission, by its very short lifetime at room temperature (sub 6 ns) and its observation only when excitation was carried out below 350 nm, it has been assigned as being due to an organic impurity. Aerated and deaerated luminescence lifetime data are presented in Table 4.1 and Table 4.2, respectively.

	τ (μs)	ϕ		τ (μs)	ϕ
$[Ru(bpy)_3]^{2+}$	1.0*	0.06*	$[Ru([D_8]\text{-}bpy)_3]^{2+}$	1.1	N/A
$[Ru(bpy)_2(ph_2phen)]^{2+}$	2.5	0.14	$[Ru([D_8]\text{-}bpy)_2(ph_2phen)]^{2+}$	3.1	0.17
			$[Ru(bpy)_2([D_{10}]\text{-}ph_2phen)]^{2+}$	2.4	N/A
			$[Ru(bpy)_2([D_{14}]\text{-}ph_2phen)]^{2+}$	2.4/2.5**	0.14**
			$[Ru(bpy)_2([D_{16}]\text{-}ph_2phen)]^{2+}$	2.6	0.15
			$[Ru([D_8]\text{-}bpy)_2([D_{16}]\text{-}ph_2phen)]^{2+}$	3.3	0.15
$[Ru(bpy)(ph_2phen)_2]^{2+}$	4.6	0.16	$[Ru([D_8]\text{-}bpy)(ph_2phen)_2]^{2+}$	4.4	0.15
			$[Ru(bpy)([D_{16}]\text{-}ph_2phen)_2]^{2+}$	5.0	0.20
			$[Ru([D_8]\text{-}bpy)([D_{16}]\text{-}ph_2phen)_2]^{2+}$	5.4	0.18
$[Ru(ph_2phen)_3]^{2+}$	6.3	0.25			
$[Ru(ph_2phen)_3]Cl_2$	5.25	N/A	$[Ru([D_{14}]\text{-}ph_2phen)_3]Cl_2$	6.4	N/A

Table 4.2 *Measurements in degassed (freeze-pump-thaw 4 cycles) acetonitrile at 25 °C. *Literature value. **Impurity detected which could possibly be involved in quenching of emission. All values assumed to have 5 % error. N/A not available. Unless indicated otherwise all complexes used are PF_6^- salts.*

For $[Ru(bpy)_2(ph_2phen)]^{2+}$ and $[Ru(bpy)(ph_2phen)_2]^{2+}$ an increase of 30 % and 17 % in emission lifetime is observed upon complete deuteriation, which is in line with the 20% increase found by Van Houten and Watts. Assuming an error of 5 % (although the actual error is much less) then the minimum % increase is 20 and 6 %, respectively.

In the case of $[Ru(bpy)(ph_2phen)_2]^{2+}$ deuteriation of bpy appears to have no effect on the observed emission lifetime, whereas deuteriation of the ph_2phen ligands results in 8 % increase in emission lifetime. This is odd in the sense that if the overall rate of decay is additive over the component decay rates then the difference in increase from single ligand deuteriation to full deuteriation should be the same as the increase found on deuteriation of two ligands. This indicates that although each ligand contributes to some extent to the overall decay rate, the contribution is dependent on the number of ligands deuteriated more than the nature of the ligands deuteriated. The results for this series of complexes show no clear evidence for the localisation of the emitting excited state on either bpy or ph_2phen. This is in agreement with the excited state resonance Raman spectra obtained by Turro *et al.*.[5c] In aqueous or acetonitrile solution features identifiable as bpy^- and ph_2phen^- were observed, indicating both excited states are populated. The relative proportion of each state populated is difficult to determine due to the large variation in resonance enhancement of Raman signals between different ligands.

The effect of increasing substitution of bpy for phen or ph_2phen on the emission lifetime is readily accounted for by two factors. Firstly the increased structural rigidity of the ligand and loss of C-H oscillators in the order bpy < phen <ph_2phen, makes vibrationally coupled deactivation via skeletal modes less important to the overall non-radiative rate constant K_{nr}. Secondly, the increased size of the ligand in the same order results in an increased spatial delocalisation of the excited electron and the excited state geometry of the complex is less distorted compared with the ground state making low frequency vibrational modes less important towards deactivation. In addition the decreased excited state distortion (S is reduced) results in a relative increase in the importance of high energy C-H stretching modes towards non-radiative deactivation and a greater deuteriation effect would be expected. These effects are particularly important for the Os(II) complexes examined.

Luminescence lifetime data for a series of homo- and heteroleptic Os(II) complexes are presented in Table 4.3.

	τ (ns) 298 K aerated	**[a]τ (ns) 298 K**	**k_{obs} *10^7**	**[b]τ (ns) 77 K**	**k_{obs} *10^5**	**[c]Lit. 298K value[15]**
$[Os(bpy)_3]^{2+}$	40	60	1.61	1150	8.69	60
$[Os(bpy)_2(d_8\text{-bpy})]^{2+}$	44	70	1.43	1560	6.41	--
$[Os(d_8\text{-bpy})_2(bpy)]^{2+}$	49	80	1.25	1990	5.03	--
$[Os(d_8\text{-bpy})_3]^{2+}$	49	100	1.00	2990	3.34	112
$[Os(bpy)_2(phen)]^{2+}$	**45**	**75**	**1.33**	**1480**	**6.76**	--
$[Os(bpy)_2(d_8\text{-phen})]^{2+}$	**46**	**77**	**1.30**	**1780**	**5.62**	--
$[Os(d_8\text{-bpy})_2(phen)]^{2+}$	**56**	**114**	**0.88**	**2650**	**3.78**	--
$[Os(d_8\text{-bpy})_2(d_8\text{-phen})]^{2+}$	**57**	**126**	**0.79**	**3800**	**2.63**	--
$[Os(bpy)(phen)_2]^{2+}$	50	97	1.03	1820	5.49	--
$[Os(d_8\text{-bpy})(phen)_2]^{2+}$	59	134	0.75	2500	4.00	--
$[Os(bpy)(d_8\text{-phen})_2]^{2+}$	50	104	0.96	2550	3.92	--
$[Os(phen)_3]^{2+}$	**62**	**228**	**0.44**	**2440**	**4.09**	**262**
$[Os(phen)_2(d_8\text{-phen})]^{2+}$	**67**	**276**	**0.36**	**3310**	**3.02**	--
$[Os(d_8\text{-phen})_2(phen)]^{2+}$	**69**	**320**	**0.31**	**4040**	**2.48**	--
$[Os(d_8\text{-phen})_3]^{2+}$	**74**	**480**	**0.21**	**6910**	**1.45**	--

Table 4.3 *Luminescence lifetime data for osmium complexes. (a) Measurements at 298 K in deaerated (Argon purge),(b) in butyronitrile (c) Literature value for dearated solutions at 298 K. All values 5 % error. N/A = not available*

In agreement with the findings of Krausz *et al.* for $[Ru(bpy)_3]^{2+}$, deuteriation of individual ligands results in a statistical decrease in the observed radiative rate constant for both $[Os(bpy)_3]^{2+}$ and $[Os(phen)_3]^{2+}$.[12]

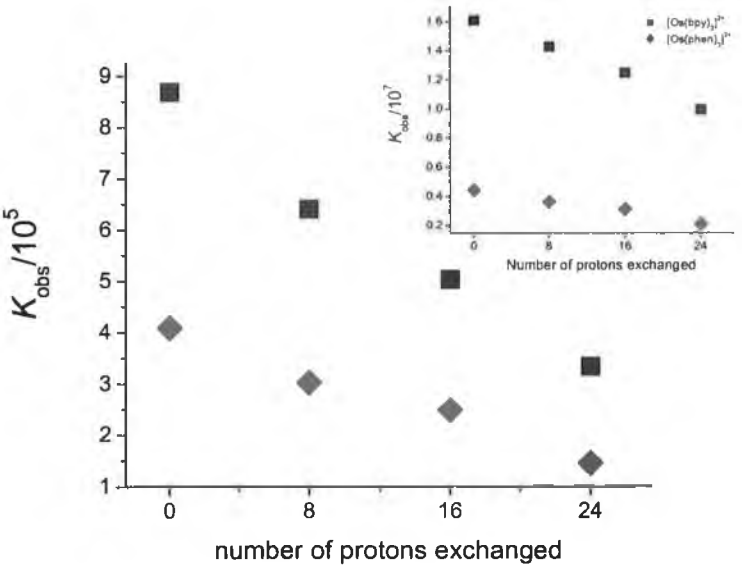

Figure 4.8 *Plot of K_{obs} against number of protons exchanged for $[Os(bpy)_3]^{2+}$ (black squares) and $[Os(phen)_3]^{2+}$ (red diamonds) at 77 K (inset at 298 K). All curves are linear {$R^2 > 0.992$}*

In contrast to the heteroleptic bpy/ph$_2$phen Ru(II) complexes described above, for the heteroleptic bpy/phen Os(II) complexes examined here at 298 K, deuteriation of the bpy ligand alone resulted in a significant increase in emission lifetime. At 77 K however the effect of deuteriation becomes nearly statistical indicating that at that temperature both phen and bpy based ^{3}MLCT excited states are involved in relaxation. The origin of the temperature dependence of the deuteriation effect may be due to, in part, the relative destabilisation of the phen ^{3}MLCT states with respect to the bpy ^{3}MLCT states in glassy media. The reduction in the energy separation of the bpy and phen ^{3}MLCT states, due to preferential destabilisation of the more solvent sensitive bpy states may explain this observation. At 77 K the bpy/phen states are both populated and become equilibrated, with a common observed radiative rate constant (k_{obs}) existing. At 298 K the energy difference between the states may be sufficient to favour population bpy based ^{3}MLCT states and hence deuteriation of the phen ligands will not affect k_{obs}.

An alternative explanation may be in the effect of deuteriation on the coupling between the bpy and phen states. Given that the two states are close in energy then coupling

between these states may be accompanied by a large barrier to internal conversion which at room temperature is easily overcome by background thermal energy. Since the bpy state has the shorter natural radiative lifetime then it is this state that dominates the overall decay rate (k_{obs}) for the complex, as evidenced by the large difference in the 298 K lifetime of the heteroleptic osmium complexes and the complex $[Os(phen)_3]^{2+}$. At 77 K many of the non-radiative processes are "frozen out" (*e.g.* CTTS contributions, skeletal vibrations *etc.*). Hence the high energy (and hence deuteriation sensitive) decay pathways from both bpy and phen ^{3}MLCT states, become important in the overall k_{obs}. Hence deuteriation of either or both the bpy and phen ligands will result in an increase in the observed radiative lifetime.

Of these two models for explaining the effect of deuteriation, the latter is the more reasonable, given that the small difference in the energy of the ^{3}MLCT states of $[Os(bpy)_3]^{2+}$ and $[Os(phen)_3]^{2+}$ would anticipate that the both bpy and phen states would be populated in all of the heteroleptic complexes. The fact that for the bpy/ph_2phen Ru complexes a similar situation is not observed can be rationalised on the basis that the greater statistical Boltzmann population of the ph_2phen ^{3}MLCT states balances the faster decay from the bpy ^{3}MLCT states.

4.2.3.3 $[Ru(bpy)_2(H_2dcb)]^{2+}$ - pH dependence of deuteriation effect.

Table 4.4 describes the effect of selective deuteriation and pH on the luminescence lifetime of both the fully deprotonated and fully protonated complexes. The lifetime values obtained for the perprotio complexes are in agreement with previously reported values.[20] On the basis of the increased basicity of the dcb^{2-}/H_2dcb ligand in the excited state, that ligand has been assigned as the location of the emissive state. For both the fully protonated and fully deprotonated complex deuteriation of the bpy ligand results in no significant increase in emission lifetime, whilst deuteriation of the H_2dcb/dcb^{2-} ligand results in an relatively large increase (compared to 5 % for $[Ru(bpy)_2([D_8]\text{-bpy})]^{2+}$).[12] The absence of a deuteriation effect on deuteriation of the bpy ligand gives strong evidence to support this conclusion. However it should be noted that complete deuteriation results in an additional increase in the observed emission lifetime. This is not unusual, but has also been observed by Kincaid *et al.* in studies on the positional dependence of deuteriation of $[Ru(bpy)_3]^{2+}$ (*vide supra*).[8c]

	Lum. λ_{max} (nm)	τ_{298K} (ns)	k_{obs} (*10^6) {Δ%}
[Ru(bpy)$_2$(dcb)]	641	562	1.78
[Ru(bpy)$_2$([D$_6$]-dcb)]	"	633	1.58 {10%}
[Ru([D$_8$]-bpy)$_2$(dcb)]	"	573	1.75 {2%}
[Ru([D$_8$]-bpy)$_2$([D$_6$]-dcb)]	"	679	1.47 {17%}
[Ru(bpy)$_2$(H$_2$dcb)]$^{2+}$	679	292	0.342
[Ru(bpy)$_2$([D$_6$]-H$_2$dcb)]$^{2+}$	"	330	0.303 {11%}
[Ru([D$_8$]-bpy)$_2$(H$_2$dcb)]$^{2+}$	"	299	0.334 {2%}
[Ru([D$_8$]-bpy)$_2$([D$_6$]-H$_2$dcb)]$^{2+}$	"	348	0.287 {16%}

Table 4.4 *Measurements in degassed (argon purged) Britton-Robinson aqueous buffer pH 1 and pH 10 at 298 K. All values assumed to have 5 % error.{Δ%} indicates %decrease in radiative rate constant relative to the perprotio complex.*

In contrast to the previous examples of heteroleptic complexes of bpy, phen and ph$_2$phen, in this case deuteriation provides strong evidence for the localization of the excited state on a particular ligand. It should be noted that in this case that the relative energies of the bpy and dcb^{2-}/H$_2$dcb 3MLCT states are considerably more different than in the previous systems.

4.2.3.4 Ru(II) polypyridyl complexes containing 1,2,4-triazoles

In this section the effect of deuteriation on emission lifetime for a series of related 1,2,4-triazole based complexes will be examined. Several of the complexes and their emission properties have been reported previously, however they have been measured again using time correlated single photon counting (TCSPC). In the case of photochemically unstable complexes the emission lifetimes obtained previously are of limited value since decomposition was observed during the measurement using laser excitation.[21] The advantage of TCSPC is that the flashlamp employed as excitation source is more suited to these systems. The results obtained are discussed in comparison with results obtained previously by Keyes *et al.* using laser excitation/PMT detection based lifetime measurements.[14]

In complexes of the type [Ru(bpy)$_2$(Xpztr)]$^+$ (where X = H or ph) and the complex [Ru(bpy)$_2$(pytr)]$^+$ deuteriation of the triazole based ligand has no effect on the excited state lifetime under deprotonated complex, whilst deuteriation of the bpy ligand leads to an increase of 20 to 25 % in the emission lifetime (see Table 4.1). This increase is similar

to the increases observed for $[Ru(bpy)_3]^{2+}$ and confirms the assignment of the lowest ^{3}MLCT state as being bpy based.

	Abs λ_{max}	Emission 298 K (77 K)	τ_{298K} (ns)		Abs λ_{max}	Emission 298 K (77 K)	τ_{298K} (ns)
$[Ru(bpy)_2(pztr)]^+$	456	668 (640)	250	$[Ru(bpy)_2(pytr)]^+$	465	650 (640)	145
$[Ru(bpy)_2(d_4\text{-pztr})]^+$	"	" (")	260	$[Ru(bpy)_2(d_5\text{-pytr})]^+$	"	" (")	147
$[Ru(d_8\text{-bpy})_2(pztr)]^+$	"	" (")	300	$[Ru(d_8\text{-bpy})_2(pytr)]^+$	"	" (")	193
$[Ru(d_8\text{-bpy})_2(d_4\text{-pztr})]^+$	"	" (")	310	$[Ru(d_8\text{-bpy})_2(d_5\text{-pytr})]^+$	"	" (")	210
$[Ru(bpy)_2(phpztr)]^+$	453	670 (640)	217	$[Ru(biq)_2(pztr)]^+$	576	782 (742)	310
$[Ru(bpy)_2(d_3\text{-phpztr})]^+$	"	" (")	210	$[Ru(biq)_2(d_4\text{-pztr})]^+$	"	" (")	310
$[Ru(bpy)_2(d_5\text{-phpztr})]^+$	"	" (")	212	$[Ru(d_{12}\text{-biq})_2(pztr)]^+$	"	" (")	330
$[Ru(bpy)_2(d_8\text{-phpztr})]^+$	"	" (")	215				
$[Ru(d_8\text{-bpy})_2(phpztr)]^+$	"	" (")	270				
$[Ru(d_8\text{-bpy})_2(d_3\text{-phpztr})]^+$	"	" (")	269				
$[Ru(d_8\text{-bpy})_2(d_8\text{-phpztr})]^+$	"	" (")	274				

Table 4.5 *Electronic data for $[Ru(LL)_2(LL')]^{x+}$ complexes in acetonitrile (error in τ is 5%)*

For the complex $[Ru(biq)_2(pztr)]^+$ an increase upon deuteriation of the biq ligand is observed, however it is barely outside the experimental error of the measurement. Since the biq ^{3}MLCT states are much lower than either bpy or pyrazine based ^{3} MLCT states then it is unlikely that the excited state is localised on the pyrazine ring. The lack of a large increase is more likely due to the absence of the H_6 and H_5 protons, which Kincaid *et al.* have shown to be the most important in vibrationally coupled deactivation of $[Ru(bpy)_3]^{2+}$.

For the protonated complexes significant barriers to the accurate determination of emission lifetime data are present. In particular for pytr$^-$ based complex, protonation results in a dramatic decrease in the observed emission lifetime while for the pyrazine based complexes the protonation of the free pyrazine nitrogen occurs quite easily in the excited state and hence the "pH window" in which the complex remains singly protonated in the excited state is very small. An additional factor affecting measurement of the protonated complexes is that of oxygen quenching. For the deprotonated complexes in every case degassing with argon purge has proven to give almost identical results compared with samples degassed by freeze-pump-thaw degassing cycles. In contrast for the protonated complexes argon purge is wholly inadequate and all samples require freeze-pump-thaw degassing to ensure reliable values are obtained. For the protonated pztr$^-$ based complexes results obtained from measurements of both the perprotio complex and the partially and fully deuteriated complexes do not agree with previously reported

values (in that the values obtained were significantly longer). These results caste doubt over the observation by Keyes *et al.* that deuteriation of the Hpztr ligand results in a doubling of emission lifetime.[14] It should be noted however that the deaeration method employed in those earlier studies was by argon purge.

Deuteriation of the pyrazine ring results in the exchange of only three C-H oscillators whilst deuteriation of the bpy ligands results in the exchange in sixteen. Unless the pyrazine C-H modes are several times more important in deactivating the excited state then it may be presumptuous to expect to be able to "see" an increase in emission lifetime upon deuteriation of that ligand. Nevertheless it has been shown for triazine based complexes that deuteriation of the bpy ligands will have no effect when the excited state is located on a non-bpy ligand (see Chapter 1).[17]

4.2.4 Resonance Raman spectroscopy

Resonance Raman spectroscopy were carried out on $[Ru(bpy)_2phpztr]^+$ and $[Ru(bpy)_2phpytr]^+$ complexes and some of their isotopologues. The use of deuteriation has allowed for both ground state and excited state resonance Raman spectra to be assigned relatively easily on the basis of isotopic shifts. The results obtained are comparable to those reported for the analogous complexes $[Ru(bpy)_2pztr]^+$ and $[Ru(bpy)_2pytr]^+$ by Hage and coworkers.[9]

4.2.4.1 Ground state resonance Raman spectroscopy

Resonance Raman (rR) provides a powerful probe of the nature of electronic absorption bands. Enhancements are observed for symmetric stretching modes of the ligand involved in the metal to ligand charge transfer transition. It allows for the identification of absorption bands which overlap extensively with other MLCT bands. The ground state rR spectra of both $[Ru(bpy)_2(Hphpztr)]^{2+}$ and $[Ru(bpy)_2(phpztr)]^+$ and several isotopologues are presented in appendix B, with significant features listed in Table 4.6 to Table 4.8 together with data for $[Ru(bpy)_3]^{2+}$ and $[Ru([D_8]\text{-}bpy)_3]^{2+}$. Spectra were recorded using two excitation wavelengths (514.5 nm and 457.9 nm).

Complex			Raman	vibrations					
[a][Ru(bpy)$_3$]$^{2+}$	1608	1563		1491		1320	1276		1176
[B][Ru(bpz)$_3$]$^{2+}$			1518		1410	1347	1161	801	
[Ru(bpy)$_2$(Hphpztr)]$^{2+}$	1610	1565	1534	1494	1429	1320	1277	1193	1175
[Ru(bpy)$_2$([D$_3$]-Hphpztr)]$^{2+}$	1610	1566		1493		1321	1278		1175
[Ru(bpy)$_2$([D$_5$]Hphpztr)]$^{2+}$	1610	1569	1528	1497		1323	1284	1191	1179
[Ru(bpy)$_2$([D$_8$]-Hphpztr)]$^{2+}$	1610	1566		1494		1324	1280		1176
[a][Ru([D$_8$]-bpy)$_3$]$^{2+}$	1575	1529	1427	1305	1202				
[Ru([D$_8$]-bpy)$_2$(Hphpztr)]$^{2+}$	1576	1532	1427	1303	1207				
[Ru([D$_8$]-bpy)$_2$([D$_3$]-Hphpztr)]$^{2+}$	1576	1531	1431	1311	1204				
[Ru([D$_8$]-bpy)$_2$([D$_8$]-Hphpztr)]$^{2+}$	1575	1532	1429	1308	1205				

Table 4.6 *Main vibrations observed in ground state rR spectra of isotopologues of [Ru(bpy)$_2$(Hphpztr)]$^{2+}$ with [Ru(bpy)$_3$]$^{2+}$ for comparison. Excitation at 457.9 nm. a) from ref 8b b) from ref 22*

For the protonated complex at 457.9 nm excitation features attributable to bpy based symmetric modes are observed at (1610, 1565, 1494, 1429, 1320, 1277 and 1175 cm^{-1}) with only very weak pyrazine features at 1534 and 1193 cm^{-1} (Table 4.6). The assignment of these bands is readily made from the isotopic shifts observed in the spectra of the seven isotopomers and by comparison with similar complexes.[9]

Complex			Raman	vibrations					
[a][Ru(bpy)$_3$]$^{2+}$	1608	1563		1491		1320	1276		1176
[B][Ru(bpz)$_3$]$^{2+}$			1518		1410	1347	1161	801	
[Ru(bpy)$_2$(phpztr)]$^{+}$	1606	1561		1487		1317	1272	1189	1170
[Ru(bpy)$_2$([D$_3$]-phpztr)]$^{+}$	1606	1562		1487		1318	1271		1169
[Ru(bpy)$_2$([D$_5$]phpztr)]$^{+}$	1609	1565		1498		1321	1277		1174
[Ru(bpy)$_2$([D$_8$]-phpztr)]$^{+}$	1608	1564		1491		1320	1276		1174
[a][Ru([D$_8$]-bpy)$_3$]$^{2+}$	1575	1529	1427	1305	1202				
[Ru([D$_8$]-bpy)$_2$(phpztr)]$^{+}$	1573	1524	1425	1299	1201				
[Ru([D$_8$]-bpy)$_2$([D$_3$]-phpztr)]$^{+}$	1574	1527	1425	1301	1203	1006			
[Ru([D$_8$]-bpy)$_2$([D$_8$]-phpztr)]$^{+}$	1578	1527	1429						

Table 4.7 *Main vibrations observed in ground state rR spectra of isotopologues of [Ru(bpy)$_2$(phpztr)]$^{+}$ with [Ru(bpy)$_3$]$^{2+}$ for comparison. Excitation at 457.9 nm. a) from ref 8b b) from ref 22*

For the deprotonated complexes at 514.5 nm excitation, a similar situation is observed with the spectrum being dominated by bpy modes (Table 4.7). However, no evidence for any pyrazine modes is present in the spectra, with only a very weak feature at 1524 tentatively assigned to a [D$_5$]-phenyl vibration.

For the protonated complex at 514.5 nm excitation again features attributable to bpy based symmetric modes are observed at (1610, 1565, 1494, 1429, 1320, 1277 and 1175 cm^{-1}) with only very weak pyrazine features at 1357 and 1190 cm^{-1} (Table 4.8). For the protonated complex an almost identical situation is observed. It should be noted however that the quality of the spectra obtained at 514.5 nm is much less than that obtained at 457.9 nm, making a detailed analysis of the spectra inadvisable.

Complexes	Raman vibrations								
[a][Ru(bpy)$_3$]$^{2+}$	1608	1563	1491			1320	1276		1176
[b][Ru(bpz)$_3$]$^{2+}$			1518		1410	1347	1161	801	
[Ru(bpy)$_2$(Hphpztr)]$^{2+}$	1606	1563	1491		1381	1316	1274		1170
[Ru(bpy)$_2$([D$_3$]-Hphpztr)]$^{2+}$	1608	1561	1491			1318	1275	1189	1173
[Ru(bpy)$_2$([D$_5$]Hphpztr)]$^{2+}$	1608	1562	1489		1380	1318	1271	1186	1127
[Ru(bpy)$_2$([D$_8$]-Hphpztr)]$^{2+}$	1586	1563	1538	1488	1449	1318	1275	1198	
[a][Ru([D$_8$]-bpy)$_3$]$^{2+}$	1575	1529	1427			1305	1202		
[Ru([D$_8$]-bpy)$_2$(Hphpztr)]$^{2+}$		1527	1424		1380			1192	
[Ru([D$_8$]-bpy)$_2$([D$_8$]-Hphpztr)]$^{2+}$	1538	1508	1425				1203	1189	

Table 4.8 *Main vibrations observed in ground state resonance Raman spectra of isotopologues of [Ru(bpy)$_2$(Hphpztr)]$^{2+}$ with [Ru(bpy)$_3$]$^{2+}$ for comparison. Excitation at 514.5 nm. a) from ref 8c b) from ref 22*

Complex	Raman Vibrations								
[a][Ru(bpy)$_3$]$^{2+}$	1608	1563		1491		1320	1276		1176
[b][Ru(bpz)$_3$]$^{2+}$			1518		1410	1347	1161	801	
[Ru(bpy)$_2$(phpztr)]$^{+}$	1604	1560		1486	1357	1316	1271	1190	1170
[Ru(bpy)$_2$([D$_3$]-phpztr)]$^{+}$	1606	1556		1486		1315	1272	1190	1170
[Ru(bpy)$_2$([D$_5$]phpztr)]$^{+}$	1605	1561	1520	1488		1316	1274	1236	1125
[Ru(bpy)$_2$([D$_8$]-phpztr)]$^{+}$	1606	1573	1521	1486	1410	1315	1274	1146	1010
[a][Ru([D$_8$]-bpy)$_3$]$^{2+}$	1575	1529			1427		1305	1202	
[Ru([D$_8$]-bpy)$_2$(phpztr)]$^{+}$	1571	1523			1420	1360	1301	1198	
[Ru([D$_8$]-bpy)$_2$([D$_8$]-phpztr)]$^{+}$	1575	1523		1485		1345	1302	1195	

Table 4.9 *Main vibrations observed in ground state resonance Raman spectra of isotopologues of [Ru(bpy)$_2$(phpztr)]$^{+}$ with [Ru(bpy)$_3$]$^{2+}$ for comparison. Excitation at 514.5 nm. a) from ref 8b b) from ref 22*

Overall it can be said that the absorption spectra of both the protonated and deprotonated complexes show predominantly bpy-based modes. The absence of evidence for pyrazine-based modes is in part due to the lower enhancement observed for pyrazine modes and the likely overlap between those modes and the bpy modes.

4.2.4.2 Excited state resonance Raman spectroscopy

The excited state resonance Raman spectra of $[Ru(bpy)_2phpytr]^+$ and $[Ru(bpy)_2phpztr]^+$ have been examined. Figure 4.9 shows the excited state resonance Raman spectrum of $[Ru(bpy)_2(phpytr)]^+$ and $[Ru([D_8]\text{-}bpy)_2(phpytr)]^+$. The spectra show clearly that the excited state is bpy with the marker bands for bpy^{*-} (bpy anion radical) at 1211 and 1285 cm^{-1} showing a very strong isotope dependence.

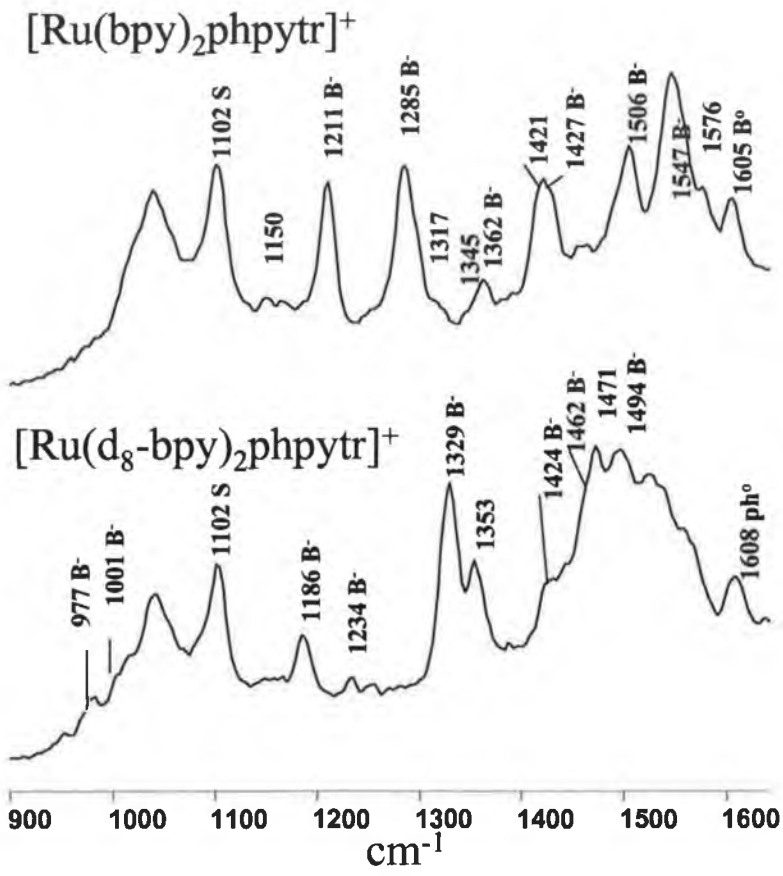

Figure 4.9 *Excited state resonance Raman spectra of $[Ru(bpy)_2(phpytr)]^+$ and $[Ru(d_8\text{-}bpy)_2(phpytr)]^+$ in CD_3CN*

For $[Ru(bpy)_2phpztr]^+$ and its isotopologues almost identical spectra are obtained with deprotonated complexes showing excited state resonances typical of bpy^- confirming that the emitting state is bpy based (see Appendix C). For the protonated complexes these marker bands are notably absent, with weak bands at 1429 and 1494 cm^{-1} suggesting that the excited state is pyrazine based. It should be noted that the marker bands for $pyrazine^{*-}$ excited state modes show considerable overlap with neutral bpy modes making their identification difficult.[9]

4.3 Conclusions

The application of deuteriation as a probe both in vibrational and electronic spectroscopy of Ru(II) and Os(II) polypyridyl complexes is clearly demonstrated in the studies described in this chapter. Together with the methodology for the preparation of deuteriated ligands in useable quantities, the further development of isotopic perturbation as a general and commonplace technique has been brought closer to realisation. Whilst the results of the resonance Raman studies presented tend to under play this, the effect of deuteriation on luminescence lifetimes is show that in every case the basic conclusions reached from the deuteriation effect are in full agreement with other studies (in particular excited state rR).

For homoleptic complexes of Os(II), the statistical effect of deuteriation shows that all three ligands are involved in excited state deactivation. For heteroleptic complexes involving bpy/phen and bpy/ph_2phen, the same conclusion has been reached, although the relative contribution of each ligand to the overall observed radiative decay rate is clearly not equal. The temperature dependence of the deuteriation effect observed, whilst initially confusing, does serve to highlight the danger in assuming the simplified excited state model where only the very lowest excited state is populated. For the H_2dcb based complexes the agreement between the deuteriation effect observed and the assignment of the lowest excited state being localised on the H_2dcb ligand is very close. However again the effect of deuteriation of ligands other than the "excited state" based ligand is demonstrated.

Several difficulties in using deuteriation as a probe of excited state properties have been encountered in this study. That of oxygen quenching is the most obvious. In the presence of a very efficient deactivation channel such as oxygen quenching and population of strongly coupled short lived excited states (*i.e.* ^{3}MC state) the observation of less competitive routes such as those due to vibrationally coupled deactivation (*e.g.* C-H, N-H and O-H modes) is not possible. In addition the possibility of excited state processes such as acid/base changes, makes the reliability of data obtained much less than for well-defined systems. This is most evident in the pyrazine-triazole based systems examined.

Nevertheless, given that contributing factors can be eliminated or accounted for then the effect of deuteriation provides a powerful and under exploited probe of the excited state properties of inorganic systems.

4.5 Experimental

$[Ru(bpy)_2(pztr)]^+$, $[Ru(bpy)_2(pytr)]^+$ and $[Ru(biq)_2(pztr)]^+$ and their isotopologues were provided by Dr. C. O'Connor (Dublin Institute of Technology). Deuteriated ligands were prepared as described in Chapters 2 and 3. Synthetic details and characterisation (NMR spectroscopic, Mass spectral and elemental analysis) are presented in appendix F.

4.6 Bibliography

1. J. P. Paris and W. W. Brandt, *J. Am. Chem. Soc.*, **1959**, *81*, 5001

2. A. Juris, V. Balzani, F. Barigelletti, S. Campagna, P. Belser and A. von Zelewsky *Coord. Chem. Rev.* **1988**, *84*, 85

3. H. Yersin, W. Humbs and J. Strasser, *Topics in Current Chemistry*, **1997**, *191* 154

4. J. R. Schoonover and G. F. Strouse, *Chem. Rev.*, **1998**, *98*, 1335

5.(a) Y. J. Chang, X. Xu, T. Yabe, S. Yu, D. R. Anderson, L. K. Orman and J. B. Hopkins, *J. Phys. Chem.*, **1990**, *94*, 729 (b) K. F. Mongey, J. G. Vos, B. D. MacCraith, C. M. McDonagh, C. Coates and J. J. McGarvey, *J. Mater. Chem.*, **1997**, *7*, 1473 (c) M. Haga, Md. M. Ali, S. Koseki, K. Fujimoto, A. Yoshimura, K. Nozaki, T. Ohno, K. Nakajima and D. J. Stufkens, *Inorg. Chem.*, **1996**, *35*, 3335

6.(a) C. V. Kumar, J. K. Barton, N. J. Turro and I. R. Gould, *Inorg. Chem.*, **1987**, *26*, 1455 (b) C. V. Kumar, J. K. Barton, I. R. Gould, N. J. Turro and J. van Houten, *Inorg. Chem.*, **1988**, *27*, 648 (c) C. Turro, S. H. Bossman, G. E. Leroi, J. K. Barton and N. J. Turro, *Inorg. Chem.*, **1994**, *33*, 1344

7.(a) S. F. McClanahan, R. F. Dallinger, F. J. Holler and J. R. Kincaid, *J Am. Chem. Soc.*, **1985**, *107*, 4853 (b) G. D. Danzer, J. A. Golus and J. R. Kincaid, *J. Am. Chem. Soc.*, **1993**, *115*, 8643 (c) M. Sykora and J. R. Kincaid, *Inorg. Chem.*, **1995**, *34*, 5852

8.(a) P. G. Bradley, N. Kress, B. A. Hornberger and R. F. Dalliger, *J. Am. Chem. Soc.*, **1981**, *103*, 7441 (b) P. K. Mallick, G. D. Danzer, D. P. Strommen and J. R. Kincaid, *J. Phys. Chem.*, **1988**, *92*, 5628 (c) K. Maruszewski, K. Bajdor, D. P. Strommen and J. R. Kincaid, *J. Phys. Chem.*, **1995**, *99*, 6286

9.(a) R. Hage, J. G. Haasnoot, J. Reedijk, R. Wang and J. G. Vos, *Inorg. Chem.*, **1991**, *30*, 3263 (b) H. P. Hughes, D. Martin, S. Bell, J. J. McGarvey and J. G. Vos, *Inorg. Chem.*, **1993**, *32*, 4402 (c) C. G. Coates, T. E. Keyes, J. J. McGarvey, H. P. Hughes, J. G. Vos and P. M. Jayaweera, *Coord. Chem. Rev.*, **1998**, *171*, 323 (d) C. G. Coates, T. E. Keyes, H. P. Hughes, P. M. Jayaweera, J. J. McGarvey and J. G. Vos, *J. Phys. Chem.*, **1998**, *102*, 5013 (e) S. Fanni, T. E. Keyes, C. M. O'Connor, H. P. Hughes, R. Wang and J. G. Vos, *Coord. Chem. Rev.*, **2000**, 208, 77

10. H. E. Nieuwenhuis, J. G. Haasnoot, R. Hage, J. Reedijk, T. L. Snoeck, D. J. Stufkens and J. G. Vos, *Inorg. Chem.*, **1991**, *30*, 48

11.(a) J. van Houten and R. J. Watts, *J. Am. Chem. Soc.*, **1975**, *97*, 3843 (b) J. van Houten and R. J. Watts, *J. Am. Chem. Soc.*, **1976**, *98*, 4853

12. E. Krausz, G. Moran and H. Riesen, *Chem. Phys. Letts.*, **1990**, *165*, 401

13. W. R. Browne, J. G. Vos, *Coord. Chem. Rev.*, **2001**, *761*, 787

14. T. E. Keyes, C. M. O'Connor, U. O'Dwyer, C. G. Coates, P. Callaghan, J. J. McGarvey and J. G. Vos, *J.Phys.Chem. A*, **1999**, *103*, 8915

15.(a) J. V. Casper, E. M. Kober, B. P. Sullivan and T. J. Meyer, *J. Am. Chem. Soc.*, **1982**, *104*, 630 (b) E. M. Kober, J. V. Casper, R. S. Lumpkin and T. J. Meyer, *J. Phys. Chem.*, **1986**, *90*, 3722

16. M. A. Bergkamp, P. Guetlich, T. L. Netzel and N. Sutin, *J. Phys. Chem.*, **1983**, *87*, 3877

17. T. E. Keyes, F. Weldon, E. Müller, P. Pechy, M. Grätzel and J. G. Vos, *J. Chem. Soc. Dalton Trans.*, **1995**, 2705

18 K. F. Mongey, J. G. Vos, B. D. MacCraith, C. M. McDonagh, C. Coates, J. J. McGarvey, *J. Mater. Chem.*, **1997**, *7*, 1479

19. H. Yersin, W. Humbs and J. Strasser, *Topics in Current Chemistry*, **1997**, *191*, 154

20. J. G. Vos, *Polyhedran*, **1992**, *11*, 2285 and ref 10 and 12 therein.

21. C. M. O'Connor, *Ph.D. Thesis*, **1999**, Dublin City University, Dublin, Ireland

22. G. D. Danzer, J. R. Kincaid, *J. Phys. Chem.*, **1990**, *94*, 3976

Chapter 5

Temperature and time resolved emission properties of mononuclear iron(II) and ruthenium(II) polypyridyl complexes: emission from coexisting excited states

In this chapter several aspects of Group VIII photophysics are explored in particular emission from excited states other than the lowest excited states. In the first part, the phenomena of temperature dependent dual luminescence reported for the mononuclear complex $[Ru(bpy)_2(pztr)]^+$ is investigated over a wide range of related complexes.[1] The effect of ligand substitution and solvent environment on the dual emissive behaviour are examined. It is found that the dual emission is not specific to $[Ru(bpy)_2(pztr)]^+$ but is in effect general to a series of pyrazine-triazole based complexes. In the second part, time resolved emission studies on the picosecond timescale are employed for the first time to study the early processes, which occur after electronic excitation of Fe(II) and Ru(II) polypyridyl complexes. Direct observation of short lived (> 3 ps) high energy emission from $[Fe(bpy)_3]^{2+}$ and $[Ru(bpy)_3]^{2+}$ is described. For the latter complex a marked sensitivity to isotopic substitution, giving a significant increase in both intensity and lifetime is observed. The results indicate that the emission in both cases is ^{1}MLCT in origin and caste a doubt as to the validity of the assumption that ISC to the lowest manifold of ^{3}MLCT excited states is unity. The results are discussed with respect to heterogeneous electron transfer reactions.

Fast, furious, frantic and fantastical photophysics!

Or to paraphrase,

Micro-, nano-, pico- and femto-second spectroscopy.

5.1 Introduction

Emission from organic molecules almost exclusively originates from the lowest excited state of a given multiplicity. This has become known as Kasha's rule.[2] However for both organic compounds and transition metal complexes this rule does not always hold and many exceptions have been reported, including $[Ru(bpy)_3]^{2+}$.[3]

"In the absence of photochemistry from the upper excited states, emission from a transition metal complex with an unfilled d shell will occur from the lowest electronic excited state in the molecule or from those states which can achieve a significant Boltzmann population relative to the lowest excited state"

Demas & Crosby made this statement in 1970 in relation to the photophysical properties of d^3 and d^6 transition metal complexes.[4] This statement implies that the rate of internal conversion and intersystem crossing from higher excited states to the lowest excited state (or states) is unity in the absence of energy loss and deactivation by photochemical reactions, *e.g.* decomposition or hapticity changes. This empirical statement in contrast to Kasha's rule does not exclude the possibility of multiple emissions since it takes into account situations where a significant population of excited molecules exist in states other than the lowest excited state and can emit from these states. A familiar example of this statement is in the simultaneous fluorescence and phosphorescence of aromatic compounds such as 2,2-bipyridyl. One of Kasha's main contributions to the development of luminescence spectroscopy was in the observation that the emission spectrum observed is independent of the 'colour' of the incident light except for the variation in its overall intensity. Or more succinctly the excitation spectrum at any wavelength of the emission band matches the absorption spectrum exactly.

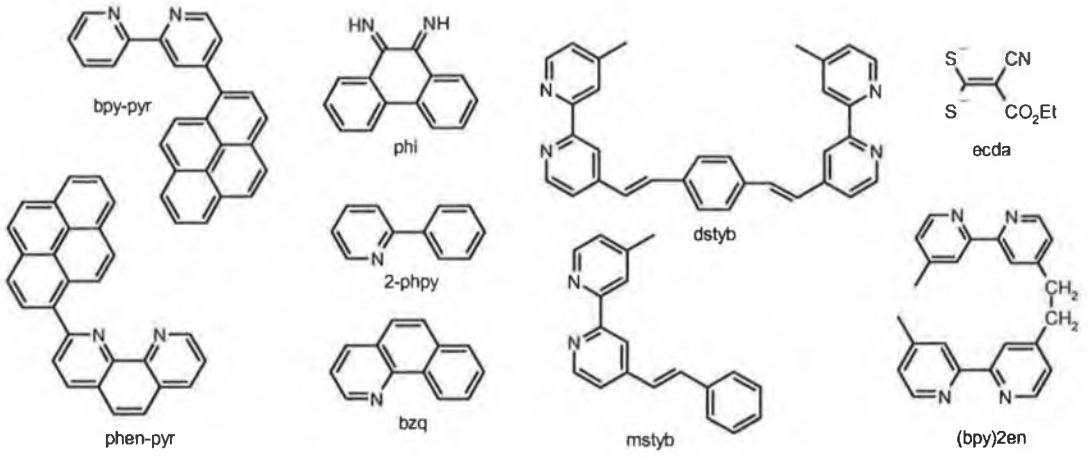

Figure 5.1 *Ligands used in dual emitting complexes*

5.1.1 Multiple emissions in transition metal complexes

Dual emission is relatively well known in organic systems where the presence of heavy atoms *e.g.* Xenon (which enhance intersystem crossing from singlet to triplet excited states) allows for the observation of phosphorescence and fluorescence at 77 K. Dual emission is, however less common in coordination compounds involving transition metals. One of the earliest reports of such behaviour is of the emission from thermally non-equilibrated ^{3}IL excited states in Rh(III) *tris*-hetereoleptic complexes containing bpy and phen ligands.[5] Since then many more cases of "dual emissive behaviour" have been reported mostly for d^6 and d^3 transition metal complexes.[6,7,8]

Incidences of dual luminescence which have been reported in the literature can be broadly categorised as follows:

a) Multiple emission from polynuclear complexes
b) Dual emission arising from non-equivalent ligands in hetereoleptic complexes
c) Emission from separate moieties of a complex
d) Emission from non-equilibrated excited states of differing orbital parentage
e) Matrix effects

There is still much controversy in the literature as regards the identification and characterization of multiple emissions. What constitutes a true dual emissive behaviour is ill defined by its nature. Ideally dual emission should involve two emissions, which are not only spectrally but also temporally resolvable. This however is often difficult and in many cases the use of various data handling techniques is required to identify multiple emission.

5.1.2 Multiple emissions in multinuclear and supramolecular systems

Dual emission from complexes of the type $[Ru(bpy)_2(LL')]^{2+}$ (where LL = bpy-pyr and phen-pyr) (see Figure 5.1) is reported by Simon *et al.*.[9] These complexes are conformationally strained resulting in reduced interaction between the pyrenyl moiety and the remainder of the complex. As a result of this, emission takes place from both the ^{3}MLCT state of the complex and the ^{3}IL of pyrenyl moiety.

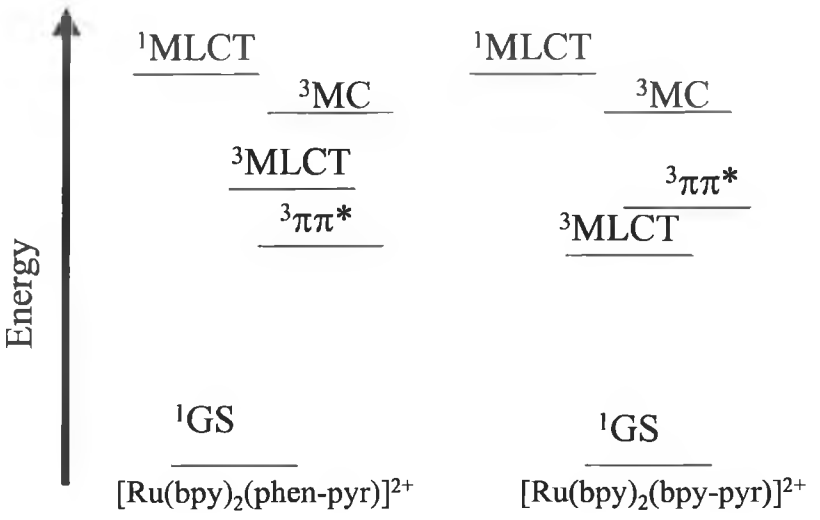

Figure 5.2 *Jablonski diagram for pyrenyl based complexes*

Although both states are almost isoenergetic for $[Ru(bpy)_2(bpy\text{-}pyr)]^{2+}$ the ^{3}MLCT excited state is lower than the ^{3}IL excited state and vice versa for $[Ru(bpy)_2(phen\text{-}pyr)]^{2+}$ (see Figure 5.2). The ^{3}IL states are not in equilibrium with the ^{3}MLCT excited states and hence double exponential emission is observed. Energy transfer is slower than relaxation of the ^{3}MLCT state but more rapid than the decay of the pyrenyl localised ^{3}IL state. Gated emission has been applied to show the spectral evolution of the emissions. Such behaviour in weakly interacting components of large molecules has been observed for $[(phenothiazine\text{-}pytr)Ru(bpy)_2]^{2+}$,[10] and for copper(I) and rhenium(I) catenate complexes.[11]

The mixed metal complex $[Ru(bpy)_2((bpy)_2en)Re(CO)_5(py)]^{3+}$ emits at both 610 nm (Ru) and 540 nm (Re) simultaneously.[12] The emissions have been assigned as ^{3}MLCT in origin and are based on each of the metal centres. Communication via the bridging ligand, $(bpy)_2en$, is poor but again sufficient to allow energy transfer between the metal centres. The emission from Ru(II)-Re(I) dimer may be modelled using a 9:1 mixture of the monomeric species $[Ru(bpy)_2(bpy)_2en)]^{2+}$ and $[(bpy)_2en)Re(CO)_5(py)]^+$.[12] Encinas *et al.* have reported dual emission from a similar Ru(II)-Re(I) binuclear complex, $[Ru(bpy)_2((Dystb)Re(CO)_5(Cl)]^{3+}$.[13] In this case energy transfer from the Re moiety is efficient but is mediated by the bridging ligand which itself emits (^{3}IL).

Serroni *et al.* have reported dual emission from the tetranuclear dendrimer $[Ru(bpy)_2(\mu\text{-}bpt)Ru\{\mu\text{-}dppRu(bpy)_2\}_2]^{7+}$ at 77 K, which is excitation wavelength dependent. [14] At 420

nm excitation, two emissions are observed at 600 and 700 nm, whilst at 530 nm irradiation only a single emission at 700 nm is observed. The emission lifetimes and excitation spectra are very different. At 300 K only one emission at 800 nm with a monoexponential lifetime is observed.

5.1.3 Dual emission arising from non-equivalent ligands in hetereoleptic rhodium, iridium and ruthenium complexes

Perhaps the earliest example of dual emissive behaviour falls into this category. In 1970, van Houten and Watts reported emission from thermally non-equilibrated ^{3}IL excited states in rhodium (III) tris hetereoleptic complexes containing bpy and phen ligands.[5] Although the ^{3}IL excited states of bpy and phen are separated by only 100 cm^{-1}, efficient energy transfer between the states does not occur. Dual emission is observed for the complexes $[Rh(bpy)_x(phen)_{3-x}]^{3+}$ (where x = 1 or 2) at 77 K in MeOH/H_2O. Identification of the each emission was achieved by comparison of emission lifetimes of the two components of the emission decay (2 and 38 ms) with the parent tris-homoleptic complexes. For the mixed ligand complexes containing the Me_2phen ligand only single emission was observed. The origin of this behaviour can be explained on the basis of both the energy gap between the excited states and the geometric constraints on such energy transfer. Since each excited state is localised on a single ligand internal conversion from one state to another requires an efficient energy acceptor to mediate the conversion. For the mixed ligand bpy/phen complexes no acceptors are readily available for the 100 cm^{-1} energy gap between the states, inhibiting the conversion. The Me_2phen excited state is 1600 cm^{-1} lower than either the bpy or phen ligands. The energy gap is very close to the energy to the skeletal vibrations observed for bpy, phen and Me_2phen ligands. In bpy/Me_2phen and phen/Me_2phen mixed ligand complexes internal conversion is efficient and only emission from the Me_2phen ligand is observed.

Similarly, multiple emission was observed from $[Rh(phi)_2(LL)]^{3+}$ (LL = bpy or phen, phi = 1,10-phenanthroline-5,6-dione) at 77 K.[15] Again both emissions have been assigned as π-π^* (^{3}IL) transitions from each ligand at 2.8 (440 nm) and 3 eV (410 nm) (phen is higher). Biexponential decay {5 ns 98 % (bpy/phen emission) and 60 ns 2% (phi emission)} is observed and the two emissions are spectrally resolvable.

Sprouse *et al.* have reported dual emission at 77 K for orthometallated iridium(III) complexes of the type $[Ir(LL)(LL')_2]^+$ where LL = bpy or phen and LL' = 2-

phenylpyridine or benzo[h]quinoline.[6] These emissions have been assigned as ^{3}MLCT in origin and the effect has been ascribed to the viscosity dependent Franck-Condon barrier to energy transfer between charge transfer states which show large geometric differences (each ^{3}MLCT state is based on a different ligand).[i] Spectral resolution was achieved by exciting directly into the lower of the two states with a tuneable laser, showing the lower energy emissions to be bpy or phen based. Above the glass transition region only a single emission is observed indicating that efficient energy transfer occurs in fluid environments. The equivalent rhodium(III) complexes in every case exhibits only single emission which is ^{3}IL in origin. Other orthometallated iridium(III) complexes have been shown to exhibit similar multiple emission.[16]

Dual emission at 77 K from the complex $[Ru(bpy)(HDPA)_2]^{2+}$ has been reported by Blakely and DeArmond.[17] The emissions are observed at 600 and 650 nm and an excitation wavelength dependence in EtOH and *i*-PrOH (but not in MeOH) has been demonstrated. In addition in H_2O this dual emission is not observed. This is not totally unexpected as solvent environment is important in determining the relative energy of excited states in particular CT states.[18] The high-energy (600 nm) emission has been assigned as ^{3}ILCT on the basis of its longer lifetime (13 μs) and small Stoke's shift. This excited state has been characterized as a n_{HDPA}-$\pi^*_{bpy/phen}$ ^{3}ILCT state. The second emission has been assigned as ^{3}MLCT in origin on the basis of its shorter lifetime at 77 K and its reduced temperature dependence. Although $[Ru(bpy)_2(HDPA)]^{2+}$ does not demonstrate similar luminescence properties, the complex $[Ru(phen)(HDPA)_2]^{2+}$ gives very similar results to the complex as $[Ru(bpy)(HDPA)_2]^{2+}$. This is not unexpected considering the small difference in the energy levels of the two ligands bpy and phen (vide infra).

5.1.4 Dual emission from mononuclear rhenium complexes

Glezen and Lees have reported multiple emission from a rhenium(I) complex $CpRe(CO)_2L$ (L = py or phpy).[19] The emission spectrum observed both a 298 K and at 77 K comprises of a ^{3}LF emission and emission from two equilibrated ^{3}MLCT states (at 77 K in frozen glass this equilibration is lost).

---

i Since electronic transitions are vertical and the reorganisational energy between excited states (MLCT) is large there is a large barrier to IC between states

Giordano *et al.* have reported that the complex *fac*-[$Re(CO)_3$(3-benzoylpyridine)$_2$] exhibits dual emission from both a ^{3}IL and a ^{3}MLCT at 77 K in EPA glass (CH_2Cl_2/DMF/MeOH).[20] The emissions are both spectrally resolvable due to the ^{3}IL transition being highly structured in contrast to the ^{3}MLCT emission. Dual emission is only observed for *fac*-[$Re(CO)_3$(3-benzoylpyridine)$_2$] and not for *fac*-$Re(CO)_3$(4-benzoylpyridine)$_2$]. The origin of this dual emissive behaviour has been assigned to the large geometric differences of the two excited states.

Dual emission from the complex [$(Re(CO)_3(CH_3CN)$(Mystb)] at 77 K has been reported by Shaw and Schmehl.[21] The emissions have been assigned as arising from ^{3}IL and ^{3}MLCT (79.4 and 3.7 μs resp.) excited states. As the temperature is raised from 77 K to 115 K (above T_g of the solvent) the lifetime of the longer-lived component drops of dramatically and is not observable above 250 K. This drop in lifetime has been attributed to increasing competition of cis-trans isomerisation of the Mstyb ligand and has lead to the assignment of the emission band as ^{3}IL in origin. For a similar dimeric complex [$(Re(CO)_3CH_3CN)_2$(Dystb)] only the ^{3}IL emission is observed.

5.1.5 Copper(I) and platinum polypyridyl complexes

Although the first report of luminescence from [$Ru(bpy)_3$]$(PF_6)_2$ was reported in the 1950's by Paris and Brandt,[22] the first report of luminescence from a Cu(I) polypyridyl complex was not until the 1980's, when McMillin and coworkers reported dual emission from $[Cu(dmp)_2]^+$.[23,24] Unusually emission from Cu(I) complexes occurs from both the lowest ^{1}MLCT and the lowest ^{3}MLCT states.

Zuleta *et al.* have observed multiple emission from a Pt(II) diimine dithiolate (ecda) complex (dimine = me_2bpy or ph_2phen).[25] Above 140 K only a single emission is observed (DMF/CH_2Cl_2/MeOH T_g ~ 165 to 175 K). However below 140 K two new bands appear at higher energies and are assigned to ^{3}IL diimine transitions by comparison with [Pt(diimine)Cl_2]. Between 6 and 80 K, the emission lifetime of the room temperature emission increases but emission intensity decreases suggesting closely spaced excited states are responsible for this multiple emission. Strong excitation wavelength dependence was observed, indicating the existence of different relaxation pathways to each emissive state (excitation at 500 nm only gives CT emission). The low energy emission observed above 140 K has been assigned to a charge transfer transition.

5.1.6 Dual luminescent behaviour from [Ru(bpy)$_2$(pztr)](PF$_6$).

Recently an example of a dual luminescent behaviour has been reported by Keyes *et al.*.[1] Temperature dependent emission studies and lifetime measurements on the complex $[Ru(bpy)_2(pztr)]^{2+}$ demonstrated that below 170 K a second unexpected emission could be identified. The second emission, found at higher energy than the emission observed at 292 K, was observable from below 170 K. Similar studies on the protonated complex, on its partially and fully deuteriated analogues and on the complex $[Ru(bpy)_2(pytr)]^{2+}$, were also reported.

The absence of dual emission under protonating conditions and in the complex $[Ru(bpy)_2(pytr)]^{2+}$, suggested strongly that the observations were not due to impurities. Such impurities would be expected to be similar for complexes prepared under the same conditions and with the only difference in reagents used being the ligand. In addition levels of impurities required for to produce the emissions observed for the dual emitting complex would be expected to be quite high and hence detectable by HPLC and NMR spectroscopic analysis. This was not the case. There are many examples of biexponential excited state decay for ruthenium complexes in EtOH/MeOH glasses,[26] which arise due to the inequivalence of sites in the frozen matrices and from solvation products. Ostensibly this could be the source of the dual luminescence observed by Keyes *et al.*, however two observations can discount this.[1] Firstly dual emission is observed at least 30 K above the upper limit of the glass transition temperature (115 to 130 K) and hence in the liquid state. Secondly both emissions have differing emission lifetimes and there spectra can be easily resolved This would not normally be possible if the emissions were as a result of inhomogenicities in the glass matrix (a range of emission lifetimes would be observed).

5.1.7 Rigidochromic effects

Since different excited states exhibit different changes in charge distribution then the rigido-chromic effects displayed on lowering temperature will differ. This can potentially lead to a "switching" of the lowest excited state with an excited state or states close in energy to it. In intermediate regions when the energy of each of the switching states is similar then two emissions may be observed. However resolution of the states both spectrally and temporally in this crossover region is generally not possible. This form of dual emissive behaviour is generally confined to the glass transition region by its very nature and is generally simple to distinguish from other forms of dual emissive behaviour

outlined above by the presence of only a single emitting state above and below the glass transition region.

5.1.8 Ruthenium polypyridyl complexes: internal conversion and intersystem crossing

Ruthenium(II) polypyridine complexes are playing a key role for the development of multi-component (supramolecular) systems capable of performing photo- and/or redox-triggered useful functions such as charge separation devices for photochemical solar energy conversion[27] and information storage devices.[28] With regard to application of these complexes as sensitisers in solar cell devices, interest in the early photophysical processes has increased dramatically in recent years.

Over the last half century $[Ru(bpy)_3]^{2+}$ has been the focus of intensive interest and its electronic excited state structure has been extensively investigated.[29] In particular the assignment of the emission at 610 nm in acetonitrile as being ^{3}MLCT in nature has been central to the photophysical investigations of not only Ru(II) but also Os(II) polypyridyl complexes.[29e] Initially assignment of the emission bands for both ruthenium and osmium complexes ranged from ^{1}MLCT emission to ^{3}dd emission. The now universally accepted ^{3}MLCT assignment is in itself not entirely accurate since spin orbit coupling is significant for ruthenium complexes resulting in efficient intersystem crossing (ISC) to the lowest ^{3}MLCT excited state(s). The efficiency of ISC is generally taken to be unity, however there is strong evidence that this is not entirely the case and estimates as low as 0.65 have been made based on electron transfer reactions.[30] More recently interest in the early processes, which occur after excitation have shown that a short-lived high energy emission together with the ^{3}MLCT emission is observable.

5.1.9 $[M(bpy)_3]^{2+}$ (M = Fe, Ru): evidence for ^{1}MLCT emission

The application of Ru(II) polypyridyl complexes as dye sensitisers in photovoltaics in recent years has drawn attention to the study of the higher lying MLCT states.[31,32] This interest arises from the proposal that direct injection of electrons from those states is a competitive process to intersystem crossing to the lowest ^{3}MLCT manifold. Improving the quantum efficiency of electron transfer to semiconductors and thereby improving conversion efficiency is desirable, as is a better understanding of these short-lived states. The timescale of injection of an electron into nanocrystalline TiO_2 has been estimated at less than 1 ps, with some estimates as low as 25 fs. It has been suggested that fast electron transfer from states energetically higher than the lowest ^{3}MLCT excited states not only

increases the efficiency of the sensitisers but also precludes deactivation by potentially photoreactive ^{3}MC states.

For $[Ru(bpy)_3](PF_6)_2$ (in single crystal form) ^{1}MLCT luminescence has been reported by Yersin *et al.*.[33] The emission was observed during the course of polarised steady state emission measurements, as a very weak high energy (λ_{max} 545 nm) shoulder of the more intense ^{3}MLCT emission.

The observation of a very weak steady state emission band at 510 nm was recently reported by Bhasikuttan *et al.*, however, the band was subject to overlap with the much more intense ^{3}MLCT emission band.[34] They have employed sub-picosecond fluorescence upconversion techniques to study this high-energy emission band in more detail and have reported a biphasic decay (~40 and ~700 fs)[ii] with considerable wavelength dependence between 500 and 620 nm. However in contrast to the ^{1}MLCT assignment made by Yersin *et al.* they have assigned the more prominent early emission (700 fs) as being from vibrational excited "hot" ^{3}MLCT states. This assignment shows some agreement with femtosecond transient absorption spectroscopy reported by McCusker and coworkers.[35] In these latter studies on the 100 to 5000 fs timescale the decay kinetics were found to be biphasic and were attributed to ISC to the ^{3}MLCT state followed by vibrational cooling dynamics.

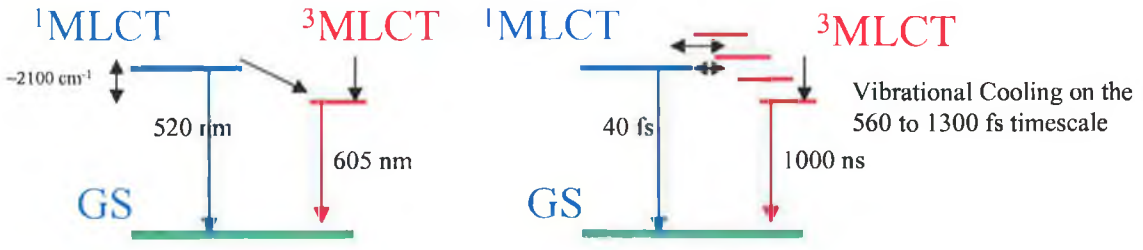

Figure 5.3 *(a) Model proposed by Yersin et al.[33] (b) Model proposed by Bhasikuttan et al.[34]*

5.1.9 Summary

Since the early 1970's, the empirical findings of Demas & Crosby have been confirmed for many d^6 transition metal systems.[4] It is clear that in order for a multiple emission to be observed, two or more emissive excited states must have a significant Boltzman population. In addition these states must either have quite similar natural decay lifetimes

iiThis short lived component has been assigned as emission from the Franck-Condon ^{1}MLCT excited state giving a rate of ISC to the vibrationally excited ^{3}MLCT state. It should be noted that this is well within the instrument response function (FWHM) of 150 fs.

or more commonly there must be a significant barrier to equilibration of the excited states. This is generally found to be achieved by significant differences in excited state geometry and/or dipole moment. In the case of the latter equilibration is generally prevented by solvent immobilisation in glass matrices. Although the majority of examples of dual emissive behaviour have been in glass matrices, the phenomenon is by no means restricted to such an environment.

In the first part of this chapter the temperature dependence of the photo-physical properties of a pyridyl- and pyrazyl-1,2,4-triazole based complexes are examined. The occurrence of a dual emissive behaviour from $[Ru(bpy)_2(pztr)]^+$ below 200 K is investigated further in this chapter not only for $[Ru(bpy)_2(pztr)]^+$ but also for other structurally related complexes. Variation in solvent is employed in order to probe the origin of these emissions. Temperature dependent emission lifetime studies and time resolved emission spectroscopies are also described.

In the second part, picosecond time resolved luminescence spectroscopy is employed to study the early time processes which occur subsequent to excitation of $[M(bpy)_3]^{2+}$ (M =Fe, Ru, Os). The effect of ligand deuteriation on the time dependence of the very short-lived emission is also examined. Whilst the results obtained for the perprotio complex are in broad agreement with the observations made by Yersin *et al.*, Bhasikuttan *et al.* and McCusker and coworkers, the emission properties of $[Ru([D_8]\text{-}bpy)_3]^{2+}$ reported below do not support the assignment of the 500-540 nm emission as being from vibrationally excited "hot" ^{3}MLCT excited states (Figure 5.3).

5.2 Results and discussion

5.2.1 Temperature dependent emission studies on Ru(II) polypyridyl complexes containing 1,2,4-triazoles

The complexes that are included in this study are divided into three groups. Group A are structurally analogous to the complex $[Ru(bpy)_2(pytr)](PF_6)$ with variations on the peripheral C5 position of the 1,2,4-triazole, group B are of the type $[Ru(LL)_2(pztr)](PF_6)$ where LL = phen, ph_2phen *etc.*) and group C complexes are structurally related to $[Ru(bpy)_2(pztr)]^+$ and are substituted in the C5 position of the 1,2,4-triazole.

Temperature dependent emission spectra for all complexes together with time resolved emission spectra for $[Ru(bpy)_2(phpztr)]^+$ are given in Appendix D. Temperature dependent lifetime data obtained for $[Ru(bpy)_2(phpztr)](PF_6)$ are given in Figure 5.5 and Figure 5.6. The results of these studies are presented and discussed below. The nature of the emitting states is of considerable interest; in particular whether the second emission is bpy based or pyrazine based. The solvatochromic behaviour of the emissions is examined as an aid to assignment. Excited states, which involve significant changes in dipole moment, are particularly sensitive to the solvent environment. Charge transfer states thus exhibit significant solvatochromic behaviour (MLCT and LMCT excited states). Intra ligand (IL) and metal centred transitions do not involve significant changes in charge distribution and hence no large changes in the compounds dipole moment occur, hence these transitions tend to vary very little with changes in solvent polarity.

Group A	Group B	Group C
$[Ru(bpy)_2(ppt1)]^+$	$[Ru(biq)_2(pztr)]^+$	$[Ru(bpy)_2(pztr)]^+$
$[Ru(bpy)_2(bpbt)]^{2+}$	$[Ru(ph_2phen)_2(pztr)]^+$	$[Ru(bpy)_2(Mepztr)]^+$
$[Ru(bpy)_2(pytr)]^+$	$[Ru(phen)_2(pztr)]^+$	$[Ru(bpy)_2(Brpztr)]^+$
$[Ru(bpy)_2(phpytr)]^+$	$[Ru(phen)_2(d_4\text{-pztr})]^+$	$[Ru(bpy)_2(phpztr)]^+$
$[Ru(bpy)_2(Brpytr)]^+$		$[Ru(bpy)_2\{3\text{-}(2,4\text{-dimethoxyphenyl})pztr\}]^+$
$[Ru(ph_2phen)_3]^{2+}$		$[Ru(bpy)_2(ppt2)]^+$
		$[Ru(bpy)_2(bpzbt)]^{2+}$

Table 5.1 *Complexes studied (see glossary for definition of ligands)*

5.2.1.1 Group A complexes

$[Ru(ph_2phen)_3](PF_6)_2$ is examined as a model complex in this study for several reasons (see Figure D.1). As for $[Ru(bpy)_3](PF_6)_2$, the excited state structure and processes are relatively well understood. Its emission properties are "normal" in that it exhibits a single monoexponential emission above 70 K and hence can be used to verify that the observed properties of other systems are not due to an artefact of the conditions and the instrumentation used. $[Ru(ph_2phen)_3](PF_6)_2$ is particularly sensitive to quenching by oxygen as can be seen from the results presented in chapter 4 and hence in a rigid matrix, *e.g.* a glass, where oxygen diffusion is inhibited the emission quantum yield, lifetime and intensity will be much greater than in fluid solution. The glass transition temperature for the EtOH/MeOH solvent system employed in the majority of these studies can be estimated from the sudden change (decrease) in observed emission λ_{max} and intensity, and luminescence lifetime as the temperature is raised. This effect is due to solvent melting

will allows vibrationally coupled deactivation with solvent modes acting as energy acceptors to become important in the term Σk_{nr}. In addition rigidochromic effects are observed on moving through the glass transition (T_g) region (*i.e.* red-shift in emission maxima on raising temperature). Rigidochromic effects arise from the inability of the solvent sphere to move to respond to the change in dipole caused by charge transfer transitions. Hence for charge transfer excited states a red shift upon melting of a glass matrix is observed. This red shift in itself may contribute significantly to the decrease in emission lifetime due to the reduction in energy gap between ground and the emissive excited state. Based on decreases observed for $[Ru(ph_2phen)_3](PF_6)_2$, the glass transition region (T_g) has been estimated at 100 to 125 K for EtOH/MeOH 1/4 v/v. In the temperature range below 120 K a strong blue shift on decreasing temperature is observed. Above the T_g (120 K to 180 K) the change in emission energy is of the order <10 nm and the dramatic change in emission intensity observed below 120 K is replaced by a gradual change in emission intensity, which is due to population of thermally accessible excited states (*e.g.* a fourth ^{3}MLCT state)).

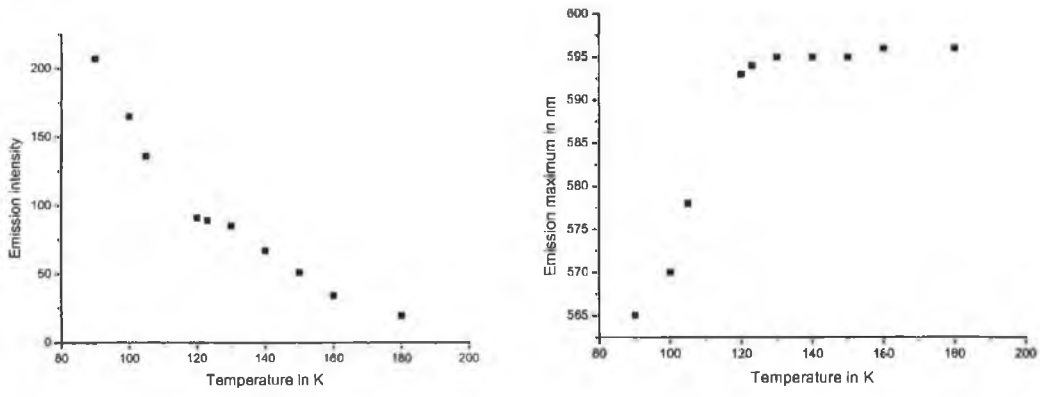

Figure 5.4 Effect of temperature on emission intensity and λ_{max} of the emission spectrum of $[Ru(ph_2phen)_3](PF_6)_2$.

For the other solvent systems used, $LiCl/H_2O$ (T_g = 180-200 K), $LiCl/D_2O$, NaCl/MeOH (T_g = 150-160 K), and CH_2Cl_2/DMF (T_g = 105-130 K) the glass transition temperatures have been estimated from the change in intensity observed for the complex under examination.

The complexes $[Ru(bpy)_2(ppt1)]^+$, $[Ru(bpy)_2(bpbt)]^{2+}$, $[Ru(bpy)_2(pytr)]^+$, and $[Ru(bpy)_2(phpytr)]^+$ were examined in the temperature region 90-220 K in EtOH/MeOH matrices. In all cases a single emission was observed with similar behaviour to

$[Ru(ph_2phen)_3]^{2+}$. This is in complete agreement with observations made for $[Ru(bpy)_2(pytr)]^+$, made by Keyes *et al.* and form a basis to be certain that the dual emissive properties observed for Group B and Group C complexes is not an artefact of the matrix employed nor due to impurities.[1]

5.2.1.2 Group B complexes

The effect of ligand variation for the pyrazine based complexes (exchanging bpy for another symmetric diimine ligand) was examined. Interestingly the temperature dependence of the emission spectrum of $[Ru(biq)_2(pztr)]^+$ and $[Ru(ph_2phen)_2(pztr)]^+$ are similar to those observed for $[Ru(bpy)_2(pytr)]^+$ and the other complexes of group A (see Figure D2 to 4). No evidence was obtained for dual emission in the 90 to 250 K temperature range. In addition no excitation wavelength dependence was observed in the shape and the λ_{max} of the emission spectra at any temperature. In contrast the temperature dependence of the emission spectrum of $[Ru(phen)_2(pztr)]^+$ (and $[Ru(phen)_2(d_4\text{-pztr})]^+$) showed dual emission almost identical to that reported by Keyes *et al.* for $[Ru(bpy)_2(pztr)]^+$ (see Figure D.5 to 7).[1] Time resolved luminescence studies at several temperatures have been carried out (see Figure D.20 to 23). It is clear from these studies that the high and low energy emissions are not equilibrated and show very much different emission lifetimes. The solvatochromic behaviour of the dual emission was investigated further for $[Ru(phen)_2(pztr)]^+$ and $[Ru(phen)_2(d_4\text{-pztr})]^+$.

$[Ru(phen)_2(pztr)](PF_6)$ and $[Ru(phen)_2(d_4\text{-pztr})](PF_6)$ under deprotonating conditions in EtOH /MeOH (4:1 v/v): The effect of solvent and the different glass transition temperatures (T_g) on the dual luminescent behaviour was examined (see Figure D5.8 to 13). It is possible that dual emission is an artefact of the glassy state or the increasing solvent viscosity as the temperature is lowered. If this were so then the temperature range over which the two emissions are observed would be expected to vary with the solvent system employed. This would be particularly noticeable for the $LiCl/H_2O$, $LiCl/D_2O$ and NaCl/MeOH systems as the T_g is considerably higher for these solvents than it is for the EtOH/MeOH and CH_2Cl_2/DMF systems.

The temperature dependence of the emission spectrum of the complex $[Ru(phen)_2(pztr)](PF_6)$ has been examined in the following solvent systems. CH_2Cl_2/DMF 4/1 v/v with 2% diethylamine, NaCl/MeOH with Et_2NH, H_2O or D_2O 9 M LiCl solution Et_2N, N-ethylmorpholine or Et_3N, EtOH/MeOH 4:1 solution N-ethylmorpholine or Et_3N,

EtOH/MeOH 4:1 solution with no added base (native pH). Dual emission was observed in each case and found not to be affected by the base added.

In CH_2Cl_2/DMF, an aprotic polar solvent, dual emission was observed under 150 K (possibly higher) (see Figure D.8 and D.9). However the evidence for dual emission is not immediately apparent as in EtOH/MeOH glasses. At both 90 K and 130 K, the excitation wavelength dependence of the emission spectrum is very noticeable. As the excitation energy is lowered from 450 nm to 520 nm the lower energy emission becomes more dominant in the overall emission spectrum. In NaCl/MeOH with Et_2NH, dual emission is also observed below 150 K ($T_g \sim 150 - 160$ K) (see Figure D.10). However, again the lower energy emission is most obvious at low energy excitation.

In aqueous glasses, at 450 nm excitation, no dual emission is "observed" however dual emission is observed following 520 nm excitation. The excitation wavelength dependence is shown in Figure A5.11/12.

[Ru(phen)$_2$(pztr)](PF$_6$) under protonating conditions in EtOH/MeOH with CF_3CO_2H: As for in basic aqueous solution the evidence for dual emission is found by excitation at 520 nm (Figure D.13). In contradiction to the findings of Keyes *et al.* dual emission is observed at and below 120 K (*i.e.* in the glassy state) in EtOH/MeOH with CF_3CO_2H.[1] The emissions are well resolved at 520 nm excitation with the high energy emission decreasing rapidly as the temperature is raised. At 430 nm excitation dual emission is not observable.

5.2.1.3 Group C complexes

The temperature dependence of the emission spectra of the complexes $[Ru(bpy)_2(phpztr)]^+$, $[Ru(bpy)_2(ppt2)]^+$, $[Ru(bpy)_2(3\text{-}(2,4\text{-dimethoxyphenyl})pztr)]^+$, $[Ru(bpy)_2(Brpztr)]^+$, $[Ru(bpy)_2(Mepztr)]^+$ and $[Ru(bpy)_2(bpzbt)]^{2+}$ have been examined in the methanol/ethanol (1/4 v/v) with 2% diethylamine (Figure D.14 to 19). In each case very similar temperature dependencies have been found to those found for $[Ru(bpy)_2(pztr)](PF_6)$ and $[Ru(phen)_2(pztr)](PF_6)$. The energies of both the high and low energy emissions are very similar for each complex suggesting that the substituent in the 5 position of the 1,2,4-triazole ring is not a significant source of perturbation of the excited state structure.

One case in particular is worth discussing in more detail. Figures D.18 and D.19 show the temperature dependence of the emission spectra of $[(Ru(bpy)_2)_2(bpbt)]^{2+}$ and $[(Ru(bpy)_2)_2(bpzbt)]^{2+}$. Both of these complexes are prepared by a coupling reaction or two mononuclear complexes and not directly from the ligand.[36] Being binuclear complexes exhibiting moderate interaction between the metal centres, it would be expected that their electronic properties would show considerable differences compared to their mononuclear analogues.[36] Room temperature absorption and emission spectroscopy indicate that this is not the case and not surprisingly both these binuclear complexes show emission temperature dependence akin to their mononuclear analogues. This may have implications for the localisation/ delocalisation of the excited state over the two metal centres, in that the excited states may be localised on a single metal centre (however since both metal centres are identical then this is near impossible to prove either way).

$[Ru(bpy)_2(phpztr)]^+$. More detailed studies into the low temperature luminescence of this complex, including lifetime dependence and solvatochromic effects, were carried out. Between 180 K and 292 K a single emission (~660 nm) is observed. Over this range a red shift is observed in the emission maximum as the temperature is reduced. This is not unusual and is related to the ability of the solvent to stabilise the excited state. As the temperature is raised the solvent sphere surrounding the complex becomes increasingly randomised and hence the state is destabilised and the emission shifts to higher energy. Below 180 K a second emission appears at higher energy (~ 620 nm). Above 140 K it is seen as a shoulder on the room temperature emission, and is very apparent in time resolved spectra. Below 135 K the 660 nm emission rapidly becomes a shoulder of the high temperature emission and below 110 K the high-energy emission is the only emission "observed". However emission lifetime measurements at 77 K show biexponential behaviour with emission lifetimes of 1.9 (55 %) and 5.4 (45 %) μs. This biexponential behaviour has been found to be emission wavelength dependent, in that the relative contributions of each of the component lifetimes changes, although the lifetimes show only minor variations. This suggests that both emissions are ^{3}MLCT based since ^{3}dd and ^{3}IL emission general exhibit much longer emission lifetimes at 77 K.

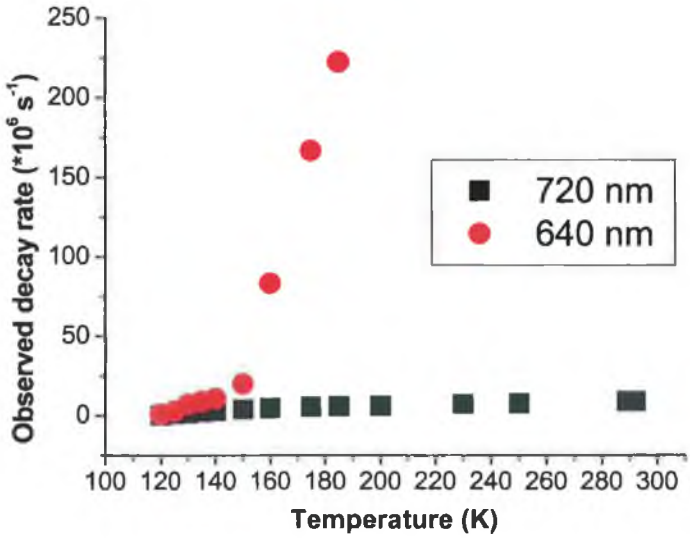

Figure 5.5 *Chart showing the temperature dependence of the observed emission decay rate (k_{obs}) of [Ru(bpy)$_2$(phpztr)](PF$_6$) monitored at 640 nm and 720 nm*

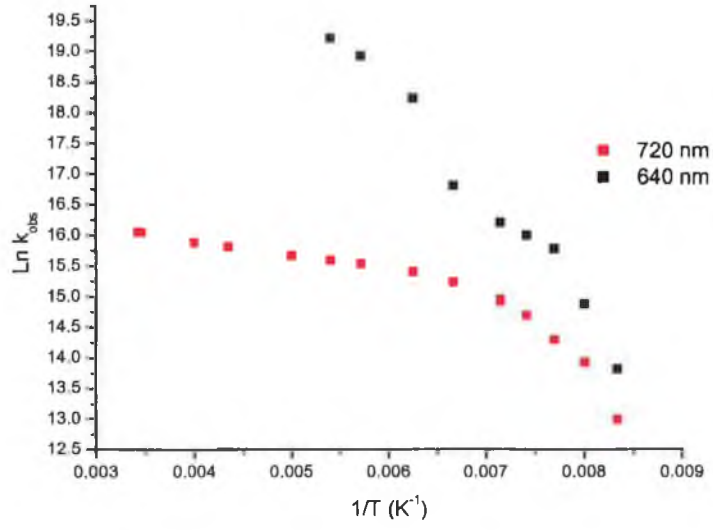

Figure 5.6 *Chart showing the temperature dependence of the natural log. Of the observed emission decay rate (ln k_{obs}) of [Ru(bpy)$_2$(phpztr)](PF$_6$) monitored at 640 nm and 720 nm*

Figure 5.5 and Figure 5.6 show the temperature dependence of the observed emission decay rate. Monitoring at 640 and 720 nm allows for the measurement of each emission with only minimal contribution from the other emission. The high-energy emission undergoes a dramatic increase in the rate of decay above 140 K but is still measurable up to 190 K. The low energy emission has much less dramatic temperature dependence.

However Figure 5.6 shows that below 140 K the temperature dependence of the emission is altered. This change is common and has been found to be due to the viscosity of the solvent (rigidochromic effect), which decreases rapidly on increasing temperature. This effect has been observed previously for similar compounds.[29]

5.2.1.4 Summary of results and discussion

As expected the pyridyl-triazole based complexes (group A) exhibit normal temperature dependent emission behaviour in the temperature range 80 to 298 K. This provides strong evidence that the dual luminescence observed for the pyrazine based complexes is not due to impurities or more importantly due to experimental artifacts. All complexes in group A show no wavelength dependence of the emission spectra (except in intensity). Changes in emission energy occur only in glass transition region and above 200 K (where an increase in emission energy is observed due to thermal randomisation of the solvent sphere preventing the solvent relaxing to its most stable state).[29]

Substitution of the bpy ligands in $[Ru(bpy)_2(pztr)]^+$ with phen results in very little change in the emission properties of the complexes. In contrast substitution with ph_2phen or biq results in a complete loss in dual emissive behaviour.

For $[Ru(biq)_2(pztr)]^+$ a significant lowering in the emission energy is observed. The biq based ^{3}MLCT excited state is significantly stabilised relative to either bpy or phen. As a result the driving force for population of the biq ^{3}MLCT states from pyrazine based ^{3}MLCT states is large. In addition, the ^{3}MC excited state of the biq complex is lower than for the bpy complex. This provides more efficient deactivation of pyrazine ^{3}MLCT states than in $[Ru(bpy)_2(pztr)]^+$. In consideration of these effects it is therefore, unsurprising that $[Ru(biq)_2(pztr)]^+$ does not exhibit the dual emission properties seen in $[Ru(bpy)_2(pztr)]^+$.

In contrast to biq, the relative energies of the bpy, phen and ph_2phen based ^{3}MLCT states are quite similar (see Chapter 4) and hence substitution of bpy for phen or ph_2phen would not be expected to alter the emissive properties dramatically. It is unusual therefore that whilst substitution with phen does not affect the emission properties, substitution with ph_2phen results in a normal temperature dependent emissive behaviour being observed.

That phen substitution does not alter the emission properties dramatically has been observed previously for the dual emitting complexes $[Rh(LL)_2phi]^{3+}$ and

$[Ru(LL)(HDPA)_2]^{2+}$ (where LL = bpy or phen) (vide supra).[17] For ph_2phen, the ^{3}MLCT excited states are considerably more delocalised than for bpy or phen and hence the dipole change barrier to internal conversion is reduced. In addition the ph_2phen ^{3}MLCT state is less distorted relative to the ground state, which may increase the coupling with the pyrazine ^{3}MLCT state.

Variation of the –H in the 5 position of the 1,2,4-triazole ring with bromide, phenyl *etc.* has been examined. The effect of substitution on the acid/base and electrochemical properties of the complexes is significant due to the perturbation of the σ-donor properties of the triazole ring. As a result, it is somewhat surprising that the emissive properties of all the complexes examined in this group are relatively unperturbed. That the emission properties and hence the lowest excited states are relatively unperturbed by substitution of the triazole ring indicates that the interaction between the two emitting states is also unperturbed. This is found to be so with dual emission observed in each case in the same temperature range.

The solvatochromic behaviour of the complex $[Ru(phen)_2(pztr)]^+$ shows that the dual emissive behaviour is strongly affected by the solvent environment. The wavelength dependence of the emission of the deprotonated complex shows the low energy emission becomes more pronounced upon excitation at longer wavelength. This indicates that population of each of the emitting states from higher states is not equal and once populated the two states do not equilibrate at low temperature.

The dipole change on switching between the pyrazine and bpy ^{3}MLCT states is expected to be considerable since in involves a switching between $[(bpy)_2Ru^{III}(pztr^{2-})]^{+}$* and $[(bpy)(bpy^{-})Ru^{III}(pztr^{-})]^{+}$*. This provides a considerable barrier to internal conversion. For the protonated complex the dipole change for such a transition is reduced and hence the barrier reduced. In addition upon protonation, the pyrazine ^{3}MLCT state is stabilised relative to the bpy ^{3}MLCT states. This suggest for the protonated complexes only single emission will be observed. This is found experimentally. However, in glassy media (*i.e.* below the T_g of the solvent system), the emission was found to be wavelength dependent with a low energy emission gaining in relative intensity with excitation at longer wavelength.

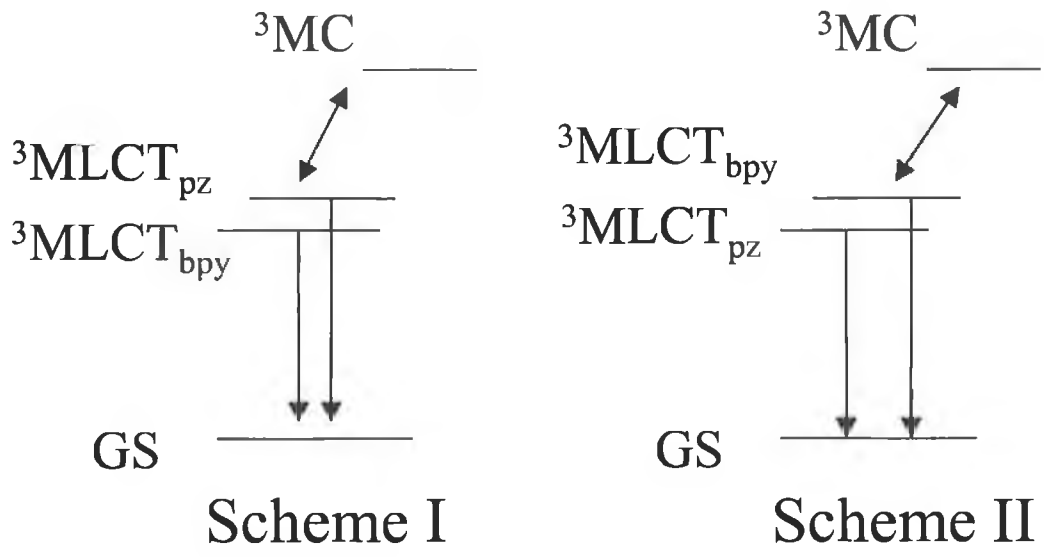

Figure 5.7 *Proposed models for excited state structure of deprotonated dual emitting complexes.*

Based on the complex $[Ru(bpy)_2(pypz)]^{2+}$,[37] it would be expected that the lowest emissive state is pyrazine based (*i.e.* Scheme II). Excited state resonance Raman studies and the effect of deuteriation on the excited state lifetimes strongly suggest that the emissive state at room temperature is bpy based (*i.e.* Scheme I). Above 180 K the two excited states are equilibrated, hence given that the pyrazine excited state Raman enhancement is much lower than for bpy^{*-}, if both states are populated in equilibrium, the excited state resonance Raman spectrum will be dominated by bpy^{*-} vibrational modes. A second consideration is the proximity of the ^{3}MC state, which facilitates rapid deactivation of ^{3}MLCT states with which it is strongly coupled. This deactivation is a thermally activated process and its importance is strongly dependent on the relative energies of the ^{3}MLCT states to it. Based on the relative insensitivity of the emission lifetime to deuteriation of the pyrazine ring for the deprotonated complex (see Chapter 4), it would be expected that the higher excited state is the pyrazine based ^{3}MLCT state. For the protonated complex the absence of evidence for population of the bpy based ^{3}MLCT at room temperature form excited state resonance Raman studies suggests that the lowest excited state in this case is pyrazine based.

5.2.2 Picosecond time resolved luminescence spectroscopy of $[Fe(bpy)_3]^{2+}$, $[Ru(bpy)_3]^{2+}$ and $[Os(bpy)_3]^{2+}$: ^{1}MLCT emission vs. emission from vibrationally hot ^{3}MLCT states

5.2.2.1 $[Ru(bpy)_3]^{2+}$

The emission spectrum recorded from time resolved luminescence studies 2 ps after excitation together with the steady state absorption and emission (^{3}MLCT) spectra for $[Ru(H_8\text{-bpy})_3]^{2+}$ are shown in Figure 5.8.

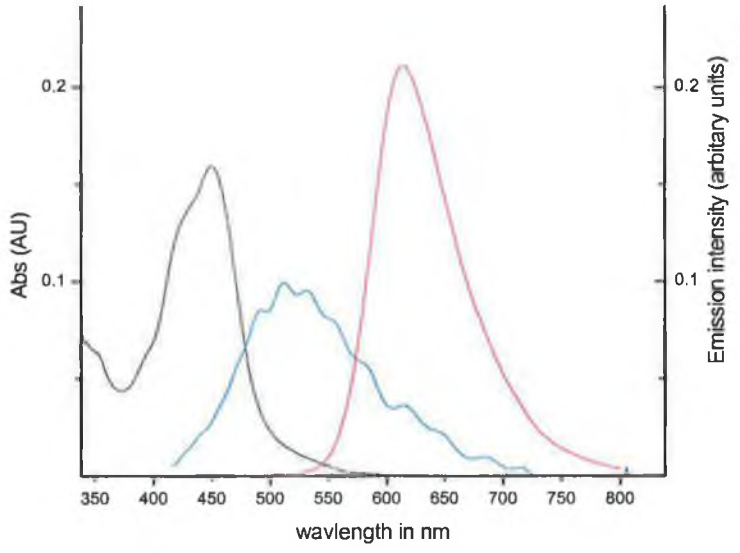

Figure 5.8 *Absorption spectrum (black), steady state emission spectrum (red) of $[Ru([D_8]\text{-bpy})_3]^{2+}$ and emission spectrum at 6 ps after laser excitation in H_2O at 289 K (spectral intensity is adjusted for clarity).*

For $[Ru(bpy)_3]^{2+}$ the emission at 520 nm rapidly decay to the long lived ^{3}MLCT emission. The decay is less than 3 ps and shows no change in emission λ_{max} during the course of its decay.[iii] Time resolved spectra for $[Ru([D_8]\text{-bpy})_3]^{2+}$ between 0 and 1000 ps are shown in Figure 5.9. It is immediately apparent that the effect of deuteriation on the 525 nm emission intensity relative to the 615 nm emission is very large. Although the number of data points available precludes the fitting of exponential curves an estimation of the emission lifetime can still be made, albeit with inherently large uncertainty associated. {< 3 ps for $[Ru([H_8]\text{-bpy})_3]Cl_2$ and 90 ps for $[Ru([D_8]\text{-bpy})_3]Cl_2$, Figure 5.10}. Similar results are obtained for the hexafluorophosphate salts in acetonitrile.

iii The decay is less than the limit of resolution of the picosecond systems

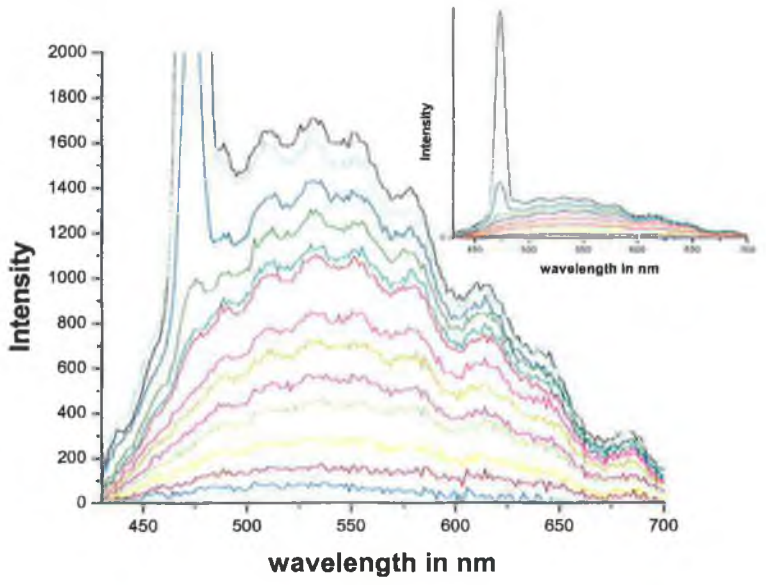

Figure 5.9 *Time resolved emission spectra of [Ru([D_8]-bpy)$_3$]Cl_2 in H_2O at 0, 2, 4, 6, 8, 10, 20, 30, 50, 100, 500 and 1000 ps (inset shows full H_2O Raman signal at 480 nm). λ_{max} excitation at 410 nm*

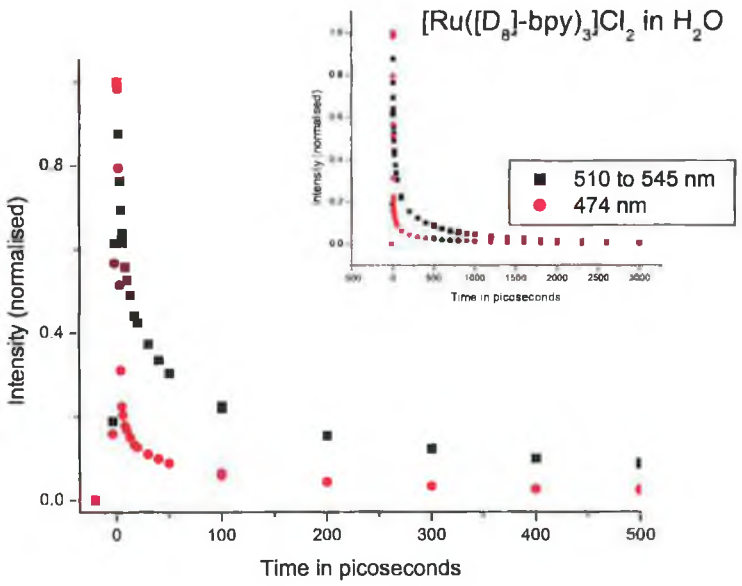

Figure 5.10 *Evolution of emission spectrum of [Ru([D_8]-bpy)$_3$]$^{2+}$ monitored at 474 nm (H_2O Raman Band) and between 510 and 545 nm. Inset shows decay between –20 and 3000 ps.*

The results obtained for $[Ru(bpy)_3]^{2+}$ are in good agreement with the results obtained on the femtosecond timescale by McCusker and coworkers using transient absorption spectroscopy[35] and by Basikuttan *et al.* using fluorescence upconversion spectroscopy.[34]

However the model proposed by Basikuttan *et al.*, *i.e.* emission from vibrationally hot excited states, is not consistent with the results obtained for the fully deuteriated complex $[Ru([D_8]\text{-bpy})_3]^{2+}$. The model previously proposed suggested that the higher vibrionic states of the lowest ^{3}MLCT excited state relaxed relatively slowly in comparison to relaxation from higher states and ISC processes. The λ_{max} of the short lived luminescence reported here and elsewhere is ~ 530 nm and is at least 2900 cm^{-1} higher that the λ_{max} of emission from the lowest ^{3}MLCT state. This energy gap corresponds to C-H and O-H stretching modes and it is therefore conceivable that slow vibrational cooling is responsible for this emission.

However, the effect of deuteriation on the 520 nm emission is somewhat perplexing. An increase in emission lifetime from >3 ps to 90 ps upon deuteriation is not consistent with slow vibrational cooling (the longest reported in solvents with very low thermal diffusivity rates is 25 ps for completion[38]). Deuteriation will reduce the energy of the C-H vibrational modes (as well as ring breathing and other modes) by approximately 800 cm^{-1}. Assuming the effect of deuteriation on ground and excited state vibrational modes is approximately the same then only minor changes in emission energy (less than the experimental error in any case) are expected. The rate of deactivation is related to the ability of the solvent to dissipate the excess vibrational energy. Deuteriation of the ligands would be expected to perturb this process. However in most solvents and especially hydrogen bonding solvents deuteriation should not affect the rate of vibrational cooling to any significant extent and no increase in emission lifetime should be observed. In order to explain the effect of deuteriation on this system then comparison with a the well known $[Pt(POP)_4]^{4-}$ (where POP = μ-$P_2O_5H_2$) is made. This system exhibits a very long lived $^3A_{2u}$ (9.8 μs at 20 °C) and very short lived weak fluorescence from the $^1A_{2u}$ (740 ps at 77 K). The fluorescence shows a marked deuteriation effect (increases to 2100 ps). This increase has been attributed to the reduction in the overlap of vibrionic functions between the singlet and triplet states and hence reduces the rate of ISC.

Since the distortion between the ^{1}MLCT and the ^{3}MLCT states in ruthenium complexes show relatively little distortion relative to the ground state (hence they are weakly coupled) then transitions such as intersystem crossing will rely on high energy vibrational modes such as O-H and C-H to mediate ISC. Hence for weakly coupled systems a strong deuteriation effect would be expected on the rate of ISC.

5.2.2.2 $[Fe(bpy)_3]^{2+}$

Picosecond time resolved spectra for $[Fe([H_8]\text{-bpy})_3]^{2+}$ and $[Fe([D_8]\text{-bpy})_3]^{2+}$ are shown in Figure 5.11. Both emissions are within < 3 ps and in contrast to $[Ru(bpy)_3]^{2+}$, no effect of deuteriation is observed on the lifetime of the Fe(II) emission.

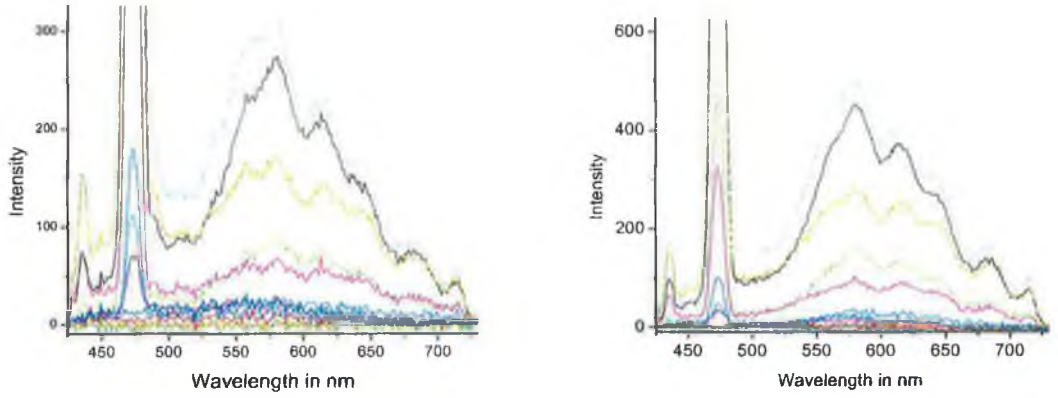

Figure 5.11 *Background subtracted time resolved emission spectra between –2 and 500 ps for $[Fe([H_8]\text{-bpy})_3]^{2+}$ (left) and $[Fe([D_8]\text{-bpy})_3]^{2+}$ (right) in aqueous solution (Sharp bands at 480 nm are due to Raman scattering from the solvent).*

5.2.2.3 $[D_8]$-bpy, $[Os([H_8]\text{-bpy})_3]^{2+}$ and $[Os([D_8]\text{-bpy})_3]^{2+}$

As a control experiment picosecond time resolved emission studies were carried out on $[D_8]$-bpy and a scattering solution. As expected no emission was observed and in addition very little Raleigh scattering was detected. Like wise for both $[Os([H_8]\text{-bpy})_3]^{2+}$ and $[Os([D_8]\text{-bpy})_3]^{2+}$ no evidence of sub nanosecond emission was observed. These latter results are not unexpected considering the very large spin-orbit coupling observed for osmium, compared with ruthenium. The assignment of spin to any state in osmium complexes has little meaning and the rate of relaxation to the lowest excited state would be expected to be faster than for ruthenium.

Overall the results of for the complexes $[Fe(bpy)_3]^{2+}$, $[Ru(bpy)_3]^{2+}$ and $[Os(bpy)_3]^{2+}$, and in particular the effect of deuteriation may be rationalised in terms of weak and strong coupling between excited states (see Chapter 1). As discussed above the coupling between the MLCT states is weak, *i.e.* the ground and excited state geometries are

similar. In contrast the coupling between the MLCT states and the lowest metal centred excited states (^{3}MC/^{1}MC) is strong (*i.e.* the MC states show a large geometric distortion compared with the ground state to the population of the e_g orbitals). For Ru(II) the weak coupling between the lowest ^{1}MLCT excited state and ^{3}MLCT results in high energy vibrational modes being important in facilitating ISC. For Fe(II) the lowest excited state is metal centred and hence ISC from the ^{1}MLCT excited state to the ^{3}MC excited state is fast due to the strong coupling between those two states. Since all vibrational modes facilitate ISC/IC in the strong coupling limit then the effect of deuteriation on the rate of these processes would be expected to be negligible.

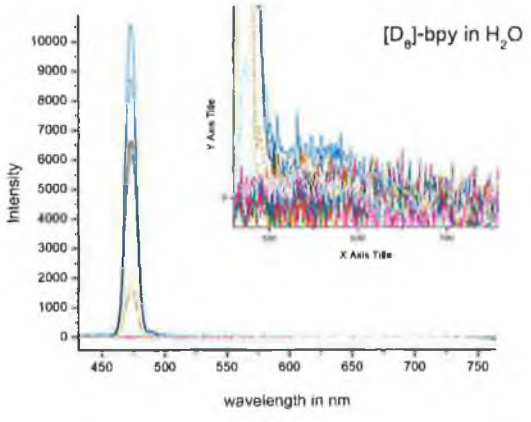

Figure 5.12 *Time resolved emission spectra of [D_8]-bpy in aqueous solution*

5.3 Conclusions

5.3.1 Dual emission in 1,2,4-triazoles

It is clear that the dual emissive behaviour observed for $[Ru(bpy)_2(pztr)]^+$ is a phenomenon general to this class of compound and is quite insensitive to perturbation by minor substitution of the triazole ring. In addition the observation of dual emission for the protonated complexes and in media other than Ethanol/Methanol confirms that this behaviour is also not due to solvent properties. The presence of two non-equilibrated states in mononuclear complexes is not unique, however in the majority of cases these states are somewhat spatially separated. For $[Ru(bpy)_2(pztr)]^+$ the barrier to internal conversion due to excited state localisation on specific ligands is of relevance. In future studies, the effect of deuteriation and triazole substitution (in 5 position) on the temperature dependence of the lifetimes of both emissions are be of interest. In addition the use of techniques such as Stark effect spectroscopy to measure the dipole moment of

each of the emissive excited states could prove useful in understanding the importance of dipole barrier in this phenomenon.

5.3.2 Picosecond spectroscopy of group VIII polypyridyl complexes

The studies described in this chapter, are of interest in understanding the fundamental, early, processes, which occur upon excitation of Group VIII polypyridyl complexes. The identification of the picosecond emissions as being ^{1}MLCT in origin is tentative and requires further investigation, in particular in examining the solvatochromic effects on the emission lifetimes using picosecond time correlated single photon counting techniques.

5.4 Experimental

All solvents used were of spectroscopic grade. The preparation of $[Ru(bpy)_2phpztr)](PF_6)$ is described in Appendix F. The complexes $[Ru(biq)_2(pztr)](PF_6)$, $[Ru(bpy)_2(pztr)](PF_6)$, $[Ru(bpy)_2(pytr)](PF_6)$, $[Ru(bpy)_2(ppt1)](PF_6)$ and $[Ru(bpy)_2(ppt2)](PF_6)$ together with the partially and fully deuteriated analogues were provided by Dr. C. O'Connor (Dublin Institute of Technology). The complexes $[Ru(bpy)_2(5\text{-}Brpztr)](PF_6)$, $[Ru(bpy)_2(5\text{-}Brpytr)](PF_6)$, $[(Ru(bpy)_2)_2(bpbt)](PF_6)_2$, $[(Ru(bpy)_2)_2(bpzbt)](PF_6)_2$ were provided by Dr. C. De Pietro (Univerity of Messina).[36] The complex $[Ru(bpy)_2$(3-(2,5-dimethoxy-phenyl)-5-(pyrazin-2-yl)-1,2,4-triazole)$](PF_6)$ was prepared Dr. D. Hughes (DCU). All complexes have been characterised by NMR, UV.Vis and emission spectroscopies. Purity has been determined by analytical HPLC. The synthesis and characterisation of all other complexes is described in Chapters 2 and Appendix F. Details for experimental techniques are given in Chapter 2. $[Fe([H_8]\text{-}bpy)_3]^{2+}$ and $[Fe([D_8]\text{-}bpy)_3]^{2+}$ were prepared *in situ* by reaction of $Fe(SO_4).7H_2O$ with 3 mole equivalents of $[H_8]$-bpy and $[D_8]$-bpy respectively in double distilled water.

5.6 Bibliography

1. T. E. Keyes, C. M. O'Connor, U. O'Dwyer, C.G. Coates, P. Callaghan, J. J. McGarvey and J. G. Vos, *J. Phys. Chem. A*, **1999**, *103*, 8915

2. M. Kasha, *Discuss. Faraday Soc.*, **1950**, *9*, 14

3. C. D. Hoger, G. A. Crosby, *J. Am. Chem. Soc.*, **1975**, *97*, 7031

4. J. N. Demas and G. A. Crosby, *J. Am. Chem. Soc.*, **1970**, *92*, 7262

5. R. J. Watts and J. van Houten, *J. Am. Chem. Soc.*, **1978**, *100*, 1718

6. S. Sprouse, K. A. King, P. J. Spellane and R. J. Watts, *J. Am. Chem. Soc.*, **1984**, *106*, 6647

7. A. I. Baba, J. R. Shaw, J. A. Simon, R. P. Thummel and R. H. Schemhl, *Coord. Chem. Rev.*, **1998**, *171*, 43

8. M. K. DeArmond and C. M. Carlin, *Coord. Chem. Revs.*, **1981**, *36*, 325

9. J. A. Simon, S. L. Curry, R. H. Schmehl, T. R. Schatz, P. Piotrowiak, X. Jin and R. Thummel, *J. Am. Chem. Soc.*, **1997**, *119*, 11012

10. S. Fanni, T. E. Keyes, S. Campagna and J. G. Vos, *Inorg. Chem.*, **1998**, *37*, 5933

11. J-M. Kern, J-P. Sauvage, J-L. Weidmann, N. Armaroli, L. Flamigni, P. Ceroni and V. Balzani, *Inorg. Chem.*, **1997**, *36*, 5329

12. S. W. Wallendael, D. P. Rillema, *J Chem. Soc., Chem. Commun.*, **1990**, 1081

13. S. Encinas, A. M. Barthram, M. D. Ward, F. Bargelletti and S. Campagna, *Chem. Commun*, **2001**, 277

14. S. Serroni, S. Campagna, G. Denti, T. E. Keyes, and J. G. Vos, *Inorg. Chem.*, **1996**, *35*, 4513

15. C. Turrro, A. Evenzahav, S. H. Bossmann, J. K. Barton and N. J. Turro, *Inorganica Chimica Acta*, **1996**, *243*, 101

16. (a) P. Didier, I. Ortmans, A. Kirsch-De Mesmaeker and R.J. Watts, *Inorg. Chem.*, **1993**, *32*, 5239 (b) A. P. Wilde, K. A. King and R. J. Watts, *J. Phys. Chem.*, **1991**, *95*, 629 (c) R. J. Watts, *J. Am. Chem. Soc.*, **1974**, *96*, 6186 (d) R. J. Watts, T. P. Watts and B. G. Griffith, *J. Am. Chem. Soc.*, **1975**, *97*, 6914 (e) R. J. Watts, M. J. Brown, B. G. Griffith and J. S. Harrington, *J. Am. Chem. Soc.*, **1975**, *97*, 6029

17. R. L. Blakely and M. K. DeArmond, *J. Am. Chem. Soc.*, **1987**, *109*, 4895

18. S. R. L. Fernando and M.Y. Ogawa, *Chem. Commun.*, **1996**, 637

19. M. M. Glezen and A. Lees, *J. Am. Chem. Soc.*, **1989**, *111*, 6602

20. P. J. Giordano, S. M. Fredericks, M. S. Wrighton and D. L. Morse, *J. Am. Chem. Soc.*, **1978**, *100*, 2257

21. J. R. Shaw and R. H. Schmehl, *J. Am. Chem. Soc.*, **1991**, *113*, 390

22. J. P. Paris and W. W. Brandt, *J. Am. Chem. Soc.*, **1959**, *81*, 5001

23. M. W. Blaskie and D. R. McMillin, *Inorg. Chem.*, **1980**, *19*, 3519

24. R. M. Everly and D. R. McMillin, *J. Phys. Chem.*, **1991**, *95*, 9071

25. J. A. Zuleta, J. M. Bevilacqua, J. M. Rehm and R. Eisenberg, *Inorg. Chem.*, **1992**, *31*, 1332

26. C. Bignozzi, C. Chiorboi, Z. Murtaza, W. E. Jones and T. J. Meyer, *Inorg. Chem.*, **1993**, *32*, 1036

27. (a) K. Kalyanasundaram, *Coord. Chem. Rev.*, **1982**, *46*, 159 (b) J.M. Lehn, *Angew. Chem., Int. Ed. Engl.*, **1988**, *27*, 89 (c) V. Balzani, S. Campagna, G. Denti, A. Juris, S. Serroni and M. Ventura, *Coord. Chem.Rev.* **1994**, *132*, 1 (d) V. Balzani, A. Juris, M. Venturi, S. Campagna and S. Serroni, *Chem. Rev.*, **1996**, *96*, 759 (e) V. Balzani, A. Juris, M. Venturi, S. Campagna and S. Serroni, *Acc. Chem. Res.* **1998**, *31*, 26 (f) C. A. Slate, D. R. Striplin, J. A. Moss, P. Chen, B. W. Erickson and T. J. Meyer, *J. Am. Chem. Soc.* **1998**, *120*, 4885 (g) Y-Z. Hu, S. Tsukiji, S. Shinkai, S. Oishi and I. Hamachi, *J. Am. Chem. Soc.* **2000**, *122*, 241 (h) J-P. Sauvage, J-P. Collin, J.-C. Chambron, S. Guillerez, C. Coudret, V. Balzani, F. Bargelletti, L. De Cola and L. Fannigni, *Chem. Rev.*, **1994**, *94*, 993 (i) J.N. Demas and D.A. DeGraff, *Analytical Chem.*, **1991**, *63*, 829

28. (a) V. Balzani and F. Scandola, *Supramolecular Photochemistry*, Ellis Horwood: Chichester, UK, **1991** (b) V. Balzani, Ed., *Supramolecular Photochemistry*, Reidel, Dordrecht, **1997** (c) J.-M. Lehn, *Supramolecular Chemistry*, Wiley-VCH, Weinheim, **1995**

29. (a) C. A. Slate, D. R. Striplin, J. A. Moss, P. Chen, B. W. Erickson and T. J. Meyer, *J. Am. Chem. Soc.* **1998**, *120*, 4885 (b) Y.-Z. Hu, S. Tsukiji, S. Shinkai, S. Oishi and I. Hamachi, *J. Am. Chem. Soc.* **2000**, *122*, 241 (c) A. Juris, V. Balzani, F. Barigelletti, S. Campagna, P. Belser and A. von Zelewsky, *Coord. Chem. Rev.* **1988**, *84*, 85. (d) T. J. Meyer, *Acc. Chem. Res.* **1989**, *22*, 163. (e) B. O'Regan and M. Graetzel, *Nature,* **1991**, *335*, 737. (f) L. De Cola, P. Belser, *Coord. Chem. Rev.* **1998**, *177*, 301 (g) C. A. Bignozzi, J. R. Schoonover, F. Scandola, *Progr. Inorg. Chem.*, **1997**, *44*, 1 (h) M-J. Blanco, M. C. Jiménez, J-C. Chambron, V. Heitz, M. Linke and J-P. Sauvage, *Chem. Soc. Rev.* **1999**, *28*, 293.

30. (a) R. Bensasson, C. Salet and V. Balzani, *J. Am. Chem. Soc*, **1976**, *98*, 3722 (b) F. Bolletta, M. Maestri and V. Balzani, *J. Phys. Chem.*, **1976**, *80*, 2499

31. (a) I. Martini, J. H. Hodak, G.V. Hartland, *J. Phys. Chem. B*, **1998**, *102*, 9508 (b) B. Burfeindt, T. Hannappel, W. Storck and F. Willig, *J. Phys. Chem.*, **1996**, *100*, 16463

32. (a) M. Hilgendorff and V. Sundstrom, *J. Phys. Chem. B*, **1998**, *102*,10505 (b) R. J. Ellingson, J. B. Asbury, S. Ferrere, H. N. Ghosh, J. R. Sprague, T. Lian and A. J. Nozik, *J. Phys. Chem. B* **1998**, *102*, 6455 (c) T. Hannappel, B. Burfeindt, W. Storck, F. Willig, *J. Phys. Chem. B,* **1997**, *101*, 6799 (d) R.W. Fessenden and P.V. Kamat, *J. Phys. Chem.* **1995**, *99*, 12902 (e) J. B. Asbury, R.J. Ellingson, H.N. Ghosh, S. Ferrere, A. J. Nozik and T. Lian, *J. Phys. Chem. B*, **1999**, *103*, 3110 (f) Y. Tachibana, S. A. Haque, I. P. Mercer, J. R. Durrant and D. R. Klug, *J. Phys. Chem. B.* **2000**, *104*, 1198

33. (a) H. Yersin, E. Gallhuber, A. Vogler and H. Kunkley, *J. Am. Chem. Soc.* **1983**, 105, 4155 (b) H. Yersin and Gallhuber, E. *J. Am. Chem. Soc.* **1984**, *106*, 6582

34. A. C. Basikuttan, M. Suzuki, S. Nakashima and T. Okada, *J. Am. Chem. Soc.*, **2002**, *in press*

35. (a) A. T. Yeh, C. V. Shank and J. K. McCusker, *Science*, **2000**, *289*, 935 (b) N. H. Damrauer, G. Cerullo, A. Yeh, T. R. Boussie, C. V. Shank, J. K. McCusker, *Science*, **1997**, *275*, 54 (c) J. E. Monat and J. K. McCusker, *J. Am. Chem. Soc.*, **2000**, *122*, 4092 (d) N. H. Damrauer and J. K. McCusker, *J. Phys. Chem. A*, **1999**, *103*, 8440 (e) N. H. Damrauer, T. R. Boussie, M. Devenney and J. K. McCusker, *J. Am. Chem. Soc.*, **1997**, *119*, 8253 (f) N. H. Damrauer, B. T. Weldon and J. K. McCusker, *J. Phys. Chem. A*, **1998**, *102*, 3382

36. C. Di Pietro, S. Serroni, S. Campagna, M. T. Gandolfi, R. Ballardini, S. Fanni, W. R. Browne and J. G. Vos, *Inorg. Chem.*, **2002**, *41*, 2871

37. G. D. Danzer, J. A. Golus and J. R. Kincaid, *J. Am. Chem. Soc.*, **1993**, *115*, 8643

38. M. L. Horng, J. A. Gardecki, A. Papazyan and M. Maroncelli, *J. Phys. Chem.*, **1995**, *99*, 17311

Chapter 6

Separation and photophysical properties of the stereoisomers of mononuclear and binuclear ruthenium(II) complexes

In this chapter the separation, characterisation and photophysical properties of the stereoisomers of mono- and bi-nuclear Ru(II) polypyridyl complexes are examined. In particular the importance of chirality both in terms of solvent and complex in ^{1}H NMR spectroscopy and photophysical properties is investigated.

6.1 Introduction

As interest in both polynuclear and asymmetric Ru(II) complexes increases, so too does the issue of isomerism, in terms of both connectivity[1,2] and stereochemistry.[3,4,5] Since through-space interactions are often as significant as through-bond interaction.[6] Obtaining inorganic complexes with well-defined spatial as well as electronic structures is generally viewed as a prerequisite for the successful development of molecular devices.[6] Ru(II) polypyridyl complexes have been extensively investigated for their photochemical, photophysical and molecular recognition properties and a wide range of multinuclear complexes based on bpy and related ligands are reported in the literature.[7,8] It has been recognised for some time that the use of bidentate ligands results in formation of stereoisomers.[3] The importance of stereochemistry and, in particular, chirality is well illustrated in the studies carried out on the stereoselective intercalation of ruthenium polypyridyl complexes into DNA[4,9,10] and proteins.[11]

The isolation of the stereoisomers of mono- and polynuclear Ru(II) and Os(II) diimine complexes has been reviewed recently.[3] The more common approaches used in preparing stereochemically pure systems can be described as: reagent induced stereochemical control,[12,13,14] the use of chiral precursors,[15,16,17,18] chromatographic techniques[10,19,20,21,22,23,24,25,26] recrystallization[27,28] or a combination of these.

There are however relatively few studies which address the relationship between stereochemistry and the photophysical properties of Ru(II) and Os(II) polypyridyl complexes and to the best of my knowledge no studies have been carried out using chiral solvents. Several studies suggest that enantiomers exhibit no observable differences in their electrochemical or electronic properties. In addition only minor, if any, differences in the properties of diastereoisomers have been reported.[20,21,22,23,24,28,29,30] However, Hesek *et al.*[13] observed a significant difference in the UV-Vis spectra of the diastereoisomers of the complex $[Ru(bpy)_2Cl(L)]^+$ (where L = (*R*)-(+)- or (*S*)-(-)-methyl-*p*-tolyl sulphoxide), while Rutherford *et al.*[23] have reported significant differences in luminescence lifetime between the meso- and homo-chiral isomers for the binuclear $[(Ru(bpy)_2)_xHAT]^{2x+}$ complex[23a] (see Figure 6.1) and for the charge separated states of a series of four geometric isomers of a Ru(II) mononuclear chromophore quencher system.[23b] In each case where differences were observed between stereoisomers these were small compared with the inherent uncertainties in the techniques used.

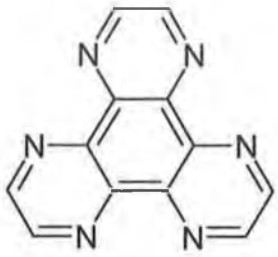

HAT

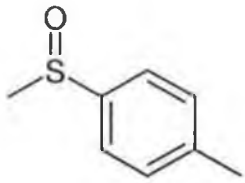

methyl-*p*-tolyl-sulfoxide

Figure 6.1 *Ligands discussed in this chapter*

In this chapter, the separation, ^{1}H NMR spectra and photophysical properties of the enantiomers of **1a/1b** $[Ru(bpy)_2(phpztr)](PF_6)$ and **2a/2b** $[Ru(phen)_2(pztr)](PF_6)$ of the four stereoisomers (**3a-d**) of the complex $[(Ru(bpy)_2)_2(bpt)](PF_6)_3$ are reported (for structure of complexes see Figure 6.2 and Figure 6.3). To assess the importance of stereochemistry on the photophysical properties of the stereoisomers, the electronic spectra and emission lifetimes were measured in both racemic and enantiomerically pure *sec*-1-phenylethanol, at 298 K and 77 K.

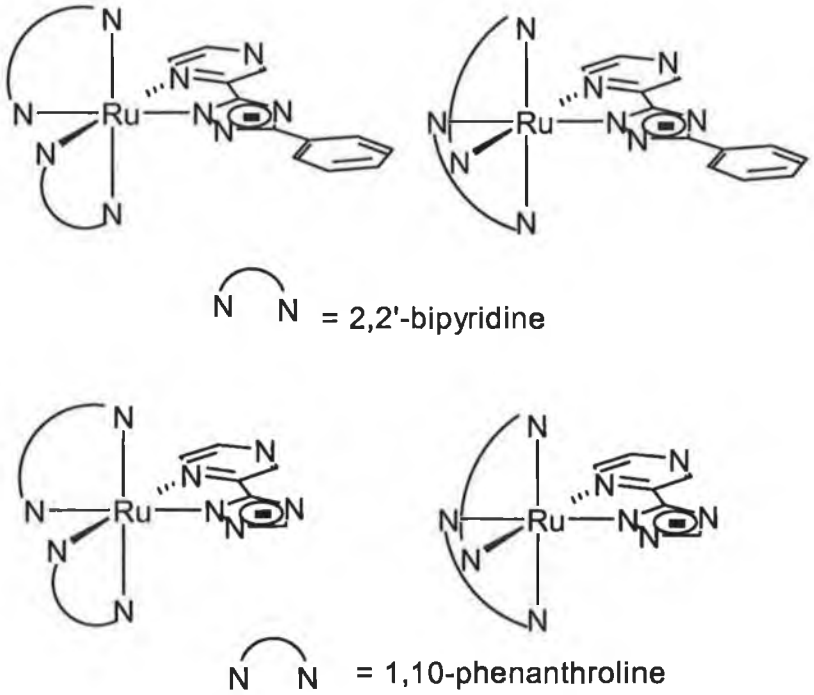

Figure 6.2 *Structure of the stereoisomers of 1 and 2. (ion charges omitted for clarity)*

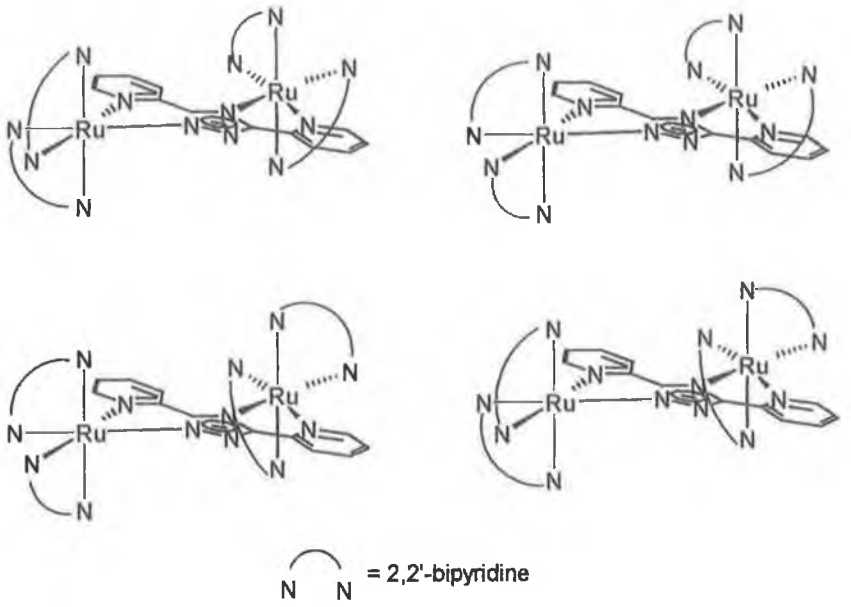

Figure 6.3 *Structure of the four stereoisomers of* ***3****. (ion charges omitted for clarity)*

6.2 Results and Discussion

6.2.1 Chromatographic resolution of stereoisomers

In contrast to the separation of **2** and **3**, the separation of **1** was carried out on both an analytical and semipreparative scale with a commercial column (CHIRACEL OD-RH) using aqueous $NaPF_6$/ acetonitrile 50/50 as mobile phase.

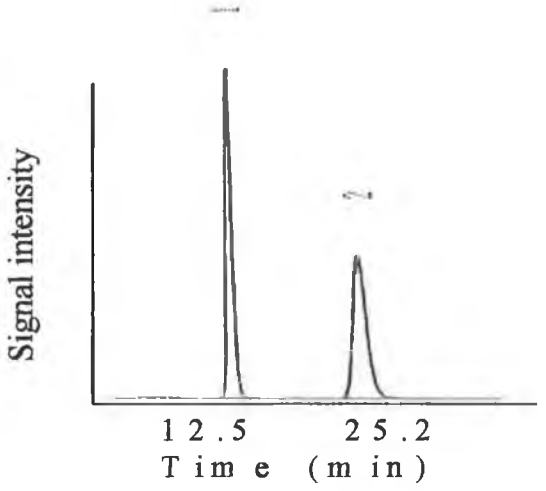

Figure 6.4 *Analytical HPLC chromatogram of* ***1a/1b****. see text for conditions.*

As can be seen from the chromatogram (Figure 6.4) the separation achieved using this column is excellent. Similar results were observed on an analytical column for the complex $[Ru(bpy)_2(5\text{-mepztr})]PF_6$ however it is very noticeable that the retention times for this complex were much shorter than for **1**. This is not unexpected as the column used

is reverse phase (*i.e.* the packing material is hydrophobic) and the substitution of a phenyl group for a methyl group would be expected to reduce the organic nature of the complex. It is of interest to note that for the achiral cation exchange column generally employed (see Chapter 2) the less "organic" the complex the shorter the retention time observed.

The analytical separation of the stereoisomers of **2** and **3** has been reported by Gasparrini *et al.*.[31,32] The separation of the Λ and Δ enantiomers of **2** was carried out on a semipreparative scale using a teicoplanin based column. The resolution obtained using this system is less than that observed for **1**, but is sufficient to allow for isolation of each stereoisomers in enantiomerically pure amounts. The separation of the stereoisomers of **3** was carried on a semi-preparative scale in two steps. In a first set of the separations (Figure 6.5), using $CH_3CN/CH_3OH/AcONH_4$ 0.5 M 60/20/20 as eluent delivered at a flow rate of 4 mL/min, three fractions were collected.

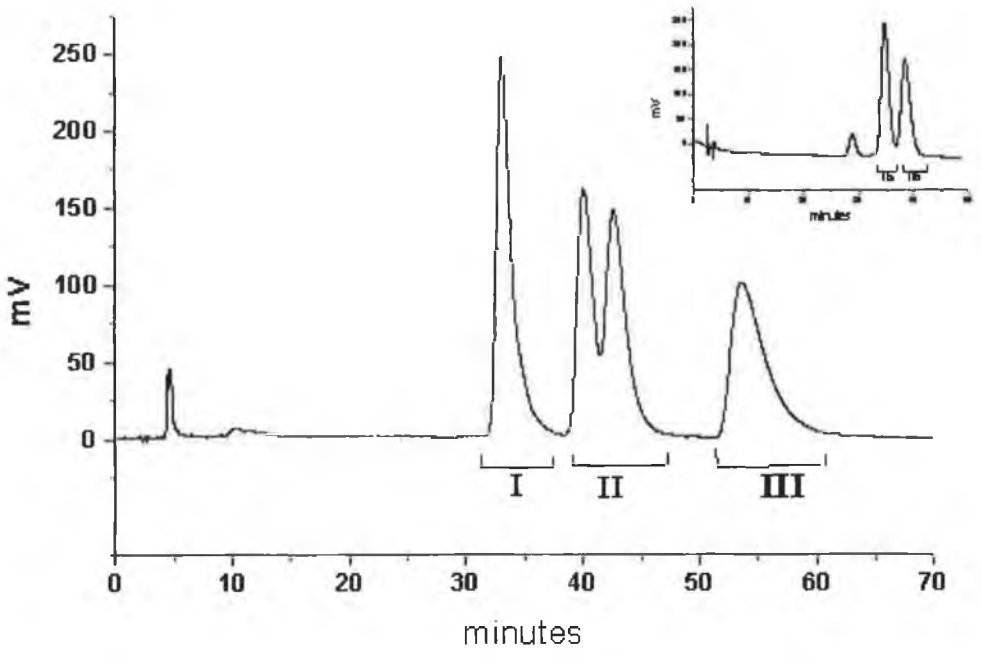

Figure 6.5 *Chromatogram of 3 on CSP1. The insert shows the chromatogram obtained for the separation of the heterochiral isomers.*

The first contained one of the homochiral stereoisomers **3a** (fraction I), the second the two heterochiral stereoisomers **3b** and **3c** (fraction II) and the last the second homochiral stereoisomer **3d** (fraction III) (see Figure 6.5). In a second set of separations (see figure 9.3, inset), the two heterochiral stereoisomers collected as fraction II, were resolved using

a different eluent ($CH_3CN/CH_3CH_2OH/AcONH_4$ 0.5 M 60/20/20), yielding fractions IIa (**3b**) and IIb (**3c**). Yields from four replicate runs and purity check are described in Table 6.1. Purity was estimated by integration of chromatogram peak areas, with control analytical runs being carried out. With the exception of I, the preceding peak contaminated each fraction.

	Yield /mg[#] (impurities)[##]	rac-1-phenylethanol τ /ns	(S)-(-)-1-phenylethanol τ /ns
3a	17(-)	146	163
3b	11(4% of **3a**)	145 (145*)	156
3c	21(27 % of **3b**)	144	155
3d	15(4% of **3c**)	140	156

Table 6.1 *Yield, estimated purity and emission lifetimes (samples deaerated by 20 min Ar purge) of the separated stereoisomers of complex 3. [#] total mass of isomer recovered [##]impurities as a % of peak area relative to the peak due to main stereoisomer *Sample degassed by four freeze-pump-thaw degassing cycles.*

6.2.2 Circular dichroism (CD) spectroscopy

CD spectra of all resolved complexes are presented in this section. Figure 9.5 shows the CD spectra for the Δ and Λ stereoisomers of **1**. As expected both stereoisomers exhibit very strong opposite (but equal) cotton effects.

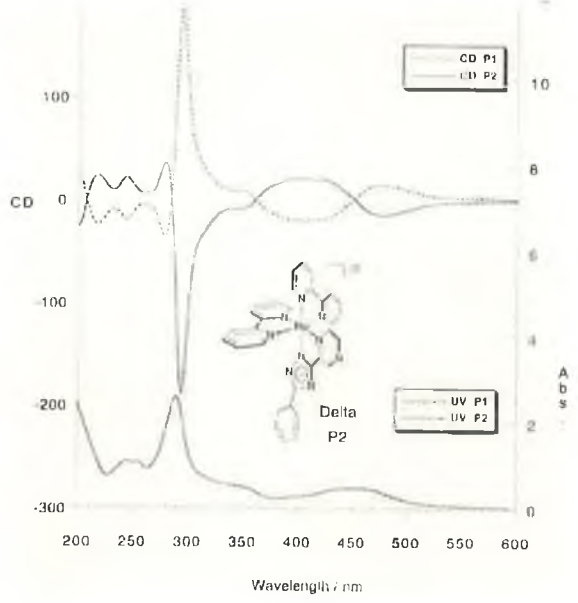

Figure 6.6 *CD and UV.Vis spectra for the Δ and Λ stereoisomers of 1 in acetonitrile {P1 is theΛ isomer/**1a** and P2 is the Δ isomer/**1b**). Spectrum provided by Dr. D. Hesek*

The CD spectra of the stereoisomers of **1** and **2** are, to a first approximation, very similar and show only very minor differences in the position of maxima and minima complexes (see Figure 6.6 and Figure 6.7). Identification of each of the stereoisomers as either Λ or Δ is made on the basis of comparison with $[Ru(bpy)_3]^{2+}$ and related. [5,33]

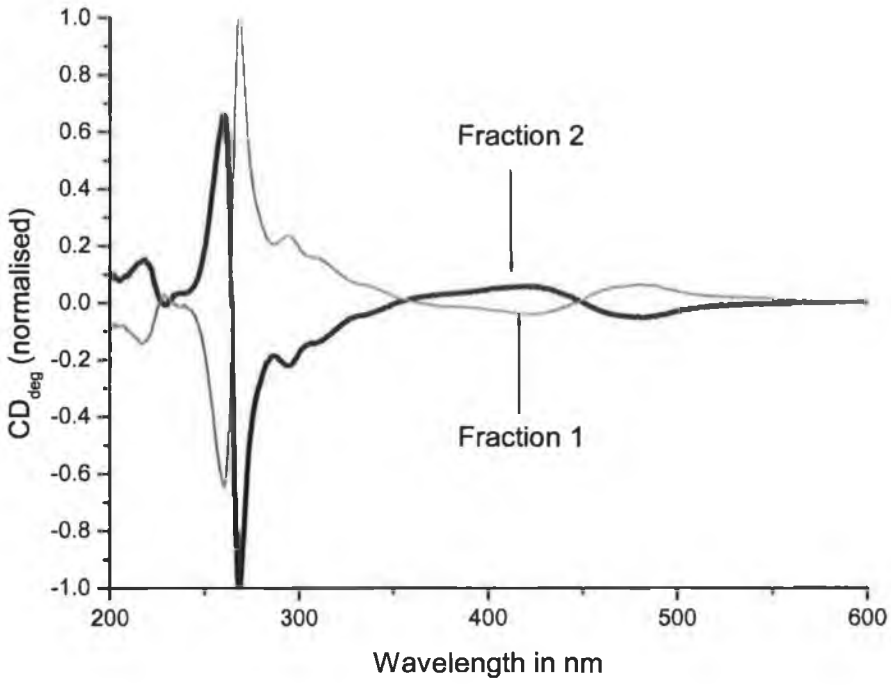

Figure 6.7 *CD and UV.Vis spectra for the Δ and Λ stereoisomers of 2 in acetonitrile {Fraction 1 is the Λ isomer/**2a** and Fraction 2 is the Δ isomer/**2b**}.*

On the basis of single wavelength CD detection of the HPLC traces, the two homo- and heterochiral isomers of **3** are identifiable.[32] It is expected that the homochiral complexes show a much stronger Cotton effect than the heterochiral pair. For the heterochiral pair each of the chiral centres has an opposite effect on the rotation of circularly polarised light. If the centres were identical than the net result would be that no CD spectra would be obtained for the two isomers. However given that the N2 and N4 sites are inequivalent then the net result is a small but observable CD effect. On this basis the first and last fractions may be assigned as the homochiral enantiomers and the 2nd and 3rd fractions as the heterochiral enantiomeric pair. The CD spectra of the **3a** and **3b** are shown in Figure 6.8. From their CD spectra and on the basis of comparison with the CD spectra of $[Ru(LL)_3]^{2+}$ (where LL = bpy or phen), **3a** and **3d** may be assigned as the ΛΛ isomer and the ΔΔ isomer respectively (*vide infra*). This is in agreement with the known selectivity of

the Teicoplanin packing material for the Δ isomer over the Λ isomer of these tris-homoleptic complexes.[32] Fractions IIa and IIb cannot be assigned to either of the two heterochiral isomers (**3b**/**3c**).

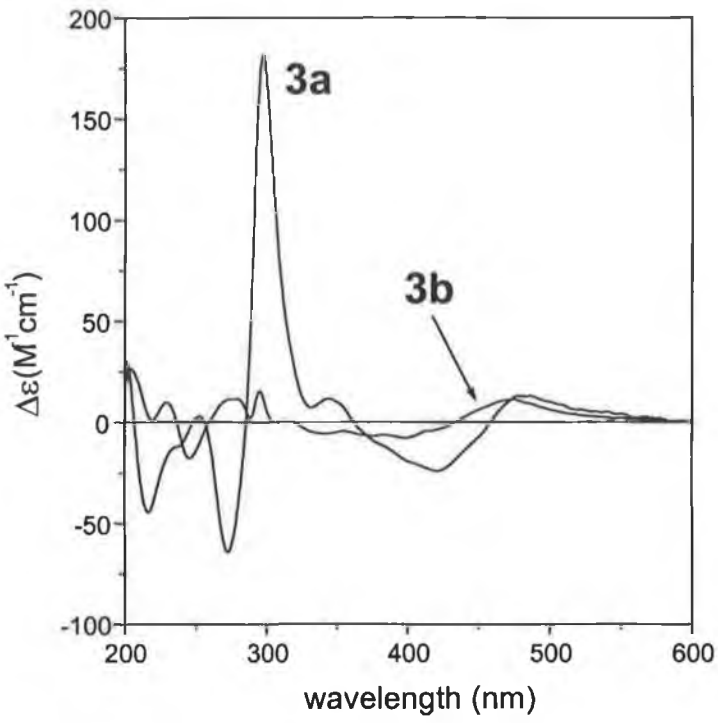

Figure 6.8 *CD spectra of **3a** and **3b** measured in CH_3CN. Provided by Dr. C. Villiani*

In Figure 6.8, the two diagnostic couplets for the Λ configuration are observed in the LCT (ligand centred transition) (272 nm negative and 298 nm positive) and MLCT (421 nm negative and 480 nm positive) regions. There is no significant mutual influence of the two chromophoric units of **3a** and the spectrum of **3a** is simply the sum of that of two mononuclear units. The original heterochiral assignment to **3b** and **3c** is confirmed by their CD spectra. The spectrum of **3b** shows very weak bands, especially in the ππ* region, presumably as a result of the near complete compensation of the two metal centres of opposite chirality. A stronger effect is observed in the MLCT region, which is not surprising since significant differences between the N2 and N4 isomers of pyridyl-1,2,4-triazole based complexes are observed.[34] Hence since a poor overlap of the absorption spectra of each centre is expected then the complete compensation of the two metal centres of opposite chirality is not anticipated.

In order to reliably assign the heterochiral stereoisomers of **3** (*i.e.* **3b**/**3c**) a comparison of the CD spectra of the N4 bound mononuclear isomers of $[Ru(bpy)_2bpt]^+$ with that of the N2 bound isomers is required. If the N2 isomer exhibits a significantly stronger Cotton effect that the N4 isomer then the isomer **3b** may be assigned as the ΛΔ isomer and *vice versa*. The preparation of the N4 isomers useful amounts is possible using high temperatures and pressures to force the isomerisation form N2 to N4 bound making such a determination possible.[34]

6.2.3 ^{1}H NMR spectroscopy

The ^{1}H NMR spectra obtained for the stereoisomers **1** and **2** show no significant differences. This is expected since they are enantiomeric pairs and the spectra were carried out in an achiral solvent. The ^{1}H NMR spectra obtained for the stereoisomers **3a** and **3b** are shown in Figure 6.9. The spectra obtained are in agreement with those reported by Hage *et al.* for materials obtained from fractional crystallisation.[2] The nature of the two species obtained was at that stage however uncertain.[2]

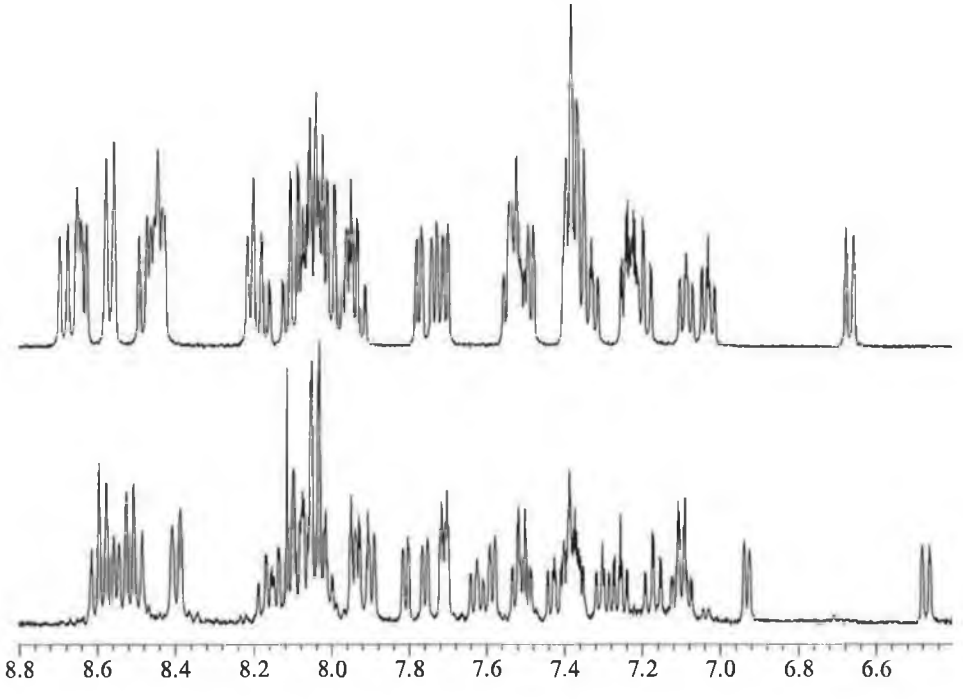

Figure 6.9 *^{1}H NMR Spectra of **3a** (homochiral isomer ΛΛ) and **3b** (heterochiral isomer ΛΔ) in CD_3CN*

As expected the ^{1}H NMR spectra of the homochiral stereoisomers **3a** and **3d** (ΛΛ and ΔΔ) are identical as are the spectra of the heterochiral stereoisomers **3b** and **3c** (ΛΔ and ΔΛ).

The spectra obtained are assignable using ^{1}H COSY techniques and are in full agreement with previously reported assignments.[2] Since there is substantial through space interaction between the bridging ligand and the bpy rings and between the bpy ligands themselves the complexity of this spectrum does not allow a detailed discussion of the differences observed. It is however clear that the fractions obtained by Hage *et al.* can be assigned as the homochiral and heterochiral enantiomeric pairs.[2]

6.2.4 Electronic properties

It is surprising that despite the considerable interest in stereochemical control of Ru(II) and Os(II) complexes, few studies of the differences in photophysical properties between stereoisomers have been reported and no comparative study of the emissive properties of enantiomeric pairs and diastereoisomers in racemic and enantiomerically pure environments has been carried out. The photophysical properties of the four stereoisomers of **1**, **2** and **3** have been examined in racemic 1-phenylethanol, in (*S*)-(-)-1-phenylethanol and in acetonitrile (butyronitrile at 77 K). 1-phenylethanol as a solvent was chosen for two reasons. Firstly the solvent is inherently chiral and can be obtained in enantiomerically pure form. Secondly the presence of a phenyl group and a hydroxy moiety allows for the possibility of a π-stacking interaction and hydrogen bonding interaction between the pyridyl rings of the complex and the solvent phenyl group and hydroxyl group respectively. That such interactions may occur has been observed both intermolecularly by Patterson *et al.*[25] and intramolecularly by Hesek *et al.*.[13]

For both **1** and **2** no differences in the electronic or photophysical properties between the enantiomeric pairs and a racemic mixture were observed as is apparent from Table 6.2. Likewise for **3**, in both rac- and (S)-(-)-1-phenylethanol no significant changes in the electronic spectra were observed, with the absorption and emission maxima for all isomers within experimental error (±2 nm) at 452 and 640 nm respectively, and with no differences in band shape. At 77 K in butyronitrile a value of 610 nm and 604 nm in both rac- and (S)-(-)-1-phenylethanol (±5 nm) was observed for all the stereoisomers of **3**. The emission lifetime data at 298 K for **3a-d** in 1-phenylethanol are presented in Table 6.1. No significant differences were observed between the lifetimes of the four stereoisomers. The values given in Table 6.1 are average values for a set of four measurements each and no differences greater than the experimental error were observed between measurements. The slight increase in lifetime observed in (S)-(-)-1-phenylethanol compared with the racemic solvent is probably due to different H_2O contents in the solvents employed. In

each case measurements were recorded under identical conditions of solvent and temperature. In order to confirm that deaeration using argon gas was sufficient in precluding any excited state quenching by oxygen, the heterochiral **3b** was subjected to four freeze-pump-thaw degassing cycles prior to lifetime measurements being made. Again no difference was observed using either method of de-oxygenation.

	rac-1-phenylethanol τ (λ_{max} Lum.)	(S)-(-)-1-phenylethanol τ (λ_{max} Lum.) 298 K	(S)-(-)-1-phenylethanol τ (λ_{max} Lum.) 77K
1a	160 ns (680 nm)	165 ns (680 nm)	5000 ns (610 nm)
1b	161 ns (680 nm)	168 ns (680 nm)	5200 ns (610 nm)
2c	230 ns (657 nm)	223 ns (657 nm)	N/A ns (590 nm)
2d	229 ns (656 nm)	219 ns (657 nm)	N/A ns (590 nm)

Table 6.2 *Emission lifetimes (samples deaerated by 20 min Ar purge) of the separated stereoisomers of complexes **1** and **2**. (N/A not available)*

The excited ^{3}MLCT state of $[Ru(bpy)_3]^{2+}$ is known to possess a considerable amount of charge transfer to solvent character (CTTS)[35] and this is expected to be the case for other Ru(II) polypyridyl complexes. Hence for the system under examination, excited state interaction with the solvent would be expected to be substantial. The use of chiral solvents amenable to intermolecular interactions such as ππ-stacking and hydrogen bonding could in principle, effect the electronic structure of stereoisomers of transition metal complexes. However, for such interactions to produce measurable differences in the photophysical properties of such complexes, the interactions must be sufficiently strong/non-random to affect the complex over the timescale of the lifetime of the excited states of such molecules. Since in fluid solutions and indeed in glassy matrices the randomness of the solvent orientation around the complex would be almost complete and hence solvent interactions significantly effect the excited state lifetime, multi-exponential behaviour would be anticipated. Changes in symmetry may result in the loss or diminishment of deactivating vibrationally linked pathways. This is not observed in any of the measurements carried out in this study. In achiral environments the differences in spectroscopic properties between the homo- (**3a/3d**) and hetero-chiral (**3b/3c**) stereoisomers of **3** are almost entirely due to differences in intramolecular interactions. Only if such intramolecular interactions are significant will differences in the photophysical properties of the homo- and hetero-chiral stereoisomers be observed. For each of the enantiomeric pairs of **1**, **2** or **3**, both intramolecular and intermolecular

interactions (in achiral solvents) are identical and hence no differences in their photophysical properties are expected. However, the use of enantiomerically pure hosts could in principle result in differential stabilization of the enantiomers. No differences are observed in photophysical properties of the stereoisomers of **1**, **2** or **3** in both achiral and chiral solvents.

The results obtained indicate that the presence of stereoisomers does not affect the general photophysical properties of either the mononuclear complex **1** and **2** or the binuclear complex **3**. That no differences in the photophysical properties of the stereoisomers are observable either at 77 K or at room temperature in both achiral, racemic and enantiomerically pure solvents, suggests strongly that the differences between the stereoisomers in either ground or excited state structure are not significant. In strained systems, differences in intramolecular interactions have been shown to effect differences in electrochemical and photophysical properties between stereoisomers, however, no such differences should occur between enantiomeric pairs.[21,23] Hence differences in intermolecular rather than intramolecular interactions are of most concern.

In the present study differences in intermolecular interactions do not result in measurable differences in photophysical properties. In contrast, Meskers *et al.* have found significant enantio-selectivity in the quenching of chiral lanthanide complexes by vitamin B_{12}.[36] In this case the lanthanide complex forms a close association with B_{12} molecule. This strongly suggests that only where the environments of the stereoisomers of an inorganic complex are significantly different, *e.g.* in the case of DNA intercalation, or photosystem II, and differences in photophysical properties may become observable.

6.3 Concluding remarks.

Overall, it may be concluded that the presence of stereoisomers in multinuclear supramolecular assemblies is unlikely to affect the photophysical properties of these assemblies, and that the importance of stereochemistry in solution is relatively low in comparison to electronic factors. Recently, differences in the thermochromic behaviour of the IT bands of the binuclear complexes (bridged by dpp type ligands) were reported by D'Alessandro *et al.*.[37] The investigation of the chirooptical properties of the LMCT and IT bands of the partially and completely oxidised forms of 1 to 3 would therefore form a natural progression to the work presented in this chapter.

One aspect which is of note is the differences in separation efficiency of the various stationary phases employed in HPLC towards the retention of Ru(II) polypyridyl complexes. This is in itself an interesting area and opens up the prospect of the use of reverse phase chromatography instead of cation exchange for purification of ruthenium complexes on a semipreparative scale.

6.4 Experimental

All solvents used for spectroscopic measurements were of Uvasol (Merck) grade. Racemic and enantiomerically pure (S)-(-)-1-phenyl-ethanol (Aldrich) were used as received. The synthesis and purification of $[Ru(bpy)_2(phpztr)](PF_6)$ **1**, has been described in Appendix E. The synthesis and purification of $[Ru(phen)_2(pztr)](PF_6)$ **2** and $[(Ru(bpy)_2)_2(bpt)](PF_6)_3$ **3**, were carried out by Dr. C. O'Connor (DIT) using previously reported methods.[2] Separation of the stereoisomers was carried out by Dr D. Hesek (**1**) and Dr. C. Villani (**2** and **3**) as described in Chapter 2. CD spectra of **1** were provided by Dr. D. Hesek, of **3** by Dr. C Villani. CD spectra of **2** were obtained in the Dublin Institute of Technology, Dublin 2 with the assistance of Dr. C. O'Connor. All other spectroscopic data were obtained in DCU as described in Chapter 2.

6.5 Bibliography

1. R. Hage, R. Prins, J. G. Haasnoot and J. Reedijk, *J. Chem. Soc., Dalton Trans.*, **1987**, 1389

2. R. Hage, A. H. J. Dijkhuis, J. G. Haasnoot, R. Prins, J. Reedijk, B. E. Buchanan and J. G. Vos, *Inorg. Chem.*, **1988**, *27* , 2185

3. (a) F. R. Keene, *Coord. Chem. Rev.*, **1997**, *166*, 121 (b) F. R. Keene, *Chem. Soc. Rev.*, **1998**, *27*, 185 (c) E. C. Constable, O. Eich, C. E. Housecroft, D. C. Rees, *Inorg. Chim. Acta,* **2000**, *300*, 158

4. P. Belser, S. Bernhard, E. Jandrasics, A. von Zelewsky, L. De Cola and V. Balzani, *Coord. Chem. Rev.*, **1997**, *159*, 1

5. (a) M. Ziegler and A. von Zelewsky, *Coord. Chem. Rev.,* **1998,** *177*, 257 (b) N. C. Fletcher, F. R. Keene, H. Viebrock and A. von Zelewsky, *Inorg. Chem.,* **1997**, *36*, 1113

6. V. Balzani and F. Scandola, *Supramolecular Photochemistry*; Ellis Horwood: Chichester, UK, **1991**

7. K. Kalyanasundaram, *Coord. Chem. Rev.*, **1982**, *46*, 159

8. A. Juris, V. Balzani, F. Barigelletti, S. Campagna, P. Belser and A. von Zelewsky, *Coord. Chem. Rev.* **1988**, *84*, 85

9. S-D. Choi, M-S. Kim, S. K. Kim, P. Lincoln, E. Tuite and B. Norden, *Biochem.*, **1997**, *36*, 214

10. C. M. Dupureur and J. K. Barton, *J. Am. Chem. Soc.*, **1994**, *116*, 10286

11. I. J. Dmochowski, J. R. Winkler and H. B. Gray, *J. Inorg. Biochem.*, **2000**, *81*, 221

12. E. C. Riesgo, A. Credi, L. De Cola and R. P. Thummel, *Inorg. Chem.*, **1998**, *37*, 2145

13. D. Hesek, Y. Inoue, S. R. L. Everitt, H. Ishida, M. Kunieda and M. G. B. Drew, *Inorg. Chem.*, **2000**, *39*, 317

14. K. Wärnmark, P. N. W. Baxter and J-M. Lehn, *Chem. Commun.*, **1998**, 993

15. A. S. Torres, D. J. Maloney, D. Tate, Y. Saad and F. M. MacDonnell, *Inorg. Chim. Acta*, **1999**, *293*, 37

16. D. Hesek, Y. Inoue and S. R. L. Everitt, *Chem. Lett.*, **1999**, 109

17. D. Hesek, Y. Inoue, S. R. L. Everitt, M. Kunieda, H. Ishida and M.G.B. Drew, *Tet.: Asymmetry*, **1998**, *9*, 4089

18. D. Hesek, Y. Inoue, S. R. L. Everitt, H. Ishida, M. Kunieda and M.G.B. Drew, *Chem. Commun.*, **1999**, 403

19. D. Hesek, Y. Inoue, H. Ishida, S. R. L. Everitt and M.G.B. Drew, *Tet. Lett.*, **2000**, 41, 2617

20. D. Hesek, Y. Inoue, S. R. L. Everitt, H. Ishida, M. Kunieda and M.G.B. Drew, *J. Chem. Soc., Dalton Trans.*, **1999**, 3701

21. (a) L. S. Kelso, D. A. Reitsma and F. R. Keene, *Inorg. Chem.*, **1996**, *35*, 5144 (b) T. J. Rutherford and F. R. Keene, *Inorg. Chem.*, **1997**, *36*, 2872

22. (a) N. C. Fletcher, P. C. Junk, D. A. Reitsma and F.R. Keene, *J. Chem. Soc., Dalton Trans.*, **1998**, 133 (b) S. Campagna, S. Serroni, S. Bodgie and F. M. MacDonnell, *Inorg. Chem.*, **1999**, *38*, 692

23. (a) T. J. Rutherford, O. van Gijte, A. Kirsch-De Mesmaeker and F. R. Keene, *Inorg. Chem.*, **1997**, *36*, 4465 (b) J. A. Treadway, P. Chen, T. J. Rutherford, F. R. Keene and T. J. Meyer, *J. Phys. Chem. A*, **1997**, *101*, 6824 (c) B. D. Yeomans, L. S. Kelso, P. A. Tregloan and F. R. Keene, *J. Euro. Inorg. Chem.*, **2001**, 239

24. T. J. Rutherford and F. R. Keene, *Inorg. Chem.*, **1997**, *36*, 3580

25. B. T. Patterson and F. R. Keene, *Inorg. Chem.*, **1998**, *37*, 645

26. K. Shinozaki, Y. Hotta, T. Otsuka and Y. Kaizu, *Chem. Lett.*, **1999**, 101

27. J. Breu, C. Kratzer and H. Yersin, *J. Am. Chem. Soc.*, **2000**, *122*, 2548

28. O. Morgan, S. Wang, S-A. Bae, R. J. Morgan, A.D. Baker, T.C. Strekas and R. Engel, *J. Chem. Soc., Dalton Trans.*, **1997**, 3773

29. M. Ruben, S. Rau, A. Skirl, K. Krause, H. Görls, D. Walther and J.G Vos, *Inorg. Chim. Acta*, **2000**, *303*, 206

30. S. Rau, M. Ruben, T. Büttner, C. Temme, S. Dautz, H. Görls, M. Rudolph, D. Walther, A. Brodkorb, M. Duati, C. O'Connor and J. G. Vos, *J. Chem. Soc., Dalton Trans.*, **2000**, 3649

31. I. D'Acquarica, F. Gasparrini, D. Misiti, C. Villani, A. Carotti, S. Cellamare and S. Muck, *J. Chromatogr. A*, **1999**, *857*, 145

32. F. Gasparrini, I. D'Acquarica, J. G. Vos, C. M. O'Connor and C. Villani, *Tet.: Assymetry*, **2001**, *11*, 3535

33. (a) F. H. Burstall, F. P. Dwyer and E. C. Gyarfas, *J. Chem. Soc.*, **1950**, 953 (b) W. W. Brandt, F. P. Dwyer and E. C. Gyarfas, *Chem. Rev.*, **1954**, *54*, 959

34. Thermal isomerisation from N2 to N4 coordination mode has been observed at high temperatures and pressures for a series of 1,2,4-triazole complexes. W.R. Browne, J.G. Vos, unpublished results

35. J. van Houten and R.J. Watts, *J. Am. Chem. Soc.*, **1975**, *97*, 3843

36. S. C. J. Meskers and H. P. J. M. Dekkers, *Spectrochim. Acta Part A*, **1999**, *55*, 1857

37. D. M. D'Alessandro, L. S. Kelso and F. R. Keene, *Inorg. Chem.*, **2001**, *40*, 6841

Chapter 7

Binuclear Ruthenium complexes - *controlling* ground state interactions

In this chapter systems containing 1,2,4-triazole base moieties, where the triazole is directly between the metal centres of binuclear systems, are examined. In these systems, the ground state interaction is found to be critically dependent on both the protonation state of the triazole and the distance between the metal centres. The systems described are bridged by a thienyl spacer and show strong interaction, which is reduced upon protonation.

7.1 Introduction

Ruthenium(II) polypyridine complexes are playing a key role for the development of multi-component (supramolecular) systems capable of performing photo- and/or redox-triggered useful functions such as charge separation devices for photochemical solar energy conversion[1] and information storage devices.[2] In particular, with regard to the latter topic, species featuring photophysical properties and redox behaviour, which can be switched or tuned by external perturbation, are of interest in this respect.[2,3]

In recent years detailed studies of mononuclear and multinuclear complexes such as Hbpt and Hbpzt, have been carried out.[4,5] Binuclear compounds featuring these ligands show strong interaction between the metal centres. This interaction has been attributed to the negative charge on the triazole ring, which promotes metal-metal interaction through hole transfer mechanism.[6] Recent studies of binuclear complexes containing related 1,2,4-triazole based ligands such as H_2L1, H_2L2 H_2bpbt and H_2bpzbt (see Figure 7.1) show that the extent of interaction is strongly dependent on the nature of the bridging ligand, both in terms of the internuclear separation, the presence of moieties other than triazoles directly between the metal centres and on the protonation state of the metal centres (*vide infra*).[7]

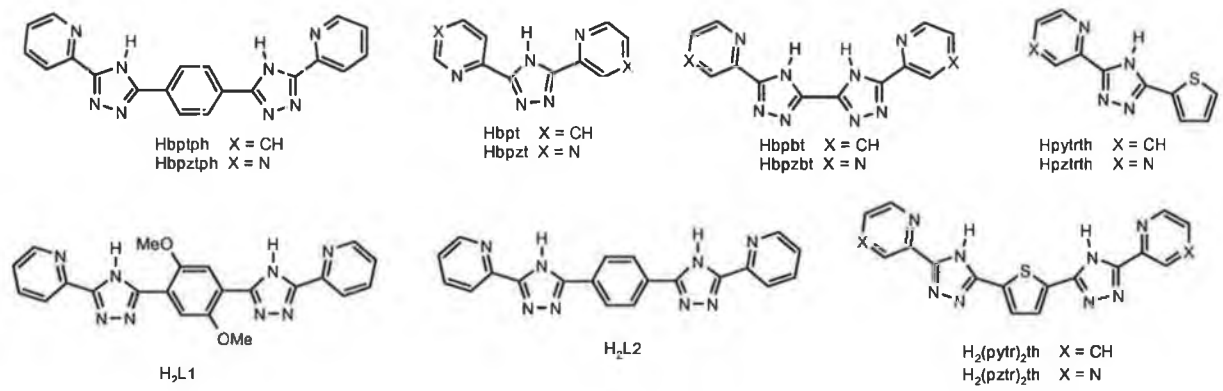

Figure 7.1 *1,2,4-triazole based ligands*

7.1.1 Homo- and hetero- binuclear complexes – from large molecules to supramolecular chemistry

The extent of intercomponent interaction, and more importantly the determination of such, is of central importance in the area of supramolecular chemistry. For multinuclear systems, which exhibit metal-based redox activity, the most direct method for measuring the interaction is through electrochemical studies. However this method is somewhat

limited in identifying the true strength of the electronic delocalisation (α^2) and coupling (H_{ab}), if any, which is present. An additional spectroscopic tool available is in the study of metal-to-metal charge transfer bands (MMCT) or intervalence transition (IT) bands of mixed valence systems. The mixed valence species may be generated either by bulk electrolysis of a solution of the analyte or by chemical oxidation *e.g.* with Ce(IV), see chapter 2.

7.1.2 Hush theory and classification of interaction type

For any binuclear system the mixed valence species may be considered as either valence localised (M^{II}-M^{III}) or valence delocalised ($M^{2½}M^{2½}$). In practice however these representations are the limiting cases and more usually mixed valence systems show interaction, which is intermediate between these limits. A theoretical basis for the study of IT bands was developed by Hush[8] and by Robin and Day[9] and latter by Creutz, Meyer and others.[10]

Appendix E covers several theoretical aspects relevant to this chapter in more detail, including some derivations of the equations used below in studying metal-metal interactions. Probably the most famous Ru(II) based binuclear system is the so called Creutz-Taube (*CT*) ion ($[(NH_3)_5Ru(\mu\text{-pyrazine})Ru(NH_3)_5]^{5+}$), which was first reported in 1969.[11] This binuclear system has been extensively investigated and is still not fully understood, however it does serve to illustrate the use of electrochemical and spectroscopic properties in investigating internuclear interactions and in demonstrating the strengths and failures in the classification of interaction proposed by Robin and Day.[9] The classification of the *CT* ion was initially determined to be Type III, however since this molecule shows characteristics of both Type II and Type III complexes then a new classification type (*i.e.* Type II/III) has been proposed by Meyer and coworkers.[12]

7.1.3 Synthesis of triazole based homo and hetero binuclear complexes

In recent years there has been considerable interest in the study of mononuclear and multinuclear ruthenium(II) polypyridyl complexes containing asymmetric ligands such as Hbpt,[4] and Hbpzt[5] (Figure 7.1), and on multidentate ligands such as dpp.[13] One of the major drawbacks of large molecular assemblies is that of control over their formation and homogeneity. The design of ever more complex systems must take into account the possibility of the formation of different isomers, be they coordination isomers or

stereoisomers. The latter form of isomerism is dealt with in Chapter 6 and will be mentioned only in respect to characterisation by NMR spectroscopy in this chapter. Of relevance here is the possibility of coordination isomerisation, which is most notable when inherently asymmetric systems are involved *e.g.* Hbpt or Hbpzt.[4,5]

The simplest example of this problem is that of the possibility of a single metal ion binding to one of two non-equivalent sites on an asymmetric ligand *e.g.* Hbpt. The asymmetry is due to both structural and chemical differences between the N2 and N4 sites of the triazole. The separation of the two coordination isomers formed is fortuitously relatively simple and is normally carried out by column chromatography. The formation of the two isomers in equal amounts is only observed when N4 coordination is not precluded by steric hindrance from a substituent in the C5 of the 1,2,4-triazole.[14] In the case of homo-binuclear systems only one coordination isomer is formed and purification is trivial. Similarly for hetero-binuclear complexes, since either of the possible coordination isomers are prepared from the mononuclear precursor, then full control over the coordination mode is easily achieved.

By increasing the asymmetry of the bridging ligand compared with bpt^- (*e.g.* ppt^-) the preparation of both mononuclear and binuclear complexes with complete control over coordination mode becomes somewhat more difficult.[15] The four mononuclear isomers of the ppt^- ligand that are formed are also separable by standard column chromatography, however, in contrast, the efficient separation of the two possible binuclear isomers is effectively impossible even by semipreparative HPLC. As a result preparation of both the homo and hetero- binuclear complexes is not possible directly from the ligand but must be via the purified mononuclear complexes.

In the preparation of both homo- and hetero- multinuclear systems several different approaches have been reported. In particular the so-called 'complexes as ligands/complexes as metals' strategy has been of particular use in the building of some of the larger assemblies reported to date.[13] This strategy involves the stepwise metal coordination of multidentate ligands, often with iterative protection and deprotection methods.[13] This approach has been used successfully in the case of symmetric bridging ligands, which limit the number of coordination isomers, however in the case of ligands containing multiple binding sites or asymmetry this approach is not always practical due

to the number of isomers formed and the requirement for the development of separation techniques. An alternative strategy has been to 'synthesise' the bridging ligand by coupling metal complex subunits together.[7] This approach has been used by several groups recently and has proven quite successful in particular for symmetric systems.[16] An alternative route to either 'the complexes as ligands/complexes as metals' or the 'coupling' approaches is to attach a metal subunit to a precursor of the bridging ligand, followed by building up of the bridging ligand before coordinating further metal subunits.

7.1.4 Ruthenium(II) and osmium(II) multinuclear complexes containing 1,2,4-triazole moieties - Internuclear interaction

In binuclear metal complexes, the metal oxidation behaviour is quite a powerful tool to gain information on the ground state electronic interaction between the metal subunits. In principle, because two redox active sites are present (*i.e.* the two metal centres), two metal-centred processes are possible, and their separation (ΔE) is related to the stability of the mixed-valence species by the comproportionation constant, K_c, (see Appendix A7).[10] However, it is often the case that when the interaction is weak, the separation between successive metal oxidation waves, in symmetric multinuclear systems, is so low as to allow only a single multi-electronic oxidation wave to be observed by cyclic voltammetry. For asymmetric systems several redox waves may be observable but at potentials close to their related mononuclear analogues and whilst generation of the mixed valence species is relatively easy in the latter case, the observation of an IT band is not necessarily so straightforward.

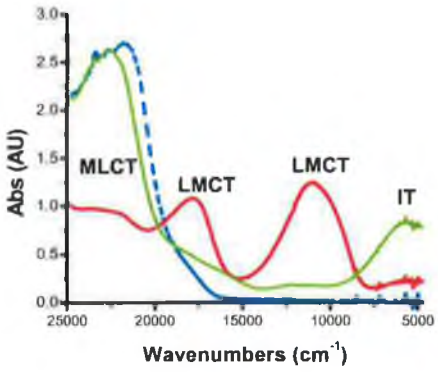

Figure 7.2 *Visible and near-IR absorption spectra of $[(Ru(bpy)_2)_2bpzbt]^{2+}$ generated electrochemically in acetonitrile with 0.1 M TEAP at 0.60 V ($Ru^{II}Ru^{II}$ blue), 1.00 V (mixed valence ($Ru^{II}Ru^{III}$), green), and 1.10 V ($Ru^{III}Ru^{III}$ red) vs SCE.*[7]

Of interest here are bridging ligands that incorporate the 1,2,4-triazole moiety directly between the metal centres. Examples of such bridging ligands are given in Figure 7.1. The electrochemical and spectroelectrochemical properties of the binuclear ruthenium complexes of some of these ligands have been investigated in detail.[4,5,17,18] In each case the metal centres are bridged by the triazolato anion. The interaction in these systems is found to be very dependent on the distance between the metal centres and on the relative energies of the metal d-orbitals and the ligand orbitals involved in the superexchange mediated communication between the metal centres.

Table 7.1 describes the spectroscopic properties of a series of mixed valence ruthenium binuclear complexes. For the systems described, it can be said that in every case the interaction between the metal centres is best classified as Type II for deprotonated complexes and borderline Type I/II for the protonated complexes. A feature of these systems is the presence of a strong IT band between 4000 cm^{-1} and 10000 cm^{-1} (*e.g.* Figure 7.2). For binuclear complexes bridged by a single triazolato anion a strong interaction is observed both in the separation of the 1st and 2nd metal oxidation waves (ΔE) and in the value of H_{ab} determined from spectroscopic parameters. Separation by two triazolato anions shows a decreased level of interaction. This increase is due to reduced orbital overlap and therefore decreased superexchange mediate interaction.[19] Inclusion of a phenyl spacer further increases the distance between the metal centres.

	H_{ab} (cm^{-1})	α^{2} [a]	ΔE (mV) ± 10 mV	K_c	$\Delta\nu_{½calc}$ (cm^{-1})	$\Delta\nu_{1/2}$ (cm^{-1})[b]	ε_{max} ($M^{-1}cm^{-1}$) ± 20 %	E_{op} (cm^{-1}) ± 100 cm^{-1}
[c] $[(Ru(bpy)_2)_2bpt]^{3+}$	700	0.016	300	117,910	3341	3300	2400	5556
[c] $[(Ru(bpy)_2)_2bpzt]^{2+}$	745	0.019	300	117,910	3260	4200	2200	5405
[d] $[(Ru(bpy)_2)_2L1]^{2+}$	480	0.0055	0	4	3865	5100	>2400	6470
[e] $[(Ru(bpy)_2)_2L2]^{2+}$	295	0.0014	0	4	4263	4262	1042	7870
[f] $[(Ru(bpy)_2)_2bpbt]^{2+}$	459	0.007	180	1,100	3060	4690	1820	5490
[f] $[(Ru(bpy)_2)_2Hbpbt]^{3+}$	435	0.0025	110	72	4250	5600	1000	8700
[f] $[(Ru(bpy)_2)_2bpzbt]^{2+}$	352	0.004	170	750	3120	4360	1120	5580
[f] $[(Ru(bpy)_2)_2Hbpzbt]^{3+}$	425	0.0025	60	10	4300	5300	1000	8500

Table 7.1 *Spectroelectrochemical data for complexes discussed in text. (a) extent of electronic delocalisation, (b) taken as double the width at half maximum of the high energy side of the absorption band, (c) from ref. 20, (d) from ref. 17, (e) from ref 18, (f) from ref.7.*

The level of interaction for these systems is much lower than would be expected on the basis of the increased distance and reflects the poor ability of phenyl groups in mediating

interaction. Protonation of the triazole moiety in each case results in a significant reduction in the level of interaction, which manifests itself in an increase in the energy of the IT band together with a decrease in its intensity and a reduction in the value of ΔE (see ***Table 7.1***). Protonation results in a destabilisation of both the ligand HOMO and metal t_{2g} orbitals of the bridging ligands resulting in a perturbation in the overlap of the metal orbitals and the ligand HOMO orbitals. If the mechanism of interaction is via hole transfer superexchange, then the perturbation will be manifested by a change in both α^2 and H_{ab}. It is interesting to note that the presence of ancillary groups such as pyrazine or pyridine have little effect on the ground state electronic properties of any of the triazole bridged systems.

7.1.5 LMCT transitions

Ligand to metal charge transfer transitions are generally observed for d^5 polypyridyl complexes. Preparation of the ruthenium(III) and osmium(III) species by bulk electrolysis or by chemical oxidation is relatively easy, however for N6 complexes such states are not normally very stable and revert back to the d^6 ion. Nevertheless they are stable enough to allow for spectroscopic examination (*e.g.* Figure 7.2).

Nazeeruddin *et al.* have examined the effects of increasing electron-donating capacity of the donor ligand on the intensity of the LMCT transition.[21] They have found that the larger the σ-donor capacity of the ligand the more intense the band observed. Similar results have been found by Vos and co-workers, where the intensities of the LMCT of protonated complexes are lower than for the corresponding deprotonated complexes.[7,18] Protonation also results in an increase in the energy of the band. These observations are not unexpected and can be rationalised in terms of the relative energies of the donor (ligand based) and acceptor (metal based) orbitals. The effect of protonation and the subsequent decrease in the σ-donor properties of the bridging ligand is to increase the energy of both the donor and acceptor orbitals leading to the observed shift in the LMCT transition. In addition upon protonation there is a noticeable decrease in the intensity of the LMCT band, which reflects the decreased electron density of the triazole ligands.

7.1.6 Ruthenium(II) and osmium(II) multinuclear complexes containing 1,2,4-triazole moieties - Energy vectoring and excited state interactions

In Table 7.2 the spectroscopic properties of a series of ruthenium(II) polypyridyl complexes incorporating 1,2,4-triazole moieties is presented. In contrast to the ground state electronic properties of the binuclear complexes, the excited state properties are very much dependent on the nature of ancillary moieties (*i.e.* pyrazyl- and pyridyl- groups). With the exception of the bpt$^-$ and bpzt$^-$ based complexes, the spectroscopic properties of the binuclear complexes are very similar to those of their mononuclear analogues.

	Absorption λ_{max} nm	Luminescence, 298 K λ_{max} nm, (τ, ns) {$\Phi*10^{-3}$}	Metal oxidation potent. (in V),
[a][(bpy)$_2$Ru(bpbt)Ru(bpy)$_2$]$^{2+}$	480	690 (102) {2.4}	+0.80 [1], +0.98 [1]
[a] [(bpy)$_2$Ru(Hbpbt)Ru(bpy)$_2$]$^{4+}$	440	660 (344) {2.1}	+1.06 [1], +1.17 [1]
[a] [(bpy)$_2$Ru(H$_2$bpbt)Ru(bpy)$_2$]$^{3+}$	431	630 (< 5)	+1.10 [2]
[b][(Ru(bpy)$_2$)$_2$L1]$^{2+}$	481	683 (105)	+0.82 [2] (1.26, 1.45)
[b] [(Ru(bpy)$_2$)$_2$H$_2$L1]$^{4+}$	412	612 (< 5)	+1.25 [2] (1.5)
[c] [(Ru(bpy)$_2$)$_2$L2]$^{2+}$	481	690 (54)	+0.84 [2]
[c][(Ru(bpy)$_2$)$_2$H$_2$L2]$^{4+}$	420	614 (<20)	+1.14 [2]
[d][(bpy)$_2$Ru(bpt)Ru(bpy)$_2$]$^{3+}$	452	648 (80)	+1.04 [1], +1.34 [1]
[d][(bpy)$_2$Ru(pytr)]$^+$	467	650 (145)	+0.83 [1]
[d][(bpy)$_2$Ru(Hpytr)]$^+$	438	612 (< 1 ns)	+ 1.14[1]
[a] [(bpy)$_2$Ru(bpzbt)Ru(bpy)$_2$]$^{2+}$	455	670 (214) {3.4}	+0.92 [1], +1.09 [1]
[a] [(bpy)$_2$Ru(Hbpzbt)Ru(bpy)$_2$]$^{3+}$	436	675 (764)	+1.09 [1], +1.15 [1]
[a] [(bpy)$_2$Ru(H$_2$bpzbt)Ru(bpy)$_2$]$^{4+}$	430	678 (1000) {7.2}	+1.13 [2]
[d][(bpy)$_2$Ru(bpzt)Ru(bpy)$_2$]$^{3+}$	449	690 (106)	+1.16 [1], +1.46 [1]
[d][(bpy)$_2$Ru(pztr]$^{2+}$	458	660 (250)	+1.01 [1]
[d][(bpy)$_2$Ru(Hpztr]$^{2+}$	441	665 (430)	+ 1.25[1]
[e][Ru(bpy)$_3$]$^{2+}$	452	620 (1000)	+1.26 [1]

Table 7.2 *Redox and electronic data for complexes discussed in text. (a) from ref.7, (b) from ref. 18 , (c) from ref. 17 , (d) from ref. 20, (e) from ref.1a.*

Figure 7.3 shows the effect of protonation on the emission spectrum of the bpbt$^-$ based binuclear complex.[7] As for mononuclear pyridyl-triazole complexes complete protonation results in a blue shift in the emission spectrum and a dramatic decrease in the emission lifetime. Unusually the monoprotonated complex shows an increase in emission energy and an increase in emission lifetime. This may be rationalised by considering that

although protonation destabilises the ligand based ^{3}MLCT states, the reduction in the level of the deactivating ^{3}MC state is not sufficient to balance the effect of an increased ground/excited state energy gap.[22]

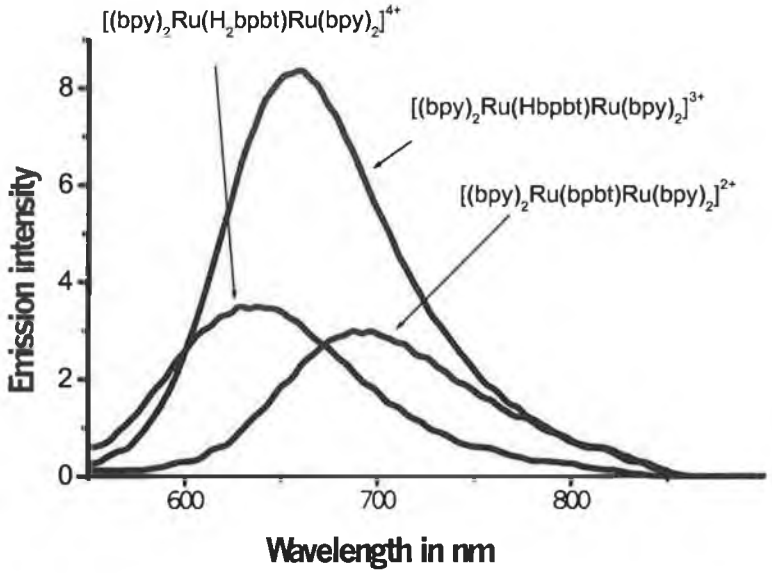

Figure 7.3 Emission spectra of $[(Ru(bpy)_2)_2(bpbt)]^{2+}$ in its three different protonation states

In this chapter efforts towards the preparation of systems, which allow for control of both ground and excited state properties by external perturbation are continued in preparation of complexes based on the ligands $H_2(pytr)_2th$ and $H_2(pztr)_2th$ (see Figure 7.1). The mononuclear analogues of both complexes have been prepared both as model complexes and as potential building blocks for hetero-binuclear complexes. The complexes formed are inherently symmetric and are similar to previously reported systems. The internuclear separation is comparable with that of H_2L1 and H_2L2 and hence the extent of interaction observed will provide information on the effect of variation of the relative energy of the metal orbitals to those of the ligand HOMO orbitals (see Figure 7.1).[7,18]

7.2 Results

7.2.1 Syntheses, NMR and mass spectral characterisation

The ligands were prepared by standard methods as described in Chapter 2. Preparation and purification of the mononuclear complexes $[(Ru(bpy)_2(pytrth)]^+$ and $[(Ru(bpy)_2(pztrth)]^+$ and the binuclear complexes $[(Ru(bpy)_2)_2((pytr)_2th)]^{2+}$ and

$[(Ru(bpy)_2)_2((pztr)_2th)]^{2+}$ was carried out by standard chromatographic techniques as described in the experimental section. Mass spectral data were obtained for the mononuclear complexes and are given in the experimental section. The molecular ions were identified by the distinctive isotopic pattern for ruthenium complexes. ^1H NMR spectral data are presented in the experimental section. Comparison of the ^1H NMR spectra of the symmetric binuclear complexes based on the ligands $H_2(pytr)_2th$ and $H_2(pytr)_2th$ and their respective mononuclear analogues are presented in Figure 7.4 and Figure 7.5.

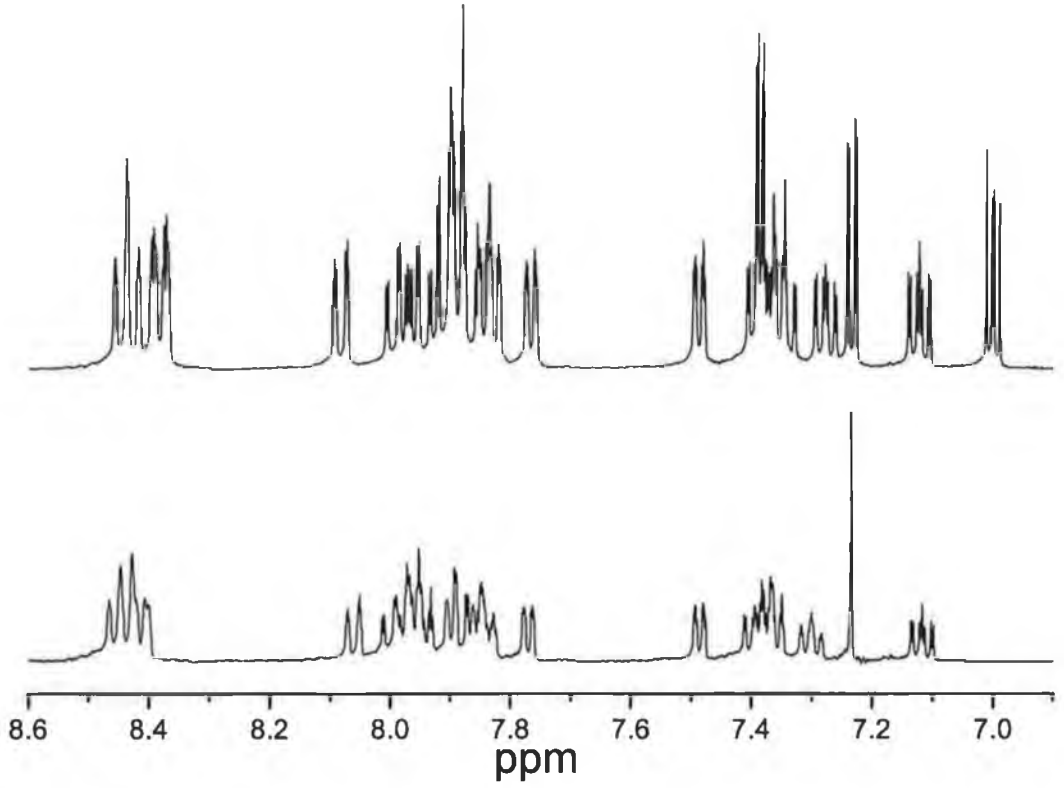

Figure 7.4 ^1H NMR spectra of $[(Ru(bpy)_2(pytrth)]^+$ and $[\{Ru(bpy)_2\}_2\{(pytr)_2th\}]^{2+}$ in CD_3CN

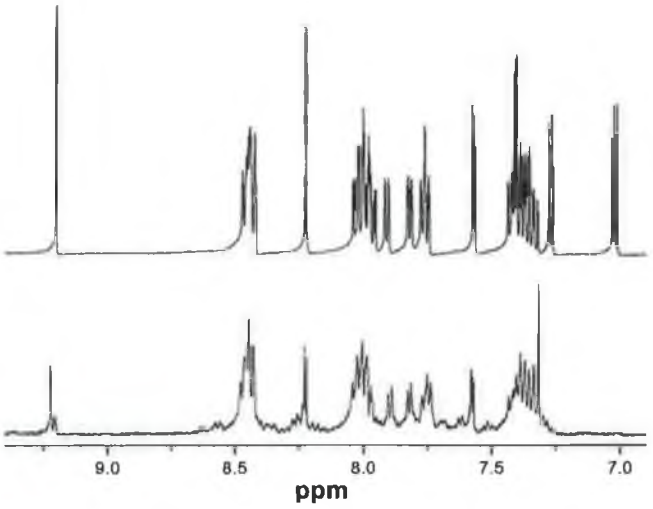

Figure 7.5 *^{1}H NMR spectra of $[(Ru(bpy)_2(pztrth)]^{2+}$ and $[\{Ru(bpy)_2\}_2\{(pztr)_2th\}]^{2+}$ in CD_3CN*

7.2.2 Electronic and Photophysical properties

All spectroscopic data for both mononuclear and binuclear complexes are presented in Table 7.3.

	Abs. λ_{max} /nm (log ε)	Lumin. λ_{max} /nm	pK_a
$[Ru(bpy)_2(pytrth)]^+$	245 (4.45), 291(4.79), 480 (3.93)	687	3.05
$[(Ru(bpy)_2)_2((pytr)_2th)]^{2+}$	243 (4.64), 290 (4.98), 360 (4.6), 430 (4.23)	680	2.50
$[Ru(bpy)_2(Hpytrth)]^{2+}$	242, 286 (4.77), 439 (4.03)	613	
$[(Ru(bpy)_2)_2((Hpytr)_2th)]^{4+}$	237, 287(5.00), 417 (4.45)	627	
$[Ru(bpy)_2(pztrth)]^+$	244 (4.48), 289 (4.86), 455 (4.15)	664	2.15
$[(Ru(bpy)_2)_2((pztr)_2th)]^{2+}$	242 (4.5), 288 (4.85), 344 (4.33), 438 (4.19), 510 (sh)	671	1.25
$[Ru(bpy)_2(Hpztrth)]^{2+}$	245, 284 (4.86), 438 (4.18)	672/648	
$[(Ru(bpy)_2)_2((Hpztr)_2th)]^{4+}$	285, 428, 515(sh)	758	

Table 7.3 *Electronic properties for mono- and bi-nuclear thienyl containing complexes (in CH_3CN). pK_a data for complexes was determined in Britton-Robinson Buffer*

The absorption and emission spectra for the mono- and bi-nuclear complexes are shown in Figure 7.7 and Figure 7.9. All complexes exhibit intense absorption bands in the UV region ~ 245 and 290 nm and moderately intense bands in the visible region ~360 – 480

nm, which are typical for this type of complex.[4,5] All complexes are luminescent in acetonitrile at 298 K.

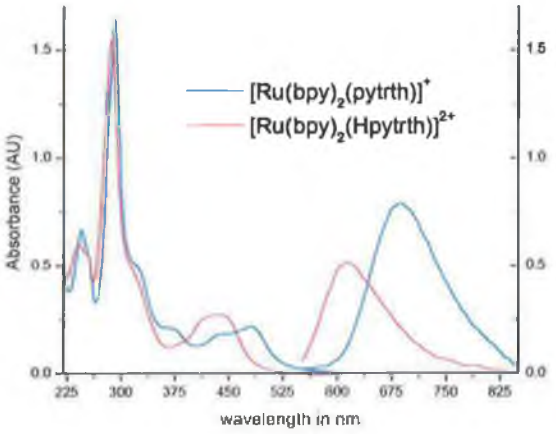

Figure 7.6 *Absorption and emission spectra for $[(Ru(bpy)_2(pytrth)]PF_6$ in acetonitrile solution*

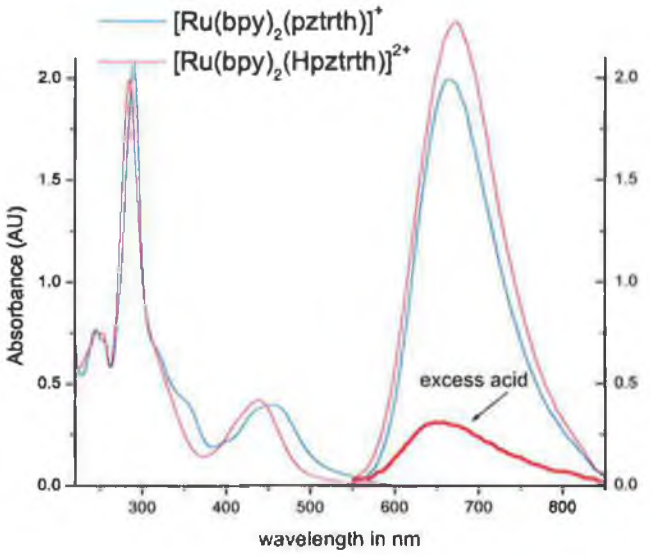

Figure 7.7 *Absorption and emission spectra for $[(Ru(bpy)_2(pztrth)]PF_6$ in acetonitrile solution*

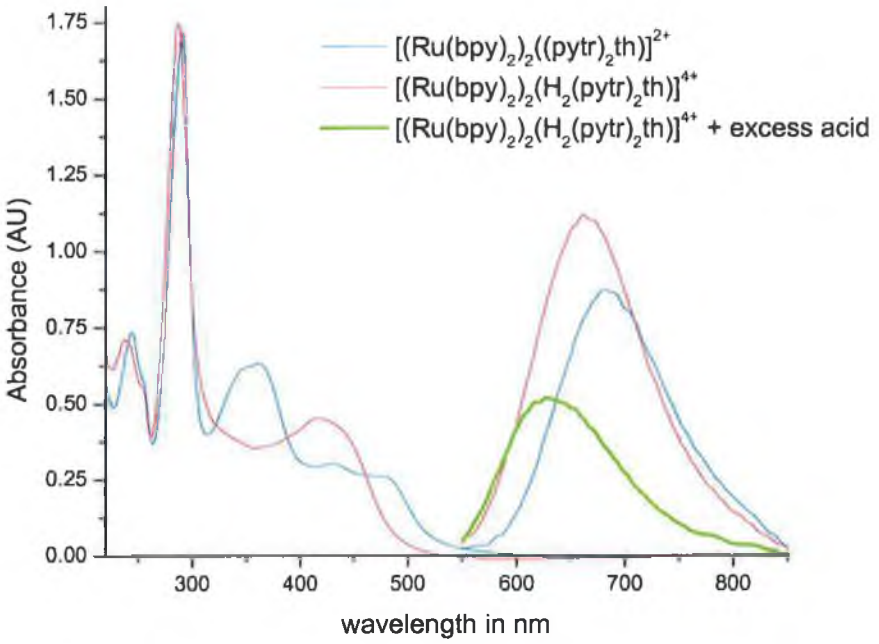

Figure 7.8 *Absorption and emission spectra for $[(Ru(bpy)_2)_2((pytr)_2th)](PF_6)_2$ in acetonitrile solution*

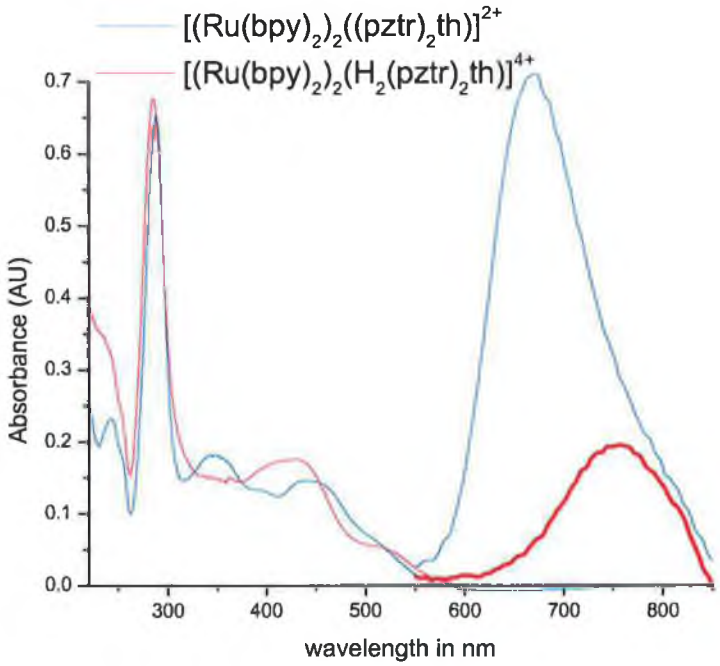

Figure 7.9 *Absorption and emission spectra for $[(Ru(bpy)_2)_2((pztr)_2th)](PF_6)_2$ in acetonitrile solution*

7.2.3 Acid base properties

The acid dissociation constants (pK_a) for all complexes are given in Table 7.4. The values were obtained from the change in the absorption spectra of the complexes with changing pH (see Figure 7.11 and Figure 7.13).

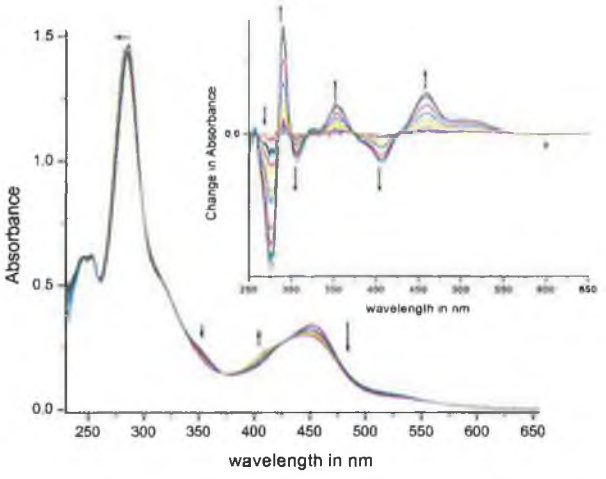

Figure 7.10 *Changes in UV.vis spectra of $[Ru(bpy)_2(pztrth)]^+$ between pH 0.5 and 10. (inset differences spectra compared with completely the protonated complexes)*

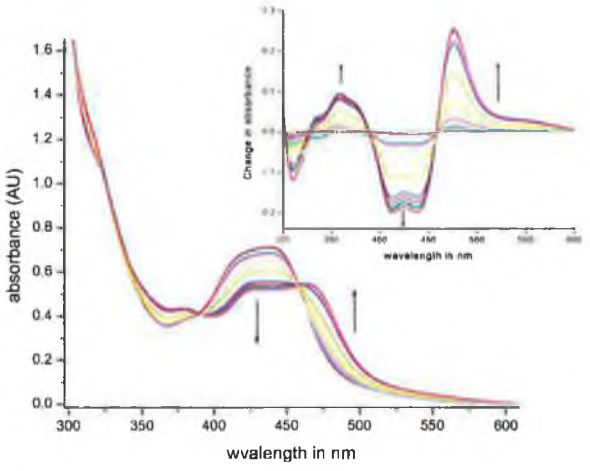

Figure 7.11 *Changes in UV.vis spectra of $[Ru(bpy)_2(pytrth)]^+$ between pH 0.5 and 10. (inset differences spectra compared with completely the protonated complexes)*

For the mononuclear complexes a progressive modification of the absorption spectrum was observed +/- 1 pH unit either side of the pK_a point with isosbestic points being maintained throughout the titration. For the binuclear complexes a similar situation is observed indicating a single step protonation process is observed in each case.

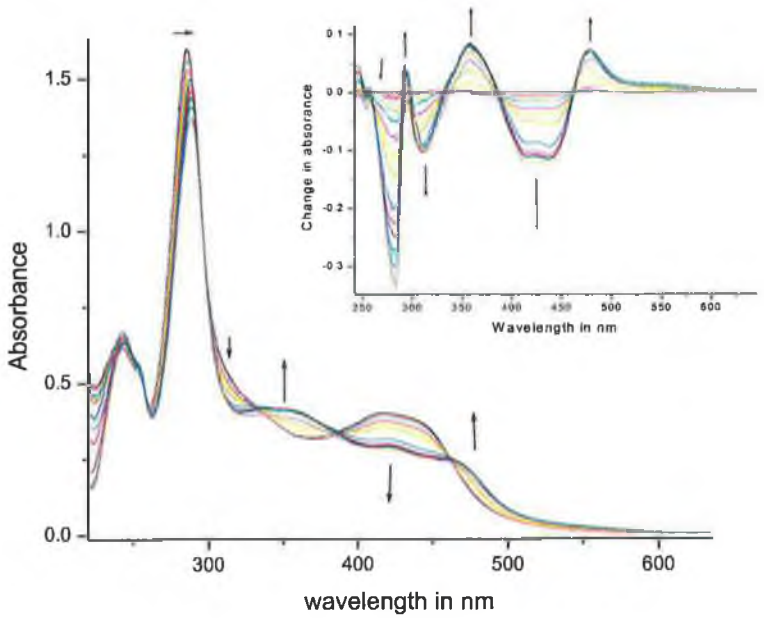

Figure 7.12 *Changes in UV.vis spectra of $[(Ru(bpy)_2)_2((pztr)_2th)]^{2+}$ between pH 0.5 and 10. (inset differences spectra compared with completely the protonated complexes)*

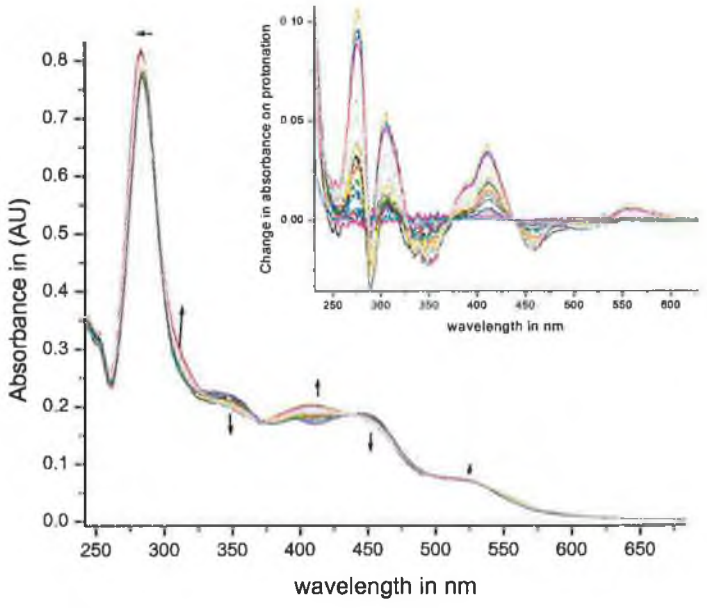

Figure 7.13 *Changes in UV.vis spectra of $[(Ru(bpy)_2)_2((pytr)_2th)]^{2+}$ between pH 0.5 and 10. (inset differences spectra compared with completely the protonated complexes)*

7.2.4 Redox properties

Oxidation and reduction potentials of all complexes are presented in Table 7.4.

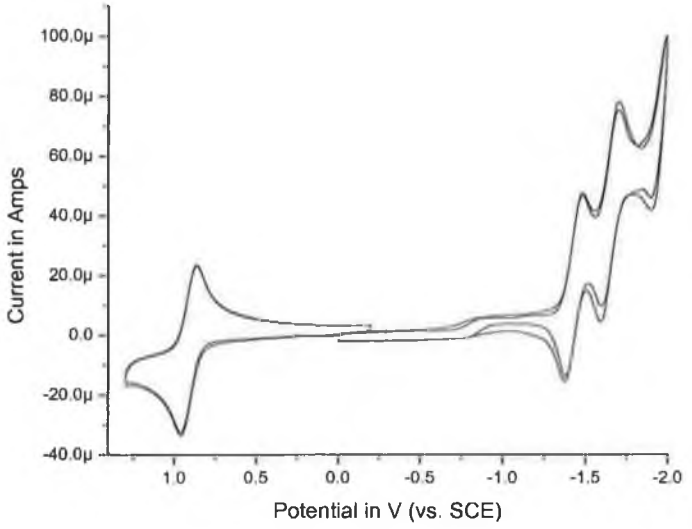

Figure 7.14 *Cyclic voltammogram of $[Ru(bpy)_2(pztrth)]^+$ in 0.1 M TEAP/CH_3CN at 200 mVs^{-1}.(Ligand oxidation not shown).*

	Ru^{II}/Ru^{III} oxid. (in V) {thienyl oxid.}	Ligand red. (in V)
$[Ru(bpy)_2(pytrth)]^+$	0.86 (1.62 *irr*)	-1.36, -1.67
$[(Ru(bpy)_2)_2((pytr)_2th)]^{2+}$	0.78, 0.87 (1.45 *irr*)	-1.44, -1.67
$[Ru(bpy)_2(Hpytrth)]^{2+}$	1.19 (1.67 *irr*)	*not measured*
$[(Ru(bpy)_2)_2((Hpytr)_2th)]^{4+}$	1.08 (1.45 *irr*)	*not measured*
$[Ru(bpy)_2(pztrth)]^+$	0.95 (1.55 *irr*)	-1.43, -1.65
$[(Ru(bpy)_2)_2((pztr)_2th)]^{2+}$	0.85, 0.95 (1.41 *irr*)	-1.49, -1.70
$[Ru(bpy)_2(Hpztrth)]^{2+}$	1.23 (1.55 *irr*)	*not measured*
$[(Ru(bpy)_2)_2((Hpztr)_2th)]^{4+}$	1.18 (1.58 *irr*)	*not measured*

Table 7.4 *Redox data for mono- and bi-nuclear complexes containing thienyl-groups.*

For the mononuclear deprotonated complexes and all protonated complexes single redox waves (with a E_{an}-E_{cat} of 70 mV) are observed, however for the fully deprotonated binuclear complexes a small separation (ΔE) between the first and second metal oxidation wave of approximately 100 mV is observed (Figure 7.15). This separation is close to that observed for the monoprotonated binuclear $bpbt^-$ and $bpzbt^-$ based complexes (see ***Table***

7.1). From this the comproportionation constant for the deprotonated complexes (K_c) is ~ 60. For the protonated binuclear complexes a value of 4 is assumed since there is no separation between the first and second metal oxidation wave.

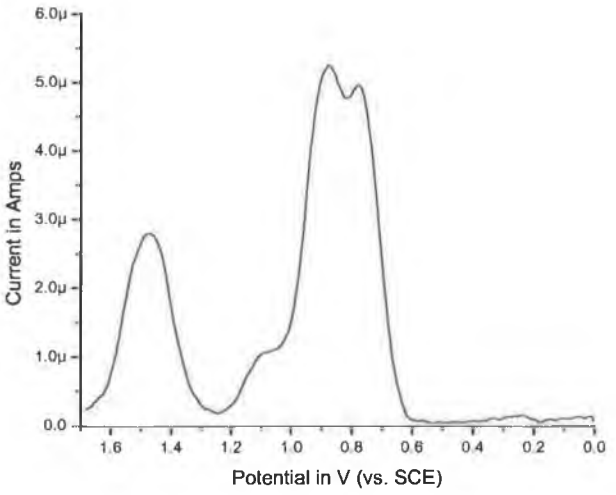

Figure 7.15 *DPV scan of $[(Ru(bpy)_2)_2((pytr)_2th)]^{2+}$ in 0.1 M TEAP/CH_3CN at 20 mVs^{-1} (peak at 1.1 V is due to small amount of protonated complex)*

7.2.5 Electronic spectroscopy of mixed valence and Ru(III) complexes

In situ preparation of both mixed valence and fully oxidised complexes was carried out using both spectroelectrochemistry and by chemical oxidation with Ce^{4+} as described in Chapter 2. For both the mononuclear complexes, both electrochemical and chemical oxidation, resulted in the depletion of the absorption bands at ~ 450 nm with a concomitant growth in lower energy bands at 425, 569 and 1049 nm. A full recovery of the original spectrum was observed upon electrochemical reduction of the oxidised species, indicating the first oxidation process is reversible. Further oxidation (at potentials above the second oxidation wave) results in an irreversible depletion of all absorption features. For the protonated complexes similar changes were observed, with a slight blue-shift in the energy of the Ru(III) absorption features and a small decrease in their intensity.

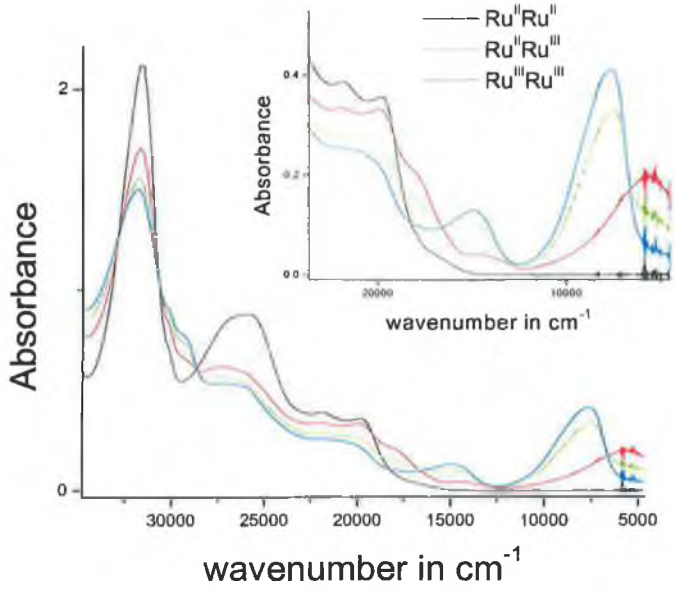

Figure 7.16 *Changes in UV.Vis-NIR absorption spectrum of* $[Ru(bpy)_2)_2((pytr)_2th)]^{2+}$ *upon successive additions of* Ce^{4+}.

For the fully deprotonated complex $[Ru(bpy)_2)_2((pytr)_2th)]^{2+}$ oxidation at 0.7 V results in a growth of a band at 1750 nm (5720 cm^{-1}) followed by the growin of two bands at 1310 nm (7610 cm^{-1}) and 675 nm (14,800 cm^{-1}) at 0.85 V (Figure 7.16). At both potentials a steady depletion of the MLCT bands of the $Ru^{II}Ru^{II}$ species was observed. Upon returning to 0.3 V a full recovery of the initial spectrum was achieved, indicating that the system was fully reversible.

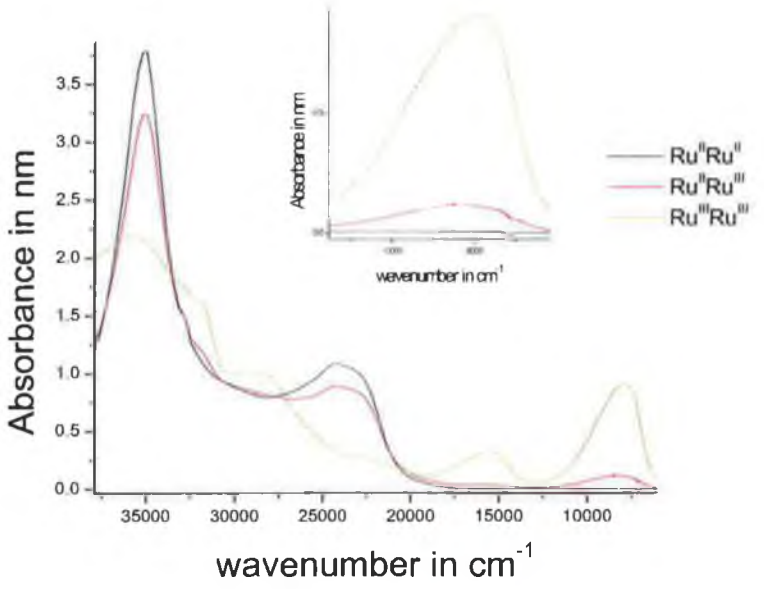

Figure 7.17 *Changes in UV.Vis-NIR absorption spectrum of* $[Ru(bpy)_2)_2(H_2(pytr)_2th)]^{4+}$ *upon successive additions of* Ce^{4+}. *Protonation with* CF_3CO_2H.

For the fully protonated complex $[Ru(bpy)_2)_2(H_2(pytr)_2th)]^{4+}$ oxidation at 0.9 V results in a growth of a band at 1190 nm (8400 cm^{-1}) followed by the grow in of two bands at 1270 nm (7890 cm^{-1}) and 645 nm (15,490 cm^{-1}) at 0.95 V (Figure 7.17). At both potentials a steady depletion of the MLCT bands of the $Ru^{II}Ru^{II}$ species was observed. Upon returning to 0.0 V a full recovery of the initial spectrum was achieved indicating again that the system is fully reversible. For $[Ru(bpy)_2)_2((pztr)_2th)]^{2+}$ an almost identical behaviour is observed with only minor differences in the λ_{max} of the absorption bands.

7.3 Discussion

7.2.1 Structural characterisation

In the preparation of the mononuclear complexes $[(Ru(bpy)_2(pytrth)]^+$ and $[(Ru(bpy)_2(pztrth)]^+$, ^1H NMR spectra and HPLC of the crude materials indicate that the product obtained before purification was already in quite a pure state with only a single isomer being observed. Chromatography on neutral alumina was employed to ensure complete removal of residual impurities. For the binuclear complexes $[(Ru(bpy)_2)_2((pytr)_2th)]^{2+}$ and $[(Ru(bpy)_2)_2((pztr)_2th)]^{2+}$ a similar situation was observed, however following chromatography on neutral alumina a dramatic increase in the levels

of a specific impurity was detected by ^{1}H NMR spectroscopy. In order to remove this impurity chromatographic separation on silica gel was carried out. The identity of the impurity is unclear however appear to be related to the use of ethylene glycol as a reaction solvent.

The molecular ions of each of the mononuclear complexes were identified by the distinctive isotopic pattern exhibited by ruthenium complexes (see Figure 8.3 for example). Although the molecular formulae of the complexes are confirmed by mass spectroscopy, no information as to the coordination mode of the mononuclear or binuclear complexes may be obtained by this technique (*vis-à-vis N2 vs. N4 coordination).*[14] In order to confirm the coordination mode of both mono and bi-nuclear complexes ^{1}H NMR spectroscopy was employed. Comparison of the ^{1}H NMR spectra of the symmetric binuclear complexes based on the ligands $H_2(pytr)_2th$ and $H_2(pytr)_2th$ and their respective mononuclear analogues are presented in Figure 7.4 and Figure 7.5. It is clear that the spectra of the mono and binuclear complexes are almost identical, which confirms that the binuclear complexes are N2N2 bound (in agreement with similar complexes).[6,17,18] The only significant differences between the complexes arise from the differences in the proton signals due to the thienyl moieties. For the mononuclear complexes 3 signals corresponding to the H3 (d), H4 (dd) and H5 (d) of the monosubstituted thienyl ring are observed at between 7.0 and 7.6 ppm. For both binuclear complexes a single resonance at ~7.45 ppm is observed. It would be expected (see chapter 6) that the binuclear complexes would exhibit twice the number of proton signals due to the presence of diastereoisomers, however given that the distances between the metal centres are large then no appreciable differences between the spectra of the diastereoisomers are observed.

7.3.2 Electronic and acid/base properties

The UV.Vis absorption and emission properties of the mononuclear complexes show a close comparison with those of the analogous $[Ru(bpy)_2(pytr)]^+$ and $[Ru(bpy)_2(pztr)]^+$, but are slightly red shifted. Upon protonation for both complexes a blue shift in the absorption spectra is observed. For $[Ru(bpy)_2(pytrth)]^+$ protonation results in large blue shift (~70 nm), in agreement with other mononuclear pyridyl-1,2,4-triazole complexes. For $[Ru(bpy)_2(pztrth)]^+$ protonation results in first a very minor red shift, followed by a blue shift in the emission λ_{max} with a concomitant reduction in intensity. Again the acid-base emission properties bare close agreement with similar systems. The pK_a values

determined for both complexes are lower than for $[Ru(bpy)_2(pytr)]^+$ and $[Ru(bpy)_2(pztr)]^+$. This suggests that the thienyl moiety is an electron withdrawing group. As is typical the pyrazine complex is more acidic than the analogous pyridine complex, due to the greater electron withdrawing nature of the pyrazine ring.

For both of the binuclear complexes protonation results in a general blue-shift in the absorption spectrum. Two absorption bands are observed at around 360 nm and 500 nm for both $[Ru(bpy)_2((pytr)_2th)]^{2+}$ and $[Ru(bpy)_2((pztr)_2th)]^{2+}$, which are absent in the spectra of both $[Ru(bpy)_2(pytr)]^+$ and $[Ru(bpy)_2(pztr)]^+$. These bands are likely to be due to the thienyl group and have been observed for terpy based thienyl bridged systems.[23] Upon protonation these absorption features are blue shifted indicating a destabilisation of the thienyl based π-π^* bands.

The effect of protonation on the emission spectra of both complexes is more complicated than for the mononuclear complexes. For $[Ru(bpy)_2((pytr)_2th)]^{2+}$ protonation initially results in a small blue shift and an increase in intensity in emission followed by a further blue shift and a decrease in emission intensity. For $[Ru(bpy)_2((pztr)_2th)]^{2+}$ protonation results in a very large red shift in the emission spectrum. These observations indicate that the interaction in the excited state between the triazole moieties may be larger than in the ground state.

7.3.3 Redox properties

Interest in multinuclear complexes lies largely in the possibility of electronic interaction between the metal centres.[1] To obtain information as to the nature and extent of the interaction electrochemical and spectroelectrochemical studies have been carried out. Assignment of redox processes is relatively straightforward by comparison with previously reported 1,2,4-triazole and thienyl containing complexes.[4,5,6,7,23] Thienyl oxidation is usually irreversible and the oxidation processes at 1.4-1.6 V (Table 7.4) are assigned as ligand oxidations on the basis of their potential and their irreversibility.[23] The Ru^{II}/Ru^{III} redox couples for 1,2,4-triazoles are expected to be at around 0.85 and 0.95 for pyridyl and pyrazyl based complexes respectively.[20] These processes are fully reversible and show an increase upon protonation of ~ 200 - 250 mV, which is due to the loss of σ-donor capacity of the 1,2,4-triazole ring. The redox waves at ~ -1.4 and -1.65 V are typical of bpy-based reductions and are therefore assigned so. The electron rich nature of

the thienyl moiety (as indicated by its low oxidation potential) makes reduction more difficult and is not observed below –2.0 V (vs. SCE).

Of particular interest are the metal oxidation processes of the binuclear systems. Based on 1,2,4-triazole based binuclear complexes, which have a metal to metal distance close to the complexes described here, it would be expected that only a single reversible redox wave would be observed.[17,18] For the protonated complexes this is the case with a single redox wave (with a E_{an}-E_{cat} of 70 mV), however for the fully deprotonated complexes a small separation ($\Delta E \sim 100$ mV) between the first and second metal oxidation wave is observed (Figure 7.15). This separation is close to that observed for the monoprotonated binuclear bpbt$^-$ and bpzbt$^-$ based complexes (see Table 7.1). From this the comproportionation constant for the deprotonated complexes (K_c) is ~ 60 (see Appendix E). For the protonated binuclear complexes a value of 4 is assumed since there is no separation between the first and second metal oxidation wave. The effect of protonation, *i.e.* in reducing ground state metal to metal communication, is consistent with trends observed for other 1,2,4-triazole bridged systems, however the observation of a single two electron redox wave for the protonated complexes does not exclude the possibility of a weak interaction still being present.[7,17,18,24] In order to investigate the possibility of weak/moderate communication between the metal centres for both the protonated and deprotonated complexes the properties of the mixed valence and fully oxidised complexes have been examined.

The use of a chemical oxidant such as Ce(IV) is a fast convenient method for the generation of stable mixed valence and oxidised species, however it is subject to several drawbacks in that it is sometimes not chemically or spectroscopically innocent. As a result all measurements were verified by electrochemical oxidation using the OTTLE setup described in Chapter 2.

Compared with systems of similar metal to metal separation, such as those based on L_1^{2-} and L_2^{2-} (see Figure 7.1), both of the deprotonated thienyl bridged complexes show very strong coupling. Unusually the intensities of both LMCT and IT bands are comparable with that of the MLCT bands. Upon protonation the IT moves to higher energy and is reduced in intensity relative to the LMCT band of the fully oxidised species. This indicates a reduction in the level of communication between the metal centres upon

protonation. It should be noted that in the case of the protonated complexes observing the IT band is very difficult as it shows almost complete overlap with the much stronger LMCT band. The low energy of the LMCT band is in itself unusual and reflects the better energy match between the ligand HOMO and metal t_{2g} orbitals. Examination of Table 7.5 shows that protonation results in a reduction in the extent of electronic delocalisation (α^2) by an order of magnitude. However it should be noted that the degree of electron coupling is only moderately reduced. The interaction strength both in terms of delocalisation and coupling for both the protonated and deprotonated complexes is comparable to that of the complexes based on the ligands bpt$^-$ and bpzt$^-$ (see Table 7.1) and is much greater than for any of the complexes described in section 7.1 which show a comparable metal to metal distance. This increased interaction strength may be attributable to the ability of the thienyl HOMO to overlap effectively with both the 1,2,4-triazoles and the metal d-orbitals (as evidenced by the low energy of the LMCT bands) facilitating much greater superexchange interaction.[23] The pH chemistry of the complexes supports a hole transfer superexchange mechanism. Protonation results in a significant decrease in the electronic delocalisation (α^2) and a significant decrease in the electronic coupling (H_{ab}). It should be noted that the value of the extinction coefficient used for the deprotonated complexes is likely to be considerably lower than the real value. Hence the value of both α^2 and H_{ab} present the lower limit of the values. Since only a single protonation step, involving protonation of both triazole moieties is observed then the extent of electrostatic interaction between the metal centres in these complexes is minimal.

	H_{ab} (cm^{-1})	$\alpha^{2\,a}$	ΔE (mV) ± 10 mV	K_c	$\Delta\nu_{1/2}$ (cm^{-1})^b	ε_{max} ($M^{-1}cm^{-1}$) ± 20 %	E_{op} (cm^{-1}) ± 100 cm^{-1}
$[(Ru(bpy)_2)_2((pytr)_2th)]^{2+}$	577	0.0102	110	72	4572	5000	5720
$[(Ru(bpy)_2)_2((pztr)_2th)]^{2+}$	565	0.0105	100	50	4520	5000	5530
$[(Ru(bpy)_2)_2(H_2(pytr)_2th)]^{4+}$	444	0.0028	0	4	3430	2600	8400
$[(Ru(bpy)_2)_2(H_2(pztr)_2th)]^{4+}$	430	0.0026	0	4	3400	2600	8450

Table 7.5 *Spectroelectrochemical data for complexes discussed in text. (a) Extent of electronic delocalisation, (b) taken as double the width at half maximum of the high-energy side of the absorption band. (c) For the deprotonated complexes the value of ε_{max} is the lowest estimate, for protonated complexes the ε_{max} is adjusted to account for $K_c = 4$. A metal to metal distance of 12.8 Å is estimated (based on non-optimised Hyperchem models)*

7.4 Conclusions

As described in the introduction, the ability to control interaction between metal centres both by external stimuli such as pH, solvent and by variation of the spacer group between metal centres is central to the development of molecular devices. In the systems described above it is clear that the presence of a thienyl spacer allows for a dramatic increase in the distance between metal centres compared with systems such as bpt$^-$ and bpzt$^-$ with only a small loss in the interaction strength. In addition in these systems the presence of moieties which allow for external manipulation of the interaction strength, make these systems much more applicable to the building of supramolecular devices.

An aspect of this study not discussed above is the potential of the mononuclear complexes in forming hetero-bimetallic systems, in particular with Pd(II), Pt(II), Cu(I) and Au(I), all of which show affinity for sulphur containing ligands. These systems should show strong interaction between the metal centres and allow for efficient energy vectoring.[4,5]

7.4 Experimental

The synthesis and characterisation of all ligands are described in Chapter 2.

[Ru(bpy)$_2$(pytrth)](PF$_6$).H$_2$O. 230 mg (0.44 mmol) of *cis*-[Ru(bpy)$_2$Cl$_2$] and 130 mg (0.57 mmol) of Hpytrth were heated at reflux for 8 h in 50 cm^3 ethanol/water (50/50 v/v). The reaction was evaporated to dryness and redissolved in the minimum of water and filtered to remove unreacted ligand. 3 drops of concentrated NH_4OH_{aq} and 2 cm^3 of saturated ammonium hexafluorophosphate were added to the filtrate and the precipitate collected under vacuum and air-dried. Purification by column chromatography on neutral alumina (CH_3CN as eluent) yielded a single red fraction. Solvent was removed in vacuo and the precipitate rerystallised from methanol/water. Yield 240 mg (0.31 mmole, 70 %). Mass spec. 640.9 m/z (calc. for $RuC_{31}H_{23}N_8S$ M^+ = 641). ^{1}H NMR in CD_3CN; 8.48 (1H,d), 8.46 (1H,d), 8.42 (2H, d), 8.10 (1H, d), 8.015 (1H, dd), 7.98 (1H, dd), 7.93 (4H, m), 7.86 (2H, m), 7.79 (1H, d), 7.51 (1H, d), 7.4 (4H, m), 7.31 (1H, dd), 7.26 (1H, d), 7.15 (1H, dd), 7.03 (1H, dd). CHN analysis: % found (% calc. for $RuC_{31}H_{23}N_8SPF_6.H_2O$); C 46.32 % (46.33 %), H 2.84 % (2.99 %), N 13.80 % (13.95 %).

[Ru(bpy)$_2$(pztrth)](PF$_6$).2H$_2$O. As for [Ru(bpy)$_2$(pytrth)](PF$_6$) except 230 mg (0.44 mmol) of *cis*-[Ru(bpy)$_2$Cl$_2$] and 130 mg (0.56 mmol) of Hpztrth were used. Yield 200 mg

(0.25 mmole, 57 %). Mass spec. 641.9 m/z (calc. for $RuC_{30}H_{22}N_9S$ M^+ = 642). ^1H NMR in CD_3CN; 9.23 (1H, d), 8.5 (4H, m), 8.25 (1H, d), 8.01 (4H, m), 7.93 (1H, d), 7.86 (1H, d), 7.80 (2H, dd), 7.59 (1H, d), 7.40 (5H, m), 7.31 (1H, d), 7.05 (1H, dd). CHN analysis: % found (% calc. for $RuC_{30}H_{22}N_9SPF_6.2H_2O$); C 43.60 % (43.80 %), H 2.73 % (2.92 %), N 14.97 % (15.33 %).

$[(Ru(bpy)_2)_2((pytr)_2th)](PF_6)_2.6H_2O$ As for $[Ru(bpy)_2(pytrth)](PF_6)$ except 300 mg (0.58 mmol) of *cis*-$[Ru(bpy)_2Cl_2]$ and 100 mg (0.27 mmol) of $H_2(pytr)_2th$ were heated at reflux in ethylene glycol/water (3/1 v/v). Yield 150 mg (0.09 mmole, 36 %). ^1H NMR in CD_3CN; 8.3 (8H, m), 7.90 (2H, d), 7.8 (9H, m), 7.74 (2H, d), 7.7 (5H, m), 7.62 (2H, d), 7.33 (2H, d), 7.24 (6H, m), 7.15 (2H, dd), 7.08 (2H, s), 6.97 (2H, dd). CHN analysis: % found (% calc. for $Ru_2C_{58}H_{42}N_{16}SP_2F_{12}.6H_2O$); C 43.80 % (43.66 %), H 2.77 % (3.01%), N 13.68 % (14.05 %).

$[(Ru(bpy)_2)_2((pztr)_2th)](PF_6)_2$. As for $[Ru(bpy)_2(pytrth)](PF_6)$ except 290 mg (0.56 mmol) of *cis*-$[Ru(bpy)_2Cl_2]$ and 90 mg (0.24 mmol) of $H_2(pztr)_2th$ were heated at reflux in 25 cm^3 ethylene glycol/water (3/1 v/v). Yield 120 mg (0.085 mmole, 33 %). ^1H NMR in CD_3CN; 9.28 (2H, d), 8.5 (8H, m), 8.27 (2H, d), 8.01 (8H, m), 7.91 (2H, d), 7.80 (2H, m), 7.76 (4H, d), 7.62 (2H, d), 7.40 (8H, m). CHN analysis: % found (% calc. for $Ru_2C_{56}H_{38}N_{18}SP_2F_{12}$); C 27.50 % (%), H 1.68 % (%), N 12.87 % (%). CHN analysis unsuccessful due to presence of PF_6^- salt in excess.

7.5 Bibliography

1. (a) K. Kalyanasundaram, *Coord. Chem. Rev.*, **1982**, *46*, 159 (b) J.M. Lehn, *Angew. Chem., Int. Ed. Engl.*, **1988**, *27*, 89, (c) V. Balzani, S. Campagna, G. Denti, A. Juris, S. Serroni and M. Ventura, *Coord. Chem. Rev.* **1994**, *132*, 1 (d) V. Balzani, A. Juris, M. Venturi, S. Campagna and S. Serroni, *Chem. Rev.*, **1996**, *96*, 759 (e) V. Balzani, A. Juris, M. Venturi, S. Campagna and S. Serroni, *Acc. Chem. Res.* **1998**, *31*, 26 (f) C. A. Slate, D. R. Striplin, J. A. Moss, P. Chen, B. W. Erickson and T. J. Meyer, *J. Am. Chem. Soc.* **1998**, *120*, 4885 (g) Y-Z. Hu, S. Tsukiji, S. Shinkai, S. Oishi and I. Hamachi, *J. Am. Chem. Soc.* **2000**, *122*, 241 (h) J-P. Sauvage, J-P. Collin, J-C. Chambron, S. Guillerez, C. Coudret, V. Balzani, F. Barigelletti, L. De Cola and L. Fannigni, *Chem. Rev.*, **1994**, *94*, 993 (i) J.N. Demas and D. A. DeGraff, *Analytical Chem.*, **1991**, *63*, 829

2. (a) V. Balzani and F. Scandola, *Supramolecular Photochemistry*, Ellis Horwood: Chichester, UK, **1991** (b) V. Balzani, Ed., *Supramolecular Photochemistry*, Reidel, Dordrecht, **1997** (c) J.-M. Lehn, *Supramolecular Chemistry*, Wiley-VCH, Weinheim, **1995**

3. (a) P.D. Beer, F. Szemes, V. Balzani, C.M. Salà, M.G. Drew, S. W. Dent and M. Maestri, *J. Am. Chem. Soc.*, **1997**, *119*, 11864. (b) F. Barigelletti, L. Flamigni, J.-P. Collin and J.-P. Sauvage, *Chem. Commun.*, **1997**, 333. (c) O. Waldmann, J. Hassmann, P. Müller, G.S. Hanan, D. Volkmer, U.S. Schubert and J.-M. Lehn, *Phys. Rev. Lett.*, **1997**, *78*, 3390. (d) E. Zahavy, and M.A. Fox, *Chem. Eur. J.*, **1998**, *4*, 1647. (e) V. Balzani, A. Credi and M. Venturi, *Curr. Opin. Chem. Biol.*, **1997**, *1*, 506.

4. (a) R. Hage, R. Prins, J. G. Haasnoot, J. Reedijk and J. G. Vos, *J. Chem. Soc., Dalton Trans.* **1987**, 1389 (b) H. A. Nieuwenhuis, J. G. Haasnoot, R. Hage, J. Reedijk, T.L. Snoeck, D. J. Stufkens and J. G. Vos, *Inorg. Chem.*, **1991**, *30*, 48 (c) B. E. Buchanan, R. Wang, J. G. Vos, R. Hage, J. G. Haasnoot, and J. Reedijk, *Inorg. Chem.*, **1990**, *29*, 3263 (d) W. R. Browne, C. M. O'Connor, C. Villani and J. G. Vos, *Inorg. Chem.* **2001**, *40*, 5461

5. (a) R. Hage, A.H.J. Dijkhuis, J.G. Haasnoot, R. Prins, J. Reedijk, B.E. Buchanan and J.G. Vos, *Inorg. Chem.*, **1988**, *27* , 2185 (b) F. Barigelletti, L. De Cola, V. Balzani, R. Hage, J.G. Haasnoot, J. Reedijk and J.G. Vos, *Inorg. Chem.*, **1989**, *28* , 4344

6. R. Hage, J.G. Haasnoot, H.A. Nieuwenhuis, J. Reedijk, D.J.A. De Rider and J.G. Vos, *J. Am. Chem. Soc.* **1990**, *112*, 9249

7. C. Di Pietro, S. Serroni, S. Campagna, M.T. Gandolfi, R. Ballardini, S. Fanni, W.R. Browne and J.G. Vos, *Inorg. Chem.*, **2002**, 41, 2871

8. (a) N. S. Hush, *Prog. Inorg. Chem.*, **1967**, *8*, 391 (b) N. S. Hush, *Electrochim. Acta*, **1968**, *13*, 1005

9. M. P. Robin and P. Day, *Adv. Inorg. Chem. Radiochem.*, **1967**, *10*, 247

10. C. Creutz, *Prog. Inorg. Chem.*, **1980**, *30*, 1

11. C. Creutz and H. Taube, *J. Am. Chem. Soc.*, **1969**, *91*, 3988

12. K. D. Demadis C. M. Hartshorn and T. J. Meyer, *Chem. Rev.*, **2001**, *101*, 2655

13. H. A. Goodwin and F. Lions, *J. Am. Chem. Soc.*, **1959**, *81*, 6415

14. R. J. Foster, A. Boyle, J. G. Vos, R. Hage, A. H. J. Dujkhuis, R. A.G. Graaf, J.G. Haasnoot and J. Reedijk, *J. Chem. Soc., Dalton Trans.*, **1990**,

15. W. R. Browne, C. M. O'Connor, H. P. Hughes, R. Hage, O. Walter, M. Doering, J. F. Gallagher and J. G. Vos, *J. Chem. Soc., Dalton Trans.*, accepted – Sept. **2002**, see Appendix A

16. M. Tiecco, M. Tingoli, L. Testaferri, D. Chianelli and E. Wenkert, *Tetrahedron*, **1986**, *42*, 1475

17. F. Weldon, *Ph.D. Thesis*, Dublin City University, Ireland, **1998**

18. P. Passaniti, W. R. Browne, F. C. Lynch, D. Hughes, M. Nieuwenhuyzen, P. James, M. Maestri and J. G. Vos, *J. Chem. Soc. Dalton Trans.*, **2002**, 1740

19. (a) J.T. Hupp, *J. Am. Chem. Soc.*, **1990**, *112*, 1563 (b) S.B. Piepho, *J. Am. Chem. Soc.*, **1990**, *112*, 4197 (c) V. Petrov, J.T. Hupp, C. Mottley and L.C. Mann, *J. Am. Chem. Soc.*, **1994**, *116*, 2171

20. R. Hage, *Ph.D. Thesis*, Leiden University, The Netherlands, **1991**

21. M. K. Nazeeruddin, S. M. Zakeeruddin, and K. Kalyanasundaram, *J. Phys. Chem.*, **1993**, *97*, 9607

22. (a) J. V. Casper and T. J. Meyer, *Inorg. Chem.*, **1983**, *22*, 2444 (b) J. V. Casper and T. J. Meyer, *J. Am. Chem. Soc.*, **1983**, *105*, 5583

23. (a) S. Encinas, L. Flamigni, F. Barigelletti, E. C. Constable, C. E. Housecroft, E. R. Scholfield, E. Figgmeier, D. Fenske, M. Neuburger, J. G. Vos and M. Zehnder, *Chem. Eur. J.*, **2002**, *8*, 137 (b) T. M. Pappenfus and K. R. Mann, *Inorg. Chem.*, **2001**, *40*, 6301 (c) A. Harriman, A. Mayeux, A. De Nicola and R. Ziessel, *Phys. Chem. Chem. Phys.*, **2002**, *4*, 2229

24. J. Bonvision, J-P Launay, M Van der Auweraer and F. C. De Schryver, *J. Phys. Chem.* **1994**, *98*, 5052

Chapter 8

The Creutz-Taube ion revisited- Binuclear complexes containing non-bridging 1,2,4-triazole moieties

The Creutz-Taube ion $\{[(NH_3)_5Ru\text{-}(\mu\text{-pyrazine})\text{-}Ru(NH_3)_5]^{4+}\}$ is easily the $[Ru(bpy)_3]^{2+}$ of binuclear Ru(II) complexes, and has been the subject of intense interest for over 30 years. In the previous chapter systems containing 1,2,4-triazole base moieties, where the triazole formed a direct bridge between the metal centres, were the focus of attention. In these systems, the ground state interaction was shown to be critically dependent on the protonation state of the triazole. In this chapter attention is focused on systems, which contain non-bridging 1,2,4-triazole moieties, in which the metal centres are bridged by pyrazine. As expected these systems show a strong interaction (as observed by electrochemistry). The effect of protonation on the level of interaction and the photochemical reactivity is examined.

8.1 Introduction

Multinuclear systems, in particular those based on Ru(II), are of significant interest in the development of models for the water splitting component of photosystem II.[1] In this area the development of polynuclear systems capable of multi-electron transfer has received considerable attention. In chapter 7, the area of multinuclear complexes and in particular, metal-metal interactions are introduced. In this chapter attention is focused on pyrazine-bridged systems, such as those shown in Figure 8.1.

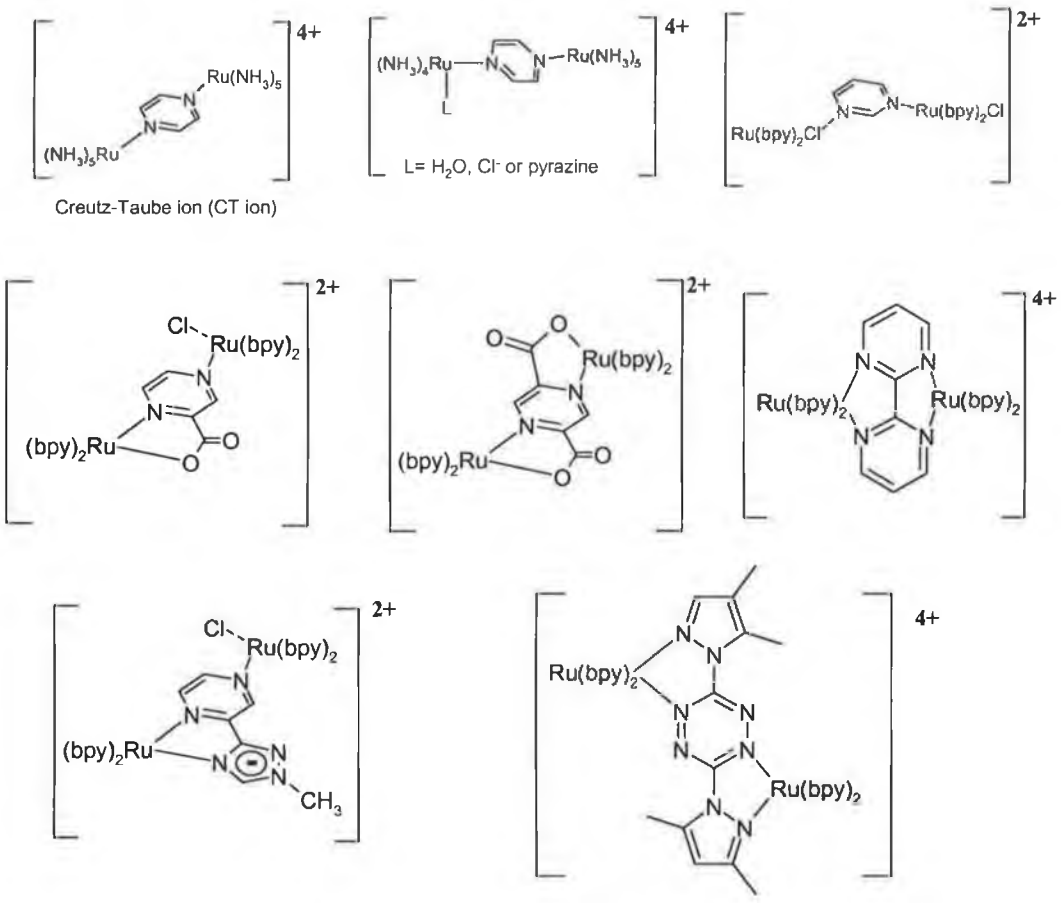

Figure 8.1 *CT ion and related complexes discussed in the text.*

The Creutz-Taube (*CT*) ion $\{[(NH_3)_5Ru\text{-}(\mu\text{-pyrazine})\text{-}Ru(NH_3)_5]^{4+}\}$ reported by Creutz and Taube in 1969,[2] is arguably the archetypal binuclear complex and both itself and similar pyrazine bridged multinuclear systems have been the focus of significant levels of attention (*vide infra*). The *CT* ion shows two fully reversible oxidation waves at 0.4 V and 0.76 V (ΔE = 360 mV) and for the mixed valence species a band in the visible region at 565 nm (the fully reduced species shows an absorption at 547 nm) and a distinct band assigned as the intervalence transition at 1570 nm are observed. Substitution of one NH_3

for H_2O resulted in a very slight shift in the λ_{max} of the IT band (to 1530 nm). However, substitution with chloride anion or pyrazine resulted in a large blue shift in the λ_{max} of the IT band to 1450 and 1160 nm respectively (Figure 8.1). The changes in the energy of the IT band have been interpreted on the basis of the effect of substitution on the barrier to electron transfer as the reduction of electron density on the substituted metal centre makes that centre more difficult to oxidize. Increasing the asymmetry in the complex by replacement of one of $Ru(NH_3)_5$ moieties by $RuCl(bpy)_2$ (960 nm), $Ru(NO_2)(bpy)_2$ (790 nm) or $Ru(CH_3CN)(bpy)_2$ (750 nm) results in a further blue-shift in the energy of the IT band.[3] Similar studies on the 4,4'-bipyridine bridged analogue of the *CT* ion have also been reported and show a much reduced level of interaction for symmetric systems (based on electrochemistry).[3,4] The mechanism for the interaction between the metal centres in pyrazine-bridged binuclear complexes is generally agreed to be via a bridge mediated superexchange process rather than by direct overlap of metal based orbitals.[5]

Meyer and coworkers have examined the intervalence properties of the *CT* ion analogues $[(bpy)_2ClM\text{-}(\mu\text{-pyrazine})\text{-}MCl(bpy)_2]^{2+}$ (where M = Ru or Os).[6] In these ions the extent of electron delocalisation in the mixed valence state is very small. The difference between successive metal oxidation waves (ΔE) for the ruthenium dimer is 120 mV and an intervalence transition at 1300 nm (ε = 455 $M^{-1}cm^{-1}$) is observed for this ion. Importantly the mixed valence and fully oxidized species show some instability, which prevented their observation initially.[7] Similarly for the osmium complexes only weak absorptions were observed for the mixed valance species. For the related complex $\{[(bpy)_2ClRu\text{-}pyrimidine\text{-}RuCl(bpy)_2]^{2+}$ the interaction observed is considerably reduced with an IT band observed at 1360 nm (ε = 34 $M^{-1}cm^{-1}$) and a calculated delocalisation parameter (α^2) an order of magnitude lower than for the pyrazine bridged dimer.[8] Again the stability of the mixed valence and fully oxidized species is poor and decomposition is observed.

Pyrazine carboxylate bridged systems such as those shown in Figure 8.1 have been examined.[9] The differences in redox potentials of the 1st and 2nd metal oxidation process are similar to those found for the pyrazine and pyrimidine bridged binuclear complexes described above. It is clear that the interaction between the metal centres in terms of the IT band is dependent on the nature of the non-bridging moieties of the complex, whilst the value of ΔE from electrochemical analysis is less so. Toma *et al.* have reported a tetra- and hepta- nuclear complexes based around a central $[Ru(bpz)_3]^{2+}$ moieties with the remaining centres being Ru(II) pentaamine groups.[10] Pavinato *et al.* have reported a

similar system based on $Ru(bpy)_2$bipyrimidine-.[11] In these systems no IT bands were observed, however the low energy absorption bands of the mixed valence species and the very low values of ε expected may result in the IT band being unobservable due to the overlap with other bands. Multinuclear complexes employing ligands based on 2,3-(dipyrid-2'-yl)-pyrazine have been reported by several groups.[12] IT absorption bands at between 5000 and 8000 cm^{-1} are typical of these classes of complex and the interaction in every case has been classified as Type II.[13]

Sarkar *et al.* have recently reported a tetrazine based binuclear ruthenium polypyridyl complex (see Figure 8.1), which shows very strong interaction between the two metal centres.[14] The strong coupling observed has been attributed to the low-energy LUMO of the ligand and the high coefficient of the LUMO on the nitrogen atoms, which facilitates effective overlap of the metal based and ligand based orbitals (*i.e.* facilitates superexchange processes). In this complex a separation between the first and second metal oxidation wave of 450 mV was observed, indicating that the interaction is very strong. A very narrow IT band observed at 1534 nm confirms that the interaction is Type III. The pH chemistry of this complex shows a pK_a of 1.0 (measured in acetonitrile: water 2:1) with a large red shift in the absorption spectrum on protonation, attributable to a stabilization of the bridging ligands' LUMO.

Hage *et al.* have reported asymmetric pyrazine bridged homo- and hetero- binuclear complexes (Figure 8.1).[15] Due the inherent differences in the oxidation potentials of the mononuclear analogues $[Ru(bpy)_2(pz)Cl]^+$ and $[Ru(bpy)_2$(1-methyl-3-(pyrazin-2'-yl)-1,2,4-triazole)$]^+$, a large separation (ΔE) between the 1st and 2nd oxidation waves (490 mV) is expected. As for the 2-pyrazine-carboxylic acid bridged dimer described above an IT band is observed for the ruthenium based dimer at 962 nm ($\varepsilon = 480\ M^{-1}cm^{-1}$) and for the ruthenium/osmium based dimers at around 1300 to 1600 nm ($\varepsilon \sim 800\ M^{-1}cm^{-1}$).

In this chapter the synthesis and characterisation of the complexes **1** (in the case of **1a** the bpy ligands are replaced with $[D_8]$-bpy) and **2** are described (see Figure 8.2). These systems have the potential to show modulation of the interaction between the metal centres by external perturbation (*e.g.* variations in the protonation state). Of interest is the effect of protonation on the ground and excited state properties of the complexes and the possibility of a two-step protonation process. 1,2,4-triazole bridged binuclear systems

(*e.g.* those based on the ligands bpt⁻, bpbt⁻ etc.) show a dramatic decrease in the strength of the interaction upon protonation. This decrease has been ascribed to the loss of interaction via superexchange, by the stabilization of the triazole LUMO.

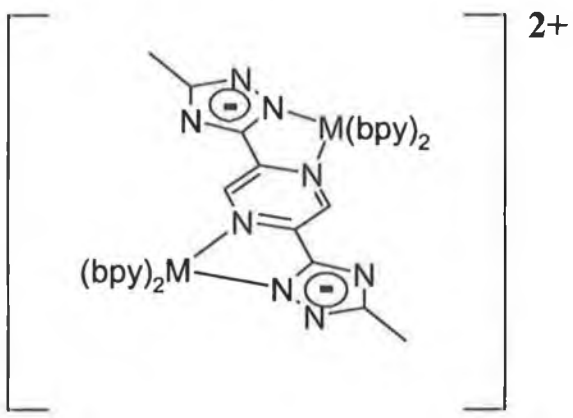

1 M = Ru
2 M =Os

Figure 8.2 *Structure of complex 1 and 2 (N2N2 bound isomer).*

8.2 Results

8.2.1 Synthesis and structural characterisation

The synthesis of the ligand was achieved following standard routes as outlined in Chapter 2. Preparation of homo-binuclear complexes by direct reaction of the ligand with two equivalents of *cis*-$[M(bpy)_2Cl_2]$ (where M = Ru or Os) is relatively straightforward with purification by column chromatography on neutral alumina using acetonitrile as eluent. For **2**, an additional purification step using silica gel was required, resulting in contamination of the isolated material being contaminated with KPF_6.

8.2.2 Mass spectrometry

Characterisation of all complexes by mass spectrometry has been carried out (see Experimental Section). Both ruthenium and osmium complexes have distinctive isotopic patterns depending on the number of metal atoms in the molecular ion detected. Deuteriation allows for additional confirmation of the molecular ion as it results in a predictable increase in the molecular ion m/z value. Similarly osmium complexes give predictable but quite complex isotopic patterns.

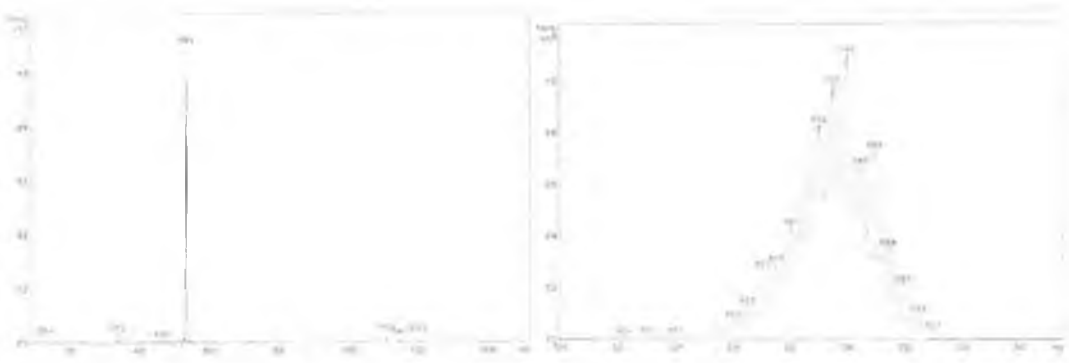

Figure 8.3 *Mass spectrum of complex 1^{2+} (right: expansion of molecular ion 100%)*

For $[(Ru(bpy)_2)_2(metr)_2pz]^{2+}$ (1) the molecular ion is observed at 534 m/z and increment of 0.5 m/z units indicates it is a divalent cation. The calculated value for $(Ru_2C_{50}H_{40}N_{16})^{2+}$ is 534.0814.

8.2.3 ^1H NMR spectroscopy

The ^1H NMR spectra of $[(Ru(bpy)_2)_2(metr)_2pz]^{2+}$ is shown in Figure 8.4. Two methyl resonances are observed at 2.175 ppm and 2.18 ppm and a total of 34 aromatic resonances are observed. For the partially deuteriated complex two pyrazinyl protons are observed at 7.92 ppm and 7.98 ppm with equal intensity indicating the formation of each diastereoisomer occurs with equal probability. ^1H NMR data are given in the experimental section.

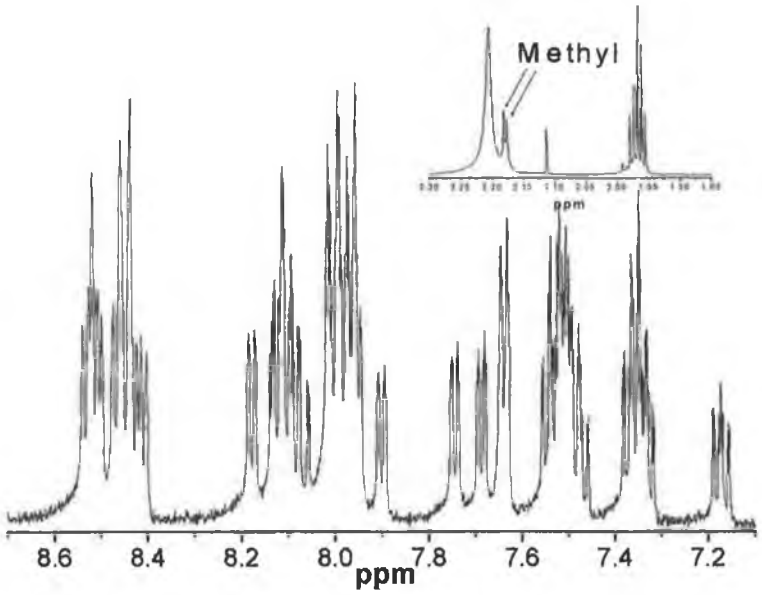

Figure 8.4 *^1H NMR spectrum (400 MHz) in CD_3CN of 1*

8.2.4 Electronic spectroscopy

The absorption spectrum (see Figure 8.6) of the deprotonated complex **(1)** shows strong absorption features at ~520 nm with several overlapping bands. Both mono- and di-protonation results in a red shift of the lowest absorption bands to 565 nm (**$H_2$1**) whilst the higher energy bands (~ 460 nm) undergoes a blue-shift to (~425 nm) upon protonation to **$H_2$1**. This results in an overall simplification of the absorption spectrum.

	Absorption λ_{max} in nm (log ε)	Emission λ_{max} in nm (τ/ns) at 298K	Emission λ_{max} in nm (τ/μs) at 77 K[a]
1	241 (4.56), 290 (4.89), 467 (4.22), 530 (4.38)	748 (191)	697 (2.32)
$H_2$1	282 (4.88), 424 (4.21), 565 (4.34)	780 (124)	756 (1.65)
1a	241(4.64), 290 (4.98), 467 (4.25), 530 (4.35)	749 (220)	700 (3.15)
$H_2$1a	282 (4.80), 424 (4.24), 565 (4.33)	779 (142)	750 (2.23)
2	240 (4.55), 474 (4.79), 547 (4.04), 792 (3.61)	Not obs.	Not obs.
$H_2$2	291 (4.79), 443 (4.06), 600 (4.04), 853 (3.52)	"	"

Table 8.1 *Spectroscopic data for **1**, **1a** and **2** and their protonated forms in acetonitrile (protonation with CF_3CO_2H). a) in butyronitrile.*

For **2** similar absorption bands are observed (see Figure 8.6), with additional absorption features in the near-IR region (700 – 900 nm). Again protonation results in a blue shift in the 470 nm absorption and a red shift in the absorption features at 540 nm and 800 nm.

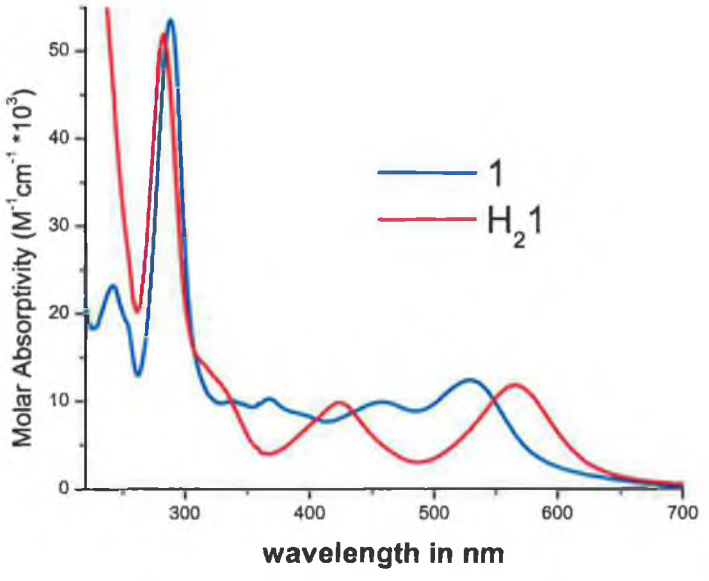

Figure 8.5 *UV.vis spectra of **1** and **$H_2$1** in acetonitrile (protonation with CF_3CO_2H)*

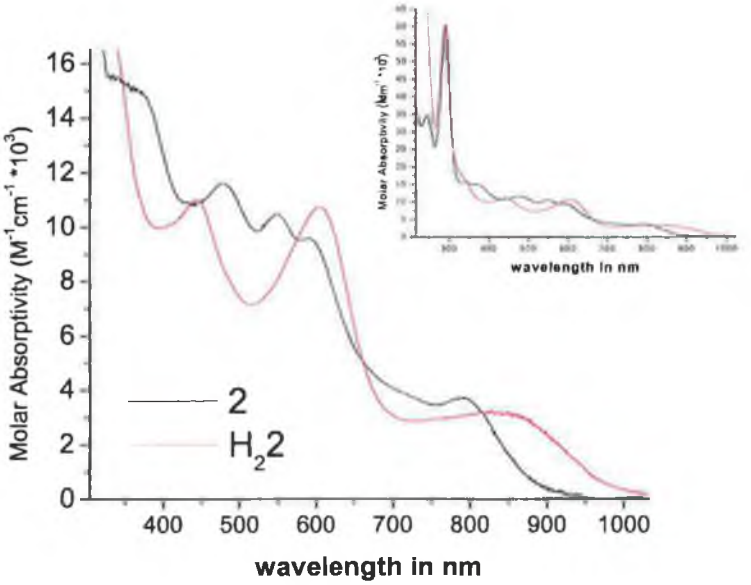

Figure 8.6 *UV.vis spectra of* ***2*** *and* $\boldsymbol{H_2 2}$ *in acetonitrile (protonation with* CF_3CO_2H*)*

As for the lowest energy absorption band of **1**, upon protonation to **H1** and then $\mathbf{H_2 1}$ the emission spectrum of the complex undergoes a red shift from 748 nm to 800 nm (see Table 8.1). For **2** as would be expected no emission is observed within the detector range of the spectrometer (< 850 nm). Table 8.1 shows the luminescence lifetime data for **1a** and **1b**. It is notable that deuteriation of the bpy ligands has a significant effect (~ 14 % at 298 K and 35% at 77K increase) on the observed emission lifetime of both **1** and $\mathbf{H_2 1}$.

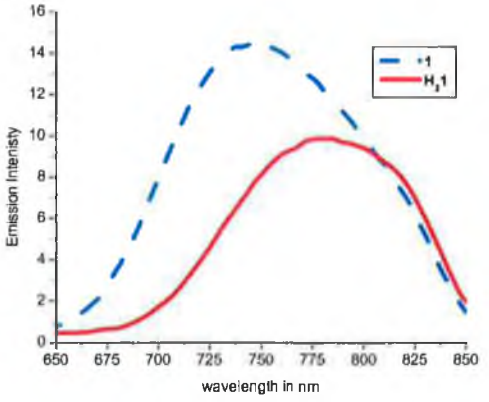

Figure 8.7 *Emission spectra of* ***1*** *and* $\boldsymbol{H_2 1}$ *in acetonitrile*

Acid base properties

The acid base chemistry of both **1** and **2** show very large changes upon protonation. For **1,** two protonation steps are observed at pK_{a1} = 2.7, pK_{a2} = 4.68 pH units (see Figure 8.8 to Figure 8.10).

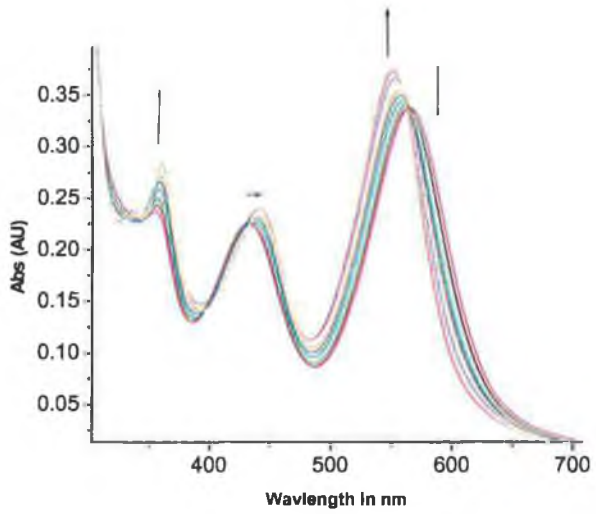

Figure 8.8 *Changes in absorption spectrum of 1 over the pH range 3.4 to 12.9, in Britton-Robinson Buffer. (Inset: Expansion of visible region)*

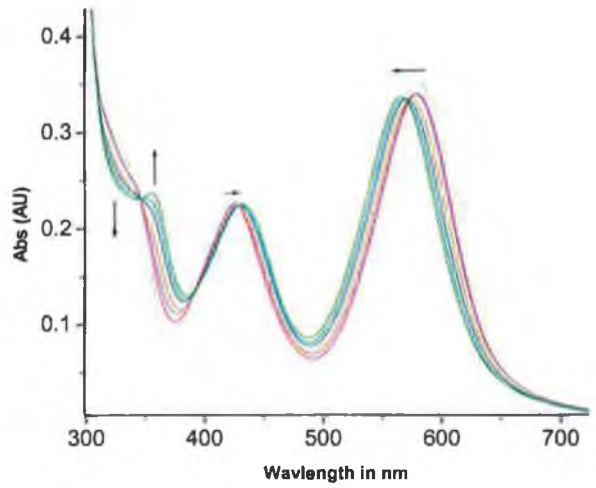

Figure 8.9 *Changes in absorption spectrum of 1 over the pH range 1.0 to 3.4, in Britton-Robinson Buffer. (Inset: Expansion of visible region)*

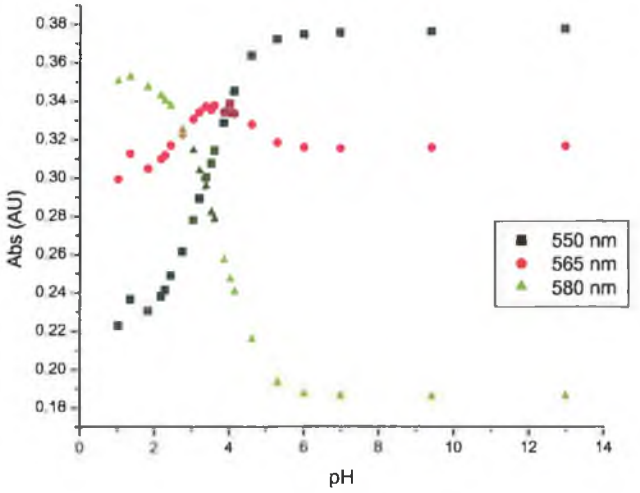

Figure 8.10 *Plot of absorbance against pH for* ***1*** *at 550 nm, 565 nm, and 580 nm.*

When followed by emission spectroscopy the pH_i of each protonation step is determinable. pH_{i1} = 2.45 and pH_{i2} = 4.85 (*N.B.* A large error in the former value is inherent due to a large signal to noise ratio from the relatively very weak emission of both **H1** and $\mathbf{H_21}$). Combined with emission lifetime data the excited state pK_a (pK_a*) values may be estimated, however given the large errors in the values obtained for the pH_i values and the lack of accurate lifetime data for the **H1**, then reliable values are not calculable (see Chapter 2). Nevertheless considering Equation 2.10 the assuming the lifetime of **H1** is intermediate of **1** and $\mathbf{H_21}$, it is likely that the correction will result in the pK_a* values being lower than the pH_i values obtained and hence lower than the ground state pK_a's.

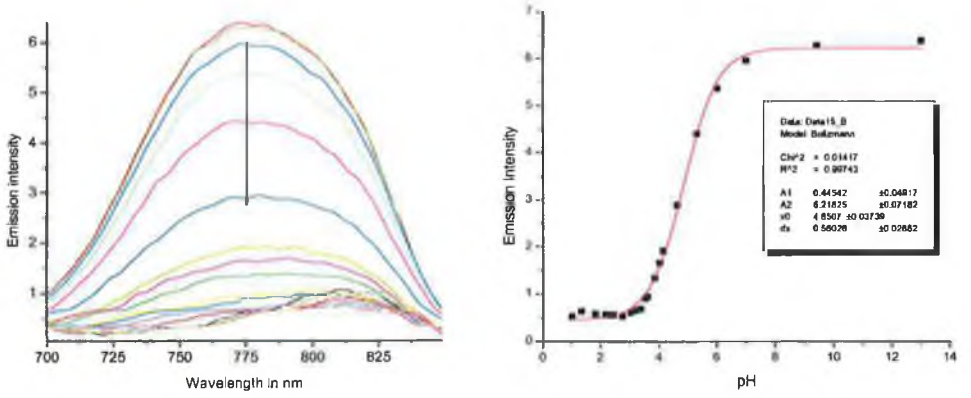

Figure 8.11 *Changes in emission spectrum of* ***1*** *over the pH range 1.0 to 12.0, in Britton-Robinson Buffer. Plot of intensity vs. pH shows only the first protonation step.*

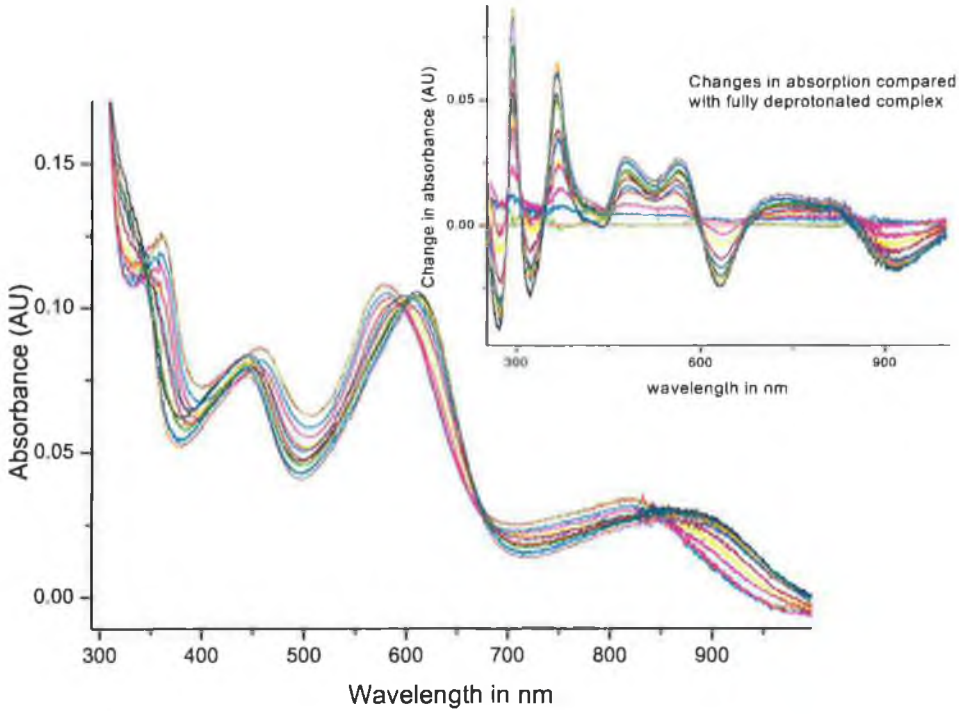

Figure 8.12 *Changes in the absorption spectrum of* ***2*** *over the pH range 1.0 to 12.0, in Britton-Robinson Buffer*

For **2**, pK_a values of 1.8 and 3.9 have been estimated which are lower than for **1**. This is not unexpected and has been observed for similar systems.[18] It should be noted however in this case the quality of the data available is not sufficient to allow for accurate determination of the pK_a values and the values presented are subject to large errors (+/- 0.3 pH units).

8.2.5 Photochemistry

The photochemical stability of the $\mathbf{H_21}$ and fully deprotonated complex **1** in acetonitrile was examined. Examination of the photochemistry of the mono-protonated complex is not practical due to the small separation between the first and second protonation steps. The reason for this is that as the photochemistry of any of the three protonation states could be observed in this region. Photodecomposition was not observed for either **2** or $\mathbf{H_22}$.

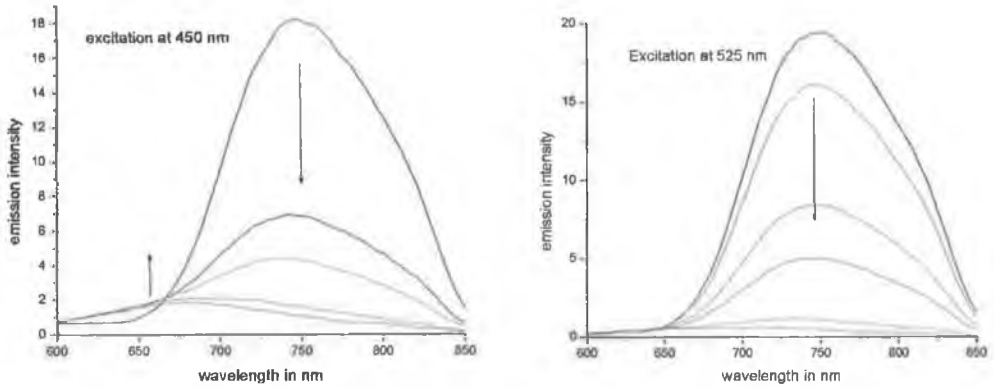

Figure 8.14 *Changes observed in the emission spectrum of 1 upon photolysis in acetonitrile*

8.2.6 Electrochemistry

Both Ru(II) (**1**) and Os(II) (**2**) binuclear complexes show reversible electrochemistry,

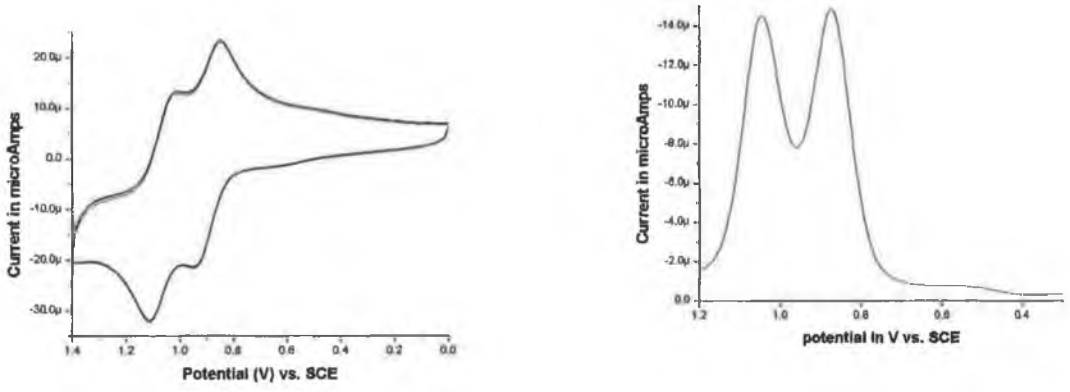

with two metal oxidation waves observable in each case.

Figure 1.15 *Metal based oxidation processes for **1** in 0.1 M TEAP/CH_3CN (left CV scan rate 200 mVs^{-1}, right DPV scan rate 20 mVs^{-1})*

Metal-based oxidation waves for **1** were observed at 0.875 V and 1.05 V (ΔE 175 mV) and are both reversible (E_{cat}-E_{an} = 80 mV). Upon protonation the oxidation potentials are raised to ~1.28 and 1.45 mV.

For **$H_2$1** no evidence for photodecomposition was observed after extended photolysis in acetonitrile. In contrast, **1** was found to undergo rapid decomposition as is seen from the collapse of the absorption band at 530 nm (Figure 8.13) and the loss of emission intensity (Figure 8.14). Surprisingly the remainder of the absorption spectra remained quite stable showing only very minor changes. Emission spectra recorded with 450 nm excitation again showed a diminishment in the emission intensity at 750 nm however a second weaker emission appeared at 680 nm and under extended photolysis became the dominant emission.

Attempts at following the reaction by ^{1}H NMR spectroscopy were only partially successful in elucidating the photoproducts formed. The most significant new feature after photolysis is a new band at 9.9 ppm, indicative of the presence of the H3 position of pyrazine adjacent to uncoordinated nitrogen. Overall a significant increase in the complexity of the spectrum as a whole is observed.

In order to verify that the complex was fully deprotonated during photolysis, a sample in acetonitrile containing Et_3N was also photolysed. Almost identical changes in the absorption spectra were observed, however, the changes in the emission spectrum were somewhat different. As for the deprotonated sample in the absence of Et_3N, the emission at 750 nm diminished, but a second emission appeared at 630 nm (possibly $[Ru(bpy)_2(Et_3N)_2]^{2+}$. This second emission was very intense relative to the initial emission spectrum and hence it is impossible to say that the emission at 680 nm did not appear also. Nevertheless it is clear that the photochemistry observed was that of the deprotonated complex in both cases.

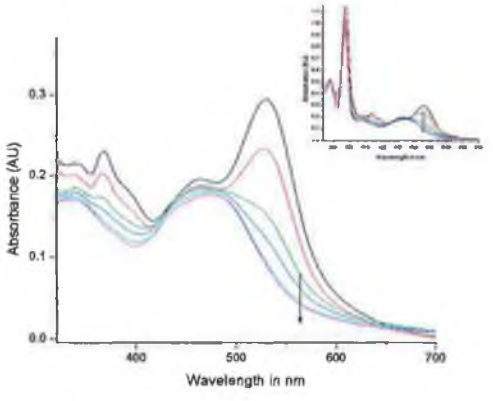

Figure 8.13 *Changes observed in the UV.Vis absorption spectrum of* ***1*** *upon photolysis in acetonitrile (inset: full spectrum)*

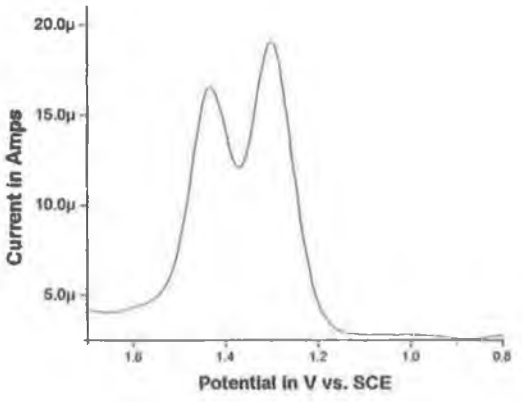

Figure 1.16 *Metal based oxidation processes for* $\mathbf{H_2 1}$ *in 0.1 M TEAP/CH_3CN (left DPV scan rate 20 mVs^{-1})*

Reduction waves for **1** are observed at –1.18 V [1], -1.58 V [2], -1.80 V [1], 1.91 V [1]. Due to the low electron density the pyrazine ring the first reduction process is most likely pyrazine based followed by bpy based reductions.

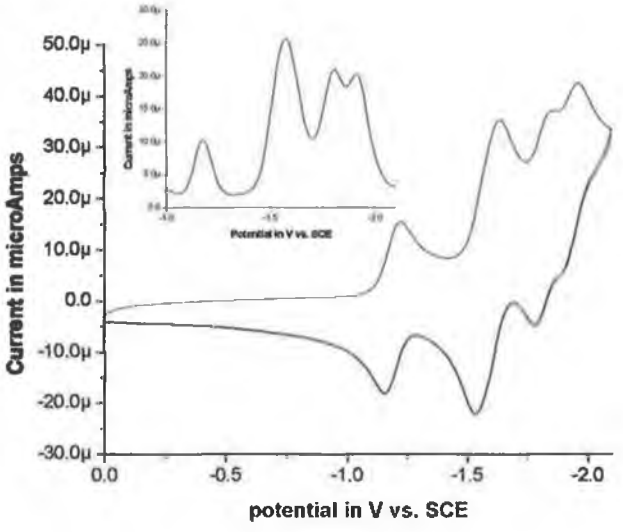

Figure 1.17 *Ligand based processes for* ***1*** *in 0.1 M TEAP/CH_3CN (CV scan rate 200 mVs^{-1}, inset: DPV scan rate 40 mVs^{-1})*

For the osmium complex, similar behaviour was observed with metal-based oxidations at 0.53 and 0.77 V (ΔE = 240 mV) for **2** and at 0.81 and 1.09 V (ΔE = 280 mV) for $\mathbf{H_2 2}$.

8.2.7 Spectroelectrochemistry

The preparation of the mixed valence and fully oxidized complex by bulk electrolysis is hampered by the lack of stability of the fully oxidized species. Nevertheless some information may still be obtained using this technique.

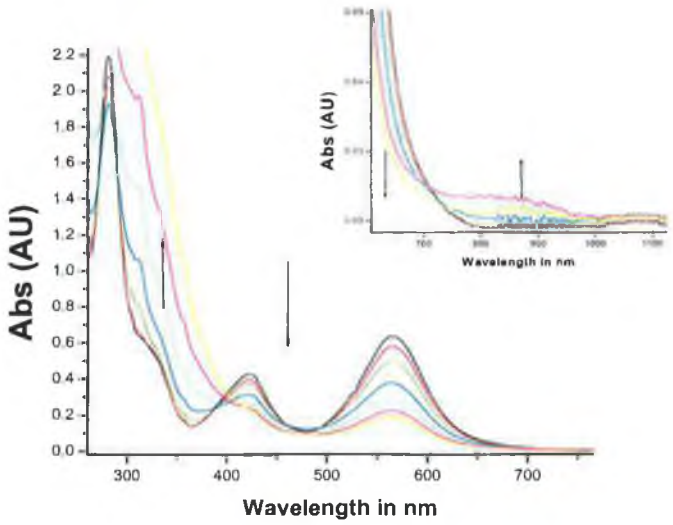

Table 8.2 *Changes in UV.vis-NIR spectrum of* $\mathbf{H_2 1}$ *($[(Ru(bpy)_2)_2(H_2(metr)_2pz]^{4+}$) upon successive additions of cerium(IV).*

In agreement with similar systems (*vide supra*) for $[(Ru(bpy)_2)_2(H_2(metr)_2pz]^{4+}$ only a very weak band is observed at ~ 850 nm. Oxidation above the second oxidation wave results in a depletion of the 850 nm band. For **1**, **2** and $\mathbf{H_2 2}$ no clear evidence for an IT band was obtained by either spectroelectrochemistry of chemical oxidation. The absorption edge below 400 nm has been assigned to the added cerium(IV) reagent. This assignment is based on its absence when electrochemical oxidation employed.

8.3 Discussion

8.3.1 General synthetic considerations and structural characterisation

Although preparation of the homo-binuclear complexes has been carried out, preparation of the mononuclear and hetero-binuclear complexes was not achieved due to the insolubility of the ligand, which aids formation of binuclear complexes over mononuclear

complexes. Identification of the molecular ion for all three complexes was achieved by mass spectral analysis.

The coordination mode of the 1,2,4-triazole in the binuclear complexes has not been considered yet. Although mass spectrometry identifies the molecular ion, the identification of the coordination mode of the complexes, *i.e.* N2/N2, N2/N4 and N4/N4 isomers, is not possible. For the mononuclear complex based on the ligand Hmepztr the N2 bound isomer is found to form in greater than 90 % excess over the sterically less favourable N4 bound isomer.[16] Assuming that the same selectivity is observed for the ligand $H_2(metr)_2pz$, the *N2N2* bound isomer would be expected to form in about ~ 90%. As can be seen from the ^1H NMR spectrum of $[Ru(bpy)_2)_2((metr)_2pz)]^{2+}$ no detectable amounts of any other isomer is observed, indicating the complexes is isomerically pure.

In contrast with many 1,2,4-triazole based bridging ligands which form asymmetric binuclear complexes (*e.g.* bpt$^-$ and bpzt$^-$ dimers), binuclear complexes based on ligands such as bipyrimidine, bisbenzimidazole and $H_2(metr)_2pz$ are symmetric with respect to the coordination mode of the metal centres (*i.e.* both centres a bound via the N2 nitrogen of the 1,2,4-triazole ring and a pyrazine ring). This results in relatively simple ^1H NMR spectrum with only two instead of four geometric isomers (see chapter 6). Nevertheless the ΔΔ (or ΛΛ), and ΔΛ (or ΛΔ) diastereoisomers show significant differences in the interactions between the bpy ligands of the metal centres (see Figure 8.18). This lends a particular problem in characterisation by ^1H NMR spectroscopy. Instead of 17 aromatic proton resonances (8 from each of the bpy rings and 1 from the pyrazine ring) and 1 methyl resonance a total of 34 aromatic resonances and 2 methyl resonances are expected to be observed. This is found to be the case for both **1** (see Figure 8.4) and **2**.

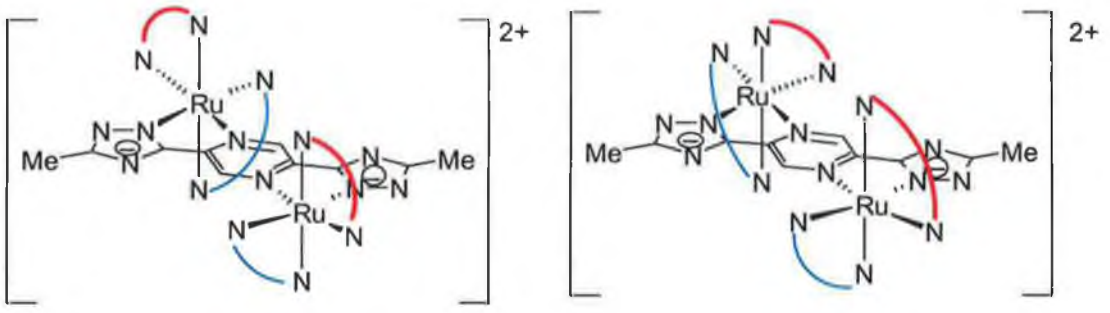

Figure 8.18 *Figure showing the two stereoisomers of* $[(Ru(bpy)_2)_2((metr)_2pz)]^{2+}$.

8.3.2 Electronic properties and acid base behaviour

The absorption spectrum of **1** shows bands at 467 and 530 nm (see Figure 8.6) which are assigned to ^{1}MLCT transitions on the basis of comparison with other Ru(II) polypyridyl complexes.[17] By comparison with the absorption spectrum of similar mononuclear complexes (*e.g.* $[Ru(bpy)_2(mepztr)]^+$ and the di-protonated complex $[Ru(bpy)_2(H_2mepztr)]^{3+}$) the low energy band at 530 nm may be assigned as being a pyrazine$^+$ based ^{1}MLCT transition, whilst the higher energy bands at around 467 nm can be assigned as bpy based ^{1}MLCT transitions.[9,18] For $\mathbf{H_21}$ a red shift in the 530 nm band to 565 nm and a blue shift of the 467 nm band to 424 nm is observed. The blue shift of the 467 nm band upon protonation of the triazole ring is not unexpected and is typical of 1,2,4-triazole based complexes.[18] The red shift of the 530 nm band (assigned as pyrazine$^+$ based ^{1}MLCT) is most likely due to the stabilization of the pyrazine LUMO and is in agreement with the acid-base behaviour reported by Sarkar *et al.* for a tetrazine based binuclear complex.[14]

The emission spectrum of **1** and $\mathbf{H_21}$ are at similar energies to those reported for $[Ru(bpy)_2(\mu\text{-}1Mepztr)Ru(bpy)_2Cl]^{3+}$ (730 nm at 298 K). The red shift observed upon protonation is in agreement with the stabilization of the pyrazine based LUMO, however assignment of the emitting state as pyrazine based is not so clear. A significant isotope effect on the emission lifetimes for **1** and $\mathbf{H_21}$ (at 298 K and 77 K) is observed upon deuteriation of the bpy ligands (see Table 8.1). The implications of this increase are unclear and require investigation by resonance Raman and excited state resonance Raman before a definitive assignment may be made as to the localization of the emitting excited state. In this regard deuteriation presents a powerful tool in the identification of vibrational bands (see Chapter 4). A second point of note is that the excited state pK_a is lower than the ground state pK_a. This indicates that the excited state is located on the bpy ligands (as this would reduce electron density on the bridging ligand and hence the basicity of the ligand).

8.3.5 Photochemistry

The most striking and indeed interesting property of the binuclear ruthenium complex described in this chapter is its photochemical reactivity. It is expected for ruthenium 1,2,4-triazole based complexes that photochemistry is much less and even completely absent for the deprotonated complexes relative to the protonated complexes (see Chapter 1). The increase in photoreactivity of mononuclear 1,2,4-triazole based complexes upon

protonation has been attributed to the lowering in energy of the gap between the lowest ^{3}MLCT state and the ^{3}MC. For **1**, the reverse situation is observed, with protonation serving to increase the stability of the complex. An explanation for this behaviour becomes apparent by examination of the effect of protonation of the UV.vis absorption spectrum of **1** (*vide supra*). In agreement with mononuclear complexes the bpy-based ^{1}MLCT absorption bands undergo a blue shift upon protonation, however the pyrazine$^+$ based MLCT bands undergo a red shift (this is also apparent from the emission spectra). This results in a net increase in the energy gap between the lowest ^{3}MLCT excited state and the ^{3}MC excited state (which is itself lowered in energy upon protonation) (see Figure 8.19).

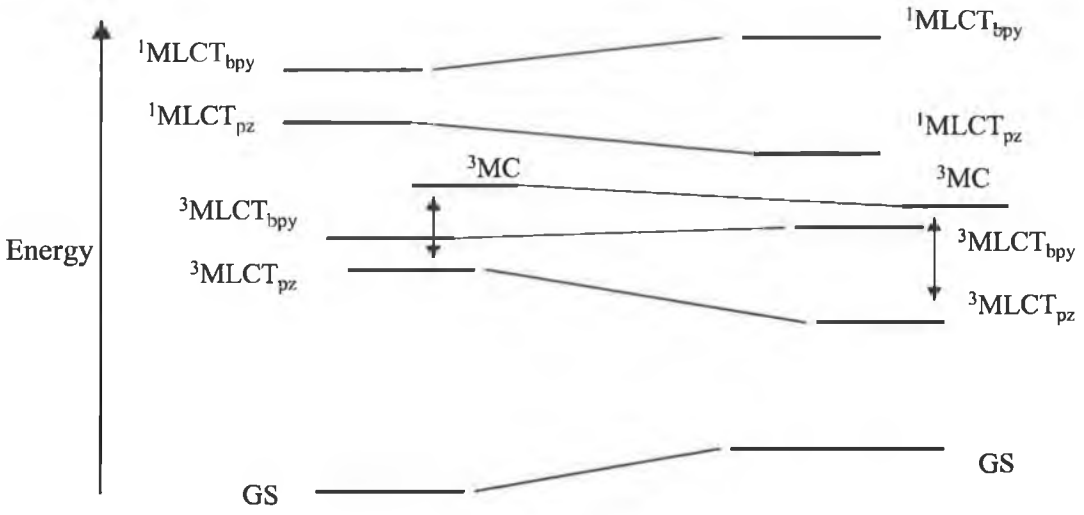

Figure 8.19 *Jablonski diagram showing relative position of electronic states for 1 (left) and* H_2*1 (right)*

The identity of the photoproducts is likely to be $[Ru(bpy)_2((metr)_2pz)]^+$ and $[Ru(bpy)_2(CH_3CN)_2]^{2+}$ (or $[Ru(bpy)_2(Et_3N)_2]^{2+}$). Although it is possible complete decomposition occurs, this can be ruled out by the presence of an emission at 680 nm, which is characteristic of a mononuclear 1,2,4-triazole based complex.[18] Preparative photochemistry followed by chromatographic separation of the photoproducts is required to confirm this. It is notable that if the mononuclear complex is formed then it would be expected to be quite stable and this could allow for the preparation of heteroleptic complexes by further reaction of the isolated mononuclear complex.

8.3.6 Redox properties and Spectroelectrochemistry

The electrochemical properties of both **1/H$_2$1** and **2/H$_2$2** are generally as would be expected for pyrazine bridged binuclear complexes (*vide supra*). In each case two well-defined metal oxidation waves were observed with a separation of ~ 150 and ~250 mV respectively. The increased separation observed for **2/H$_2$2** may be rationalized on the basis of the greater direct overlap of metal orbitals compared with their ruthenium analogues. For $[Ru(bpy)_2(\mu\text{-}1Mepztr)Ru(bpy)_2Cl]^{3+}$ two redox waves at 0.92 and 1.41 V were observed.[15] That such a large separation between the first and second oxidation process was observed, was accounted for partially by the inherent asymmetry in the system with the RuN_5Cl moiety being more easily oxidised than the electron poor RuN_6 moiety. The asymmetry does not account for all of the difference observed as significant interaction between the metal centres results in a 100 mV increase in the oxidation potential of the RuN_6 moiety relative to the mononuclear analogue $[Ru(bpy)_2(1Mepztr)]^{2+}$ (1.32 V). On this basis the separation between the 1st and 2nd redox processes of both **1/H$_2$1** and **2/H$_2$2** indicates that the interaction is larger than for the asymmetric system.

Similarly the reduction process observed for one can be interpreted on the basis of comparison with similar systems. The first reduction wave observed at –1.18 V is reversible and is assigned as a pyrazine$^+$ based reduction process by comparison with similar systems and by its absence in the mononuclear complex $[Ru(bpy)_2(5\text{-}Mepztr)]^+$.[18] Subsequent reduction processes are assigned as bpy based reductions.[19]

The most striking aspect of the electrochemical properties of both **1** and **2** is that the effect of protonation on ΔE is minimal; indicating the change in the degree of interaction is quite small. This is in stark contrast to 1,2,4-triazole[18] and benzimidazole[20] bridged systems which show marked changes of the degree of interaction upon protonation. Since protonation shows a strong effect on the π-donor properties of the metal centres (as evidenced by the large change in metal oxidation potentials) then it is unlikely that the energy of the pyrazine HOMO/LUMO orbitals will be unaffected. This suggests that the mechanism for interaction between the metal centres may not be predominantly via a ligand mediated hole transfer superexchange mechanism, but by rather by direct interaction between the metal centres or through an electron transfer superexchange mechanism mediated by the ligands unoccupied molecular orbitals. It is also likely that

the large value of ΔE may be due in large part to electrostatic interactions rather than delocalisation.

As has been demonstrated in Chapter 7, spectroelectrochemistry and the study of IT transitions is an invaluable tool in determining the extent of electronic delocalisation between metal centres. Unfortunately a characteristic of pyrazine bridged binuclear Ru(II) and Os(II) complexes is that when IT bands are observed they are at quite high energy and their observation is subject to significant interference from other bands (in particular LMCT and LMCT bands). On the basis of the high oxidation potentials of the metal centres relative to the *CT* ion, it is likely the barrier to electron transfer in the mixed valence state will be considerable. Hence the oscillator strength of the intervalence transition would be expected to be low and the energy of the band much higher. This is also the case for both **1** and **2** and their protonated analogues. The observation of a weak band at 850 nm for $\mathbf{H_2 1}$ is consistent with the expected energy of an IT band for this class of compounds however the exact nature of the species responsible for the band is not clear since the fully oxidized species is quite unstable.

8.4 Conclusions and outlook

The pyrazine bridged binuclear systems described in this chapter represent a significant change in the direction of recent research into multinuclear systems incorporating 1,2,4-triazole moieties. It is the first example of a multinuclear 1,2,4-triazole based system in which the triazole moieties are not positioned directly between the metal centres. As for other pyrazine bridged systems the degree of metal-metal interaction is quite large. Interestingly deprotonation/protonation of the 1,2,4-triazole moieties has only a minor influence on the degree of internuclear interaction.

In contrast to its effect on spectroelectrochemical properties, the effect of the 1,2,4-triazole on the complexes (**1** and **2**) spectroscopic and photochemical properties are very significant. The photochemical properties of **1** are also quite interesting and show a reversal of expected behaviour in that protonation renders the complex photostable whilst for all other 1,2,4-triazole systems examined protonation increases their photoreactivity. The photophysical properties of these systems are also perplexing. Given that the lowest excited ^{1}MLCT states for **1** and $\mathbf{H_2 1}$ then it would be expected that the lowest ^{3}MLCT excited states are also pyrazine based. The effect of deuteriation contradicts this assumption suggesting that the lowest excited state is bpy based! In order to confirm the

location of the lowest excited emissive state the excited state resonance Raman spectroscopic studies are necessary. In such a study deuteriation should prove invaluable in definitively assigning bands (see chapter 4).

The results presented here indicate that further investigation of these systems is warranted. In particular the preparation of asymmetric systems both in terms of the metals employed and also in the substituents present on the 1,2,4-triazole moiety (*e.g.* replacement of the methyl groups). It would be expected that the combination of a phenyl moiety and a bromide moiety would result in a sufficient separation of the 1st and 2nd protonation steps to allow for the investigation of the properties of the monoprotonated complex.

8.5 Experimental

The synthesis of $H_2(Metr)_2Pz$ is described in Chapter 2.

$[Ru(bpy)_2)_2(Metr)_2Pz](PF_6)_2.3H_2O$ 350 mg (0.67 mmol) of *cis*-$[Ru(bpy)_2Cl_2]$ was heated at reflux with 50 mg (0.21 mmol) of $H_2(metr)_2pz$ ligand in ethanol/water for 24 h. The cooled reaction mixture was reduced *in vacuo,* diluted with water and filtered to remove unreacted material. A few drops of conc. ammonia solution and then conc. aqueous ammonium hexafluorophosphate was added to the purple solution and the precipitate filtered, washed with diethyl ether and allowed to air-dry. The complex was purified by column chromatography on neutral alumina using acetonitrile as eluent. Yield 120 mg (0.089 mmol, 24 %) ^{1}H NMR spectroscopy (in CD_3CN): 8.52 (m, 3H), 8.44 (m, 5H), 8.175 (d, 1H), 8.12 (m, 4H), 8.05 (d, 1H), 7.99 (m, 6H), 7.89 (d, 1H), 7.75 (d, 1H), 7.68 (d, 1H), 7.64 (m, 2H), 7.51 (m, 5H), 7.35 (m, 3H), 7.175 (dd, 1H), 2.18 (s, methyl, 3H), 2.175 (s, methyl, 3H). Mass spec. Mol^{2+} (calc for $C_{50}H_{40}N_{16}Ru_2$: 534) found: 534 m/z. Elemental Analysis (calc. for $C_{50}H_{40}N_{16}RuP_2F_{12}.3H_20$) C: 42.64 % (42.55%), H: 2.75 % (3.05 %), N 15.64 % (15.89 %).

$[Ru(d_8\text{-}bpy)_2)_2(Metr)_2Pz](PF_6)_2$. As for $[Ru(bpy)_2)_2(Metr)_2Pz](PF_6)_2$ except 200 mg (0.37 mmol) of *cis*-$[Ru(d_8\text{-}bpy)_2Cl_2]$ and 30 mg (0.124 mmol) of $H_2(metr)_2pz$ was used. Yield 41 mg (0.027 mmol, 22 %) ^{1}H NMR spectroscopy (in CD_3CN); 7.98 (s, 1H), 7.92 (s, 1H), 2.18 (s, methyl, 3H), 2.175 (s, methyl, 3H). Mass spec. Mol^{2+} (calc for $C_{50}D_{32}H_8N_{16}Ru_2$: 550) found: 548.6 m/z. (deviation due to incomplete H/D exchange assuming 85 % deuteriation of bpy ligands then peak at 548 expected) Elemental Analysis not available.

$[Os(bpy)_2)_2(Metr)_2Pz](PF_6)_2.2H_2O.4KPF_6$ As for $[Ru(bpy)_2)_2(Metr)_2Pz](PF_6)_2$ except 300 mg (0.49 mmol) of *cis*-$[Os(bpy)_2Cl_2]$ and 35 mg (0.145 mmol) of $H_2(metr)_2pz$ was used. Yield 60 mg (0.039mmol, 27 %) ^1H NMR spectroscopy (in CD_3CN); 8.58 (m, 10H), 8.18 (d, 1H), 8.01(m, 12H), 7.74 (m, 4H), 7.56 (m, 5H), 7.42 (m, 3H), 7.21 (dd, 1H), 2.165 (s, methyl, 3H), 2.16 (s, methyl, 3H). Mass spec. Mol^{2+} (calc for $C_{50}H_{40}N_{16}Os_2$: 623) found: 623 m/z. Elemental Analysis (calc. for $C_{50}H_{40}N_{16}OsP_2F_{12}.2H_2O.4KPF_6$) C: 25.5 % (26.01 %), H: 1.77 % (1.82 %), N 7.41 % (9.71 %). Elemental analysis was affected due to excess PF_6^- salts present.

8.6 Bibliography

1. (a) H. Dürr and S. Bossmann, *Acc. Chem. Res.*, **2001**, *34*, 905 (b) T. J. Meyer, *Acc. Chem. Res.*, **1989**, *22*, 163. (c) B. O'Regan and M. Graetzel, *Nature*, **1991**, *335*, 737 (d) L. De Cola and P. Belser, *Coord. Chem. Rev.* **1998**, *177*, 301 (e) C. A. Bignozzi, J. R. Schoonover and F. Scandola, *Progr. Inorg. Chem.* **1997**, *44*, 1 (f) M-J. Blanco, M. C. Jiménez, J-C. Chambron, V. Heitz, M. Linke and J.-P. Sauvage, *Chem. Soc. Rev.* **1999**, *28*, 293 (g) L. Sun, L. Hammarström, B. Åkermark and S. Styring, *Chem. Soc. Rev.*, **2001**, *30*, 36 (h) A. Magnunson, Y. Frapart, M. Abrahamsson, O. Horner, B. Åkermark, L. Sun, J-J Girerd, L. Hammarström, and S. Styring, *J. Am. Chem. Soc.*, **1999**, *121*, 89

2. C. Creutz and H. Taube, *J. Am. Chem. Soc.*, **1969**, *91*, 3988

3. (a) R. W. Callahan, G. M. Brown and T. J. Meyer, *J. Am. Chem. Soc.*, **1974**, *96*, 7829 (b) R. W. Callahan, G. M. Brown and T. J. Meyer, *Inorg. Chem.*, **1975**, *14*, 1443

4. G. M. Tom, C. Creutz and H. Taube, *J. Am. Chem. Soc.*, **1974**, *96*, 7827

5. (a) J. T. Hupp, *J. Am. Chem. Soc.*, **1990**, *112*, 1563 (b) S. B. Piepho, *J. Am. Chem. Soc.*, **1990**, *112*, 4197 (c) V. Petrov, J. T. Hupp, C. Mottley and L. C. Mann, *J. Am. Chem. Soc.*, **1994**, *116*, 2171

6. (a) R. W. Callahan, F. R. Keene, T. J. Meyer and D. J. Salmon, *J. Am. Chem. Soc.*, **1977**, *99*, 1064 (b) M. J. Powers and T. J. Meyer, *J. Am. Chem. Soc.*, **1980**, *102*, 1979 (c) K. D. Demadis, G. A. Neyhart, E. M. Kober, P. S. White and T. J. Meyer, *J. Am. Chem. Soc.*, **1999**, *38*, 5948

7. S. A. Adeyemi, J. N. Braddock, G. M. Brown, J. A. Ferguson and T. J. Meyer, *J. Am. Chem. Soc.*, **1972**, *94*, 300

8. M. J. Powers and T. J. Meyers, *Inorg. Chem.*, **1978**, *17*, 2955

9. (a) K. A. Goldsby and T. J. Meyer, *Inorg. Chem.*, **1984**, *23*, 3002 (b) D. Sedney and A. Ludi, *Inorg. Chim. Acta*, **1981**, *47*, 153

10. H. E. Toma, P. R. Auburn, E. S. Dodsworth, M. N. Golovin and A. B. P. Lever, *Inorg. Chem.* **1987**, *26*, 4257

11. R. A. Pavinato, J. A. Walk and M. E. McGuire, *Inorg. Chem.*, **1993**, *32*, 4982

12. (a) C. H. Braunstein, A. D. Baker, T. C. Strekas and H. D. Gafney, *Inorg. Chem.*, **1984**, *23*, 857 (b) M. Milkevitch, E. Brauns and K. J. Brewer, *Inorg. Chem.*, **1996**, *35*, 1737 (c) S. Campagna, S. Serroni, S. Bodige and F. M. MacDonell, *Inorg. Chem.*, **1999**, *38*, 692 (d) M. M. Richter, G. E. Jensen, K. J. Brewer, *Inorg. Chim. Acta*, **1995**, *230*, 35 (e) J. Sherborne, S .M. Scott and K. C. Gordon, *Inorg. Chim. Acta*, **1997**, *260*, 199

13. (a) B. D. Yeomans, L. S. Kelso, P. A. Tregloan, and F. R. Keene, *Eur. J. Inorg. Chem.*, **2001**, 239 (b) D. M. D'Alessandro, L. S. Kelso and F. R. Keene, *Inorg. Chem.*, **2001**, *40, 6841*

14. B. Sarkar, R. H. Laye, B. Mondal, S. Chakraborty, R. L. Paul, J. C. Jeffrey, V. C. Puranik, M. D. Ward and G. K. Lahiri, *J. Chem. Soc., Dalton Trans.*, **2002**, 2097

15. R. Hage, H. E. B. Lempers, J. G. Haasnoot, J. Reedijk, F. Weldon and J. G. Vos, *Inorg. Chem.*, **1997**, *36*, 3139

16. R. J. Foster, A. Boyle, J. G. Vos, R. Hage, A. H. J. Dujkhuis, R. A. G. Graaf, J. G. Haasnoot and J. Reedijk, *J. Chem. Soc., Dalton Trans.*, **1990**, 21

17. A. Juris, V. Balzani, F. Barigelletti, S. Campagna, P. Belser and A. von Zelewsky *Coord. Chem. Rev.* **1988**, *84*, 85

18. R. Hage, *Ph.D. Thesis*, Leiden University, The Netherlands, **1991**

19. B. K. Ghosh, A. Chakravorty, *Coord. Chem. Revs.*, **1989**, *95*, 239

20. (a) M. Haga, T. Ano, K. Kano and S. Yamabe, *Inorg. Chem.*, **1991**, *30*, 3843 (b) M. Haga, Md. M. Ali, S. Koseki, K. Fujimoto, A. Yoshimura, K. Nozaki, T. Ohno, K. Nakajima and D. J. Stufkens, *Inorg. Chem.*, **1996**, *35*, 3335 (c) M. Haga, Md. M. Ali and R. Arakawa, *Angew. Chem. Int. Ed. Engl.*, **1996**, *35*, 77

Chapter 9

Concluding remarks and future work

"Sometimes if all you've got are old words,

the best you can do is put them together,

and hope something new comes out."

9.1 Concluding remarks

The studies described in this thesis cover a diverse range of topics. These include; the development of methods for the selective deuteriation of organic aromatic and heteroaromatic compounds; the application of deuteriation in probing both spectroscopic characterisation and in probing excited state electronic structure; the use of temperature and time resolved spectroscopy in elucidating the ISC and IC processes of polypyridine complexes; the investigation of the importance of stereochemistry in both mono- and bi-nuclear ruthenium complexes; and finally the use of electrochemistry and spectroelectrochemistry to investigate intramolecular interactions in binuclear complexes. The common thread within these studies however is in improving understanding of the fundamental processes that occur in Ru(II) and, to a lesser extent, Os(II) polypyridine complexes.

In Chapter 1, a brief review of Group VIII polypyridine photophysics and photochemistry is presented. A complete review of this area is impractical due to the considerable length such an undertaking would amount to (as evidenced by the many reviews cited throughout this thesis). In contrast the application of deuteriation to inorganic photophysics is a much less developed area and as a result a more detailed and comprehensive review of this area has been attempted. In chapter 2, a summary of the physical techniques and standard synthetic procedures is presented. Where possible a brief discussion of the basis of the techniques employed and of problems encountered is included.

In Chapter 3, a methodology for the regioselective (on a preparative scale) deuteriation is presented. The methods developed build on earlier procedures developed by Vos and coworkers.[1] The use of the deuteriated materials, not only as ligands, but also as reagents for further synthesis is demonstrated in the preparation of $[D_6]$-dcb from $[D_{12}]$-dmb in good yields (Chapter 2). The ability to prepare deuteriated material containing thermally unstable functional groups such as carboxylic acids, in useful amounts, expands further the potential range of these techniques.

The preparation of isotopically substituted material (often with regioselectively) allows for a much wider application of deuteriation in Ru(II) and Os(II) polypyridine photophysics. It is this area, which is considered in Chapter 4, where the effect of partial deuteriation of both homo- and hetero-leptic complexes on the luminescence decay and ground and excited state resonance Raman is examined. The effect of deuteriation of inorganic complexes on non-radiative deactivation processes has been found to mirror that found for organic systems. However, whereas X-H vibrational modes can dominate the overall rate of non-radiative deactivation (k_{nr}) in organic systems, for inorganic complexes other vibrational modes such as skeletal vibrations and solvent modes can dominate. Despite this, the application of deuteriation as a probe of the nature of electronically excited states has been demonstrated and shows considerable potential. The most striking features of the study are the difference in deuteriation effect for Ru(II) and Os(II) polypyridyl complexes. As discussed in the introduction the effect of deuteriation depends on the importance of $k_{C\text{-}H}$ to the overall non-radiative rate constant (k_{nr}). For Ru(II) complexes thermally activated population of the ^{3}MC excited state is an important deactivation pathway, whilst for Os(II) complexes the same process is relatively insignificant and vibrationally coupled deactivation is more important.

The effectiveness of deuteriation in determining the location of the ^{3}MLCT emissive excited state is on initial inspection, quite poor. However, considering that in many heteroleptic complexes all ligands to a greater or lesser extent contribute to the lowest excited state then deuteriation should provide "inconclusive" results. For heteroleptic complexes, in which large differences in the LUMO energies of the ligands are present, then the effect of deuteriation would be expected to be specific to the ligands deuteriated. This is observed for the mixed ligand complexes, containing the ligands bpy/dcb^{2-}, bpy/phpztr$^-$ *etc.*

In Chapter 5, two areas of ruthenium photophysics are examined. The first is that of temperature dependent dual emission in pyrazine-triazole based Ru(II) polypyridine complexes. The observation of dual emission in a range of structurally similar complexes and the observation of dual emission for the protonated complex has confirmed the observations made by Keyes *et al.*.[1c] Due to the large temperature dependence of both emissions (in terms of emission λ_{max}), the assignment of each emission as being charge transfer is justified. It is also apparent that the emissions originate from ^{3}MLCT states localised on pyrazine and bpy

moieties, with the large dipole change associated with IC between these states resulting in a large barrier to that process. The second area examined is of more general interest than the first, and involves the probing of the early processes which occur upon excitation in Fe(II) and Ru(II) polypyridine complexes. The observation of luminescence from an Fe(II) complex was unexpected and in itself challenges the general perception that Fe(II) complexes are non-emissive. Similarly the observation by time resolved emission spectroscopy of emission at high energy from $[Ru(bpy)_3]^{2+}$ confirms earlier steady state observations. The effect of deuteriation on this emission provides compelling evidence that this emission is not due to slow vibrational cooling but rather from a higher lying excited state. The orbital parentage of the emitting state is as yet unknown, however it is probable it is ^{1}MLCT in character owing to the small Stoke's shift between it and the ^{1}MLCT absorption bands.

The photophysical properties of stereoisomers of mono- and bi-nuclear Ru(II) complexes are the subject examined in Chapter 6. Stereochemistry, in particular in relation to multinuclear and supramolecular photophysics, is a relatively new area. No differences in the spectroscopic properties of the either the mononuclear or binuclear complexes were observed in both achiral and chiral solvents. In all cases the excited states of the complexes are located on the peripheral bpy ligands, hence that no differences are observed does not presuppose that no differences would be expected for binuclear complexes in which the excited state is localised on the bridging ligand. In order to investigate this, separation and examination of the stereoisomers of the complex $[Ru(bpy)_2)_2(bpzt)]^{3+}$ may be worthwhile. In this complex the excited state has been determined to be localised on the bridging bpzt$^-$ ligand (see Chapter 1).

In Chapters 7 and 8, attention is turned to binuclear Ru(II) and Os(II) systems. The complexes examined in each chapter differ fundamentally in the mode of bridging between the metal centres. In Chapter 7, the metal centres are bridged by a thienyl- group and two 1,2,4-triazole groups. The interaction between the two centres was expected to be weak by comparison with similar complexes where the thienyl- group is replaced by a phenyl- or dimethoxyphenyl- group. In contrast the degree of electronic delocalisation and the electronic coupling is found to be very large despite the relatively small electrostatic interaction between the metal centres (as evidenced by the small difference (ΔE) in the 1st and 2nd

oxidation process). In Chapter 8, the metal centres are bridged by a pyrazine moiety rather than 1,2,4-triazole groups. The electrostatic interaction in these systems is large however the high energy and low molar absorptivity of the IT bands (only observed for **H1**) indicates that the barrier to electron transfer is quite large. The effect of protonation in these latter systems, in contrast to the triazole bridged systems, is to alter the spectroscopic properties dramatically, however the effect of protonation on ground state interaction strength is quite minimal. These studies demonstrate the versatility of 1,2,4-triazole based systems in not only mediating internuclear interaction but also in perturbing the excited state properties.

9.2 Further work

The main areas of future work recommended are as follows.

Chapter 3. One area neglected in this thesis is in the photophysical properties of the ligands employed (and their isotopologues) and there Zn(II) salts. In future studies the investigation of their photophysical properties, in particular the effect of deuteriation on their phosphorescence lifetimes should be examined, given that for bpy deuteriation results in a doubling of its phosphorescence lifetime.

Chapter 4. The use deuteriation in photophysical studies of Ru(II) complexes forms the bulk of the studies reported in Chapter 4. The investigation of the deuteriation effect of the Os(II) complexes shows that in comparison to the ruthenium complexes, deuteriation can result in a doubling of emission lifetime. In future studies the use of deuteriation in studying the photophysical properties of the Os(II) analogues of the 1,2,4-triazole based Ru(II) complexes may be of value, considering that the shorter luminescence lifetimes make other techniques less amenable (*e.g.* excited state resonance Raman and transient absorption spectroscopy).

Chapter 5. The determination of Arhenius parameters for the complexes examined in chapter 5 in particular for their partially deuteriated analogues should be carried out. In addition the measurement of the lifetimes of the short lived (sub-nanosecond) emissions observed for $[Fe(bpy)_3]^{2+}$ and $[Ru(bpy)_3]^{2+}$ by time correlated single photon counting techniques would be of particular benefit in understanding these systems.

Chapter 6. The stereoisomers of mono- and bi-nuclear complexes are examined in Chapter 6 with respect to their UV.Vis absorption and luminescence properties. Future studies on these complexes recommended are in the determination of the effect of stereochemistry (*e.g.* in their CD spectra) on the LMCT transitions of the mononuclear complexes and the LMCT and IT transitions of the binuclear complex. Additionally, rR and excited state rR spectra of the complexes may prove to be more sensitive to the steric effects.

Chapter 7. The thienyl- bridged binuclear complexes examined Chapter 7 show Type II interaction between the metal centres. The solvatochromic behaviour of the IT band for these complexes should be investigated in order to confirm the interaction classification (*i.e.* as type II). Future work in this area recommended is in the preparation metal complexes and in introducing asymmetry into the bridging ligand by variation of the terminal pyridine/pyrazine moiety.

Chapter 8. The most immediate progression of the study reported in Chapter 8 is in the preparation of the mononuclear complex photochemically, followed by reaction with *cis*-$[Os(bpy)_2Cl_2]$ to prepare the mixed metal binuclear complex. The properties of the monoprotonated complex (H1) were not investigated due to the small difference between the first and second protonation step. By variation substitution of the methyl groups on the triazole rings with an electron-withdrawing group (*e.g.* Br-) and an electron-donating group (*e.g.* phenyl-) should create sufficient perturbation to increase the pH difference between the 1^{st} (pka_1) and 2^{nd} (pk_{a2}) protonation steps of the complex. This would allow for examination of the monoprotonated complex.

9.3 Bibliography

1. (a) T. E. Keyes, F. Weldon, E. Müller, P. Pechy, M. Grätzel and J. G. Vos, *J. Chem. Soc. Dalton Trans.*, **1995**, 2705 (b) S. Fanni, T. Keyes, C. M. O'Connor, H. Hughes, R. Y. Wang and J. G. Vos, *Coord. Chem. Rev.*, **2000**, *208*, 77 (c) T. E. Keyes, C. M. O'Connor, U. O'Dwyer, C. G. Coates, P. Callaghan, J. J. McGarvey and J. G. Vos, *J. Phys. Chem. A*, **1999**, *103*, 8915

Appendix A1

Publications

"*Ruthenium(II) and Osmium(II) Polypyridyl Complexes of asymmetric pyrazinyl- and pyridinyl-1,2,4-triazole based ligands. Connectivity and physical properties of mononuclear complexes*"
Wesley R. Browne, Christine M. O'Connor, Helen P. Hughes, Ronald Hage, Olaf Walter, Manfred Doering, John F. Gallagher and Johannes G. Vos, *J. Chem. Soc., Dalton Trans.*, **2002,** accepted Sept.

"*Routes to regioselective deuteriation of heteroaromatic compounds*"
Wesley R. Browne, Christine M. O'Connor, J. Scott Killeen, Adrian L. Guckian, Micheal Burke, Paraic James, Maurice Burke and Johannes G. Vos, *Inorg. Chem.*, **2002**, 41, 4245

"Proton Controlled Intramolecular Communication in Dinuclear Ruthenium(II) Polypyridine Complexes"
Cinzia Di Pietro, Scolastica Serroni, Sebastiano Campagna, Maria Teresa Gandolfi, Roberto Ballardini, Stefano Fanni, Wesley Browne, Johannes G. Vos, *Inorg. Chem.*, **2002,** *41*, 2871

"*Synthesis, spectroscopic and electrochemical properties of mononuclear and dinuclear bis(bipy)ruthenium(II) complexes containing dimethoxyphenyl-(pyridin-2-yl)-1,2,4-triazole ligands"*
Paolo Passaniti, Wesley R. Browne, Fiona C. Lynch, Donal Hughes, Mark Nieuwenhuyzen, Paraic James, Mauro Maestri, Johannes G. Vos, *J. Chem. Soc., Dalton Trans.*, **2002,** 1740

"*The separation and photophysical properties of the ΛΛ, ΔΔ, ΛΔ and ΔΛ stereoisomers of a dinuclear ruthenium(II) complex*"
Wesley R. Browne, Christine O'Connor, Claudio Villani, Johannes G. Vos, *Inorg. Chem.*, **2001,** *40*, 5461

"The Effect of Deuteriation on the Emission Lifetime of Inorganic Compounds"
Wesley R. Browne, Johannes G. Vos, *Coord. Chem. Rev.*, **2001**, *761*, 787.

"*Photochemically Induced Isomerisation in Ruthenium Polypyridyl Complexes"*
Stefano Fanni, Francis Weldon, Leif Hammarstrom, Emad Muktar, Wesley R. Browne, Tia E. Keyes and Johannes G. Vos, *Euro. J. Inorg. Chem.*, **2001,** 529.

Presentations

"*Proton Controlled Intramolecular Communication in binuclear Ruthenium(II) Polypyridine Complexes*"
Wesley R. Browne, Johannes G. Vos, Poster presentation, 54th Irish Universities Chemistry Colloquium, The Queen's Univeristy, Belfast, April **2002**

"Structural and photophysical characterisation of deuteriated ruthenium(II) polypyridyl complexes."
Oral presentation, 53rd Irish Universities Chemistry Colloquium, University College Dublin, June **2001**.

"Regioselective deuteriation of asymmetric diimine ligands: probing electronic excited state structure"
Poster Presentation: International Symposium on the Photophysics and Photochemistry of Coordination Compounds, Vesprem, Hungary, July **2001**

"Studying Metal-Metal Interactions: Techniques and applications"
Wesley R. Browne, Oral Presentation, Chemistry Research Seminar Series, Dublin City University, November **2001**

"*The application of spectro-electrochemistry in the study of binuclear Ruthenium (II) dimine complexes containing triazole based bridging ligands.*"
Wesley R. Browne, Johannes G. Vos, Poster Presentation, Electrochem. 2000, Dublin City University Sept. **2000**.

Ruthenium(II) and Osmium(II) Polypyridyl Complexes of asymmetric pyrazinyl- and pyridinyl-1,2,4-triazole based ligands. Connectivity and physical properties of mononuclear complexes.

Wesley R. Browne,[a] Christine M. O'Connor,[a,b] Helen P. Hughes,[a,c] Ronald Hage,[d] Olaf Walter,[e] Manfred Doering,[e] John F. Gallagher,[f] and Johannes G. Vos[a]*

[a] *National Centre for Sensor Research, School of Chemical Sciences, Dublin City University, Dublin 9, Ireland. E-mail: johannes.vos@dcu.ie*
[b] *Present Address; Department of Chemistry, Dublin Institute of Technology, Dublin 2, Ireland*
[c] *Present Address; Department of Chemistry, Waterford Institute of Technology, Waterford, Ireland*
[d] *Unilever Research Laboratory, Olivier van Noortlaan 120, 3133 AT, Vlaardingen, The Netherlands*
[e] *ITC-CPV, Forshungszentrum Karlsruhe, PO Box 3640, 76021 Karlsruhe, Germany*
[f] *National Institute for Cellular Biotechnology, School of Chemical Sciences, Dublin City University, Dublin 9, Ireland.*

Keywords: Ruthenium / Osmium / Deuteriation / Coordination modes / acid base properties

Abstract

The synthesis, purification and characterisation of two coordination isomers of ruthenium(II) and osmium (II) complexes containing the ligand 3-(pyrazin-2'-yl)-5-(pyridin-2''-yl)-1,2,4-triazole (Hppt) are described. The x-ray and molecular structure of the complex $[Ru(bipy)_2(ppt)]PF_6.CH_3OH$ (**1a**) is reported, where the $Ru(bipy)_2$ centre is bound to the ppt^- ligand via the pyridine nitrogen and the N1 atom of the triazole ring. ^1H NMR spectroscopic measurements confirm that in the second isomer (**1b**) the $Ru(bipy)_2$-moiety is bound via the N2 atom of the triazole ring and the pyrazine ring. Partially deuteriated metal complexes are utilised to facilitate interpretation of ^1H NMR spectra. The redox and electronic properties indicate that there are significant differences in the electronic properties of the two coordination isomers obtained. The acid-base properties of the compounds are also reported and show that the pK_a of the 1,2,4-triazole ring varies systematically depending on the nature of the non-coordinating substituent. Analysis of these data indicates a significant electronic interaction between the pyridyl/pyrazyl rings and the 1,2,4-triazole ring in the coordinated ppt^- ligand.

Introduction

For many years, Ruthenium(II) and Osmium(II) polypyridyl complexes have attracted attention due to their well-defined spectroscopic, photophysical, photochemical, and electrochemical properties.[1] These properties are of particular use in the construction of supramolecular systems[2] and in the development of photochemically driven molecular devices.[3] Ruthenium(II) polypyridyl complexes have also received extensive attention as functional models for water-oxidation catalysis in photo-system II[4] and in the catalytic photochemical cleavage of water.[5] Of particular interest is their incorporation into the design of multinuclear structures capable of directing and modulating electron and energy transfer processes.[3] The ability to tune the excited state properties of these complexes is central to their potential for practical applications.

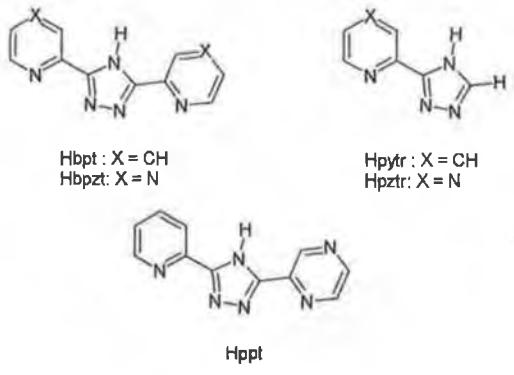

Figure 1 *Ligands described in text*

For these reasons there has been a detailed investigation of the synthesis and characterisation of multinuclear ruthenium(II) and osmium(II) polypyridyl complexes using negatively charged triazole based bridging ligands.[6,7] It was shown that with these ligands relatively strong interaction can be obtained between metal centres, so that both electron transfer and energy transfer processes can occur efficiently.[8] The immobilisation of such dinuclear complexes on nanocrystalline TiO_2 has also been reported.[9] In these studies the importance of the 1,2,4-triazole bridge in mediating electron transfer was demonstrated. By systematically changing the nature of the bridge, the effect on the nature of the lowest excited states of these multinuclear compounds and on metal-metal interaction has been examined in detail. It was found that by using ligands such as 3,5-bis(pyridin-2'-yl)-1,2,4-triazole (Hbpt, Figure 1) the lowest energy excited state is located on the polypyridyl ligands (i.e. bipy) whilst with the ligand 3,5-bis(pyrazin-2'-yl)-1,2,4-triazole (Hbpzt, Figure 1) the emitting state is located on the pyrazine bridging ligand.[6,7] This has important consequences for the photochemical properties of these compounds and indeed dinuclear bpt^- and $bpzt^-$ complexes show different products when photolysed under the same conditions.[10] In addition, resonance Raman evidence suggested that in the dinuclear $bpzt^-$ complexes the excited state is located on *one* of the pyrazine rings of the bridge.[11] These results show clearly that the photophysical properties of these dinuclear structures can be manipulated by a careful choice of the bridging ligand.

References

1. (a) V. Balzani, A. Juris, M. Venturi, S. Campagna and S. Serroni, *Acc. Chem. Res.*, 1998, **31**, 26; (b) C. A. Slate, D. R. Striplin, J. A. Moss, P. Chen, B. W. Erickson and T. J. Meyer, *J. Am. Chem. Soc.*, 1998, **120**, 4885; (c) Y.-Z. Hu, S. Tsukiji, S. Shinkai, S. Oishi and I. Hamachi, *J. Am. Chem. Soc.*, 2000, **122**, 241; (d) V. Balzani, A. Juris, M. Venturi, S. Campagna and S. Serroni, *Chem. Rev.*, 1996, **96**, 759.
2. (a) A. Juris, V. Balzani, F. Barigelletti, S. Campagna, P. Belser and A. von Zelewsky, *Coord. Chem. Rev.*, 1988, **84**, 85; (b) T. J. Meyer, *Acc. Chem. Res.* 1989, **22**, 163; (c) B. O'Regan and M. Graetzel, *Nature*, 1991, **335**, 737; (d) L. De Cola and P. Belser, *Coord. Chem. Rev.*, 1998, **177**, 301; (e) C. A. Bignozzi, J. R. Schoonover and F. Scandola, *Progr. Inorg. Chem.*, 1997, **44**, 1; (f) M.-J. Blanco, M. C. Jiménez, J.-C.Chambron, V. Heitz, M. Linke and J.-P. Sauvage, *Chem. Soc. Rev.*, 1999, **28**, 293.
3. (a) V.Balzani, F. Scandola, *Supramolecular Photochemistry*, Ellis Horwood, Chichester, UK, 1991; (b) V. Balzani, Ed., *Supramolecular Photochemistry*, Reidel, Dordrecht, 1997.
4. H. Dürr and S. Bossmann, *Acc. Chem. Res.*, 2001, **34**, 905.
5. P. R. Rich, *Faraday Discuss., Chem. Soc.*, 1982, **75**, 349.
6. (a) R. Hage, R. Prins, J. G. Haasnoot, J. Reedijk and J. G. Vos, *J. Chem. Soc., Dalton Trans.* 1987, 1389; (b) H. A. Nieuwenhuis, J. G. Haasnoot, R. Hage, J. Reedijk, T. L. Snoeck, D. J. Stufkens and J. G. Vos, *Inorg. Chem.*, 1990, **30**, 48; (c) B. E. Buchanan, R. Wang, J. G. Vos, R. Hage, J. G. Haasnoot and J. Reedijk, *Inorg. Chem.*, 1990, **29**, 3263; (d) W. R. Browne, C. M. O'Connor, C. Villani and J. G. Vos, *Inorg. Chem.*, 2001, **40**, 5461.
7. (a) R. Hage, A.H.J. Dijkhuis, J.G. Haasnoot, R. Prins, J. Reedijk, B.E. Buchanan and J. G. Vos, *Inorg. Chem.*, 1988, **27**, 2185; (b) F. Barigelletti, L. De. Cola, V. Balzani, R. Hage, J. G. Haasnoot, J. G. Vos, *Inorg. Chem.*, 1989, **28**, 4344.
8. R. Hage, J. G. Haasnoot, H. A. Nieuwenhuis, J. Reedijk, D. J. A. De Ridder and J. G. Vos, *J. Am. Chem. Soc.*, 1990, **112**, 9249.
9. A. C. Lees, C. J. Kleverlaan, C. A. Bignozzi and J.G. Vos, *Inorg. Chem.*, 2001, **40**, 5343.
10. H. P. Hughes and J. G. Vos, *Inorg. Chem.*, 1995, **34**, 4001.
11. C. G. Coates, T. E. Keyes, H. P. Hughes, P. M. Jayaweera, J. J. McGarvey and J. G. Vos., *J. Phys. Chem. A*, 1998, **102**, 5013

To further investigate these systems we have extended our study to include the ligand 3-(pyrazin-2'-yl)-5-(pyridin-2''-yl)-1,2,4-triazole (Hppt) (See Fig. 1). The synthesis of these dinuclear complexes presents a major synthetic challenge. The asymmetry of the ligand may result in the formation of up to 4 different mononuclear coordination isomers as shown in Fig. 2 and as expected the reaction of one equivalent of the bridging ligand with two equivalents of a $[M(bipy)_2]$ precursor leads to the formation of a mixture of different coordination isomers. Therefore in order to obtain well-defined dinuclear complexes an indirect route via the formation of mononuclear precursors has to be developed.

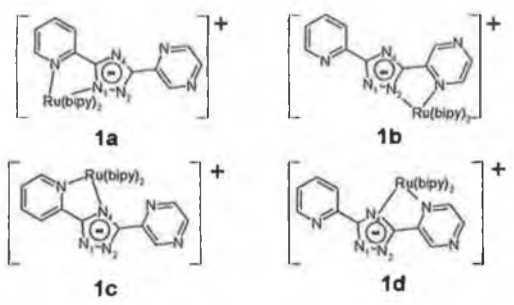

Figure 2 *Possible coordination isomers of* $[Ru(bipy)_2ppt]^+$.

In this contribution the synthesis, purification and characterisation of two mononuclear coordination isomers of $Ru(bipy)_2$ and $Os(bipy)_2$ complexes with Hppt are reported. The compounds obtained have been separated using chromatographic techniques and were characterised using ^1H NMR, electronic spectroscopy and electrochemistry. The X-ray crystal structure of one of the coordination isomers is reported. The acid-base properties of the coordination isomers are also investigated and are discussed, together with data obtained for related complexes. In particular the effect of substitution in the C5 position of the 1,2,4-triazole on the acid base properties is rationalised on the basis of the electron withdrawing/donating properties of the substituent.

Results and Discussion

Synthesis and purification. The synthesis of the ligand Hppt[28] and of the mononuclear complexes[6,7] were carried out by previously reported procedures. Hppt is inherently asymmetric and as a result the synthesis of its mononuclear complexes is complicated by the possibility of the formation of four coordination isomers (Fig. 2). The metal centre may be bound via N1 of the triazole ring and the pyridine ring (**1a**), via N2 of the triazole ring and the pyrazine ring (**1b**), via N4 of the triazole ring and the pyridine ring (**1c**) and finally via N4 of the triazole ring and the pyrazine ring (**1d**). It has been shown for several 1,2,4-triazoles that the presence of bulky substituents in the 5- position of the 1,2,4-triazole ring results in preferential formation of the N2 isomer. The ratio of N4 bound isomers varies from 50% (5 position occupied by H)[12] to less than 5% (5 position occupied by Br).[13] HPLC analysis of reaction products before purification shows that, in agreement with this observation, the amount of N4 bound isomers present is estimated at less than 5% and these are removed by recrystallisation. The remaining two coordination isomers **1a** and **1b** were subsequently separated by column chromatography as detailed in the experimental part.

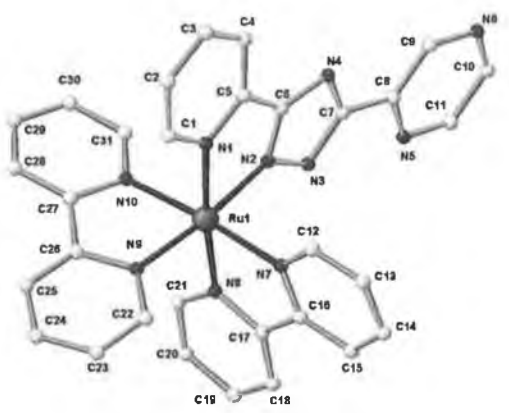

Figure 3 *Molecular structure of* ***1a*** *cation*

X-ray Crystallography.

The molecular structure of **1a** is shown in Fig. 3. Complex **1a** co-crystallised with a molecule of methanol and a hexafluorophosphate counter anion (not shown). From the crystal structure it is clear that the ligand is bound through the pyridine-N and N1 of the triazole ring (via N(1) and N(2) in Fig. 3). The bite angle of the N(1)-Ru(1)-N(2) is 77.98 (6)°, which corresponds well with the bite angle obtained by Hage et al. of 78(1)° for $[Ru(bipy)_2$(3,5-bis(pyridin-2-yl)-1,2,4-triazole)$]PF_6.½H_2O$,[6] and of 77.9(1)° for

12. (a) H. A. Nieuwenhuis, J. G. Haasnoot, R. Hage, J. Reedijk, T. L. Snoeck, D. J. Stufkens and J. G. Vos, *Inorg. Chem.*, 1991, **30**, 48; (b) S. Fanni, T. E. Keyes, C. M. O'Connor, H. Hughes, R. Wang and J.G. Vos, *Coord. Chem. Revs.*, 2000, **208**, 77.

13. S. Fanni, C. Di Pietro, S. Serroni, S. Campagna and J. G. Vos, *Inorg. Chem. Commun.*, 2000, **3**, 42.

[Ru(bipy)$_2$(3-(2-hydroxy-phenyl)-5-(pyridin-2-yl)-1,2,4-triazole)]PF_6.CH_3COCH_3.[14]

	1a.PF_6.MeOH
Empirical Formula	$C_{32}H_{27}F_6N_{10}OPRu$
Formula weight 30 g mol^{-1}	812.67
Temperature	200 (2) K
Wavelength in Å	0.71073
Space group	Triclinic P-1 (No. 2)
Unit cell dimensions	
a Å - α	9.9097(7) - 93.8570(10) °
b Å - β	12.5731(9) -93.4100(10)°
c Å - γ	14.1156(10) -111.4390(10)°
Volume Å^3, Z	1626.6(2), 2
Density (calc.) Mg/m^3	1.659
Crystal dimensions (mm)	0.6 x 0.5 x 0.4
Absorption coeff. mm^{-1}	0.611
F(000)	818
θ range for data collection	1.45°-28.30°
Limiting indices	$-12 \le h \le 12$; $-15 \le k \le 16$; $-18 \le l \le 18$
No. Reflections collected	17142
Independent reflec. (R_{int})	734 (0.0185)
Data/restraints/parameters	7634 / 0 / 469
GOF F^2	1.048
Final R indices [I > 2σ(I)] R1 (wR2)	0.0293, (0.0726)
R indices all data R1 (wR2)	0.0342, (0.0749)
Largest difference peak and hole (eÅ^{-3})	0.702 and -0.524

Standard deviations in parentheses.

Table 1. *X-ray parameters*

Bite angles of 78.87(7)° and 78.72(7)° for bipyridyl ligands are also typical for this class of complex. Ruthenium-nitrogen distances of 2.0398(16)-2.1033(17) Å are also comparable to those found in other complexes.[15] The ruthenium-pyridine distance Ru(1)-N(1) at 2.1033(17) Å is the longest Ru-N bond in the complex and the ruthenium-triazole distance Ru(1)-N(2) at 2.0398(16) Å is the shortest, in agreement with previously reported structures (e.g. 2.03(2) Å [Ru(bipy)$_2$(3,5-bis(pyridin-2-yl)-1,2,4-triazole)]PF_6.$\frac{1}{2}H_2O$.[6] The isomer obtained is therefore identified as **1a**, where the metal centre is bound to N1 of the triazole ring and the pyridine moiety (Fig. 2).

^{1}H NMR spectroscopy

It as been shown previously that ^{1}H NMR spectroscopy can be used effectively to determine the coordination mode of triazole based ligands.[16] To this end, ^{1}H and ^{1}H COSY NMR spectroscopy together with specific deuteriation have been employed. In Table 1, the chemical shifts (δ) of the ppt$^-$ proton resonances are presented together with those of the free ligand and of the analogous bpt$^-$ and bpzt$^-$ Ru(bipy)$_2$- complexes. The bipy resonances are as expected and are not listed (see supplementary material for spectra of **1a/1b**).[16]

Results obtained for the analogous bpt$^-$ and bpzt$^-$ mononuclear compounds show that coordination of a pyridyl/pyrazyl moiety results in a significant change in the chemical shift of its H6 proton while only minor changes to the H6 proton of the free ring are observed.[6,12] This is illustrated in the ^{1}H NMR spectra of the partially deuteriated analogues **2a** and **2b** (Fig. 4).

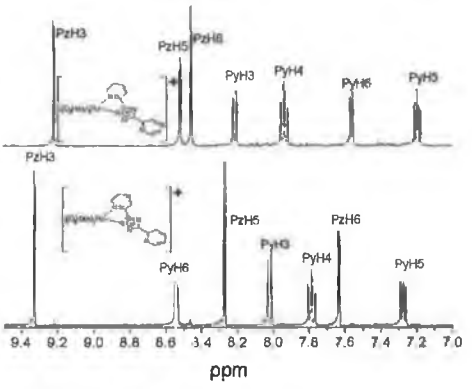

Figure 4 *^{1}H NMR (400 MHz) spectra of **2a** (upper spectrum) and **2b** (lower spectrum) in CD_3CN*

Partial deuteriation simplifies the analysis of the spectra, since ppt$^-$ based signals can be identified with ease. For **2a**, the H6 resonance of the coordinated pyridyl ring at 7.56 ppm is significantly different from the free ligand value of 8.72 ppm, in agreement with coordination being via the N2 of the 1,2,4-triazole ring and the pyridine moiety. Similarly for **2b** the change in the H6 resonance of the pyrazyl ring from 8.73 ppm in the free ligand to 7.63 ppm shows that coordination in this case, and for **1b**, is via the triazole N2 atom of and the pyrazine ring.

For the osmium(II) complexes **3a/3b** the upfield shift of the H6 proton of the coordinated ring is greater than for the ruthenium complexes. This has been observed previously, and has been attributed to increased π-backbonding to the ligands by osmium(II) compared with ruthenium(II), which increases the ring current of the aromatic rings and hence the shielding effect felt by the H6 proton.[22]

14. R. Hage, J. G. Haasnoot, J. Reedijk, R. Wang, E. M. Ryan, J. G. Vos, A. L. Spek, and A. J. M. Duisenberg, *Inorg. Chim. Acta*, 1990, **174**, 77.
15. D. P. Rillema, D. S. Jones, C. Woods and H. A. Levy, *Inorg. Chem.*, 1992, **31**, 2935.
16 R. Hage, R. Prins, J. G. Haasnoot, J. Reedijk and J. G. Vos, *J. Chem. Soc., Dalton Trans.*, 1987, 1389

Table 2 ^{1}H NMR resonances observed for the mononuclear ppt complexes in CD_3CN, together with bpt and bpztanalogues.

Compound			H^3	H^4	H^5	H^6
Hppt		pz	9.42 s	----	8.68 d	8.73 d
		py	8.26 d	8.00 m	7.52 m	8.72 d
2a	$[Ru(d_8\text{-bipy})_2(ppt)]^+$	pz	9.20 (-0.22) s	----	8.52 (-0.16) d	8.46 (-0.27) d
		py	8.22 (0.04) d	7.94 (-0.06) m	7.20 (-0.32) m	7.56 (-1.16) d
2b	$[Ru(d_8\text{-bipy})_2(ppt)]^+$	pz	9.33 (-0.09) s	----	8.28 (-0.40) d	7.63 (-1.10) d
		py	8.02 (-0.14) d	7.78 (-0.22) m	7.27 (-0.25) m	8.54 (-0.18) d
3a	$[Os(bipy)_2(ppt)]^+$	pz	9.19 (-0.16) s	----	8.50 (-0.22) d	8.43 (-0.29) d
		py	8.13 (-0.07) d	7.75 (-0.28) m	7.07 (-0.49) m	7.42 (-1.37) d
3b	$[Os(bipy)_2(ppt)]^+$	pz	9.25 (-0.10) s	----	7.64 (-1.08) d	8.13 (-0.59) d
		py	8.46 (+0.26) d	7.31 (-0.72) m	7.75 (+0.19) m	8.53 (-0.26) d
$[Ru(bipy)_2(bpt)]^+$		Ring A[a]	8.23 (+0.08) d	8.01 (+0.01) m	7.26 (-0.26) m	7.74 (-0.98) d
		Ring B[b]	8.06 (-0.09) d	7.74 (-0.26) m	7.20 (-0.32) m	8.45 (-0.22) d
$[Ru(bipy)_2(bpzt)]^+$		Ring A[a]	9.30 (-0.04) s	--	8.36 (-0.42) d	7.61 (-1.17) d
		Ring B[b]	9.23 (-0.09) s	-	8.46 (-0.32) d	8.46 (-0.32) d
[c]$[Os(bipy)_2(bpt)]^+$		Ring A[a]	8.32 (+0.17) d	7.94 (-0.06) m	7.30 (-0.26) m	7.74 (-0.97) d
		Ring B[b]	8.23 (+0.08) d	8.14 (+0.07) m	7.59 (-0.07) m	8.65 (-0.02) d
$[Os(bipy)_2(bpzt)]^+$		Ring A[a]	9.23 (-0.11) s	--	8.06 (-0.72) d	7.57 (-1.21) d
		Ring B[b]	9.20 (-0.14) s	--	8.46 (-0.32) d	8.46 (-0.32) d

Values in parantheses are change with respect to free ligand {*i.e.* Hppt (in CD_3CN), Hbpt (in $(CD_3)_2SO$), Hbpzt (in $(CD_3)_2SO$)}. pz = pyrazine ring, py is pyridine ring; {s = singlet, d = doublet, dd = doublet of doublets and m = multiplet}. [a]coordinated ring, [b]free ring. [c]From ref. 18 measured in $(CD_3)_2CO$.

In conclusion, with the x-ray structure of **1a** as reference, the coordination mode of mononuclear ppt complexes in general can be determined conveniently by ^{1}H NMR spectroscopy.

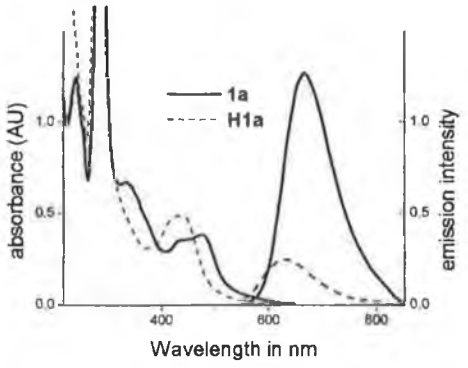

Figure 5 *UV.vis absorption and emission spectra of* ***1a****,* ***H1a*** *in acetonitrile.*

Electronic properties

The visible absorption and emission data for the compounds obtained are listed in Table 3. The lowest energy absorption feature for the ruthenium complexes is assigned to a singlet metal-to-ligand-charge-transfer (^{1}MLCT) transition (log ε ~ 4.2) by comparison with other ruthenium polypyridyl complexes.[2] All compounds show strong absorptions (log ε ~ 5) at about 280 nm which are π-π* in nature. For the osmium(II) complexes **3a/3b** formally forbidden ^{3}MLCT transitions are present at longer wavelengths (550 nm to 750 nm) similar to those observed for $[Os(bipy)_3]^{2+}$.[17] Overall the electronic properties are typical for pyridyl and pyrazine triazole complexes,[6,7] however, there are some significant differences

[17] G. M. Bryant, J. E. Fergusson and H. J. K. Dowell, *Aust. J. Chem.*, 1971, **24**, 257,

in the electronic properties of the two isomers as the comparison below shows.

For the pyridine bound complexes **1a** and bpt⁻, the absorption spectra of the protonated and deprotonated species are very different, with a substantial blue shift in the λ_{max} occurring upon protonation (~ 40 nm) (see fig. 5). However, for the pyrazine bound complexes (**1b** and bpzt-) only a small blue shift in the λ_{max} of the ^{1}MLCT absorption bands occurs upon protonation (~ 10 nm) (Fig. 6). The effect of protonation on the pyridine and pyrazine bound isomers are similar to those of related complexes mononuclear complexes (see Table 3).

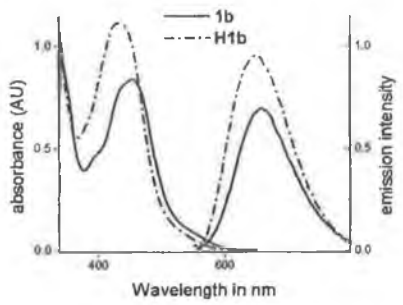

Figure 6 *UV.vis absorption and emission spectra of **1b**, **H1b** in acetonitrile.*

For the osmium analogues a similar behaviour is observed, however, the presence of formally spin forbidden transitions (^{3}MLCT) results in more complex spectra.

Table 3 *Redox and electronic data for non-deuteriated complexes.*

Compound	**Oxidation Pot. (V)**	**Reduction Pot. (V)**	**Absorption (log ε) (nm)**	**[a]Emission / nm 298 K (τ_{us})**
$[Ru(bipy)_2(ppt)]^+$ (**1a**)	0.95	-1.45, -1.70	475 (4.04)	670 (72)
$[Ru(bipy)_2(Hppt)]^{2+}$ (**H1a**)	1.25	—	438	640 (5)
$[Ru(bipy)_2(ppt)]^+$ (**1b**)	1.05	-1.50, -1.75	457 (4.35)	657 (82)
$[Ru(bipy)_2(Hppt)]^{2+}$ (**H1b**)	1.20	—	432	647 (29)
[b]$[Ru(bipy)_2(bpt)]^+$	0.85	-1.47, -1.72	475 (4.05)	678 (72)
[b]$[Ru(bipy)_2(Hbpt)]^{2+}$	1.06	—	429 (4.19)	645 (45)
[c]$[Ru(bipy)_2(bpzt)]^+$	0.99	-1.42, -1.62	453 (4.15)	654 (88)
[c]$[Ru(bipy)_2(Hbpzt)]^{2+}$	1.24	—	446 (4.07)	675 (28)
$[Os(bipy)_2(ppt)]^+$ (**3a**)	0.52	-1.42, -1.69	385 (3.95) 446 (3.74) 498 (3.82) 620	750 (45)
$[Os(bipy)_2(Hppt)]^{2+}$ (**H3a**)	0.80	—	392 432 470 600	730 (39)
$[Os(bipy)_2(ppt)]^+$ (**3b**)	0.63	-1.44, -1.72	408 (4.04) 432 (4.07) 474 (4.11) 610	760 (16)
$[Os(bipy)_2(Hppt)]^{2+}$ (**H3b**)	0.77	—	408 450 600	743 (5)
[b]$[Os(bipy)_2(bpt)]^+$	0.49	-1.41, -1.69	392 (1.34) 438 (1.06) 486 (1.08) 610 (0.28)	762 (55)
[b]$[Os(bipy)_2(Hbpt)]^{2+}$	0.89	—	394 (1.45) 438 (1.38) 476 (1.42) 570 (sh)	n/a (n/a)
$[Os(bipy)_2(bpzt)]^+$	0.64	-1.41, -1.69	404, 436 (3.66), 483 (3.70), 600	783 (14)
$[Os(bipy)_2(Hbpzt)]^{2+}$	1.08	—	416, 452	791 (n/a)

Redox potentials (vs. SCE) were obtained using CV and DPP in 0.1 M TEAP/acetonitrile (scan rate:10 mV/s). Protonation by addition of concentrated $HClO_4$. [a]measured in aerated acetonitrile. [b]values obtained from ref. 6. [c]values obtained from ref. 7.

All complexes examined are luminescent in acetonitrile at room temperature and at 77 K. The ruthenium complexes examined all emit in the 650 to 700 nm region and a large blue shift is observed between 300 and 77 K, typical for ^{3}MLCT emission.[2] As for the absorption spectra, the emission maximum of **1a** (676 nm) is close to that of the analogous bpt$^-$ complex (678 nm). Upon protonation of **1a**, a blue shift in the spectrum and a reduction in the emission lifetime is observed for the pyridine bound isomer. For **1b** a 10 nm blueshift in the λ_{max} occurs upon protonation, however, the reduction in emission lifetime is somewhat less dramatic than for **1a**. For the osmium complexes emission is observed at much lower energy (> 700 nm) as expected.[17] Both **3a** and **3b** undergo a blueshift in both absorption and emission spectra upon protonation.

Acid-base properties.

The acid-base properties of all compounds have been investigated by studying the pH dependence of their absorption spectra. The pK_a values obtained from these studies and of some related complexes are presented in Table 4. The behaviour observed can be explained by protonation/deprotonation of the triazole moiety as indicated in equation 1;

$$[Ru(bipy)_2(ppt)]^+ + H^+ \leftrightarrow [Ru(bipy)_2(Hppt)]^{2+} \quad (1)$$

Although protonation of the coordinated pyrazine ring is possible, this occurs at only at negative pH ($pK_a \sim -1.5$).[8]

Given the structural similarities between the pyridine bound complex **1a** and the bpt$^-$ based mononuclear complex (and likewise the pyrazine bound isomer **1b** and the bpzt$^-$ based complex) it would be expected that the pKa values for the related complexes would be quite similar. Unusually the acid-base properties of **1a/1b** are found to display behaviour quite different to this expectation.

Table 4 shows that the acidity of the coordinated triazole ring is strongly dependent on the nature of the non-coordinated substituent in the C5 position. This dependence is reflected in the ΔpK_a values, with respect to the unsubstituted C-H analogues, given in Table 4. The effect of the introduction of a pyridine or pyrazine ring is particularly relevant. A comparison of the pK_a values of the pztr$^-$ and bpzt$^-$ complexes shows that the triazole ring becomes more acidic by 1.7 pH units in the presence of an additional, free, pyrazine ring. A comparison of the values observed for the pytr$^-$ and bpt$^-$ complexes shows that the effect of the introduction of a pyridine ring is far less dramatic and does not result in a significant change in the pK_a (+ 0.1 pH unit). This indicates that the free pyrazine group acts as a strong electron-withdrawing group. Within this framework the pK_a values are as expected and indicate that there is substantial interaction between the different components of the Hppt ligand. Similar trends are observed for the analogous osmium(II) complexes. It is interesting to note the comparison of the substituent effect on the acid base properties of the complexes and "Hammett" effects observed for organic systems such as substituted benzoic acids.

Table 4 ***Ground state pK_a values of 1,2,4-triazole based mononuclear complexes.***

Pyrazine complexes	pK_a	ΔpK_a	Pyridine complexes	pK_a	ΔpK_a
[a][Ru(bpy)$_2$(pztr)]$^+$	3.7	0	[a][Ru(bpy)$_2$(pytr)]$^+$	4.1	0
[a][Ru(bpy)$_2$(bpzt)]$^+$	2	-1.7	**1a**	2.7	-1.4
1b	3.8	0.1	[a][Ru(bpy)$_2$(bpt)]$^+$	4.2	0.1
[a][Ru(bpy)$_2$(Mepztr)]$^+$	4.2	0.5	[a][Ru(bpy)$_2$(Mepytr)]$^+$	4.9	0.8
[b][Ru(bpy)$_2$(Brpztr)]$^+$	1.4	-2.3	[b][Ru(bpy)$_2$(Brpytr)]$^+$	1.3	-2.8
[Os(bpy)$_2$(bpzt)]$^+$	1.2	-2.5	**3a**	2.1	-2
3b	3.5	-0.2	[a][Os(bpy)$_2$(bpt)]$^+$	4	-0.1

All measurements are carried out in Britton-Robinson buffer, values ± 0.1. a) from ref 18, b) from ref 19

Electrochemical properties

Electrochemical potentials for pyridine bound and pyrazine bound complexes are presented together with those of their analogous bpt$^-$ and bpzt$^-$ complexes in Table 4. As expected the pyrazine bound isomer (**1b**) has a more positive metal-based oxidation potential than the pyridine bound isomer (**1a**). This is due mainly to the weaker σ-donor/stronger π-acceptor properties of the pyrazine over the pyridine ligand.[20] The first two reduction potentials of the deprotonated complexes are reversible and are similar to those of $[Ru(bipy)_3]^{2+}$, suggesting they are bipy based reductions.[21] Due to hydrogen formation

18. R. Hage, *Thesis Ph.D.*, Leiden University, The Netherlands, 1991.
19. C. Di Pietro, S.Serroni, S. Campagna, M. T. Gandolfi, R. Ballardini, S. Fanni, W. Browne and J. G. Vos, Inorganic Chemistry, *in press*, **2002**
20. (a) E. S. Dodsworth and A. B. P. Lever, *Chem. Phys. Letts.*,1986, **124**, 152; (b) D.P. Rillema, G. Allen, T.J. Meyer and D. Conrad, *Inorg. Chem.*, 1983, **22**, 1617
21. (a) C. M. Elliot and E.J. Hershenhart, *J. Am. Chem. Soc.*, 1982, **104**, 7519; (b) R. Hage, J.G. Haasnoot, D. J. Stufkens, T.L. Snoeck, J.G. Vos and J. Reedijk, *Inorg. Chem.*, 1989, **28**, 1413.

reduction potentials could not be obtained for the protonated complexes. The oxidation potentials of the osmium complexes, **3a** and **3b**, are approximately 400 mV lower than those of the corresponding ruthenium complexes. This is normal behaviour for these types of systems and is attributed to the higher energy of the 5d orbitals compared to the 4d orbitals.[22]

Overall the redox properties of all complexes are as expected. However the influence of the free pyrazine ring of **1a** and the bpzt- based complexes is of note with the redox potentials of these complexes being in every case significantly higher than for their –H substituted analogues. This is in agreement with the acid-base properties of these complexes, with the electron withdrawing influence of the pyrazine ring resulting in a reduction in the σ-donor strength of the 1,2,4-triazole ring (resulting in a lowering of the pK_a) and consequently a stabilisation of the metal centre towards oxidation.

Conclusions

In this contribution the synthesis, structural, electrochemical and electronic characterisation of a series of ruthenium(II) and osmium(II) $(bipy)_2$- complexes based on the ligand Hppt are reported. The acid-base properties of the two major coordination isomers, taken together with a series of related complexes, provide for a much improved understanding of the effect of "spectator" or non-coordinated substituents on the 1,2,4-triazole ring. It is shown that these substituents are of major importance in determining the ground state properties of both the ruthenium(II) and osmium(II) based complexes. Overall the effect of protonation on the electronic and electrochemical properties of the complexes examined are as expected and confirm the assignments of coordination mode of the ppt⁻ ligand made on the basis of ^{1}H NMR spectroscopy and X-ray crystallography.

The isolation and identification of the major coordination isomers formed has been achieved and allows for the preparation of both homo- (RuRu, OsOs) and hetero- (RuOs) binuclear complexes of the ligand Hppt in a systematic and controlled manner. The inherent asymmetry of the Hppt ligand results in important differences in the ground state properties of the mononuclear coordination isomers. In further studies the effects of these differences on the excited state properties of the two parts of the ppt⁻ ligand will be investigated in greater detail. Of particular interest is the location of the excited state and, for binuclear complexes, the degree of interaction between the metal centres mediated by the bridging ppt⁻ ligand. In these studies selective deuteriation will be invaluable in understanding the excited state properties of mono- and bi-nuclear complexes, in particular in the interpretation of their resonance Raman spectra.[23]

Experimental

Materials: All solvents employed were of HPLC grade or better and used as received unless otherwise stated. For all spectroscopic measurements Uvasol (Merck) grade solvents were employed. All reagents employed in synthetic procedures were of reagent grade or better. $[D_8]$-2,2'-bipyridine,[24] *cis*-$[Ru(bipy)_2Cl_2].2H_2O$,[25] *cis*-$[Ru([D_8]\text{-}bipy)_2Cl_2].2H_2O$,[25] *cis*-$[Os(bipy)_2Cl_2].2H_2O$,[26] and tetraethylammonium perchlorate (TEAP)[27] were prepared by previously reported methods.

Syntheses

3-(pyrazin-2'-yl)-5-(pyridin-2''-yl)-1H-1,2,4-triazole (**Hppt**) was prepared by standard procedures.[28]

2-pyrazylhydrazide. 15 g of 2-pyrazylcarboxylic acid (0.12 mol) were heated at reflux for 3 hours in 90 cm^3 ethanol and 15 cm^3 concentrated H_2SO_4. The solution was neutralised with saturated Na_2CO_3 solution and filtered. The volume was reduced *in vacuo* and extracted with four 30 cm^3 aliquots of dichloromethane. The combined fractions were washed with 10 cm^3 of water and dried over $MgSO_4$. The dichloromethane was removed *in vacuo* to yield the ethyl-2-pyrazylcarboxylate, which crystallised on cooling. The ester was dissolved in 20 cm^3 of ethanol and an equimolar amount of hydrazine monohydrate was added drop-wise. The solution was then kept a –4 °C for 12 h and crystalline 2-

22. (a) G. M. Bryant and J. E. Fergusson, *Aust. J. Chem.*, 1971, **24**, 441; (b) Y. Ohsawa, M. K. DeArmond, K. W. Hanck and C. G. Moreland, *J. Am. Chem. Soc.*, 1985, **107**, 5383; (c) J. M. de Wolf, R. Hage, J. G. Haasnoot, J. Reedijk and J.G. Vos, *New J. Chem.*, 1991, **15**, 501.

23. W. R. Browne and J. G. Vos, *Coordination Chemistry Reviews*, 2001, **761**, 787.

24. W. R. Browne, C. M. O'Connor, J. S. Killeen, A. L. Guckian, M. Burke, P. James, M. Burke, J. G. Vos, *Inorg. Chem.*, in press, 2002

25. B. P. Sullivan, D. J. Salmon and T. J. Meyer, *Inorg. Chem.*, 1978, **17**, 3334.

26. E. M. Kober, K. A. Goldsby, D. N. S. Narayana and T. J. Meyer, *J. Am. Chem. Soc.*, 1983, **105**, 4303.

27. R. Wang, J. G. Vos, R. H. Schmehl and R. Hage, *J. Am. Chem. Soc.*, 1992, **114**, 1964.

28. R. Prins, R. A. G. de Graaff, J. G. Haasnoot, C. Vader and J. Reedijk, *J. Chem. Soc., Chem. Commun.*, 1986, 1430.

pyrazylhydrazide formed. The solid 2-pyrazyl-hydrazide was filtered and air-dried. Yield 12 g, 74 %. ^{1}H NMR in $(CD_3)_2SO$: δ ppm 10.15 (1H, s, N-H), 9.11 (1H, s), 8.81 (1H, d), 8.67 (1H, d), 4.65 (2H, s).

1-(pyrazin-2'-yl)-4-(pyridin-2''-yl)-acylamidrazone. Equimolar amounts of 2-cyanopyridine (as to the 2-pyrazylhydrazide, 12g) were dissolved in 30 cm^3 of methanol with 0.7 g of sodium and heated under reflux for 3 hours. The 2-pyrazylhydrazide was added to the solution and heated for 15 min. The solution was cooled to room temperature and the precipitate formed (yellow) was filtered and air-dried for 2 h. Yield 12.4 g, 67%. ^{1}H NMR in $(CD_3)_2SO$: δ ppm 9.19 (1H, d, H3''), 8.73 (1H, d, H6''), 8.60 (1H, dd, H5''), 8.19 (1H, d, H3'), 7.90 (1H, t, H4'), 7.51 (1H, t, H5'), 8.84 (1H, d, H6').

*3-(pyrazin-2'-yl)-5-(pyridin-2''-yl)-1H-1,2,4-triazole (**Hppt**)*. 12.4 g (0.05 mol) of 1-(pyrazin-2'-yl)-4-(pyridin-2''-yl)-acylamidrazone was heated under reflux for 1 hour in 10 cm^3 of ethylene glycol to yield the Hppt ligand. The ligand (white) was recrystalised from hot ethanol. Yield: 8 g (52%). ^{1}H NMR in $(CD_3)_2SO$ δ ppm 9.33 (1H, d, H3''), 8.72 (2H, m, H5'', H6''), 8.17 (1H, d, H3'), 8.01 (1H, t, H4'), 7.54 (1H, t, H5'), 8.77 (1H, d, H6').

$[Ru(bipy)_2(ppt)]PF_6.3H_2O$ ***1a*** */ $[Ru(bipy)_2(ppt)]PF_6.H_2O.CH_3OH$* ***1b***. 520 mg (1 mmol) of *cis*-$[Ru(bipy)_2Cl_2].2H_2O$ was added to 0.45 g (2.1 mmol) **Hppt** dissolved in 50 cm^3 of hot ethanol:water (1:1).The solution was heated at reflux for 4 h and evaporated to dryness. The residue dissolved in 10 cm^3 of water. 3 drops of conc. aqueous ammonia and 5 cm^3 of saturated aqueous ammonium hexafluorophosphate were added to precipitate **1a/1b**. The isomers were separated by column chromatography using neutral alumina and acetonitrile as eluent. The pyridine bound isomer (**1a**) eluted first followed by the pyrazine bound isomer (**1b**). Only very small amounts of the N4 bound isomers were obtained subsequently by elution with methanol and were not further investigated. Further purification took place by recrystallisation from acetone:water (1:1 v/v). Yield of combined fractions: 420 mg (51 %). Mass spec: m/z **1a** - 637 (M^+), **1b** - 637 (M^+). Elemental analysis: Found (calc. for $C_{31}H_{23}F_6N_{10}PRu.3H_2O$: **1a)**: C 44.6 (44.55); H 3.2 (3.11); N 16.2 (16.77)%. Found (calc. for $C_{31}H_{23}F_6N_{10}PRu.H_2O.CH_3OH$: **1b)**: C 45.0 (46.10); H 3.3 (3.36); N 17.2 (16.81)%. Crystals of **1a** suitable for X-ray analysis were grown from a methanol solution of **1a**.

$[Ru([D_8]\text{-}bipy)_2(ppt)]PF_6.CH_3OH.2H_2O$ ***2a*** */ $[Ru([D_8]\text{-}bipy)_2(ppt)]PF_6.2H_2O$* ***2b***
As for **1a/1b**. Yield of combined fractions: 712 mg (93%). Mass spec: m/z **2a** - 653 (M^+), **2b** - 653 (M^+). Elemental analysis: Found (calc. for $C_{31}H_7D_{16}F_6N_{10}PRu.CH_3OH.2H_2O$): **2a)**: C 44.60 (44.29); H 2.85 (3.34); N 15.84 (16.15)%. Found (calc. for $C_{31}H_7D_{16}F_6N_{10}PRu.2H_2O$): **2b)**: C 44.46 (44.66); H 2.77 (3.00); N 16.32 (16.81)%.

$[Os(bipy)_2(ppt)]PF_6.2H_2O$ ***3a*** */ $[Os(bipy)_2(Hppt)](PF_6)_2.2H_2O$* ***3b.*** As for **1a/1b** except 575 mg (1 mmol) of *cis*-$[Os(bipy)_2Cl_2]$ was heated at reflux with 223 mg (1 mmol) of Hppt for 4 days with 50 mg of zinc powder. Yield of combined fractions: 0.82 g (78 %). Mass spec: m/z **3a** - 725 (M^+), Elemental analysis: Found (calc. for $C_{31}H_{23}F_6N_{10}POs.2H_2O$: **3a)**: C 41.1 (41.05); H 2.80 (2.76); N 15.28 (15.45)%. Found (calc. for $C_{31}H_{24}F_{12}N_{10}P_2Os.2H_2O$: **3b)**: C 35.6 (35.35); H 2.6 (2.47); N 13.5 (13.31)%.

$[Os(bipy)_2(Hbpzt)](PF_6)_2.H_2O$
As for **4a/4b** except 440 mg (2 mmol) of Hbpzt was heated at reflux with 575 mg (1 mmol) of *cis*-$[Os(bipy)_2Cl_2].2H_2O$. Yield: 470 mg (0.42 mmol, 42%). Elemental analysis: Found (calc. for $C_{30}H_{23}F_{12}N_{11}P_2Os.H_2O$): C 35.6 (34.78); H 2.34 (2.32); N 14.93 (14.83) %.

Elemental analysis on C, H and N was carried out at the Microanalytical Laboratory at University College Dublin using an Exador analytical CE440.

X-ray Crystallography: Data for **1a** were collected on a Siemens SMART 1000 CCD-diffractometer fitted with a molybdenum tube (K_α, λ = 0.71073 Å) and a graphite monochromator. Relevant experimental data is presented in Table 1. A full sphere of data was collected with the irradiation time of 4s per frame. The structures were solved with direct methods and all non hydrogen atoms refined anisotropically with the SHELX programm[29] (refinement by least-squares against F2). Crystallographic data of the structures have been deposited at the Cambridge Crystallographic Database Centre, supplementary publication No. CCDC xxxxxx (**1a**). Copies of this information may be

29. G. M. Sheldrick, SHELX-97, Universität Göttingen 1997.

obtained free of charge form The Director, CCDC, 12 Union Road, Cambridge CB2 1EZ, UK (Fax: +44-1223-336033; email: deposit@ccdc.cam.ac.uk or http://www.ccdc.cam.ac.uk).

Instrumental Methods: NMR Spectroscopy. ^{1}H and ^{1}H COSY spectra were recorded on a Bruker Avance (400 MHz) NMR Spectrometer. Peak positions are relative to residual solvent peaks. Electrochemical measurements were carried out on a Model 660 Electrochemical Workstation (CH Instruments). Typical complex concentrations were 0.5 to 1 mM in anhydrous acetonitrile (Aldrich 99.8%) containing 0.1 M TEAP. A Teflon shrouded glassy carbon or platinum working electrode, a Pt wire auxiliary electrode and SCE reference electrode were employed. Solutions for reduction measurements were deoxygenated by purging with N_2 or Ar gas for 15 min prior to the measurement. Measurements were made in the range of –2.0 to 2.0 V (w.r.t SCE electrode). Protonation of complexes was achieved by addition of 0.1 M $HClO_4$ to the electrolyte solution. The scan rates used were typically 100 or 200 mV/s. UV/Vis absorption spectra were recorded on a Shimadzu UV/Vis-NIR 3100 spectrophotometer interfaced with an Elonex PC466 using UV/Vis data manager. Absorption maxima, ±2 nm Molar absorption coefficients are ± 10%. Emission spectra (accuracy ± 5 nm) were recorded at 298 K using a LS50B luminescence spectrophotometer, equipped with a red sensitive Hamamatsu R928 PMT detector, interfaced with an Elonex PC466 employing Perkin-Elmer FL WinLab custom built software. Emission and excitation slit widths were 10 nm at 298 K. Emission spectra are uncorrected for photomultiplier response. 10 mm pathlength quartz cells were used for recording spectra. pH titrations were carried out in Britton-Robinson buffer (0.04 M H_3BO_3, 0.04 M H_3PO_4, 0.04 M CH_3CO_2H) (pH was adjusted using concentrated sulphuric acid or sodium hydroxide solution.

Supplementary material

S1 *^{1}H NMR (400 MHz) spectra of **1a** (upper spectrum) and **1b** (lower spectrum) in CD_3CN*

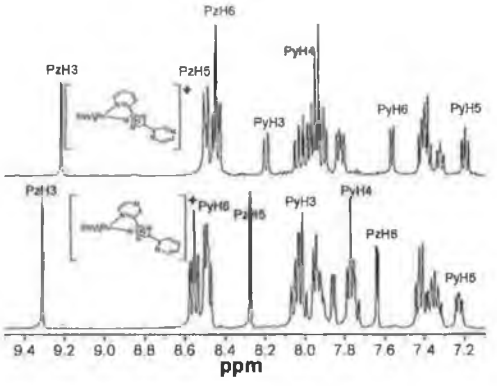

Acknowledgements
The authors thank Enterprise Ireland for financial assistance.

Inorg. Chem. **2002**, *41*, 4245–4251

Routes to Regioselective Deuteriation of Heteroaromatic Compounds

Wesley R. Browne,[†] Christine M. O'Connor,[‡] J. Scott Killeen,[†] Adrian L. Guckian,[†] Micheal Burke,[§] Paraic James,[∥] Maurice Burke,[§] and Johannes G. Vos*[,†]

National Centre for Sensor Research, School of Chemical Sciences, Dublin City University, Dublin 9, Ireland, Department of Chemistry, Dublin Institute of Technology, Dublin 2, Ireland, School of Chemical Sciences, Dublin City University, Dublin 9, Ireland, and National Institute for Cellular Biotechnology, Dublin City University, Dublin 9, Ireland

Received March 22, 2002

A systematic approach to the deuteriation of polypyridyl type ligands is reported. A range of isotopologues of heteroaromatic compounds containing pyrazyl, pyridyl, 1,2,4-triazole, thienyl, methyl, and phenyl moieties, have been prepared in a cost-effective manner, using a range of methods based on subcritical aqueous media. Selectively and fully deuteriated ligands are characterized by mass spectrometry and ^{1}H, ^{2}D, and ^{13}C NMR spectroscopy. The application of deuteriation to supramolecular chemistry is discussed.

Introduction

The application of transition metal complexes incorporating polypyridyl type ligands in inorganic photochemistry and supramolecular chemistry, in particular, has increased rapidly since the mid 1970s.[1] In particular, ruthenium(II) and osmium(II) based polypyridyl complexes have been utilized as building blocks for large multinuclear structures, mostly because of their synthetic versatility and suitable photophysical and electrochemical properties.[2] However, with the ever-increasing complexity of supramolecular systems, the ability to characterize these molecules fully by standard NMR techniques has become difficult.[3] An additional challenge often encountered is the identification of the nature of the emitting state, which, for heteroleptic compounds, may be located on different parts of the molecular assembly. Deuteriation of ligands has been proposed as a tool to help overcome these problems, at least in part.[4]

To date, however, the widespread use of deuteriation as a general spectroscopic aid has been limited, primarily because of the lack of generally applicable, high yield, and low cost H/D exchange procedures for polypyridyl type ligands. In this contribution, a general and systematic approach to the deuteriation of polypyridyl type heteroaromatic compounds is reported. This approach is based on the use of subcritical D_2O. The methods reported in this contribution are a significant improvement on traditional routes reported for the deuteriation of 2,2′-bipyridyl, which require several synthetic steps or the use of the environmentally unfriendly material asbestos.[5,6] Both methods yield only fully deuteriated compounds, in low to moderate yields. With the systematic approach reported in this contribution, more than 30 partially and fully deuteriated compounds (Figure 1) are obtained in high yields (~90%). The procedures used are relatively low cost and straightforward and can be carried out on at least gram scale. The approach reported is of a general nature and can be applied to a wide range of compounds, and as a result, the widespread use of partial deuteriation to elucidate the properties of supramolecular structures is now possible.

* To whom correspondence should be addressed. E-mail: johannes.vos@dcu.ie. Fax: 00353 1 7005503. Phone: 00353 1 7005307.
† National Centre for Sensor Research.
‡ Dublin Institute of Technology.
§ School of Chemical Sciences, Dublin City University.
∥ National Institute for Cellular Biotechnology.

(1) (a) Juris, A.; Balzani, V.; Barigelletti, F.; Campagna, S.; Belser, P.; von Zelewsky, A. *Coord. Chem. Rev.* **1988**, *84*, 85. (b) Balzani, V.; Campagna, S.; Denti, G.; Juris, A.; Ventura, M. *Coord. Chem. Rev.* **1994**, *132*, 1. (c) Balzani, V.; Scandola, F. *Supramolecular Photochemistry*; Ellis Horwood: Chichester, U.K., 1991. (d) *Supramolecular Photochemistry*; Balzani, V., Ed.; Reidel: Dordrecht, The Netherlands, 1997. (e) Kalyanasundaram, K. *Coord. Chem. Rev.* **1962**, *46*, 159.

(2) (a) Balzani, V.; Juris, A.; Venturi, M.; Campagna, S.; Serroni, S. *Acc. Chem. Res.* **1998**, *31*, 26. (b) Slate, C. A.; Striplin, D. R.; Moss, J. A.; Chen, P.; Erickson, B. W.; Meyer, T. J. *J. Am. Chem. Soc.* **1998**, *120*, 4885. (c) Hu, Y.-Z.; Tsukiji, S.; Shinkai, S.; Oishi, S.; Hamachi, I. *J. Am. Chem. Soc.* **2000**, *122*, 241. (d) Balzani, V.; Juris, A.; Venturi, M.; Campagna, S.; Serroni, S. *Chem. Rev.* **1996**, *96*, 759.

(3) (a) Thummel, R. P.; Williamson, D.; Hery, C. *Inorg. Chem.* **1993**, *32*, 1587. (b) Chirayil, S.; Thummel, R. P. *Inorg. Chem.* **1989**, *28*, 812. (c) O'Brien, J. E.; McMurry, T. B. H.; O'Callaghan, C. N. *J. Chem. Res., Synop.* **1998**, 448 and references therein.

(4) For a recent review see: Browne, W. R.; Vos, J. G. *Coord. Chem. Rev.* **2001**, *219*, 761 and references therein.

(5) Cook, M. J.; Lewis, A. P.; McAuliffe, G. S. G.; Skarda, V.; Thomson, A. J.; Glasper, J. L.; Robbins, D. J. *J. Chem. Soc., Perkin Trans. 2* **1984**, 1293.

(6) Fischer, G.; Puza, M. *Synthesis* **1973**, *4*, 218.

10.1021/ic020226y CCC: $22.00
Published on Web 07/09/2002

Table 1. Conditions, Yields, and Extent of Isotope Exchange Reactions

	compound	overall % H−D exchange (site)[a]	method[b]	% yield[c]	reaction time (days)
1b	[D_8]-2,2′-bipyridine	>98	A	80	2 × 3 days
		>98	C	90	6
2b	[D_4]-4,4′-bipyridine	>98 (C2/C6); <15 (C3/C5)	B	95	3
2c	[D_8]-4,4′-bipyridine	>98	A	80	4
		>98	C	90	6
3b	[D_{12}]-4,4′-dimethyl-2,2′-bipyridine	>98 (50% exchange at C3)	A	70	4
		>98	C	95	6
4b	[D_8]-1,10-phenanthroline	>98	A	70	4
		>98	C	95	6
5b	[D_6]-4,7-diphenyl-1,10-phenanthroline	>98 phenanthroline protons (<5% for phenyl rings, C5/C6 show incomplete exchange)	C	95	6
5c	[D_{10}]-4,7-diphenyl-1,10-phenanthroline	~95% for phenyl rings	D (from **5d**)	95	6
5d	[D_{14}]-4,7-diphenyl-1,10-phenanthroline	>98 (<5 at C5/C6)	A	60	6
5e	[D_{16}]-4,7-diphenyl-1,10-phenanthroline	>98	A then C	80	2 × 3 days
6b	[D_{12}]-2,2′-biquinoline	>98	A	80	3
6c	[D_4]-2,2′-biquinoline	>98 C2/C3/C4 (<10 at remaining positions)	C	60	4
7b	[D_{10}]-2,3-di-(pyrid-2yl)-pyrazine	> 98	C	90	6
8b	[D_2]-2-(thien-2′-yl)-pyridine	>98 (py-H6/th-H5′)	B	85	6
8c	[D_7]-2-(thien-2′-yl)-pyridine	>98	C	95	6

[a] In the case of partially deuteriated compounds, exchange at individual positions is given in parentheses. [b] **A** 0.1 g of 10% Pd/C in 20 mL of D_2O at 200 °C; **B** in 20 mL of D_2O at 200 °C; **C** in 20 mL of 1 M NaOD/D_2O at 200 °C; **D** in 20 mL of 1 M NaOH/H_2O at 200 °C. [c] Based on recovered yield.

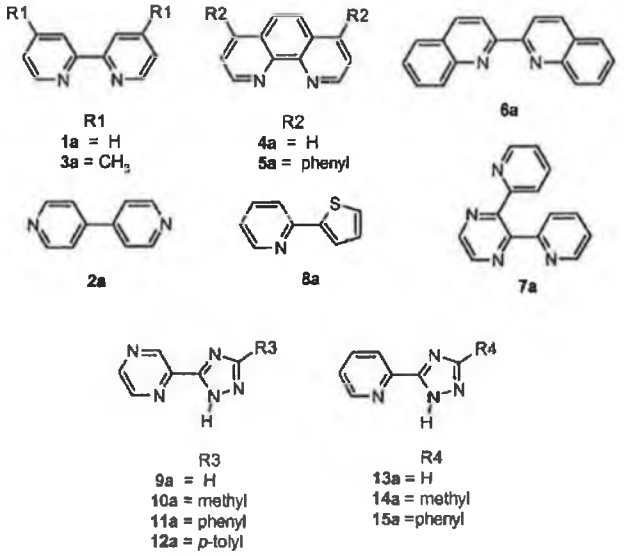

Figure 1. Structures of compounds examined.

Preliminary results on the deuteriation of 2,2′-bipyridyl using a Pd/C catalyst and D_2O as deuterium source were reported in an earlier communication.[7] Subsequently, this approach was applied to the full deuteriation of 1,10-phenanthroline,[7,8] pyridyl- and pyrazyl-1,2,4-triazole,[9] imidazole,[10] and 2-(thien-2′-yl)-pyridine.[11]

Results

As outlined in the Experimental Section, several H/D exchange procedures, methods A, B, and C, have been developed. In method A, Pd/C is used as a catalyst in the presence of D_2O, and in method B, only D_2O is used, while method C is based on the use of basic D_2O (pD = 10/11). In addition, "reverse" D/H exchange has been used to achieve further regioselectivity. The approaches taken are basic H_2O, method D, neutral H_2O, method E, and neutral H_2O in the presence of Pd/C, method F. In all methods, the reaction is carried out in a sealed steel container with a Teflon liner at 200 °C. The products obtained, together with yields, the degree of deuteriation, and experimental conditions are given in Tables 1 and 2. Spectroscopic characterization of the products has been carried out using mass spectrometry and ^1H, ^2D, and ^{13}C NMR spectroscopy. Data are given as Supporting Information. The degree of deuteriation was determined using both ^1H NMR spectroscopy and mass spectrometry. In Tables 1 and 2 (and for convenience throughout this paper), the exchange of the N−H proton of 1,2,4-triazole rings is not considered because exchange at this position is fast and occurs under ambient conditions in protic solvents.

Discussion

General. The application of high temperature and supercritical aqueous media in organic reactions has attracted significant interest in recent years.[12] Much less attention has been focused on medium temperature (150−250 °C) aqueous media despite it being the more accessible temperature range. H/D exchange of pyridine under acidic, neutral, and basic conditions was investigated in some detail in the medium (150−250 °C) and low (<150 °C) temperature range.[13−15] The usefulness of transition metal catalysts was examined,

(7) Keyes, T. E.; Weldon, F.; Müller, E.; Pechy, P.; Grätzel, M. J. G. Vos, J. *J. Chem. Soc., Dalton Trans.* **1995**, 2705.
(8) Coates, C. G.; Callaghan, P. L.; McGarvey, J. J.; Kelly, J. M.; Kruger, P. E.; Higgins, M. E. *J. Raman Spectrosc.* **2000**, *31*, 283.
(9) Fanni, S.; Keyes, T.; O'Connor, C. M.; Hughes, H.; Wang, R. Y.; Vos, J. G. *Coord. Chem. Rev.* **2000**, *208*, 77.
(10) Hardacre, C.; Holbrey, J. D.; McMath, S. E. J. *Chem. Commun.* **2001**, 367.
(11) Yersin, H.; Humbs, W. *Inorg. Chem.* **1999**, *38*, 5820.
(12) (a) Katritzky, A. R.; Nichols, D. A.; Siskin, M.; Murugan, R.; Balasubramanian, M. *Chem. Rev.* **2001**, *101*, 837. (b) Junk, T.; Catallo, W. J. *Chem. Soc. Rev.* **1997**, *26*, 401.
(13) (a) Zoltewicz, J. A.; Smith, C. L. *J. Am. Chem. Soc.* **1967**, *89*, 3358. (b) Yao, J.; Evilia, R. F. *J. Am. Chem. Soc.* **1994**, *116*, 11229. (c) Riesen, H.; Wallace, L.; Krausz, E. *J. Phys. Chem.* **1996**, *100*, 17138.

Table 2. Conditions, Yields, and Extent of Hydrogen/Deuterium Exchange Reactions

	compound	overall % H−D exchange (site)[a]	method[b]	% yield[c]	reaction time (days)
9b	$[D_4]$-Hpztr	>98%	B	95	3
10b	$[D_6]$-Hmepztr	>98%	B	95	3
11b	$[D_3]$-Hphpztr	>98% (pz)	B	95	3
11c	$[D_5]$-Hphpztr	>98% (ph)	E (#)	95	3
11d	$[D_8]$-Hphpztr	>98%	A	80	2 × 3 days
12b	$[D_3]$-Htolpztr	>98% (pz)	B	95	3
12c	$[D_3]$-Htolpztr	>98% (Me)	E (prepared from **12e**)	95	2
12d	$[D_4]$-Htolpztr	>80% (tolyl, see Scheme 2)	F (#)	95	6
12e	$[D_6]$-Htolpztr	>98% (pz and Me)	A	95	6
12f	$[D_7]$-Htolpztr	>98% (tolyl)	E (#)	95	3(§)
12g	$[D_{10}]$-Htolpztr	>98%	C	95	2 × 10 days
13b	$[D_5]$-Hpytr	>98%	C	80	3
14b	$[D_7]$-Hmepytr	>98%	C	80	3
15b	$[D_1]$-Hphpytr	>95% (py H6)	B	95	30
15c	$[D_4]$-Hphpytr	>95% (py), <15% (ph)	C	90	3
15d	$[D_5]$-Hphpytr	>95% (ph), <15% (py)	E (#)	90	3
15e	$[D_9]$-Hphpytr	>98%	A	80	6
	$[Ru(bpy)_2(\mathbf{11a})](PF_6)$	>98% pz C3/5, <20% at pz C6	B	70	3
	$[Ru(bpy)_3](PF_6)$	no exchange obsd	B	90	3
		no exchange obsd	B	90	3

[a] In the case of partially deuteriated compounds, exchange at individual positions is given in parentheses. [b] **E** in 20 mL of H_2O at 200 °C; **F** 0.1 g of 10% Pd/C in 20 mL of H_2O at 200 °C; # indicates preparation from perdeuteriated reagents (see Experimental Section). For other reaction conditions, see Table 1. [c] On the basis of recovered yield, § indicates that when species reacted for 30 days, no further exchange was observed. For **12b**−**g**, see Scheme 2 for further information.

with Pt and Pd receiving the most attention.[15] However, to the authors' knowledge, no detailed study on the general application of such methods has been reported. The motivation behind the interest in the deuteriation of polypyridyl ligands is their potential applicability in the study of supramolecular systems. One approach taken has been the direct deuteriation of the metal complexes.[16−18] For example, deuteriation of $[Ru(bpy)_3]^{2+}$ in 0.1 M $NaOCD_3/(CD_3)_2SO/CD_3OD$ at 35 °C was found to occur rapidly at the 3,3′-positions and more slowly at the 5,5′-positions. In the present study, $[Ru(bpy)_3]^{2+}$ is found to be inert to H/D exchange in both neutral and basic D_2O (Table 2). When using method B, $[Ru(bpy)_2(\mathbf{11a})]^+$ shows a very slow exchange at the H6 position of the pyrazyl ring (adjacent to the coordinating nitrogen), whereas the H3 and H5 positions of the pyrazine ring undergo complete exchange. Overall deuteriation of metal complexes is slow and has severe limitations, especially in the case of heteroleptic complexes; for this reason, a general strategy for the H/D exchange of ligands is needed.

With the strategy reported in this contribution, deuteriation has been achieved on the gram scale, with high yields (typically >80% after purification) and to high degrees of isotopic purity (typically >98%). No impurities were observed for any of the reactions listed in Tables 1 and 2. The yields reported are recovered yields, and the less than quantitative values obtained for method A reflect the difficulty of removing the substrates from the Pd/C catalyst. It is also important to realize that there is a theoretical limit to the extent of deuteriation. This limit is dependent on the molar ratio between the substrate and the solvent D_2O. For example, 3 g of 2,2′-bipyridine contains 0.1538 mol equiv of protons, and 20 mL of D_2O contains 2.214 mol equiv of deuterons; for this reaction mixture, the maximum theoretical deuteriation is 93.5%. When 1 g of bpy is employed, the maximum theoretical limit is raised to 98%. When large amounts are deuteriated (>1 g) by any of the procedures, the sample is subjected to two cycles rather than one, and after the second cycle, the equilibrium limit rises to greater than 99.5%. This is indicated in the tables. We thank one of the reviewers for highlighting this issue. By careful manipulation of the conditions employed and by the combination of different methods, regioselective deuteriation is achieved. The behavior of the compounds studied is discussed in more detail in the next sections.

Deuteriation of Heterocyclic Groups. Compounds **1a**−**8a** (Figure 1) are among the most commonly employed bidentate ligands in the preparation of inorganic polypyridyl complexes.[1] Table 1 shows that Pd/C is not needed to achieve full deuteriation. Neutral and basic D_2O solutions also yield high deuteriation ratios and high yields. The absence of a catalyst has the advantage that the workup of the reaction mixture is easier, and hence, yields improve (See Table 1).

The effect of the reaction conditions used (e.g., time, pH/pD and catalyst) is found to be dependent on the type of proton to be exchanged. For example, as shown in Figure 2,

(14) (a) Wong, J. L.; Heck, J. H., Jr. *J. Org. Chem.* **1974**, *39*, 2398. (b) Buncel, E.; Clement, O.; Onyido, I. *J. Am. Chem. Soc.* **1994**, *116*, 2679. (c) Clement, O.; Roszak, A. W.; Buncel, E. *J. Am. Chem. Soc.* **1996**, *118*, 612. (d) Hardacre, C.; Holbrey, J. D.; McMath, S. E. J. *Chem. Commun.* **2001**, 367. (e) Anto, S.; Getvoldsen, G. S.; Harding, J. R.; Jones, J. R.; Lu, S.-Y.; Russell, J. C. *J. Chem, Soc., Perkin Trans. 2* **2000**, 2208.

(15) (a) Buncel, E.; Clement, O. *J. Chem. Soc., Perkins Trans. 2* **1995**, 1333. (b) Olofson, R. A.; Landesberg, J. M. *J. Am Chem. Soc.* **1966**, *88*, 4263. (c) Olofson, R. A.; Landesberg, J. M.; Houk, K. N.; Michealman, J. S. *J. Am Chem. Soc.* **1966**, *88*, 4265. (d) Coburn, R. A.; Landesberg, J. M.; Kemp, D. S.; Olofson, R. A. *Tetrahedron* **1970**, *26*, 685.

(16) Constable, E. C.; Seddon, K. R. *J. Chem. Soc., Chem. Commun.* **1982**, 34.

(17) McClanahan, S. F.; Kincaid, J. R. *J. Am Chem. Soc.* **1986**, *108*, 3840.

(18) Strommen, D. P.; Mallick, P. K.; Danzer, G. D.; Lumpkin, R. S.; Kincaid, J. R. *J. Phys. Chem.* **1990**, *94*, 1357.

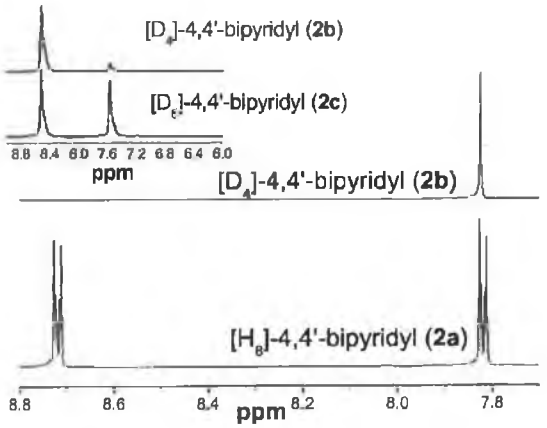

Figure 2. ^{1}H NMR spectra of [H_8]-4,4′-bipyridine (**2a**) (lower spectrum) and [D_4]-4,4′-bipyridine (**2b**) (upper spectrum) in [D_6]-acetone. Inset: ^{2}D NMR spectra of [D_8]-4,4′-bipyridine (**2c**) (lower spectrum) and [D_4]-4,4′-bipyridine (**2b**) (upper spectrum) in [D_6]-acetone).

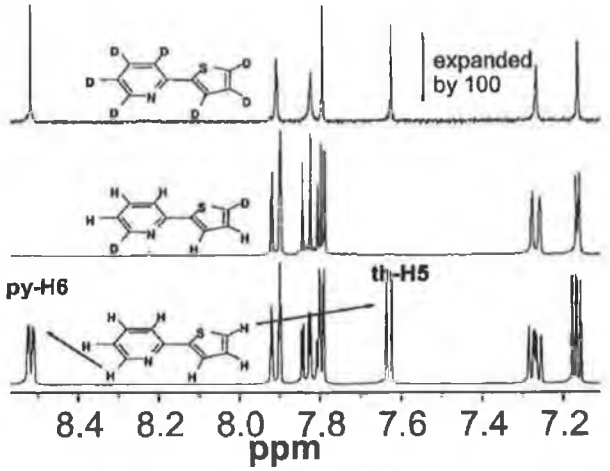

Figure 3. ^{1}H NMR spectra of [H_7]-2-(thien-2′-yl)-pyridine (**8a**) (lower spectrum), [D_2]-2-(thien-2′-yl)-pyridine (**8b**) (middle spectrum), and [D_7]-2-(thien-2′-yl)-pyridine (**8c**) (upper spectrum) in [D_6]-DMSO (all spectra were obtained at equal concentrations).

by using method B, little exchange is observed for the H3/H5 position of 4,4′-bipyridine (**2a**). Another example is illustrated in Figure 3 for compounds **8a**−**c**. This figure shows that after use of method B only the pyridine H6 and the thienyl H5 are exchanged, while full exchange is obtained with method C. In general, with method B, only exchange at the positions adjacent to heteroatoms (e.g., N and S) takes place even with extended reaction times (see Tables 1 and 2). Pyrazyl groups (compounds **9a**−**12a**) readily undergo complete exchange. This is not unexpected because every position can be considered as analogous to the H2/H6 position of pyridine.

Under basic conditions, much less variation is observed in exchange rates at different positions, with thienyl, pyridyl, and pyrazyl groups showing complete H/D exchange. However, with this method, a significant level of control over the deuteriation of the aryl and pyridyl moieties in **5a** and **6a** can be achieved. It should be noted that with method C the regioselectively observed for **5a** is different than that observed with method B. This is discussed later in more detail.

Deuteriation of Aromatic and Aliphatic Groups. H/D exchange of methyl groups depends on the nature of the moiety to which they are attached. When bound directly to pyridyl (**3a**) or 1,2,4-triazole (**10a**, **14a**) groups, complete exchange occurs under all conditions examined (Tables 1 and 2). In contrast, methyl groups attached to phenyl rings (**12a**) show no exchange using method B but deuteriate completely in basic media and with method A. Phenyl (**5a**, **11a**, and **15a**) and tolyl groups (**12a**) are the least reactive moieties. No exchange of aromatic protons was observed using method B, but phenyl groups do exchange in the presence of Pd/C catalyst (method A). Using method C, complete exchange of both phenyl and methyl protons is observed, albeit at a much slower rate than for heteroaromatic groups.

Regioselective Deuteriation. The differences in the reactivities of the various moieties allow for the development of strategies for the regioselective isotope exchange. Two examples of how different methods can be combined to achieve particular selectively deuteriated compounds are shown in Schemes 1 and 2. Scheme 1 (and Table 1) illustrates the routes taken in the preparation of four isotopologues of 4,7-diphenyl-1,10-phenanthroline (ph_2phen), namely [D_6]-ph_2phen, [D_{10}]-ph_2phen, [D_{14}]-ph_2phen, and [D_{16}]-ph_2phen. H/D exchange of the phenyl groups is achieved in the presence of the Pd/C catalyst in neutral D_2O but occurs only very slowly in basic D_2O. Consequently, using method A, the D_{14}- isotopologue (**5d**) is obtained in good yield with excellent regioselectivity. Interestingly, it is the phenanthroline H5 and H6 positions, which do not exchange under these conditions. However, deuteriation of the complete phenanthroline moiety takes place using method C. The fact that these reactions are high yield and can be carried out on a gram scale opens the possibility to use the products obtained as materials for further reaction. Therefore, a reverse D/H exchange as shown in Scheme 1 becomes a viable option. With this approach, compounds such as **5c** can be prepared from **5d**. In this process, the moiety that is most easily exchanged, namely the phenanthroline grouping, is regenerated in the perprotio form.

In Scheme 2, the different reactivities of pyrazine, aromatic, and methyl groupings are illustrated. On the basis of the behavior observed in Scheme 1, it is surprising that the tolyl aromatic protons do not exchange in any significant manner using method A, and this suggests that the methyl group deactivates the tolyl ring toward H/D exchange. Exchange of these protons is more efficient in the presence of base, albeit at a slower rate than for methyl or pyrazinyl protons. In contrast to the results obtained for **3a** and **10a**, the protons of the methyl group in **12a** can be exchanged using method A, but not by the use of method B. Again, the reverse D/H exchange can be used to yield isotopologues, such as **12c**, **12d**, and **12f**, which contain deuterium atoms in positions, which undergo H/D exchange with most difficulty.

Scheme 1. Routes Examined in the Deuteriation of **5a**

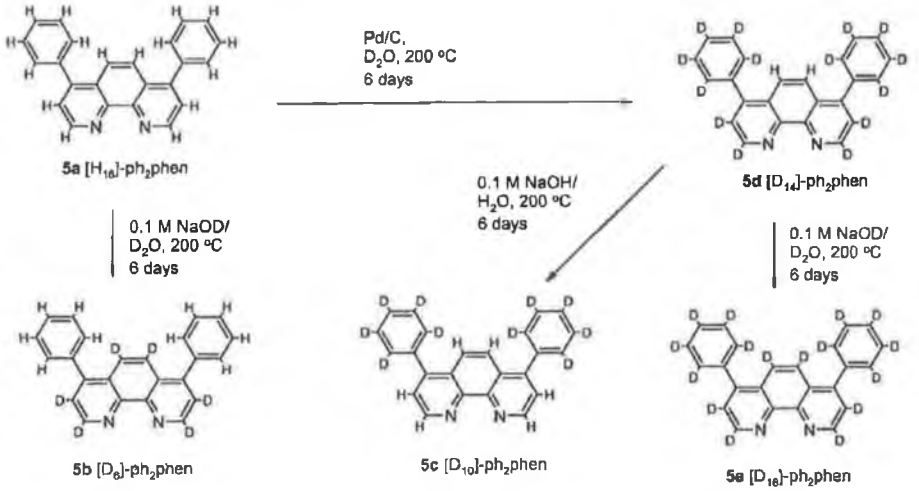

Scheme 2. Routes Examined for the Deuteriation of **12a**

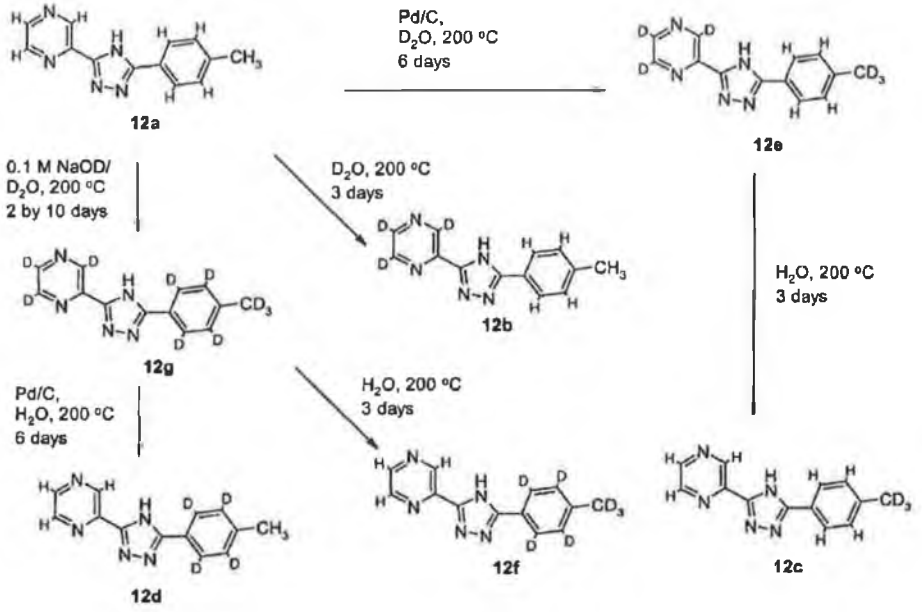

Application of Deuteriation in Supramolecular Systems. The effect of deuteriation on ^{1}H and ^{13}C NMR spectroscopy is already well-known.[3,4] Deuteriation results not only in a loss in intensity but also in the splitting of ^{13}C signals into multiplets. An example of this is shown in Figure 4, which shows the ^{13}C spectra for **4a** and **4b**. In the spectrum of **4b**, only the signals that can be attributed to the quaternized carbon atoms remain as singlets; the others appear as triplets. Selective deuteriation is therefore useful in the assignment of ^{13}C resonances.[3c] In addition, ^{2}D NMR spectroscopy can be used to monitor specific sites in complexes, which have complicated ^{1}H NMR spectra (see Figure 2 and Supporting Information). Furthermore, for large molecules such as ruthenium(II) and osmium(II) polypyridyl complexes, deuteriation has been shown to be very useful in simplifying ^{1}H NMR spectra,[3] and an example of this can be seen in Figure 5 (and Supporting Information), where ^{1}H NMR resonances are eliminated by selective deuteriation. The spectra shown illustrate how well-defined NMR based information can be obtained for compounds, which contain a large number of hydrogen atoms. It is also important to point out that no evidence for H/D exchange was observed, under the reaction conditions employed to prepare ruthenium complexes from deuteriated ligands.[9] This is in agreement with the observed temperature dependence of the deuteriation methods discussed, which indicates that no measurable exchange occurs below 140 °C.[19]

The application of deuteriation is not limited to structural characterization. Isotope exchange has found application as a probe for studying excited-state processes in transition metal complexes in time-resolved resonance Raman spectroscopy.[18] In addition, deuteriation has received considerable attention, in the study of the excited-state properties of rare earth ions and ruthenium(II) polypyridyl complexes.[4] Selec-

(19) O'Dwyer, U. MSc Thesis., Dublin City University, Dublin, Ireland, 1997.

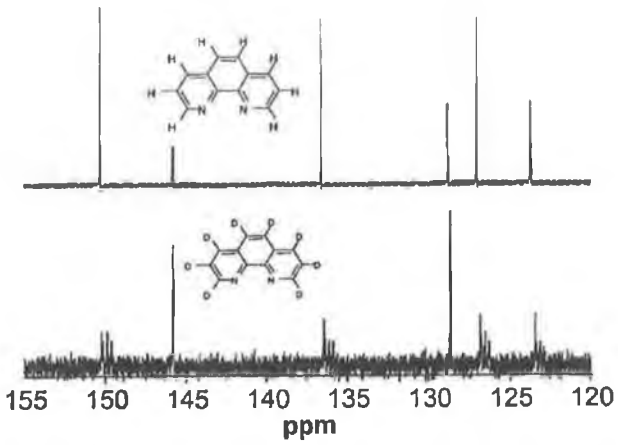

Figure 4. ^{13}C (proton decoupled) NMR spectra of [H_8]-1,10-phenanthroline (**4a**) (upper spectrum) and [D_8]-1,10-phenanthroline (**4b**) (lower spectrum) in [D_6]-DMSO.

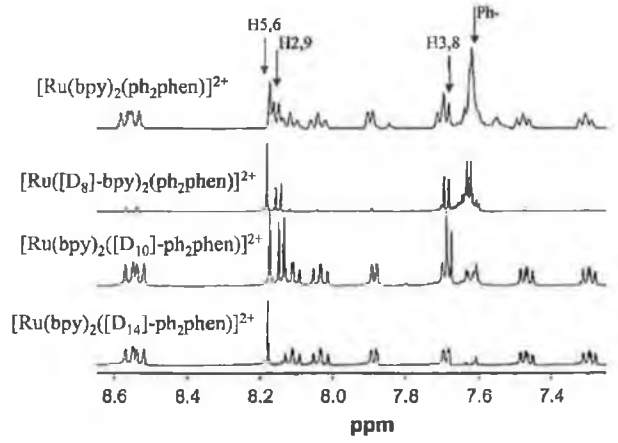

Figure 5. ^1H NMR spectra (400 MHz) of [Ru([D_x]-bpy)([D_y]-ph_2phen)]-$(PF_6)_2$ in [D_3]-acetonitrile. ($x = 0$ or 8, $y = 10$, 14, 16). Resonances due to ph_2phen ligand are indicated.

tive deuteration of mixed ligand complexes was shown to yield important information about the location of the emitting state in mixed ligand complexes by its effect on emission lifetime.[7,8] For example, this approach can now be applied in the study of 2,3-bis(pyrid-2′-yl)-pyrazine (**7a**) based multinuclear ruthenium and osmium based bis(bipyridyl) complexes.[20] Deuteration of either **7a** or **1a** would allow for the detailed study of the possible isomers present, and selective deuteration could also be used to study the excited-state behavior of such compounds.

Limitations. During the course of this study, 1,2,4-triazines and compounds containing functional groups (e.g., carboxylic acids, esters, and carbonitriles) were found to decompose under the conditions employed. However, the deuteration of relatively large amounts of material (up to 3 g in this study), coupled with high yields, allows for the preparation of a much larger range of deuteriated compounds through the deuteration of precursors in synthetically useful amounts. Therefore, the preparation of perdeuteriated compounds containing thermally unstable functional groups such as carboxylic acids, carbonitriles, amides, and so forth may be achieved indirectly via perdeuteriated methyl precursors (e.g., [D_6]-4,4′-dicarboxy-2,2′-bipyridine can be prepared from **3b**).

(20) Campagna, S.; Giannetto, A.; Serroni, S.; Denti, G.; Trusso, S.; Mallamace, F.; Micalli, N. *J. Am. Chem. Soc.* **1995**, *117*, 1754.

Conclusions

In this contribution, a general approach to the deuteration of heteroaromatic compounds is described. The potential for regioselective deuteration is identified. The procedures employed allow for the reduction and often the complete elimination of the requirement for catalysts or derivatization (e.g., via *N*-oxide intermediates[5]) and much improved yields. The applicability of deuteration in inorganic photophysics and supramolecular chemistry is already well-known.[4] However, its use has been severely limited by the cost and difficulty in preparing well-defined deuteriated materials. In this regard, the methods described here allow for the widespread application of deuteration in such studies and provide an additional tool for the study of the spectroscopic and photophysical properties of supramolecular compounds.

Experimental Section

Materials. All reagents for synthesis were used as received without further purification. D_2O (99.9%) and 10% w/w Pd/C (Sigma-Aldrich) were used as received. NaOD/D_2O solution (1 M) was prepared in situ by addition of 460 mg of sodium metal to 20 mL of D_2O. 2,2′-Bipyridine (**1a**), 4,4′-bipyridine (**2a**), 4,4′-dimethyl-2,2′-bipyridine (**3a**), 1,10-phenanthroline (**4a**), 4,7-diphenyl-1,10-phenanthroline (ph_2phen) (**5a**), 2,2′-biquinoline (**6a**) (Sigma-Aldrich), and 2-(thien-2′-yl)-pyridine (2-thpy) (**8a**) (Lancaster) were obtained from commercial sources and used as received without further purification. The syntheses of 2,3-bis(pyrid-2′-yl)-pyrazine (**7a**),[21] 3-(pyrazin-2′-yl)-1,2,4-triazole (Hpztr) (**9a**), 3-methyl-5-(pyrazin-2′-yl)-1,2,4-triazole (Hmepztr) (**10a**), 3-(pyridin-2′-yl)-1,2,4-triazole (Hpytr) (**13a**), 3-methyl-5-(pyridin-2′-yl)-1,2,4-triazole (Hmepytr) (**14a**),[22] and 3-phenyl-5-(pyridin-2′-yl)-1,2,4-triazole (Hphpytr) (**15a**)[7] have been carried out using previously reported procedures. [Ru(bpy)$_3$]$(PF_6)_2$,[23] [Ru(d_x-bpy)$_2$(d_y-ph_2phen)]$(PF_6)_2$,[24] and [Ru(bpy)$_2$(**11a**)]$(PF_6)_2$[25] (where bpy = **1a**, ph_2phen = **5a**, x = 0 or 8 and y =0, 10, and 14) were prepared by literature procedures. The compounds 3-phenyl-5-(pyrazin-2′-yl)-1,2,4-triazole (Hphpztr) (**11a**) and 3-tolyl-5-(pyrazin-2′-yl)-1,2,4-triazole (Htolpztr) (**12a**) were carried out by previously reported procedures.[22]

Hydrogen−Deuterium Exchange Reactions. H−D exchange reactions were carried out using a Teflon cup contained in a general purpose dissolution Bomb P/N 4744 from Scientific Medical Products. Typical examples of each reaction type A−F are given in following paragraphs. Spectroscopic data for each partially and fully deuteriated compound are summarized as Supporting Information. In the case of method A, the solvent employed to remove deuteriated compound from the catalyst varied depending on the solubility of the compound. The extent of isotope exchange was determined from the isotopic pattern of the mass spectra of the compounds and by comparison of the ^1H NMR spectra of the

(21) Goodwin, H. A.; Lions, F. *J. Am. Chem. Soc.* **1959**, *81*, 6415.
(22) Hage, R. Ph.D. Thesis, Leiden University, The Netherlands, 1991.
(23) Casper, J. V.; Meyer, T. J. *J. Am. Chem. Soc.* **1983**, *105*, 5583.
(24) Baggot, J.; Gregory, G.; Piling, M.; Anderson, S.; Seddon, K. R.; Turp, J. *J. Chem. Soc., Faraday Trans. 2* **1983**, *79*, 195.
(25) Browne, W. R.; Guckian, A.; Vos, J. G. To be published.

deuteriated compound with its perprotio analogue at known concentrations using the residual solvent peak as an internal standard.

Method A. [D_8]-2,2′-Bipyridine (1b). 2,2′-Bipyridine (**1a**) (3 g) was reacted with 50 mg of 10% Pd/C in 20 mL of D_2O at 200 °C under pressure for 3 days. On cooling, the reaction mixture was filtered, and the catalyst was washed with 2 × 50 mL of diethyl ether to remove any 2,2′-bipyridine from the catalyst surface. The diethyl ether washings and the aqueous filtrate were evaporated to dryness to yield [D_8]-2,2′-bipyridine. It should be noted that with this method yields are sometimes lower than quantitative because of difficulty in removing the product from the catalyst.

Method B. [D_3]-Hphpztr (11b). A 1 g portion of 3-phenyl-5-(pyrazin-2-yl)-1,2,4-triazole (**11a**) was reacted at 200 °C in 20 mL of D_2O for 3 days. After cooling, the compound precipitated and was filtered and air-dried.

Method C. [D_4]-Hphpytr (15c). A 1.5 g portion of 3-phenyl-5-(pyridin-2-yl)-1,2,4-triazole (**15a**) was reacted at 200 °C in 20 mL of 1 M NaOD/D_2O for 3 days. On cooling, the reaction mixture was neutralized with concentrated HCl. and the white precipitate was filtered and air-dried.

Method D. [D_5]-Hphpytr (15d). A 0.5 g portion of [D_9]-3-phenyl-5-(pyridin-2-yl)-1,2,4-triazole (**15e**) was reacted at 200 °C in 20 mL of 1 M NaOH/H_2O for 3 days. On cooling, the reaction mixture was neutralized with concentrated HCl, and the white precipitate was filtered and air-dried.

Method E. [D_5]-Hphpztr (11c). A 0.5 g portion of [D_8]-3-phenyl-5-(pyrazin-2-yl)-1,2,4-triazole (**11d**) was reacted at 200 °C in 20 mL of H_2O for 3 days. On cooling the reaction mixture, the white precipitate was filtered and air-dried.

Method F. As for method A except H_2O was used in place of D_2O.

^{1}H,^{13}C, and ^{2}D NMR Spectroscopic and Mass Spectral Data. Assignments of ^{1}H and ^{2}D NMR resonances were made by comparison with assignments made for ^{1}H NMR spectra of their perprotio analogues and are available as Supporting Information. Assignments of ^{13}C spectra were made on the basis of comparison with assignments made for their perprotio analogues using HMQC and HMBC NMR experiments and on the basis of the loss of intensity and splitting upon deuteriation. ^{1}H, ^{2}D, ^{13}C and ^{1}H COSY, HMQC, and HMBC spectra were recorded on a Bruker Avance 400 (400 MHz) NMR spectrometer equipped with a QNP probe (a broad band probe was employed for ^{2}D NMR spectroscopy). All measurements were carried out in [D_6]-acetone or [D_6]-dimethyl sulfoxide. ^{2}D NMR spectra were acquired in [H_6]-acetone or [H_6]-dimethyl sulfoxide. Peak positions are relative to residual solvent peaks. Mass spectra were obtained using a Bruker-Esquire-LC_00050 electrospray ionization mass spectrometer at positive polarity with cap-exit voltage of 167 V. Spectra were recorded in the scan range of 50−2200 *m/z* with an acquisition time of between 300 and 900 μs and a potential between 30 and 70 V. Each spectrum was recorded by summation of 20 scans. The limited solubility of some compounds precluded the measurement of their ^{2}D and ^{13}C NMR spectra.

Acknowledgment. The authors thank Enterprise Ireland for financial support.

Supporting Information Available: ^{1}H NMR spectra and characterization information. This material is available free of charge via the Internet at http://pubs.acs.org.

IC020226Y

DALTON
FULL PAPER

Synthesis, spectroscopic and electrochemical properties of mononuclear and dinuclear bis(bipy)ruthenium(II) complexes containing dimethoxyphenyl(pyridin-2-yl)-1,2,4-triazole ligands†

Paolo Passaniti,[a] Wesley R. Browne,[b] Fiona C. Lynch,[b] Donal Hughes,[b] Mark Nieuwenhuyzen,[c] Paraic James,[d] Mauro Maestri[a] and Johannes G. Vos*[b]

[a] *Dipartimento di Chimica "G.Ciamician", University of Bologna Via Selmi 2, 40126 Bologna, Italy*
[b] *National Centre for Sensor Research, School of Chemical Sciences, Dublin City University, Dublin 9, Ireland. E-mail: johannes.vos@dcu.ie*
[c] *School of Chemistry, Queen's University of Belfast, Belfast, Northern Ireland, UK BT9 5AG*
[d] *National Institute for Cellular Biotechnology, Dublin City University, Dublin 9, Ireland*

Received 25th September 2001, Accepted 12th February 2002
First published as an Advance Article on the web 26th March 2002

The ligands **HL1** and H_2**L2** and the complexes $[Ru(bipy)_2L1]PF_6 \cdot 2H_2O$ **1**, $[(Ru(bipy)_2)_2L2](PF_6)_2 \cdot 7H_2O$ **2**, {where **HL1** = 3-(2′,5′-dimethoxyphenyl)-5-(pyridin-2″-yl)-1H-1,2,4-triazole, H_2**L2** = 1,4-bis(5′-(pyridin-2″-yl)-1′H-1′,2′,4′-triazol-3′-yl)-2,5-dimethoxybenzene and bipy = 2,2′-bipyridyl}, have been prepared and characterised, by NMR, UV–vis and emission spectroscopies and by electrochemical measurements. X-Ray crystal structures of ligands **HL1**, H_2**L2** and of the complex **1** are also reported. The dinuclear complex (**2**) exhibits a weak electronic interaction between the metal centres, which is modulated by the protonation state of the 1,2,4-triazole rings. The extent of the metal–metal interaction in these systems is compared with that observed in other pyridyl-1,2,4-triazole based dinuclear compounds of differing metal–metal distances.

Introduction

Ruthenium(II) polypyridyl complexes are of interest for their spectroscopic, photophysical, photochemical, and electrochemical properties.[1–3] These properties are of particular use in the construction of supramolecular systems and photochemically driven molecular devices.[4,5] Ruthenium(II) polypyridyl complexes have also received extensive attention as models for photo-system II and in the catalytic photochemical cleavage of water.[6]

Of particular interest is the design of multinuclear structures capable of directing and modulating electron and energy transfer processes.[4,5] In this regard many studies of ruthenium complexes covalently bound to electron acceptors or donors have been reported. The general approach taken in electron transfer studies has been to bind the electron acceptor/donor to the ruthenium polypyridyl centre *via* the polypyridyl ligands.[7–9] However, since the excited state in such compounds is normally based on these ligands a strong coupling between the metal centre and the electron donor/acceptor is usually observed, which precludes a long-lived charge separation.[9,10] In our laboratories we have taken a different approach aimed at weakening the direct electronic coupling between the electron donor/acceptor and the sensitiser, consequently slowing down the back reaction and achieving a longer lived charge separated state.[11] This approach is based on the attachment of groupings to spectator ligands, such as 3-(pyridin-2′-yl)-1,2,4-triazoles. In addition, the pH dependent properties of the 1,2,4-triazole ligands are shown to be useful in applications such as molecular switches.[12]

Due to its role as redox relay in biological systems, the hydroquinone/quinone redox couple is of particular interest. In an earlier study on ruthenium polypyridyl complexes incorporating pyridyltriazole ligands with pendent hydroquinone groupings an electrochemically induced intramolecular protonation of the ruthenium centre was observed upon oxidation of the hydroquinone.[13] We are presently involved in a systematic study of this unusual observation and also of the photophysical properties of molecular dyads of this type. In the present contribution, the spectroscopic and electrochemical properties of the mono-nuclear complex **1** based on the $Ru(bipy)_2$-complex of 3-(2′,5′-dimethoxyphenyl)-5-(pyridin-2″-yl)-1H-1,2,4-triazole (**HL1**) and the dinuclear complex **2** based on the $Ru(bipy)_2$-complex of 1,4-bis(5′-(pyridin-2″-yl)-1′H-1′,2′,4′-triazol-3′-yl)-(2,5-dimethoxybenzene) (H_2**L2**) are reported (bipy = 2,2′-bipyridyl). The electrochemical, spectroelectrochemical and photophysical properties of the compounds are compared with those reported for analogous mononuclear and dinuclear complexes based on 3-(pyridin-2′-yl)-1H-1,2,4-triazole (Hpytr) (**3**) and 3,5-bis(pyridin-2′-yl)-1H-1,2,4-triazole (Hbpt) (**4**). For structures of complexes **1**–**4** see Fig. 1. The compounds reported are synthetic precursors to the analogous hydroquinone/quinone compounds and serve as model compounds. The results obtained for the hydroquinone/quinone analogues will be reported in a further publication.

Experimental

Materials

All solvents employed were of HPLC grade or better and used as received unless otherwise stated. For all spectroscopic measurements Uvasol (Merck) grade solvents were employed. All reagents employed in synthetic procedures were of reagent grade or better. *Cis*-$[Ru(bipy)_2Cl_2] \cdot 2H_2O$,[14] (pyridin-2-yl)-

† Electronic supplementary information (ESI) available: figures showing the molecular structures and intermolecular interactions for **HL1** and H_2**L2**; ^{1}H COSY NMR spectrum of **2**. See http://www.rsc.org/suppdata/dt/b1/b108728m/

 DOI: 10.1039/b108728m

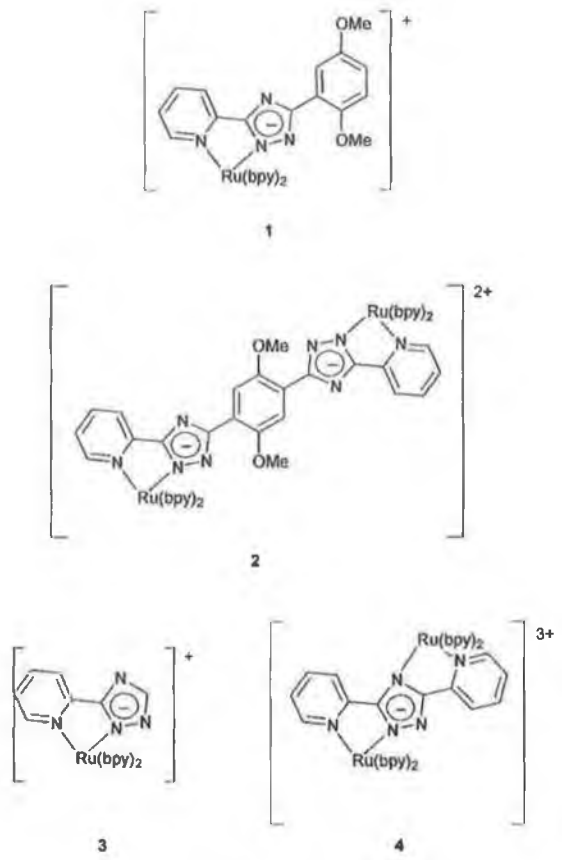

Fig. 1 Structures of compounds **1**–**4**.

amidrazone and tetraethylammoniumperchlorate (TEAP)[15] were prepared by previously reported procedures.

Syntheses

3-(2′,5′-Dimethoxyphenyl)-5-(pyridin-2″-yl)-1H-1,2,4-triazole (HL1). 2,5-Dimethoxybenzoic acid (10 g, 55 mmol) and PCl_5 (11.45 g, 55 mmol) were reacted together to form a clear yellow product. The $POCl_3$ formed was removed by distillation with slight heating (40 °C) under a weak vacuum leaving a clear yellow liquid, which crystallised overnight under vacuum. The acid chloride (11.03 g, 50 mmol) formed was dissolved in 30 cm^3 of dry tetrahydrofuran and added dropwise to (pyridin-2-yl)amidrazone (6.85 g, 50 mmol) and sodium carbonate (2.65 g, 25 mmol) in 40 cm^3 of tetrahydrofuran, resulting in immediate precipitation of the pale yellow acylamidrazone. The reaction mixture was stirred for a further 4 h and the yellow product collected by vacuum filtration and stirred in ice water for 30 min followed by recovery using vacuum filtration. The yellow product was dried overnight at 80 °C. Yield of 1-(2′,5′-dimethoxyphenyl)-4-(pyridin-2″-yl)acylamidrazone: 10.95 g, (73%), mp 190 °C. The amidrazone (6 g, 20 mmol) was dissolved in a minimum of ethylene glycol and heated at reflux for 30 min. On cooling, the ligand **HL1** precipitated from solution and was collected by filtration. The product was decolourised over charcoal and crystallised from dichloromethane. Yield: 3.4 g, 60%. ^{1}H NMR (d_6-acetone): δ 12.54 (1H, s), 8.69 (1H, d, 3.9 Hz), 8.20 (1H, d, 7.9 Hz), 7.87 (1H, t, 7.9 Hz), 7.82 (1H, s, 3.0 Hz), 7.39 (1H, t, 4.9 Hz), 7.12 (1H, d, 9.9 Hz), 7.04 (1H, dd, 3.0 Hz, 8.9 Hz), 3.99 (3H, broad s), 3.83 (3H, s). Elemental analysis: Found (Calc. for $C_{15}H_{14}N_4O_2$) C 63.62 (63.83), H 5.15 (4.96), N 18.74 (19.86)%.

1,4-Bis(5′-(pyridin-2″-yl)-1′H-1′,2′,4′-triazol-3′-yl)-2,5-dimethoxybenzene (H_2L2). Diethyl-2,5-dihydroxyterephthalate (5.09 g, 20 mmol) and potassium carbonate (13.8 g, 100 mmol) were stirred with 100 cm^3 dry acetone in a flask fitted with reflux condenser and $CaCl_2$ drying tube. Iodomethane (14.2 g, 100 mmol) was added and the mixture heated to reflux for 48 h. The reaction was followed by TLC (mobile phase: pet. ether (40/60) : diethyl ether 2 : 1 v/v). On cooling, the white precipitate was filtered and washed with acetone. Yield of diethyl-2,5-dimethoxyterephthalate: 5.36 g (95%). ^{1}H NMR (d_1-chloroform): δ 7.36 (1H, s), 4.36 (2H, q, 7.4 Hz), 3.87 (3H, s), 1.37 (3H, t, 7.4 Hz).

Diethyl-2,5-dimethoxyterephthalate (5 g, 18 mmol) was added to 5 g (9 mmol) of potassium hydroxide in 15 cm^3 ethylene glycol, and heated at 100 °C until the mixture became homogenous. The ethanol formed during heating was removed by distillation at reduced pressure. The reaction mixture was then cooled, H_2O (20 cm^3) was then added and the reaction mixture was made slightly acidic by the addition of 20% H_2SO_4, which resulted in a white precipitate of 2,5-dimethoxyterephthalatic acid forming. This was filtered and washed with water (10 cm^3) and then acetone (5 cm^3). The 2,5-dimethoxyterephthalatic acid was dried in a Kugelrohr apparatus *in vacuo* over P_2O_5 at 100 °C. Yield: 3.9 g (94%), mp 265 °C. ^{1}H NMR (d_6-dimethylsulfoxide): δ 7.28 (1H, s), 3.77 (3H, s).

Phosphorous pentachloride (6.25 g, 30 mmol) was added to 2,5-dimethoxyterephthalic acid (3.5 g, 15 mmol) and the solids stirred with gentle heating. After evolution of gas had ceased, the phosphoryl oxychloride was removed by distillation at normal pressure and then under reduced pressure. The 2,5-dimethoxyterephthaloyl dichloride (3.95 g, 15 mmol) formed was dissolved in 50 cm^3 tetrahydrofuran and added with stirring to a solution of (pyridin-2-yl)amidrazone (4.76 g, 35 mmol) and sodium carbonate (1.59 g, 15 mmol) in 30 cm^3 of dry tetrahydrofuran at 0 °C. After stirring for 24 h, the reaction contents were added to 100 g of ice water and stirred for 30 min. The yellow solid was filtered, washed with water and acetone, and dried under vacuum. Impurities were removed by heating the crude product in dimethylsulfoxide, filtering and washing with acetone (10 cm^3). Yield of 1,4-bis(acylpyridin-2′-ylamidrazone)-2,5-dimethoxybenzene: 5 g (10 mmol, 67%), mp 189 °C. ^{1}H NMR (d_6-dimethylsulfoxide): δ 10.21 (2H, s, –NH), 8.61 (2H, d, 5.6 Hz, H6), 8.17 (2H, d, 7.4 Hz, H3), 7.76 (2H, t, 7.4 Hz, H4), 7.50(2H, t, 7.4 Hz, H5), 7.38 (2H, s, Benz-H), 6.81(4H, s, $-NH_2$), 4.03 (6H, s, $-OCH_3$).

1,4-Bis(acylpyridin-2′-ylamidrazone)-2,5-dimethoxybenzene (5 g, 10 mmol) was heated to reflux in ethylene glycol until the reaction mixture turned to a clear brown colour. The product (**H_2L2**), a tan solid, precipitated from solution overnight and was recrystallised from dimethylsulfoxide. Yield of **H_2L2**: 2.3 g (5.4 mmol, 54%). ^{1}H NMR (d_6-dimethylsulfoxide): δ 14.11 (2H, broad s, –NH), 8.70 (2H, broad s, H6), 8.18 (2H, d, H3), 7.94 (4H, broad s, H4 and Benz-H); 7.47 (2H, s, H5); 4.03 (6H, broad s, $-OCH_3$). Elemental analysis: Found (Calc. for $C_{22}H_{18}N_8O_2 \cdot 1H_2O$) C 59.46 (59.46), H 4.20 (4.50), N 25.42 (25.23)%.

[Ru(bipy)$_2$(L1)]PF$_6$·2H$_2$O (1). *Cis*-[Ru(bipy)$_2$Cl$_2$]·2H$_2$O (370 mg, 0.71 mmol) and **HL1** (200 mg, 0.71 mmol) were heated at reflux for 8 h in 150 cm^3 EtOH–H_2O (2 : 1 v/v). The hot solution was filtered and evaporated to dryness after which 10 cm^3 of water was added to the dark red product. **1** was precipitated with an excess aqueous solution of NH_4PF_6. The product was purified by column chromatography with activated neutral alumina (Brockmann 1, std grade, 150 mesh, Aldrich) and acetonitrile as eluent. The product obtained was recrystallised from acetone–H_2O (with 1 drop of conc. ammonia). Single crystals for X-ray structure determination were grown from an acetone solution of the product. Yield: 495 mg (82%). ^{1}H NMR (d_3-acetonitrile). δ 8.45 (2H, t, 8.9 Hz), 8.38 (2H, t, 8.9 Hz), 8.08

Table 1 X-Ray experimental crystal data for **HL1**, H_2L2 and **1**

	HL1	H_2L2	1
Empirical formula	$C_{15}H_{14}N_4O_2$	$C_{28}H_{18}N_8O_2$	$C_{38}H_{35}F_6N_8O_3PRu$
M/g mol^{-1}	282.30	426.44	897.78
T/K	293(2)	153(2)	293(2)
Wavelength/Å	1.54178	0.71073	1.54178
Crystal system, space group	Monoclinic, $P2_1/n$	Monoclinic, $P2_1/c$	Triclinic, $P\bar{1}$
a/Å, α/°	10.664(2), 90	9.235(3), 90	11.704(7), 69.92
b/Å, β/°	17.689(7), 96.96	11.636(3), 106.44	12.915(7), 88.60
c/Å, γ/°	15.057(3), 90	10.096(3), 90	15.631(9), 63.14
V/Å^3, Z	2819.4(14), 8	1040.5(5), 2	1956(2), 2
Crystal dimensions/mm	0.85 × 0.19 × 0.12	0.76 × 0.21 × 0.30	0.32 × 0.11 × 0.15
μ/mm^{-1}	0.754	0.093	4.358
No. reflections collected	3763	1853	7006
Independent reflec. (R_{int})	3540 (0.0549)	1359 (0.0528)	4917 (0.0501)
Final R indices [$I > 2\sigma(I)$] $R1$ ($wR2$)	0.065 (0.1599)	0.0610 (0.0991)	0.0655 (0.1639)
R indices all data $R1$ ($wR2$)	0.1103 (0.1952)	0.1398 (0.1258)	0.0761 (0.1724)

(1H, d, 7.9Hz, H3), 7.95 (7H, m, containing H4), 7.79 (2H, t, 4.9 Hz), 7.51 (1H, d, 5.9 Hz, H6), 7.42(1H, t, 6.9 Hz), 7.38 (2H, t, 5.9 Hz), 7.27 (1H, t, 5.9 Hz), 7.20 (1H, d, 2.9 Hz, H3″), 7.12 (1H, t, 6.9 Hz, H5), 6.93 (1H, d, 8.9 Hz, H6″), 6.83 (1H, dd, 2.9 Hz, 8.9, H5″), 3.71(3H, s, –OCH_3 1″), 3.61(3H, s, –OCH_3 4″). Elemental analysis: Found (Calc. for $C_{35}H_{33}N_8O_4PF_6Ru$) C 48.2 (48.0), H 4.0 (3.8), N 12.4 (12.8)%.

[(Ru(bipy)$_2$)$_2$(L2)](PF$_6$)$_2$·7H$_2$O (2). **2** was prepared in a similar manner to **1**, except that 0.25 g (0.48 mmol) of *cis*-[Ru(bipy)$_2$(Cl)$_2$]·2H$_2$O was heated at reflux with 0.1 g (0.24 mmol) of H_2L2. Yield: 0.32 g (89%). ^{1}H NMR (d_3-acetonitrile): δ 8.47 (2H, d, 7.4 Hz), 8.68 (2H, d, 7.4Hz), 8.59 (4H, t, 7.4 Hz), 8.29 (2H, d, 7.4 Hz, H3), 8.07 (8H, m), 7.96 (10H, m, H4), 7.71 (2H, d, 5.5 Hz, H6), 7.50 (8H, m, Benz-H), 7.37 (2H, t, 7.4 Hz), 7.24 (2H, t, 7.4 Hz, H5), 3.54 (6H,s,–OCH_3). Elemental analysis: Found (Calc. for $C_{62}H_{62}N_{18}O_9P_2F_{12}Ru_2$) C 44.7 (44.65), H 3.4 (3.72), N 13.1 (13.44)%.

Elemental analysis was performed at the Microanalytical Laboratory at University College Dublin.

X-Ray crystallography

Data for **HL1**, H_2L2 and **1** were collected on a Siemens P4 diffractometer using the XSCANS[16] software with graphite monochromated Mo-K_α radiation (Table 1) Relevant experimental data is presented in Table 1.

The structures were solved using direct methods and refined with the SHELXTLPC and SHELXL-93 program packages[17] and the non-hydrogen atoms were refined with anisotropic thermal parameters.

CCDC reference numbers 171755–171757.

See http://www.rsc.org/suppdata/dt/b1/b108728m/ for crystallographic data in CIF or other electronic format.

NMR spectroscopy

^{1}H and ^{1}H COSY spectra were recorded on a Bruker AC400 (400 MHz) NMR spectrometer. All measurements were carried out in d_6-dimethylsulfoxide, d_1-chloroform or d_6-acetone for ligands and d_3-acetonitrile for complexes. Peak positions are relative to residual solvent peaks.

Photophysical measurements

UV-vis absorption spectra were recorded on a Shimadzu UV.vis-NIR 3100 spectrophotometer interfaced with an Elonex-466 PC using UV-vis data manager software. Emission spectra were recorded using a LS50-B Luminescence spectrophotometer, equipped with a red sensitive Hamamatsu R928 PMT detector, interfaced with an Elonex-466 PC using Windows based fluorescence data manager software. Emission/excitation slit widths were 5 nm. Emission spectra are uncorrected for photomultiplier response. 1 cm path length quartz cells were used for recording spectra. Luminescence lifetime measurements were obtained using an Edinburgh Analytical Instruments (EAI) Time Correlated Single Photon Counting apparatus (TCSPC) comprising of two model J-yA monochromators (emission and excitation), a single photon photomultiplier detection system model 5300, and a F900 nanosecond flashlamp (N_2 filled at 1.1 atm pressure), interfaced with a personal computer *via* a Norland MCA card. Data correlation and manipulation was carried out using EAI F900 software version 5.1.3. Emission lifetimes were calculated using a single exponential fitting function (Edinburgh instruments F900 software). pH titrations of **1** and **2** were carried out in Britton–Robinson buffer (0.04 M H_3BO_3, 0.04 M H_3PO_4, 0.04 M CH_3CO_2H) (pH was adjusted using concentrated sulfuric acid or sodium hydroxide solution). The appropriate isosbestic point from the absorption spectra was used as the excitation wavelength for emission titrations.

Electrochemical and spectroelectrochemical measurements

Electrochemical measurements were carried out on a Model 660 Electrochemical Workstation (CH Instruments). Typical complex concentrations were 0.5 to 1 mM in anhydrous acetonitrile (Aldrich 99.8%) containing 0.1 M TEAP. A Teflon shrouded glassy carbon working electrode, a Pt wire auxiliary electrode and SCE reference electrode were employed. Solutions for reduction measurements were deoxygenated by purging with N_2 or Ar gas for 15 min prior to the measurement. Measurements were made in the range of −2.0 to 2.0 V (w.r.t SCE electrode). Protonation of complexes was achieved by addition of 0.1 M trifluoroacetic acid (in acetonitrile) to the electrolyte solution. The scan rates used were typically 100 or 200 mV s^{-1}. Spectroelectrochemistry was carried out using an OTTLE set-up comprising of a home made Pyrex glass, thin layer cell (1 mm pathlength). The optically transparent working electrode was made from platinum–rhodium gauze, the counter electrode used was a platinum wire, and the reference electrode was a pseudo Ag/AgCl reference electrode. 0.1 M TEAP in anhydrous acetonitrile was used as electrolyte. The working electrode was held at the required potential throughout the measurement using an EG&G PAR Model 363 potentiostat. Absorption and emission spectra were recorded as described above.

Results and discussion

As noted in the introduction, the ultimate aim of our investigations is the study of metal complexes having pendent hydroquinone or quinone groupings. In earlier studies hydroquinone type ligands such as the hydroquinone analogue of **HL1**, 3-(2′,5′-dihydroxyphenyl)-5-(pyridin-2″-yl)-1,2,4-triazole were

prepared directly using 2,5-dihydroxybenzoic acid.[13] With this approach however, low yields were generally obtained. For this reason a new synthesis has been developed based on methoxy precursors with subsequent deprotection of these groups to form the required hydroquinone complex. In this contribution we report on the synthesis and properties of these dimethoxy-'protected' complexes. The synthesis of the ligands **HL1** and H_2**L2** and complexes **1** and **2** (Fig. 1) have been carried out by modification of general procedures.[18] In this manner dimethoxy precursors can be obtained in high yield.

X-Ray crystallography

The molecular structures obtained for **HL1** and H_2**L2** confirm the structural features of the two ligands. Figures showing the molecular structure and intermolecular interactions are given as ESI.† The molecular structure of **1** is shown in Fig. 2. In the

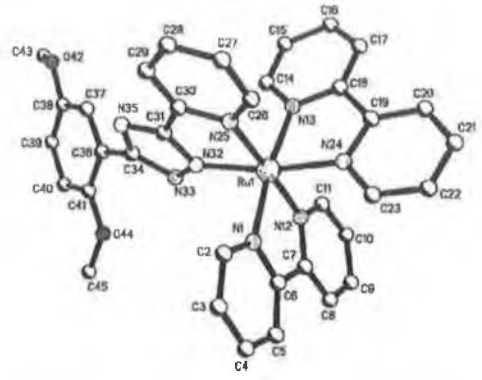

Fig. 2 Molecular structure and labelling scheme for **1**.

X-ray analysis of **1** the protons on one of the methoxy groups are disordered. Complex **1** cocrystallised with a molecule of acetone and a hexafluorophosphate counter anion. From the crystal structure it is clear that the ligand is bound through the pyridine-N and N2 of the triazole ring (or *via* N(25) and N(32)). The bite angle of the N(25)–Ru(1)–N(32) is 77.8(2)°, which corresponds well with the bite angle of 77.9(1)° obtained by Hage *et al.* for [Ru(bipy)$_2$(3-(2-hydroxy-phenyl)-5-(pyridin-2-yl)-1,2,4-triazole)]PF_6·CH_3COCH_3.[19] Bite angles of 79.5(3) and 78.8(3)° for bipyridine ligands and Ru–N distances of 2.033(7)–2.098(7) Å are also comparable to those found in other complexes.[19,20] Ru(1)–N(25) at 2.098(7) Å is the longest Ru–N bond in the complex. One factor contributing to this increased length is limited π-backbonding to the π-electron rich 1,2,4-triazole ring from the metal centre. The intermolecular X-ray structure is dominated by interaction between two C(3)–H atoms and the N2 nitrogen of the triazole ring forming a hydrogen bonded dimer (Fig. 3). The dimers form a three-dimensional network *via* π ··· π interactions and hydrogen bonding involving the bipy and pyridyltriazole ligands. The packing of these dimers creates cavities within the lattice in which the PF_6 anions and acetone molecules are located.

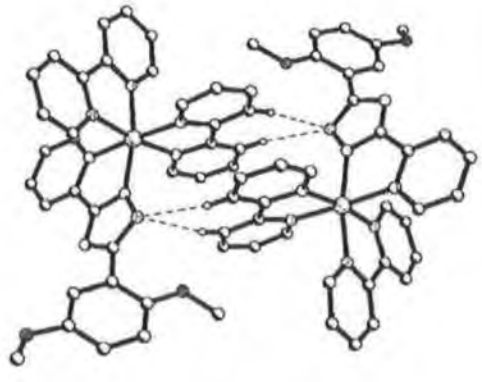

Fig. 3 Diagram of the hydrogen bonded dimer for **1**.

^{1}H NMR spectroscopy

^{1}H NMR spectra have been used extensively to determine the coordination mode of pyridyltriazoles and other types of chelating ligands.[21] The spectra obtained for **1** and **2** are shown in Fig. 4. Due to the complexity of the ^{1}H NMR spectra of the

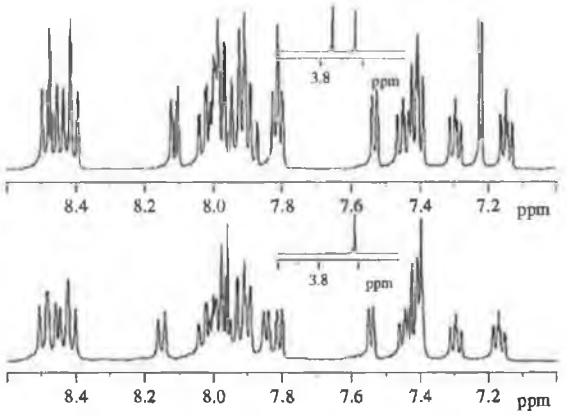

Fig. 4 ^{1}H NMR spectra of **1** (upper spectrum) and **2** (lower spectrum) in d_3-acetonitrile (400 MHz). –OCH_3 signals are shown as insets.

complexes ^{1}H COSY NMR spectroscopy (see ESI†) has been performed of both ligands and complexes and the spectra have been assigned by comparison with data previously reported for similar ligands and complexes.[21] It is worth pointing out that for **1** two non-equivalent methoxy signals are observed at 3.61 and 3.74 ppm. The spectrum obtained for **2** is strikingly simple. The dinuclear compound obtained is clearly highly symmetric as indicated by the presence of only one methoxy signal at 3.64 ppm and by the fact that the phenyl protons are equivalent and found as a singlet at 7.40 ppm. In contrast for the mononuclear complex **1** the three phenyl protons are all non-equivalent and appear at 6.83, 6.93 and 7.20 ppm. The crystal structure obtained for **1** (Fig. 2) shows that the coordination mode of the triazole ring in this compound is *via* the N2 nitrogen atom. For **3** it has been shown previously that the ^{1}H NMR spectra of the N2 and N4 bound coordination isomers are significantly different.[21] The symmetric ^{1}H NMR of **2** together with steric considerations and its similarity with the spectrum of **1**, point therefore strongly to a N2 coordination of both the 1,2,4-triazole rings in the dinuclear species.

Photophysical and acid–base properties

The photophysical data obtained for **1** and **2** are summarised in Table 2, together with data for $[Ru(bipy)_3]^{2+}$ and complexes **3** and **4** for comparison. For both **1** and **2**, the absorption and emission maxima are red-shifted with respect to $[Ru(bipy)_3]^{2+}$ [1] but are in agreement with those reported for **3** and **4**.[21] This is not unexpected as π-electron rich 1,2,4-triazole containing ligands such as **HL1** and H_2**L** are stronger σ-donors and weaker π-acceptors than 2,2′-bipyridine and destabilise the filled metal d-orbitals and hence raise the energy of the ground state metal based orbitals.[21] On protonation of both **1** and **2** a blue shift of both the lowest energy absorption bands and the emission maxima are observed, as would be expected due to the stabilisation of the filled metal d-orbitals by the reduction in the σ-donor strength of the protonated triazole ligand. In addition, on protonation of both **1** and **2** the emission lifetime decreases to the sub-nanosecond timescale. This decrease (in

interaction parameter a^2 for the system is found to be 0.0055 cm^{-1} (H_{ab} = 480 cm^{-1}), compared with 0.016 for **4** (H_{ab} = 700 cm^{-1}). This confirms that although an interaction is present it is at most very weak and hence the system is best described as type II. For the protonated complex the absence of an IT band and the single bielectronic redox wave confirms it to be type I *i.e.* no interaction.

Concluding remarks

Complexes **1** and **2** are synthetic intermediates in the preparation of hydroquinone and quinone containing complexes. The present study forms therefore a basis for the investigation of quinone complexes, which will be reported in a later publication. X-Ray and molecular structures of **HL1** and **H_2L2** and of **1** facilitate detailed studies of these and similar compounds with respect to the distance dependence of electron and energy transfer processes in the quinone/hydroquinone target compounds. The electrochemical, acid–base, spectroscopic and photophysical results reported in this study for **1** and **2**, indicate that for the dinuclear species the individual metal centres behave independently and in an almost identical fashion to the mononuclear complex **1**. Importantly they show only a single two electron metal-based oxidation. This indicates that the interaction between the two metal centres is weak. In the deprotonated complex **2** the presence of an intervalence band in the spectroelectrochemical data confirm the presence of a weak interaction. The results obtained show that the electronic interaction (H_{ab}) in **2** is considerable less than observed in **4**. This is not unexpected on the basis of the increased distance (d) between the metal centres and the presence of the 'phenyl spacer', which has been found in previous studies to provide poor electronic communication.[19] This study allows for more successful prediction of the supramolecular aspects of analogous systems containing hydroquinone and quinone moieties where direct electrochemical and spectroelectrochemical investigations are not possible due to the presence of ligand based oxidations at potentials lower than that of the metal centres.[12] The present study is aimed at providing a base for the comparison of the electrochemical and photophysical properties of such compounds and assesses the potential of the hydroquinone/quinone redox couple to act as an electrochemical switch.

Acknowledgements

The authors thank Enterprise Ireland and the EU TMR Grant no. CT96076 for financial assistance.

References

1 A. Juris, V. Balzani, F. Barigelletti, S. Campagna, P. Belser and A. von Zelewsky, *Coord. Chem. Rev.*, 1988, **84**, 85.
2 K. Kalyanasundaram, *Coord. Chem. Rev.*, 1982, **46**, 159.
3 E. A. Seddon and K. R. Seddon, *The Chemistry of Ruthenium*, Elsevier, Amsterdam, 1984, ch. 15.
4 V. Balzani, F. Scandola, *Supramolecular Photochemistry*, Ellis Horwood, Chichester, UK, 1991.
5 *Supramolecular Photochemistry*, ed. V. Balzani, Reidel, Dordrecht, 1997.
6 P. R. Rich, *Faraday Discuss. Chem. Soc.*, 1982, **75**, 349.
7 K. S. Schanze and K. Sauer, *J. Am. Chem. Soc.*, 1998, **110**, 1180.
8 V. Goulle, A. Harriman and J.-M. Lehn, *J. Chem. Soc., Chem. Commun.*, 1993, 1034.
9 K. A. Opperman, S. L. Mecklenburg and T. J. Meyer, *Inorg. Chem.*, 1994, **33**, 5295.
10 V. Balzani, S. Campagna, G. Denti, A. Juris and M. Venturi, *Coord. Chem. Rev.*, 1994, **132**, 1.
11 S. Fanni, T. E. Keyes, S. Campagna and J. G. Vos, *Inorg. Chem.*, 1998, **37**, 5933.
12 T. E. Keyes, P. M. Jayaweera, J. J. McGarvey and J. G. Vos, *J. Chem. Soc., Dalton Trans.*, 1997, 1627.
13 R. Wang, T. E. Keyes, R. Hage, R. H. Schmehl and J. G. Vos, *J. Chem. Soc., Chem. Commun.*, 1993, 1652.
14 B. P. Sullivan, D. J. Salmon and T. J. Meyer, *Inorg. Chem.*, 1978, **17**, 3334.
15 R. Wang, J. G. Vos, R. H. Schmehl and R. Hage, *J. Am. Chem. Soc.*, 1992, **114**, 1964.
16 J. Fait, XSCANS, Program for Data Collection and Processing, 1993, Bruker, Madison, WI.
17 G. M. Sheldrick, SHELXTL version 5.10, University of Gottingen, Germany, 1997.
18 F. Barigelletti, L. De Cola, V. Balzani, R. Hage, J. G. Haasnoot, J. Reedijk and J. G. Vos, *Inorg. Chem.*, 1989, **28**, 4344.
19 R. Hage, J. G. Haasnoot, J. Reedijk, R. Wang, E. M. Ryan, J. G. Vos, A. L. Spek and A. J. M. Duisenberg, *Inorg. Chim. Acta*, 1990, **174**, 77.
20 D. P. Rillema, D. S. Jones, C. Woods and H. A. Levy, *Inorg. Chem.*, 1992, **31**, 2935.
21 R. Hage, A. H. J. Dijkhuis, J. G. Haasnoot, R. Prins, J. Reedijk, B. E. Buchanan and J. G. Vos, *Inorg. Chem.*, 1988, **27**, 2185.
22 T. J. Meyer, *Pure Appl. Chem.*, 1984, 630.
23 M. P. Robin and P. Day, *Adv. Inorg. Chem. Radiochem.*, 1967, **10**, 247.
24 D. E. Richardson and H. Taube, *Inorg. Chem.*, 1981, **20**, 1278.
25 (*a*) N. S. Hush, *Prog. Inorg. Chem.*, 1967, **8**, 391; (*b*) N. S. Hush, *Electrochim. Acta*, 1968, **13**, 1005.
26 C. Creutz, O. N. Marshall and N. Sutin, *J. Photochem. Photobiol., A: Chem.*, 1994, **82**, 47.
27 M. K. Nazeeruddin, S. M. Zakeeruddin and K. Kalyanasundaram, *J. Phys. Chem.*, 1993, **97**, 9607.
28 J. Bonvision, J.-P Launay, M Van der Auweraer and F. C. De Schryver, *J. Phys. Chem.*, 1994, **98**, 5052.

Table 3 Absorption bands observed for complexes **1**, **2** and **4** in Ru^{II}, $Ru^{II}Ru^{III}$ (mixed valence) and Ru^{III} oxidation states

Complex	Ru^{II} MLCT bands/nm (cm^{-1})	$Ru^{II}Ru^{III}$ IT bands/nm (cm^{-1})	Ru^{III} LMCT bands/nm (cm^{-1})
[a] $[Ru(bipy)_3]^{2+}$	452 (22075)	—	675 (14810)
1 $[Ru(bipy)_2(L1)]^+$	485 (20620)	—	1075 (9300)
$[Ru(bipy)_2(HL1)]^{2+}$	440 (22725)	—	825 (12120)
2 $[(Ru(bipy)_2)_2(L2)]^{2+}$	482 (20745)	1540 (6470)	1220 (8220)
$[(Ru(bipy)_2)_2(H_2L2)]^{2+}$	412 (24270)	—	840 (11930)
4 $[(Ru(bipy)_2)_2(bpt)]^{3+}$	453 (22075)	1800 (5556)	753 (13280)

[a] Value obtained from ref. 27

depletion in the MLCT band at 485 nm, coupled with the formation of a new band at 1075 nm. This band is comparable to the ligand to metal charge transfer bands (LMCT) observed for other $[Ru(LL)_3]^{3+}$ complexes (where LL = substituted-2,2-bipyridine).[27] Upon increasing the oxidation potential to 1.3 V, the depletion of the MLCT band continues, while the band at 1075 nm also decreases in intensity. The depletion of the MLCT bands at 485 nm and the appearance of the LMCT band at 0.8 V is consistent with the oxidation of the metal centre. Further increase of the oxidation potential to 1.3 V is irreversible and results in decomposition of the complex in agreement with data obtained from cyclic voltammetry (*vide supra*). The reversibility of the initial oxidation process has been confirmed by reformation of the initial spectrum upon bulk electrolysis at 0.3 V, subsequent to electrolysis at 0.8 V.

For **2** the situation is similar except that for this compound an additional broad feature at 1545 nm is formed at 0.75 V prior to formation of the expected LMCT absorption band at 1216 nm (Fig. 7). Further oxidation at higher potentials results

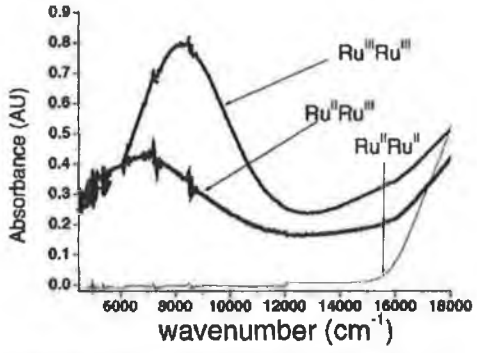

Fig. 7 Near-IR absorption spectra of the fully reduced ($Ru^{II}Ru^{II}$) mixed valence ($Ru^{II}Ru^{III}$) (electrolysis at 0.75 V *vs.* pseudo Ag/AgCl) and full oxidised ($Ru^{III}Ru^{III}$) (electrolysis at 0.85 V *vs.* pseudo Ag/AgCl) complex **2**.

in depletion of all spectroscopic bands as was observed for **1**. The band initially formed at 1545 nm is assigned as an IT band on the basis of its absence in the spectra of **1** and its energy and bandwidth which are comparable to those observed for $[(Ru(bipy)_2)_2bpt]^{4+}$.[19] The depletion of the 1545 nm band and the formation of the LMCT band at higher energy occur with the presence of a sharp isosbestic point at 1490 nm. The situation is similar to that of Bonvoisin *et al.*[28] for the formation of an IT band of an organic aromatic polyamine system, which exhibited a single reversible three electron oxidation wave. Emission-spectroelectrochemistry has also been used to investigate the species, which are present during formation of both IT and LMCT bands of the partially and fully oxidised species, respectively. Oxidation of **2** up to 0.85 V (*vs.* pseudo Ag/AgCl) results in depletion of the emission at 683 nm. The initial emission spectrum completely recovered upon returning the potential to 0.3 V. In contrast when **2** is oxidised at 1.3 V and the potential returned to 0.3 V the original emission spectrum is not reformed rather a new emission is observed at higher energy, indicating irreversible ligand oxidation of **2**. The nature of the product formed was not further investigated.

Under acidic conditions, at which the triazole ring is protonated, no IT band is observed for **2**. The LMCT bands observed are shifted to higher energy compared with the LMCT bands observed for the deprotonated complexes, from 1075 nm to 825 nm for **1** and from 1220 nm to 840 nm for **2**. The intensities of these bands relative to the LMCT bands of the deprotonated complexes is also much reduced. These observations are not unexpected and can be rationalised in terms of the relative energies of the donor (ligand based) and acceptor (metal based) orbitals. The effect of protonation and the subsequent decrease in the σ-donor properties of the bridging ligand is to increase the energy of both the donor and acceptor orbitals leading to the observed shift in the LMCT transition. In addition upon protonation there is a noticeable decrease in the intensity of the LMCT band, which reflects the decreased electron density of the triazole ligands. These results are consistent with the findings of Nazeeruddin *et al.*,[27] who have found that the intensity of the LMCT transition increases with increasing electron-donating capacity of the donor ligand.

Estimation of electronic coupling (H_{ab})

Hush theory may be applied to multinuclear systems exhibiting IT bands in their mixed valence states[25] to quantify the level of interaction between the metal centres of the dinuclear complex. A measure of the interaction between the two metal centres in the mixed valence state can be obtained *via* the determination of the resonance exchange integral H_{ab}, as shown in eqn. 2.[26]

$$H_{ab} = [\alpha^2 \cdot E_{op}^{\ 2}]^{1/2} \quad (2)$$

where α^2 is a measure of the extent of electron delocalisation and can be obtained from the intervalence band using eqn. 3;

$$\alpha^2 = \frac{(4.2 \times 10^{-4}) \cdot \varepsilon_{max} \cdot \Delta\nu_{1/2}}{d^2 \cdot E_{op}} \quad (3)$$

where ε_{max} is the extinction coefficient of the IT band (M^{-1} cm^{-1}), $\Delta\nu_{1/2}$ is the peak width at half maximum, d is the estimated internuclear distance in Å, E_{op} is the maximum of the IT band expressed in cm^{-1}.

As noted above, the absence of two resolvable metal oxidation waves in the CV of **2** indicates that any interaction if present is weak. As a result, it is also expected that K_c will be very small and hence at equilibrium only a small proportion of the total concentration of **2** in solution comprises of the mixed valence species. Since the concentration of the $Ru^{II}Ru^{III}$ species is difficult to accurately calculate, the evaluation of ε_{max} (and thence α^2) can only be approximate. Based on the crystal structure of **1**, the internuclear distance of **2** can be estimated as 12 Å. E_{op} is taken directly from the spectra of the mixed valence species (6470 cm^{-1}) and $\Delta\nu_{1/2}$ is taken as double the width at half maximum of the high energy side of the IT band (5100 cm^{-1}). Assuming a maximum extinction coefficient of 2400 M^{-1} cm^{-1} (that of the IT band of **4**) the upper limit of the

Table 2 Spectroscopic and redox data for complexes described in text

	Abs. λ max/ nm ($\varepsilon/10^{-3}$ M^{-1} cm^{-1})	Em. λ max 298 K/nm	[b]Lifetime at 298 K/ns	[c]Ru^{II}/Ru^{III} oxid. (ligand)/V	Ligand based red./V
[Ru(bipy)$_3$]$^{2+}$	452	608	1000	1.26	−1.33, −1.55, −1.8
1 [Ru(bipy)$_2$(**L1**)]$^{+}$	485 (10.7) 290 (80.7)	685	110	0.80 (1.20, 1.40)	−1.48, −1.76
[Ru(bipy)$_2$(**HL1**)]$^{2+}$	441 (15.3) 286 (86.8)	612	—	1.2 (1.45)	*Not measured*
2 [(Ru(bipy)$_2$)$_2$(**L2**)]$^{2+}$	481 (18.9) 290 (148)	683	105	0.82 (1.26, 1.45)	−1.48, −1.73
[(Ru(bipy)$_2$)$_2$**HL2**]$^{4+}$	412 (28.3) 285 (153)	612	—	1.25 (1.5)	−1.49, −1.73
3 [Ru(bipy)$_2$(pytr)]$^{+}$	465 (11.0)	650	145	0.83	−1.47, −1.72, −2.25
[Ru(bipy)$_2$(pytr)]$^{2+}$	437 (12.9)	620	—	1.14	−1.49, −1.73, −2.25
[d]**4** [(Ru(bipy)$_2$)$_2$(bpt)]$^{3+}$	453 (22.6)	648	100	1.04, 1.34	−1.40, −1.62, −1.67

[a] From l. [b] Lifetimes measured in deaerated acetonitrile at 298 K (lifetimes for protonated species are sub-nanosecond and were not measured). [c] All redox potentials are *vs.* SCE in 0.1 M TEAP–acetonitrile, 100 mV s^{-1} scan rate. [d] Value obtained from ref. 19.

contravention of the energy gap law[22]) is a result of the reduction in the ^{3}MLCT − ^{3}MC gap, which facilitates fast thermally activated radiationless deactivation of the emissive ^{3}MLCT excited state *via* population of the ^{3}MC state.[21] The acid–base properties of **1** and **2** (pK_a = 4.0 and 4.1, respectively) have been determined using absorption spectroscopy by titration both in Britton–Robinson buffer and in acetonitrile and are similar to those reported previously for **3** (pK_a = 4.07).[21] In the case of complex **2**, a two-step protonation process is possible however only a single protonation step is observed in aqueous media in the range of pH 1.5 to 10 (Fig. 5). Titration in acetonitrile

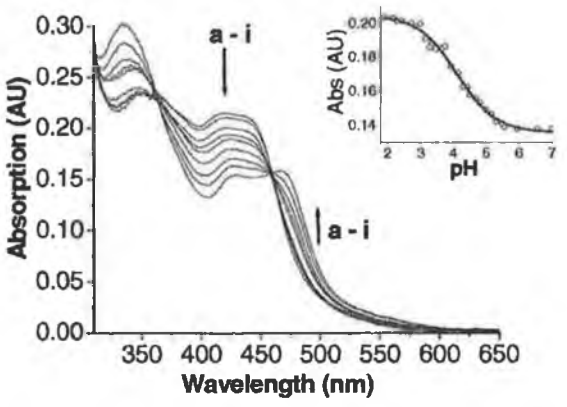

Fig. 5 Titration of **2** in Britton–Robinson buffer pH (a) 1.84; (b) 2.50; (c) 2.84; (d) 3.16; (e) 3.62; (f) 3.92; (g) 4.29; (h) 4.79; (i) 10.06 (inset; pH titration plot monitored at 415 nm).

shows complete protonation with two equivalents of trifluoroacetic acid, indicating that in aqueous media both protonation steps occur at essentially the same pH.

Electrochemical and spectroelectrochemical properties

Redox properties of **1** and **2** are presented in Table 2. $E_{1/2}$ values were determined by cyclic voltammetry (CV). For each of the deprotonated complexes a single reversible redox wave was observed at low oxidation potentials followed by two quasi-reversible oxidation waves at higher potentials. The reversible peaks at 0.8 (**1**) and 0.82 V (**2**) (*vs.* SCE) are attributed to oxidation of the metal centre (*vide infra*), while the quasi-reversible peaks at 1.2 (**1**) and 1.26 V (**2**) are assigned to the first oxidation of the dimethoxyphenyl grouping (Fig. 6). No clear electrochemistry was obtained for the free dimethoxy ligand, most likely because of adsorption on the electrode surface. The metal oxidation potentials are considerably lower (~300 mV) than for [Ru(bipy)$_3$]$^{2+}$, as is expected for the stronger σ-donating 1,2,4-triazoles. The larger peak-to-peak separation (E_p) in the first oxidation wave of **2** compared with **1** reflects the bi-electronic process involved in the metal oxidation ($Ru^{II}Ru^{II}$ to $Ru^{III}Ru^{III}$). For the protonated complexes all redox waves are observed at a

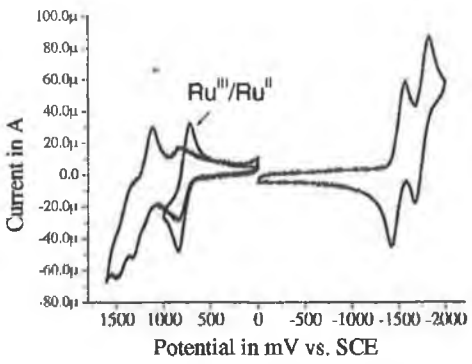

Fig. 6 Cyclic voltammogram of **1** showing reversibility of Ru^{II}/Ru^{III} redox couple and subsequent irreversible ligand oxidation couples (in 0.1 M TEAP–acetonitrile, 100 mV s^{-1} scan rate, ref. SCE).

higher oxidation potential for both **1** and **2**, which arises from the reduced σ-donor capacity of the protonated triazole moieties. Comparison of the first oxidation potential of **2** with those of **1**, **3** and **4**, indicates that Ru(bipy)$_2$(1,2,4-triazole)-units of the dimer behave independently and have properties similar to monomeric species and are quite different from those observed for the dinuclear complex **4**.

The extent of interaction between metal centres in polynuclear complexes has been classified by Robin and Day as Type I, II or III.[23] In dinuclear metal complexes, the metal redox properties are useful in investigating electronic interaction between metal subunits. In principle, because two redox-active sites are present (the two metal centres), two metal-centred oxidation processes are possible, and their separation (ΔE) is related to the stability of the mixed-valence species by the comproportionation constant, K_c, as defined in eqn. 1. The

$$K_c = \exp(\Delta E/25.69) \quad (1)$$

absence of a measurable difference (ΔE < 40 mV) in the two metal-based oxidations of **2** indicates that little or no communication between the metal centres exists, and the value of K_c for **2** is therefore reported to be less than 5.[24]

However, since fast electron transfer between metal centres can occur with an electronic coupling as low as tens of wavenumbers,[10] the absence of two resolvable redox waves does not automatically indicate that the coupling between the metal centres is absent. The most direct measure of the metal–metal electronic coupling in a mixed valence system, $Ru^{II}Ru^{III}$, can be obtained from intervalence transitions (IT).[25,26] For this reason the spectroelectrochemical investigations have been carried out. The electronic properties of partially and completely oxidised complexes, **1** and **2**, together with data from model systems are presented in Table 3.

Applying a potential of 0.8 V (*vs.* pseudo Ag/AgCl reference electrode) to a basic acetonitrile solution of **1** results in

Notes

Separation and Photophysical Properties of the ΔΔ, ΛΛ, ΔΛ, and ΛΔ Stereoisomers of a Dinuclear Ruthenium(II) Complex

Wesley R. Browne,[†] Christine M. O'Connor,[†,#] Claudio Villani,[‡,§] and Johannes G. Vos*[,†]

National Centre for Sensor Research, School of Chemical Sciences, Dublin City University, Dublin 9, Ireland, and Dipartimento di Scienze del Farmaco, Università di Chieti, Via dei Vestini 31, 66013 Chieti, Italy

Received May 4, 2001

Introduction

As interest in both polynuclear and asymmetric ruthenium(II) complexes increases, so too does the issue of isomerism, in terms of both connectivity[1,2] and stereochemistry.[3−5] Since through-space interactions are often as significant as through-bond interactions,[6] obtaining inorganic complexes with well-defined spatial and electronic structures is viewed as a prerequisite for the successful development of molecular devices. Ruthenium(II) polypyridyl complexes have been extensively investigated for their photochemical, photophysical, and molecular recognition properties, and a wide range of multinuclear complexes based on 2,2′-bipyridyl (bpy) and related ligands have been prepared.[7,8] It has been recognized for some time that the use of bidentate ligands results in formation of stereoisomers.[3] The importance of stereochemistry and, in particular, chirality is well illustrated in the studies carried out on the stereoselective intercalation of ruthenium polypyridyl complexes into DNA[4,9,10] and proteins.[11] The isolation of the stereoisomers of mono- and polynuclear ruthenium(II) and osmium(II) diimine complexes has been reviewed recently.[3] The more common approaches used in preparing stereochemically pure systems can be described as: reagent induced stereochemical control,[12−14] the use of chiral precursors,[15−18] chromatographic techniques,[10,19−26] recrystallization,[27,28] or a combination of these.

There are however relatively few studies which address the relationship between stereochemistry and the photophysical properties of ruthenium(II) and osmium(II) polypyridyl complexes, and to the best of our knowledge, no studies have been carried out in chiral solvents. Several studies suggest that enantiomers exhibit no observable differences in their electrochemical or electronic properties. In addition only minor, if any, differences in the properties of diastereoisomers have been reported.[20−24,28−30] However, Hesek et al.[13] have reported a significant difference in the UV−Vis spectra of the diastereoisomers of the complex $[Ru(bpy)_2Cl(L)]^+$ (where L = (*R*)-(+)- or (*S*)-(−)-methyl-*p*-tolyl sulfoxide), while Keene and co-workers[23] have reported significant differences in luminescence lifetimes between the meso- and homochiral isomers for the dinuclear $[(Ru(bpy)_2)_xHAT]^{2x+}$ complex[23a] (where $x = 1-3$, LL = 2,2′-bipyridine or 1,10-phenanthroline, and HAT = 1,4,5,8,9,12-hexaazatriphenylene) and for the charge separated states of a series of four geometric isomers of a ruthenium(II) mononuclear chromophore quencher system[23b].

In this contribution, the separation, ^{1}H NMR spectra, and photophysical properties of the four stereoisomers (**1a**−**d**) of the complex $[(Ru(bpy)_2)_2(bpt)](PF_6)_3$ are reported. (For structure of complex see Figure 1). To assess the importance of stereochemistry on the photophysical properties of the four

* To whom correspondence should be addressed. E-mail: johannes.vos@dcu.ie.
† Dublin City University.
‡ Università di Chieti.
# Current address: School of Chemistry, Dublin Institute of Technology, Dublin 8, Ireland.
§ E-mail: villani@unich.it.

(1) Hage, R.; Prins, R.; Haasnoot, J. G.; Reedijk, J. *J. Chem. Soc., Dalton Trans.* **1987**, 1389.
(2) Hage, R.; Dijkhuis, A. H. J.; Haasnoot, J. G.; Prins, R.; Reedijk, J.; Buchanan, B. E.; Vos, J. G. *Inorg. Chem.* **1988**, *27*, 2185.
(3) (a) Keene, F. R. *Coord. Chem. Rev.* **1997**, *166*, 121. (b) Keene, F. R. *Chem. Soc. Rev.* **1998**, *27*, 185.
(4) Belser, P.; Bernhard, S.; Jandrasics, E., De Cola, L., Balzani, V. *Coord. Chem. Rev.* **1997**, *159*, 1.
(5) Ziegler M.; von Zelewsky A. *Coord. Chem. Rev.* **1998**, *177*, 257.
(6) Balzani, V.; Scandola, F. *Supramolecular Photochemistry*; Ellis Horwood: Chichester, UK, **1991**.
(7) Kalyanasundaram, K. *Coord. Chem. Rev.* **1962**, *46*, 159.
(8) Juris, A.; Balzani, V.; Barigelletti, F.; Campagna, S.; Belser, P.; Von Zelewsky, A. *Coord. Chem. Rev.* **1988**, 86.
(9) Choi, S.-D.; Kim, M.-S.; Lincoln, P.; Tuite, E.; Norden, B. *Biochemistry* **1997**, *36*, 1, 214.
(10) Dupureur, C. M.; Barton, J. K. *J. Am. Chem. Soc.* **1994**, *116*, 10286.
(11) Dmochowski, I. J.; Winkler, J. R.; Gray, H. B. J. *Inorg. Biochem.* **2000**, *81*, 221.
(12) Riesgo, E. C., Credi, A.; De Cola, L.; Thummel, R. P. *Inorg. Chem.* **1998**, *37*, 2145.
(13) Hesek, D.; Inoue, Y.; Everitt, S. R. L.; Ishida, H.; Kunieda, M.; Drew, M. G. B. *Inorg. Chem.* **2000**, *39*, 317.
(14) Wärnmark, K.; Baxter, P. N. W.; Lehn, J.-M. *Chem. Commun.* **1998**, 993.
(15) Torres, A. S.; Maloney, D. J.; Tate, D.; Saad, Y.; MacDonnell, F. M. *Inorg. Chim. Acta* **1999**, *293*, 37.
(16) Hesek, D.; Inoue, Y.; Everitt, S. R. L. *Chem. Lett.* **1999**, 109.
(17) Hesek, D.; Inoue, Y.; Everitt, S. R. L.; Ishida, H.; Kunieda, M.; Drew, M. G. B. *Tetrahedron: Asymmetry* **1998**, *9*, 4089.
(18) Hesek, D.; Inoue, Y.; Everitt, S. R. L.; Ishida, H.; Kunieda, M.; Drew, M. G. B. *Chem. Commun.* **1999**, 403.
(19) Hesek, D.; Inoue, Y.; Ishida, H.; Everitt, S. R. L.; Drew, M. G. B. *Tetrahedron Lett.* 2000, *41*, 15, 2617.
(20) Hesek, D.; Inoue, Y.; Everitt, S. R. L.; Ishida, H.; Kunieda, M.; Drew, M. G. B. J. *Chem. Soc., Dalton Trans.* **1999**, 3701.
(21) Kelso, L. S.; Reitsma, D. A.; Keene, F. R. *Inorg. Chem.* **1996**, *35*, 5144.
(22) Fletcher, N. C.; Junk, P. C.; Reutsma, D. A.; Keene, F. R. *J. Chem. Soc., Dalton Trans.* **1998**, 133.
(23) (a) Rutherford, T. J.; Gijte, O. V.; Kirsch-DeMesmacker, A.; Keene, F. R. *Inorg. Chem.* **1997**, *36*, 4465. (b) Treadway, J. A.; Chen, P., Rutherford, T. J.; Keene, F. R., Meyer, T. *J. Phys. Chem. A* **1997**, *101*, 6824. (c) Yeomans, B. D.; Kelso, L. S.; Tregloan, P. A.; Keene, F. R. *Eur. J. Inorg. Chem.* **2001**, 239.
(24) Rutherford, T. J.; Keene, F. R. *Inorg. Chem.* **1997**, *36*, 3580.
(25) Patterson, B. T.; Keene, F. R. *Inorg. Chem.* **1998**, *37*, 645.
(26) Shinozaki, K.; Hotta, Y.; Otsuka, T.; Kaizu, Y. *Chem. Lett.* **1999**, 101.
(27) Breu, J.; Kratzer, C.; Yersin, H. *J. Am. Chem. Soc.* **2000**, *122*, 2548.
(28) Morgan, O.; Wang, S.; Bae, S.-A.; Morgan, R. J.; Baker, A. D.; Strekas, T. C.; Engel, R. *J. Chem. Soc., Dalton Trans.* **1997**, 3773.
(29) Ruben, M.; Rau, S.; Skirl, A.; Krause, K.; Görls, H.; Walther, D.; Vos, J. G. *Inorg. Chim. Acta* **2000**, *303*, 206.
(30) Rau, S.; Ruben, M.; Büttner,; T. Temme,; C. Dautz,; S. Görls, H.; Rudolph, M.; Walther, D.; Brodkorb, A.; Duati, M.; O'Connor, C.; Vos, J. G. *J. Chem. Soc., Dalton Trans.* **2000**, 3649.

10.1021/ic010473m CCC: $20.00
Published on Web 09/07/2001

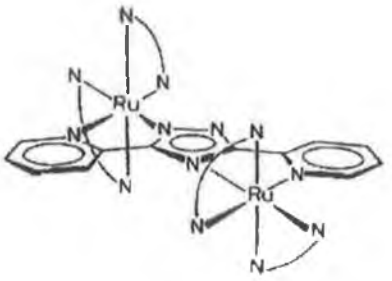

Figure 1. Structure of one of the four stereoisomers of **1**.

stereoisomers, the electronic spectra and emission lifetimes were measured in both racemic and enantiomerically pure 1-phenylethanol, at 298 and 77 K.

Experimental Section

Materials. All solvents used for spectroscopic measurements were of Uvasol (Merck) grade. Racemic and enantiomerically pure {(*S*)-(−)-} 1-phenyl-ethanol (Aldrich) were used as received. The synthesis and purification of $[(Ru(bpy)_2)_2(bpt)](PF_6)_3$ **1** (bpy = 2,2′-bipyridine, Hbpt = 3,5-bis(pyridin-2-yl)-1*H*-1,2,4-triazole) were carried out using previously reported methods.[2]

Chromatography. Separation of the four stereoisomers of **1** was achieved with semipreparative HPLC using a chiral stationary phase (CSP 1) containing Teicoplanin bonded to silica gel microparticles,[31,32] packed in a 250 × 10 mm I.D. column. A Waters Delta Prep 3000 preparative HPLC apparatus, equipped with Knauer UV and RI detectors and a 7010 Rheodyne injector, was employed for the separation. Analytical control of the collected fractions was carried out on a Waters 2690 Separation Module equipped with a UV 481 detector set at 288 nm. Samples of **1** were dissolved in the eluent (40 mg/mL) and filtered through a 0.45 micron filter prior to injection. Typical column loadings were 20−30 mg per run, using $CH_3CN/RCH_2OH/AcONH_4$ 0.5 M 60/20/20 mobile phase (where R = H or CH_3).

Spectroscopy. ^1H NMR Spectra were obtained in [D_3]acetonitrile or [D_6]acetone and recorded on a Bruker AC400 (400 MHz) NMR spectrometer. UV−vis absorption spectra (accuracy ± 2 nm) were recorded on a Shimadzu UV−vis−NIR 3100 spectrophotometer interfaced with an Elonex PC466, using UV−vis data manager. Emission spectra (accuracy ± 5 nm) were recorded at 298 and 77 K using a Perkin-Elmer LS50B luminescence spectrophotometer, which was equipped with a red sensitive Hamamatsu R298 PMT detector and interfaced with an Elonex PC466 employing Perkin−Elmer FI WinLab custom built software. Emission and excitation slit widths were 5 nm at 77K and 10 nm at 298 K. Emission spectra are uncorrected for photomultiplier response. 10 or 2 mm path length quartz cells were used for recording spectra. Emission measurements at 77 K were carried out in a liquid nitrogen filed glass cryostat, with the sample held in a borosilicate NMR tube.

Circular Dichroism (CD) Spectroscopy. CD spectra of the four stereoisomers were recorded on a Jasco J-710 spectropolarimeter in CH_3CN at 25 °C. For these measurements, impure fractions were reprocessed by HPLC on the chiral stationary phase to obtain single stereoisomers with greater than 99% purity. After removal of the solvent at reduced pressure, complexes **1a**−**d** were dissolved in water and converted to their PF_6 salts by addition of a concentrated solution of KPF_6. Acetonitrile solutions of the complexes **1a**−**d** (as PF_6 salts) were used at concentrations in the 5−8 × 10^{-6} M range.

Emission Lifetime Measurements. Luminescence lifetime measurements were obtained using an Edinburgh Analytical Instruments (EAI) time-correlated single-photon counting apparatus (TCSPC) comprised of two model J-yA monochromators (emission and excitation), a single photon photomultiplier detection system model 5300, and a F900 nanosecond flashlamp (N_2 filled at 1.1 atm pressure, 40 kHz) interfaced with a personal computer via a Norland MCA card. A 500 nm cut off filter was used in emission to attenuate scatter of the excitation light (337 nm); luminescence was monitored at 640 nm. Data correlation and manipulation was carried out using EAI F900 software version 5.1.3. Samples were deaerated for 20 min using Argon prior to measurements followed by repeated purging to ensure complete oxygen exclusion. Emission lifetimes were calculated using a single-exponential fitting function, Levenberg−Marquardt algorithm with iterative deconvolution (Edinburgh instruments F900 software). The reduced χ^2 and residual plots were used to judge the quality of the fits. Lifetimes are ± 5%.

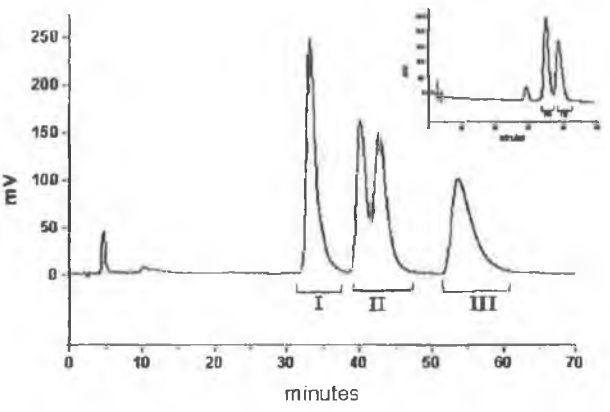

Figure 2. Chromatogram of $[(Ru(bpy)_2)_2(bpt)]^{3+}$ on CSP1. The insert shows the chromatogram obtained for the separation of the heterochiral isomers.

Table 1. Yield, Estimated Purity, and Emission Lifetimes (Samples Deaerated by 20 min Ar Purge) of the Separated Stereoisomers of Complex **1**

	yield/mg[a] (impurities)[b]	*rac*-1-phenylethanol (τ/ns)	(*S*)-(−)-1-phenylethanol (τ/ns)
1a	17(−)	146	163
1b	11(4% of **1a**)	145 (145[c])	156
1c	21(27% of **1b**)	144	155
1d	15(4% of **1c**)	140	156

[a] Total mass of isomer recovered. [b] Impurities as a % of peak area relative to the peak due to the main stereoisomer. [c] Sample degassed by four freeze−pump−thaw degassing cycles.

Results and Discussion

Chromatographic Resolution of Stereoisomers. The analytical separation of the stereoisomers of **1** has been reported in an earlier study.[32] The separation of the stereoisomers was carried out on a semipreparative scale in two steps. In a first set of the separations (Figure 2), using $CH_3CN/CH_3OH/AcONH_4$ 0.5 M 60/20/20 as eluent delivered at a flow rate of 4 mL/min, three fractions were collected. The first contained one of the homochiral stereoisomers **1a** (fraction I), the second contained the two heterochiral stereoisomers **1b** and **1c** (fraction II), and the last fraction contained the second homochiral stereoisomer **1d** (fraction III) (see Figure 2). In a second set of separations (see Figure 2, inset), the two heterochiral stereoisomers, collected as fraction II, were resolved using a different eluent ($CH_3CN/CH_3CH_2OH/AcONH_4$ 0.5 M 60/20/20), yielding fractions IIa (**1b**) and IIb (**1c**). Yields from four replicate runs and a purity check are described in Table 1. Purity was estimated by integration of chromatogram peak areas, with control analytical runs being carried out. With the exception of I, the preceding peak contaminated each fraction.

Circular Dichroism. On the basis of single wavelength CD detection of the HPLC traces, the two homo- and heterochiral

(31) D'Acquarica, I.; Gasparrini, F.; Misiti, D.; Villani, C.; Carotti, A.; Cellamare, S.; Muck, S. *J. Chromatogr., A* **1999**, *857*, 145.
(32) Gasparrini, F.; D'Acquarica, I.; Vos, J. G.; O'Connor, C. M.; Villani, C. *Tetrahedron: Asymmetry* **2001**, *11*, 3535.

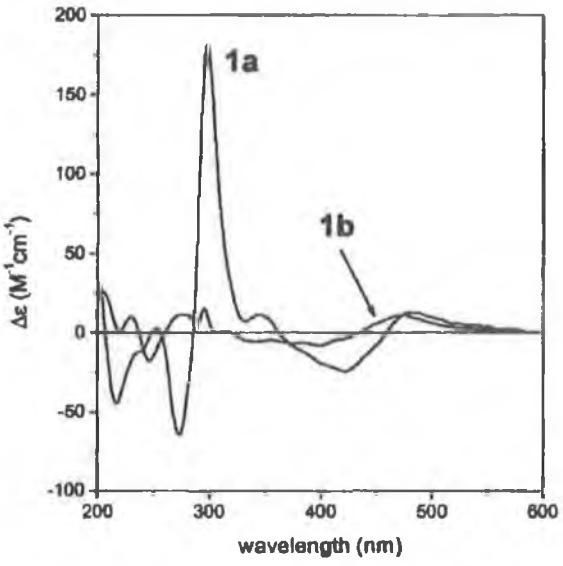

Figure 3. CD spectra of **1a** and **1b** measured in CH_3CN.

isomers are identifiable.[32] The CD spectra of the **1a** and **1b** (Figure 3) further suggest that the ΛΛ isomer (**1a**) is obtained as the first fraction, followed by the two heterochiral isomers, and finally the ΔΔ (**1d**) isomer, on the basis of comparison with the CD spectra of $[Ru(LL)_3]^{2+}$ (where LL = 2,2′bipyridine or 1,10-phenathroline) and the known selectivity of the Teicoplanin packing material for the Δ isomer over the Λ isomer of these tris-homoleptic complexes.[32] Since for the present semipreparative separation the same stationary phase, packed into a 10 mm I.D. column, that was employed for analytical separation was used, the same elution order is obtained. The stereoisomers of **1** are named in accordance with previously assigned labels as homochiral (ΛΛ (**1a**) and ΔΔ (**1d**)) and heterochiral (ΛΔ/ΔΛ, **1b**/**1c**).[32] The origin of the differences, which allow for resolution of the heterochiral stereoisomers, is the inherent asymmetry of the complex. The N2 and N4 coordination sites of the triazole ring are nonequivalent, and hence, the ΛΔ and ΔΛ stereoisomers form an enantiomeric pair. Fractions IIa and IIb cannot be assigned to either of the two heterochiral isomers (**1b**/**1c**).

CD spectra of **1a** and **1d** (and those of **1b** and **1c**) show a mirror image relationship as expected for enantiomeric pairs. The spectrum of **1a** is very similar to that of the parent mononuclear $[Ru(bpy)_3]^{2+}$ having Λ configuration,[5] thus confirming the original assignment of ΛΛ configuration to the first eluted homochiral complex. The two diagnostic couplets for the Λ configuration were found in the LCT (ligand centered transition) (272 nm negative and 298 nm positive) and MLCT (421 nm negative and 480 nm positive) regions. There is no significant mutual influence of the two chromophoric units of **1a**, and the spectrum of **1a** is simply the sum of that of two mononuclear units. The original heterochiral assignment to **1b** and **1c** is confirmed by their CD spectra. The spectrum of **1b** shows very weak bands, especially in the LCT region, presumably as a result of the near complete compensation of the two metal centers of opposite chirality.

^{1}H NMR Spectroscopy. The ^{1}H NMR spectra obtained for the stereoisomers **1a** and **1b** are shown in Figure 4. The spectra obtained are in agreement with those reported by Hage et al.[2] for materials obtained from fractional crystallization. The nature of the two species obtained was at that stage, however, uncertain.[2] As expected, the ^{1}H NMR spectra of the homochiral

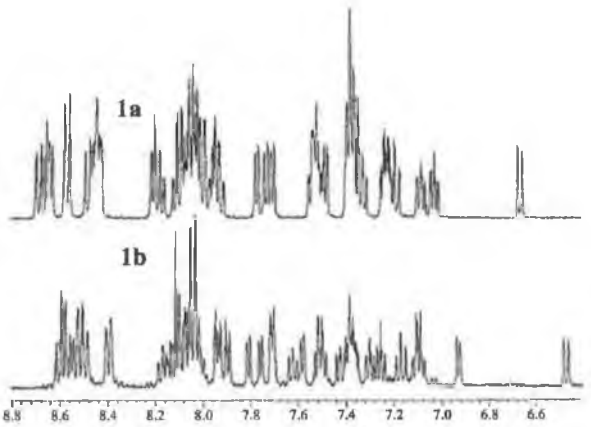

Figure 4. ^{1}H NMR Spectra of **1a** (homochiral isomer ΛΛ) and **1b** (heterochiral isomer ΛΔ) in [D_3]acetonitrile.

stereoisomers **1a** and **1d** (ΛΛ and ΔΔ) are identical, as are the spectra of the heterochiral stereoisomers **1b** and **1c** (ΛΔ and ΔΛ). The spectra obtained are assignable using ^{1}H COSY techniques and are in full agreement with previously reported assignments.[2] Since there is substantial through space interaction between the bridging ligand and the bpy rings and between the bpy ligands themselves, the complexity of this spectrum does not allow for a detailed discussion of the differences observed. It is, however, clear that the fractions obtained by Hage et al. can be assigned as the homochiral and heterochiral enantiomeric pairs.[2]

Electronic Properties. It is surprising that despite the considerable interest in stereochemical control of ruthenium(II) and osmium(II) complex, few studies of the differences in photophysical properties between stereoisomers have been reported, and to the authors knowledge, no comparative study of the emissive properties of enantiomeric pairs and diastereoisomers in racemic and enantiomerically pure environments has been carried out. The photophysical properties of the four stereoisomers of **1** have been examined in racemic 1-phenylethanol, (*S*)-(−)-1-phenylethanol, and acetonitrile (butyronitrile at 77 K). The 1-phenylethanol was chosen as a solvent for two reasons. First, the solvent is inherently chiral and can be obtained in enantiomerically pure form. Second, the presence of a phenyl group and a hydroxy moiety allows for the possibility of a π-stacking interaction and hydrogen bonding interaction between the pyridyl rings of the complex and the solvent phenyl group and hydroxy group, respectively. That such interactions may occur has been observed both intermolecularly by Patterson et al.[25] and intramolecularly by Hesek et al.[13] In both *rac*- and (*S*)-(−)-1-phenylethanol, no significant changes in the electronic spectra were obtained; the absorption and emission maxima for all four isomers was within experimental error (±2 nm) at 452 and 640 nm, respectively, with no differences in band shape. At 77 K in butyronitrile, a value of 610 and 604 nm in both *rac*- and (*S*)-(−)- 1-phenylethanol (±5 nm) was observed for all stereoisomers. The emission lifetime data at 298 K for **1a**−**d** in 1-phenylethanol are presented in Table 1. No significant differences were observed between the lifetimes of the four stereoisomers. The values given in Table 1 are average values for a set of four measurements each, and no differences greater than the experimental error were observed between measurements. The slight increase in lifetime observed in (*S*)-(−)-1-phenylethanol compared with the racemic solvent is probably due to different H_2O contents in the solvents employed. In each case, measurements were recorded under identical conditions

of solvent and temperature. To confirm that deaeration using argon gas was sufficient in precluding any excited-state quenching by oxygen, the heterochiral **1b** was subjected to four freeze−pump−thaw degassing cycles prior to the lifetime measurements being made. No difference was observed using either method of deoxygenation.

The excited ^{3}MLCT state of $[Ru(bpy)_3]^{2+}$ is known to possess a considerable amount of charge transfer to solvent character (CTTS),[33] and this is expected to be the case for other ruthenium(II) polypyridyl complexes. Hence, for the system under examination, excited-state interaction with the solvent would be expected to be substantial. The use of chiral solvents amenable to intermolecular interactions such as π-stacking and hydrogen bonding could, in principle, effect the electronic structure of stereoisomers of transition metal complexes. However, for such interactions to produce measurable differences in the photophysical properties of such complexes, the interactions must be sufficiently strong/nonrandom to affect the complex over the time scale of the lifetime of the excited states of such molecules. Since in fluid solutions and glassy matrixes the randomness of the solvent orientation around the complex would be almost complete, and solvent interactions significantly affect the excited state lifetime, then multiexponential behavior would be expected. Changes in symmetry may result in the loss or diminishment of deactivating vibrationally linked pathways. This is not observed in any of the measurements carried out in this study. In achiral environments the differences between the homo- (**1a/1d**) and heterochiral (**1b/1c**) stereoisomers of **1** are almost entirely due to differences in intramolecular interactions. Only if such intramolecular interactions are significant will differences in the photophysical properties of the homo- and heterochiral stereoisomers be observed. For each enantiomeric pair, both intramolecular and intermolecular interactions (in achiral solvents) are identical, and hence, no differences in their photophysical properties are expected. However, the use of enantiomerically pure hosts could in principle result in differential stabilization of the enantiomers. No differences are observed in the photophysical properties of the stereoisomers of **1** in both achiral and chiral solvents.

The results obtained indicate that the presence of stereoisomers does not affect the general photophysical properties of the dinuclear complex **1**. That no differences in the photophysical properties of the stereoisomers of **1** are observable either at 77 K or at room temperature in both achiral, racemic, and enantiomerically pure solvents, suggests strongly that the differences in either ground or excited-state structures are not significant. In strained systems,[21,23] differences in intramolecular interactions have been shown to effect differences in electrochemical and photophysical properties between stereoisomers; however, no such differences should occur between enantiomeric pairs. Hence, differences in intermolecular rather than intramolecular interactions are of most concern. In the present system differences in intermolecular interactions do not result in measurable differences in photophysical properties. Meskers et al.[34] have found significant enantioselectivity in the quenching of chiral lanthanide complexes by vitamin B_{12}. In this case the lanthanide complex forms a close association with the B_{12} molecule. This strongly suggests that only where the environments of the stereoisomers of an inorganic complex are significantly different, i.e., in the case of DNA intercalation or photosystem II, differences in photophysical properties may become observable.

Conclusions

These results suggest that the presence of stereoisomers in multinuclear supramolecular assemblies is unlikely to affect the photophysical properties of these assemblies, and the importance of stereochemistry in solution is relatively low in comparison to electronic factors.

Acknowledgment. The authors thank Enterprise Ireland for financial assistance.

1C010473M

(33) Van Houten, J.; Watts, R. J. *J. Am. Chem. Soc.* **1975**, *97*, 3843.

(34) Meskers, S. C. J.; Dekkers H. P. J. M. *Spectrochim. Acta Part A* **1999**, *55*, 1857.

Inorg. Chem. **2002**, *41*, 2871–2878

Proton Controlled Intramolecular Communication in Dinuclear Ruthenium(II) Polypyridine Complexes

Cinzia Di Pietro,[†] Scolastica Serroni,[†] Sebastiano Campagna,[†] Maria Teresa Gandolfi,[‡] Roberto Ballardini,[‡] Stefano Fanni,[§] Wesley R. Browne,[§] and Johannes G. Vos*[,§]

Dipartimento di Chimica Inorganica, Chimica Analitica e Chimica Fisica dell'Università, Via Sperone 31, I-98166 Messina, Italy, Dipartimento di Chimica, "G. Ciamician", Via Selmi 2, I-40126 Bologna, Italy, and National Centre for Sensor Research, School of Chemical Science, Dublin City University, Dublin 9, Ireland

Received December 18, 2001

The synthesis and characterization of two dinuclear ruthenium polypyridyl complexes based on the bridging ligands 5,5′-bis(pyridin-2″-yl)-3,3′-bis(1H-1,2,4-triazole) and 5,5′-bis(pyrazin-2″-yl)-3,3′-bis(1H-1,2,4-triazole) and of their mononuclear precursors are reported. The dinuclear compounds have been prepared by a Ni(0) catalyzed coupling of a mononuclear ruthenium(II) polypyridyl complex containing a brominated triazole moiety. Electrochemical and photophysical studies indicate that, in these dinuclear complexes, the protonation state of the bridge may be used to tune the intercomponent interaction between the two metal centers and that these species act as proton driven three-way molecular switches that can be read by electrochemical or luminescence techniques.

Introduction

Ruthenium(II) polypyridine complexes are playing a key role for the development of multicomponent (supramolecular) systems capable of performing photo- and/or redox-triggered functions. Examples are artificial antenna systems,[1] charge separation devices for photochemical solar energy conversion,[1] and information storage devices.[2] Of particular interest in this regard are molecular components with well-defined photophysical and redox properties, which can be switched or tuned by external perturbation.[3]

For the past number of years, there has been considerable interest in the study of mononuclear and multinuclear ruthenium(II) polypyridyl complexes containing ligands such as 3,5-bis(pyridin-2′-yl)-1H-1,2,4-triazole (Hbpt)[4] and 3,5-bis(pyrazin-2′-yl)-1H-1,2,4-triazole) (Hbpzt)[5] (Figure 1). It has been shown that for dinuclear compounds featuring these ligands strong interaction is observed between metal centers.[6]

In this contribution, the syntheses and spectroscopic, photophysical, and redox properties of two new dinuclear ruthenium(II) complexes $[(bpy)_2Ru(bpbt)Ru(bpy)_2]^{2+}$ (**1**) (where H_2bpbt is 5,5′-bis(pyridin-2″-yl)-3,3′-bis(1H-1,2,4-triazole)) and $[(bpy)_2Ru(bpzbt)Ru(bpy)_2]^{2+}$ (**2**) (where H_2-

* Corresponding author. E-mail: johannes.vos@dcu.ie. Fax: 00353 1 7005503. Phone: 00353 1 700 5307.
† Chimica Analitica e Chimica Fisica dell'Università.
‡ "G. Ciamician".
§ Dublin City University.

(1) (a) Balzani, V.; Juris, A.; Venturi, M.; Campagna, S.; Serroni, S. *Acc. Chem. Res.* **1998**, *31*, 26. (b) Slate, C. A.; Striplin, D. R.; Moss, J. A.; Chen, P.; Erickson, B. W.; Meyer, T. J. *J. Am. Chem. Soc.* **1998**, *120*, 4885. (c) Hu, Y.-Z.; Tsukiji, S.; Shinkai, S.; Oishi, S.; Hamachi, I. *J. Am. Chem. Soc.* **2000**, *122*, 241. (d) Balzani, V.; Juris, A.; Venturi, M.; Campagna, S.; Serroni, S. *Chem. Rev.* **1996**, *96*, 759.

(2) (a) Juris, A.; Balzani, V.; Barigelletti, F.; Campagna, S.; Belser, P.; von Zelewsky, A. *Coord. Chem. Rev.* **1988**, *84*, 85. (b) Meyer, T. J. *Acc. Chem. Res.* **1989**, *22*, 163. (c) O'Regan, B.; Graetzel, M. *Nature* **1991**, *335*, 737. (d) De Cola, L.; Belser, P. *Coord. Chem. Rev.* **1998**, *177*, 301. (e) Bignozzi, C. A.; Schoonover, J. R.; Scandola, F. *Prog. Inorg. Chem.* **1997**, *44*, 1. (f) Blanco, M.-J.; Jiménez, M. C.; Chambron, J.-C.; Heitz, V.; Linke, M.; Sauvage, J.-P. *Chem. Soc. Rev.* **1999**, *28*, 293.

(3) (a) Beer, P. D.; Szemes, F.; Balzani, V.; Salà, C. M.; Drew, M. G.; Dent, S. W.; Maestri, M. *J. Am. Chem. Soc.* **1997**, *119*, 11864. (b) Barigelletti, F.; Flamigni, L.; Collin, J.-P.; Sauvage, J.-P. *Chem. Commun.* **1997**, 333. (c) Waldmann, O.; Hassmann, J.; Müller, P.; Hanan, G. S.; Volkmer, D.; Schubert, U. S.; Lehn, J.-M. *Phys. Rev. Lett.* **1997**, *78*, 3390. (d) Zahavy, E.; Fox, M. A. *Chem.—Eur. J.* **1998**, *4*, 1647. (e) Balzani, V.; Credi, A.; Venturi, M. *Curr. Opin. Chem. Biol.*, **1997**, *1*, 506.

(4) (a) Hage, R.; Prins, R.; Haasnoot, J. G.; Reedijk, J.; Vos, J. G. *J. Chem. Soc., Dalton Trans.* **1987**, 1389. (b) Nieuwenhuis, H. A.; Haasnoot, J. G.; Hage, R.; Reedijk, J.; Snoeck, T. L.; Stufkens, D. J.; Vos, J. G. *Inorg. Chem.* **1990**, *30*, 48. (c) Buchanan, B. E.; Wang, R.; Vos, J. G.; Hage, R.; Haasnoot, J. G.; Reedijk, J. *Inorg. Chem.* **1990**, *29*, 3263. (d) Browne, W. R.; O'Connor, C. M.; Villani, C.; Vos, J. G. *Inorg. Chem.* **2001**, *40*, 5461. (e) Wang, R.; Vos, J. G.; Schmehl, R. H.; Hage, R.; *J. Am Chem. Soc.* **1992**, *114*, 1964.

(5) (a) Hage, R.; Dijkhuis, A. H. J.; Haasnoot, J. G.; Prins, R.; Reedijk, J.; Buchanan, B. E.; Vos, J. G. *Inorg. Chem.* **1988**, *27*, 2185. (b) Barigelletti, F.; De Cola, L.; Balzani, V.; Hage, R.; Haasnoot, J. G.; Vos, J. G. *Inorg. Chem.* **1989**, *28*, 4344.

(6) Hage, R.; Haasnoot, J. G.; Nieuwenhuis, H. A.; Reedijk, J.; De Ridder, D. J. A.; Vos, J. G. *J. Am. Chem. Soc.* **1990**, *112*, 9249.

10.1021/ic0112894 CCC: $22.00
Published on Web 04/30/2002

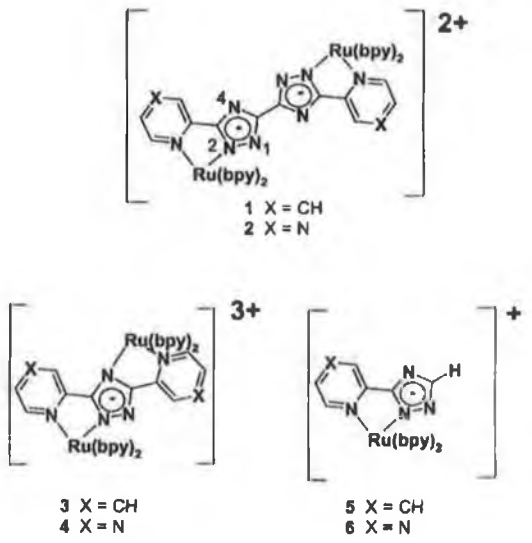

Figure 1. Complex structures.

bpzbt = 5,5′-bis(pyrazin-2″-yl)-3,3′-bis(1H-1,2,4-triazole)) are reported, together with the synthesis and characterization of their mononuclear precursors. The structures of **1** and **2**, of the dinuclear compounds $[(Ru(bpy)_2)_2(bpt)]^{3+}$ (**3**) and $[(Ru(bpy)_2)_2(bpzt)]^{3+}$ (**4**), and of some other mononuclear analogues, used for comparison, are shown in Figure 1.

A first feature of this study is the manner in which the title compounds have been synthesized. The N2 and N4 coordination sites of the triazole ring are nonequivalent,[7] and direct synthesis of the dinuclear species from the bridging H_2bpbt and H_2bpzbt ligands leads in our hands to the formation of an ill defined mixture of products. Possible isomers are shown in Figure 2. The dinuclear compounds have been prepared by a Ni(0) catalyzed homonuclear coupling of a bromine substituted ruthenium(II) polypyridyl complex. With this synthetic method, a single well-defined product is obtained.

The second purpose is the investigation of the intercomponent processes in **1** and **2** as a function of the protonation state of the bridging ligand. The important observation is that by control of the protonation of the bridge a three-way proton controlled molecular switch is obtained, which can be read by electrochemical or spectroscopic methods. A preliminary communication on this work has recently appeared.[8]

Experimental Section

Materials. All solvents used for spectroscopic measurements were of Uvasol (Merck) grade. All other reagents were HPLC grade or better. *cis*-$[Ru(bpy)_2Cl_2]\cdot 2H_2O$ was prepared by standard procedures.[9] Complexes **3**−**6** have been prepared by previously reported procedures.[4−7]

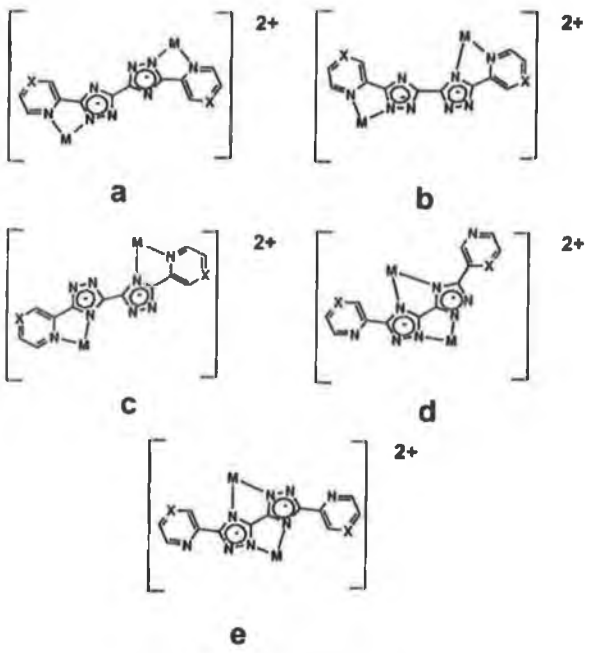

Figure 2. Possible coordination isomers formed by direct reaction of H_2-bpbt or H_2bpzbt with *cis*-$[Ru(bpy)_2Cl_2]$ (X = CH or N).

Synthetic Methods. 3-Bromo-5-(pyridin-2′-yl)-1H-1,2,4-triazole (HBrpytr). A suspension of 3-(pyridin-2′-yl)-1H-1,2,4-triazole (880 mg, 6 mmol) in H_2O (15 mL) was dissolved by slow addition of 10 M NaOH (pH ~ 12). Subsequently, 0.6 mL of Br_2 (99%; d = 3.199 g/mL) was added slowly while maintaining a pH of 12 by addition of concentrated NaOH solution. After stirring for 3 h, the solution was acidified to pH 3−4 with 5 M HCl (aq), resulting in precipitation of the brominated ligand, which was collected by suction filtration. Yield: 945 mg (70%). ^{1}H NMR data d_6-DMSO: H3, 8.60 ppm (d); H4, 7.85 ppm (t); H5, 7.49 ppm (t); H6, 8.00 ppm (d).

3-Bromo-5-(pyrazin-2′-yl)-1H-1,2,4-triazole (HBrpztr). This compound was obtained from 3-(pyrazin-2-yl)-1H-1,2,4-triazole using the method described for HBrpytr. Yield: 920 mg (65%). ^{1}H NMR data *d*-chloroform: H3, 9.40 ppm (s); H5, 8.72 ppm (d); H6, 8.65 ppm (d).

$[Ru(bpy)_2(Brpytr)]PF_6\cdot H_2O$. A suspension of HBrpytr (200 mg, 0.9 mmol) and *cis*-$[Ru(bpy)_2Cl_2]\cdot 2H_2O$ (348 mg, 0.67 mmol) in 20 mL of EtOH/H_2O (1:1, v/v) was heated at reflux for 2 h. After cooling to room temperature, the reaction mixture was filtered and reduced in volume in vacuo. Two drops of a 30% NH_4OH solution were added prior to addition of saturated aqueous solution of NH_4PF_6 (3 mL) to induce precipitation. The solid was separated by vacuum filtration and washed with 20 mL of diethyl ether. The red-orange product was obtained in a pure form by recrystallization from acetone/water (1:1, v/v). Yield: 59%. ^{1}H NMR data d_3-acetonitrile: 7.15 ppm (dd, 1H), 7.30 ppm (dd, 1H), 7.42 ppm (dd, 2H), 7.51 ppm (dd, 1H), 7.59 ppm (d, 1H), 7.70 ppm (d, 1H), 7.83 ppm (d, 1H), 7.85 ppm (dd, 1H), 7.9 ppm (m, 3H), 7.99 ppm (m, 3H), 8.03 ppm (dd, 1H), 8.52 ppm (dd, 1H), 8.56 ppm (d, 1H), 8.6 ppm (dd, 2H). UV−vis absorption spectroscopy: λ_{max} = 475 nm (ϵ = 11600 M^{-1} cm^{-1}). Luminescence spectroscopy: λ_{max} = 665 nm, τ = 250 ns at 298 K in deaerated acetonitrile. Acid/base properties: pK_a 1.3, pH_i 0.9. Anal. Calcd for $C_{27}H_{22}OBrF_6N_8PRu$: C, 40.50%; H, 2.75%; N, 14.06%. Found: C, 40.79%; H, 2.57%; N, 13.94%. Mass spectroscopy: molecular$^+$ ion (for $C_{27}H_{20}N_8$-

(7) (a) Niewenhuis, H. A.; Haasnoot, J. G.; Hage, R.; Reedijk, J.; Snoeck, T. L.; Stufkens, D. J.; Vos, J. G. *Inorg. Chem.* **1991**, *30*, 48. (b) Fanni, S.; Keyes, T. E.; O'Connor, C. M.; Hughes, H.; Wang, R.; Vos, J. G. *Coord. Chem. Rev.* **2000**, *208*, 77.

(8) Fanni, S.; Di Pietro, C.; Serroni, S.; Campagna, S.; Vos, J. G. *Inorg. Chem. Commun.* **2000**, *3*, 42.

(9) Sullivan, B. P.; Salmon, D. J.; Meyer, T. J. *Inorg. Chem.* **1978**, *17*, 3334.

$RuBr^+$) at 637/639 *m/z* units ($^{79}Br/^{81}Br$). The isotopic pattern is in agreement with theoretical values.

[Ru(bpy)$_2$(Brpztr)]PF$_6$·H$_2$O. *cis*-[Ru(bpy)$_2$Cl$_2$]·2H$_2$O (519 mg, 0.67 mmol) with 300 mg (0.9 mmol) of HBrpztr was heated at reflux in 20 mL of EtOH/H$_2$O (1:1, v/v) for 3 h. The pure complex was obtained using the method described for [Ru(bpy)$_2$(Brpytr)]-PF$_6$·H$_2$O. Yield: 64%. ^{1}H NMR d_3-acetonitrile: 7.35 ppm (dd, 1H), 7.41 ppm (dd, 1H), 7.45 ppm (dd, 1H), 7.53 ppm (dd, 1H), 7.71 ppm (d, 1H), 7.76 ppm (d, 1H), 7.83 ppm (d, 1H), 7.9 ppm (m, 3H), 8.06 ppm (m, 3H), 8.22 ppm (d, 1H), 8.58 ppm (dd, 2H), 8.65 ppm (dd, 2H), 9.02 ppm (d, 1H). UV−vis absorption spectroscopy: λ_{max} = 450 nm (ϵ = 12900 M^{-1} cm^{-1}). Luminescence spectroscopy: λ_{max} = 647 nm, τ = 200 ns at 298 K in deaerated acetonitrile. Acid/base properties: pK_a 1.4, pH$_i$ 1.1/5.5. Anal. Calcd for $C_{23}H_{21}OBrF_6N_9PRu$: C, 39.00%; H, 2.62%; N, 15.73%. Found: C, 39.47%; H, 2.69%; N, 15.24%. Mass spectroscopy: molecular$^+$ ion (for $C_{26}H_{19}N_9RuBr^+$) at 638/640 *m/z* units ($^{79}Br/^{81}Br$). The isotopic pattern is in agreement with theoretical values.

[{Ru(bpy)$_2$}$_2$bpbt](PF$_6$)$_2$·4H$_2$O (1). In a 5 mL round-bottomed, two-necked flask equipped with magnetic stir bar and rubber septum were placed 124 mg (0.524 mmol) of NiCl$_2$·6H$_2$O and 549 mg (2.1 mmol) of PPh$_3$. The flask was purged with nitrogen prior to addition of dry DMF (2 mL) via a syringe. The blue reaction mixture was stirred at room temperature, under nitrogen, for 30 min followed by addition of 33 mg (0.524 mmol) of zinc powder. To the dark-brown catalyst formed (1 h, under nitrogen) was added 410 mg (0.524 mmol) of [(bpy)$_2$Ru(Brpytr)]PF$_6$·H$_2$O, and the resulting mixture was heated at 95 °C for 4 h. After the reaction mixture cooled to room temperature, Et$_2$O was added to induce precipitation; the crude product so obtained was dissolved in acetone/water (1:1, v/v) with 2 drops of 30% NH$_4$OH and 3 mL of a saturated aqueous solution of NH$_4$PF$_6$. The product was separated by filtration, dissolved in a small volume of MeCN/MeOH (50:1, v/v), and purified by chromatography on neutral alumina with MeCN/MeOH (50:1, v/v). The second red-orange band was collected, and the solvent was evaporated under reduced pressure. The deep-red product obtained was recovered by filtration and was purified by recrystallization from acetone/water (1:1, v/v). Yield: 40%. Anal. Calcd for $C_{54}H_{48}O_4F_{12}N_{16}P_2Ru_2$: C, 43.91%; H, 3.28%; N, 15.17%. Found: C, 44.21%; H, 3.32%; N, 15.56%. Mass spectroscopy: *m/z* 558 (M^{2+} ion calculated for $C_{54}H_{40}N_{16}Ru_2^{2+}$: 558). ^{1}H NMR data ($d_6$-acetone) δ ppm: 8.73 (dd, 4H), 8.64 (m, 4H), 8.07 (m, 12H), 7.95 (dd, 2H), 7.87 (dd, 2H), 7.64 (d, 2H), 7.52 (m, 6H), 7.40 (dd, 2H), 7.36 (dd, 2H), 7.19 (dd, 4H).

[{Ru(bpy)$_2$}$_2$bpzbt](PF$_6$)$_2$·4H$_2$O (2). This complex was obtained using the method described for **1**. Yield: 50%. Anal. Calcd for $C_{52}H_{46}O_4F_{12}N_{18}P_2Ru_2$: C, 42.22%; H, 3.11%; N, 17.05%. Found: C, 42.80%; H, 2.75%; N, 16.80%. Mass spectroscopy: 559 *m/z* units (M^{2+} ion calculated for $C_{52}H_{38}N_{18}Ru_2^{2+}$: 559).^{1}H NMR data ($d_6$-acetone/NaOD) δ ppm: 9.3 (d, 1H), 9.25 (d, 1H), 8.76 (dd, 4H), 8.67 ppm (dd, 4H), 8.31 (d, 2H), 8.10 (m, 8H), 7.92 (dd, 2H), 7.85 (dd, 2H), 7.82 (dd, 2H), 7.56 (m, 4H), 7.44 (m, 8H).

Instrumentation. ^{1}H NMR spectra were recorded on a Bruker AC400 (400 MHz) NMR spectrometer. All measurements were carried out in d_6-DMSO or *d*-chloroform for ligands and in d_6-acetone for complexes. Peak positions are relative to residual solvent peaks. UV−vis absorption spectra were recorded on a Shimadzu UV−vis−NIR 3100 spectrophotometer interfaced with an Elonex PC466 using UV−vis data manager. Absorption maxima are ±2 nm; molar absorption coefficients are ±10%. Emission spectra (accuracy ±5 nm) were recorded at 298 K using an LS50B luminescence spectrophotometer, equipped with a red sensitive Hamamatsu R928 PMT detector, interfaced with an Elonex PC466 employing Perkin-Elmer Fl WinLab custom built software. Emission spectra are uncorrected for photomultiplier response. Quartz cells (10 mm path length) were used. Emission quantum yields were measured at room temperature with the optically dilute method using $[Ru(bpy)_3]^{2+}$ in aerated aqueous solution as a quantum yield standard, assuming a value of 0.028,[10,11] and are ±10%. pH titrations of **1** and **2** were carried out in Britton−Robinson buffer (0.04 M H_3BO_3, 0.04 M H_3PO_4, 0.04 M CH_3CO_2H) (pH was adjusted using concentrated sulfuric acid or sodium hydroxide solution). pH$_i$ refers to the inflection point of the emission titration curve. The appropriate isobestic point from the absorption spectra was used as the excitation wavelength for emission titrations.

Luminescence lifetime measurements were obtained using an Edinburgh Analytical Instruments (EAI) time-correlated single-photon counting apparatus (TCSPC) composed of two model J-yA monochromators (emission and excitation), a single photon photomultiplier detection system model 5300, and a F900 nanosecond flashlamp (N_2 filled at 1.1 atm pressure, 40 kHz), interfaced with a personal computer via a Norland MCA card. A 500 nm cut off filter was used in emission to attenuate scatter of the excitation light (337 nm). Data correlation and manipulation were carried out using EAI F900 software version 5.1.3. Samples were deaerated for 20 min using Ar gas before measurements were carried out. In the case of complex **2**, samples were deaerated via three freeze−pump−thaw cycles. Emission lifetimes were calculated using a single-exponential fitting function; a Levenberg−Marquardt algorithm with iterative reconvolution Edinburgh instruments F900 software was used; uncertainty is ±10%. The reduced χ^2 and residual plots were used to judge the quality of the fits.

Mass spectra were obtained using a Bruker-Esquire LC 00050 electrospray ionization mass spectrometer at positive polarity with cap-exit voltage of 167 V. Spectra were recorded in the scan range 50−2200 *m/z* with an acquisition time of between 300 and 900 μs and a potential of between 30 and 70 V. Each spectrum was recorded by summation of 20 scans.

Elemental analysis has been carried out at the Microanalytical Laboratory at University College Dublin.

Electrochemical measurements were carried out on a Model 660 electrochemical workstation (CH Instruments). Typical complex concentrations were 0.5−1 mM in anhydrous acetonitrile containing 0.1 M tetraethylammonium perchlorate (TEAP). A Teflon shrouded glassy carbon working electrode, a Pt wire auxiliary electrode, and an SCE reference electrode were employed. Solutions for reduction measurements were deoxygenated by purging with N_2 or Ar gas for 15 min prior to the measurement. Measurements were made in the range −2.0 to 2.0 V versus SCE. Protonation of complexes was achieved by addition of 0.1 M trifluoromethanesulfonic acid in acetonitrile. pH cyclic voltammograms were obtained at sweep rates of 20, 50, 200, and 500 mV s^{-1}; differential pulse voltammetry (DPV) experiments were performed with a scan rate of 20 mV s^{-1}, a pulse height of 75 mV, and a duration of 40 ms. For reversible processes, the half-wave potential values are reported; identical values are obtained from DPV and CV measurements. Redox potentials are ±10 mV. Spectroelectrochemistry was carried out using an OTTLE setup composed of a homemade Pyrex glass, thin layer cell (2 mm). The optically transparent working electrode was made from platinum−rhodium gauze, a platinum wire counter electrode, and the reference electrode, which was a pseudo-Ag/AgCl reference electrode. The working electrode was held at the

(10) Demas, J. N.; Crosby, G. A. *J. Phys. Chem.* **1971**, *75*, 991.
(11) Nakamaru, N. *Bull. Chem. Soc. Jpn.* **1982**, *55*, 2697.

Table 1. Electronic, Photophysical, and Redox Data for Complexes **1**−**6**[a]

		absorption λ_{max}[b] nm	emission, 298 K λ_{max}[b] nm, (τ, ns) {Φ*10^{-3}}	E (ox) V vs SCE
1	$[(bpy)_2Ru(bpbt)Ru(bpy)_2]^{2+}$	480	690 (102) {2.4}	+0.80 [1], +0.98 [1]
H1	$[(bpy)_2Ru(Hbpbt)Ru(bpy)_2]^{3+}$	440	660 (344) {2.1}	+1.06 [1], +1.17 [1]
$H_2$1	$[(bpy)_2Ru(H_2bpbt)Ru(bpy)_2]^{4+}$	431	630 (<5 ns)	+1.10 [2]
3	$[(bpy)_2Ru(bpt)Ru(bpy)_2]^{3+}$	452	648 (80)	+1.04 [1], +1.34 [1]
5	$[(bpy)_2Ru(pytr)]^{+}$	467	650 (145)	+0.83 [1]
H5	$[(bpy)_2Ru(Hpytr)]^{2+}$	438	612 (<1 ns)	+1.14[1]
2	$[(bpy)_2Ru(bpzbt)Ru(bpy)_2]^{2+}$	455	670 (214) {3.4}	+0.92 [1], +1.09 [1]
H2	$[(bpy)_2Ru(Hbpzbt)Ru(bpy)_2]^{3+}$	436	675 (764)	+1.09 [1], +1.15 [1]
$H_2$2	$[(bpy)_2Ru(H_2bpzbt)Ru(bpy)_2]^{4+}$	430	678 (1000) {7.2}	+1.13 [2]
4	$[(bpy)_2Ru(bpzt)Ru(bpy)_2]^{3+}$	449	690 (106)	+1.16 [1], +1.46 [1]
6	$[(bpy)_2Ru(pztr)]^{2+}$	458	660 (250)	+1.01 [1]
H6	$[(bpy)_2Ru(Hpztr)]^{2+}$	441	665 (430)	+1.25[1]
	$[Ru(bpy)_3]^{2+}$	452	620 (1000)	+1.26 [1]

[a] Bracketed numbers ([ ]) refer to the number of electrons under the wave. [b] In acetonitrile at 298 K. Data for the mononuclear pyridine and pyrazine model compounds $[Ru(bpy)_2(pytr)]^{2+}$ (**5**) and $[Ru(bpy)_2(pztr)]^{2+}$ (**6**), respectively, (where Hpytr = 3-(pyridin-2′-yl)-1H-1,2,4-triazole and Hpztr = 3-(pyrazin-2′-yl)-1H-1,2,4-triazole) are included for comparison.

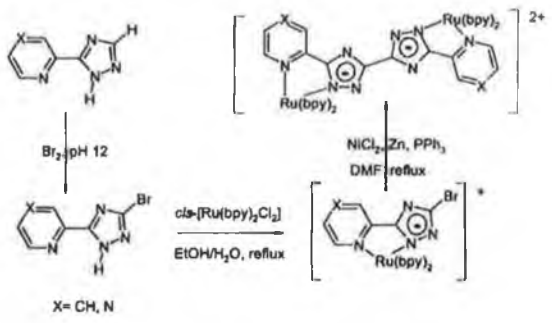

Figure 3. Synthetic scheme employed in preparation of **1** and **2**.

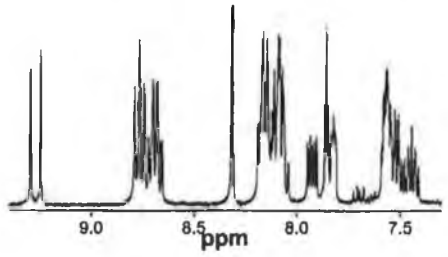

Figure 4. ^{1}H NMR spectra of **2** in d_3-acetone.

required potential throughout the measurement using an EG&G PAR Model 362 potentiostat. Absorption spectra were recorded as described previously. Protonation of complexes under bulk electrolysis was achieved by the addition of a dry 1 M trifluoroacetic acid solution in acetonitrile.

Results

General. The approach taken in this study to obtain pure, well-defined products is outlined in Figure 3. The synthesis of the brominated precursors has been carried out following procedures normally applied to the synthesis of triazole containing ruthenium(II) polypyridyl complexes.[4,5] The mono- and diprotonated complexes of **1** and **2**, which are produced in situ by the addition of an appropriate amount of triflic acid, are referred to as **H1**/**H2** and **$H_2$1**/**$H_2$2**, respectively. The materials obtained from this approach have been fully characterized using spectroscopic measurements. The ^{1}H NMR spectral data shown in Figure 4 illustrate the symmetric nature of the complexes. Spectral assignments are given in the Experimental Section.

Photophysical Properties. All spectroscopic data for complexes **1** and **2** are presented in Table 1, together with data for model complexes **3**−**6**. The absorption spectra of complexes **1** and **2** show intense bands in the UV region [**1**, λ_{max} = 243 nm (ϵ = 52500 M^{-1} cm^{-1}), 290 nm (ϵ = 124100 M^{-1} cm^{-1}); **2**, 244 nm (ϵ = 53400 M^{-1} cm^{-1}), 288 nm (ϵ = 126600 M^{-1} cm^{-1})] and moderately intense bands in the visible region [(**1**, 480 nm (ϵ = 17400 M^{-1} cm^{-1}); **2**, 455 nm (ϵ = 25400 M^{-1} cm^{-1})], which are typical for these types of complexes.[4,5] The complexes are luminescent in acetonitrile at 298 K, and excitation spectra match closely the absorption spectra. Luminescence lifetimes at room temperature are strictly single exponential and are in the 100−1000 ns time domain. Luminescence quantum yields at room temperature are of the order of 10^{-3} (Table 1).

Acid−Base Properties. The spectroscopic, photophysical, and redox properties (vide infra) of **1** and **2** are dependent on the protonation state of the complex. For **1**, in aqueous buffered solution, UV−vis spectroscopy as a function of pH yields two reversible protonation steps with pK_a values of 1.1 and 3.8. On the basis of former protonation studies on Ru(II) complexes containing triazolate ligands,[12] the protonation processes can be attributed to protonation of the triazole rings. However, the two successive pK_a values obtained suggest that the triazole rings interact and the monoprotonated species is better viewed as a compound where the added proton is shared between the two triazole units of the bridging ligand. As with the structurally similar mononuclear complexes **5** and **6**, protonation results in a blue shift in the UV−vis absorption spectra. Complex **2**, as observed for **6**, shows only minor changes in its UV−vis spectra upon protonation, and hence, reliable determination of pK_a values is not possible. For **2**, additional protonation states exist via protonation of pyrazine; however, such protonation occurs only at very negative pH and need not be considered in the pH range studied.[7]

The emission properties of **1** and **2** also show pH dependence (see Table 1). Emission spectra obtained for **1**

(12) (a) Vos, J. G. *Polyhedron* **1992**, *11*, 2285. (b) Hossain, Md. D.; Ueno, R.; Haga, M. *Inorg. Chem. Commun.* **2000**, *3*, 35. (c) Haga, M.; Ali, Md. M.; Maegawa, H.; Nozaki, K.; Yoshimura, A.; Ohno, T. *Coord. Chem Rev.* **1994**, *132*, 99.

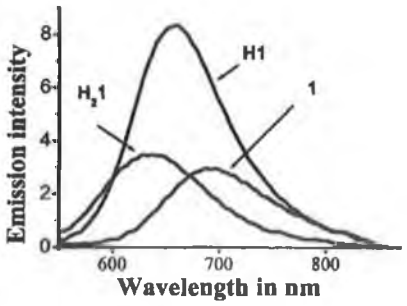

Figure 5. Emission spectra of **1**, **H1**, and $\mathbf{H_21}$ in acetonitrile (protonation with CF_3SO_3H acid).

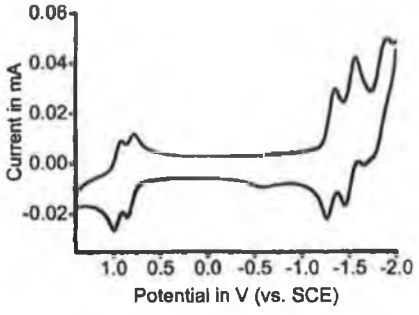

Figure 6. Cyclic voltammogram of **1** in acetonitrile solution.

at three different protonation states are shown in Figure 5. The emission spectrum of **1** undergoes a blue shift from 690 nm (**1**) to 660 nm (**H1**) to 630 nm ($\mathbf{H_21}$) in acetonitrile. The inflection points of the emission titration curves (pH_i) are observed at pH 0.45 and 2.7 in buffered aqueous solution (see Experimental Section). Single protonation of **1** to **H1** results in an increase of emission lifetime, in contrast with the effect of the protonation of the mononuclear complex **5**. However, the doubly protonated complex $\mathbf{H_21}$ compares well in terms of emission energy and emission lifetime with **H5**.

For **2**, protonation results in a small red shift in the emission spectrum (~10 nm) in agreement with similar pyrazine based complexes (e.g., **6**/**H6**).[13] Compared with **1**, the changes in emission energy are much smaller, but the emission lifetime of the emitting state increases with each protonation step. It should be noted that protonation of the pyrazine ring in the exited state is easier than in the ground state. For $\mathbf{H6/H_26}$, a pH_i value of 2.0 has been reported. Because this process leads to quenching of the emission, the acidity of the measuring solution needs to be controlled carefully.

Redox Properties. The metal based oxidation potentials for **1** and **2** and for their protonated forms together with those of the model compounds are collected in Table 1. Both **1** and **2** undergo several reversible oxidation and reduction processes within the redox window investigated (between +2.0 and −2.0 V vs SCE) (see Figure 6). For both **1** and **2**, the first metal oxidation potential is close to that of monomers **5** and **6**, respectively, and at lower potential than those of dinuclear complexes **3** and **4**. For both **1** and **2**, an increase

(13) Hage, R.; Haasnoot, J. G.; Nieuwenhuis, H. A.; Reedijk, J.; Wang, R.; Vos, J. G. *J. Chem. Soc., Dalton Trans.* **1991**, 3271.

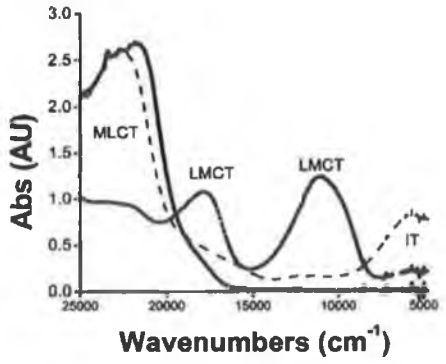

Figure 7. Visible and near-IR absorption spectra of **2** in acetonitrile with 0.1 TEAP at 0.60 V (solid line), 1.00 V (dashed line), and 1.10 V (dotted line) vs SCE.

in the metal based oxidation potentials is observed upon protonation, together with a significant decrease in the gap between the first and second oxidation waves, from ~135 mV for both **1** and **2** to less than 70 mV for **H1** and **H2**. Both $\mathbf{H_21}$ and $\mathbf{H_22}$ exhibit a single two electron metal oxidation wave at potentials comparable to those observed for **H5** and **H6**. The ligand based reduction processes are as expected for ruthenium polypyridyl complexes and are not further discussed.[4,5]

Spectroelectrochemistry. The visible−near-infrared spectra of **2**, of the electrochemically generated mixed valence and fully oxidized species, are shown in Figure 7. Only minor differences are observed in the energy of the intervalence (IT) and ligand-to-metal-charge-transfer (LMCT) bands in **1** and **2** and in **H1** and **H2**. For **1** and **2**, the formation of the mixed valence species is identified by a decrease in the intensity of the ^{1}MLCT bands at ~22220 cm^{-1} (450 nm) and the formation of new bands at ~5500 cm^{-1} and at 11000 and 17500 cm^{-1}. Bulk electrolysis at a potential above the second oxidation wave results in the complete depletion of the 22220 cm^{-1} band coupled with a concomitant depletion of the band at 5500 cm^{-1} and a further increase in both bands at 11000 and 17500 cm^{-1}. All processes are fully reversible.

Reversible spectroelectrochemistry is also observed for **H1** and **H2**. For both compounds, after applying a potential of 1.2 V (vs pseudo-Ag/AgCl), the formation of a band at about 8700 cm^{-1} is observed; further increase of the potential past the second oxidation potential of the complex results in the formation of spectral features at 17860 and 11175 cm^{-1} with concomitant depletion of the band at 8700 cm^{-1}. However, analysis of the IT bands is difficult, because they are located in an area of the spectrum where both LMCT and IT bands are expected. For the fully protonated complexes $\mathbf{H_21}$ and $\mathbf{H_22}$, no evidence for intervalence bands was found. However, in the presence of triflic acid, the fully oxidized $\mathbf{H_21}$ and $\mathbf{H_22}$ exhibit spectral features, most likely LMCT bands at 23360 and 12550 cm^{-1} that are, however, less intense and blue-shifted with respect to those of the mono- and deprotonated species.

Discussion

Synthesis and Characterization. As pointed out in the Introduction, the preparation of complexes with ligands such

as H_2bpbt and H_2bpzbt is by no means straightforward. Because the N2 and N4 nitrogen atoms of the triazole ring are chemically nonequivalent, direct synthesis of the complexes from these ligands can yield five possible coordination isomers, on the basis of the binding mode of the five-membered ring (Figure 2). In three of these isomers (isomers **a**−**c** in Figure 2), the $Ru(bpy)_2$ moiety is bound to a pyridine (or pyrazine) and a triazole ring; in the other two isomers, coordination takes place via the two central triazole rings and does not involve the pyridine and pyrazine rings (isomers **d** and **e** in Figure 2).[14] To avoid the formation of so many different coordination isomers, a new synthetic method was developed.[8] This method is based on the Ni(0) catalyzed coupling reported for bromide containing organic compounds.[15]

In this synthetic approach, brominated pyridine and pyrazine triazole ligands were prepared by adapting procedures previously reported for the bromination of 1,2,4-triazoles.[16] These brominated ligands were subsequently complexed with *cis*-$[Ru(bpy)_2Cl_2]\cdot 2H_2O$, and the products obtained from this complexation reaction were reacted with Ni(0) to produce the dinuclear complexes. With this method, the formation of complexes where the metal centers are coordinated to the two central triazole rings is prevented.

As already noted, the N2 and N4 coordination sites of the triazole ring (see Figure 2) are not equivalent, and therefore, the formation of coordination isomers is expected.[7] The introduction of the bromine atom, although primarily for use in the coupling reaction, has the secondary effect that the presence of this bulky atom in the 3-position results in the formation of the N2 isomer (>95%) over the N4 isomer (<5%), with the N4 isomer being lost during subsequent recrystallization. Therefore, as a result of the synthetic strategy employed, **1** and **2** have been obtained as well-defined symmetrical dinuclear compounds where both metal centers are coordinated to a pyridine (**1**) or pyrazine (**2**) ring and N2 of the triazole moiety (isomer **a** in Figure 2). This is confirmed by the relative simplicity of the ^{1}H NMR spectra. The spectra are very similar to those obtained for the N2 isomers of mononuclear model complexes **5** and **6**.[7] This similarity confirms that N2 coordination is retained in the coupling reaction, and the symmetry of the spectrum furthermore confirms that both metal centers are equivalent. This observation is not unexpected. Earlier studies have shown that the pyridyl- and pyrazyltriazoles are extremely stable under normal synthetic conditions and that isomerization is only observed for protonated complexes. Deprotonated complexes were found to be photostable.[4c] Both compounds are isolated fully deprotonated, and the protonated species are obtained in situ by the addition of the appropriate amount of acid (Table 1).

Both **1** and **2** exhibit absorption and emission properties, which are characteristic for triazole based ruthenium polypyridyl complexes[4,5] (Table 1). For **1** and its protonated species, the emissive state can be assigned as a bpy based ^{3}MLCT state.[4,5] $\mathbf{H_21}$ emits weakly at 630 nm in acetonitrile, and its emission lifetime is significantly shorter (<5 ns) than that observed for **H1** and **1** (Table 1). The dramatic reduction in emission lifetime is related to the increase in the energy of the luminescent ^{3}MLCT state upon double protonation of the "spectator" bridging ligand and to the simultaneous decrease in the σ-donor strength of the 1,2,4-triazole moiety. This results in a lowering in the energy of the ^{3}MC level, which is known to deactivate the luminescent ^{3}MLCT state by a thermally activated surface crossing process.[2a,7] Somewhat surprisingly, **H1** has an increased emission lifetime. While the luminescent ^{3}MLCT state is undoubtedly raised in energy, it appears that the decrease in the σ-donor strength of the 1,2,4-triazole moieties in **H1** is not as significant as for $\mathbf{H_21}$ or the mononuclear analogue **H5**. As a result, the energy between the ^{3}MLCT and ^{3}MC levels is not sufficiently reduced to allow for more efficient deactivation of the emissive ^{3}MLCT excited state via population of the non-emissive ^{3}MC state. Consequently, the prolonged lifetime of the emitting state of **H1** compared with **1** can be attributed to the energy gap law.[17]

For **2**, the situation is more complex as the effect of protonation is to increase the emission lifetime with a small red shift in emission energy of the order of 10 nm. The difference in luminescence properties of the pyridine (**1** and **5**) and pyrazine (**2** and **6**) based complexes has been attributed to the switching of excited-state localization upon protonation, from a bpy based excited state to a pyrazine based excited state in the case of pyrazine based complexes.[7] Because the acceptor orbitals of the MLCT emitting level(s) in nonprotonated and protonated species of **2** are significantly different, no direct comparison can be made. Luminescence lifetimes for $\mathbf{2/H2/H_22}$ are longer than those of the mononuclear complex **6**/**H6**, and this may be indicative of charge delocalization within the dinuclear structures (Table 1).

By comparison with literature data, the oxidation waves at about 1.0 V versus SCE can be assigned as metal centered (Ru^{II}/Ru^{III}) processes.[4,5] Variations in the potential values of the various complexes may be explained on the basis of differences in the donor/acceptor properties of the ligands (Table 1). The oxidation processes of **2** occur at more positive potential than that of **1**, because of the better π-acceptor properties of the pyrazine ring. It is immediately apparent that for both **1** and **2** first metal oxidation potentials are very close to those of monomers **5** and **6**, respectively, and at much lower potential than those of the dinuclear complexes **3** and **4**. The presence of two metal based oxidation processes for both deprotonated and monoprotonated species indicates the presence of a significant intramolecular communication. This is discussed in more detail in the next section.

Intramolecular Interactions. The spectroscopic and electrochemical data discussed previously provide direct

(14) Fennema, B. D. J. R.; Hage, R.; Haasnoot J. G.; Reedijk, J. *J. Chem. Soc., Dalton Trans.* **1990**, 2425.
(15) Tiecco, M.; Tingoli, M.; Testaferri, L.; Chianelli, D.; Wenkert, E. *Tetrahedron* **1986**, *42*, 1475.
(16) Krüger, C.-F.; Miethchen, R. *Chem. Ber.* **1967**, *100*, 2250.
(17) Caspar, J. V.; Kober, E. M.; Sullivan, B. P.; Meyer, T. *J. Am. Chem. Soc.* **1982**, *104*, 630.

Table 2. Spectroelectrochemical Data for Complexes **1**–**4** in 0.1 M TEAP/Acetonitrile

	$\Delta E \pm$ 10 mV	K_c	$\Delta\nu_{1/2}$calcd (cm^{-1})	$\Delta\nu_{1/2}$ (cm^{-1})[b]	ϵ_{max} (M^{-1} cm^{-1}) ± 20%	$E_{op} \pm$ 100 cm^{-1}	α^2
1	180	1100	3060	4690	1820	5490	0.007
H1	110	72	4250	5600	1000	8700	0.0025
2	170	750	3120	4360	1120	5580	0.004
H2	60	10	4300	5300	1000	8500	0.0025
3[a]	300	117910	3341	3300	2400	5556	0.016
4[a]	300	117910	3260	4200	2200	5405	0.019

[a] Taken from ref 6. [b] Taken as double the width at half maximum of the high energy side of the absorption band.

evidence for communication between the two metal centers. They also indicate that this interaction is strongly dependent on the protonation state of the bridging ligand. The presence of two protonation steps with different pK_a values provides further confirmation of this. The effect of communication on the emission behavior is most clearly demonstrated for **H1** (Figure 5) and **H2**. In the absence of any interaction, two emission signals are expected for a monoprotonated species. For **H1**, where the emission energy values expected for the deprotonated (690 nm) and protonated species (630 nm) are significantly different, this would be particularly straightforward to detect. Instead, a single-exponential decay of the emitting state is observed, and the emission at 660 nm is intermediate between that of **1** and $\mathbf{H_21}$. This indicates the presence of a new emitting species, in which the effect of monoprotonation is shared by both metal centers.

Electrochemical and spectroelectrochemical studies can be used to quantify this interaction. The first parameter of interest is the separation between the two metal based oxidation processes (ΔE). This separation is related to the stability of the intervalence compound Ru(II)Ru(III) as defined in eq 1[18]

$$K_c = \exp(\Delta E/25.69) \tag{1}$$

where K_c is the comproportionation constant as defined in eq 2

$$Ru^{II}Ru^{II} + Ru^{III}Ru^{III} \overset{K_c}{\rightleftharpoons} 2Ru^{II}Ru^{III} \tag{2}$$

The ΔE values obtained for the deprotonated compounds of 180 mV for **1** and 170 mV for **2** are indicative of a significant intramolecular communication (Table 2). This interaction is, however, less than that observed for **3** and **4**, for which values of about 300 mV were obtained. For **H1** and **H2**, the difference between first and second metal oxidation waves decreases to 110 mV for **H1** and 60 mV in **H2**. This leads to significantly reduced K_c values indicating a decreased interaction. This decrease in interaction upon protonation is even more prevalent for both $\mathbf{H_21}$ and $\mathbf{H_22}$ for which only a single two-electron oxidation wave is observed. This indicates that for the fully protonated species K_c is less than 5 and that a mixed valence species does not form in detectable amounts.

(18) Richardson, D. E.; Taube, H. *Inorg. Chem.* **1981**, *20*, 1278.

More detailed information about the nature of this interaction can be obtained from spectroelectrochemical investigations. On the basis of the electrochemical results outlined previously, intervalence bands can be expected for the deprotonated and the singly protonated species. Analysis of the spectroscopic properties of the intervalence band allows for the estimate of the interaction parameter (α^2) as in eq 3[19]

$$\alpha^2 = \frac{(4.2 \times 10^{-4})\epsilon_{max}\nu_{1/2}}{d^2 E_{op}} \tag{3}$$

where ϵ_{max} is the extinction coefficient of the IT band (M^{-1} cm^{-1}), $\Delta\nu_{1/2}$ is its peak width at half-height, d is the estimated metal to metal distance, 9.5 Å for these compounds, and E_{op} is the energy of the absorption maximum of the intervalence band. Additional information can be obtained by estimating the theoretical peak width at half-height, $\Delta\nu_{1/2calcd}$ using eq 4.[19]

$$\Delta\nu_{1/2calcd} = [2310(E_{op} - \Delta E)]^{1/2} \tag{4}$$

If the value of $\Delta\nu_{1/2}$ obtained from this equation correlates well with the value found from direct measurement, then the system can be described as valence localized $Ru^{II}Ru^{III}$, that is, Type II. If the IT band is narrower then the system, it is better described as type III (valence delocalized).[20] The values obtained from eqs 1–4 are presented in Table 2. On the basis of these data and, in particular, because $\Delta\nu_{1/2}$ observed is larger than $\Delta\nu_{1/2calcd}$, it seems clear that the mixed valence compounds behave as type II (or valence trapped) dinuclear species. Another important observation is that the ΔE, E_{op}, and α^2 values obtained for **1** and **2** are the same within experimental error (Table 2). This observation and the similarity of the energies of the LMCT bands observed for the mixed valence compounds indicate that LUMO of the bridging ligand plays at best minor roles in determining intercomponent interaction. Instead, it is expected that interaction between the metal centers is taking place via a hole transfer mechanism involving the HOMO of the metal units and bridging ligand.[6] This is confirmed by the decrease in interaction observed upon protonation of the bridging ligand. In a hole transfer mechanism, the extent of the interaction depends on the energy gap between the dπ-metal orbitals (metal based HOMO) and the σ-orbitals of the bridge.[21] The spectroscopic and electrochemical data show that the ligand based σ-orbitals are stabilized upon protonation, so that the energy gap between the relevant orbitals *increases*, leading to *decreased* superexchange-assisted electronic interactions.

The α^2 values given in Table 2 indicate that the amount of electron delocalization in **1** and **2** is considerably less than that observed in **3** and **4**. This observation can be explained

(19) (a) Hush, N. S. *Prog. Inorg. Chem.* **1967**, *8*, 391. (b) Hush, N. S. *Electrochim. Acta* **1968**, *13*, 1005.
(20) Robin, M. P.; Day, P. *Adv. Inorg. Chem. Radiochem.* **1967**, *10*, 247.
(21) (a) Giuffrida, G.; Campagna, S. *Coord. Chem. Rev.* **1994**, *135–136*, 517. (b) Laye, R. H.; Couchman, S. M.; Ward, M. D. *Inorg. Chem.* **2001**, *40*, 4089 and references therein.

by considering the difference in the distance between the two metal centers. Crystallographic data have shown that *d* in **3** is 6.5 Å, while preliminary molecular modeling suggests that in **1** and **2** this distance is 9.5 Å. An additional factor may be that in **3** and **4** the negative charge of the bridge is shared between the two metal centers, while in **1** and **2** the triazole based negative charge is expected to be more localized.

Finally, the difference in the redox and luminescence properties of the deprotonated (**1** and **2**), monoprotonated (**H1** and **H2**), and the diprotonated ($\mathbf{H_21}$ and $\mathbf{H_22}$) species warrants some additional comments. On looking at Table 1 and Figure 5, it is clear that the luminescence output of **1** can be switched between three "states" in terms of emission energy and lifetime. It should be stressed, however, that the excited-state responsible for the emission remains the same in all three cases. So, the behavior observed cannot be explained by a switching process between different electronic states. It is rather a stepwise protonation, which perturbs the emitting excited state in such a way that three different outputs are generated. In principle, the same also occurs for **2**; however, the changes in luminescence energy are almost negligible. While the switching of the luminescence output between two "states" is common,[12] the possibility of switching luminescence between three different outputs is less so. In addition, the redox properties of both compounds can also be employed in this respect. For example, by monitoring of the current at 0.8, 1.05, and 1.15 V, the protonation state of **1** may be "read". In view of the future development in the design of systems capable of manipulating information (e.g., light or electrons) at the molecular level, our results offer new lines toward this goal, in terms of both synthetic methods and physical properties.

Conclusions

With the ever-increasing interest in multinuclear metal complexes as supramolecular systems, the assemblies investigated are becoming ever more complex. As a result, the formation of isomers and side products is an increasing problem. The Ni(0) catalyzed homonuclear coupling reported in this contribution is simple and leads to pure compounds in a high yield, in cases where direct reaction of the bridging ligand with the metal centers leads to a mixture of products.[22] To the best of our knowledge, this is the first time such a coupling has been carried out with ruthenium(II) polypyridyl complexes.[8] The method can be adapted to many other systems and constitutes, therefore, together with some related methods,[23] an important tool for the design of novel supramolecular assemblies.

The electrochemical and photophysical studies of the dinuclear compounds obtained illustrate the "tunable nature" of the properties of these supramolecular systems and their potential as molecular switches. The close proximity of the two triazole rings creates interaction between the two parts of the molecule, and the three protonation states obtained show different levels of intercomponent interaction. It is, furthermore, important to note that while the differences in ground-state properties and metal−metal interaction between the pyridine (**1**) and pyrazine (**2**) based complexes are minor, their luminescence properties are substantially different. Relatively small changes in the composition of the compounds, that is, pyridine versus pyrazine, lead to compounds with different excited-state properties. Taking into account the synthetic procedures used in this investigation, this opens the possibility for extensive variation in the components that can be used to build up a range in proton gated redox active and emitting compounds.

Acknowledgment. The authors thank Mr. Maurice Burke and Mr. Michael Burke of Dublin City University for assistance in Mass Spectrometry and ^{1}H NMR spectroscopy. The authors thank MURST (Progetto Artificial photosynthesis), CNR, Enterprise Ireland, and the EU, TMR Grant 96CT-0031, for financial assistance.

IC0112894

(22) Müller, E.; Nazeeruddin, Md. K.; Graetzel, M.; Kalyanasundaram, K.; Prome, J.-C. *New J. Chem.* **1996**, *20*, 759.

(23) (a) Tzalis, D.; Tor, Y. *J. Am. Chem. Soc.* **1997**, *119*, 852. (b) Connors, P. J., Jr.; Tzalis, D.; Dunnick, A. L.; Tor, Y. *Inorg. Chem.* **1998**, *37*, 1121. (c) Chodorowski-Kimmes, S.; Beley, M.; Colin, J.-P.; Sauvage, J.-P. *Tetrahedron Lett.* **1996**, *37*, 2963. (d) Dunne, S. J.; Constable, E. C. *Inorg. Chem. Commun.* **1998**, *1*, 167. (e) Johansson, K. O.; Lotoski, J. A.; Tong, C. C.; Hanan, G. S. *Chem. Commun.* **2000**, 819. (f) Griffiths, P. M.; Loiseau, F.; Puntoriero, F.; Serroni, S.; Campagna, S. *Chem. Commun.* **2000**, 2297.

Ground state resonance Raman spectra

Protonated complexes at 457.9 nm excitation

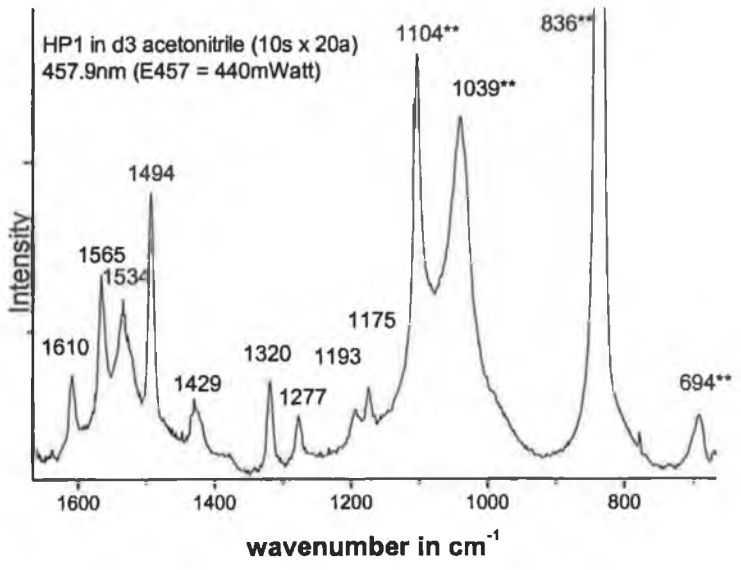

Figure B.1 *Resonance Raman spectrum of $[Ru(bpy)_2(Hphpztr)]^{2+}$ in CD_3CN; protonation with CF_3CO_2H.*

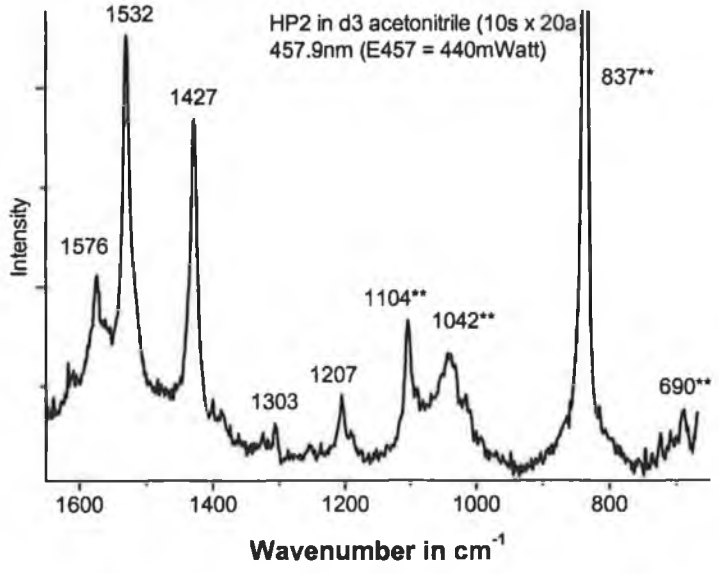

Figure B.2 *Resonance Raman spectrum of $[Ru([D_8]\text{-}bpy)_2(Hphpztr)]^{2+}$ in CD_3CN; protonation with CF_3CO_2H.*

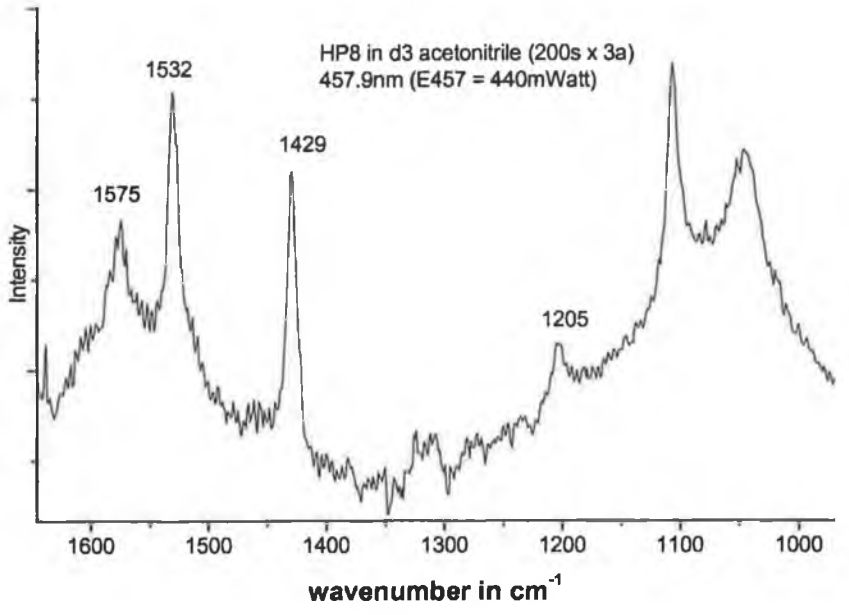

Figure B.3 *Resonance Raman spectrum of $[Ru([D_8]\text{-}bpy)_2([D_8]\text{-}Hphpztr)]^{2+}$ in CD_3CN; protonation with CF_3CO_2H.*

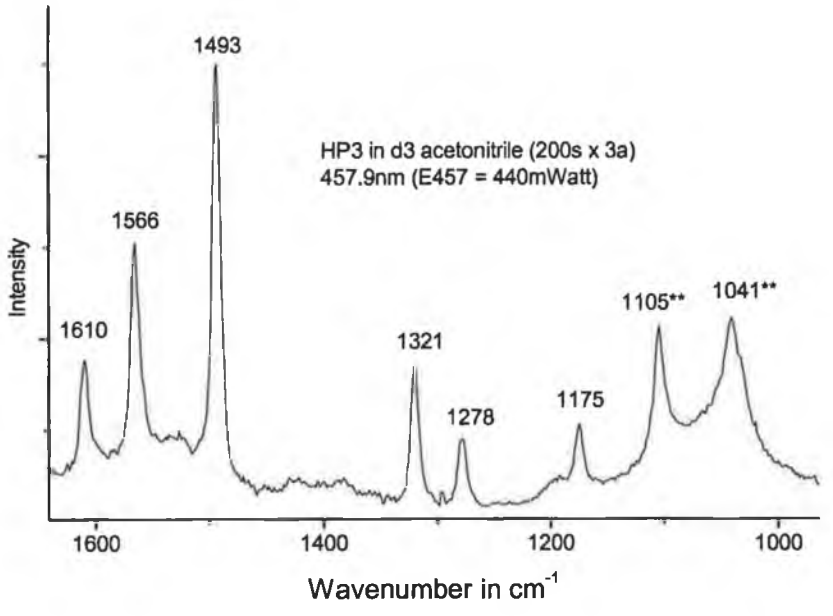

Figure B.4 *Resonance Raman spectrum of $[Ru(bpy)_2([D_3]\text{-}Hphpztr)]^{2+}$ in CD_3CN; protonation with CF_3CO_2H*

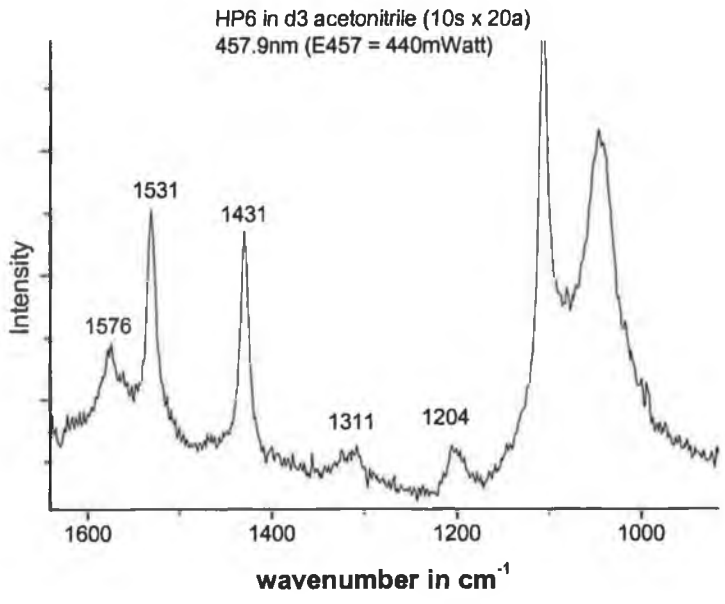

Figure B.5 *Resonance Raman spectrum of $[Ru([D_8]\text{-}bpy)_2([D_3]\text{-}Hphpztr)]^{2+}$ in CD_3CN; protonation with CF_3CO_2H*

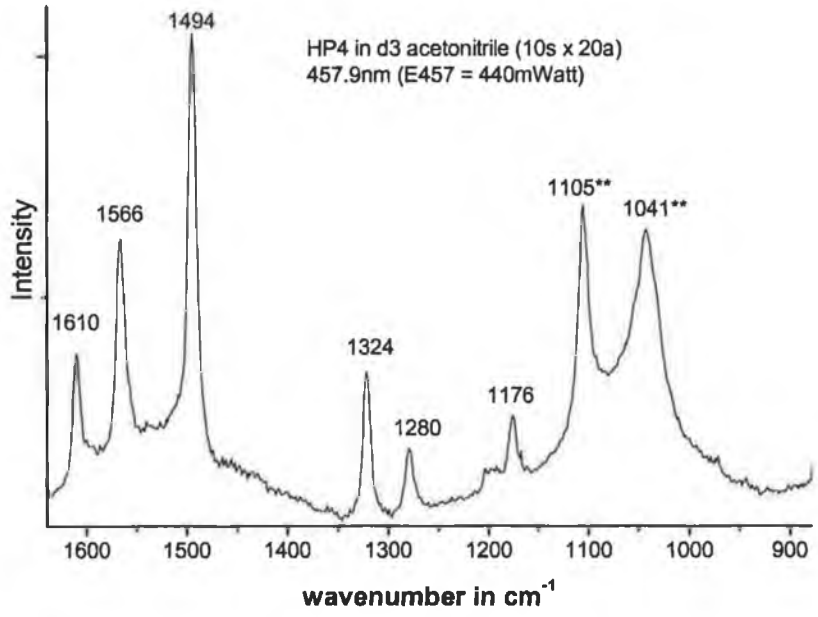

Figure B.6 *Resonance Raman spectrum of $[Ru(bpy)_2([D_8]\text{-}Hphpztr)]^{2+}$ in CD_3CN; protonation with CF_3CO_2H*

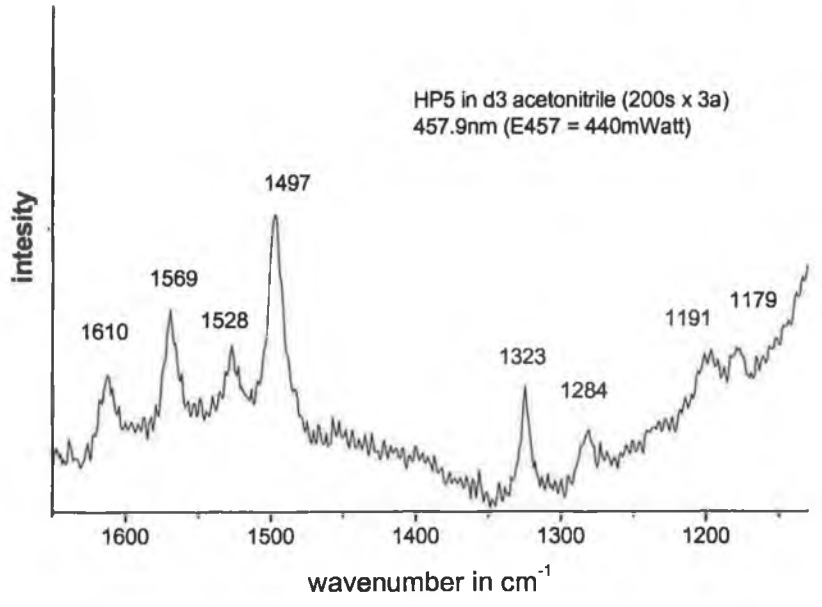

Figure B.7 *Resonance Raman spectrum of $[Ru(bpy)_2([D_5]\text{-}Hphpztr)]^{2+}$ in CD_3CN; protonation with CF_3CO_2H*

Deprotonated complexes at 457.9 nm excitation

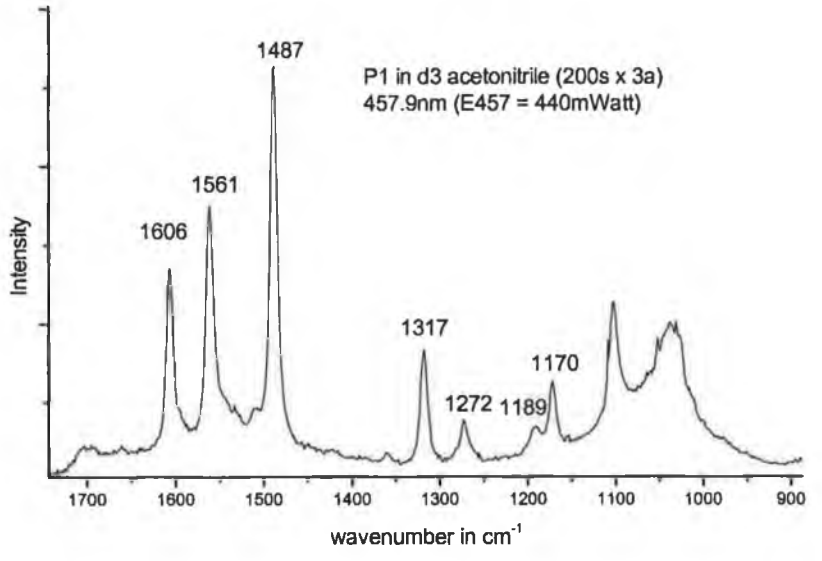

Figure B.8 *Resonance Raman spectrum of $[Ru(bpy)_2(phpztr)]^{+}$ in CD_3CN.*

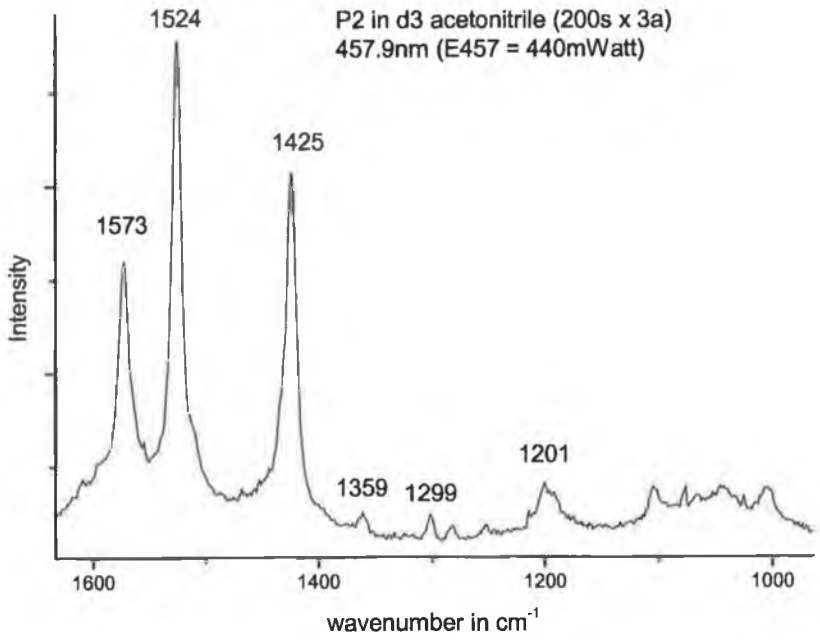

Figure B.9 *Resonance Raman spectrum of $[Ru([D_8]\text{-}bpy)_2(phpztr)]^+$ in CD_3CN.*

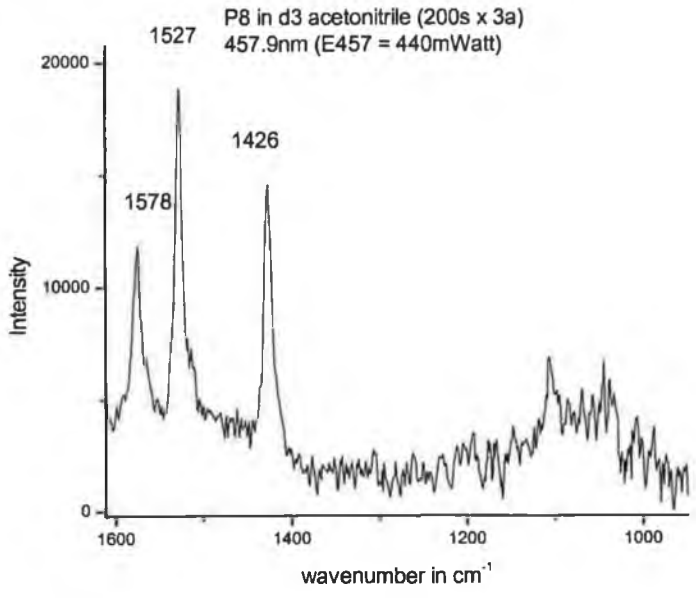

Figure B.10 Resonance Raman spectrum of $[Ru([D_8]\text{-}bpy)_2([D_8]\text{-}phpztr)]^+$ in CD_3CN.

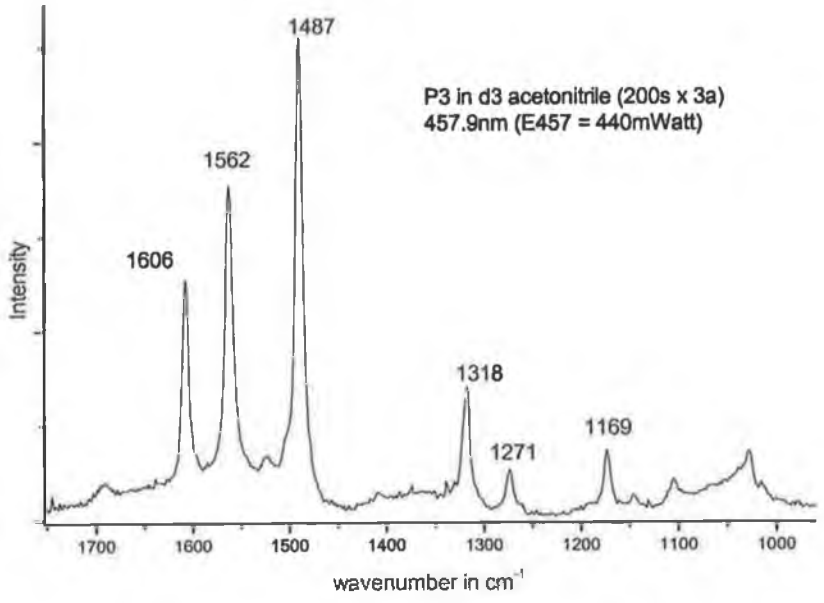

Figure B.11 *Resonance Raman spectrum of [Ru(bpy)$_2$([D$_3$]-phpztr)] in CD$_3$CN.*

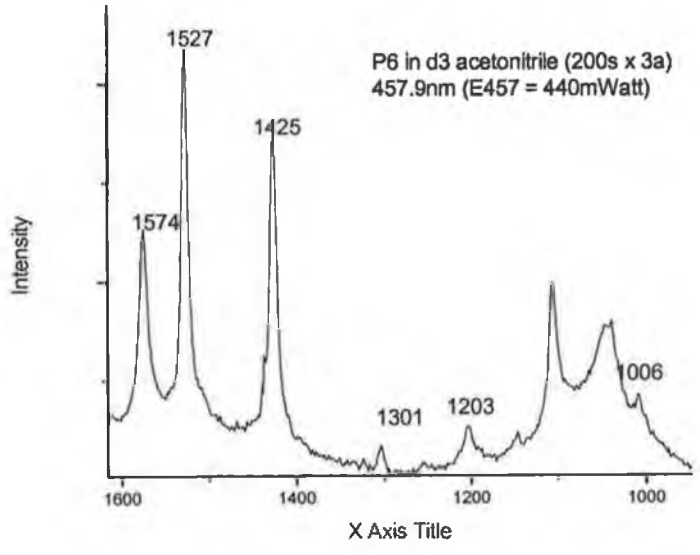

Figure B.12 *Resonance Raman spectrum of [Ru([D$_8$]-bpy)$_2$([D$_3$]-phpztr)]$^+$ in CD$_3$CN.*

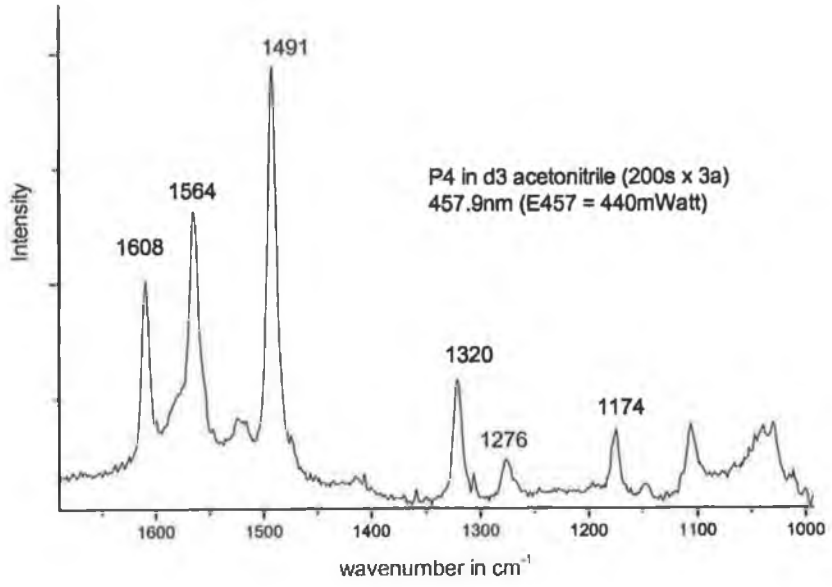

Figure B.13 *Resonance Raman spectrum of $[Ru(bpy)_2([D_8]\text{-phpztr})]^+$ in CD_3CN.*

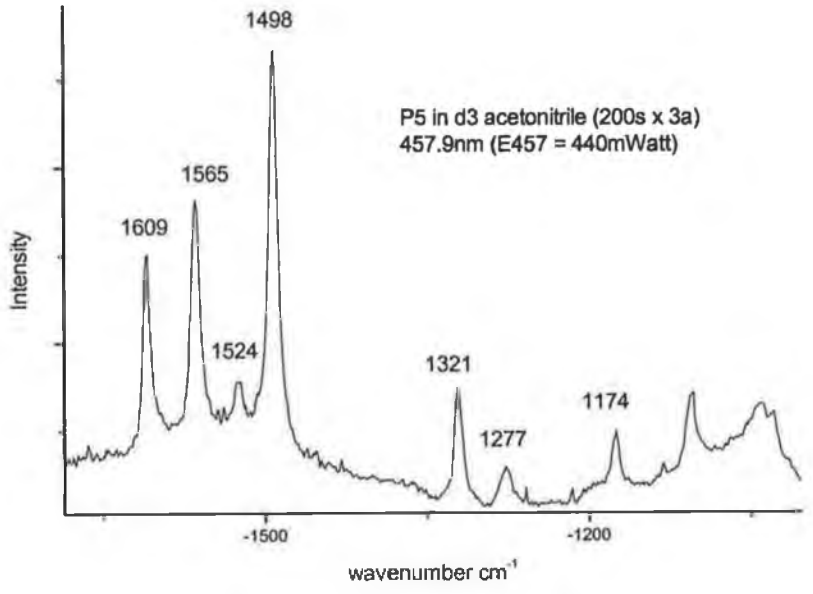

Figure B.14 *Resonance Raman spectrum of $[Ru(bpy)_2([D_5]\text{-phpztr})]^+$ in CD_3CN.*

Protonated complexes at 514.5 nm excitation

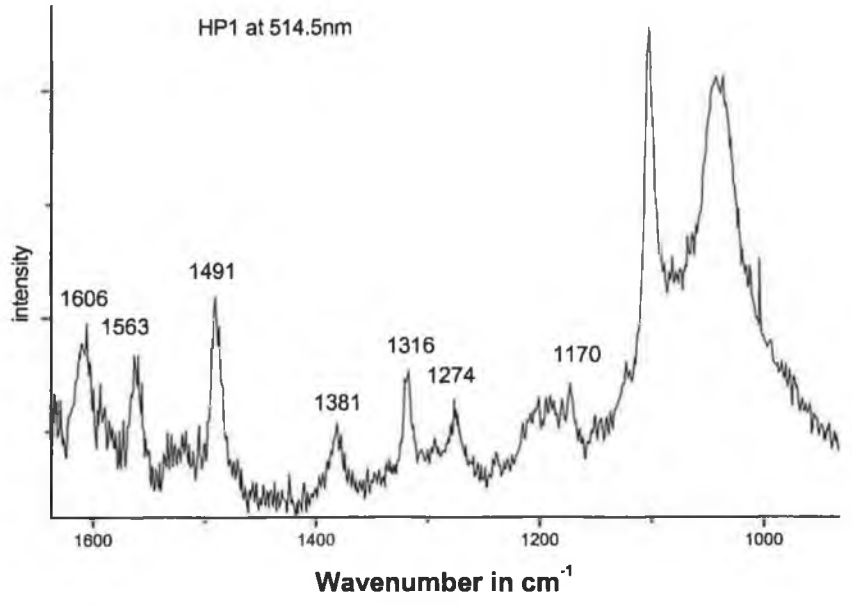

Figure B.15 *Resonance Raman spectrum of $[Ru(bpy)_2(Hphpztr)]^{2+}$ in CD_3CN; protonation with CF_3CO_2H.*

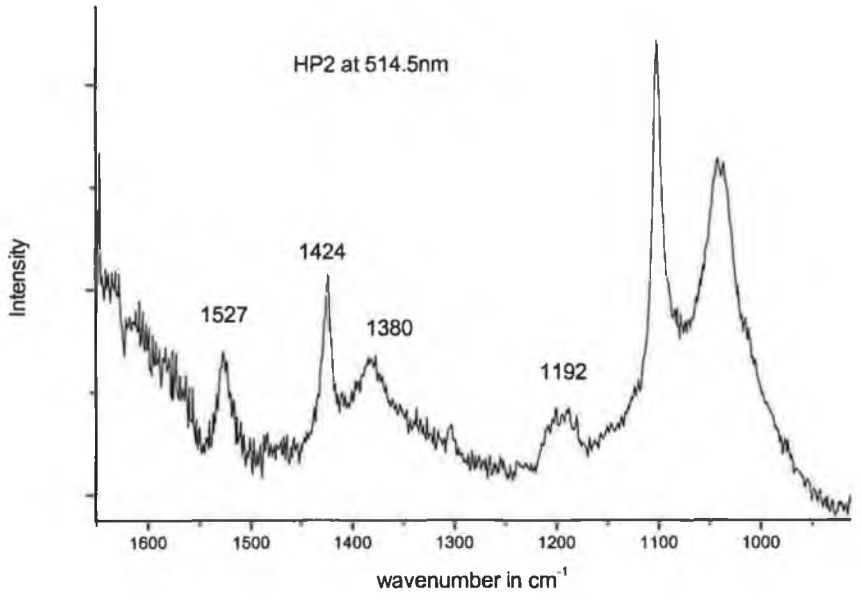

Figure B.16 *Resonance Raman spectrum of $[Ru([D_8]\text{-}bpy)_2(Hphpztr)]^{2+}$ in CD_3CN; protonation with CF_3CO_2H.*

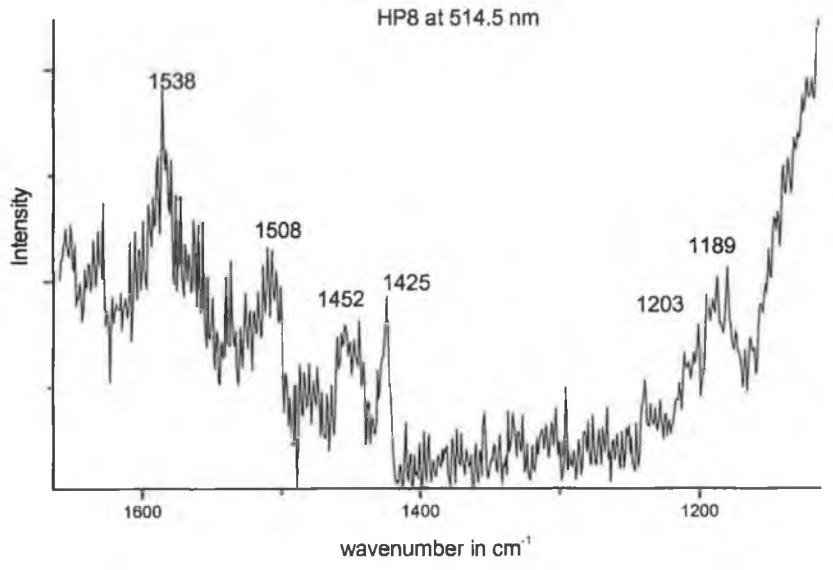

Figure B.17 *Resonance Raman spectrum of $[Ru([D_8]\text{-bpy})_2([D_8]\text{-Hphpztr})]^{2+}$ in CD_3CN; protonation with CF_3CO_2H.*

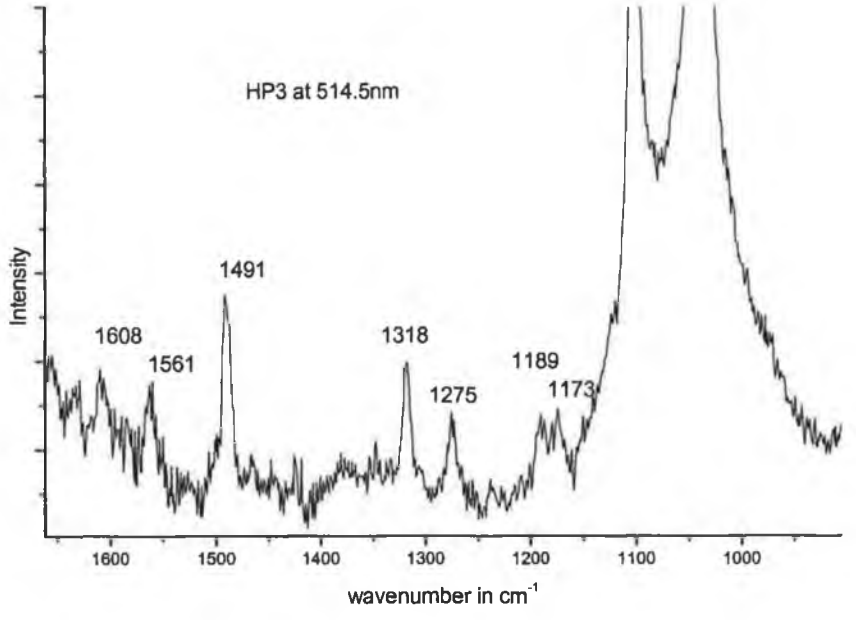

Figure B.18 *Resonance Raman spectrum of $[Ru(bpy)_2([D_3]\text{-Hphpztr})]^{2+}$ in CD_3CN; protonation with CF_3CO_2H*

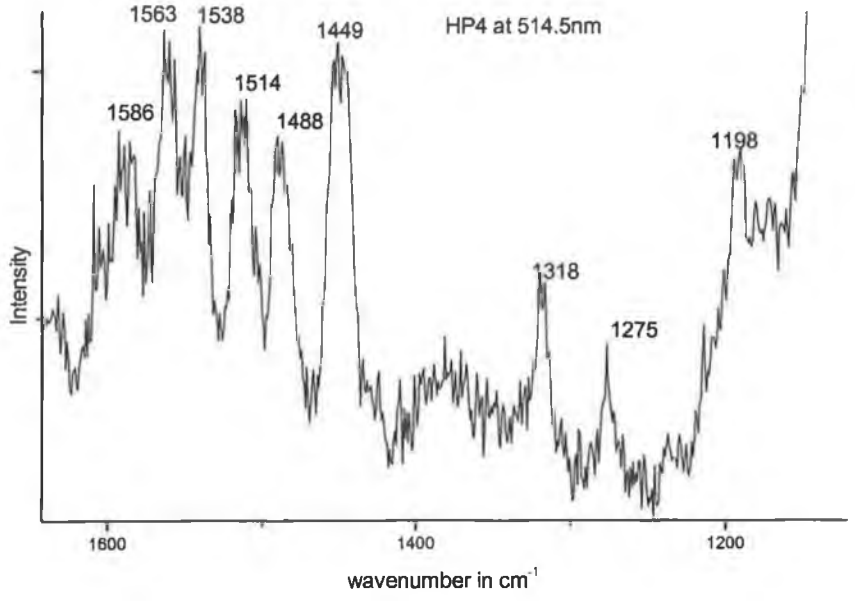

Figure B.19 *Resonance Raman spectrum of $[Ru(bpy)_2([D_8]\text{-}Hphpztr)]^{2+}$ in CD_3CN; protonation with CF_3CO_2H*

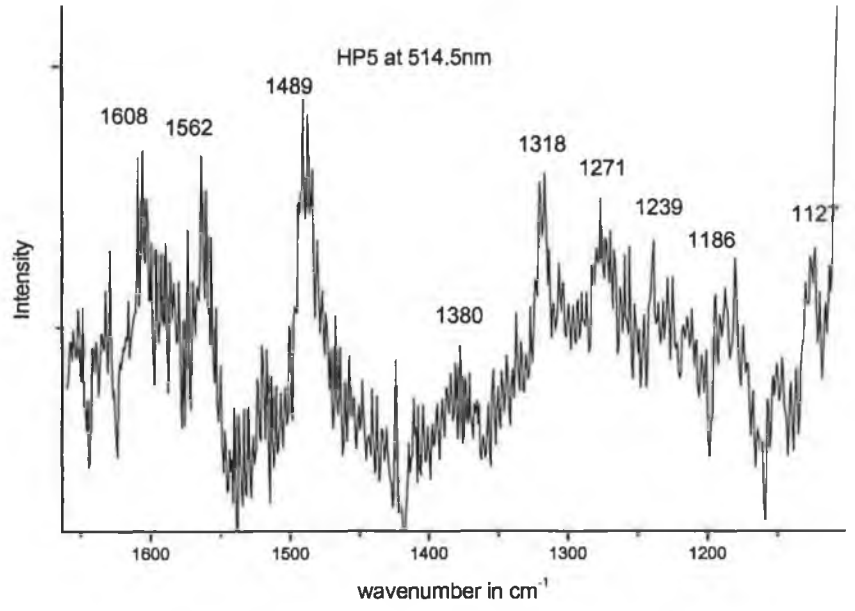

Figure B.20 *Resonance Raman spectrum of $[Ru(bpy)_2([D_5]\text{-}Hphpztr)]^{2+}$ in CD_3CN; protonation with CF_3CO_2H*

Deprotonated complexes at 514.5 nm excitation

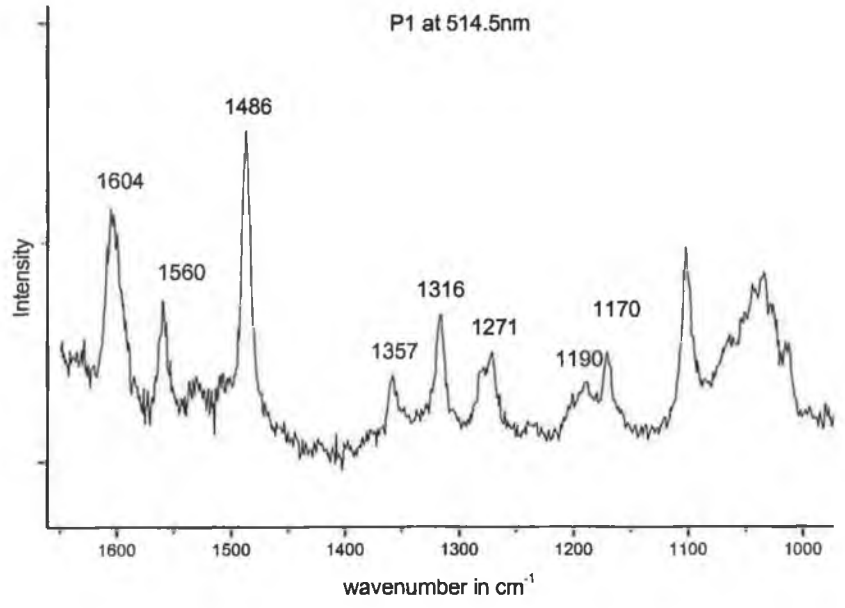

Figure B.21 *Resonance Raman spectrum of $[Ru(bpy)_2(phpztr)]^+$ in CD_3CN.*

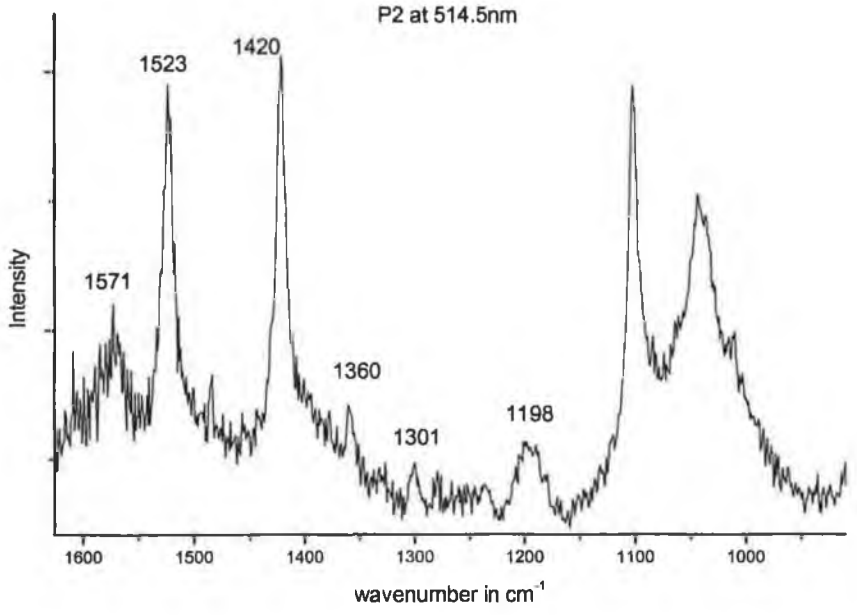

Figure B.22 *Resonance Raman spectrum of $[Ru([D_8]\text{-}bpy)_2(phpztr)]^+$ in CD_3CN.*

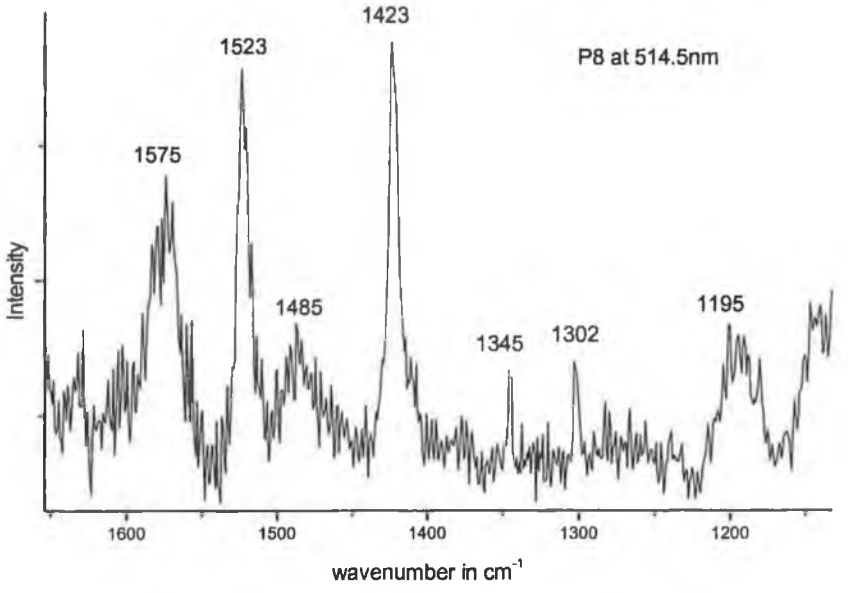

Figure B.23 *Resonance Raman spectrum of [Ru([D$_8$]-bpy)$_2$([D$_8$]- phpztr)]$^+$ in CD$_3$CN.*

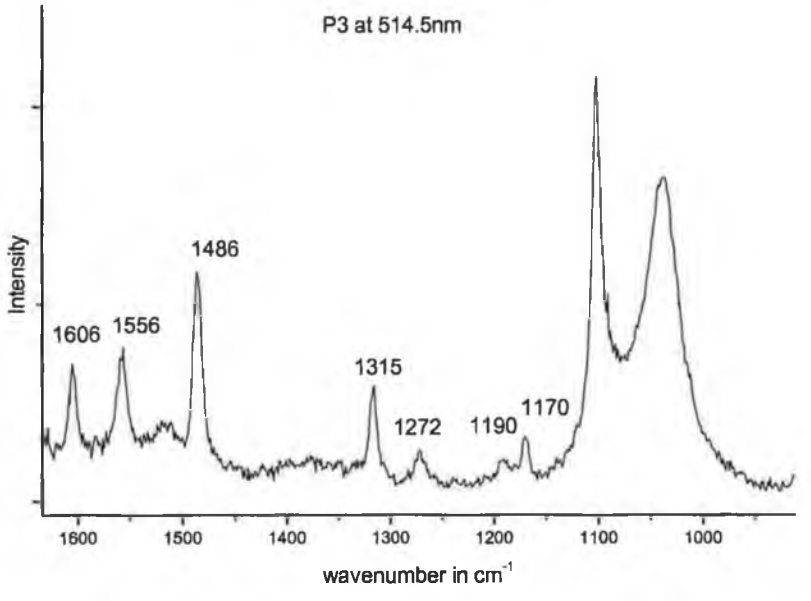

Figure B.24 *Resonance Raman spectrum of [Ru(bpy)$_2$([D$_3$]-phpztr)] in CD$_3$CN.*

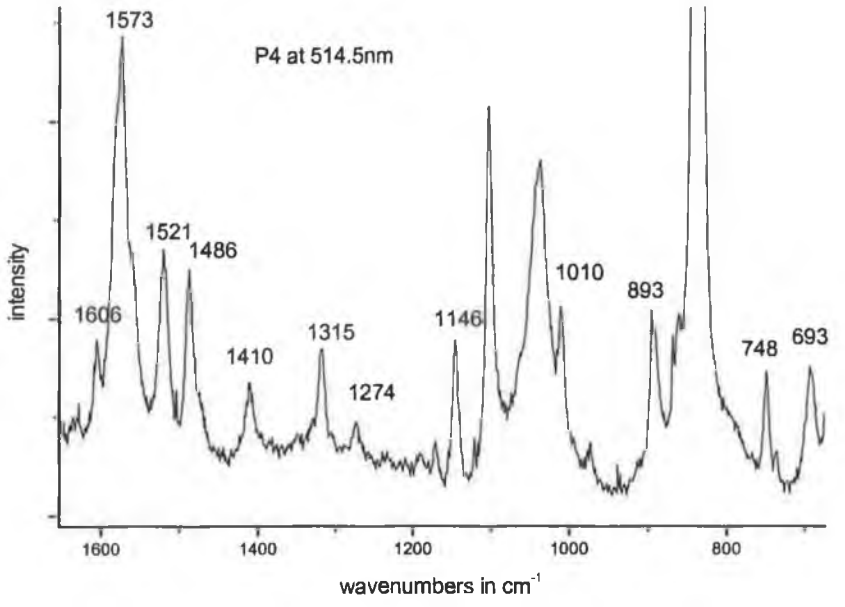

Figure B.25 *Resonance Raman spectrum of $[Ru(bpy)_2([D_8]\text{-phpztr})]^+$ in CD_3CN.*

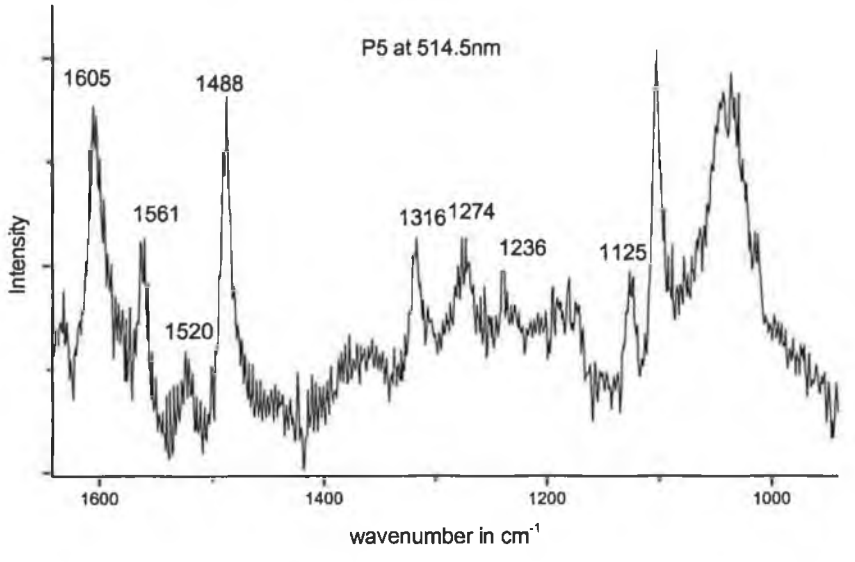

Figure B.26 *Resonance Raman spectrum of $[Ru(bpy)_2([D_5]\text{-phpztr})]^+$ in CD_3CN.*

Excited state resonance Raman spectra

Protonated complexes

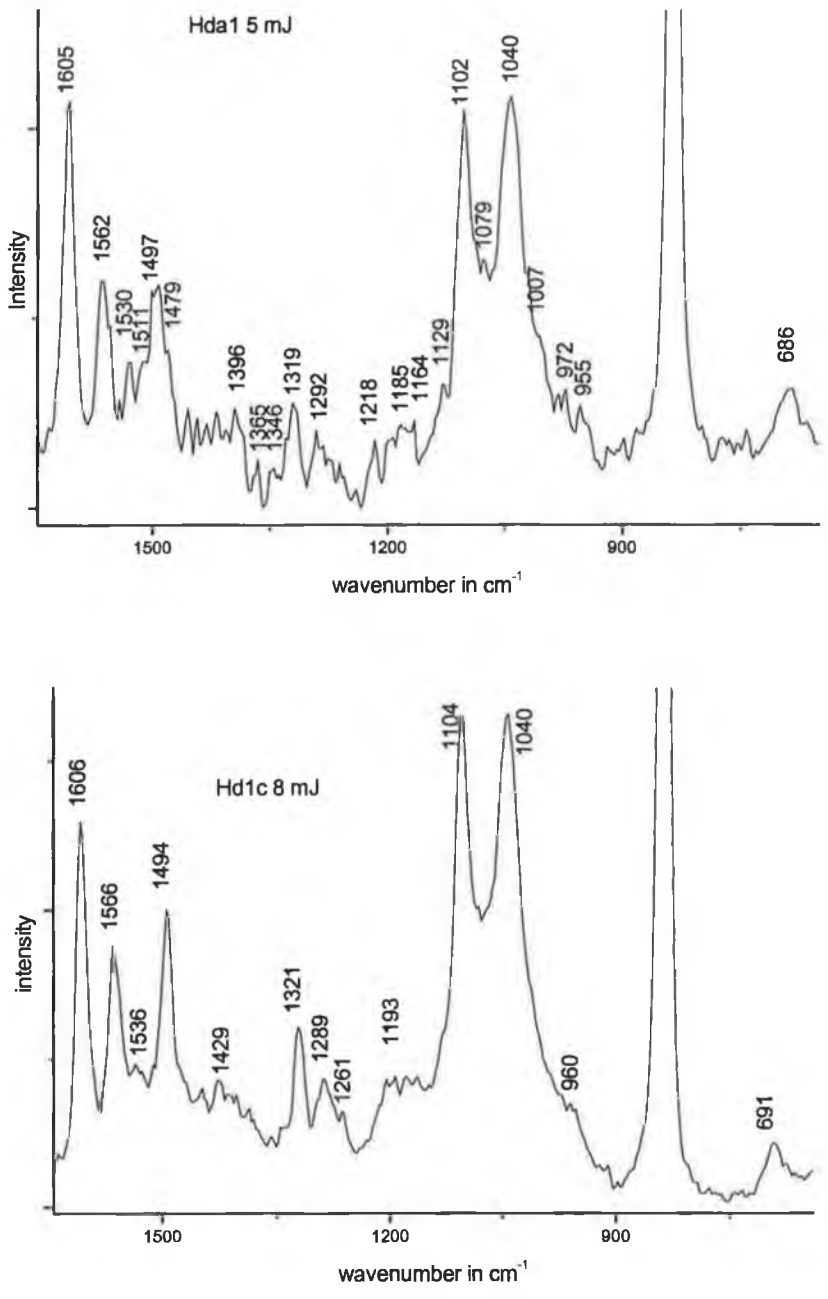

Figure C.1 *Excited state rR spectrum of $[Ru(bpy)_2(Hphpztr)]^{2+}$ in CD_3CN; protonation with CF_3CO_2H.*

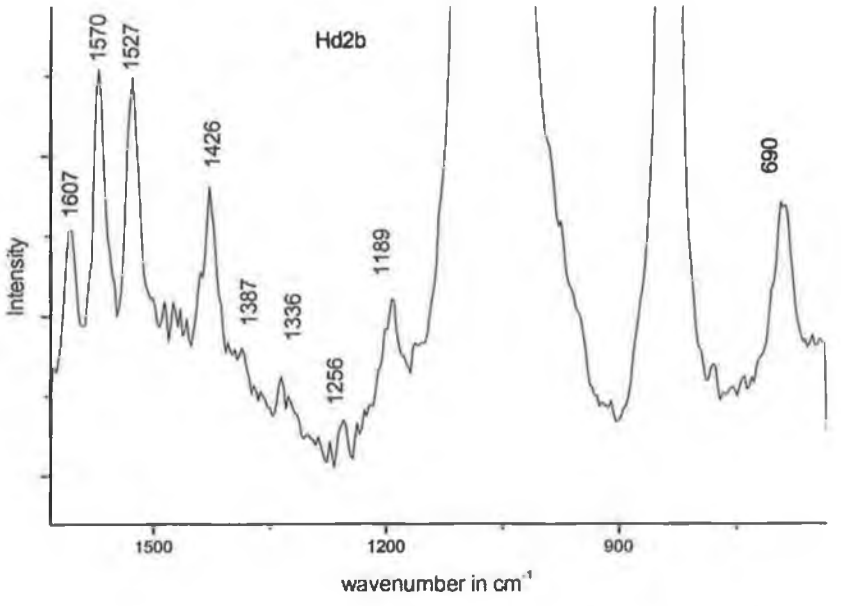

Figure C.2 *Excited state rR spectrum of $[Ru([D_8]\text{-bpy})_2(Hphpztr)]^{2+}$ in CD_3CN; protonation with CF_3CO_2H.*

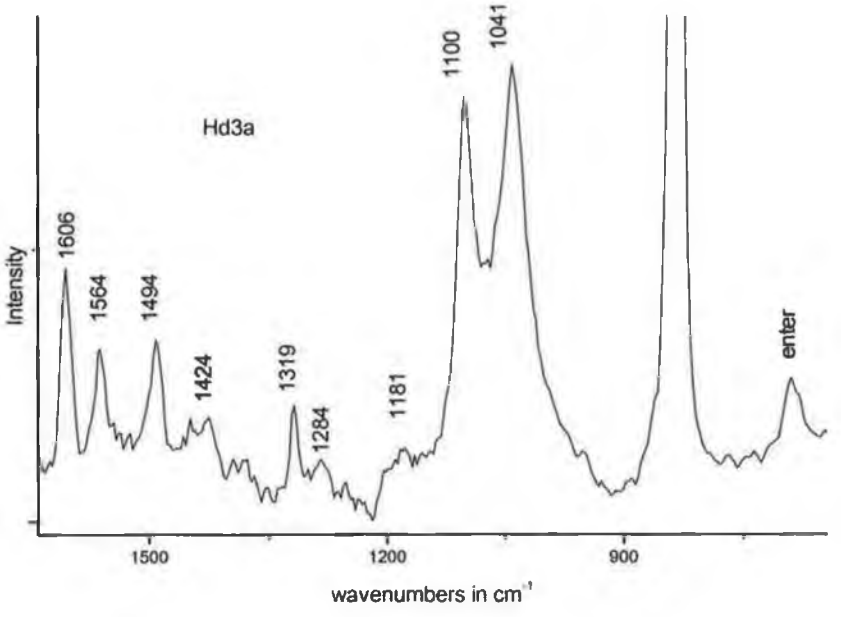

Figure C.3 *Excited state rR spectrum of $[Ru(bpy)_2([D_3]\text{-Hphpztr})]^{2+}$ in CD_3CN; protonation with CF_3CO_2H.*

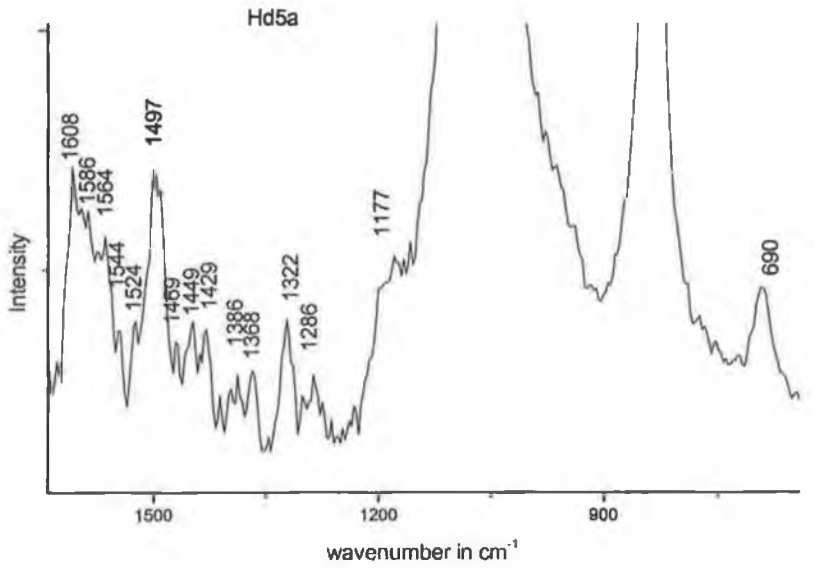

Figure C.4 *Excited state rR spectrum of $[Ru(bpy)_2([D_5]\text{-}Hphpztr)]^{2+}$ in CD_3CN; protonation with CF_3CO_2H.*

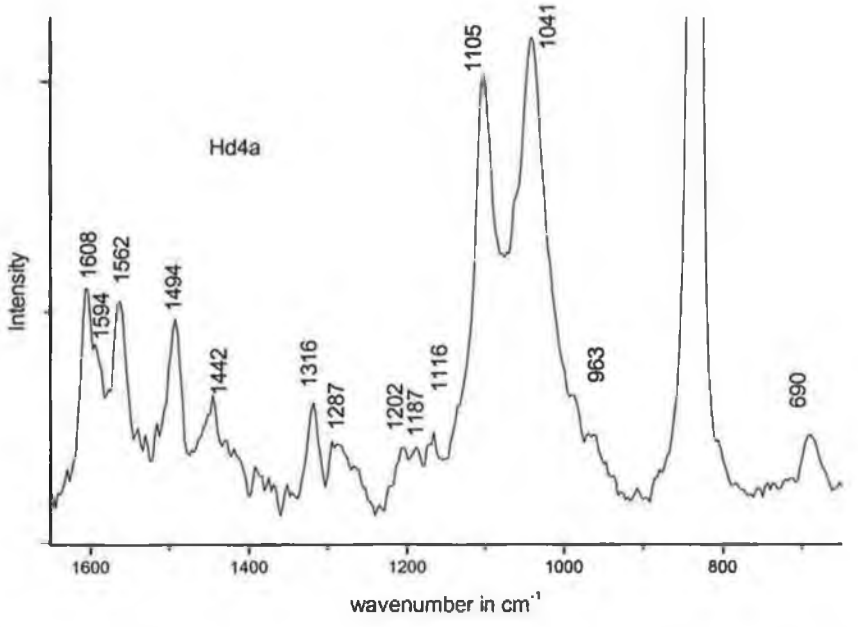

Figure C.5 *Excited state rR spectrum of $[Ru(bpy)_2([D_8]\text{-}Hphpztr)]^{2+}$ in CD_3CN; protonation with CF_3CO_2H.*

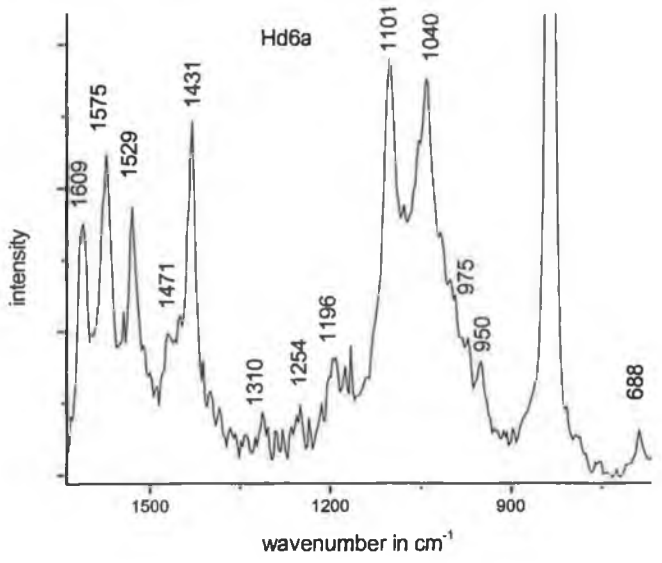

Figure C.6 *Excited state rR spectrum of $[Ru([D_8]\text{-bpy})_2([D_3]\text{-Hphpztr})]^{2+}$ in CD_3CN; protonation with CF_3CO_2H.*

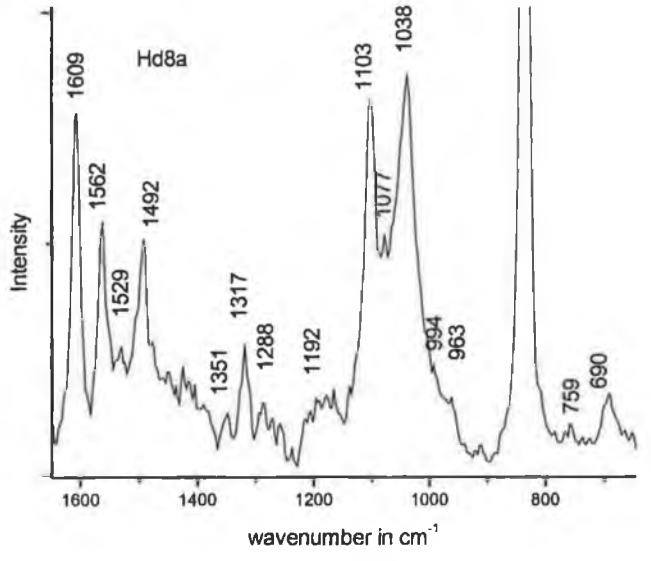

Figure C.7 *Excited state rR spectrum of $[Ru([D_8]\text{-bpy})_2([D_8]\text{-Hphpztr})]^{2+}$ in CD_3CN; protonation with CF_3CO_2H.*

Deprotonated complexes

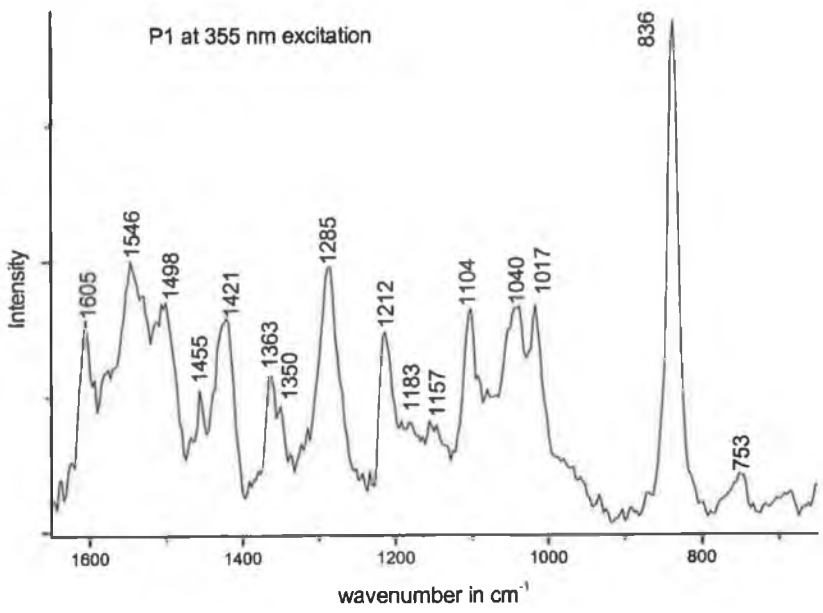

Figure C.8 *Excited state rR spectrum of $[Ru(bpy)_2(phpztr)]^+$ in CD_3CN*

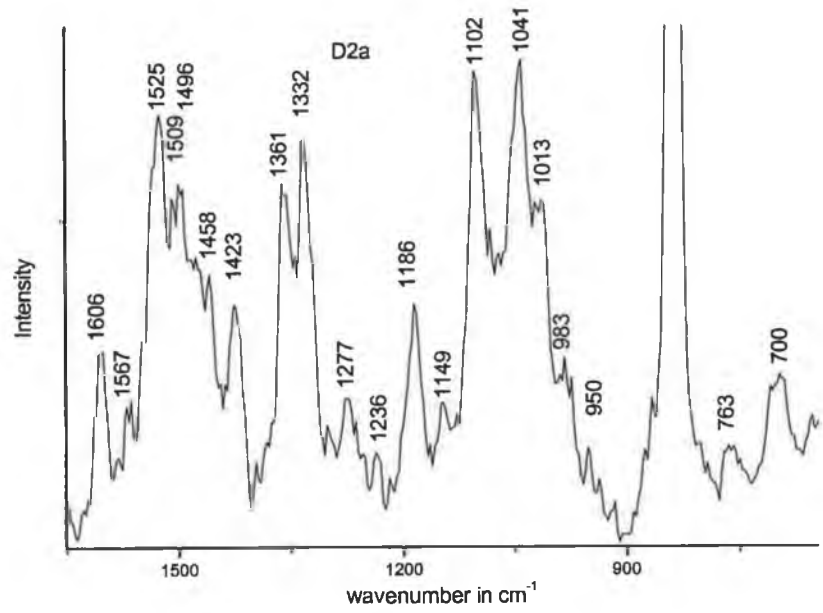

Figure C.9 *Excited state rR spectrum of $[Ru([D_8]\text{-}bpy)_2(phpztr)]^+$ in CD_3CN.*

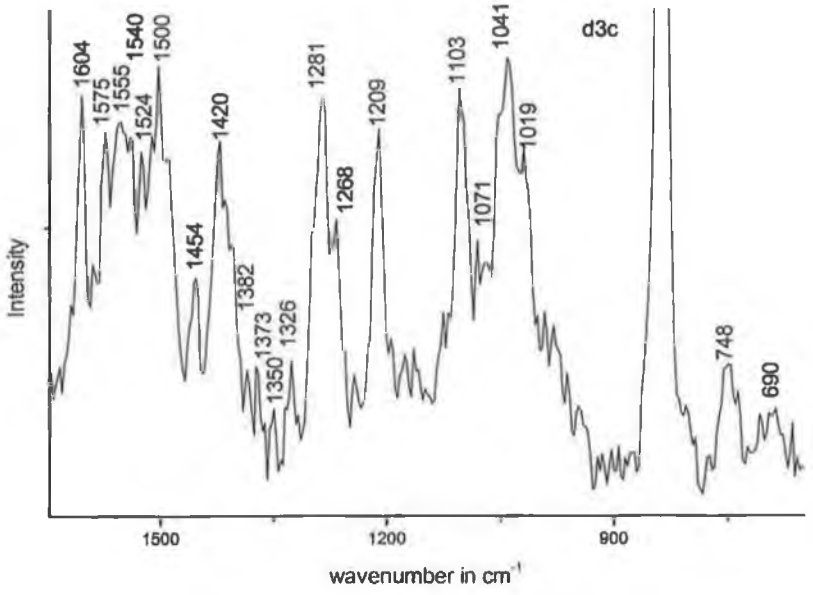

Figure C.10 *Excited state rR spectrum of $[Ru(bpy)_2([D_3]\text{-phpztr})]^+$ in CD_3CN*

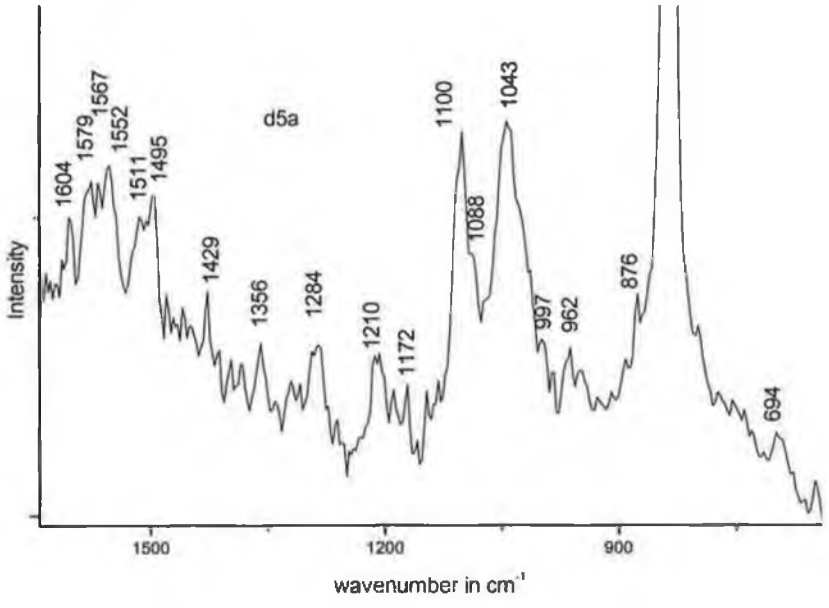

Figure C.11 *Excited state rR spectrum of $[Ru(bpy)_2([D_5]\text{-phpztr})]^+$ in CD_3CN*

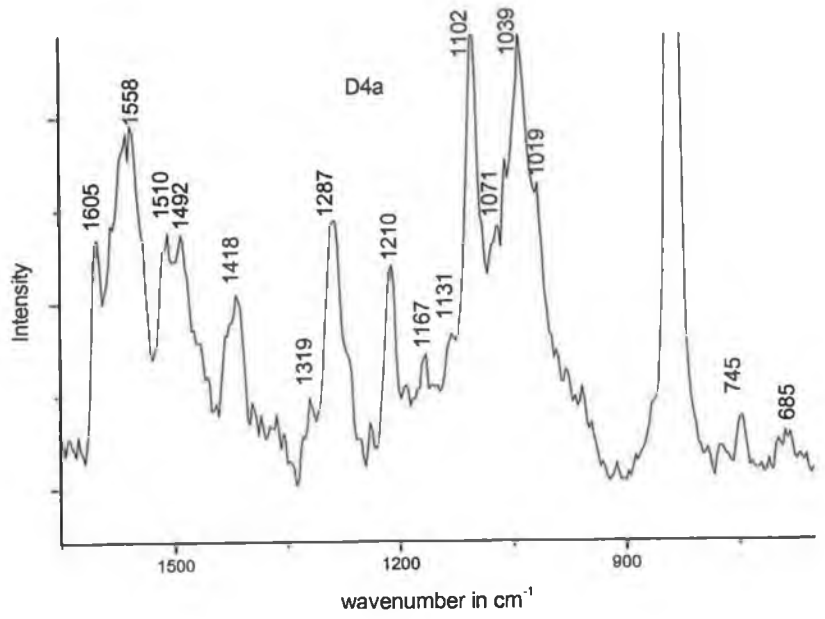

Figure C.12 *Excited state rR spectrum of $[Ru(bpy)_2([D_8]\text{-phpztr})]^+$ in CD_3CN*

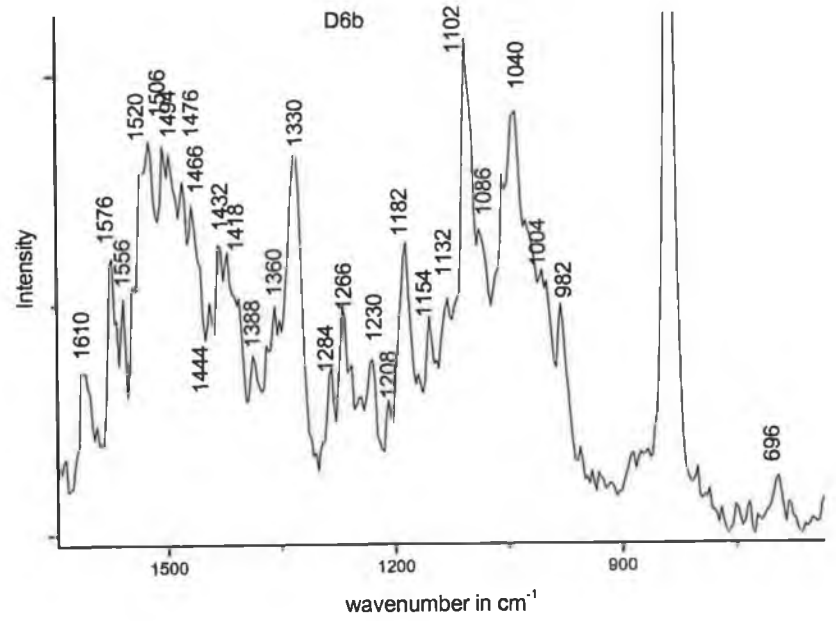

Figure C.13 *Excited state rR spectrum of $[Ru([D_8]\text{-bpy})_2([D_3]\text{-phpztr})]^+$ in CD_3CN*

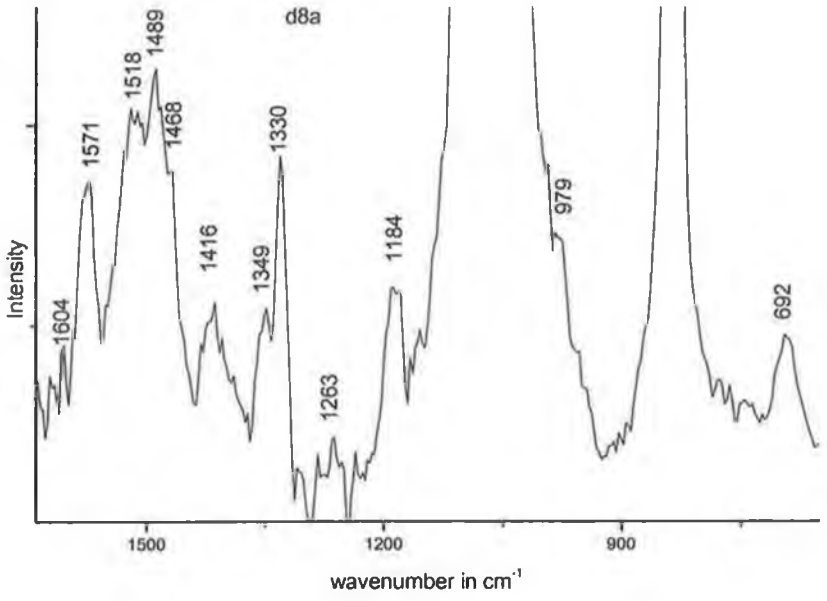

Figure C.14 *Excited state rR spectrum of* $[Ru([D_8]\text{-bpy})_2([D_8]\text{-phpztr})]^+$ *in* CD_3CN

Temperature Dependent emission studies

a) $[Ru(ph_2phen)_3](PF_6)_2$

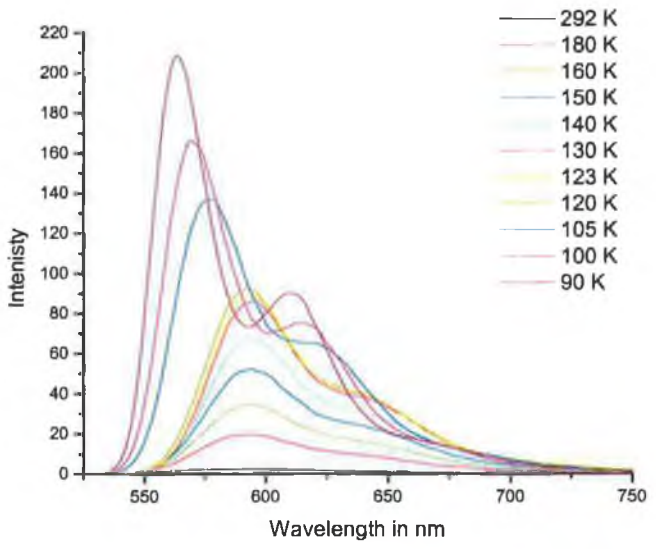

Figure D.1 *Temperature dependence of the emission spectrum of* $[Ru(ph_2phen)_3](PF_6)_2$ *in EtOH/MeOH 4/1 v/v between 90 K and 292 K.*

b) $[Ru(LL)_2(pztr)](PF_6)$ LL = biq or ph_2phen under basic conditions.

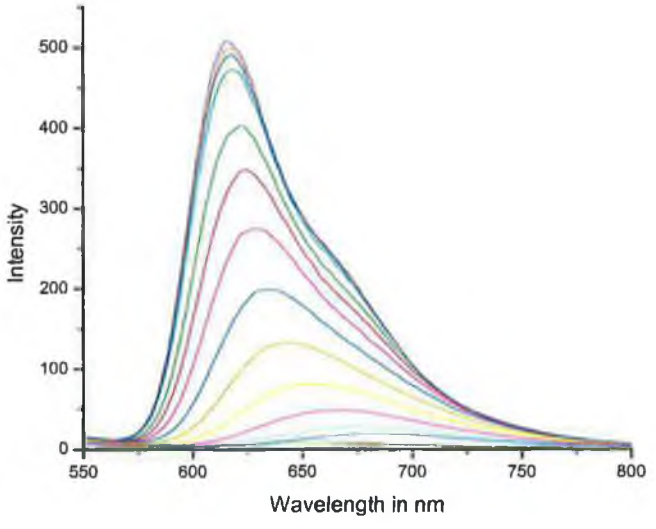

Figure D.2 *Temperature dependence of the emission spectrum of* $[Ru(ph_2phen)_2(pztr)]PF_6$ *in EtOH/MeOH 4/1 v/v 2%* Et_2NH *between 90 and 240 K.*

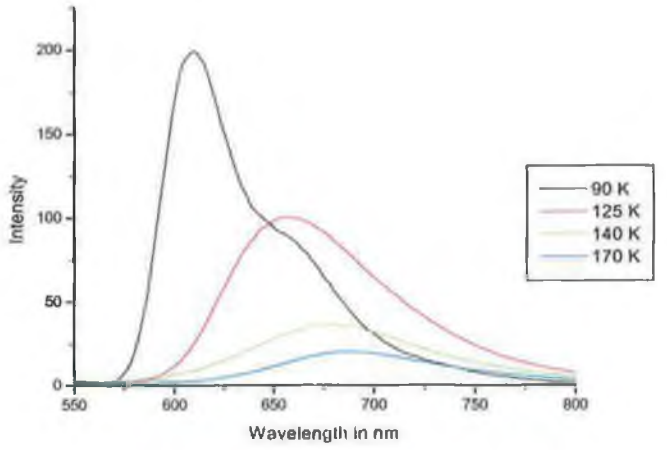

Figure D.3 *Temperature dependence of the emission spectrum of* $[Ru(ph_2phen)_2(pztr)]PF_6$ *in EtOH/MeOH 4/1 v/v 2%* Et_2NH *between 90 and 170 K.*

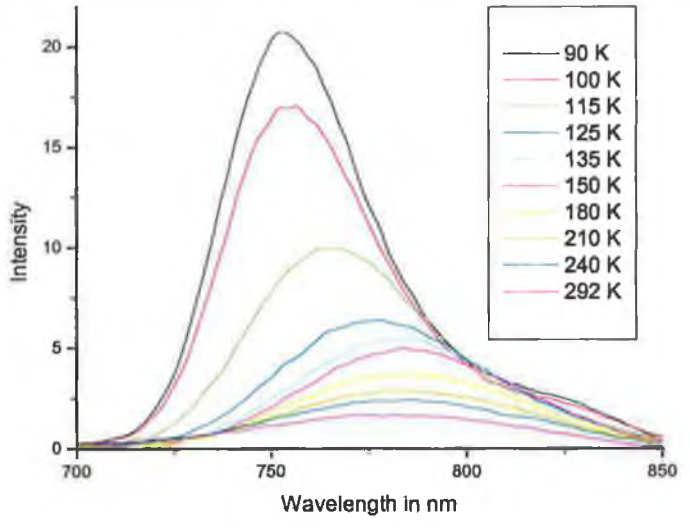

Figure D.4 *Temperature dependence of the emission spectrum of* $[Ru(biq)_2(pztr)]PF_6$ *in EtOH/MeOH 4/1 v/v 2%* Et_2NH *between 90 K and 240 K.*

c) $[Ru(phen)_2(pztr)](PF_6)$ & $[Ru(phen)_2(d_4\text{-}pztr)](PF_6)$ in EtOH/MeOH under basic conditions.

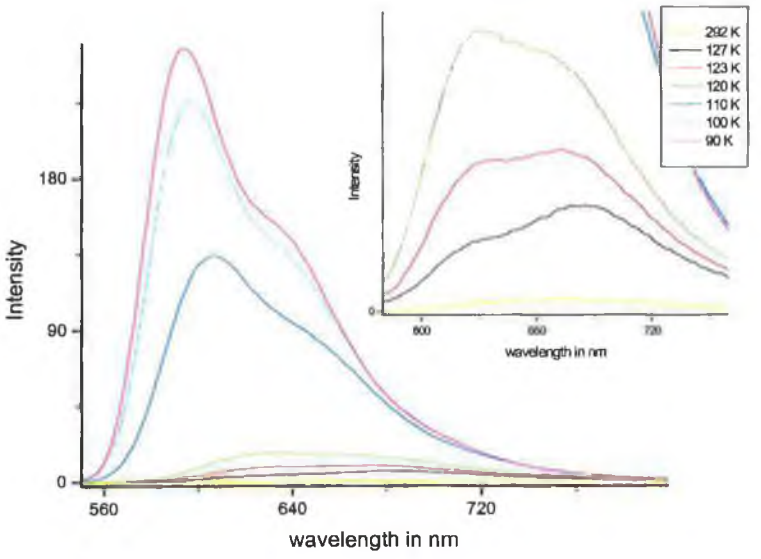

Figure D.5 *Temperature dependence of the emission spectrum of $[Ru(phen)_2(pztr)]PF_6$ in EtOH/MeOH 1/1 v/v between 90 K and 293 K. (inset: expansion of lower portion of graph)*

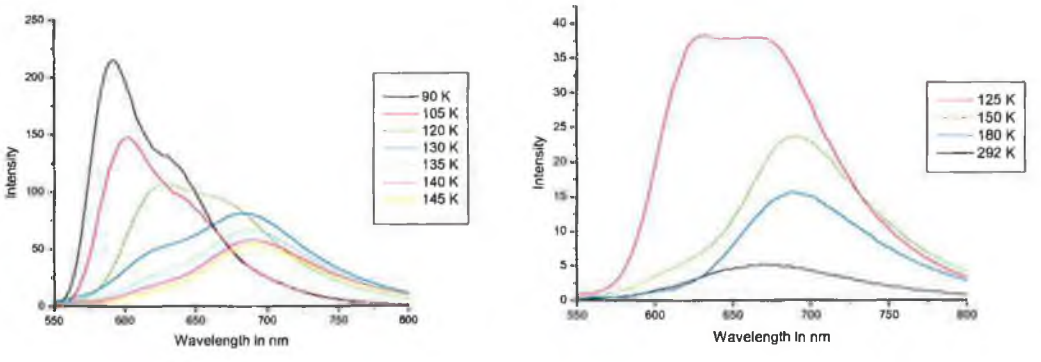

Figure D.6 *Temperature dependence of the emission spectrum of $[Ru(phen)_2(pztr)]PF_6$ in EtOH/MeOH 4/1 v/v between 90 K and 293 K. (intensity of left hand spectra are adjusted for clarity)*

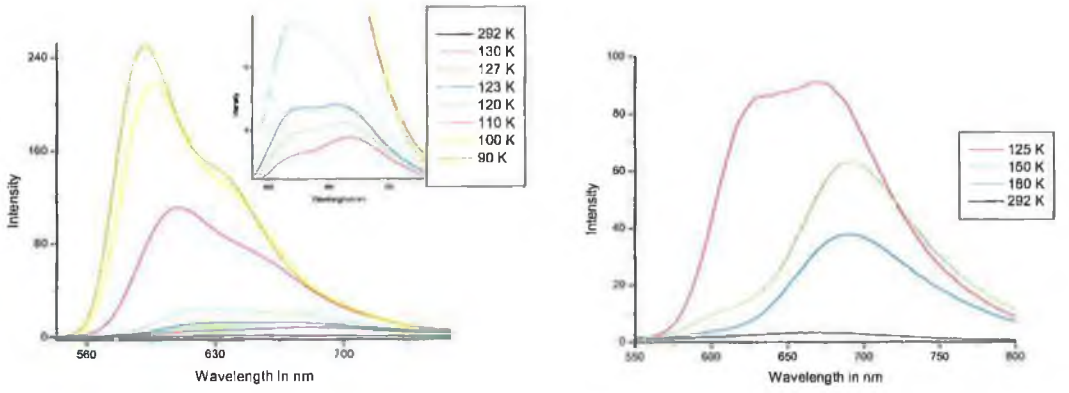

Figure D.7 *Temperature dependence of the emission spectrum of [Ru(phen)$_2$(d$_4$-pztr)]PF$_6$ in EtOH/MeOH 4/1 v/v between 90 K and 293 K. (inset: expansion of lower portion of graph)*

d) [Ru(phen)$_2$(pztr)](PF$_6$) in various glass forming matrices under basic conditions.

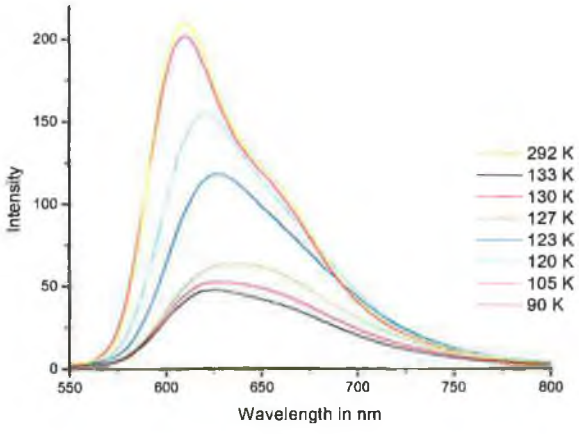

Figure D.8 *Temperature dependence of the emission spectrum of [Ru(phen)$_2$(pztr)]PF$_6$ in CH$_2$Cl$_2$/DMF 4/1 v/v between 90 K and 292 K.*

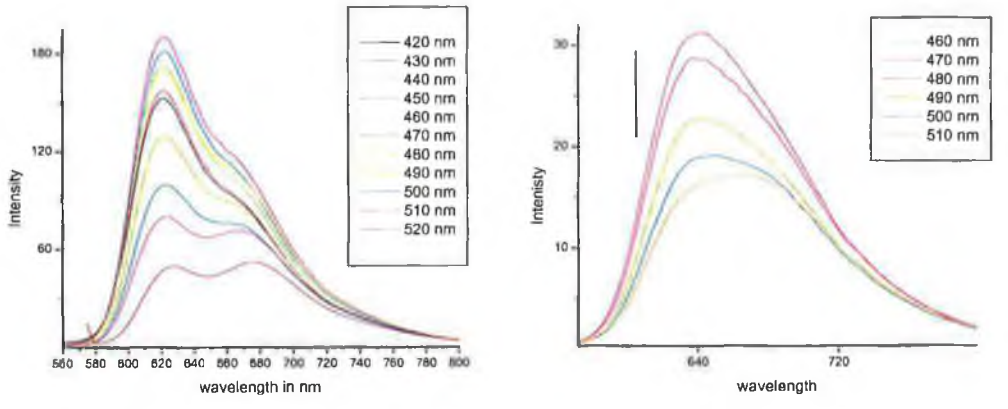

Figure D.9 *Excitation wavelength dependence of the emission spectrum of [Ru(bpy)$_2$(phpztr)]PF$_6$ in CH$_2$Cl$_2$/DMF 4/1 v/v at 90 K (left) and 130 K (right).*

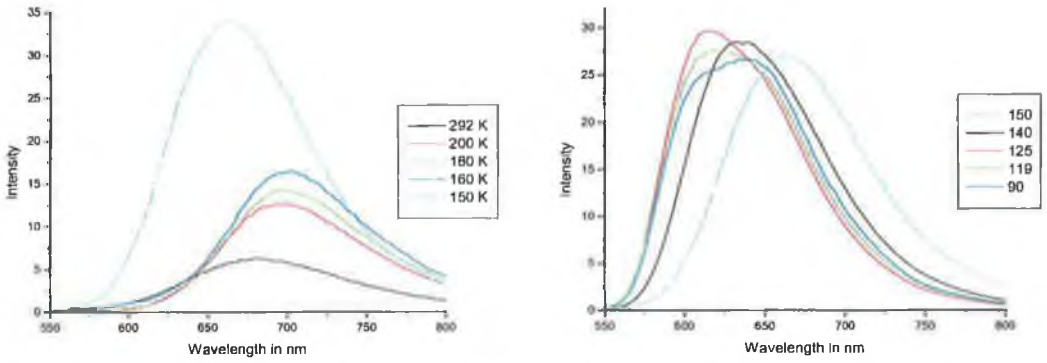

Figure D.10 *Temperature dependence of the emission spectrum of $[Ru(phen)_2(pztr)]PF_6$ in NaCl/MeOH between 90 K and 292 K. Spectra on left are normalised for comparison.*

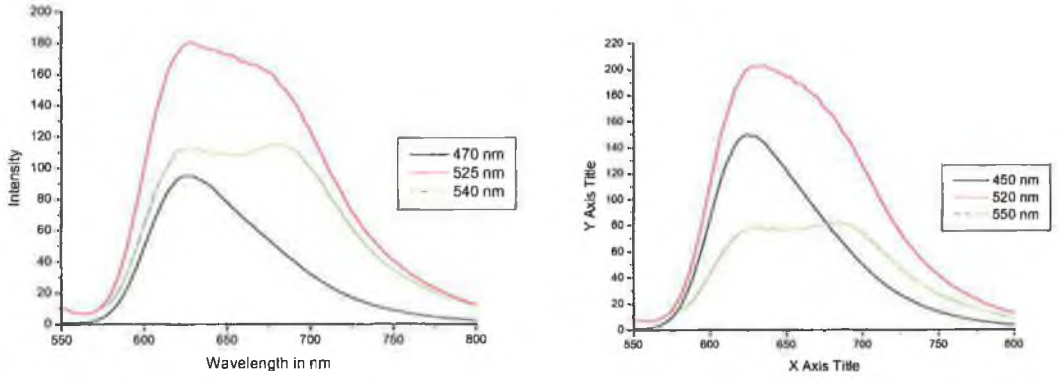

Figure D.11 *Temperature dependence of the emission spectrum of $[Ru(phen)_2(pztr)]PF_6$ in 9M $LiCl/D_2O$/2% Et_3N at between 450 and 550 nm excitation. Spectra on left at 90 K, Spectra on right at 125 K. Spectral intensity adjusted for comparison*

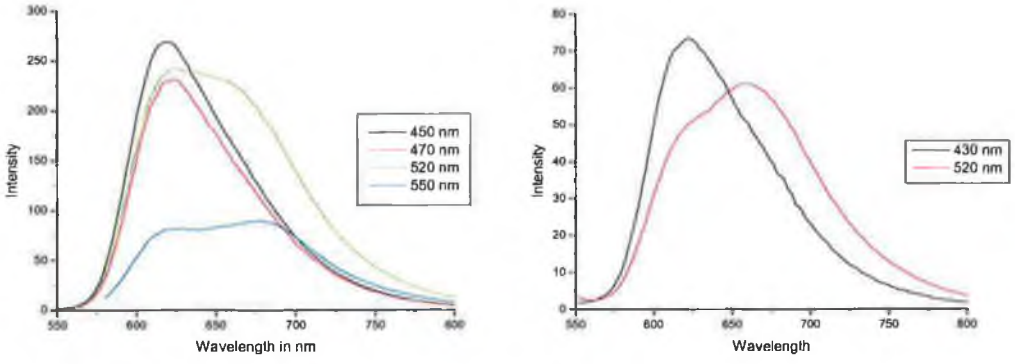

Figure D.12 *Temperature dependence of the emission spectrum of $[Ru(phen)_2(pztr)]PF_6$ in 9M $LiCl/H_2O$ between 90 K at between 450 and 550 nm excitation. Spectra on left with in D_2O no added base, Spectra on right with methyl-morpholine-N-oxide. Spectral intensity adjusted for comparison*

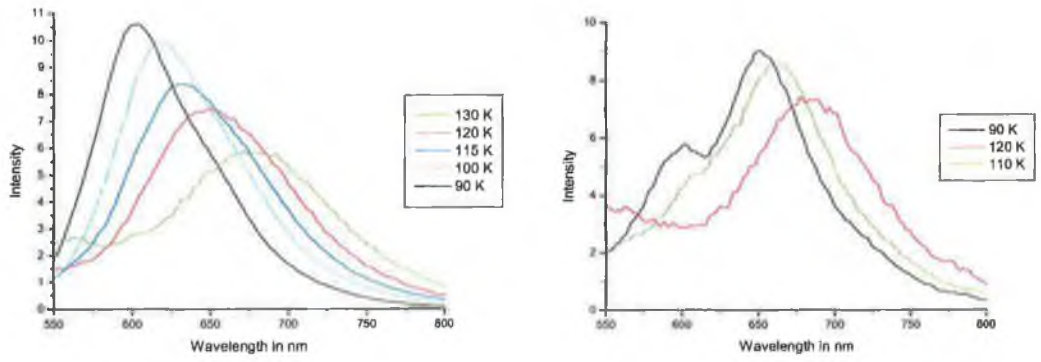

Figure D.13 *Temperature dependence of the emission spectrum of [Ru(phen)$_2$(pztr)]PF$_6$ in EtOH/MeOH 4/1 v/v with 2% CF_3CO_2H between 90 K and 130 K. Spectra on left are at 430 nm excitation. Spectra on right are at 520 nm excitation. Spectra are adjusted in intensity for comparison.*

e) [Ru(Bpy)$_2$(Xpztr)](PF$_6$) in EtOH/MeOH X = Me, Br, Ph, 2,4-dimethoxybezene.

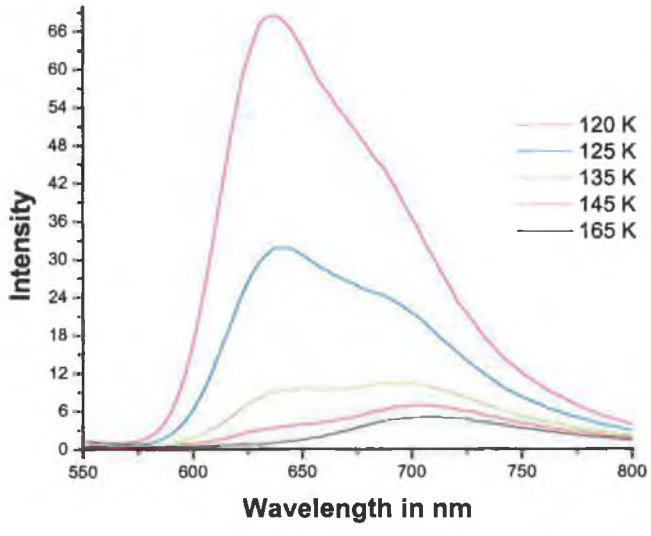

Figure D5.14 *Temperature dependence of the emission spectrum of [Ru(bpy)$_2$(mepztr)]PF$_6$ in EtOH/MeOH 4/1 v/v with 2% Et_3N between 120 and 165 K*

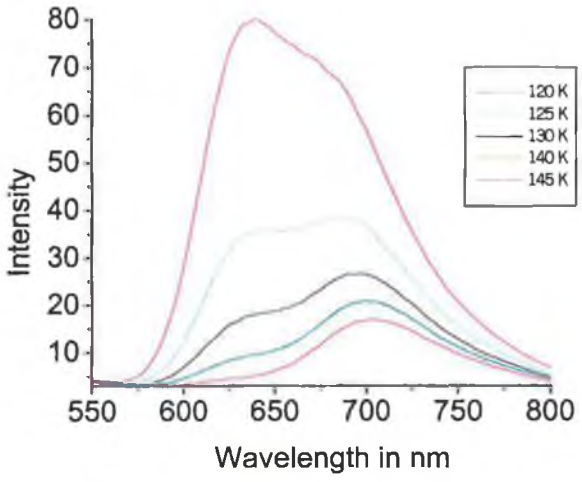

Figure D.15 *Temperature dependence of the emission spectrum of [Ru(bpy)$_2$(brpztr)]PF$_6$ in EtOH/MeOH 4/1 v/v with 2% Et$_3$N between 120 and 145 K*

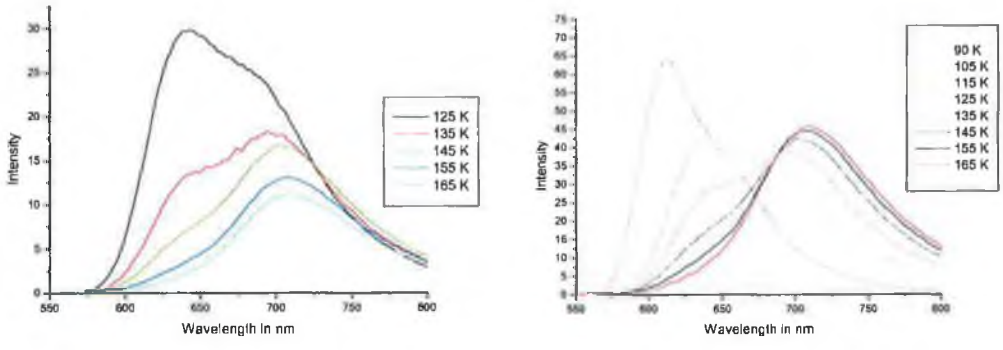

Figure D.16 *Temperature dependence of the emission spectrum of [Ru(bpy)$_2$(phpztr)]PF$_6$ in EtOH/MeOH 4/1 v/v with 2% Et$_3$N between 90 K and 165 K. Graph on left is normalised for comparison.*

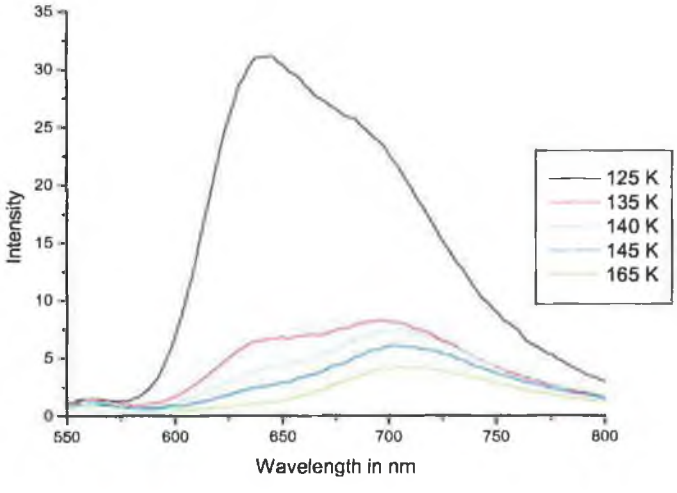

Figure D.17 *Temperature dependence of the emission spectrum of [Ru(bpy)$_2$(3-(2,5-dimethoxybezene)pztr)]PF$_6$ in EtOH/MeOH 4/1 v/v with 2% Et$_3$N between 125 K and 165 K.*

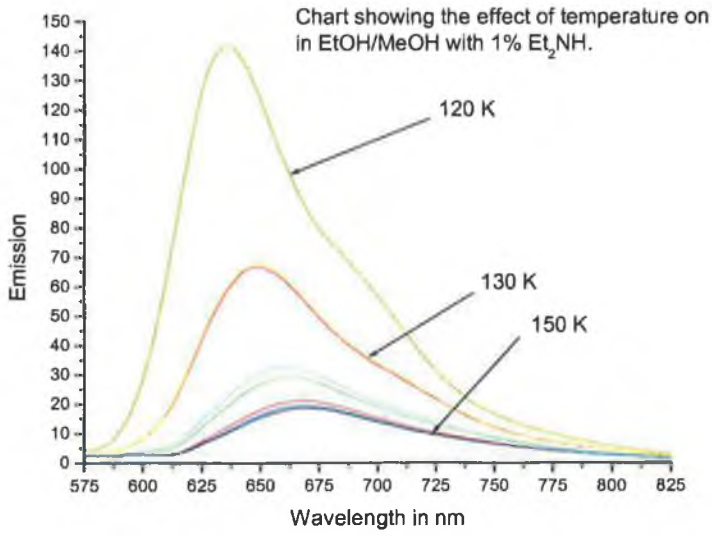

Figure D5.18 *Temperature dependence of the emission spectrum* of $[(Ru(bpy)_2)_2(bpbt)]^{2+}$ in *EtOH/MeOH 4/1 v/v with 2% Et_3N between 90 K and 165 K.*

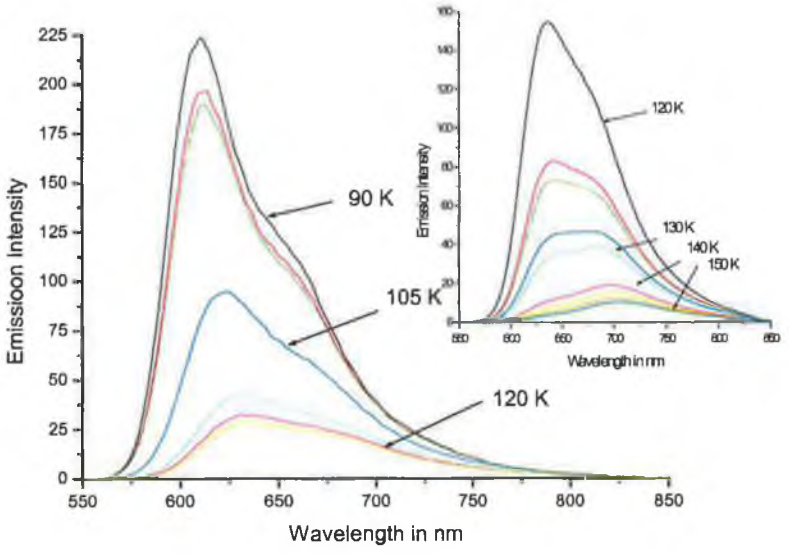

Figure D.19 *Temperature dependence of the emission spectrum of* $[(Ru(bpy)_2)_2(bpzbt)]^{2+}$ *in EtOH/MeOH 4/1 v/v with 2% Et_3N between 90 K and 165 K*

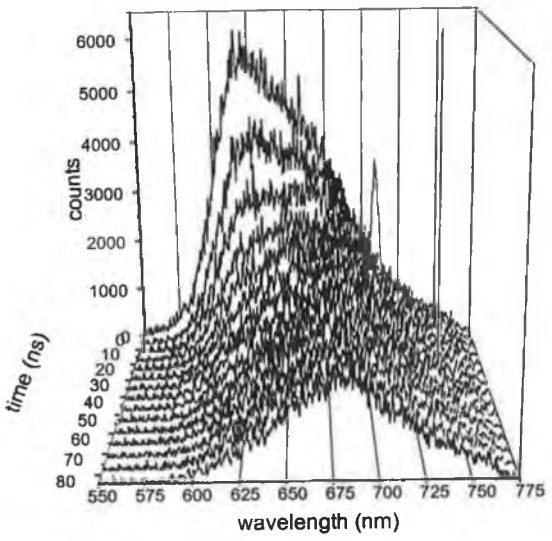

Figure D.20 *Time resolved emission spectrum of [(Ru(phen)$_2$(pztr)]PF$_6$ in EtOH/MeOH 4/1 v/v with 2% Et$_3$N at 120 K.*

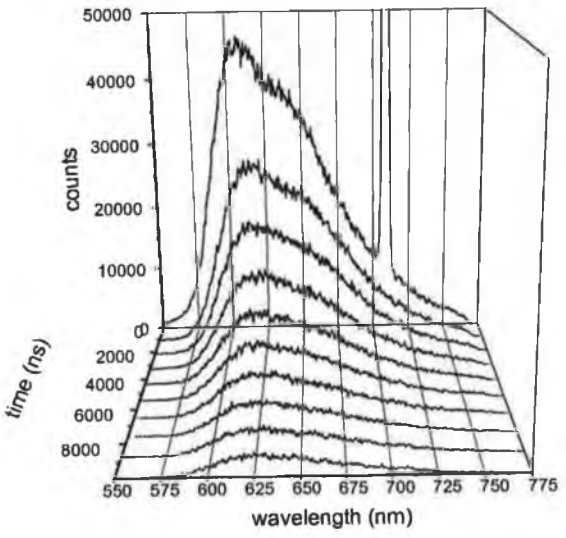

Figure D.21 *Time resolved emission spectrum of [(Ru(phen)$_2$(pztr)]PF$_6$ in EtOH/MeOH 4/1 v/v with 2% Et$_3$N at 105 K.*

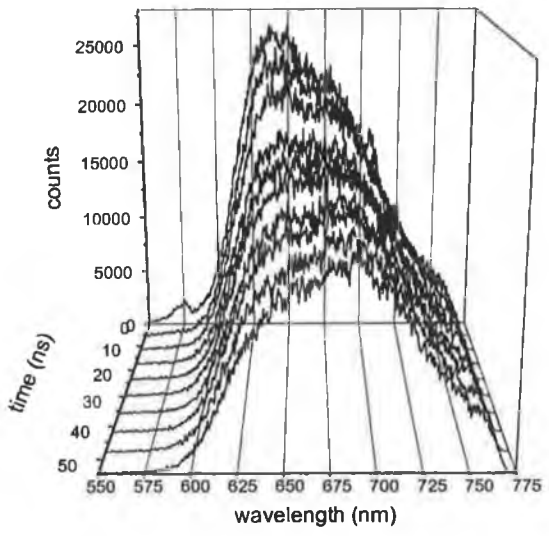

Figure D.22 *Time resolved emission spectrum of [(Ru(phen)$_2$(pztr)]PF$_6$ in EtOH/MeOH 4/1 v/v with 2% Et$_3$N at 135 K.*

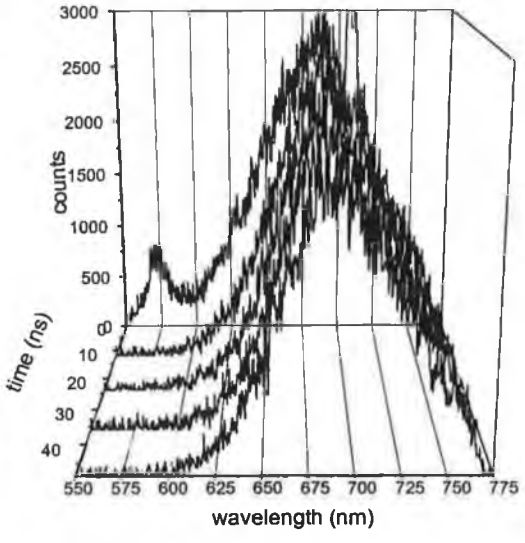

Figure D.23 *Time resolved emission spectrum of [(Ru(phen)$_2$(pztr)]PF$_6$ in EtOH/MeOH 4/1 v/v with 2% Et$_3$N at 165 K.*

Appendix E

Electron transfer

Figure E.1 describes the some of the basic electron transfer process possible, including (1) optical, (2) photoinduced and (3) thermal electron transfer. Optical electron transfer (which is observed as an intervalence transition in mixed valence systems such as those described above) uses EM radiation to move an electron spatially and is a temperature independent form of electron transfer (Equation A7.1). In contrast both thermal electron transfer processes (*i.e.* (2) and (3)), thermal energy is required to transfer electronic charge.

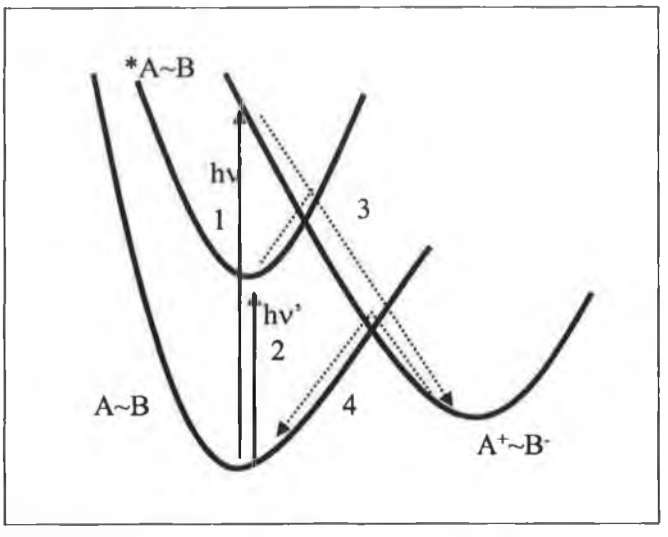

Figure E.1 *Relationship between optical (1), photo-induced (2 and 3), and thermal back (4) electron transfer processes in supramolecular species*

Equation A7.1 $A\sim B + h\nu \longrightarrow A^{+}\sim B^{-}$

The relationship between optical photo-induced and thermal back electron transfer is shown in Figure E.1. Hush Theory (vide infra) can be used to relate the parameters involved in the optical and thermal electron transfer processes.[ii] For optical electron transfer to take place the transition must be vertical (Frank Condon principle) with E_{op} being the energy of the transition. For symmetric systems the value of ΔG^{o} is zero and hence Equation E.2 becomes $E_{op} = \lambda$.[i]

Equation E.2 $E_{op} = \lambda + \Delta G^{o}$

Hush theory and classification of interaction type

For any binuclear system the mixed valence species (e.g. $[MM]^{5+}$) may be considered as either valence localised (M^{II}-M^{III}) or valence delocalised ($M^{2½}M^{2½}$). In practice however these representations are the limiting cases and frequently mixed valence systems show interaction, which is intermediate between these limits. A theoretical basis for the study of IT bands was originally developed by Hush[ii] and by Robin and Day[iii] and latter by Creutz, Meyer and others.[iii,iv]

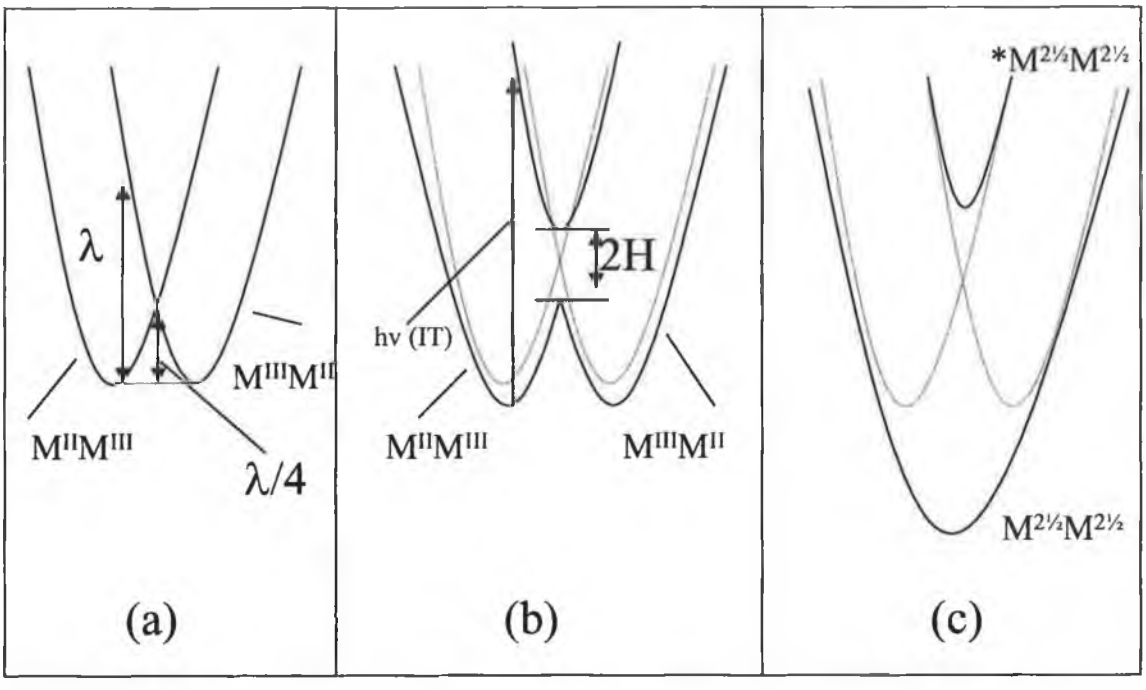

Figure E.2 *Potential energy curves for a symmetric mixed valence compound showing (a) negligible (b) weak and (c) strong electronic coupling. In the case of (b) and (c) the dashed lines represent the zero order states*[v]

If the species ($M^{II}M^{III}$) and ($M^{III}M^{II}$) are considered as "electronic isomers" the equilibrium geometry of each species can be considered in terms of both inner sphere (λ_i) and outer sphere (λ_o) effects (*vide infra*). The inner sphere effects account for the differences in the metal-ligand bond lengths between the M^{II} and M^{III} states and the outer sphere effects refer to the difference in the solvation of the two "electronic isomers". At the equilibrium geometry of each of the electronic states the other state can be considered as an electronically excited state and the possibility of an electronic transition between these states is present. The energy separation between these two states is called the reorganisational energy (λ) and is related to the intrinsic barrier to electron transfer ($\lambda/4$, *i.e.* the crossing point between the two potential wells: Figure E.2). At the crossing point there are no Franck-Condon[vi] restrictions to electron exchange since both states have the

same nuclear geometry and energy and hence thermal electron transfer is possible. If there is a large separation between the metal centres or if the bridge between the metal centres is insulating then the electronic interaction (H) between the metal centres will be negligible and the system is best represented by Figure E.2 (a). Even if the required energy for electron exchange is reached the transition probability will be close to zero and the molar absorptivity (ε) will therefore be very small. Most multinuclear systems however do show some electronic interaction, either by direct or indirect (superexchange) overlap of metal orbitals. For weakly interacting systems the electronic interaction is so small as to have little effect on the nuclear geometries of the metal centres (*i.e.* the difference in energy of the "electronic isomers" is much larger than H). However it does result in some mixing of the electronic states (Figure E.2(b)). In this situation the system retains the properties its individual components, but additional properties are observed, *i.e.* intervalence transitions. The probability of such a transition is dependent on the mixing between the two states and hence the larger the mixing the more intense the IT band. The thermal barrier to electron transfer is (when H is small) only marginally less than $\lambda/4$. When the electronic interaction is very strong (*i.e.* $H \approx \lambda$ Figure E.2(c)) then the mixing between the two electronic states results in a single ground state minimum and the system is best described as valence delocalised ($M^{2½}M^{2½}$). In such systems the properties are usually completely different from those of its individual components.

Classification of interaction

Multinuclear systems are generally divided into three classes depending on the level of electronic interaction observed. The factors determining the level of electronic interaction between the metal centres of a mixed valence system can be considered on the basis of the classification system that has developed.[ii,iii,iv]

Type I — No electronic interaction observed, no IT band observed, single redox wave. These systems have comproportionation constants at the theoretical statistical limit at $K_c = 4$, (see below) indicating very unstable mixed valence species e.g. $[Ru(bpy)_2(P2P)Ru(bpy)_2]^{5+}$ (where P2P = 1,2-di-(pyryd-4'-yl)-ethane),[ivb] shows a single two electron redox wave at 0.77 V (vs. SCE) and no evidence of a low energy band.

Type II — Moderate interaction observed although the system is best described as valence localised ($M^{II}M^{III}$), Broad IT band observed usually > 900 nm for

ruthenium binuclear complexes. Often a small difference between the first and second metal oxidation process although frequently only a single two electron oxidation wave is observed. These systems have small comproportionation constants indicating moderately stable mixed valence species *e.g.* $[Ru(bpy)_2(POP)Ru(bpy)_2]^{5+}$ (where POP = 4,4'-bipyridine),[ivb] shows two one-electron metal oxidation waves with 80 mV separation and exhibits an IT band at 1050 nm.

Type III — Strong interaction observed and system is valence delocalised ($M^{2½}M^{2½}$). Low energy absorption bands are usually observed but are narrower than for IT bands of Type II and are not charge transfer bands. These systems have large comproportionation constants indicating very stable mixed valence species. *e.g.* $([(NH_3)_5Ru(NC\text{-}CN)Ru(NH_3)_5]^{5+})$[iii] has an 800 mV separation between the first and second redox process and a strong narrow absorption at 1430 nm.

Type II/III — This is a more recent classification and describes systems with moderate interaction between the redox centres and which exhibit properties similar to both Class II and Class III systems.[vii]

The comporportionation constant: K_c

The comporportionation constant is the equilibrium constant for the reaction:

Equation E.3

$$Ru^{II}Ru^{II} + Ru^{III}Ru^{III} \overset{K_c}{\rightleftharpoons} 2Ru^{II}Ru^{III}$$

Equation E.4

$$K_c = \frac{[Ru^{II}Ru^{III}]^2}{[Ru^{II}Ru^{II}][Ru^{III}Ru^{III}]}$$

The electrostatic interaction between metal centres is an important factor in determining the stability of the mixed valence species. Since the electrostatic interaction is the product of the charges (Coulomb's law) then the equilibrium in Equation E.3 will be driven to the right in order to reduce the strength of this interaction {*i.e.* 3*3 +2*2 > 2*(2*3)}. When the interaction between the two metal centres is negligible then the system will reach a statistical equilibrium state and hence Equation E.4 will become: $K_c = 2^2/(1*1) = 4$.

Equilibrium constants may be related to other thermodynamic parameters such as the Gibbs free energy change in a system ΔG (by Equation E.5), and hence to electrochemical properties (by Equation E.6 and Equation E.7).

Equation E.5 $\Delta G = -RT \ln K_c$

Equation E.6 $\Delta G = -nF(\Delta E)$

Equation E.7 $K_c = \exp(RT\Delta E / nF) = \exp(\Delta E / 25.69)$ at 298 K

Experimental methods for the determination of extent of interaction

In addition to the electrochemistry and the study of IT bands, other methods for the determination of interaction include Stark effect spectroscopy. For the *CT* ion a dipole moment of 0.7 ± 0.1 D has been determined for the IT band. The theoretical value for the transfer of one electron over the 6.9 Å (pyrazine bridge) has been calculated to be 32.7 D.[viii] This indicates that there is extensive mixing of the metal centred and bridging orbitals and the unpaired electron is shared between the two metal centres. It should be noted at this point that the energy of the IT band may show considerable solvent dependence. In polar and hydrogen solvents the outer sphere reorganisational energy (λ_o) is much larger than for less polar and non-hydrogen bonding solvents. This results in a close correlation between the energy of the IT band and the donor number of the solvent.[ix]

Electrochemical studies

Electrochemical studies can be used to quantify the level of electronic interaction. The first parameter of interest is the separation between the two metal-based oxidation

processes (ΔE). This separation is related to the stability of the intervalence compound Ru(II)Ru(III) as defined in Equation E.7. In systems, which show strong interaction, the size of K_c will be large and vice versa. For cases where no interaction is observed then a lower limit of 4 is assumed.

The application of spectro-electrochemistry to the study of metal centre interaction in multinuclear complexes

Electrochemical data can provide direct evidence for communication between redox centres. More detailed information about the nature of this interaction can be obtained from spectroelectrochemical investigations. Analysis of the spectroscopic properties of the mixed valence species allows for the estimate of the interaction parameter (α^2) as in *Equation E.8*.

Equation E.8

$$\alpha^2 = \frac{(4.2*10^{-4}).\varepsilon_{max} \,.\, \Delta\nu_{½}}{d^2.\, E_{op}}$$

Equation E.9

$$H = [\alpha^2.E_{op}{}^2]^{½}$$

$\Delta\nu_{½}$ is its peak width at half height, d is the inter component distance in Å and E_{op} is the energy of the absorption maximum of the intervalence band. Additional information can be obtained by estimating the theoretical peak width at half height, $\Delta\nu_{½calc}$ using Equation E.10.

Equation E.10

$$\Delta\nu_{½calc} = [2310(E_{op}- \Delta E)]^{½}$$

If the value of $\Delta\nu_{1/2}$ obtained from this equation correlates well with the value found from direct measurement than the system can be described as valence localised $Ru^{II}Ru^{III}$ *i.e.* Type II. If the IT band is narrower then the system is better described as Type III (valence delocalised).

Solvatochromic effects.

The reorganisational energy (λ) can be expressed as the sum of two independent contributions: the inner sphere $\{\lambda_I\}$ (bond lengths and angles between "electronic isomers") and outer sphere $\{\lambda_o\}$ (differences in solvation between the "electronic isomers").

Equation E.11

$$\lambda = \lambda_i + \lambda_o$$

For Type III systems which are valence delocalised, no large change in the electric dipole moment upon excitation is expected and hence λ_o is expected to be small. In contrast for Type II systems the change in electric dipole moment for intervalence transitions is very large and the changes in both nuclear geometry and solvation are expected to be considerable, hence the contribution of λ_o to λ will be large. From this difference Type II can be identified by the large solvent dependence of the IT band and vice-versa. In the case of Type II/III systems, the properties of the IT band may suggest Type II and Type III simultaneously, In that a strong solvatochromic effect (indicating Type II) may be observed despite the band being very narrow (indicating Type III).

---

i. ΔG^o is the difference in the Gibbs free energy of the initial; and final electron states

ii. (a) N.S. Hush, *Prog. Inorg. Chem.*, **1967**, *8*, 391 (b) N.S. Hush, *Electrochim. Acta,* **1968**, *13*, 1005

iii. M.P. Robin and P. Day, *Adv. Inorg. Chem. Radiochem.*, **1967**, *10*, 247

iv. (a) N. S. Hush, *Prog. Inorg. Chem.*, **1967**, *10*, 247 (b) C. Creutz, *Prog. Inorg. Chem.*, **1980**, *30*, 1

v. J-P. Sauvage, J-P. Collin, J-C. Chambron, S. Guillerez, C. Coudret, V. Balzani, F. Bargelletti, L. De Cola and L. Flamigni, *Chem. Rev.*, **1994**, *94*, 993

vi. On the timescale of an electronic transition the nuclear geometry is effectively frozen. Hence all transitions must be vertical.

vii. K.D. Demadis, C.M. Hartshorm, T.J. Meyer, *Chem. Rev.*, **2001**, *101*, 2655

viii. D. H. Oh, M. Sano and S. G. Boxer, *J. Am. Chem. Soc.*, **1991**, *113*, 6880

ix. (a) T.J. Meyer, *Acc. Chem. Res.*, **1978**, *11*, 94 (b) G.A. Neyhart, J.T. Hupp, J.C. Curtis, C.J. Timpson and T.J. Meyer, *J. Am. Chem. Soc.*, **1996**, *118*, 3724 (c) P.Perez-Tejeda, P. Lopez, M.L. Moya, M. Dominquez, F. Sanchez, E. Carmona and P. Palma, *New J. Chem.*, **1996**, *20*, 95

Appendix F

Synthesis and characterisation of Ruthenium(II) and Osmium(II) polypyridyl complexes employed in Chapters 4 to 6

$[Os(bpy)_3](PF_6)_2.H_2O.KPF_6$ This complex was prepared as a side product in the preparation of *cis*-$[Os(bpy)_2Cl_2]$ (see Chapter 2). 600 mg (1.37 mmol) of $(NH_4)_2OsCl_6$ and 462 mg (2.96 mmol) of bpy were heated at reflux in 4 cm^3 of ethylene glycol for 30 mins. The solution was cooled to room temperature and 5 cm^3 of saturated sodium dithionite (aqueous) solution was added dropwise and the solution stirred overnight. The *cis*-$[Os(bpy)_2Cl_2]$ formed as a precipitate and was removed from the reaction mixture by vacuum filtration. 2 cm^3 of saturated $NH_4PF_{6(aq)}$ solution was added to the filtrate. The resulting precipitate was filtered, washed with diethyl ether and purified by column chromatography on silica gel with 65/35 CH_3CN/H_2O *sat.* KNO_3 as eluent. The solvent was reduced in vacuo and the product precipitate with 0.5 cm^3 of saturated NH_4PF_{6aq}. Yield 90 mg (0.08 mmol, 6 %). ^1H NMR (400 MHz) in CD_3CN; 8.50 (6H, d, H3), 7.87 (6H, dd, H4), 7.45 (6H, d, H6), 7.315 (6H, dd, H5). Mass spec M^+ at 330 m/z (calculated for $OsC_{30}H_{24}N_6$: 329.5). CHN analysis (Calculated for $OsP_2F_{12}N_6C_{30}H_{24}.H_2O.KPF_6$); C 31.85 (31.80 %), H 2.01 (2.12 %), N 7.32 (7.42%).

$[Os([D_8]\text{-}bpy)_3](PF_6)_2$. As for $[Os(bpy)_3](PF_6)_2$ except 300 mg (0.685 mmol) of $(NH_4)_2OsCl_6$ and 240 mg (1.46 mmol) of $[D_8]$-bpy. Yield 70 mg (0.07 mmol, 10 %) ^1H NMR (400 MHz) in CD_3CN; 8.59 (*resid.* s, H3), 7.98 (*resid.* s, H4), 7.75 (*resid.* s, H6), 7.42 (*resid.* s, H5). Mass spec M^+ at 342 m/z (calculated for $OsC_{30}D_{24}N_6$: 341.5).

$[Os(phen)_3](PF_6)_2$. As for $[Os(bpy)_3](PF_6)_2$ except 300 mg (0.68 mmol) of $(NH_4)_2OsCl_6$ and 250 mg (1.38 mmol) of phen. Yield 90 mg (0.09 mmol, 14 %). ^1H NMR (400 MHz) in CD_3CN; 8.14 (d, H4/7), 8.01 (s, H5/H6), 7.71 (d, H6), 7.42 (dd, H5).

$[Os([D_8]\text{-}phen)_3](PF_6)_2$. As for $[Os(bpy)_3](PF_6)_2$ except 300 mg (0.68 mmol) of $(NH_4)_2OsCl_6$ and 260 mg (1.38 mmol) of $[D_8]$-phen. Yield 60 mg (0.06 mmol, 9 %). ^1H NMR (400 MHz) in CD_3CN; 8.14 (*resid.* s, H4/7), 8.01 (*resid.* s, H5/H6), 7.71 (*resid.* s, H6), 7.42 (*resid.* s, H5).

$[Os(bpy)_2([D_8]\text{-}bpy)](PF_6)_2.KPF_6$ 55 mg (0.09 mmol) of *cis*-$[Os(bpy)_2Cl_2]$ and 30 mg (0.18 mmol) of $[D_8]$-bpy were heated at reflux in 4 cm^3 of ethylene glycol for 30 mins. 5 cm^3 of water was added and the reaction mixture heated at reflux for a further 8 h. The reaction mixture was cooled to room temperature and 2 cm^3 of saturated NH_4PF_{6aq} solution was added to the reaction mixture and the resulting precipitate was filtered, washed with diethyl ether and purified by column chromatography on silica gel with 65/35 CH_3CN/H_2O *sat.* KNO_3 as eluent. The solvent was reduced in vacuo and the product precipitate with 0.5 cm^3 of saturated NH_4PF_{6aq}. Yield 60 mg (0.06 mmol, 67 %). ^1H NMR (400 MHz) in CD_3CN; 8.50 (6H, d, H3), 7.87 (6H, dd, H4), 7.45 (6H, d, H6), 7.315 (6H, dd, H5).CHN analysis (Calculated for $OsP_2F_{12}N_6C_{30}H_{16}D_8.KPF_6$); C 32.30 (31.57 %), H 2.04 (2.10 %), N 7.40 (7.37 %).

$[Os([D_8]\text{-}bpy)_2(bpy)](PF_6)_2.H_2O.KPF_6$ As for $[Os(bpy)_2([D_8]\text{-}bpy)](PF_6)_2$ except 50 mg (0.08 mmol) of *cis*-$[Os([D_8]\text{-}bpy)_2Cl_2]$ and 30 mg (0.19 mmol) of bpy. Yield 40 mg (0.04 mmol, 50 %) ^1H NMR (400 MHz) in CD_3CN; 8.50 (6H, d, H3), 7.87 (6H, dd, H4), 7.45 (6H, d, H6), 7.315 (6H, dd, H5). CHN analysis (Calculated for $OsP_2F_{12}N_6C_{30}H_{24}D_6.H_2O$); C 31.68 (30.87 %), H 1.93 (2.14 %), N 7.06 (7.20 %).

$[Os(phen)_2([D_8]\text{-}phen)](PF_6)_2$. As for $[Os(bpy)_2([D_8]\text{-}bpy)](PF_6)_2$ except 50 mg (0.76 mmol) of *cis*-$[Os(phen)_2Cl_2]$ and 30 mg (0.16 mmol) of $[D_8]$-phen. Yield 35 mg (0.034 mmol, 50 %). ^1H NMR (400 MHz) in CD_3CN; 8.14 (d, H4/7), 8.01 (s, H5/H6), 7.71 (d, H6), 7.42 (dd, H5).

$[Os([D_8]\text{-}phen)_2(phen)](PF_6)_2$. As for $[Os(bpy)_2([D_8]\text{-}bpy)](PF_6)_2$ except 50 mg (0.074 mmol) of *cis*-$[Os([D_8]\text{-}phen)_2Cl_2]$ and 30 mg (0.167 mmol) of phen. Yield 37 mg (0.038 mmol, 52 %). ^1H NMR (400 MHz) in CD_3CN; 8.14 (d, H4/7), 8.01 (s, H5/H6), 7.71 (d, H6), 7.42 (dd, H5).

$[Os(bpy)_2(phen)](PF_6)_2$. As for $[Os(bpy)_2([D_8]\text{-}bpy)](PF_6)_2$ except 50 mg (0.076 mmol) of *cis*-$[Os(bpy)_2Cl_2]$ and 30 mg (0.160 mmol) of phen. Yield 42 mg (0.043 mmol, 56 %). ^1H NMR (400 MHz) in CD_3CN: 8.53 (d, 1H), 8.48 (d, 1H), 8.44 (d, 1H), 8.26 (s, 1H), 8.01 (d, 1H), 7.94 (dd, 1H), 7.81 (m, 2H), 7.7 (dd, 1H), 7.45 (d, 1H), 7.38 (dd, 1H), 7.15 (dd, 1H).

[Os([D$_8$]-bpy)$_2$(phen)](PF$_6$)$_2$. As for [Os(bpy)$_2$([D$_8$]-bpy)](PF$_6$)$_2$ except 50 mg (0.08 mmol) of *cis*-[Os([D$_8$]-bpy)$_2$Cl$_2$] and 30 mg (0.167 mmol) of phen. Yield 60 mg (0.061 mmol, 76 %). ^{1}H NMR (400 MHz) in CD_3CN: 8.44 (d, 1H), 8.26 (s, 1H), 7.79 (d, 1H), 7.38 (dd, 1H).

[Os(bpy)$_2$([D$_8$]-phen)](PF$_6$)$_2$. As for [Os(bpy)$_2$([D$_8$]-bpy)](PF$_6$)$_2$ except 50 mg (0.082 mmol) of *cis*-[Os(bpy)$_2$Cl$_2$] and 30 mg (0.16 mmol) of [D$_8$]-phen. Yield 40 mg (0.041 mmol, 50 %). ^{1}H NMR (400 MHz) in CD_3CN: 8.53 (d, 1H), 8.48 (d, 1H), 8.01 (d, 1H), 7.94 (dd, 1H), 7.81 (dd, 1H), 7.7 (dd, 1H), 7.45 (d, 1H), 7.15 (dd, 1H).

[Os([D$_8$]-bpy)$_2$([D$_8$]-phen)](PF$_6$)$_2$. As for [Os(bpy)$_2$([D$_8$]-bpy)](PF$_6$)$_2$ except 50 mg (0.08 mmol) of *cis*-[Os([D$_8$]-bpy)$_2$Cl$_2$] and 30 mg (0.16mmol) of [D$_8$]-phen. Yield 35 mg (0.041 mmol, 50 %). ^{1}H NMR (400 MHz) in CD_3CN: 8.53 (*resid.* s), 8.48 (*resid.* s), 8.44 (*resid.* s), 8.26 (*resid.* s), 8.01 (*resid.* s), 7.94 (*resid.* s), 7.81 (*resid.* s), 7.79 (*resid.* s), 7.7 7.81 (*resid.* s), 7.45 7.81 (*resid.* s), 7.38 7.81 (*resid.* s), 7.15 7.81 (*resid.* s).

[Os(phen)$_2$(bpy)](PF$_6$)$_2$. As for [Os(bpy)$_2$([D$_8$]-bpy)](PF$_6$)$_2$ except 50 mg (0.06 mmol) of *cis*-[Os(phen)$_2$Cl$_2$] and 30 mg (0.192 mmol) of bpy. Yield 34 mg (0.034 mmol, 57 %). ^{1}H NMR (400 MHz) in CD_3CN: 8.52 (d, 1H), 8.465 (d, 1H), 8.36 (d, 1H), 8.27 (s, 1H), 8.26 (s, 1H), 8.145 (d, 1H), 7.84 (dd, 1H), 7.82 (d, 1H), 7.755 (dd, 1H), 7.61 (d, 1H), 7.51 (dd, 1H), 7.20 (dd, 1H)

[Os([D$_8$]-phen)$_2$(bpy)](PF$_6$)$_2$. As for [Os(bpy)$_2$([D$_8$]-bpy)](PF$_6$)$_2$ except 50 mg (0.074 mmol) of *cis*-[Os([D$_8$]-phen)$_2$Cl$_2$] and 30 mg (0.192 mmol) of bpy. Yield 50 mg (0.049 mmol, 66 %) ^{1}H NMR (400 MHz) in CD_3CN: 8.52 (d, 1H), 7.82 (d, 1H), 7.61 (d, 1H), 7.20 (dd, 1H)

[Os(phen)$_2$([D$_8$]-bpy)](PF$_6$)$_2$. As for [Os(bpy)$_2$([D$_8$]-bpy)](PF$_6$)$_2$ except 50 mg (0.076 mmol) of *cis*-[Os(phen)$_2$Cl$_2$] and 30 mg (0.183 mmol) of [D$_8$]-bpy. Yield 53 mg (0.053 mmol, 69 %). ^{1}H NMR (400 MHz) in CD_3CN: 8.465 (d, 1H), 8.36 (d, 1H), 8.27 (s, 1H), 8.26 (s, 1H), 8.145 (d, 1H), 7.82 (d, 1H), 7.755 (dd, 1H), 7.51 (dd, 1H).

[Ru(bpy)$_3$](PF$_6$)$_2$. 350 g (2.24 mmoles) of bpy and 670 mg (1.2 mmoles) *cis*-[Ru(bpy)$_2$Cl$_2$] were dissolved in 50/50 v/v/ ethanol/water. The solution (purple) was refluxed for 4 h. Ethanol was removed under reduced pressure. The product was

precipitated with saturated ammonium hexafluorophosphate solution filtered and air-dried for 3 hours. The deep red product was rerystallised from acetone/water 5/1. Yield 690 mg (0.75 mmoles, 62%). ^{1}H NMR (400 MHz) in CD_3CN; 8.415 (6H, d, H3), 7.97 (6H, dd, H4), 6.50 (6H, d, H6), 7.31 (6H, dd, H5). CHN analysis (Calculated for $RuP_2F_{12}N_6C_{30}H_{24}$); C 41.90 (41.91 %), H 2.69 (2.79%), N 9.65 (9.78%).

[Ru([D$_8$]-bpy)$_3$](PF$_6$)$_2$. As for [Ru(bpy)$_3$](PF$_6$)$_2$ except 200 mg (1.2 mmoles) of d$_8$-bpy and 350 mg (1.0 mmoles) *cis*-[Ru([D$_8$]-bpy)$_2$Cl$_2$]. Yield 460 mg (0.52 mmoles, 52%). ^{1}H NMR (400 MHz) in CD_3CN; 8.41 (*resid.* s. H3), 7.965 (*resid.* s, H4), 6.49 (*resid.* s, H6), 7.30 (*resid.* s, H5).

[Ru(ph$_2$phen)$_3$](PF$_6$)$_2$.H$_2$O As for [Ru(bpy)$_3$](PF$_6$)$_2$ except 100 mg (0.3 mmoles) of ph$_2$phen and 160 mg (0.18 mmoles) *cis*-[Ru(ph$_2$phen)$_2$Cl$_2$]. Yield 210 mg (0.15 mmoles 83 %). ^{1}H NMR (400 MHz) in CD_3CN; 8.32 (d, 2H), 8.26 (s, 2H), 7.69 (d, 2H), 7.66 (m, 10H). CHN analysis (Calculated for $RuP_2F_{12}N_6C_{72}H_{48}.H_2O$); C 60.91 (61.49 %), H 3.36 (3.49 %), N 5.86 (5.98 %).

[Ru(ph$_2$phen)$_3$]Cl$_2$. 162 mg (0.67 mmol) of $RuCl_3.2H_2O$ and 665 mg (2.0 mmol) of ph$_2$phen. Yield 430 mg (0.37 mmol, 55 %), ^{1}H NMR; as for [Ru(ph$_2$phen)$_3$](PF$_6$)$_2$.H$_2$O

[Ru([D$_{14}$]-ph$_2$phen)$_3$]Cl$_2$. 40 mg (0.164 mmol) of $RuCl_3.2H_2O$ and 164 mg (0.47 mmol) of [D$_{14}$]-ph$_2$phen.Yield 85 mg (0.07 mmol, 43 %). ^{1}H NMR (400 MHz) in CD_3CN; 8.32 (*resid.* s), 8.26 (*resid.* s), 7.69 (*resid.* s), 7.66 (*resid.* m).

[Ru(bpy)$_2$(ph$_2$phen)](PF$_6$)$_2$.H$_2$O. As for [Ru(bpy)$_3$](PF$_6$)$_2$ except 200 mg (0.6 mmoles) of ph$_2$phen and 350 mg (0.67 mmoles) of *cis*-[Ru(bpy)$_2$Cl$_2$]. Yield 340 mg (0.33 mmoles, 49 %). ^{1}H NMR (400 MHz) in CD_3CN; 8.6 (1H, d), 8.57 (1H, d), 8.215 (s, 1H), 8.18 (d, 1H), 8.14 (dd, 1H), 8.07 (dd, 1H), 7.92 (d, 1H), 7.73 (dd, 2H), 7.65 (m, 5H), 7.50 (dd, 1H), 7.33 (dd, 1H). CHN analysis (Calculated for $RuP_2F_{12}N_6C_{44}H_{32}.H_2O$); C 51.08 (50.14 %), H 3.13 (3.13 %), N 7.64 (7.98%).

[Ru([D$_8$]-bpy)$_2$(ph$_2$phen)](PF$_6$)$_2$.2(CH$_3$)$_2$CO. As for [Ru(bpy)$_3$](PF$_6$)$_2$ except 100 mg (0.3 mmoles) of ph$_2$phen and 140 mg (0.26 mmoles) of *cis*-[Ru([D$_8$]-bpy)$_2$Cl$_2$]. Yield 190 mg (0.18 mmoles, 69 %). ^{1}H NMR (400 MHz) in CD_3CN; 8.57 (1H, d), 8.215 (s, 1H), 7.73

(dd, 2H), 7.65 (m, 5H). CHN analysis (Calculated for $RuP_2F_{12}N_6C_{44}H_{16}D_{16}.2(CH_3)_2CO$); C 51.78 (51.41 %), H 3.01 (3.77 %), N 7.11 (7.20 %).

$[Ru(bpy)_2([D_{10}]\text{-}ph_2phen)](PF_6)_2.NH_4PF_6.2H_2O$ As for $[Ru(bpy)_2(ph_2phen)](PF_6)_2$ except 90 mg (0.173 mmol) of *cis*-$[Ru(bpy)_2Cl_2]$ and 60 mg (0.175 mmol) of $[D_{10}]$-ph_2phen. Yield 125 mg (0.121 mmol, 71 %). CHN analysis (Calculated for $RuP_2F_{12}N_6C_{58}H_{22}D_{10}.2H_2O.NH_4PF_6$); C 42.83 (42.44 %), H 2.72 (3.05 %), N 7.52 (7.88 %). ^1H NMR (400 MHz) in CD_3CN; 8.6 (1H, d), 8.57 (1H, d), 8.215 (s, 1H), 8.18 (d, 1H), 8.14 (dd, 1H), 8.07 (dd, 1H), 7.92 (d, 1H), 7.73 (dd, 2H), 7.50 (dd, 1H), 7.33 (dd, 1H).

$[Ru(bpy)_2([D_{14}]\text{-}ph_2phen)](PF_6)_2.H_2O$ As for $[Ru(bpy)_3](PF_6)_2$ except 240 g (0.72 mmoles) of $[D_{14}]$-ph_2phen and 384 mg (0.73 mmoles) of *cis*-$[Ru(bpy)_2Cl_2]$. Yield 670 mg (0.65 mmoles, 89%). ^1H NMR (400 MHz) in CD_3CN; 8.6 (1H, d), 8.57 (1H, d), 8.18 (d, 1H), 8.14 (dd, 1H), 8.07 (dd, 1H), 7.92 (d, 1H), 7.50 (dd, 1H), 7.33 (dd, 1H). CHN analysis (Calculated for $RuP_2F_{12}N_6C_{42}H_{18}D_{14}.H_2O$); C 49.64 (49.48 %), H 3.03 (3.09 %), N 7.80 (7.87%).

$[Ru(bpy)_2([D_{16}]\text{-}ph_2phen)](PF_6)_2.(CH_3)_2CO$ As for $[Ru(bpy)_3](PF_6)_2$ except 100 mg (0.29 mmoles) of $[D_{16}]$-ph_2phen and 130 mg (0.25 mmoles) of *cis*-$[Ru(bpy)_2Cl_2]$. Yield 230 mg (0.22 mmoles 88 %). ^1H NMR (400 MHz) in CD_3CN; 8.6 (1H, d), 8.18 (d, 1H), 8.14 (dd, 1H), 8.07 (dd, 1H), 7.92 (d, 1H), 7.73 (dd, 2H), 7.33 (dd, 1H). CHN analysis (Calculated for $RuP_2F_{12}N_6C_{42}H_{16}D_{16}.(CH_3)_2CO$); C 50.81 (50.86 %), H 3.23 (3.43 %), N 7.54 (7.57 %).

$[Ru([D_8]\text{-}bpy)_2([D_{16}]\text{-}ph_2phen)](PF_6)_2.H_2O$ As for $[Ru(bpy)_3](PF_6)_2$ except 119 mg (0.34 mmoles) of $[D_{16}]$-ph_2phen and 140 mg (0.26 mmoles) of *cis*-$[Ru([D_8]\text{-}bpy)_2Cl_2]$. Yield 220 mg (0.21 mmoles, 80 %). CHN analysis (Calculated for $RuP_2F_{12}N_6C_{42}D_{32}.H_2O$); C 48.94 (48.66 %), H 3.01 (3.04 %), N 7.69 (7.74 %).

$[Ru(bpy)(ph_2phen)_2](PF_6)_2.2H_2O$ As for $[Ru(bpy)_3](PF_6)_2$ except 200 mg (1.28 mmoles) of bpy and 350 mg (40 mmoles) of *cis*-$[Ru(ph_2phen)_2Cl_2]$. Yield 390 mg (0.33 mmoles,82 %). ^1H NMR (400 MHz) in CD_3CN; 8.39 (1H, d), 8.095 (1H, d), 8.00 (s, 1H), 7.99 (s, 1H), 7.90 (m, 2H), 7.67 (s, 1H), 7.55 (d, 1H), 7.40 (m, 11H), 7.17 (dd, 1H). CHN

analysis (Calculated for $RuP_2F_{12}N_6C_{58}H_{40}.2H_2O$); C 56.07 (55.81%), H 2.42 (3.37%), N 5.66 (6.74%).

[Ru(bpy)([D16]-ph2phen)2](PF6)2.H2O.CH3CN. As for $[Ru(bpy)_3](PF_6)_2$ except 105 mg (0.67 mmoles) of bpy and 300 mg (0.33 mmoles) of *cis*-$[Ru([D_{16}]\text{-}ph_2phen)_2Cl_2]$. Further purification by flash precipitation from acetonitrile into diethylether was carried out. Yield 350 mg (0.29 mmoles 87 %). ^1H NMR (400 MHz) in CD_3CN; 8.39 (1H, d), 7.90 (dd, 1H), 7.67 (s, 1H), 7.17 (dd, 1H). CHN analysis (Calculated for $RuP_2F_{12}N_6C_{58}H_8D_{32}.H_2O.CH_3CN$); C 54.32 (55.21%), H 3.13 (3.37 %), N 7.43 (7.52 %).

[Ru([D8]-bpy)(ph2phen)2](PF6)2.2H2O As for $[Ru(bpy)_3](PF_6)_2$ except 103 mg (0.63 mmoles) of $[D_8]$-bpy and 350 mg (40 mmoles) of *cis*-$[Ru(ph_2phen)_2Cl_2]$. Yield 400 mg (0.34 mmoles 85 %). ^1H NMR (400 MHz) in CD_3CN; 8.095 (1H, d), 8.00 (s, 1H), 7.99 (s, 1H), 7.90 (d, 1H), 7.55 (d, 1H), 7.40 (m, 11H). CHN analysis (Calculated for $RuP_2F_{12}N_6C_{58}H_{32}D_8.2H_2O$); C 54.13 (55.46 %), H 3.17 (3.35 %), N 6.98 (6.69 %).

[Ru([D8]-bpy)([D16]-ph2phen)2](PF6)2. As for $[Ru(bpy)_3](PF_6)_2$ except 110 mg (0.67 mmoles) of $[D_8]$-bpy and 370 mg (0.4 mmoles) *cis*-$[Ru([D_{16}]\text{-}ph_2phen)_2Cl_2]$. Yield 420 mg (0.34 mmoles, 85 %). CHN analysis (Calculated for $RuP_2F_{12}N_6C_{58}D_{40}$); C 55.29 (55.64 %), H 3.15 (3.20 %), N 7.07 (6.71 %).

[Ru(bpy)2(4,4'-dcb)](PF6)2.3H2O 260 mg (0.5 mmol) of *cis*-$[Ru([bpy)_2Cl_2]$ and 122 mg (0.5 mmol) of H_2dcb were heated at reflux in 50 cm^3 of EtOH/H_2O 50/50 v/v for 4 h. The reaction mixture was cooled to room temperature and 2 cm^3 of saturated NH_4PF_{6aq} solution were added. The solution was acidified to pH 2 and the precipitate collected by vacuum filtration and washed with diethyl ether. The product was recrystallised from methanol/water (pH 1) Yield 300 mg (0.31 mmol, 62 %) ^1H NMR in $[D_6]$-DMSO/NaOD: 8.84 (1H, s), 8.70 (2H, d), 8.09 (2H, dd), 7.73 (4H, m), 7.48 (2H, m). ^{13}C NMR $[D_6]$-DMSO/NaOD: 166.44, 156.78, 156.73, 156.70, 151.375, 148.45, 138.25, 128.09, 127.07, 124.60, 123.25. CHN analysis (Calculated for $RuP_2F_{12}N_6C_{32}H_{24}O_4.3H_2O$); C 38.33 (38.36 %), H 2.53 (2.70 %), N 8.18 (8.39 %).

[Ru(bpy)2([D6]-4,4'-dcb)](PF6)2.2H2O As for $[Ru(bpy)_2(4,4'\text{-dcb})](PF_6)_2$ except 260 mg (0.5 mmol) of *cis*-$[Ru(bpy)_2Cl_2]$ and 125 mg (0.5 mmol) of $[D_6]$- H_2dcb were heated at reflux in 50 cm^3 of EtOH/H_2O 50/50 v/v for 4 h. Yield 280 mg (0.29 mmol, 58 %) ^1H

NMR in [D_6]-DMSO/NaOD: 8.84 (*resid.* s), 8.70 (2H, d), 8.09 (2H, dd), 7.73 (2H, dd), 7.48 (2H, m). ^{13}C NMR [D_6]-DMSO/NaOD: 166.01, 156.70, 156.73, 156.67, 151.41, 148.75, 138.22, 127.07, 124.65. CHN analysis (Calculated for $RuP_2F_{12}N_6C_{32}H_{18}D_6O_4.2H_2O$); C 38.52 (38.83 %), H 2.56 (2.86 %), N 8.25 (8.49 %).

[Ru([D_8]-bpy)$_2$(4,4'-dcb)](PF$_6$)$_2$.3H$_2$O As for [Ru([H_8]-bpy)$_2$([H_6]-4,4'-dcb)](PF_6)$_2$ except 260 mg (0.485 mmol) of *cis*-[Ru([D_8]-bpy)$_2Cl_2$] and 125 mg (0.51 mmol) of H_2dcb were heated at reflux in 50 cm^3 of EtOH/H_2O 50/50 v/v for 4 h. Yield 290 mg (0.30 mmol, 60 %) ^{1}H NMR in [D_6]-DMSO/NaOD: 8.825 (1H, s), 8.75 (2**resid* s), 8.12 (2**resid.* s), 7.73 (4H, d), 7.685 (1H, d), 7.49 (*resid.* s). ^{13}C NMR [D_6]-DMSO/NaOD: 166.44, 156.73, 151.19, 149.04, 127.09, 123.24. CHN analysis (Calculated for $RuP_2F_{12}N_6C_{32}H_8D_{16}O_4.3H_2O$); C 37.75 (37.76 %), H 2.48 (2.65 %), N 8.15 (8.26 %).

[Ru([D_8]-bpy)$_2$([D_6]-4,4'-dcb)](PF$_6$)$_2$.2H$_2$O As for [Ru([D_8]-bpy)$_2$([H_6]-4,4'-dcb)](PF_6)$_2$ except 260 mg (0.485 mmol) of *cis*-[Ru([D_8]-bpy)$_2Cl_2$] and 125 mg (0.5 mmol) of [D_6]-H_2dcb were heated at reflux in 50 cm^3 of EtOH/H_2O 50/50 v/v for 4 h. Yield 310 mg (0.32 mmol, 64 %) ^{1}H NMR in [D_6]-DMSO/NaOD: 8.82 (*resid* s), 8.77 (*resid.* s), 8.765 (*resid.* s), 8.127 (*resid.* s), 8.116 (*resid.* s), 7.73 (3**resid.* s), 7.686 (*resid* s), 7.50 (*resid.* s). ^{13}C NMR [D_6]-DMSO/NaOD: 165.67, 156.76 (2 peaks). CHN analysis (Calculated for $RuP_2F_{12}N_6C_{32}H_2D_{22}O_4.H_2O$); C 38.36 (38.21 %), H 2.49 (2.59 %), N 8.19 (8.36 %).

[Ru(bpy)$_2$(phpztr)]PF$_6$.2H$_2$O. 0.63 g (2.8 mmoles) of Hphpztr were added slowly to 1000 mg (2.1 mmoles) of *cis*-[Ru(bpy)$_2Cl_2$] in 80 ml Ethanol/Water 2:1 for 4 hours. The ethanol was subsequently removed in vacuo, made basic by addition of 1 drop of conc. ammonia solution and the product precipitated with concentrated aqueous ammonium hexaflourophosphate solution. The precipitate was collected under vacuum and recrystalised from 30 ml acetone /water 5:1 with 2 drops of conc. ammonia solution. The N2 isomer was isolated by chromatography with acetonitrile as eluent. Yield of N2 isomer 550 mg (0.7 mmoles, 25 %). FAB Mass Spectral analysis gives a molecular ion$^+$ at 635 m/z and an isotopic pattern in agreement with the theoretical values. CHN analysis (Calculated for $RuPF_6N_9C_{32}H_{24}.2H_2O$); C 46.92 (47.06 %), H 3.02 (3.19 %), N 15.54 (15.44 %), P 3.47 (3.80%) ^{1}H NMR in [D_3]-acetonitrile: δ ppm 9.29 (1H, d), 8.47 (4H, m), 8.255 (1H, d), 8.04 (4H, m), 7.96 (3H, m), 7.88 (1H, d), 7.80 (2H, dd), 7.61 (1H, d), 7.4 (7H, m).

[Ru([D_8]-bpy)$_2$(phpztr)]PF_6.4H_2O As for [Ru(bpy)$_2$(phpztr)]PF_6.2H_2O except 180 mg (0.8 mmoles) of Hphpztr and 230 mg (0.5 mmoles) of *cis*-[Ru([D_8]-bpy)$_2Cl_2$]. Yield of N2 isomer 180 mg (0.2 mmoles 40 %). CHN analysis (Calculated for $RuPF_6N_9C_{32}H_8D_{16}.4H_2O$); C 44.15 (44.24 %), H 2.68 (3.23 %), N 14.37 (14.52 %). ^{1}H NMR in [D_3]-acetonitrile: 9.29 (1H, d), 8.255 (1H, d), 7.96 (2H, d), 7.61 (1H, d), 7.38 (2H, dd), 7.33 (1H, dd).

[Ru(bpy)$_2$([D_3]-phpztr)]PF_6.3H_2O As for [Ru(bpy)$_2$(phpztr)]PF_6.2H_2O except 80 mg (0.35 mmoles) of [D_3]-Hphpztr and 132 mg (0.29 mmoles) of *cis*-[Ru(bpy)$_2Cl_2$].Yield of N2 isomer 90 mg (0.12 mmoles, 41%). CHN analysis (Calculated for $RuPF_6N_9C_{32}H_{21}D_3.3H_2O$); C 45.23 (45.88 %), H 2.93 (3.23 %), N 14.79 (15.05 %). ^{1}H NMR in [D_3]-acetonitrile: δ ppm 8.47 (4H, m), 8.04 (4H, m), 7.96 (3H, m), 7.88 (1H, d), 7.80 (2H, dd), 7.4 (7H, m).

[Ru(bpy)$_2$([D_5]-Hphpztr)](PF_6)$_2$.H_2O As for [Ru(bpy)$_2$(phpztr)]PF_6.2H_2O except 30 mg (0.14 mmoles) of [D_5]-Hphpztr and 68 mg (0.13 mmoles) of *cis*-[Ru(bpy)$_2Cl_2$]. Yield of N2 isomer 61 mg (0.078 mmoles, 60 %). CHN analysis (Calculated for $RuP_2F_{12}N_9C_{32}H_{20}D_5.H_2O$); C 41.54 (40.46 %), H 2.72 (2.74 %), N 13.15 (13.28 %). ^{1}H NMR in [D_3]-acetonitrile: δ ppm 9.29 (1H, d), 8.47 (4H, m), 8.255 (1H, d), 8.04 (4H, m), 7.96 (1H, d), 7.88 (1H, d), 7.80 (2H, dd), 7.61 (1H, d), 7.4 (4H, m).

[Ru(bpy)$_2$([D_8]-phpztr)]PF_6.3H_2O As for [Ru(bpy)$_2$(phpztr)]PF_6.2H_2O except 50 mg (0.22 mmoles) of [D_8]-Hphpztr and 110 mg (0.21 mmoles) of *cis*-[Ru(bpy)$_2Cl_2$]. Yield of N2 isomer 50 mg (0.06 mmoles, 20%). CHN analysis (Calculated for $RuPF_6N_9C_{32}H_{16}D_8.3H_2O$); C 45.56 (45.61 %), H 2.89 (3.21 %), N 14.66 (14.96 %). ^{1}H NMR in [D_3]-acetonitrile: δ ppm 8.47 (4H, m), 8.04 (4H, m), 7.96 (1H, d), 7.88 (1H, d), 7.80 (2H, dd), 7.4 (4H, m).

[Ru([D_8]-bpy)$_2$([D_3]-phpztr)]PF_6.3H_2O As for [Ru(bpy)$_2$(phpztr)]PF_6.2H_2O except 100 mg (0.45 mmoles) of [D_3]-Hphpztr and 150 mg (0.28 mmoles) of *cis*-[Ru([D_8]-bpy)$_2Cl_2$]. CHN analysis (Calculated for $RuPF_6N_9C_{32}H_5D_{19}.4H_2O$); C 43.27 (44.09 %), H 2.83 (3.21 %), N 14.20 (14.47 %). Yield of N2 isomer 98 mg (0.126 mmoles, 45 %).^{1}H NMR in [D_3]-acetonitrile: 7.96 (2H, d), 7.38 (2H, dd), 7.33 (1H, dd).

[Ru([D8]-bpy)2([D8-]-phpztr)]PF6. As for $[Ru(bpy)_2(phpztr)]PF_6.2H_2O$ except 45 mg (0.19 mmoles) of $[D_8]$-Hphpztr and 80 mg (0.15 mmoles) of *cis*-$[Ru([D_8]\text{-}bpy)_2Cl_2]$. Yield of N2 isomer 37 mg (0.045 mmoles, 30 %).

[Ru(bpy)2(phpytr)]PF6.2H2O As for $[Ru(bpy)_2(phpztr)]PF_6.2H_2O$ except 250 mg (1.12 mmoles) of Hphpytr and 500 mg (0.96 mmoles) of *cis*-$[Ru(bpy)_2Cl_2]$. Yield of N2 isomer 420 mg (0.53 mmoles, 55 %). CHN analysis (Calculated for $RuPF_6N_8C_{33}H_{25}.2H_2O$); C 49.52 (49.69 %), H 3.12 (3.26 %), N 13.75 (14.05 %). ^{1}H NMR in $[D_3]$-acetonitrile: δ ppm 8.78 (1H, d), 8.75 (d, 1H), 8.66 (d, 2H), 8.20 (d, 1H), 8.14 (m, 4H), 8.04 (m, 6 H), 7.94 (d, 1H), 7.72 (d, 1H), 7.57 (dd, 2H), 7.52 (dd, 1H), 7.46 (dd, 1H), 7.31 (dd, 2H), 7.26 (m, 2H).

[Ru([D8]-bpy)2(phpytr)]PF6.2H2O As for $[Ru(bpy)_2(phpztr)]PF_6.2H_2O$ except 240 mg (1.08 mmoles) of Hphpytr and 500 mg (0.93 mmoles) of *cis*-$[Ru([D_8]\text{-}bpy)_2Cl_2]$. Yield of N2 isomer 390 mg (0.49 mmoles, 53 %). CHN analysis (Calculated for $RuPF_6N_8C_{33}H_9D_{16}.2H_2O$); C 46.85 (47.65 %), H 3.07 (3.25 %), N 13.13 (13.48 %). ^{1}H NMR (400 MHz) in $[D_3]$-acetonitrile: δ ppm 8.16 (1H, d), 7.96 (2H, 9), 7.91 (1H, dd), 7.52 (1H, d), 7.37 (2H, dd), 7.29 (1H, dd), 7.15 (1H, dd).

$[Ru(ph_2phen)_2(pztr)]PF_6.(CH_3)_2CO.2H_2O$ As for $[Ru(bpy)_2(phpztr)]PF_6.2H_2O$ except 630 mg (4.3 mmol) of Hpztr and 1000 mg (1.2 mmol) of *cis*-$[Ru(ph_2phen)_2Cl_2]$. Yield 300 mg (N2 isomer) (0.31 mmol, 26 %). CHN analysis (Calculated for $RuPF_6N_9C_{54}H_{19}.(CH_3)_2CO.2H_2O$); C 58.43 (59.48 %), H 3.51 (3.83 %), N 10.73 (10.96 %). ^{1}H NMR (400 MHz) in $[D_3]$-acetonitrile: δ ppm 9.17 (1H, d), 8.72 (1H, d), 8.54 (1H, d), 8.31 (1H, d), 8.18 (2H, d), 8.15 (2H, d), 8.11 (1H, d), 8.10 (1H, s), 7.91 (3H, m), 7.77 (1H, d), 7.65 (1H, d), 7.52 (23H, m)